USGS
science for a changing world

GROUNDWATER RESOURCES PROGRAM

Groundwater Availability of the Central Valley Aquifer, California

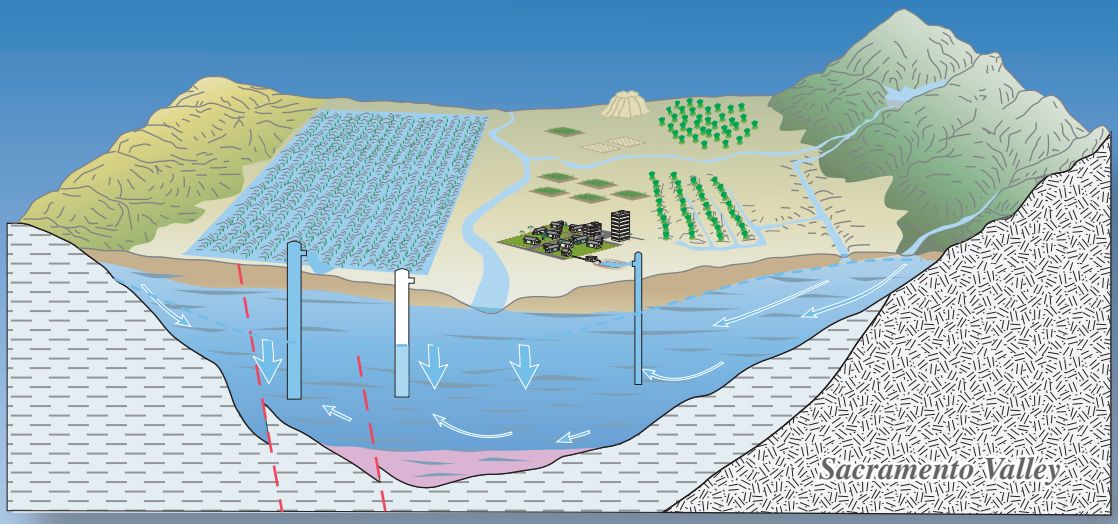

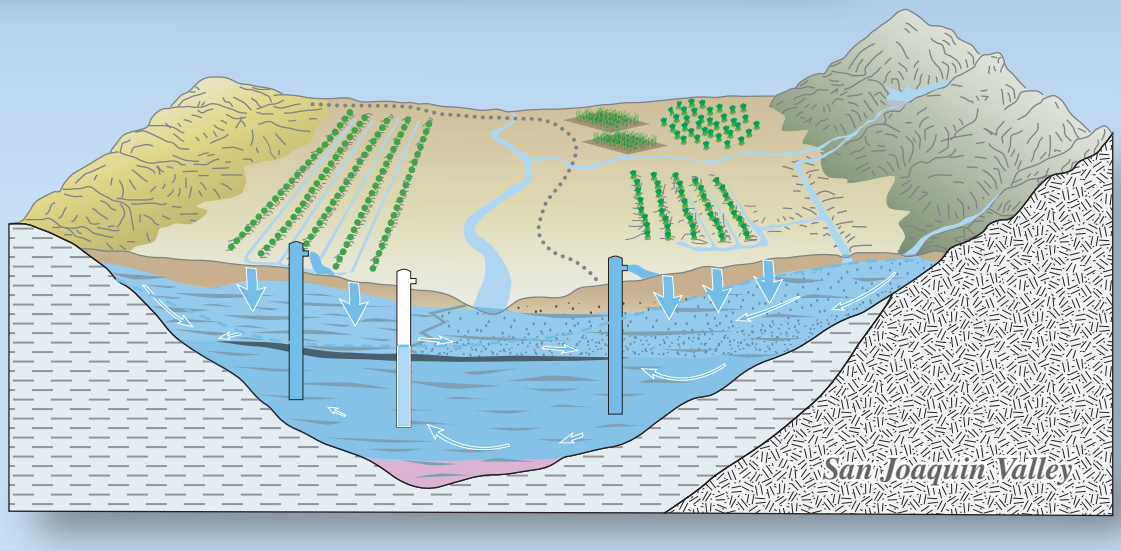

Professional Paper 1766

U.S. Department of the Interior
U.S. Geological Survey

Generalized block diagrams showing post-development hydrologeology of the Sacramento and San Joaquin Valleys, California.

Groundwater Availability of the Central Valley Aquifer, California

Edited by Claudia C. Faunt

Chapter A
Introduction, Overview of Hydrogeology, and Textural Model of California's Central Valley

By Claudia C. Faunt, Randall T. Hanson, and Kenneth Belitz

Chapter B
Groundwater Availability in California's Central Valley

By Claudia C. Faunt, Kenneth Belitz, and Randall T. Hanson

Chapter C
Numerical Model of the Hydrologic Landscape and Groundwater Flow in California's Central Valley

By Claudia C. Faunt, Randall T. Hanson, Kenneth Belitz, Wolfgang Schmid, Steven P. Predmore, Diane L. Rewis, and Kelly McPherson

Appendix 1
Supplemental Information—Modifications to Modflow-2000 Packages and Processes

By Wolfgang Schmid and R.T. Hanson

Groundwater Resources Program

Professional Paper 1766

U.S. Department of the Interior
U.S. Geological Survey

U.S. Department of the Interior
KEN SALAZAR, Secretary

U.S. Geological Survey
Suzette M. Kimball, Acting Director

U.S. Geological Survey, Reston, Virginia: 2009
For more information on the USGS—the Federal source for science about the Earth, its natural and living resources, natural hazards, and the environment, visit *http://www.usgs.gov* or call 1-888-ASK-USGS

For an overview of USGS information products, including maps, imagery, and publications, visit *http://www.usgs.gov/pubprod*

To order this and other USGS information products, visit *http://store.usgs.gov*

Suggested citation:
Faunt, C.C., ed., 2009, Groundwater Availability of the Central Valley Aquifer, California: U.S. Geological Survey Professional Paper 1766, 225 p.

ISBN 978-1-4113-2515-9

Foreword

An adequate supply of groundwater is essential for the Nation's health and economic well being. Increased use of groundwater resources and the effects of drought have led to concerns about the future availability of groundwater to meet domestic, agricultural, industrial, and environmental needs. The resulting effects of competition for groundwater from human and environmental uses need to be better understood to respond to the following basic questions that are being asked about the Nation's ability to meet current and future demands for groundwater. Do we have enough groundwater to meet the needs of the Nation? Where are these groundwater resources? Is groundwater available where it is needed? To help answer these questions, the U.S. Geological Survey's (USGS) Groundwater Resources Program is conducting large-scale multidisciplinary regional studies of groundwater availability, such as this study of the Central Valley Aquifer System, California.

Regional groundwater availability studies quantify current groundwater resources, evaluate how those resources have changed through time, and provide tools that decision makers can use to forecast system responses to future development and climate variability and change. These quantitative studies are, by design, large in scope, can include multiple aquifers, and address critical groundwater issues. The USGS has previously identified the Nation's principal aquifers and they will be used as a framework to classify and study regional groundwater systems.

The groundwater availability studies being conducted for each regional groundwater flow system emphasize the use of long-term groundwater monitoring data, in conjunction with groundwater models, to improve understanding of the flow systems and assess the status and trends in groundwater resources in the context of a changing water budget for the aquifer system. The results of these individual groundwater availability studies will be used collectively as building blocks towards a national assessment of groundwater availability. In addition, these studies will provide the foundational information and modeling tools needed to help State and local resource managers make water availability decisions based on the latest comprehensive quantitative assessment given their regional water-management constraints and goals.

Matthew C. Larsen, Associate Director for Water

U.S. Geological Survey

This page intentionally left blank.

Contents

Chapter A

Introduction, Overview of Hydrogeology, and Textural Model of California's Central Valley

Chapter B

Groundwater Availability in California's Central Valley

Chapter C

Numerical Model of the Hydrologic Landscape and Groundwater Flow in California's Central Valley

Appendix 1

Supplemental Information—Modifications to Modflow-2000 Packages and Processes

Figures

Chapter A

Chapter B

Chapter C

Appendix

Tables

Chapter A

Chapter B

Chapter C

Conversion Factors

Inch/Pound to SI

Multiply	By	To obtain
	Length	
inch (in.)	2.54	centimeter (cm)
inch (in.)	25.4	millimeter (mm)
foot (ft)	0.3048	meter (m)
mile (mi)	1.609	kilometer (km)
mile, (mi)	1.609	kilometer (km)
	Area	
acre	4,047	square meter (m^2)
acre	0.4047	hectare (ha)
acre	0.4047	square hectometer (hm^2)
acre	0.004047	square kilometer (km^2)
square foot (ft^2)	929.0	square centimeter (cm^2)
square foot (ft^2)	0.09290	square meter (m^2)
square inch (in^2)	6.452	square centimeter (cm^2)
section (640 acres or 1 square mile)	259.0	square hectometer (hm^2)
square mile (mi^2)	259.0	hectare (ha)
square mile (mi^2)	2.590	square kilometer (km^2)
	Volume	
acre-foot (acre-ft)	1,233	cubic meter (m^3)
acre-foot (acre-ft)	0.001233	cubic hectometer (hm^3)
	Flow rate	
acre-foot per day (acre-ft/d)	0.01427	cubic meter per second (m^3/s)
acre-foot per year (acre-ft/yr)	1,233	cubic meter per year (m^3/yr)
acre-foot per year (acre-ft/yr)	0.001233	cubic hectometer per year (hm^3/yr)
	Hydraulic conductivity	
foot per day (ft/d)	0.3048	meter per day (m/d)

Temperature in degrees Celsius (°C) may be converted to degrees Fahrenheit (°F) as follows:

$°F=(1.8×°C)+32$

Vertical coordinate information is referenced to the National Geodetic Vertical Datum of 1929 (NGVD 29).

Altitude, as used in this report, refers to distance above or below the NGVD 29.

NGVD 29 can be converted to the North American Vertical Datum of 1988 (NAVD 88) by using the National Geodetic Survey conversion utility available at URL *http://www.ngs.noaa.gov/TOOLS/*

Well-Numbering System

Wells are identified and numbered according to their location in the rectangular system for the subdivision of public lands. Identification consists of the township number, north or south; the range number, east or west; and the section number. Each section is divided into sixteen 40-acre tracts lettered consecutively (except I and O), beginning with "A" in the northeast corner of the section and progressing in a sinusoidal manner to "R" in the southeast corner. Within the 40-acre tract, wells are sequentially numbered in the order they are inventoried. The final letter refers to the base line and meridian. In California, there are three base lines and meridians; Humboldt (H), Mount Diablo (M), and San Bernardino (S). All wells in the study area are referenced to the San Bernardino base line and meridian (S) Well numbers consist of 15 characters and follow the format 011N001E24Q008S. In this report, well numbers are abbreviated and written 11N/1E-24Q8. Wells in the same township and range are referred to only by their section designation, 24Q8. The following diagram shows how the number for well 11N/1E-24Q8 is derived.

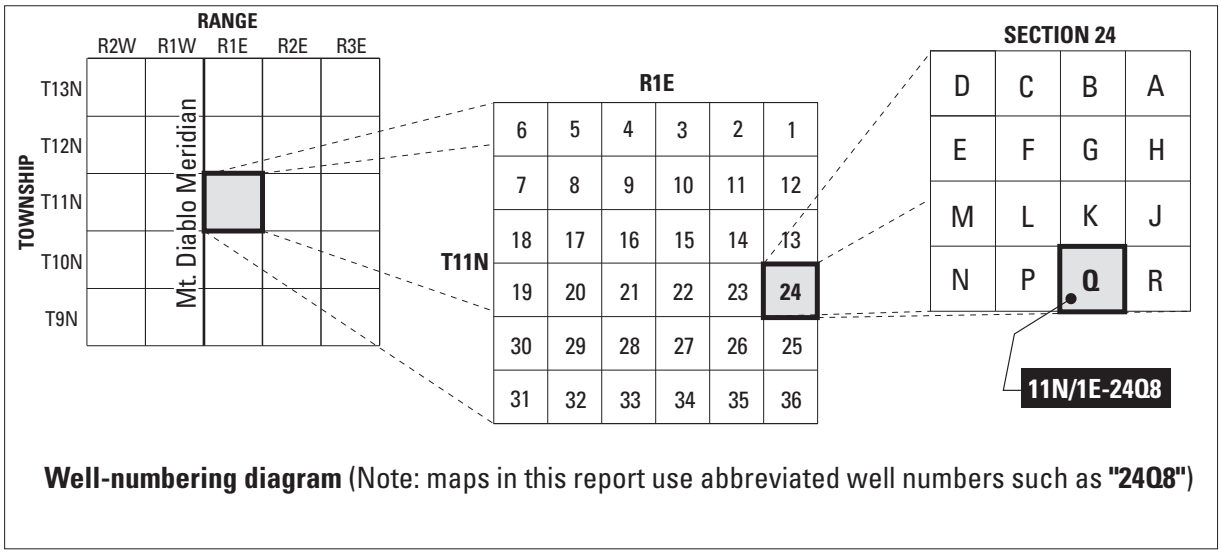

Well-numbering diagram (Note: maps in this report use abbreviated well numbers such as **"24Q8"**)

Chapter A. Introduction, Overview of Hydrogeology, and Textural Model of California's Central Valley

By Claudia C. Faunt, Randall T. Hanson, and Kenneth Belitz

Executive Summary

California's Central Valley covers about 20,000 square miles and is one of the most productive agricultural regions in the world. More than 250 different crops are grown in the Central Valley with an estimated value of $17 billion per year. This irrigated agriculture relies heavily on surface-water diversions and groundwater pumpage. Approximately one-sixth of the Nation's irrigated land is in the Central Valley, and about one-fifth of the Nation's groundwater demand is supplied from its aquifers.

The Central Valley also is rapidly becoming an important area for California's expanding urban population. Since 1980, the population of the Central Valley has nearly doubled from 2 million to 3.8 million people. The Census Bureau projects that the Central Valley's population will increase to 6 million people by 2020. This surge in population has increased the competition for water resources within the Central Valley and statewide, which likely will be exacerbated by anticipated reductions in deliveries of Colorado River water to southern California. In response to this competition for water, a number of water-related issues have gained prominence: conservation of agricultural land, conjunctive use, artificial recharge, hydrologic implications of land-use change, and effects of climate variability.

To provide information to stakeholders addressing these issues, the USGS Groundwater Resources Program made a detailed assessment of groundwater availability of the Central Valley aquifer system, that includes: (1) the present status of groundwater resources; (2) how these resources have changed over time; and (3) tools to assess system responses to stresses from future human uses and climate variability and change. This effort builds on previous investigations, such as the USGS Central Valley Regional Aquifer System and Analysis (CV-RASA) project and several other groundwater studies in the Valley completed by Federal, State and local agencies at differing scales. The principal product of this new assessment is a tool referred to as the Central Valley Hydrologic Model (CVHM) that accounts for integrated, variable water supply and demand, and simulates surface-water and groundwater-flow across the entire Central Valley system.

The development of the CVHM comprised four major elements: (1) a comprehensive Geographic Information System (GIS) to compile, analyze and visualize data; (2) a texture model to characterize the aquifer system;(3) estimates of water-budget components by numerically modeling the hydrologic system with the Farm Process (FMP); and (4) simulations to assess and quantify hydrologic conditions.

Geographic Information System (GIS)

The GIS for the CVHM is used to store, analyze, link, and visualize both the spatial and temporal model input and output data. Because the three-dimensional (3-D) groundwater-flow model of the heterogeneous Central Valley aquifer system includes complex surface-water management processes, the GIS is extremely useful for recognizing and understanding spatial relations within and between data sets. Because data transformation (including mathematical functions or logical operations), reformatting, and integration are accomplished relatively easily using GISs, the CVHM GIS was extremely valuable to the hydrologic modeling. In particular, the CVHM GIS was used to assist in the conversion of remotely sensed land-use information and topography from digital elevation models into input to the groundwater model. The link between the groundwater model and the GIS, however, was accomplished with the aid of computer programs for translating input and output data. Information from multiple, often disparate, datasets were combined, processed, and (or) resampled to produce spatial and temporal data sets needed for the groundwater model input and (or) observations. In addition, the groundwater model results can be readily visualized spatially and temporally using the CVHM GIS and accompanying translation programs.

Texture Modeling

The Central Valley is a large structural trough filled with sediments of Jurassic to Holocene age, as much as 3 miles deep in the San Joaquin Valley, which comprises the southern two-thirds of the Central Valley, and as much as 6 miles deep in the Sacramento Valley, comprising the northern one-third. Most of the freshwater, however, is contained in the upper part of the sediments consisting of post-Eocene continental rocks and deposits (Williamson and others, 1989), with thicknesses ranging from 1,000 to 3,000 feet. Aquifer-system sediments comprise heterogeneous mixtures of unconsolidated to semi-consolidated gravel, sand, silt, and clay.

In order to better characterize the aquifer-system deposits, lithologic data from approximately 8,500 drillers' logs of boreholes ranging in depth from 12 to 3,000 ft below land surface were compiled and analyzed to develop a 3-D texture model. The lithologic descriptions on the logs were simplified into a binary classification of coarse- or fine-grained. The percentage of coarse-grained sediment, or texture, then was computed from this classification for each 50-foot depth interval of the drillers' logs. A 3-D texture model was developed for the basin-fill deposits of the valley by interpolating the percentage of coarse-grained deposits onto a 1-mile spatial grid at 50-foot depth intervals from land surface to 2,800 feet below land surface.

The resulting 3-D texture model shows substantial heterogeneity and systematic variation in the texture of the sediments. These results correlate well with depositional source areas, independently mapped geomorphic provinces, and factors affecting the development of alluvial fans. In general, the Sacramento Valley predominantly is fine-grained and reflects the more fine-grained volcanic-derived sediments. However, some relatively coarse-grained deposits do occur along the river channels and the alluvial fans emanating from the Cascade Range and the northern Sierra Nevada.

In the San Joaquin Valley, especially on the eastern side, the areas of coarse-grained texture are more widespread than the areas of fine-grained texture and occur along the major rivers. In the southern part of the San Joaquin Valley, the alluvial fans derived from the glaciated parts of the Sierra Nevada are much coarser grained than the alluvial fans to the north. In contrast to the eastern San Joaquin Valley, the western San Joaquin Valley generally is finer-grained and is underlain by the Corcoran Clay Member of the Tulare Formation (hereafter referred to as the Corcoran Clay). These finer textures reflect the source material: shales and marine deposits of the Coast Range. These rocks generally yield finer-grained sediments than the granitic parent rocks that make up the alluvial fans on the eastern side of the valley. In addition, this finer-grained texture may be related to the fact that the western side of the valley has lower elevation drainage basins and is drained internally with no outlet for exporting the finer-grained materials. This area of predominately fine-grained texture is associated with the largest amount of subsidence attributed to groundwater withdrawals recorded in the valley.

Hydrologic System Modeling

The complex hydrologic system of the Central Valley is simulated using a number of advanced components of the USGS's numerical modeling code MODFLOW-2000 (MF2K). The Farm Process (FMP) for MF2K is used to simulate the groundwater and surface-water components of the hydrologic cycle and to assess and quantify the hydrologic conditions. The FMP dynamically allocates groundwater recharge and groundwater pumpage on the basis of crop water demand, surface-water deliveries, and depth to the water table. This approach is particularly useful in the Central Valley where private groundwater pumping for irrigation is not metered.

The FMP simulates un-metered historical pumpage and the delivery of surface water for 21 water-balance regions within the Central Valley for water years 1962–2003. The farm delivery requirement (irrigation requirement) is calculated from consumptive use, effective precipitation, groundwater uptake by plants, and on-farm efficiency. The FMP links with a number of existing MF2K Packages. The Streamflow Routing Package (SFR1) is linked to facilitate the simulated conveyance of surface-water deliveries. If surface-water deliveries do not meet the farm delivery requirement, the FMP invokes simulated groundwater pumping to meet the demand. Based on this demand, the FMP uses specified irrigation efficiencies to calculate irrigation return flow. Although the FMP can account for various economic and other management criteria, these criteria were not simulated in this model.

Utilizing MODFLOW and the FMP, the CVHM simulates groundwater and surface-water flow, irrigated agriculture, land subsidence, and other key processes in the Central Valley on a monthly basis. This model was developed at scales relevant to water management decisions for the entire Central Valley aquifer system, which was discretized horizontally into 20,000 model cells of 1-mi^2 areal extent, and vertically into 10 layers ranging in thickness from 50 to 1,800 ft. The texture model was used to estimate hydraulic conductivity for every cell in the model. Land subsidence, an important consequence of intense groundwater pumpage in susceptible aquifer systems, especially in the San Joaquin Valley, is simulated using the SUB Package. Intra-borehole flow, an important mechanism for vertical flow within and between hydrogeologic units in parts of the valley, is simulated across the Corcoran Clay using the MNW Package.

The hydrology of the present-day Central Valley and the CVHM model are driven by surface-water deliveries and associated groundwater pumpage, which in turn reflect spatial and temporal variability in climate, water availability, land use, and the water-delivery system. In general, the Sacramento Valley receives more precipitation than the drier, more heavily pumped San Joaquin Valley. The surface-water delivery system developed for the valley redistributes a significant part of this water from north to south. The simulated monthly water budgets indicate that precipitation and surface-water deliveries supply most of the water consumed in the initial part of the growing season, whereas increased groundwater pumpage augments these supplies later in the season. Generally, the model shows that during wet years water is taken into groundwater storage in the aquifer system, and during dry years water is released from groundwater storage. Even during dry years, however, the model shows that some recharge to the groundwater system occurs during winter or early spring precipitation.

During recent decades, changes in the surface-water delivery system have had profound effects on the hydrologic system. Because of the abundance of surface water and smaller amounts of pumpage, the Sacramento Valley and Sacramento–San Joaquin Delta generally have experienced relatively little groundwater storage depletion. The San Joaquin Valley has experienced large changes in groundwater storage. In the early 1960s, groundwater pumpage exceeded surface-water deliveries in the San Joaquin Valley, causing water levels to decline to historic lows on the west side of the San Joaquin Valley, which resulted in large amounts of subsidence. In the late 1960s, the surface-water delivery system began to route water from the wetter Sacramento Valley to the drier, more heavily pumped San Joaquin Valley. The surface-water delivery system was fully functional by the early 1970s, resulting in water-level recovery in the northern and western parts of the San Joaquin Valley. Overall, the Tulare Basin part of the San Joaquin Valley still is showing dramatic declines in groundwater levels and accompanying increased depletion of groundwater storage.

Climate variability has had profound effects on the Central Valley hydrologic system. For example, the droughts of 1976–77 and 1987–92 led to reduced surface-water deliveries and increased groundwater pumpage, thereby reversing the overall trend of groundwater-level recovery and re-initiating land subsidence in the San Joaquin Valley. Since the mid-1990s, although annual surface-water deliveries generally have exceeded groundwater pumpage, water still is being removed from storage in most years in the Tulare Basin. Other than the large loss in storage in the Tulare Basin, on average there has been little overall change in storage throughout the rest of the Central Valley.

The CVHM is designed to be coupled with forecasts from Global Climate Models (GCMs) and to allow for efficient updates using remotely sensed data. Implementation of the FMP using GIS tools facilitates the use of remotely sensed evapotranspiration data. The tools allow for the spatial and temporal input data for the model to be updated more efficiently. This capability, in turn, facilitates using the model with climate data derived from GCMs. The input data for the crop-based water budget are consistent with output data from the GCMs. This facilitates using CVHM to forecast the potential supply of surface-water deliveries, demand for groundwater pumpage, and changes in groundwater storage in the Central Valley.

In the future, with the aid of GIS tools, the CVHM also could be used as a platform to connect the simulation of hydrologic processes with water allocation/optimization models (for example, CALSIM). The CVHM could be used to evaluate sub-regional issues such as proposed exportation of water from the Sacramento Valley to Southern California, or the restoration of salmon habitat in the San Joaquin River. The relatively detailed database on texture properties coupled with water-level altitudes may make CVHM particularly useful for assessing artificial recharge sites. These types of sub-regional issues could be evaluated using sub-regional models dynamically linked to the regional CVHM through the embedded-model technology of the local grid refinement (LGR) capability within MODFLOW.

Introduction

For more than 50 years, California's Central Valley has been one of the most productive agricultural regions of the world, which is due in large part to an ample supply of irrigation water. Using fewer than 1 percent of U.S. farmland, the Central Valley supplies 8 percent of U.S. agricultural output (by value) (Great Valley Center, 1999) and produces one quarter of the Nation's food (Great Valley Center, 1998), including 40 percent of the Nation's fruits, nuts, and other table foods (Bertoldi, 1989). In 2002, 250 different crops were grown, with an estimated value of $17 billion per year (Great Valley Center, 2005). The predominate crop types are cereal grains, hay, cotton, fresh and processing tomatoes, vegetables, citrus, tree fruits, nuts, table grapes, and wine grapes.

Paradoxically, most of the area is arid to semiarid and naturally is water-deficient (Bertoldi, 1989). Agriculture has been sustained by the development of an extensive system of reservoirs and canals and also by the availability of groundwater. Approximately 75 percent of the irrigated land in California and 17 percent of the Nation's irrigated land is in the Central Valley (Bureau of Reclamation, 1994). In addition, about 20 percent of the Nation's groundwater demand is supplied from pumping Central Valley aquifers, making it the second-most-pumped aquifer system in the U.S. (Bureau of Reclamation, 1994; Planert and Williams, 1995; Alley, 2006). As impressive as these numbers are from an agricultural water-use perspective, the Central Valley is rapidly becoming an important area for California's expanding urban population. Between 1970 and 2000, the population in the Central Valley doubled, reaching 6.5 million people in 2005 (California Department of Finance, 2007) and future growth is projected to continue.

Because the Central Valley contains so many communities, industries, and ecosystems that depend directly or indirectly on groundwater, and because competition for available water is intensifying, there is a need to quantify the region's water resources and the trends affecting them so that potential future water-use conflicts can be reduced or avoided. Although the Central Valley lies entirely within the State of California (*fig. A1*), its long history of groundwater development to support agriculture, and the complexity and immensity of the local, State and National economic factors related to the availability of the Valley's groundwater, underscore the National importance of this vital resource. In response, the U.S. Geological Survey (USGS) is assessing the availability of the Central Valley's water resources, particularly its groundwater.

The availability and sustainability of groundwater as a source of supply is a function of many factors—both natural and human—that control its use. Natural factors include the quantity and quality of water, climate, and environment. Human factors include the laws, regulations, and economics (U.S. Geological Survey, 2002). Water problems in California can be categorized under three broad headings: (1) problems of natural distribution (both spatial and temporal); (2) technical-hydrologic problems; and (3) political, legal, and social problems (California Department of Water Resources, 2005). Although the third category is referred to at times, this report focuses on the first two categories. The focus of this study is on improving the fundamental knowledge of groundwater availability in the Central Valley, including water fluxes (groundwater levels and flows and surface-water inflows, diversions, and deliveries), storage, and water use by agriculture and other human activities.

Purpose and Scope

The purpose of this report is to describe groundwater availability in the Central Valley. The descriptions are derived largely from the study results, including modeling; however, they also utilize the extensive literature on California's Central Valley. The report comprises three chapters and an appendix. Chapter A (this chapter) summarizes the study's purpose and scope and provides an overview of the hydrogeology of the study area. The hydrogeologic description includes the geologic framework and regional groundwater-flow. *Chapter B* describes an analysis and assessment of groundwater availability in the Central Valley—the principal focus of this report. Included in *Chapter B* are descriptions of the effects of development on the flow system, groundwater sustainability and management, and monitoring of the groundwater system. *Chapter C* documents the development of a three-dimensional (3-D), finite-difference numerical model of the Central Valley regional groundwater-flow system. This model is used to evaluate the groundwater availability described in *Chapter B*. Relative to the previously developed Central Valley Regional Aquifer System Analysis (CV-RASA) model (Williamson and others, 1989), the current model was extended to incorporate a slightly larger geographic area (*fig. A1*), has a finer spatial and temporal discretization, uses a more-detailed depiction of subsurface geology, and simulates monthly water budgets for April 1961 through September 2003. Finally, an appendix documents modifications to MODFLOW-2000 (MF2K) that were required to align the functionality of MF2K with the landscape, hydrologic and geologic architecture of the Central Valley.

In support of the assessment of groundwater availability in the Central Valley, the study has three objectives:

1. Develop a better understanding of the 3-D internal architecture of the freshwater-bearing deposits of the Central Valley;

2. Utilize enhanced water-budget analysis techniques to estimate water-budget components (recharge, discharge, storage) for the groundwater flow system in areas dominated by irrigated agriculture; and

3. Quantify the Central Valley's groundwater-flow system to enable the forecasting of system response to stresses from human and environmental stresses at scales relevant to water-management decisions.

The first objective is achieved through the development of a texture model. This texture model is documented in the "*Aquifer Characteristics*" section of Chapter A of this report. The second objective is achieved through the development of the "Farm Process" (FMP) as an additional simulation component within MF2K. A U.S. Geological Survey Techniques and Methods report documents the Farm Process (Schmid and others, 2006). The application of the FMP within the context of simulating the irrigated agriculture and as much as possible of the hydrologic cycle in the Central Valley also is documented in *Chapter C*. The final objective is accomplished using a quantitative numerical modeling tool, referred to in this report as the Central Valley Hydrologic Model (CVHM). CVHM consists of a linked landscape-process and groundwater-flow model that is described in *Chapter C*. *Chapter B* describes the application of this model for an analysis of groundwater availability in the Central Valley.

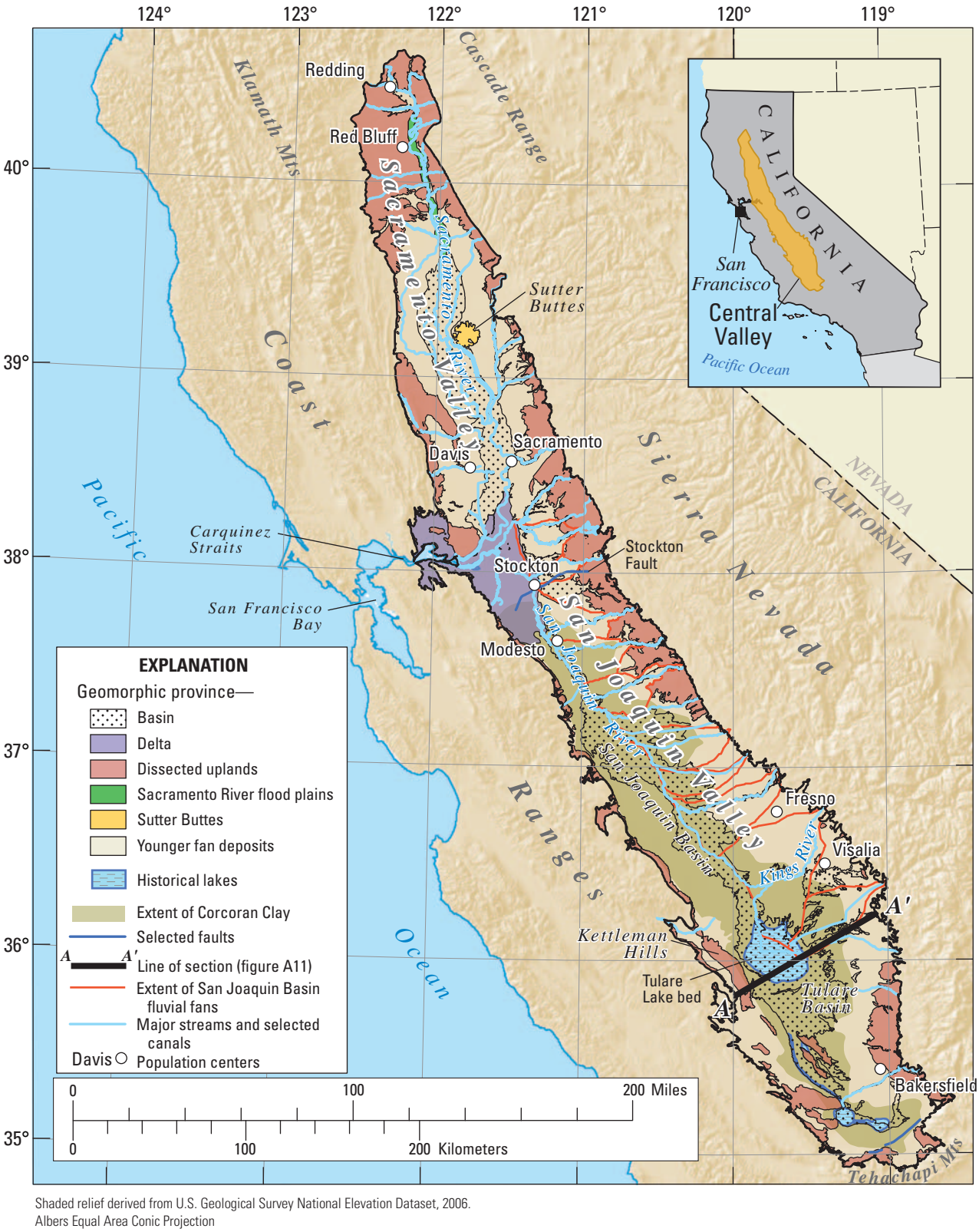

Shaded relief derived from U.S. Geological Survey National Elevation Dataset, 2006.
Albers Equal Area Conic Projection

Figure A1. Central Valley major geomorphic provinces (modified from Davis and others, 1959; Olmstead and Davis, 1961; and Jennings,1977), alluvial fans of the San Joaquin Basin (Weissmann and others, 2005), and extent and thickness of Corcoran Clay (modified from Page,1986 and Burow and others, 2004).

Methods of Analyses

Assessment of groundwater resources is an evolving process. The technology, available data, groundwater usage, spatial distribution of demand, and issues of concern all change over time (Reilly, 2005). An improved understanding of the groundwater-flow system can be developed as more data are collected and analytical tools become available. These analytical tools include improved computer simulation techniques, as well as improved data-integration and data-management practices. In order to understand the status of the Central Valley groundwater system, basic information on the geologic framework, boundary conditions, hydraulic head (water level) distribution, water quality, and the transmission and storage properties of the aquifer system must be known or estimated. Human activities, such as irrigation amounts and water withdrawals, also must be accounted for in the calculation of water availability (Reilly, 2005).

The evaluation of Central Valley water resources included the collection, integration and management of new and existing data, and the development and calibration of the CVHM. The CVHM is used to help quantify the groundwater availability. The results, conclusions, and limitations discussed in this report are based on analyses of the data and the CVHM.

Data Compilation

Six major classes of data were collected or compiled as part of this investigation: (1) borehole lithologic data regarding sediment characteristics; (2) hydrologic data consisting of precipitation records, historical water levels in wells, and streamflows; (3) compaction data related to subsidence; (4) water-use data from previous studies; (5) spatial land-use data, including crop type; and (6) surface-water deliveries and diversions. In addition, information from other modeling studies of the Central Valley was reviewed, analyzed, and compiled. In particular, the previous CV-RASA model (Williamson and others, 1989) and the current Central Valley modeling effort by the CA-DWR (C. Brush, California Department of Water Resources, written commun., February 21, 2007) were used. These data were incorporated into the CVHM. Details regarding the data are described in *Chapter C* of this report. An overview of the data types and data-integration and data-management techniques follows.

During the past decade, Geographic Information Systems (GIS) have advanced considerably as tools for storing, analyzing, manipulating, displaying, and modeling surface-water and groundwater data. GIS tools also are useful for linking spatial and temporal data to model input and output. When developing a 3-D numerical hydrologic model of a heterogeneous aquifer system having complex surface-water management processes, such as the Central Valley, compilation of a complex array of different categories and types of data is required (*figs. A2* and *A3*). Developing even one of these data types can be considered a major task on its own. For example, the steps for compiling, analyzing, and building the water-level data necessary for input data sets and observations is summarized in *figure A4*. A more detailed description of the development, compilation, and analysis of information for the hydraulic properties database is described in the "*Textural Analysis*" section of this chapter.

The geospatial database and GIS techniques were extremely valuable to the CVHM, by facilitating the transformation (including mathematical functions or logical operations), reformatting, and integration of data used in the CVHM (*figs. A2* and *A3*). The link between the CVHM and the GIS also required development of computer programs for translating input and output data. With the GIS and translation programs, information from the disparate datasets was combined, processed, and (or) re-sampled to produce spatial and temporal data sets needed for the CVHM input or observations. Utilizing GIS, the CVHM results were visualized spatially and temporally along with the observation data (*fig. A2*).

Numerical Model

Development of the CVHM resulted in a comprehensive synthesis of the hydrologic data and the capability to analyze the response of the hydrologic system to changes in stress. The CVHM provides a quantitative framework that can be used as a tool to help manage water resources.

Given the large increase in available data and major improvements in simulation tools, the CV-RASA model (Williamson and others, 1989) was updated using the U.S. Geological Survey's modular modeling software, MF2K (Harbaugh and others, 2000; Hill and others, 2000). The incorporation of the Farm Process (FMP) (Schmid and others, 2006) was integral to modeling the water budget components. Likewise, incorporation of new modules, such as the multi-node well (MNW) (Halford and Hanson, 2002), subsidence (SUB) (Hoffmann and others, 2003), and streamflow routing (SFR1) (Prudic and others, 2004) packages, aided in more realistic simulation of the system. The development and calibration of the CVHM is documented in detail in *Chapter C* of this report.

The CVHM includes simulation of groundwater-flow in a sand-silt-clay aquifer system. The system has been subject to groundwater withdrawals, land subsidence, and recharge by both natural processes and excess irrigation water. CVHM incorporates a dynamically integrated water supply-and-demand accounting system at monthly time scales for both agricultural areas and areas of native vegetation. The CVHM provides for a more accurate simulation of irrigated agriculture, surface-water, and groundwater-flow across the entire Central Valley system than the previous CV-RASA model. Analyses of the transient effects of variability in surface-water deliveries and associated groundwater pumpage are presented for three specific climatic conditions: drought, wet, and typical year conditions.

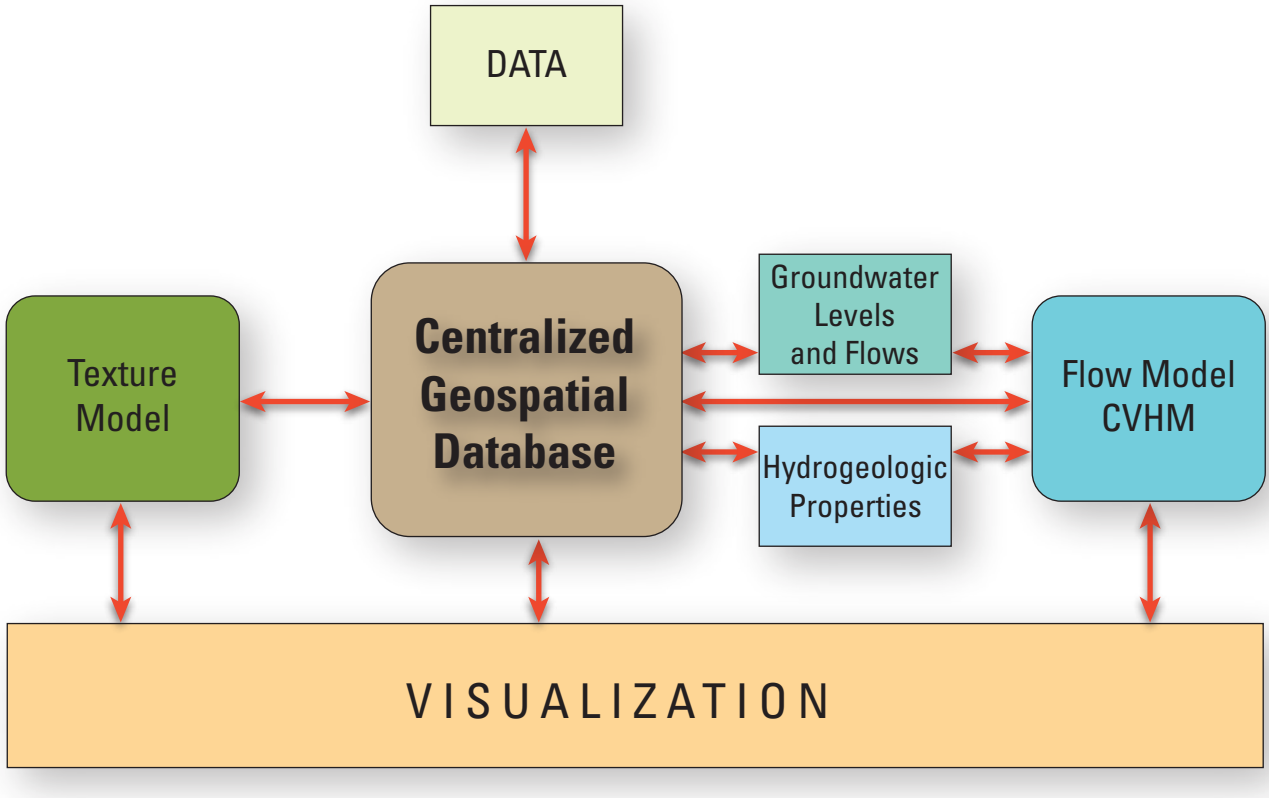

Figure A2. The relation and flow of information used in analyzing the Central Valley Hydrogeologic system. Both interpretive and modeling data flow in and out of the centralized geospatial database. The texture model, data in the geospatial database, and modeling results are visualized throughout the data gathering, analysis, and modeling stages of the project.

Previous Investigations

Because of the long history of groundwater development and its impacts in the Central Valley, there are many hydrologic investigations of the Central Valley aquifer system. The CA-DWR, the USGS, and various local and Federal agencies have all completed numerous studies. Many of these studies are summarized by Bertoldi and others (1991). The earliest systematic studies were done by California's first State Engineer, William Hall, and his staff (Hall, 1886; Hall, 1889; and Mendenhall and others, 1916). Bertoldi (1979) compiled a bibliography of nearly 600 reports on groundwater in the Central Valley. Since then, a number of site-specific and regional groundwater models have been completed by various Federal, State, and local agencies as well as private consultants. Two of these studies are regional modeling efforts and are summarized below.

Recent Regional Groundwater Models

Central Valley Regional Aquifer-System Analysis (CV-RASA)

The USGS initiated the Regional Aquifer-System Analysis (RASA) program in 1978 in response to Federal and State needs for information to improve management of the Nation's groundwater resources. The objective of the RASA program was to define the regional geohydrology and establish a framework of information that could be used for regional assessment of groundwater resources. Twenty-five regional aquifer systems were studied under the RASA program, including the Central Valley (Sun and Johnston, 1994).

The CV-RASA project provided a wealth of information on the Central Valley (Williamson, 1982; Diamond and Williamson, 1983; Hull, 1984; Mullen and Nady, 1985; Page, 1986; Williamson and others, 1989; Bertoldi and others 1991; among many others), including a regional groundwater-flow model. The groundwater-flow model simulated conditions from 1961 to 1977, a period of large and variable stresses on the groundwater-flow system, but at a relatively coarse spatial scale. The CV-RASA model grid cells were 36 mi^2, and the freshwater-bearing deposits were represented by four model layers. The resulting model represented flow conditions for large regions, but generally was inadequate at scales less than about 500 mi^2. Because water-management decisions typically are made at the scale of individual water districts, which often are smaller than 500 mi^2, the CV-RASA model cannot be used appropriately for providing information relevant to management decisions at those scales.

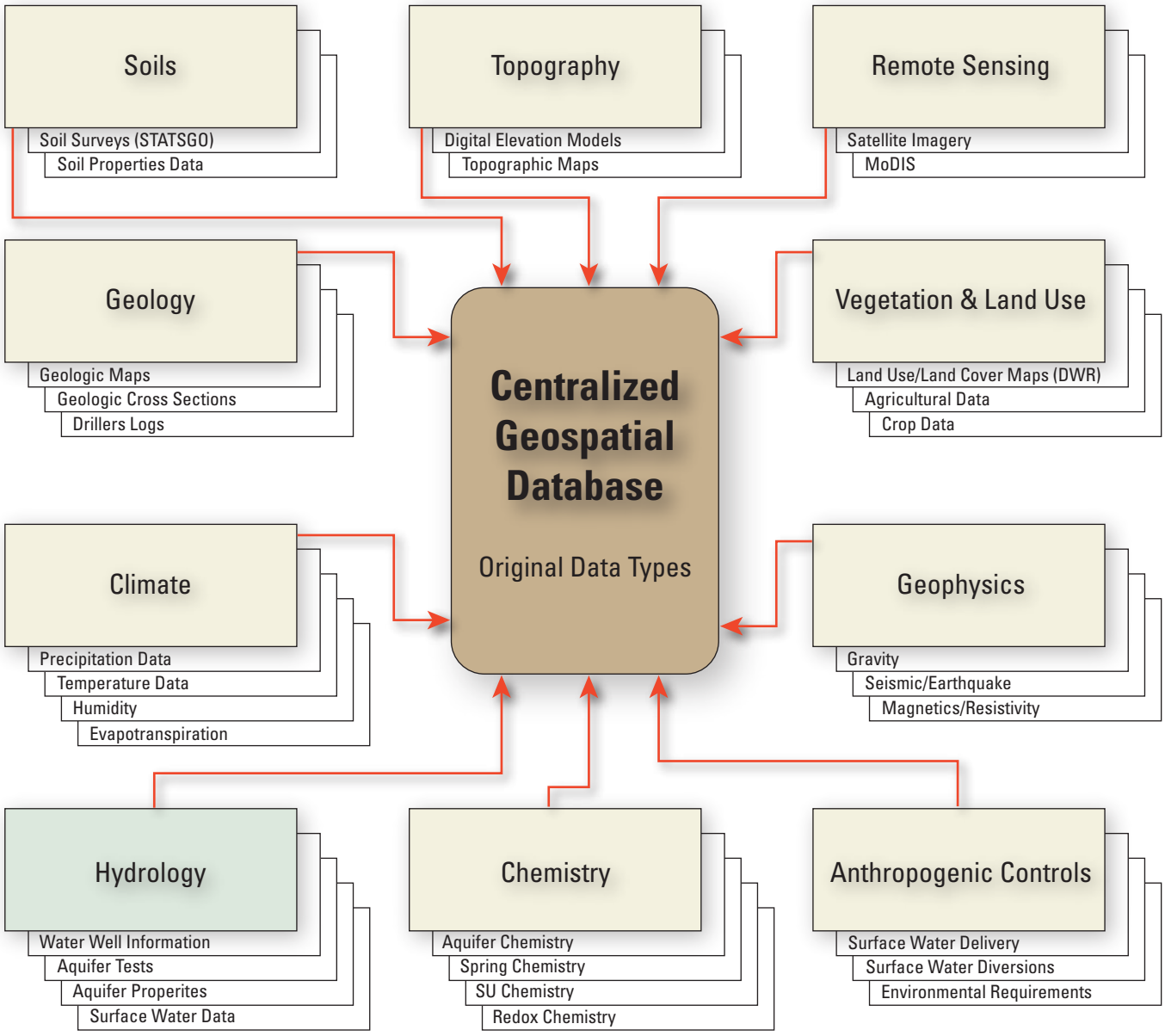

Figure A3. The diversity of data types and categories included in the centralized geospatial database. Data types in bold were used specifically in this study.

The CV-RASA model initially utilized a water budget that was based on net recharge to the flow system. During model calibration, the net recharge fluxes were changed substantially. Because the simulated water budget was significantly different from the estimated budget, it was unclear whether uncertainty in the budgets (simulated and estimated) was due to errors in the budget components or to simulation errors. As a consequence, use of the CV-RASA model to simulate variations in different budget components was not very useful, and it was clear that refined budget estimates were needed. Subsequent to the CV-RASA model, Gronberg and Belitz (1992), Belitz and others (1993), and Brush and others (2004) each developed an alternative approach to estimating the water budget based on crop water use, irrigation efficiency, and surface-water deliveries and applied the approach to parts of the San Joaquin Valley.

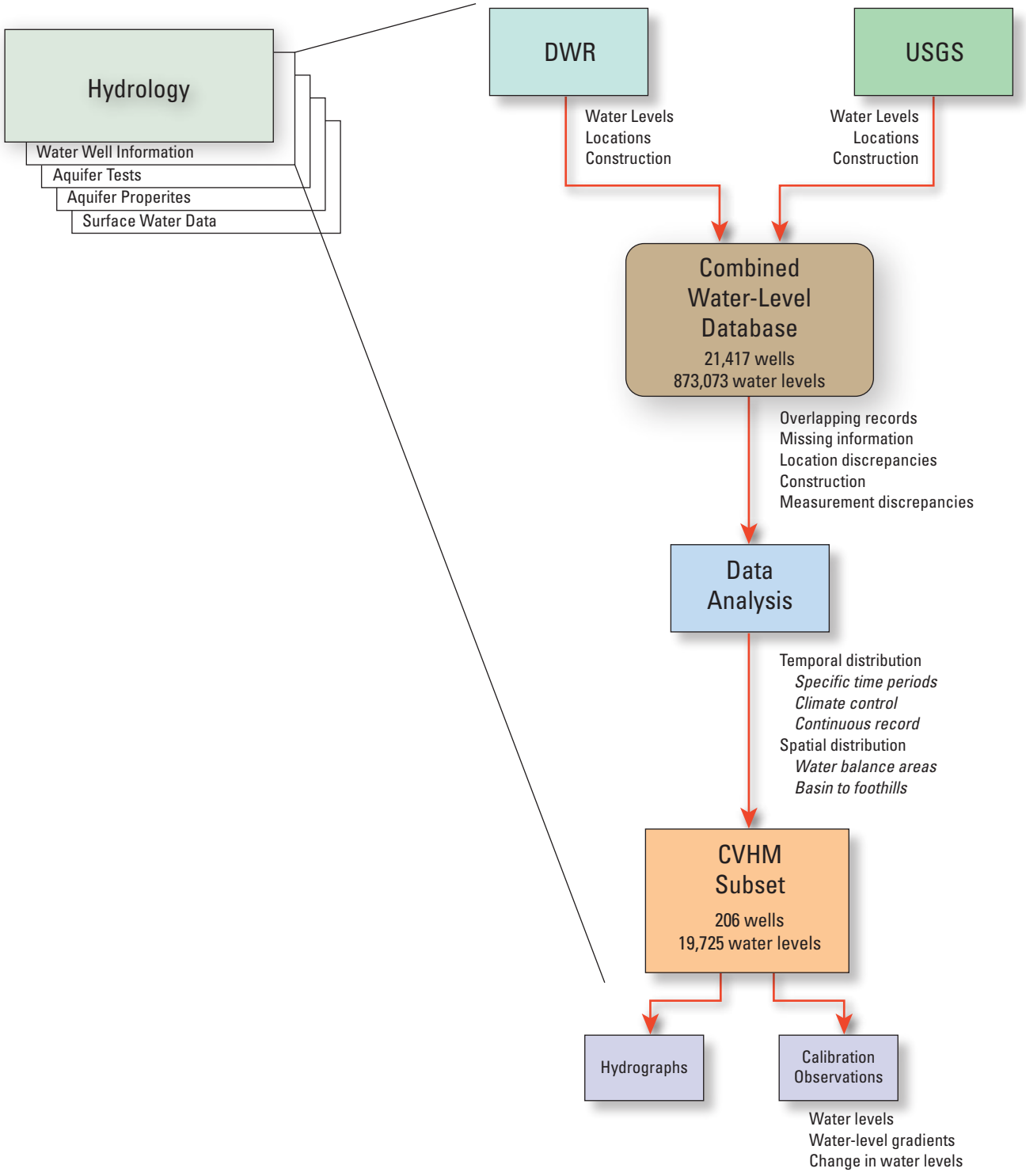

Figure A4. An example of the detail for compilation, integration, and analysis for one data type (water-level nformation).

California Central Valley Groundwater-Surface-Water Simulation Model (C2VSIM)

CA-DWR currently (2008) is using the 3-D finite element code Integrated Water Flow Model (California Department of Water Resources, 2007b) to develop an integrated groundwater-surface-water model for the Central Valley; this model is referred to as C2VSIM. C2VSIM simulates the development of the groundwater-flow system and groundwater-surface water interactions on a monthly basis from October 1921 to September 2003 (C. Brush, California Department of Water Resources, written commun., February 21, 2007). The groundwater-flow system is represented with three layers, each having 1,393 elements ranging in size from about 2 to 65 mi^2. The model of the groundwater-flow system is coupled with one-dimensional land-surface, streamflow, lake, and unsaturated-zone processes. Land-surface processes are simulated using 21 subregions corresponding to CA-DWR water-supply planning areas. The surface-water network is simulated using 449 stream nodes representing 75 stream reaches, with 80 diversion locations providing 108 deliveries. The compilation of the monthly water delivery and diversion information for these 21 subregions is a substantial contribution toward understanding the hydrology of the Central Valley. The calibrated C2VSIM model will be used to simulate the groundwater-flow system and calculate stream accretions and depletions for use in CALSIM-III (California Department of Water Resources, 2007a). CALSIM-III is a reservoir-river basin simulation model used for planning and management of the State Water Project and Central Valley Project, which are large surface-water storage and distribution networks in California's Central Valley (C. Brush, U.S. Geological Survey, written commun., 2006).

Study Area

The Central Valley, also known as the Great Valley of California, covers about 20,000 mi^2 and is one of the more notable structural depressions in the world. It occupies a central position in California—bounded by the Cascade Range to the north, the Sierra Nevada to the east, the Tehachapi Mountains to the south, and the Coast Ranges and San Francisco Bay to the west, the valley is a vast agricultural region drained by the Sacramento and San Joaquin Rivers (*fig. A1*). The valley averages about 50 miles (mi) in width and extends about 400 mi northwest from the Tehachapi Mountains to near Redding (*fig. A1*). Generally, the land surface has very low relief. Its configuration is the result of millions of years of alluvial and fluvial deposition of sediments derived from the bordering mountain ranges. Most of the valley lies close to sea level, but is higher along the valley margins. Most of the valley boundary along the eastern edge is about 500 feet (ft) above sea level and most of the western boundary ranges from 50 to 350 ft above sea level. Near the apexes of some alluvial fans in the south along the margin of the valley, the maximum elevation is about 1,700 ft.

For convenience of discussion, the valley can be divided into two large parts: the northern one-third is known as the Sacramento Valley and the southern two-thirds is known as the San Joaquin Valley (*fig. A1*). The San Joaquin Valley can be split further into the San Joaquin Basin and the Tulare Basin (*fig. A1* and *table A1*). In this report, the term San Joaquin Valley will be used to represent the southern two-thirds of the Central Valley, as a whole. Where more detail is warranted, the northern part of the San Joaquin Valley, the San Joaquin Basin, will be distinguished from southern part, the Tulare Basin. The San Joaquin and Sacramento Valleys meet in the Delta area where the combined discharge of the Sacramento and San Joaquin Rivers flows through the Central Valley's one natural outlet, the Carquinez Strait, on its way to San Francisco Bay and the Pacific Ocean (*fig. A1*). Just east of the Delta, several streams issue from the Sierra Nevada into the valley and flow to the Delta in an area referred to as the Eastside Streams.

Climate

Climate in the Central Valley is arid-to-semiarid hot, Mediterranean. Precipitation during an average year ranges from 13 to 26 inches in the Sacramento Valley (46 inches in the extreme northern part of the valley) and from 5 to 18 inches in the San Joaquin Valley (*fig. A5A*). Dramatic deviations from average climatic conditions are manifested as droughts or floods. Most of the Central Valley is prone to flooding. About 85 percent of the precipitation falls during November through April, half of it during December through February in average years (*fig. A6*). The valley is hot and dry during the summer, and cool and damp in the winter, when the area frequently is covered by a ground fog known regionally as "tule fog." Reference evapotranspiration (ETo) is relatively high, and ranges from 45 inches in the Sacramento Valley to 56 inches in the San Joaquin Valley (*fig. A5B*). In general, most of the valley is in a state of perennial water deficiency; ETo exceeds precipitation by as much as 3 ft. Overall, precipitation exceeds ETo during the winters and ETo exceeds precipitation during the summers.

Sacramento Valley

Geographically, the Sacramento Valley is bounded on the east by the Sierra Nevada and on the west by the Coast Range and Klamath Mountains. The only significant topographic feature here, or on the Central Valley floor at large, is Sutter Buttes, a volcanic remnant in the south-central part of the Sacramento Valley (*fig. A1*). The Sacramento River, which is the longest river system in the State of California, flows from the Cascade Range in the north to the San Francisco Bay/Sacramento–San Joaquin River Delta; major tributaries are the Pit (north of the study area), Feather, Yuba, Bear, and American Rivers (*fig. 5A*).

Table A1. Water-balance subregions within the Central Valley, California.

[General description based on depletion study area (DSA) names (where available) or subareas from Williamson and others (1989; fig. A27). DSA 49 is subdivided into four subregions A–D, and DSA 60 is subdivided into eight subregions A–H. Routed surface water deliveries are conveyed along streams or canals to a water-balance subregion. Non-routed surface water deliveries, or water transfers, are surface-water deliveries to a water-balance subregion not connected to a stream or major canal. This conveyance typically occurs through small canals or diversion ditches. DWR, California Department of Water Resources; mi^2, square mile]

Regions	Site identifier	General description	DWR DSA number	Total area (mi^2)	Routed surface-water deliveries	Non-routed surface-water deliveries
Sacramento Valley	1	Sacramento River above Red Bluff (Redding Basin)	DSA 58	611	2	None
	2	Red Bluff to Chico Landing (Red Bluff, Corning, Bend, Antelope, Dye Creek, Los Molinos, and Vina Basins)	DSA 10	1,163	3	None
	3	Colusa Trough (Most of Colusa Basin and Capay Valley Basin)	DSA 12	1,112	4	None
	4	Chico Landing to Knights Landing proximal to the Sacramento River	DSA 15	560	1	None
	5	Eastern Sacramento Valley foothills near Sutter Buttes (North and South Yuba, East Butte and eastern parts of West Butte and Sutter Basins)	DSA 69	957	2	6
	6	Cache-Putah area (Western Solano and most of Delta and Yolo Basins)	DSA 65	1,044	4	None
	7	East of Feather and South of Yuba Rivers (North American Basin)	DSA 70	534	4	4
Eastside Streams	8	Valley floor east of the Delta (Cosumnes and parts of South American and Eastern San Joaquin Basins)	DSA 59	1,362	6	None
Delta	9	Delta (parts of Solano, Eastern San Joaquin, South American, and most of Tracy Basins)	DSA 55	1,026	1	None
San Joaquin Basin	10	Delta-Mendota Basin	DSA 49A	1,083	1	7
	11	Modesto and southern Eastern San Joaquin Basin	DSA 49B	664	6	None
	12	Turlock Basin	DSA 49C	540	5	None
	13	Merced, Chowchilla, and Madera Basins	DSA 49D	1,648	6	2
Tulare Basin	14	Westside and Northern Pleasant Valley Basins	DSA 60A	1,071	None	3
	15	Tulare Lake and Western Kings Basin	DSA 60B	1,423	4	5
	16	Northern Kings Basin	DSA 60C	478	2	1
	17	Southern Kings Basin	DSA 60D	569	2	1
	18	Kaweah and Tule Basins	DSA 60E	1,358	4	4
	19	Western Kern County and Southern Pleasant Valley Basin	DSA 60F	1,365	2	3
	20	Northeastern Kern County Basin	DSA 60G	705	2	3
	21	Southeastern Kern County Basin (Arvin-Maricopa area)	DSA 60H	1,105	3	2
TOTAL	—	—	—	20,378	64	41

The city of Sacramento and the surrounding communities form the major population center of the region. With the exception of Redding, cities and towns north of Sacramento are located in mainly agricultural areas. The 1995 population of the Sacramento Valley was 2.4 million (California Department of Water Resources, 2003).

The Sacramento Valley has mild winters and hot, dry summers. The natural levees that border the Sacramento–Feather River system create backwater basins of heavy clay soils that sustain rice farms and duck clubs. Truck, field, orchard, and rice crops are grown on approximately 2.1 million acres; rice represents about 23 percent of the total acreage (California Department of Water Resources, 2003).

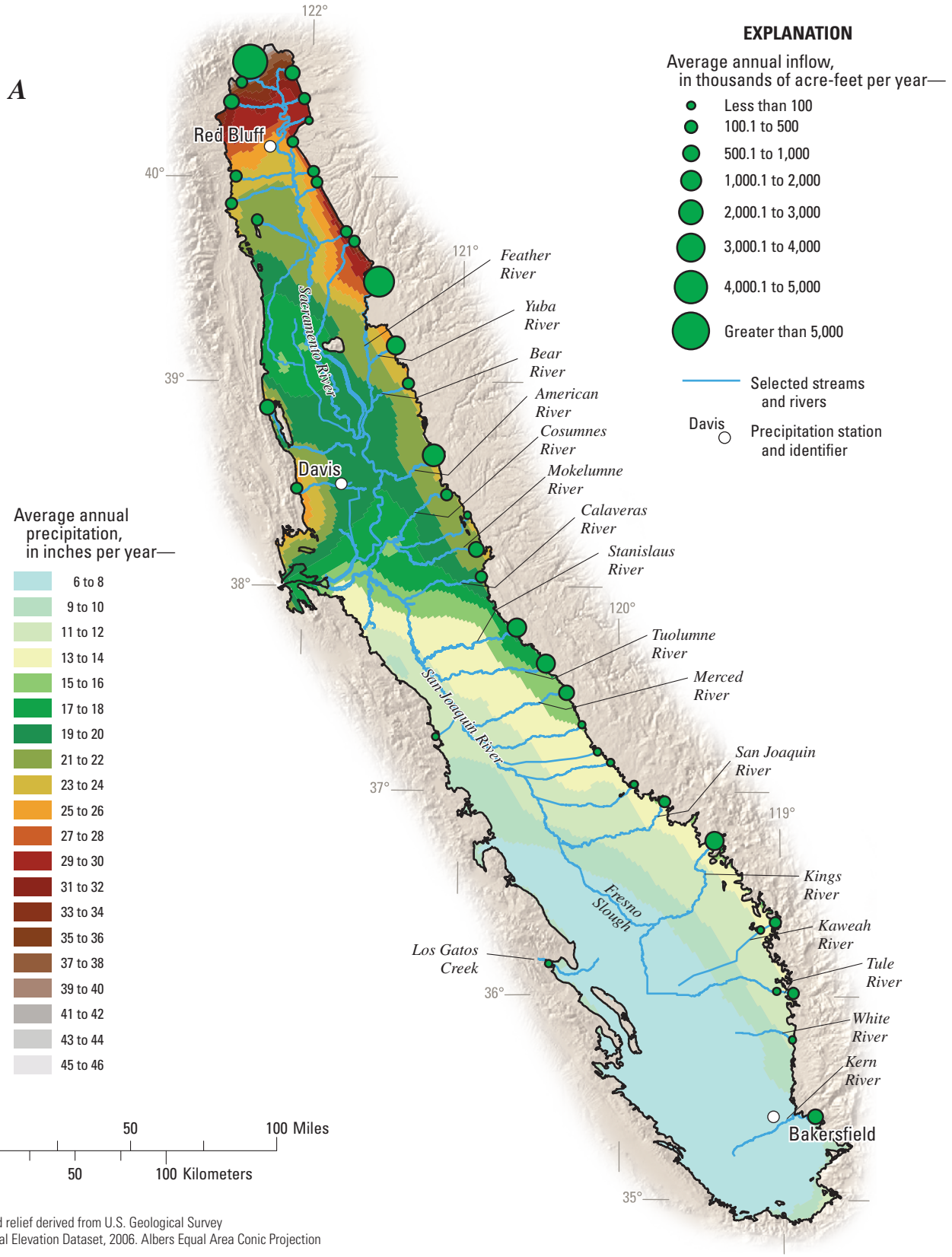

Figure A5. *A*, Surface-water inflows and average annual precipitation for September 1961 through September 2003 throughout the Central Valley, California. *B*, Average annual reference evapotranspiration (ETo) for September 1961 through September 2003 throughout the Central Valley, California. ETo data were calculated from PRISM temperature data (Climate Source, 2006). The surface-water inflows are from U.S. Geological Survey files and California Department of Water Resources (C. Brush, written commun., February 21, 2007). Precipitation data are from Parameter-Elevation Regressions on Independent Slopes Model (PRISM) data (Climate Source, 2006).

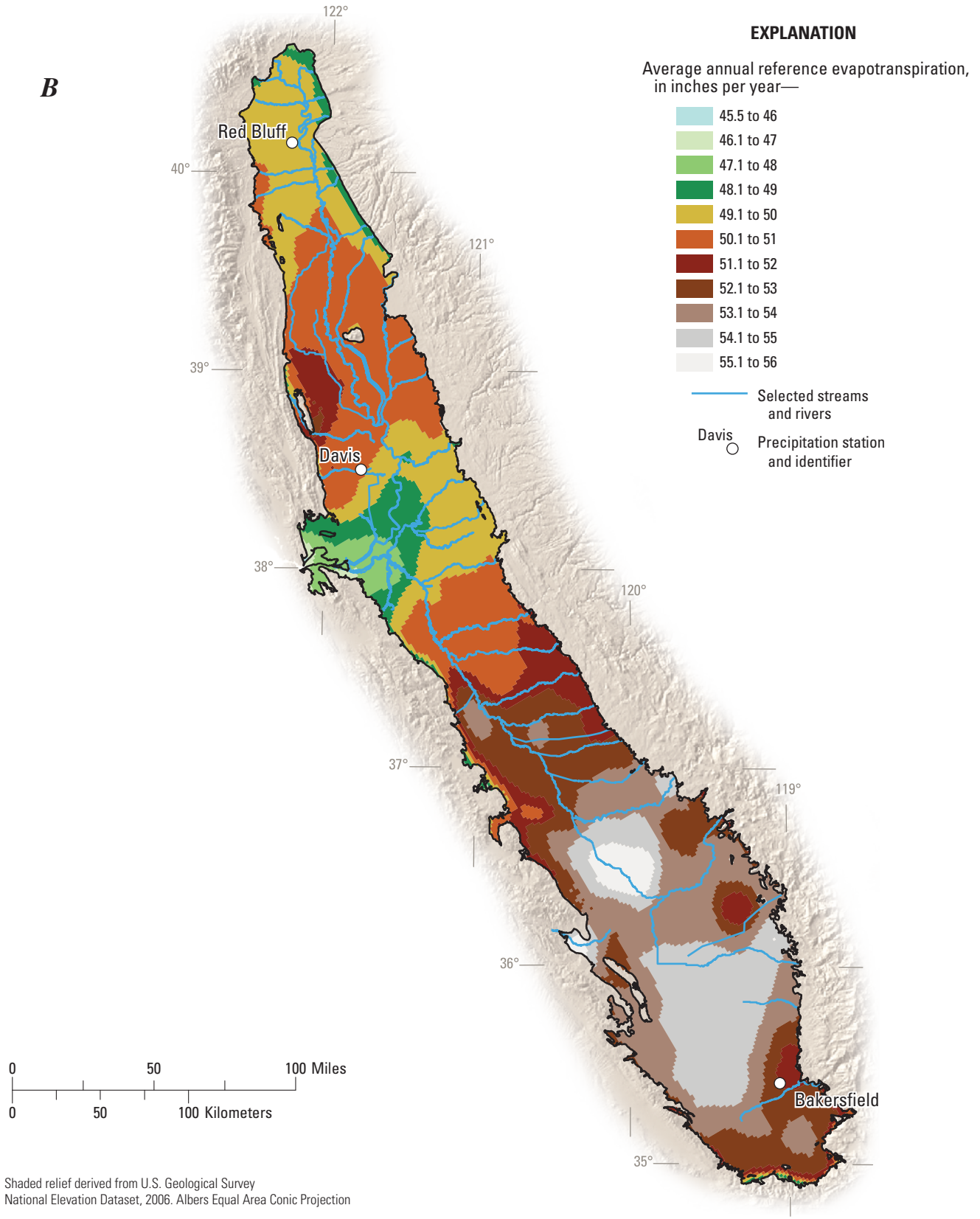

Figure A5. Continued.

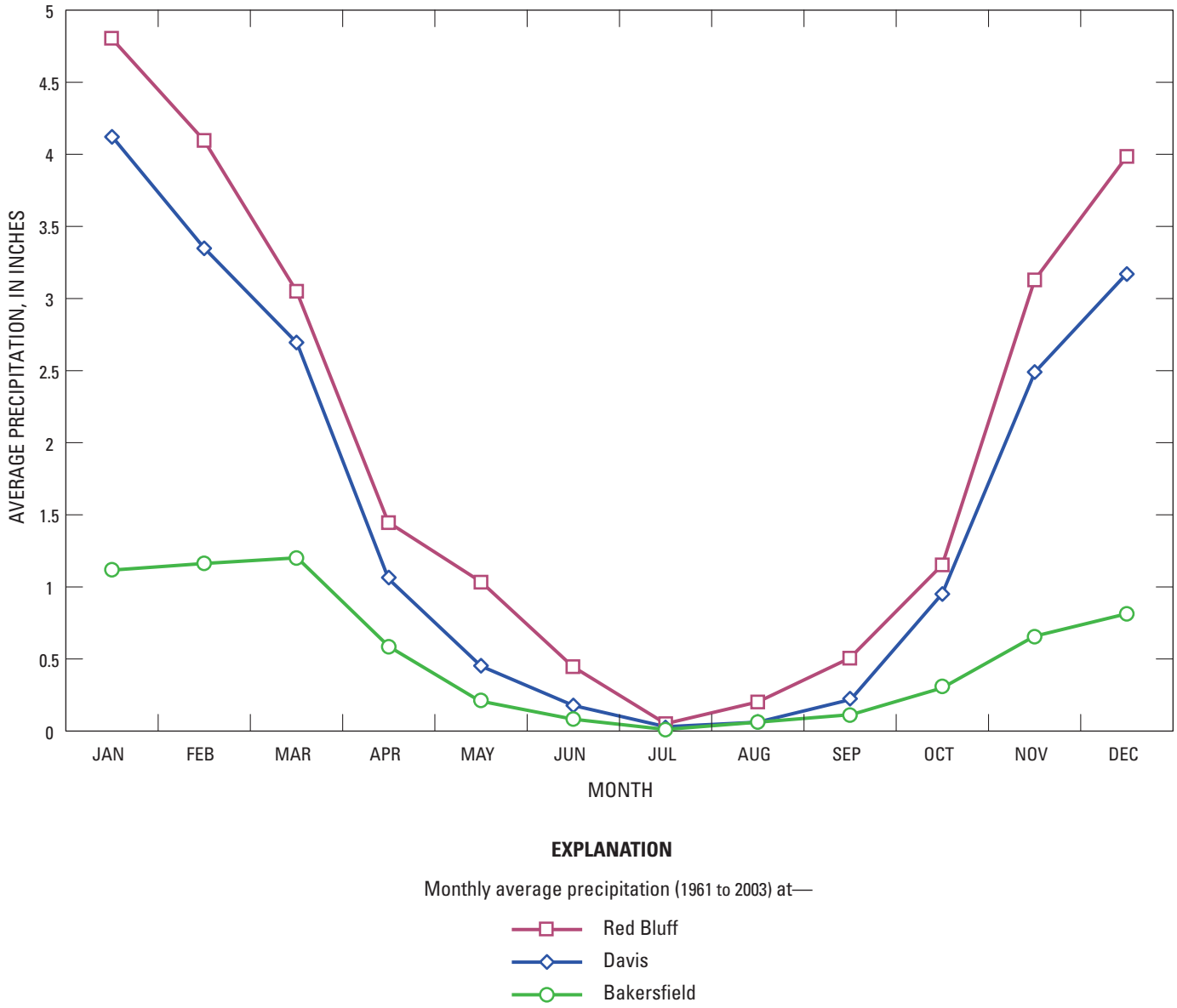

Figure A6. Average monthly precipitation for Redding, Davis, and Bakersfield, California (Climate Source, 2006).

Depending on location, agriculture in the Sacramento Valley relies on a variable combination of surface water and groundwater. Groundwater accounts for less than 30 percent of the annual supply used for agricultural and urban purposes in this area. The Sacramento Valley, generally rich in surface water, provides water for much of California's urban and agricultural needs (California Department of Water Resources, 2003). With growing demand for high-quality water throughout the state, water transfers from the Sacramento Valley to other parts of the state are being evaluated more carefully. Several areas have passed ordinances that regulate or impede these transfers. CA-DWR studies indicate that additional ecosystem protection and restoration efforts are needed to improve habitat for threatened and endangered species (California Department of Water Resources, 2003). Because these environmental efforts require additional water, they may ultimately affect the availability of water resources for other purposes.

Delta and Eastside Streams

The Sacramento and San Joaquin Rivers flow through the northern and southern parts of the valley, respectively, and join to form the San Francisco Bay/Sacramento–San Joaquin River Delta (referred to in this report as the Delta) (*fig. A1*). The Delta also receives freshwater inflow from the Cosumnes, Mokelumne, and Calaveras Rivers and other small streams on the eastside. The shared Delta is a large expanse of interconnected canals, streams, sloughs, marshes, wetlands, and peat islands just south of the State capital. The Delta is a delta in name only. In reality, it is an estuary and the reverse of a classic delta, in that multiple rivers are coming together as opposed to one river that no longer is confined to its channel and expands in width. The Delta is a major source of water for domestic, industrial, and agricultural uses as well as an important habitat to 750 animal and plant species. The Delta also supports species listed as threatened or endangered: Delta smelt, Chinook salmon, and steelhead.

The Delta covers an area of about 1,000 mi^2 of estuary. The Delta has 1,100 mi of rivers and 1,600 mi of levees. The levees protect farmlands as much as 22 ft below sea level. Approximately 70 percent of surface-water flow to the Delta comes from the Sacramento River and the remainder comes from the San Joaquin River. Water from the Sacramento River is much fresher than water from the San Joaquin River. As the freshwater moves westward through the Delta to the San Francisco Bay, it is underlain by an increasingly thick wedge of tidal salt water from the Pacific Ocean. Since the construction of major dams on rivers in the Delta drainage basin, water in the Delta has remained generally suitable for agricultural and urban uses, however, salt levels increase during dry periods.

The Delta is the heart of a massive, engineered north-to-south water-delivery system (*fig. A7*). At the southern end of the Delta, water is regulated and pumped into canals to be transported southward. State and Federal contracts provide for export of up to 7.5 million acre-ft per year, although historically they have not reached this amount. About 83 percent of water exported from the Delta is used for agriculture and the remainder is used for urban and environmental purposes in Central and Southern California (California Department of Water Resources, 1998). Because of environmental concerns, particularly the decline of the Delta smelt, the exports sometimes are curtailed. This focus on ecosystem restoration often leads to conflicts with agricultural and urban interests and regulatory droughts.

In the late 1800s, large-scale agricultural development in the Delta required levee-building to prevent historically frequent flooding on the low-lying Delta islands. An extensive network of drainage ditches prevents islands from flooding internally. The accumulated drainage is pumped through or over the levees into stream channels. Subsidence of the Delta islands, principally caused by decomposition of organic carbon in the peat soils, threatens the stability of island levees. As subsidence progresses, the levee system will become increasingly vulnerable to catastrophic failure during floods and earthquakes (Ingebritsen, and others, 2000; Lund and others, 2007). In addition, historical records show that sea level in San Francisco Bay has risen between 4 and 8 inches over the past 100 years (Ryan and others, 1999), possibly related to global warming. Whatever the reasons, water levels have risen, environmental issues have increased, and many levees have begun to fail—some have failed. As a result, the Delta has become an area of national concern resulting in the development of a major Federal-State-stakeholder effort known as the "CALFED Bay-Delta program." CALFED is a collaboration among 25 State and Federal agencies that came together with a mission: to improve water supplies in California and the ecological health of the Delta. In addition to the CALFED program, Lund and others (2007) issued a vision statement for the Delta whereby they suggest that alternatives, including a by-pass canal, may need to be considered to address the water-resource demands, water quality, and environmental issues of the Delta.

San Joaquin Basin of the San Joaquin Valley

Geographically, the San Joaquin Basin is bounded on the east by the Sierra Nevada and on the west by the Coast Ranges (*fig. A1*). The Delta borders its northern extent and the internally drained Tulare Basin borders its southern extent. Significant geographic features include the San Joaquin River and the southern part of the Delta. The San Joaquin River runs southwestward as it drains part of the Sierra Nevada, and turns northwestward as it courses along the axis of the northern San Joaquin Valley. The major tributaries, including the Stanislaus, Tuolumne, and Merced Rivers, have drainage basins in the Sierra Nevada to the east (*fig. A5A*).

The San Joaquin Basin contains a half-dozen cities with populations exceeding 50,000 in 2000 (California Department of Finance, 2007), including Stockton, Turlock, Merced, and Modesto. A large part of the population of the basin is involved in all facets of agricultural production. Gradually, the population is shifting towards supporting the large urban areas and industry. Most of the population is centered in the northern part of the basin near Stockton. The total population of the San Joaquin Basin in 2000 was approximately 2 million (Great Valley Center, 2005).

The San Joaquin Basin has mild winters. Although the summers are particularly hot and dry, the area has been extensively developed for agriculture. In 2000, approximately two-thirds of the area was used for agriculture. The southwestern half of the San Joaquin Basin has long been known for its cotton fields, but recent drops in cotton prices have caused a rapid shift to other crops, particularly almond orchards. On the eastern side of the San Joaquin Basin, alluvial fans are dominated by deciduous fruit and nut orchards. The remainder of the irrigated area is covered by pasture, truck, and field crops.

Figure A7. General features of the surface-water system in the Central Valley, California.

Although surface water is used when it is available, the region relies heavily on groundwater. Groundwater accounts for about 30 percent of the annual supply of both types of water used for agricultural and urban purposes (California Department of Water Resources, 2003; *Chapter C*). During periods of drought, the groundwater usage increases. Essentially, all natural flows in area streams are diverted for agricultural and municipal use (Moore and others, 1990). Only about 8 percent of the historic San Joaquin Valley wetland acreage remains today (Moore and others, 1990). Plans to restore the habitat and fish populations on the San Joaquin River through higher releases of water from Friant Dam have spurred growing concerns over long-term availability of the Sierra water supplies. As a result, new surface storage reservoirs in the upper San Joaquin Basin are being considered (California Department of Water Resources, 2003).

Tulare Basin of the San Joaquin Valley

Geographically, the southern part of the San Joaquin Valley, the Tulare Basin, is bounded by the Sierra Nevada on the east, the Tehachapi Mountains on the south, and by the Coast Ranges on the west (*fig. A1*). The northern extent is less well-defined, but generally corresponds to the Kings River. Significant geographic features include the Tulare Lake Basin and the Kettleman Hills. The Tulare Basin was separated from the southern end of the San Joaquin Basin by the merging of alluvial fans from the Kings River to the east and Los Gatos Creek to the west. The Kings, Kaweah, Kern, and the Tule Rivers drain into the Tulare Lake Basin; historically, the bulk of the flow is from the Kings River. At the present time, only a minor part of the flow from the Kings River enters the Tulare Lake Basin (and most of this is diverted before reaching Tulare Lake). The Kings River bifurcates in the Kings River Fan to form two rivers referred to as the North Fork and South Fork, but currently much of the flow is diverted or lost to seepage before it reaches this point. The North Fork flows into Fresno Slough and ultimately to the San Joaquin River. The South Fork flows towards Tulare Lake.

The Kings, Kaweah, Kern, and the Tule Rivers issue from steeply plunging canyons in the Sierra Nevada onto broad, extensive alluvial fans. Over many thousands of years, the natural flow of these rivers formed networks of streams and washes on the slopes of the alluvial fans and terminated in topographically closed sinks, such as Tulare Lake, Kern Lake, and Buena Vista Lake. Historically, Tulare Lake was the largest freshwater lake west of the Mississippi River (Moore and others, 1990) and the second largest (by surface area) freshwater lake in the United States (Moore and others, 1990). The lake surface fluctuated annually with the variation in rainfall, runoff, and snowmelt. Further south, the Kern River terminated in two smaller lakes that today, like the former Tulare Lake, have dried and the waters that fed them have long since diverted to irrigation.

The Tulare Basin, wider than the San Joaquin Basin and Sacramento Valley, contains the population centers of Fresno, Bakersfield, and Visalia. About 4 percent of the basin area is urban. Although most of the basin's population is focused on agricultural activities, Bakersfield is well known for its oil fields. The total population of the Tulare Basin in 2000 was approximately 4 million (Great Valley Center, 2005).

The Tulare Basin also has mild winters and hot dry summers. When first viewed by Don Pedro Fages in 1772, he described the southern-most part of the Tulare Basin as a barren desert waste with scattered saltbush (Atriplex) (Parsons, 1987). Beyond the desert area were tule marshes, fed by streams carrying Sierra snowmelt, that became the home for migrating waterfowl for several months each winter. Despite these transient marsh areas, the area is dry and the valley summer heat is intense. The present-day Tulare Basin has been developed extensively for agriculture and petroleum extraction. Agricultural fields, vineyards, and orange groves are interspersed with oil fields (Parsons, 1987). Grains, cotton, and corn are the main agricultural crops in the Tulare Basin.

Historically, groundwater has been important to both urban and agricultural users (California Department of Water Resources, 2003). Until recently, Fresno and Visalia were entirely dependent on groundwater for their supply, and Fresno was the second largest city in the U.S. reliant solely on groundwater (California Department of Water Resources, 2003). These cities are slowly adding surface water to their supplies. Water used for agriculture in the Tulare Basin constituted 69 percent of the total water use in 1998 and 86 percent of the total in 2001 (Great Valley Center, 2005).

Surface water is preferred over groundwater because of relative costs. Uncertainty and limitations of surface-water deliveries from the Delta are of growing concern. Groundwater often is used to replace much of the shortfall in surface-water supplies. Because groundwater is a finite resource, alternate sources of water either are being considered or starting to be used. For example, some of the more permeable deposits recently have been used for groundwater recharge programs. Water districts have recharged several million acre-ft of water for future use and transfer through water banking programs (California Department of Water Resources, 2003). The groundwater recharge programs store excess water during wet periods for extraction during dry periods (California Department of Water Resources, 2005).

Each of the river systems in the region (Kings, Kaweah, Tule, and Kern) has unique environmental water needs because of the arid nature of the region and extensive modifications for agriculture. There has been significant activity on the Kings and Kern Rivers to restore flows for habitat as well as for recreation.

Water-Balance Subregions

For the purpose of this work, the Central Valley was divided into 21 previously identified areas, termed "water-balance subregions" (WBSs) in this study (*fig. A8* and *table A1*). Many of the WBSs initially were identified by CA-DWR and Bureau of Reclamation (BOR) as numbered "Depletion Study Areas" (California Department of Water Resources, 1977). Since their initial identification, many of the depletion study areas have been subdivided further into the WBSs (C. Brush, California Department of Water Resources, written commun., February 21, 2007; California Department of Water Resources, 2003). The WBSs are used as accounting units for surface-water delivery and for estimation of groundwater pumpage. The boundaries generally represent hydrographic rather than political subdivisions, particularly in the San Joaquin and Tulare Basins. Where possible, the description in *table A1* identifies the hydrographic basin that generally coincides with the WBS; otherwise, a general description of the part of the valley is given. In the Sacramento Valley and the Delta, the boundaries usually do not coincide with hydrographic basin boundaries. The specifics of the water-budget delivery and diversion system are discussed in *Chapter C*. For simplicity of reporting purposes, these 21 WBSs are grouped into the five regional areas: the Sacramento Valley, Delta, Eastside Streams, San Joaquin Basin, and Tulare Basin (*table A1*).

Geologic History and Setting

The Central Valley, as its name implies, is virtually one large sediment-filled valley between the Coast Ranges and the Sierra Nevada (Farrar and Bertoldi, 1988). The Sierra Nevada, which forms the eastern side of the valley, is the eroded edge of a huge tilted block of crystalline rock. The valley fill overlies a westward-sloping surface of basement rocks that are the subsurface continuation of the Sierra Nevada. Emplacement of the Sierra Nevada batholith ended around 85 million years ago (Ma) in the Mesozoic Era. The Sierra Nevada topography is a consequence of two periods of uplift (Wakabayashi and Sawyer, 2001). The most recent and most significant uplift of the range began about 5 Ma in the Miocene Epoch; however, significant relief predates this uplift and was a result of uplift that occurred at least 50 million years earlier in the Eocene Epoch in a different tectonic setting. Throughout the orogenesis of the Sierra Nevada, the crestal elevations of the southern part of the range greatly exceeded those of the northern part of the range. The northeast corner of the valley is at the southern end of the Cascade Range and contains volcanic rocks. Geologically, this area of the valley is relatively young; most of the volcanic activity was during late Tertiary to Holocene time (last 10 million years). The only prominent non-sedimentary rock feature in the entire Central Valley is the Sutter Buttes, a Pliocene and Pleistocene volcanic plug that rises abruptly to an altitude of 2,000 ft above the flat valley floor (Farrar and Bertoldi, 1988).

A huge volume of sediments of deep marine, shallow marine, deltaic, and continental origin fill the Central Valley (Farrar and Bertoldi, 1988). The valley fill deposits range in thickness from zero on the eastern edge of the valley to more than 50,000 ft on the western edge (Wentworth and others, 1995). During and since marine deposition, sediments derived from erosion of igneous and metamorphic rocks and consolidated marine sediments in the surrounding mountains have been transported into the valley by streams. These continental sediments at the southern end of the valley have an average thickness of about 2,400 ft (Planert and Williams, 1995). The continental sediments consist mostly of basin-fill or lake deposits of sand and gravel interbedded and mixed with clay and silt. Depending on location, deposits of fine-grained materials—mostly clay and silt—compose as much as 50 percent of the thickness of the valley-fill sediments (Planert and Williams, 1995).

Alluvial fans, some of which are more than 1,000 ft thick, have formed on all sides of the Central Valley. The fine-grained detritus carried by streams is moved farther toward the valley axis, leaving the coarse-grained materials closer to the valley margins. The coarse-grained sediments in the fans typically are associated with stream channels. On the eastern side of the valley, these stream channels are large, laterally migrating distributary channels. Over time, shifting stream channels create coalescing fans, forming broad sheets of inter-fingering, wedge-shaped lenses of gravel, sand, and finer detritus. The texture of these fan deposits is controlled by many factors, including the bedrock source materials, drainage basin area, elevation, and tectonic basin subsidence rate.

Structurally, other than the Sutter Buttes, the Central Valley is rather nondescript. The valley is transected by two cross-valley faults, the Stockton Fault and White Wolf Fault (Hackel, 1966). The Stockton Fault and associated Stockton arch together form a geologic divide between the Sacramento and the San Joaquin Valleys (*fig. A1*). During an examination of water levels throughout the valley, several smaller structures were inferred as possibly affecting groundwater-flow.

Davis and others (1959) and Olmstead and Davis (1961) described geomorphic provinces of the San Joaquin and Sacramento Valleys, respectively. These geomorphic maps were combined with Jennings' (1977) map to develop a map of geomorphic provinces for the entire Central Valley (*fig. A1*). The map shows the extent of the fans in the valley as well as the dissected uplands and basins. Because the location and type of these provinces generally has been stable and continuous throughout the time of sediment deposition, the characteristics of these provinces relate to the character of the deposits.

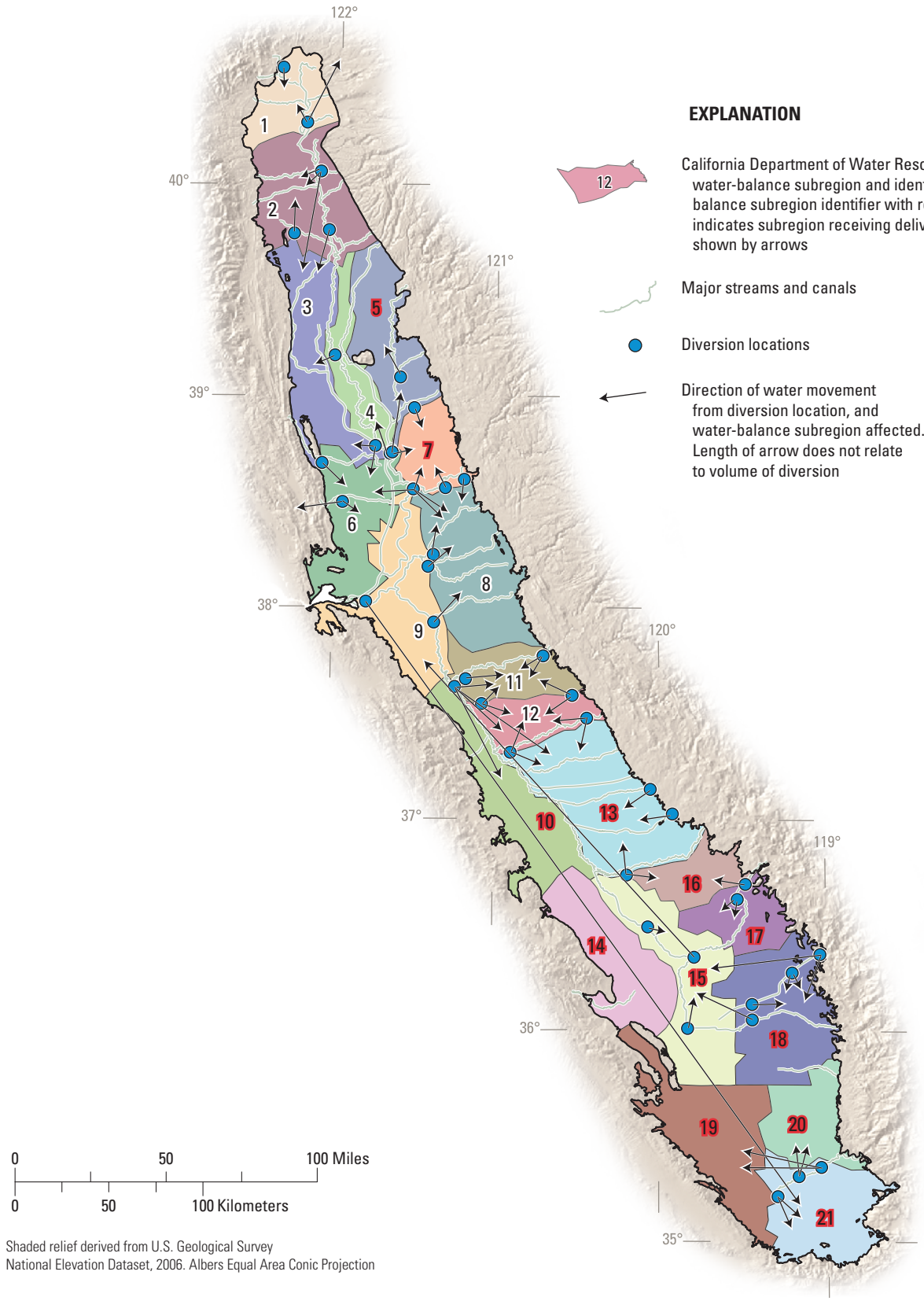

Figure A8. Distribution of water-balance subregions (WBSs) used for surface-water delivery and estimation of groundwater pumpage. These areas are based on areas defined by the California Department of Water Resources and are used as "virtual farms" for accounting by the Farm Process in the simulation of the hydrologic system of the Central Valley with MODFLOW-2000. WBSs 5, 7, 10, and 13-21 receive surface-water that is not shown in the stream network (non-routed deliveries).

Weissmann and others (2005) recently examined factors controlling sequence development of alluvial fans in the San Joaquin Basin (*fig. A1*). They determined that the character of the fans is dependent on the fan's position in the basin and its drainage-basin characteristics. In particular, four factors appear to control development of these fans: tectonic basin subsidence rates, ratio of degree of change in sediment supply to change in discharge, local base-level changes, and basin width. These characteristics ultimately control the grain size and sorting of the deposits.

The Kings River fan has relatively thick deposits with vertical stacking owing to the wide valley width, connection to glaciated parts of the Sierra Nevada, and high tectonic basin subsidence rates. Conversely, the Chowchilla River fan was not connected to a glaciated region and, as a result, had very little change in sediment supply to discharge ratios. This, in turn, resulted in thinner depositional sequences and no incised valleys. These characteristics ultimately control the grain size and sorting of the deposits. The "*Textural Analysis*" section describes the relation of the geomorphology to the textural model in more detail.

Hydrogeology

Detailed descriptions of the physical hydrogeology of the Central Valley are contained in Page (1986), Farrar and Bertoldi (1988), and Williamson and others (1989). A brief overview, based on these earlier works, is presented here. The overview contains a description of the hydrogeologic units and aquifer characteristics as well as the hydrologic system (including climate variability, surface water, and groundwater). A large part of the "Aquifer Characteristics" section is devoted to a detailed examination of the distribution of coarse- and fine-grained sediments in the valley.

Aquifer Characteristics

The sediments of the Central Valley compose an aquifer system comprising confining units and unconfined, semi-confined, and confined aquifers. This aquifer system generally consists of alluvial deposits shed from the surrounding Sierra Nevada and Coast Ranges (*fig. A9*). The chief source of groundwater in the Central Valley is located within the upper 1,000 ft of deposits (Page, 1986). Fresh groundwater (dissolved solids less than 2,000 mg/L) occurs at depths of more than 3,000 ft in the alluvial deposits that fill structural troughs along the west side of the Sacramento Valley and in the southern part of the San Joaquin Valley. Below the freshwater zone is saline water; primarily connate water contained in the thick, marine sedimentary rocks (*fig. A9*) (Planert and Williams, 1995). In places, saline water is found at shallow depths in continental deposits. Such occurrences of saline water can result from upward migration of connate water, evaporative concentration, or estuarine water trapped during sedimentation (Farrar and Bertoldi, 1988).

Traditionally, an assessment of the geologic framework of a groundwater basin focuses on a description of the hydrogeologic or stratigraphic units that compose the aquifer system. Physiography, weathering characteristics, and soils have been used on a limited basis to map formations in the Central Valley; however, defining specific stratigraphic units in the subsurface has been difficult because differences in lithology are not apparent (Bertoldi and others, 1991). As a result, most groundwater studies of the Central Valley define hydrogeologic units—aquifers and confining units, rather than stratigraphic units. Early studies simply conceived of just one unconfined aquifer in the Sacramento Valley that was not correlated with any particular stratigraphic unit (Bryan, 1923; Bloyd, 1978). Early studies of the San Joaquin Valley conceived of two aquifers separated by a regional confining unit. This confining unit is a stratigraphic unit, the Corcoran Clay Member of the Tulare Formation (referred to in this report as the Corcoran Clay. Recently, Williamson and others (1989) described the Central Valley as one continuous heterogeneous aquifer system. In general, this study follows the same conceptual framework as Williamson and others (1989).

Although a number of stratigraphic units have been identified (Tuscan, Tehama, Tulare, and San Joaquin formations), their spatial character and extent is poorly known. Dudley and others (2006) defined the extent of the Tuscan and Tehama formations in a small area near Sutter Buttes and identified them as units that appear to be locally important for groundwater resources. Unfortunately, Dudley's work is not complete. Unlike the Corcoran Clay in the south, the drillers' logs examined in the current CVHM study and prior studies, and electric logs analyzed by Page (1986), reveal no extensive, continuous fine-grained deposits in the Sacramento Valley. These studies reveal fine-grained sediments likely associated with the relatively low energy drainage basins and nearby volcanic activity interbedded with coarse-grained alluvial sediments (*fig. A9A*). In this study, no regional stratigraphic units are defined in the Sacramento Valley.

In the San Joaquin Valley, the upper semi-confined aquifer comprises three hydrogeologic units that grade into each other: Coast Ranges alluvium, Sierran alluvial deposits, and flood-basin deposits (Laudon and Belitz, 1991; Belitz and others, 1993) (*fig. A9B*). The Coast Ranges alluvium, derived from the Coast Ranges to the west, varies from sands and gravels in creek-channel deposits near the heads of fans to silts and clays in interfan and distal fan areas (Laudon and Belitz, 1991), and is 800 ft thick along the Coast Ranges and pinches out near the valley trough (Miller and others, 1971). The Sierran alluvium, generally coarser-grained than the Coast Ranges alluvium, is derived from the Sierra Nevada to the east. It consists of well-sorted medium- to-coarse-grained fluvial deposits, ranging from 400 to 500 ft thick in the valley trough, and thinning eastward and westward (Miller and others, 1971). The Coast Ranges alluvium and Sierran alluvium interfinger near the surface at the valley trough, and the contact extends

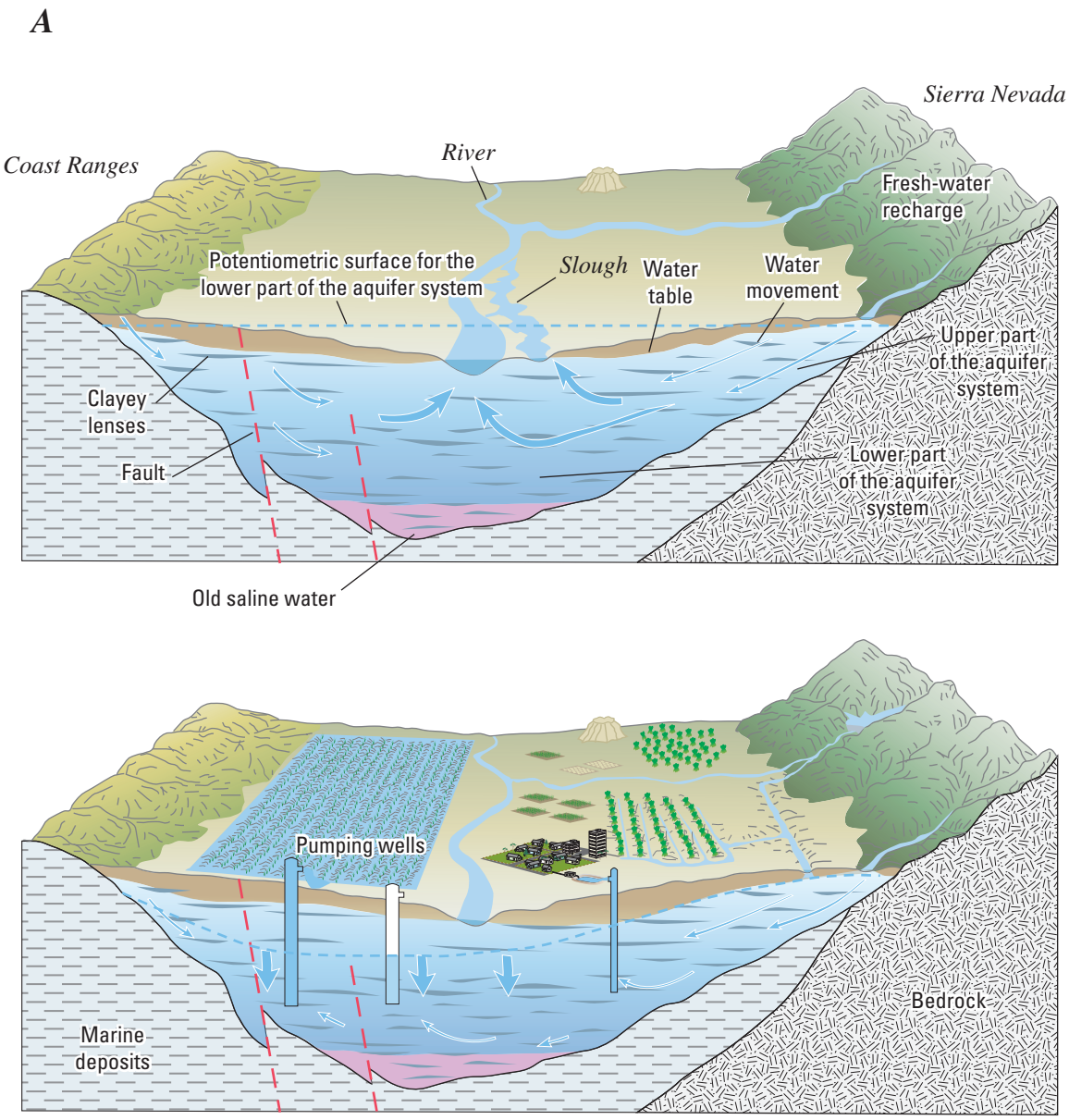

Figure A9. Pre- and post-development of the *A,* Sacramento Valley. *B*, Central part of the San Joaquin Valley, California. (Modified from Belitz and Heimes, 1990; and Galloway and others, 1999).

westward with increasing depth (*fig. A9B*). Flood-basin deposits, as much as 35 ft thick, derived from both the Coast Ranges and the Sierra Nevada, lie along and beneath the valley trough (Laudon and Belitz, 1991).

Numerous lenses of fine-grained sediments are distributed throughout the San Joaquin Valley and generally constitute more than 50 percent of the total thickness of the valley fill. Generally, these lenses are discontinuous and not vertically extensive or laterally continuous. However, during the Pleistocene, as much as 6,600 mi^2 of the San Joaquin Valley was inundated by lakes that accumulated up to 150 ft of diatomaceous clay, often referred to as the E-clay or the Corcoran Clay (Page and Bertoldi, 1983; Farrar and Bertoldi, 1988). This clay is a low-permeability, areally extensive, lacustrine deposit (Johnson and others, 1968) as much as 200 ft thick (Davis and others, 1959; Page, 1986) (*fig. A1*). This continuous clay divides the groundwater-flow system of the western San Joaquin Valley into an upper semi-confined zone and a lower confined zone (Williamson and others, 1989; Belitz and Heimes, 1990; Burow and others, 2004).

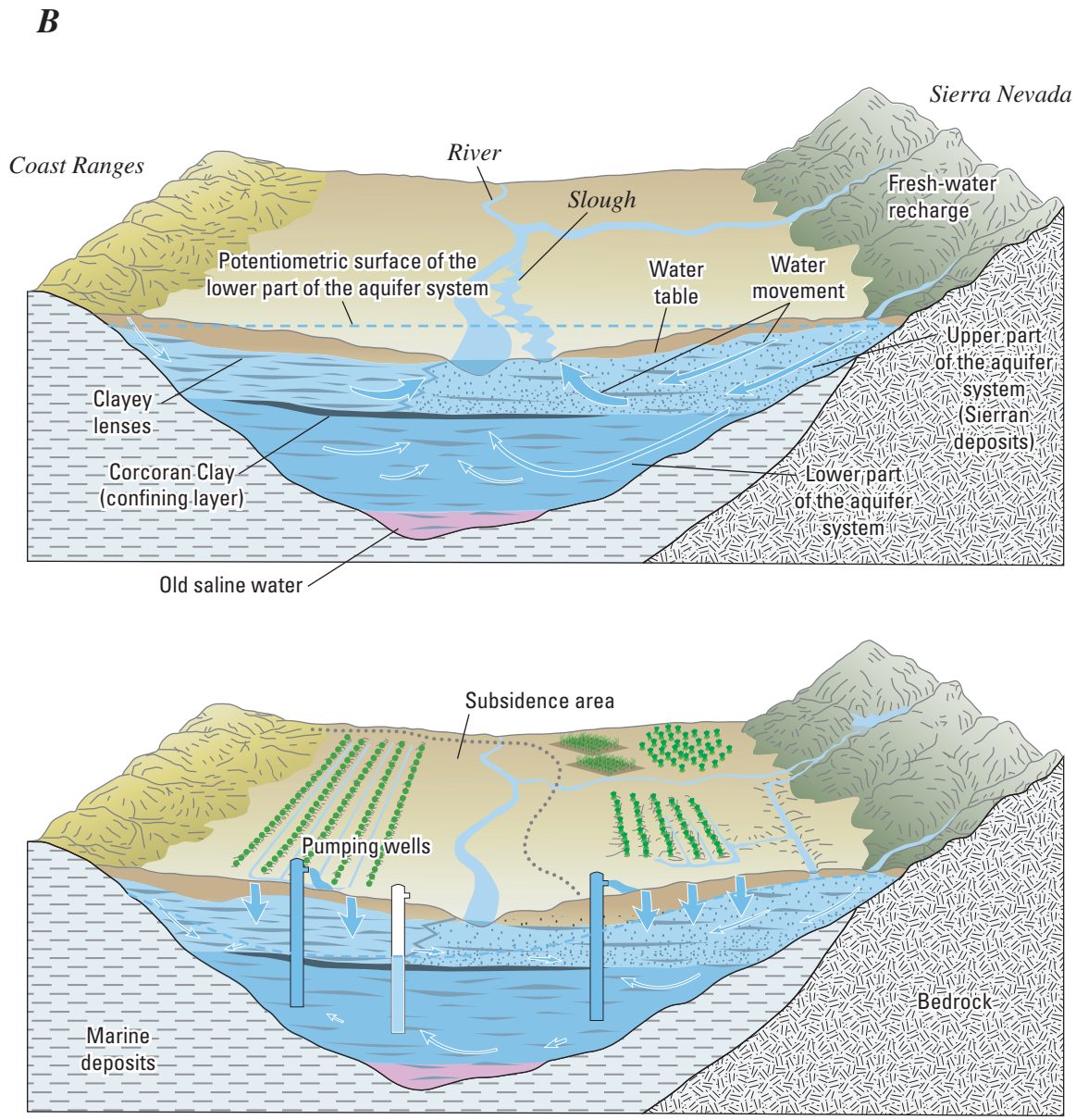

Figure A9. Continued.

The extent and distribution of the Corcoran Clay was defined for use in this study because the unit is one of the few regionally mapable deposits in the valley (*fig. A1*). The 3-D thickness and extent of the Corcoran Clay (Page, 1986; Burow and others, 2004) was used to define the domain of the clay (*fig. A1*). It generally is very fine grained; however, isolated, coarser zones are apparent from drillers' logs, particularly where the clay is less than 20 ft thick, as identified by Page (1986). In addition to its confining properties, laboratory tests indicate that the clay is highly susceptible to compaction. Since development, thousands of large-diameter irrigation wells perforated in the aquifers above and below the Corcoran Clay have increased the hydraulic connection between these aquifers and substantially has increased equivalent vertical hydraulic conductivity of the aquifer system (Williamson and others, 1989; Bertoldi and others, 1991; and Gronberg and Belitz, 1992).

In parts of the southern Coast Ranges and where it dips into the valley, the San Joaquin Formation is shallow enough to be part of the freshwater-bearing deposits. Allegra Hosford-Scheirer (U.S. Geological Survey, written commun., 2004) developed a 3-D integrated stratigraphic framework model for the San Joaquin Valley. Included in her model is the extent and thickness of the San Joaquin Formation and older units. Where the San Joaquin Formation does occur within the CVHM, the deposits are identified as such.

Locally, additional hydrogeologic units have been mapped in parts of the Central Valley (Burow and others, 2004; Phillips and others, 2007). Other than the units identified above, however, the 3-D extent of regionally extensive units generally is unavailable. Fortunately, for understanding regional and local flow patterns and to quantify groundwater in storage, the physical properties of the aquifer materials and the distribution of these properties are more important than are the delineation of formation boundaries (Bertoldi and others, 1991).

In general, the valley deposits compose an aquifer system characterized by large variations in properties. The water-transmitting properties of the aquifer sediments, as represented by hydraulic conductivity (K) and vertical anisotropy, are functions of lithology and differ according to grain size and the degree of sorting of the sediments. There is considerable variation in the hydraulic properties of the deposits from place to place. The relation between hydrogeologic units, lithology, and aquifer characteristics (hydraulic conductivity and vertical anisotropy) has been elucidated in many previous studies in the Central Valley (Davis and others, 1959 and 1964; Page, 1986; Williamson and others, 1989; Bertoldi and others, 1991; Laudon and Belitz, 1991; Phillips and Belitz, 1991; Belitz and Phillips, 1995; Burow and others, 2004; C. Brush, USGS, written commun., 2006; and Phillips and others, 2007). Because there is limited stratigraphic control and measurements of hydraulic properties of the aquifer system are scarce, material properties in many studies of the Central Valley were estimated on the basis of the distribution of sediment texture derived from drillers' logs, geologic logs, and geophysical logs (Page, 1983, 1986; Laudon and Belitz, 1991; Burow and others, 2004). Texture is defined as the percentage of coarse-grained sediment present within a specified subsurface depth interval (Laudon and Belitz, 1991).

For the purpose of evaluating the distribution of texture, the Central Valley was divided into nine regions on the basis of groups of groundwater basins and subbasins (*fig. A10*). These regions will be discussed in more detail in the "*Results of Texture Model*" section.

Textural Analysis

Lateral and vertical variations in sediment texture affect the direction and rate of groundwater-flow as well as the magnitude and distribution of aquifer-system compaction, manifested as land subsidence. Therefore, the textural distribution was used to define the vertical and lateral hydraulic conductivity and storage property distributions for the CVHM.

As in previous studies, this study relies on lithologic data from drillers' logs, which are frequently assumed to be poor sources of lithologic information. However, a number of previous studies in the Central Valley have shown that logs, particularly drillers' logs, if carefully selected, are useful sources of lithologic information. Page (1986) utilized 685 geophysical logs to investigate the texture of deposits above the base of freshwater in the entire 20,000 mi^2 area of the Central Valley. Later investigations, particularly those by Laudon and Belitz (1991), show that drillers' logs can provide valid texture information if the logs are classified and perforated on the basis of the degree of detail in the log. In addition to regional studies, different depth intervals at subregional scales ranging from 500 to 1,000 mi^2 in the west-central San Joaquin Valley have been studied (Prokopovich, 1987; Belitz and Heimes, 1990; Laudon and Belitz, 1991; Belitz and others, 1993; C. Brush, USGS, written commun., 2006). Brush and others (C. Brush, USGS, written commun., 2006) developed texture maps for a 1,000-mi^2 area in the upper part of the western San Joaquin Valley. Burow and others (2004) developed a 3-D kriged estimate of the percentages of coarse-grained texture based on more than 3,500 drillers' logs in a 900-mi^2 subregion in the Modesto area in the eastern San Joaquin Valley.

Recently, other geostatistical approaches have been applied to relatively small areas within the Central Valley. Phillips and others (2007) used applied transition-probability geostatistical approaches (TProGS) to derive the spatial distribution of sedimentary hydrofacies in a nearly 6.5-mi^2 study area of the eastern San Joaquin Valley near the Merced River (*fig. A5A*). Burow and others (2004) developed a hydrofacies model in a 19-mi^2 study area near Modesto. Weissmann and others (2002) constructed a sequence stratigraphic model of the 64-mi^2 stream-dominated Kings River alluvial fan by combining multiple adjacent individual realizations. Application of the TProGS approach to an area as large as the Central Valley is difficult because the sequence-stratigraphic boundaries largely are undefined and because there are a large number of depositional settings.

Based on a methodology developed in earlier work by Page (1983, 1986), Laudon and Belitz (1991), Phillips and Belitz (1991), and Burow and others (2004), the primary variable selected for the textural analysis in this study was the percentage of coarse-grained texture, as compiled from drillers' logs of wells and boreholes drilled in the Central Valley (*fig. A10B*).

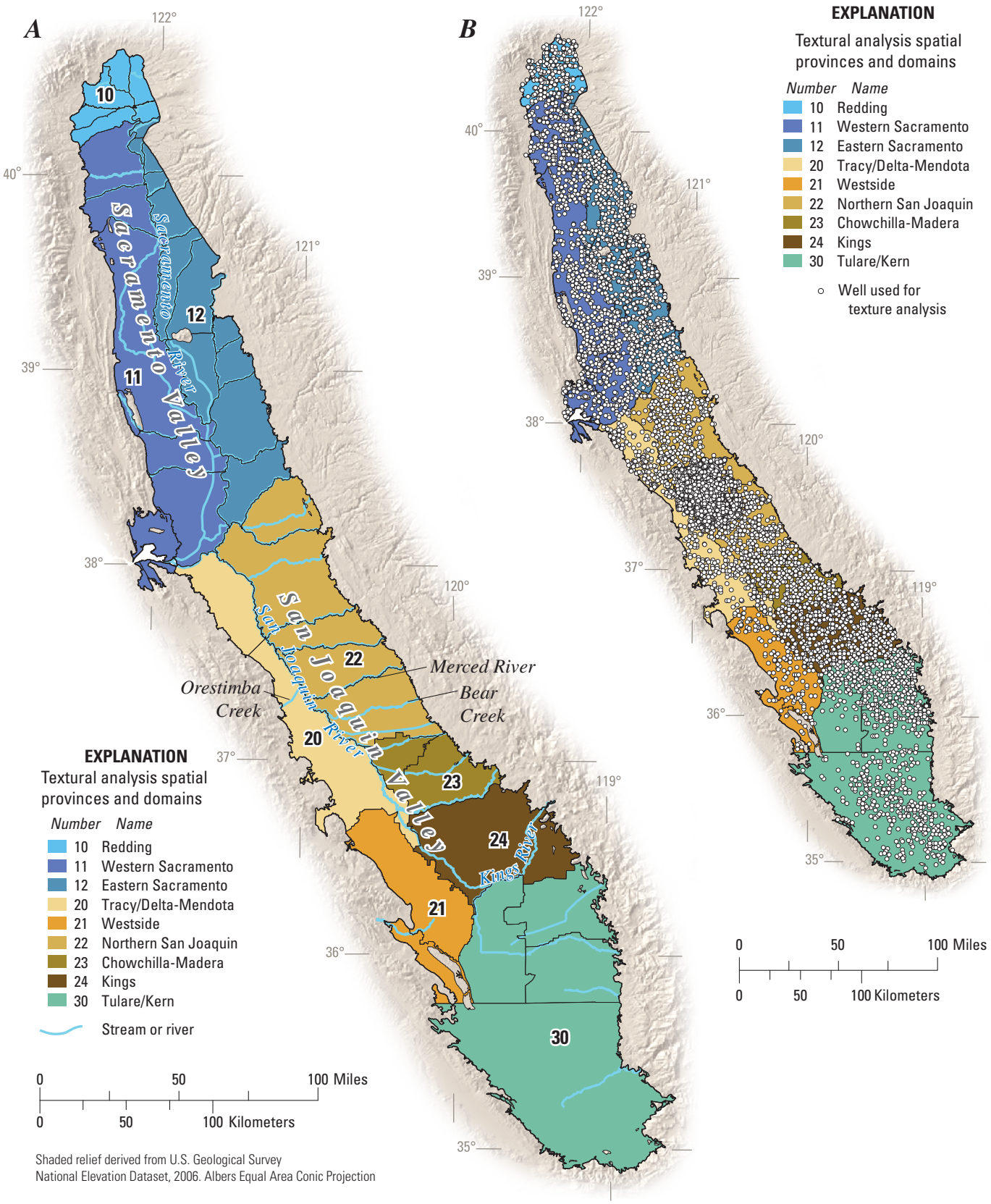

Figure A10. *A*, Central Valley showing groundwater basins and subbasins, groupings of basins and subbasins into spatial provinces and domains for textural analysis. *B*, Distribution of wells used for mapping texture. *C*, Count of wells for each depth increment by domains through 1,200 feet. Because less than 1 percent of the logs extend past 1,200 feet, increments below 1,200 feet were not shown. Detailed description of the spatial provinces and domains are in *table A2*.

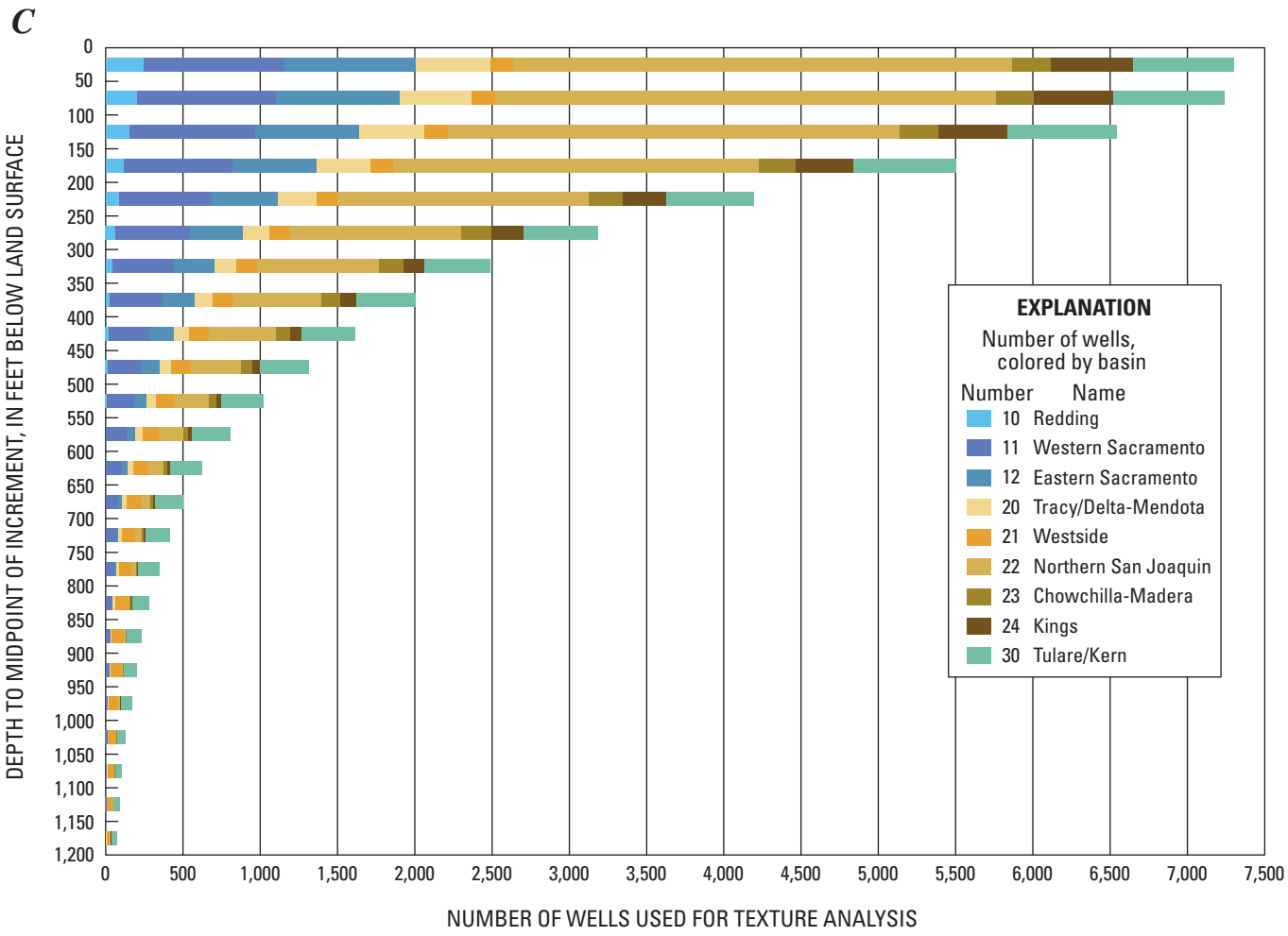

Figure A10. Continued.

Selection and Compilation of Existing Well Data

A database was constructed to organize information on well construction and subsurface lithology in the study area using the database design of Burow and others (2004). Although more than 150,000 optically scanned drillers' logs were obtained from the California Department of Water Resources, this study did not attempt to utilize all of these logs. As noted by Laudon and Belitz (1991), Belitz and others (1993), and Burow and others (2004), textural information in drillers' logs commonly is ambiguous and inconsistent because expertise, experience, and vocabulary of the describers vary greatly. For this study an algorithm was devised to select a subset of good-quality logs that were spatially distributed throughout the valley. Three criteria were considered: specificity of location, degree of detail of geologic description, and density of selected wells. Logs that lacked location information and had poor lithologic descriptions or were illegible were not selected. Lithologic descriptors were subjectively evaluated on the basis of the amount of detail in the descriptions and the depth of the log. Logs with abundant details were subjectively selected. There was no attempt to condition the data or analyses to the higher quality holes. The density of selected well logs used in the texture analysis was based on the quality of drillers' logs. If two "higher-quality" logs were available for a quarter township, the search was satisfied and the next quarter township was evaluated. If not, then up to four lesser-quality logs were selected and then the next quarter township was examined. Preliminary analysis of the drillers' logs indicated that this process resulted in logs yielding sufficient detail to map the texture at 50-ft-depth intervals on a 1-mile grid. The average thickness of the intervals in the selected drillers' logs was 15.5 feet, and 95 percent of the intervals were less than 50 feet thick. On average, 20 intervals per log were defined and more than 80 percent of the selected logs had 10 or more different lithologic characteristics.

Latitude-longitude locations were derived from the township, range, section, and quarter-quarter section given on the drillers' logs. The location was calculated to the center of the most detailed part of the township/range information. If more than one point was available for a given location, the subsequent points were located randomly within the most detailed township/range designation.

Burow and others (2004) developed a database from about 3,500 drillers' logs in the 900-mi^2 Modesto area. These logs are densely spaced and represent about one-third of the total wells drilled in the Modesto area. Therefore, this area was not resampled and their more detailed database was used where it existed. As a result, the data density for this region, which covers only about 5 percent of the Central Valley, is much higher than the rest of the valley. In this study, the sediment descriptions and depth intervals were entered into the database exactly as they appeared on the drillers' log. The database of existing wells constructed for this 20,000-mi^2 study area contains information from 8,497 drillers' logs. This represents about 5 percent of the total number of wells drilled in the Central Valley. Although the database does not include all well records, the data provides a representative sample of the existing wells. Well depths range from 13 to 3,114 ft below land surface, with a median depth of 321 ft.

Classification of Texture from Drillers' Logs and Regularization of Well Data

Each lithologic log interval was classified using a discrete binary texture classification of either "coarse grained" or "fine grained" on the basis of the description in the log. In this study, coarse-grained sediment is defined as consisting of sand, gravel, pebbles, boulders, cobbles, or conglomerate. Fine-grained sediment is defined as consisting principally of clay, lime, loam, mud, or silt. These definitions of "coarse grained" and "fine grained" are similar to those originally defined by Page (1986) and later used by Williamson and others (1989), Phillips and Belitz (1991), Laudon and Belitz (1991), Belitz and others (1993), Burow and others (2004), and Brush and others (C. Brush, USGS, written commun., 2006). For use in statistical and geostatistical analysis, the percentage of coarse-grained texture was calculated over 50-foot depth intervals in each of the 8,497 logs in the database. This regularized data set consists of 46,878 data values of percentage of coarse-grained texture, referred to in this report as "texture values". General statistical analyses were computed to examine spatial changes in percentage of coarse-grained deposits (count, mean, and standard deviation), both laterally and with depth. The global mean percentage of coarse-grained texture is 36 percent, with a standard deviation of 32 percent.

The graph in *figure A10C* shows that the majority of the texture values were for depths less than 200 ft. For many of the well logs, texture values are discontinuous from the ground surface to the bottom of the borehole. Thus, none of the depth intervals include texture values for all 8,497 logs. For depth intervals shallower than 500 ft, there are more than 1,300 texture values available within each of the nine study domains. For depths greater than 1,100 ft, less than 100 texture values exist for a given depth interval. Only 129 logs had texture values for depth intervals below 1,000 ft, and only 16 drillers' logs had data for intervals at depths greater than 1,800 ft. Analysis of the sample variance for each depth interval indicated that the variability of the average percentage of coarse-grained texture increased with increasing depth for depths greater than 300 ft. The primary reason for the increased variability is most likely the decrease in the number of drillers' logs available for wells of increasing depth (*fig. A10C*). For depth intervals with less than approximately 1,000 texture values (depth intervals greater than 550 ft), the number of drillers' logs likely is insufficient to represent the average percentage of coarse-grained texture at a given depth.

Geostatistical Modeling Approach

The geostatistical methods employed in this study are similar to those used by Burow and others (2004). Geostatistics is a set of applications and statistical techniques used to analyze spatial and (or) temporal correlations of variables distributed in space and (or) time (Isaaks and Srivastava, 1989). An advantage of using geostatistical models instead of simple spatial interpolation methods, such as inverse-distance weighted interpolation, is that the geostatistical model provides the best linear unbiased estimate and provides a set of weights that minimize estimation error (Journel and Huijbregts, 1978). In addition, the model is fitted to the observed spatial correlation structure, whereas simple interpolation methods are based on an assumed spatial correlation structure. Furthermore, anisotropy in the spatial correlation structure can be modeled by combining several different models aligned along the principal axis of anisotropy to form a nested set of models.

Regions and Domains

Because of the large size of the Central Valley and multiple depositional environments, the study area was divided into the nine regions (*fig. A10*). The mean versus the standard deviation of the texture data was evaluated for "stationarity" (Journel and Huijbregts, 1978) and to identify and remove any proportional effect. Two criteria were used to identify and remove any proportional effect: groundwater subbasins, and position relative to the Corcoran Clay (above, below, and outside). First, the study area was separated into its two dominant valleys, Sacramento and San Joaquin. The Sacramento Valley was divided into the major groundwater basins (California Department of Water Resources, 2003): the Redding Area Basin on the north, and the Sacramento Valley Basin to the south (*fig. A10A*). Although the Sacramento Valley Basin has been subdivided into 18 subbasins (California Department of Water Resources 2003), this amount of detail was not warranted; therefore, the subbasins within this basin were lumped into two domains, one east and one west of the Sacramento River.

The San Joaquin Valley was separated into three major parts: the eastern and the western parts of the San Joaquin Valley and the southern, more internally drained, part. On the western side, the Tracy and Delta–Mendota subbasins were grouped into one region, as were the Westside and Pleasant Valley sub-basins (*fig. A10A*). Likewise, the eastern side of the valley was divided into three regions that were groupings of groundwater subbasins (*fig. A10A*). The southern part, referred to here as the Tulare/Kern region in *figure A10A*, includes the four southern groundwater subbasins of the San Joaquin Valley Basin (California Department of Water Resources, 2003).

The San Joaquin Valley was divided laterally and vertically (*table A2*). Laterally, the domains consist of groupings of similar groundwater subbasins described above (*fig. A10A*). However, because the hydrogeology of the San Joaquin Valley is dominated by the Corcoran Clay, where this clay exists, the regions were subdivided above and outside the extent the Corcoran Clay (*table A2*). This resulted in two more domains: the extent and thickness of the Corcoran Clay, and the area below the clay. Thus, to assure stationarity within a domain, 17 domains were identified (9 spatial provinces, and divisions of the provinces into the 6 spatially based domains above the Corcoran Clay, a domain within the Corcoran Clay, a domain below the Corcoran Clay, and a domain where the Corcoran Clay is absent) (*figs. A10A, A10B,* and *table A2*).

Geostatistical Model of Coarse-Grained Texture

Because present-day land surface represents a depositional horizon, the spatial correlation model was developed using depth below land surface as the z axis. Three-dimensional variograms for each of the 17 domains (*table A2*) were developed. The variogram models for each domain were defined using nested structures; each model included a nugget, an exponential variogram model, and often a nested Gaussian variogram model. Horizontal anisotropy was oriented with the trend of the valley axis within each domain. Therefore, the principal axes of horizontal anisotropy of the domains are nearly north-south in the Sacramento Valley and nearly northwest-southeast in the San Joaquin Valley. Reflecting the geometry and depositional environment of the Central Valley, the variograms typically have a horizontal range in the hundreds of miles along the axis of the valley and tens of miles perpendicular to the valley axis, and a much smaller vertical range of 165 to 820 ft (*table A2*). Although nugget values range from 0 to 50 percent of the sill, the nugget typically is about one-third of the sill. The largest variance is in the northern and southern domains (Redding and Tulare/Kern outside the extent of the Corcoran Clay), where streams enter the valley from three directions.

Texture was estimated at the cell-centers of a 3-D grid. The grid is oriented with the long axis roughly parallel to the Central Valley axis and has a uniform cell spacing of 1 mi in the x and y axis directions. The resulting grid consists of 98 cells in the x-axis direction and 441 cells in the y-axis direction. The vertical discretization is defined by the established 50-foot depth intervals, starting with the midpoint of the first interval at 25 ft below land surface and extending 46 cells in the vertical direction to 2,300 ft below land surface. Because areas outside the basin boundary (*fig. A1*) were not estimated, the discretization defined a total of 20,533 grid cells in the lateral direction and a total of 944,518 grid cells for the entire 3-D grid.

Using the 3-D variogram models described above and in *table A2*, textural values for 50-foot depth intervals (the center of cell along the z axis) were estimated using 3-D kriging for each domain. The 17 domain models then were merged to form one model at 50-foot depth intervals for the entire Central Valley. Because data points for the entire model area were available for estimation within each domain, the transition from one domain to the next usually is smooth. The estimate at each grid cell-center was constrained by the number of data points, rather than by the spatial dimensions of the search neighborhood. Therefore, for locations of the estimation grid having densely spaced and relatively deep boreholes with continuous drillers' logs, the effective search neighborhood was relatively small. For locations of the estimation grid which contain sparsely spaced drillers' logs, the effective search neighborhood was expanded vertically and laterally until the threshold number of texture values was reached. The estimation neighborhood contained at least two texture values for each kriged estimate. Estimates in the corners, lower layers, and along the boundaries of the grid are extrapolated rather than interpolated values. As is indicated by the nugget and range of the variograms, the assumption that, in heterogeneous alluvial sediments, texture at a point is related to texture at surrounding points several miles away may not always be valid. Therefore, in areas where texture data are sparse, the texture maps should be regarded as showing only general trends and averages. Conversely, in areas where texture data are variable and closely spaced, the 3-D kriging may produce smoothed estimates. These results occur because the kriging algorithm used is a function of both distance and direction.

At the scale of the Central Valley, kriging was done at points instead of volumes. The point estimates were used to map the texture within the Corcoran Clay. Where the Corcoran Clay is thin and, therefore, underrepresented by the 50-foot depth intervals, the texture distribution within the Corcoran Clay showed some gridding artifacts that parallel the depth and thickness of the Corcoran Clay. These artifacts could be the result of imperfect mapping of the depth to the Corcoran Clay, the regularized 50-foot incremented data banding in and out of the Corcoran Clay, and (or) misidentification and (or) generalization of the extent and thickness of the Corcoran Clay on Page's (1986) map. To better represent the textural distribution within the Corcoran Clay, the 3-D boundary defined by Page (1986), and later modified by Burow and others (2004), was used to segregate points thought to represent the clay. These points were used to develop a two-dimensional kriged map of the percentage of coarse texture in the Corcoran Clay.

Table A2. Distribution of statistical properties for the percentage of coarse-grained deposits for the Central Valley, Calfornia, by domain, including variogram and variogram models.

[All values in feet unless noted otherwise. Spatial province numbers are used to help correlate with *figure A2*. Variogram model parameters: Slicing height, 50 feet (15.23 m); Lag, 2,000 feet (600 meters); tolerance (percent of lag), 0.5; number of lags, 50]

Valley	Spatial province	Spatial province number[2]	Domain	Area (square miles)	Variogram				Variogram models[3]								
										Model 1 - Exponential					Model 2 - Gaussian			
											Directional scales				Directional scales		
					Number of samples	Mean	Variance	Anisotropy/ rotation (degrees)	Nugget	Sill	1	2	3	Sill	1	2	3
Sacramento	Redding	10	Redding	597	1,010	39	1,348	0	1,300	2,400	5,000	15,000	500	800	98,000	328,000	700
	Western Sacramento Valley	11	Western Sacramento	3,524	6,423	25	820	10	1,100	1,200	16,000	21,000	400	300	131,000	656,000	2,300
	Eastern Sacramento Valley	12	Eastern Sacramento	2,588	4,632	32	1,069	15	1,300	1,600	20,000	28,000	400	500	164,000	492,000	500
San Joaquin	Tracy/Delta–Mendota	20	Tracy/Delta–Mendota above Corcoran Clay	1,198	1,466	45	1,029	20	1,000	2,300	16,000	59,000	800				
			Tracy/Delta–Mendota Corcoran Clay absent	508	433	29	820	20	0	2,700	16,000	8,000	200				
	Westside	21	Westside above Corcoran Clay	844	1,343	30	982	47	1,000	2,200	20,000	30,000	500				
			Westside Corcoran Clay absent	384	481	33	1,012	47	1,300	2,000	17,000	39,000	500				
	Northern San Joaquin	22	Northern San Joaquin above Corcoran Clay	865	4,470	51	876	31	1,600	1,200	459,000	33,000	600				
			Northern San Joaquin Corcoran Clay absent	2,373	8,931	34	936	31	300	2,100	3,000	4,000	200	600	66,000	164,000	300
	Chowchilla–Madera	23	Chowchilla–Madera above Corcoran Clay	375	330	37	691	35	0	2,200	30,000	20,000	200				
			Chowchilla-Madera Corcoran Clay absent	488	1,119	36	878	35	1,100	1,500	21,000	21,000	600				
	Kings	24	Kings - above Corcoran Clay	498	1,157	46	577	30	1,000	900	26,000	39,000	200				
			Kings - Corcoran Clay absent	1,027	1,560	47	837	30	1,000	1,600	39,000	30,000	500				
	Tulare/Kern	30	Tulare/Kern - above Corcoran Clay	2,788	2,562	43	1,042	28	500	2,100	11,000	8,000	300	900	164,000	295,000	2,000
			Tulare/Kern - Corcoran Clay absent	2,500	2,775	41	1,314	28	1,200	2,000	16,000	25,000	700				
	Corcoran Clay	N/A	Inside Extent of Corcoran Clay	6,568	374	26	874	33	0	2,900	20,000	20,000	0	9,800	197,000	656,00	197,000
			Below Corcoran Corcoran Clay	6,568	4,685	35	1,138	33	900	1,400	6,000	4,000	400	1,400	180,000	558,000	400

3-D Model of Percentage of Coarse-Grained Texture

The texture model was developed in two stages. In the first stage, the texture was estimated for each of the 50-ft thick layers. In the second stage, the resulting estimates were aggregated vertically into 10 model layers, resulting in approximately 205,330 nodes. Although the lateral spacing, 1 mi^2, stayed the same, the vertical spacing was increased with depth. In general, the model layers range from 50- to 400-feet thick; the thickness of each layer is 50 ft more than the layer above (*table A3*).

Where the Corcoran Clay exists, the layers above the clay were modified so that the clay was explicitly represented by layers 4 and 5 (*fig. A11*). In order to complete this representation, the relative thicknesses of layers 1–3 above the clay were modified. The vertical thickness above the clay was divided evenly between the three layers below a specified maximum thickness. The specified maximum thicknesses of layers 1

Table A3. Central Valley, California, groundwater flow model layer thicknesses and depths.

[Layers 4 and 5 represent Corcoran Clay where it exists; elsewhere a 1 foot thick phantom layer; they are kept only to keep track of layer numbers]

Layer	Thickness (feet)	Depth to base outside Corcoran Clay (feet)	Texture figure
1	50	50	A9(a)
2	100	150	—
3	150	300	A9(b)
4	Variable	301	A9(c)
5	Variable	302	A9(c)
6	198	500	A9(d)
7	250	750	—
8	300	1,050	—
9	350	1,400	A9(e)
10	400	1,800	—

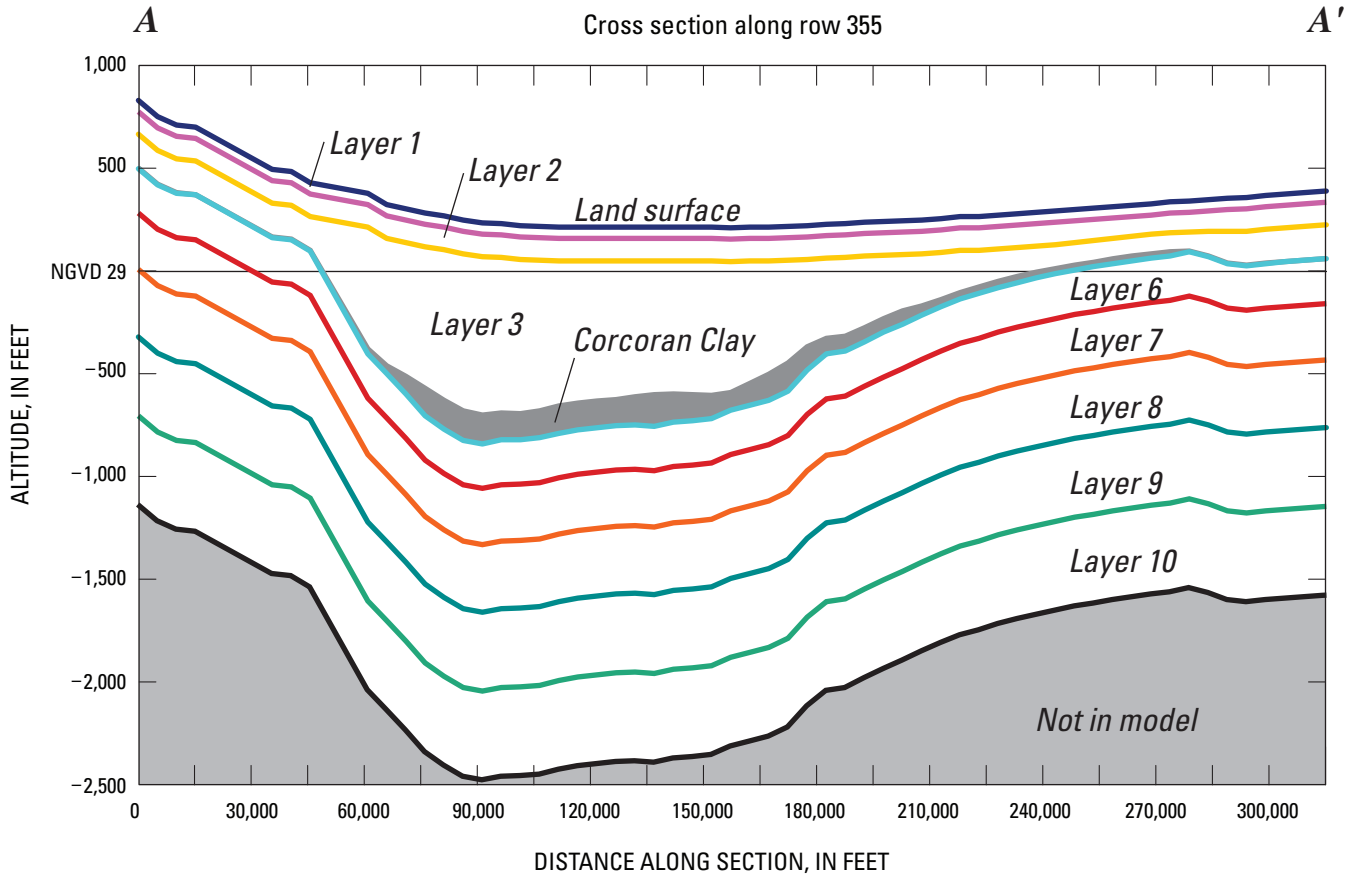

Figure A11. Generalized hydrogeologic section (*A*–*A*′) indicating the vertical discretization of the numerical model of the groundwater-flow system in the Central Valley, California. Line of section shown on *figure A1* (altitudes are along row 355; layer numbers indicate model layer).

and 2 were 50 and 100 ft, respectively. Any residual thickness was added to layer 3, as necessary, to reach the depth of the top of the Corcoran Clay. In addition, in layer 3, an area about 3-mi wide around the area of the Corcoran Clay was modified, where necessary, to allow a smooth transition from the non-uniform varying depth and thickness of the Corcoran Clay to the regular depth intervals of the model layers. The texture value for each layer was determined by averaging the percent-coarse value for the appropriate model layer. Layer 1 of the texture model is identical to that of the texture lattice. Likewise, layers 4 and 5 within the Corcoran Clay correspond to the 2D kriged values. Outside of the area of the Corcoran Clay, layers 4 and 5 do not exist and are considered phantom layers that are kept only to keep track of layer numbering (see *Chapter C*).

Results of Texture Model

The relatively low mean percentage of coarse-grained deposits indicates a prevalence of fine-grained texture throughout the region (*table A2*). This tendency was identified previously by Page (1986), Belitz and others (1993), and Burow and others (2004). The spatial patterns of the percentage of coarse-grained texture are shown in five representative layers in the texture model (*fig. A12*) and oblique views of the model (*fig. A13*). For shallow depths (0–150 ft for the upper two model layers), the large number of drillers' logs reduces the variance of the estimate. Layers 1 and 3 (*figs. A12A* and *A12B*) are quite similar in detail; layer 9 is smoothed, relative to the others, where there is a lack of drillers' logs (*figs. A12D* and *A12E*). Layer 1 represents the uppermost 50 ft, and because of the data density, is the most detailed layer in the model (*fig. A12A*). Layer 3, which still shows significant detail, represents the interval between 150 and 300 ft below the land surface (*figs. A11* and *A12B*). Layers 4 and 5 represent the Corcoran Clay and generally are very fine-grained (*fig. A12C*). Layer 6 represents the 200-foot interval directly beneath the Corcoran Clay where it is present, or the 300- to 500-foot interval below the land surface (*fig. A12D*). Finally, layer nine represents the sparsely penetrated 350-foot interval between 1,050 and 1,400 ft below the land surface (and deeper below the Corcoran Clay) (*fig. A12E* and *table A2*).

The 3-D kriged estimates of percentage coarse-grained texture show significant heterogeneity in the texture of the sediments (*figs. A14* and *A15*). Zones of very coarse-grained texture (greater than 90 percent coarse-grained) are locally significant; however, the results indicate a predominance of intermediate values of 30–70 percent coarse-grained texture (*figs. A12* and *A13*). This distribution of texture is described by the 17 domains defined in *table A2*. It also can be related to the geomorphic provinces and alluvial fan morphology of the Sacramento River (*fig. A14*). In the following paragraphs, the general textural modeling results are described for each of the domains.

Sacramento Valley

As mentioned previously, the Sacramento Valley was divided into domains equivalent to the three parts that were based on groundwater basins or subbasins: the Redding Basin, and the two groups of subbasins east and west of the Sacramento River. The Redding domain is the coarsest (mean percentage of coarse-grained deposits of 39 percent, from the interval data) of the three domains. The western part of the Redding domain becomes coarser with depth. Most of the area in the eastern and western Sacramento domains, including the Delta, is predominantly fine-grained (*figs. A12* and *A13*); the eastern Sacramento Valley domain is coarser (mean of 32 percent) than the western domain (mean of 25 percent). The fine-grained nature of the Sacramento Valley reflects a number of factors, including more fine-grained volcanic-derived source-area sediments and the lack of glacially derived deposits. Except for the drainage basins draining Lake Tahoe, the northern Sierra Nevada drainage basins have a much lower average elevation and a less-coarse depositional character than the glaciated drainage basins to the south. This resulted in a higher percentage of fine-grained texture. In addition, the lack of extensive tectonic basin subsidence in the Sacramento Valley may have resulted in most of the sediments being removed from the individual drainage basins. However, some coarse-grained isolated deposits are in the shallow part of the Sacramento Valley (layer 1; *figs. A1* and *A12A*) along the channel of the Sacramento River and the distal parts of the fans emanating from the Cascade Range, the northern Sierra Nevada, and the American River drainage basin. The coarsest deposits correlate with the Sacramento River channel and flood-plain before it widens into more of a basin-type province (*fig. A14*). Hence, the southernmost Sacramento Valley is similar to the northern San Joaquin Valley, and the character of the alluvial fans in this part of the valley is similar to that of the Tuolumne or Stanislaus River fans (*fig. A12*). Although somewhat less variable with depth, both the eastern and western Sacramento domains remain relatively fine grained with depth with some coarser areas along the western edge of the Sierra. These areas most likely represent older alluvial fans of the Sierra (*figs. A12* and *A13*).

The overall change in sediment texture between the Sacramento and San Joaquin Valleys can be seen in the cumulative distribution curves plotted in *figure A15*. Overall, the Sacramento Valley texture is more fine-grained. The fine-grained consistent texture of the Corcoran Clay is visible in *figure A15B*. In addition, the changes in sediment texture, with depth, are evident. As would be expected, there is more variability in the shallow sediments. In the Sacramento Valley, at the fine-grained end, the change is systematic from layer 1 down to 10. Toward the coarser end of the distribution curves, the change is not so systematic. In the San Joaquin Valley curves, there is more contrast between the depth layers than in the Sacramento Valley curves.

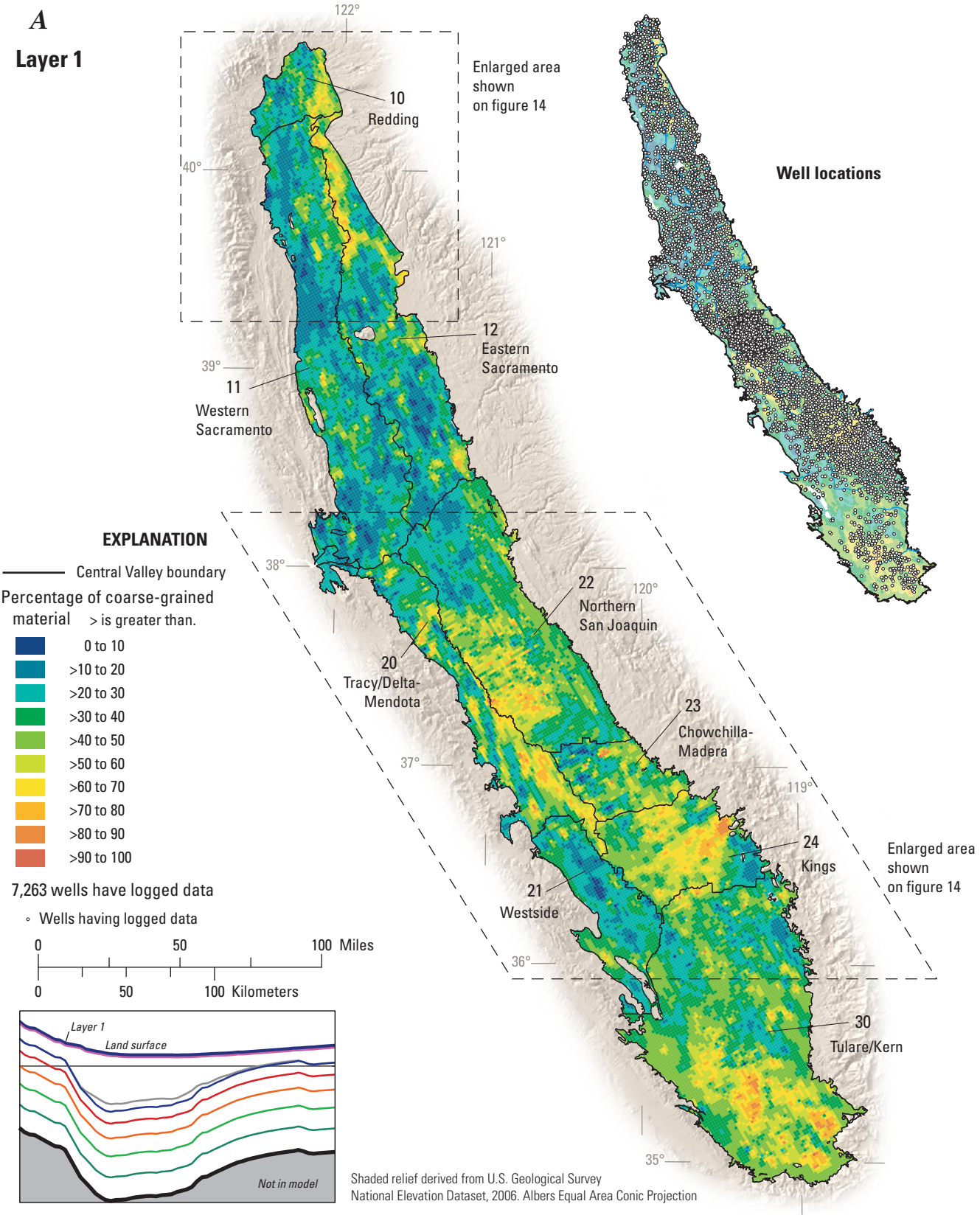

Figure A12. Kriged distribution of coarse-grained deposits for layers 1, 3, Corcoran Clay, 6, and 9 of the groundwater-flow model. Inset shows distribution of wells used in that depth interval.

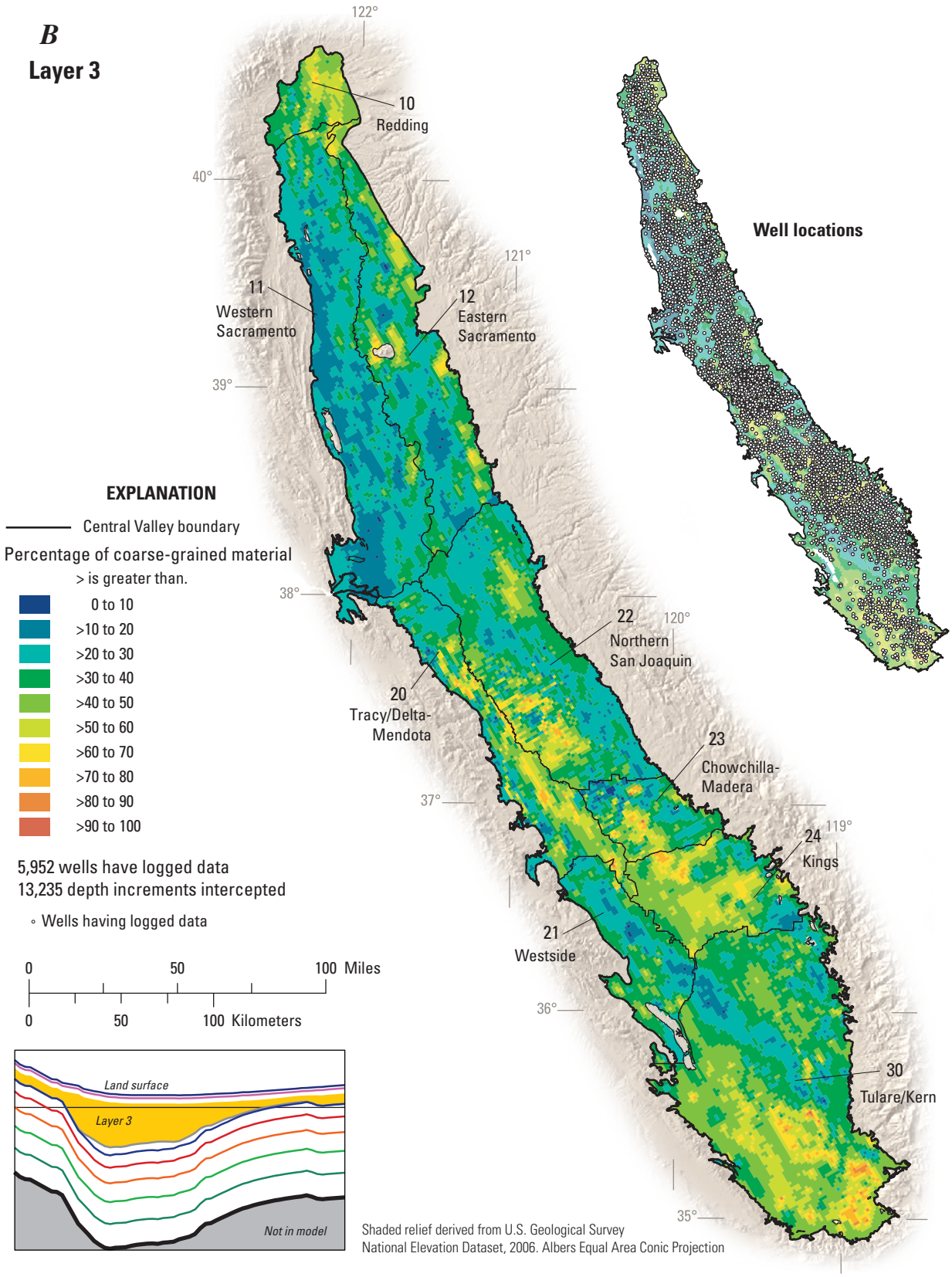

Figure A12. Continued.

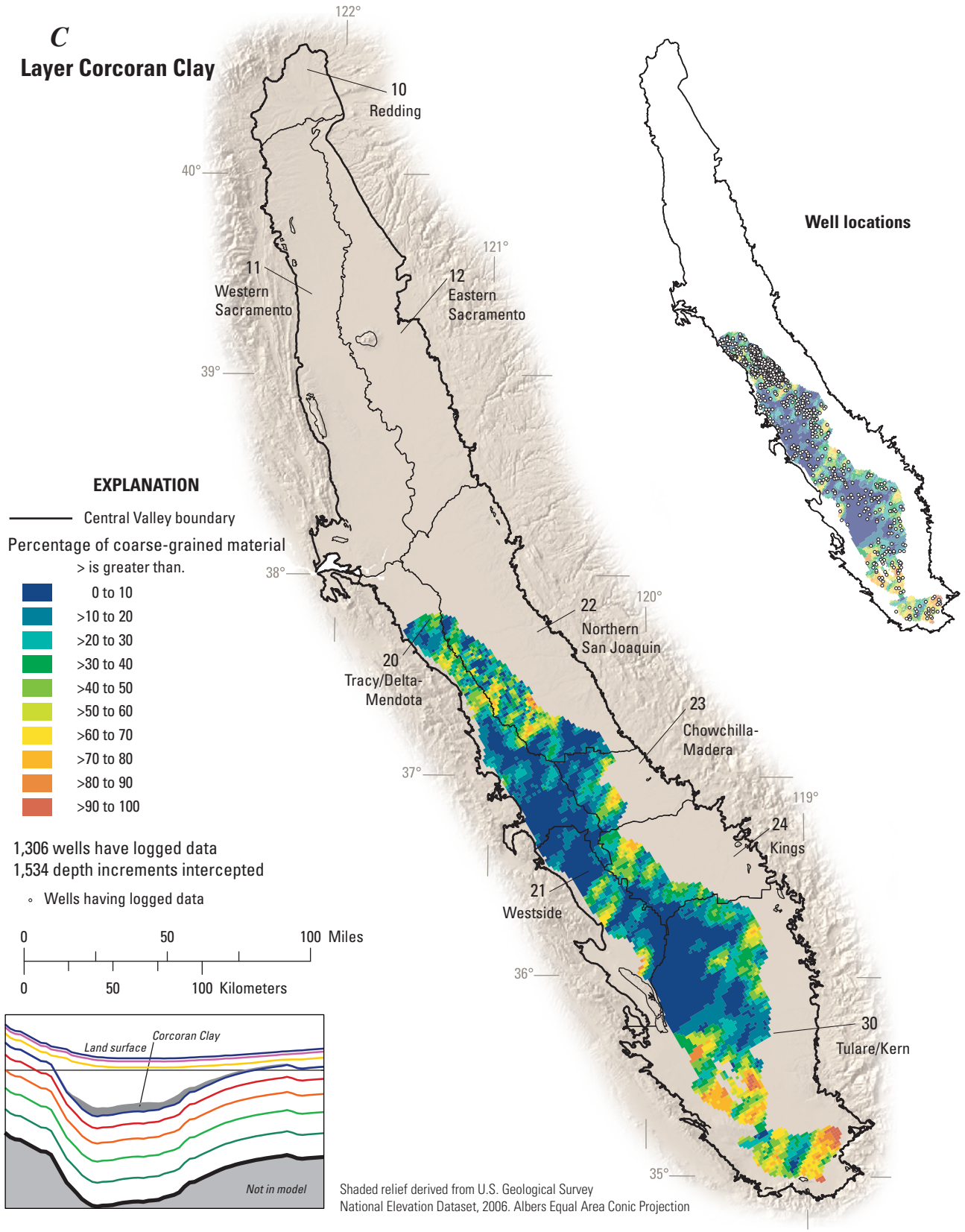

Figure A12. Continued.

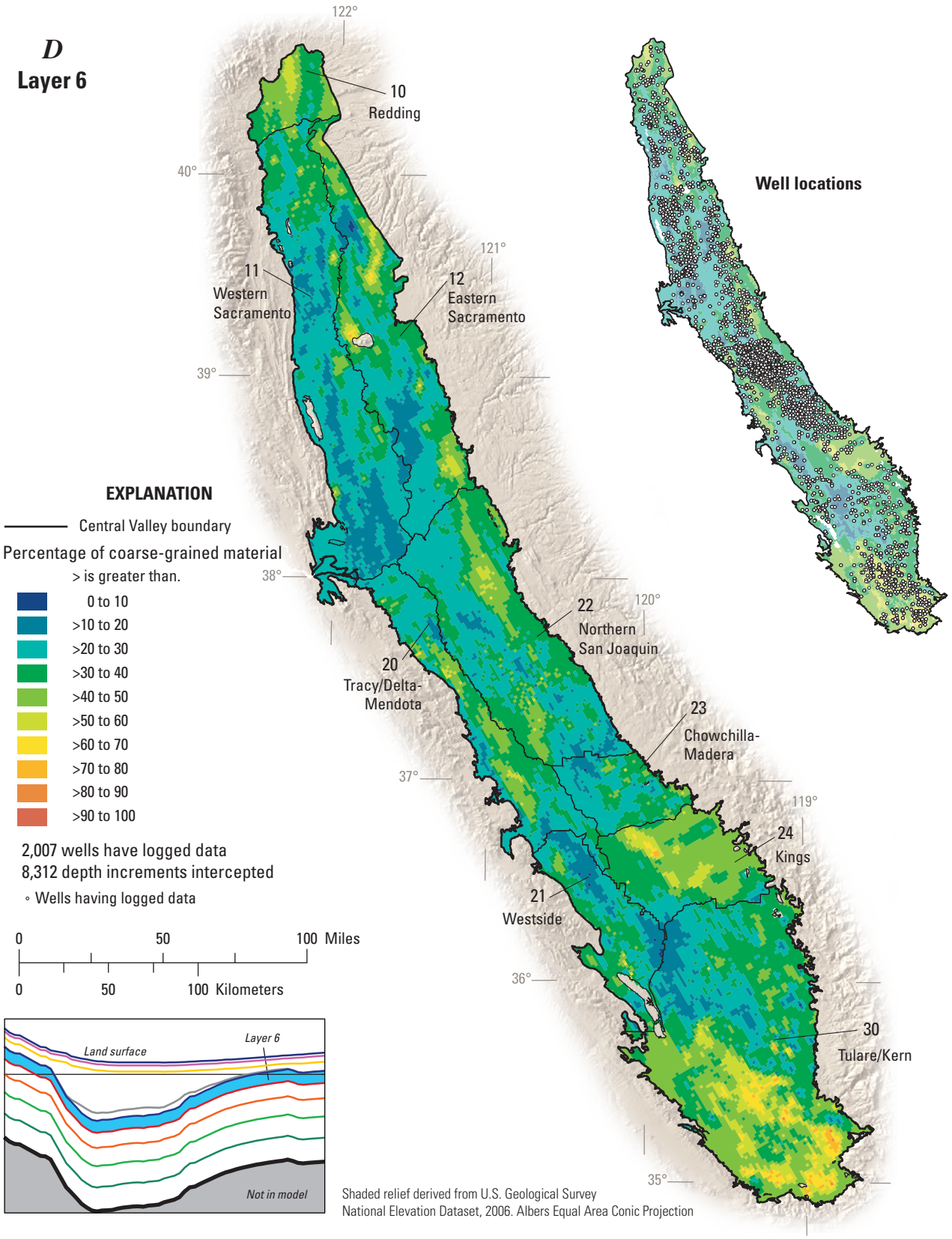

Figure A12. Continued.

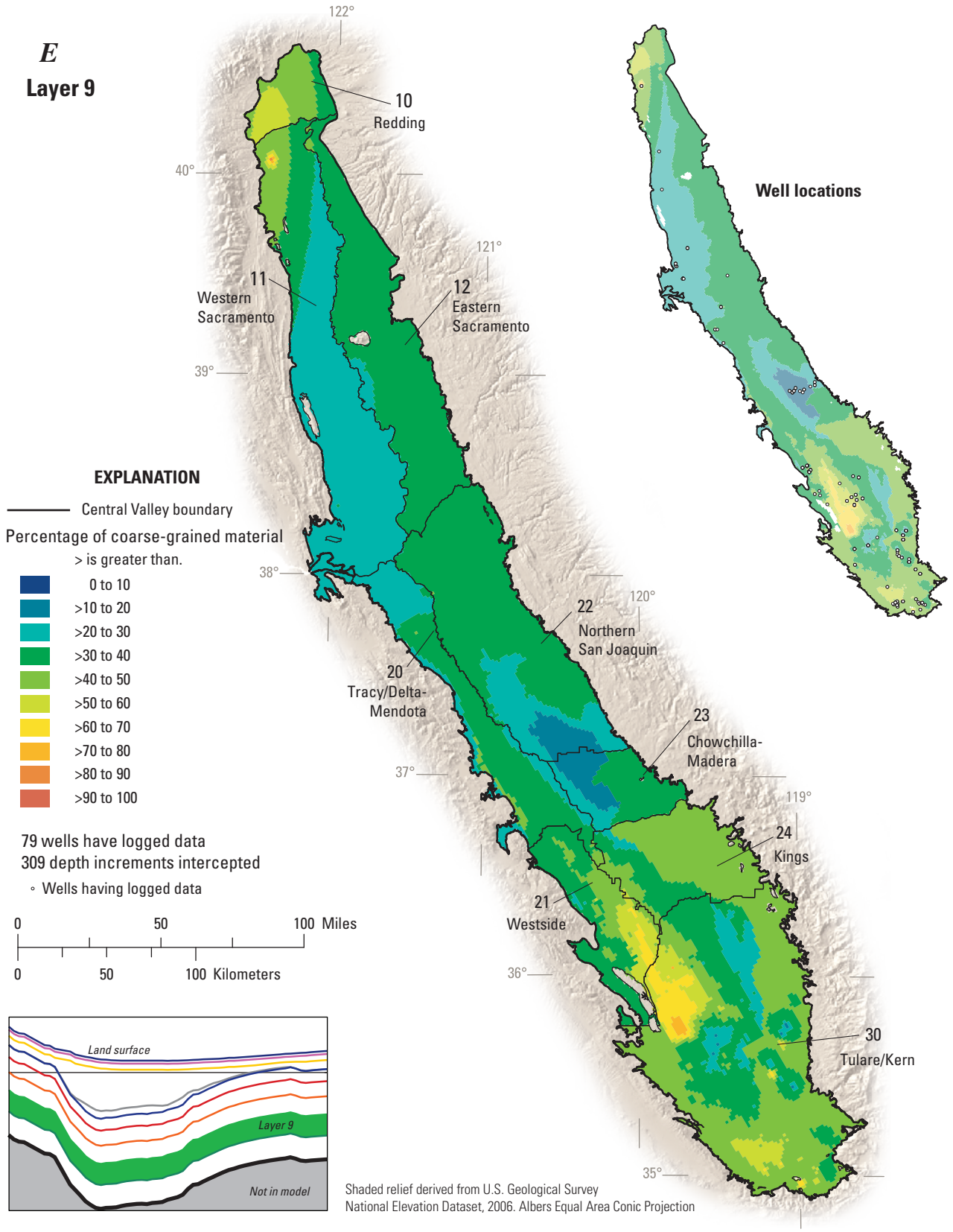

Figure A12. Continued.

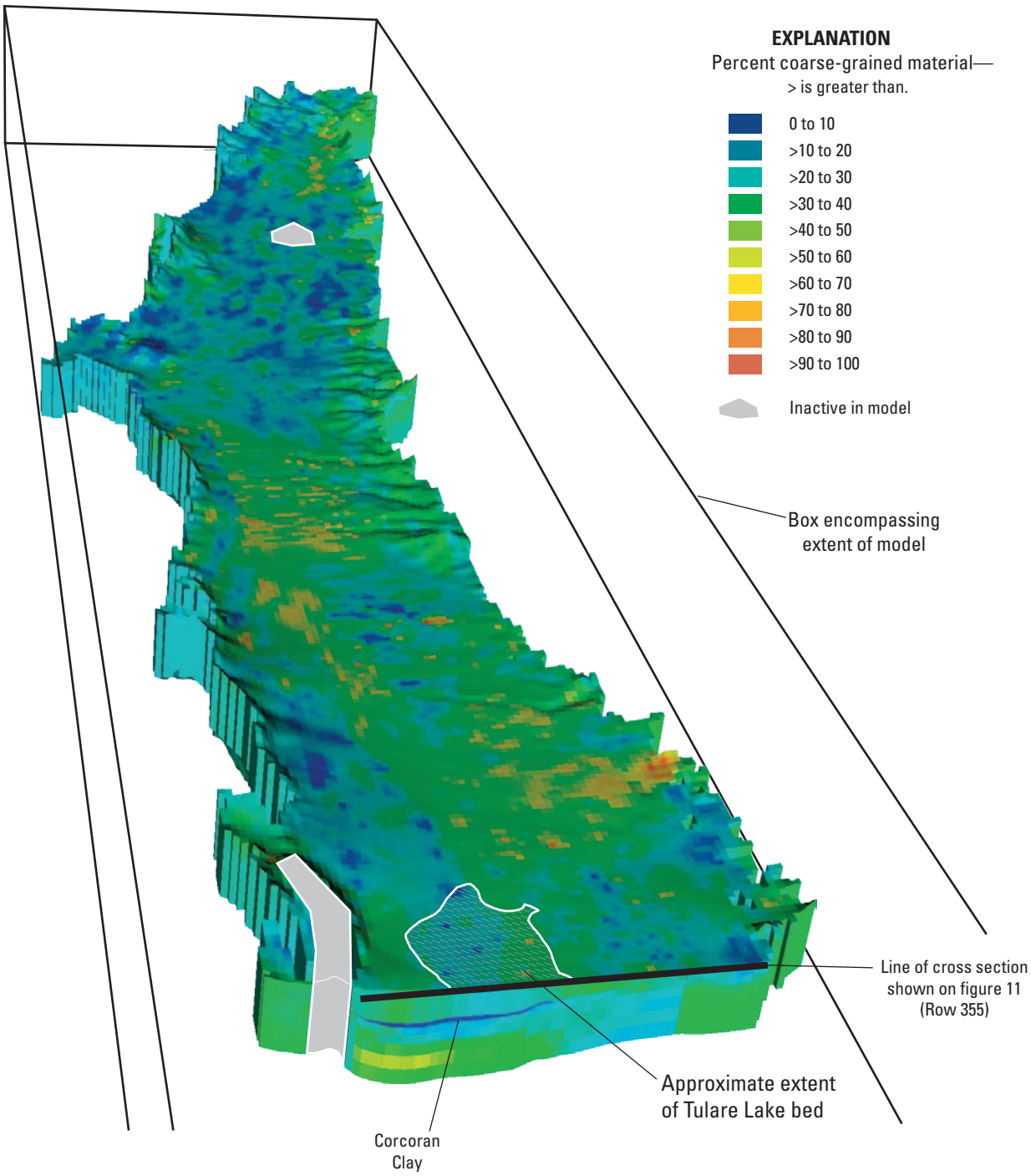

Figure A13. Kriged texture within groundwater-flow model.

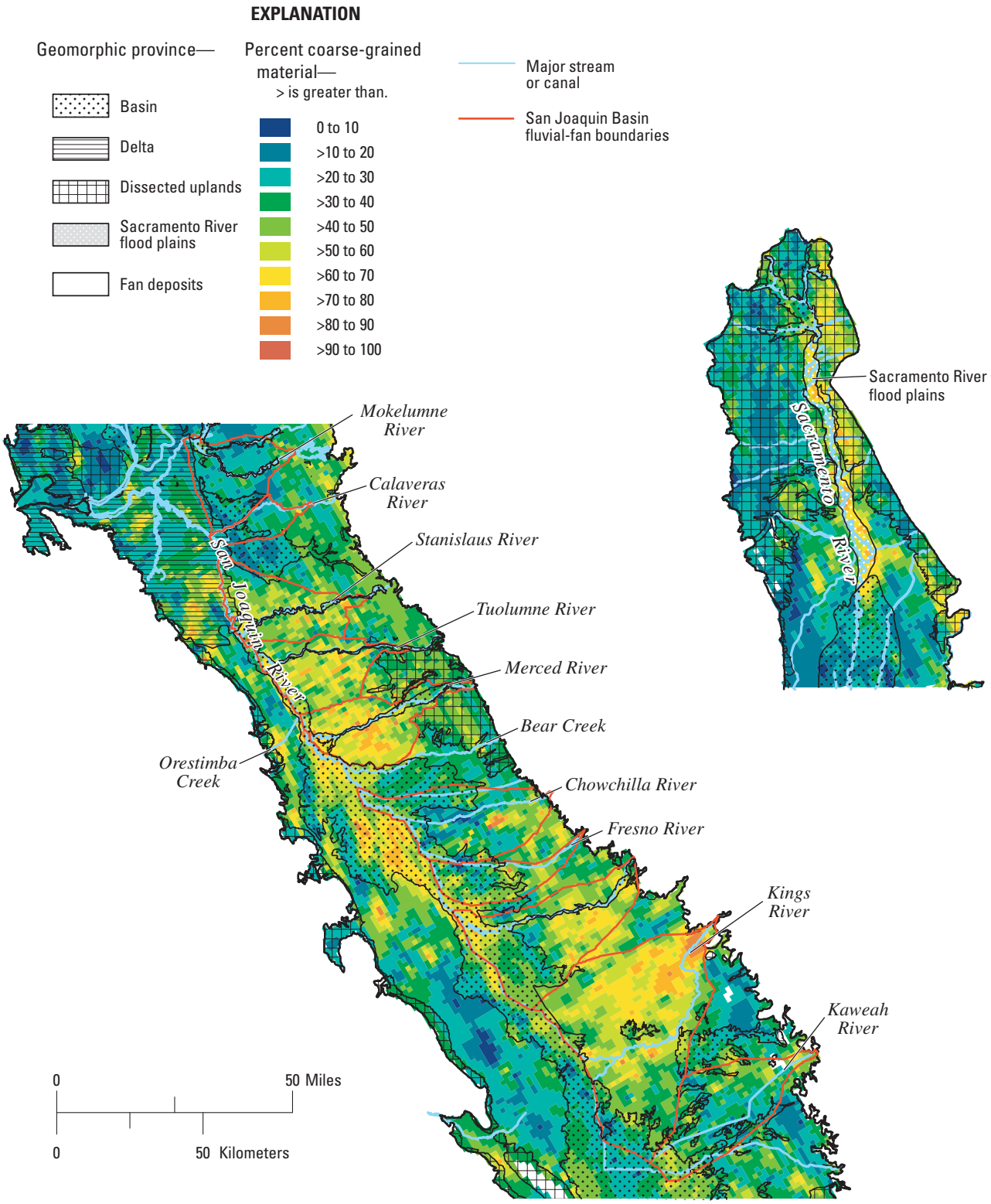

Figure A14. Distribution of coarse-grained deposits for the upper 50 feet for part of the Central Valley. The map is overlain with the major geomorphic provinces of the Central Valley and the fluvial fans of the San Joaquin Basin (modified from Davis and others, 1959; Olmstead and Davis, 1961; Jennings, 1977; and Weissmann and others, 2005).

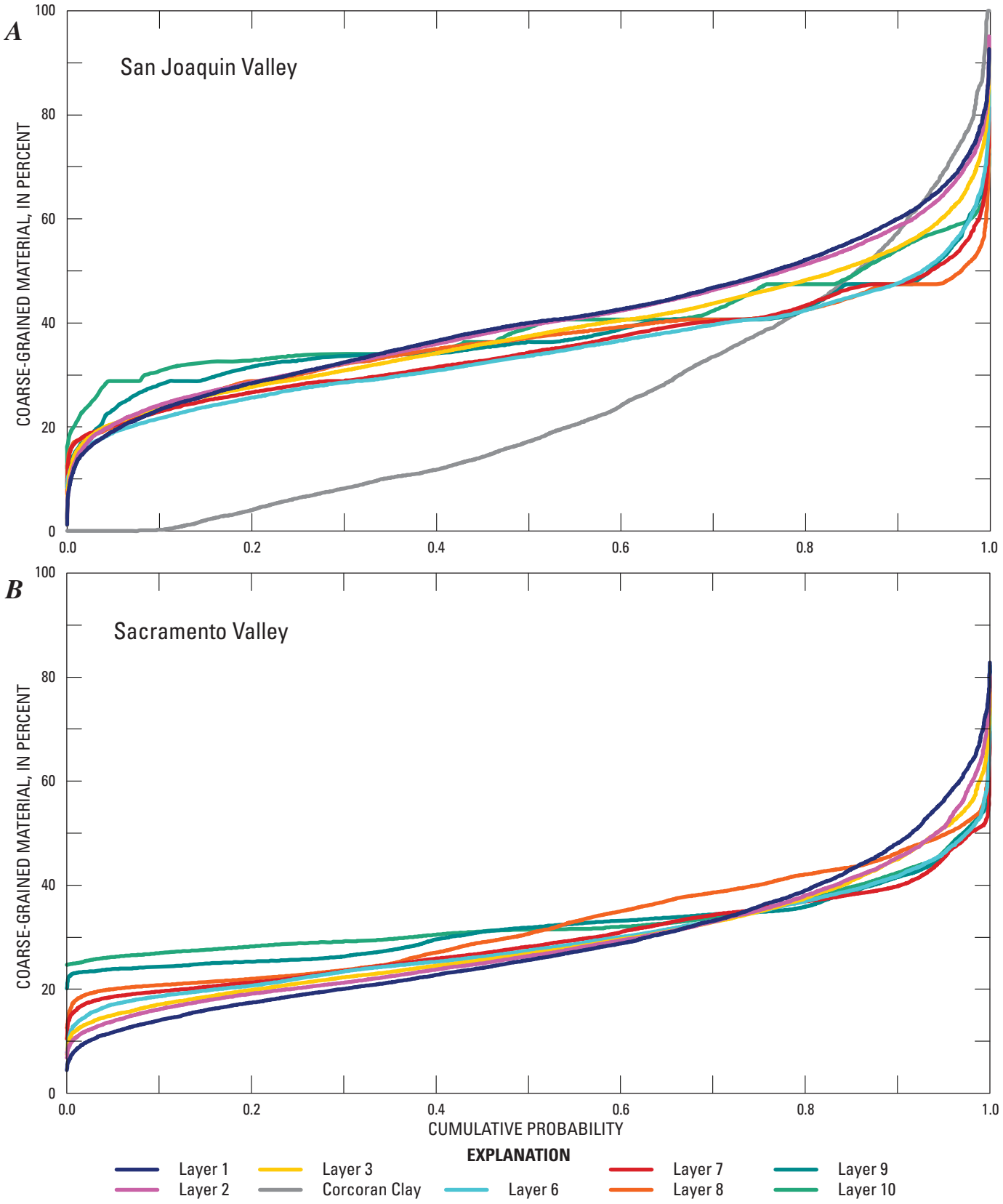

Figure A15. Cumulative distributions of kriged sediment textures for model layers in the *A*, Sacramento Valley. *B*, San Joaquin Valley and Tulare Basin.

San Joaquin Valley

Texture in the San Joaquin Valley is punctuated by the distribution of the Corcoran Clay domain. In contrast to the texture of the overlying and underlying domains (*table A2*), the Corcoran Clay domain has zones of very fine-grained texture throughout and it is the finest-grained domain (mean of 26 percent) in the San Joaquin Valley (*fig. A12C*). Despite the overall fine-grained nature of this deposit, the results of this study indicate some coarse-grained areas within areas previously defined as part of the Corcoran Clay (Page, 1986; Burow and others, 2004). These coarser areas generally occur where the Clay is thin, and partly may be an artifact of regularizing texture over the 50-foot depth intervals. Many of these thin coarser areas are found along the edges of the clay and are not laterally extensive. A more extensive coarser area is found along the northern part of the clay along the Merced River, Bear Creek, and Orestimba Creek. Adjacent to the border between the Kings and the Westside domains, the clay is particularly thin and consistently coarser grained across the clay, grading from east to west. South of the Tulare Lake bed (*fig. A12*), the clay is thin and, except for a few beds, is not very fine-grained in this model (*figs. A12C* and *A13*). In this area, it is possible that the wells penetrate the deeper Tertiary sediments. Before the Corcoran Clay was deposited, this area probably was alluvial/deltaic, as the southern seaway was open as recently as the late Pliocene, when the Coast Ranges were uplifted. As a result, the sediments are interbedded. The Pleistocene sediments may be thick here because tectonic basin subsidence, combined with the narrowness of the valley, may have forced the Kern River to deposit its sediment near the mountain front.

Below the Corcoran Clay, the mean texture is larger than that in the domain of the Corcoran Clay (*table A2* and *fig. A12D*). Except for the Westside domain, the domains below the Corcoran Clay are finer grained than the domains above. Although the area below the Tulare Lake bed usually is thought of as a clay plug, the nine wells identified in this study that extend below the base of the Corcoran Clay near the Tulare lake bed record alternating series of sands and clays (coarse and fine-grained sequences). As a result, the texture model of the lower layers (*figs. A12E* and *A13*) shows a relatively coarse-grained area in the southern part of the Central Valley.

The San Joaquin Valley, above and beyond the extent of the Corcoran Clay, is segregated laterally into three major parts: the eastern and the western parts of the San Joaquin Valley, and the southern more internally drained part of the valley. The deposits reflect the difference in source materials and surface-water influx of the Coast Ranges and the Sierra Nevada. Areas of coarse-grained texture are more widespread than the areas of fine-grained texture. The coarse-grained areas are prevalent in many of the fans in the Sierra foothills, and below the San Joaquin River channel along the axis of the valley (*figs. A12* and *A13*). Generally, the fine-grained texture zones are in the proximal interchannel and distal floodplain areas. Along the valley axis, the coarsest deposits lie west of the present-day channel of the San Joaquin River, indicating the channel may have shifted eastward.

The domains of the eastern San Joaquin Valley (Northern San Joaquin, Chowchilla–Madera, and Kings) show a different geometry and distribution of deposits. These domains generally agree with the areas mapped by Weismann and others (2005). These domains suggest a complex spatial structure that can be attributed to the effects of the east-west alignment of the tributary rivers and the fans (*fig. A14*) along the Sierra Nevada foothills, combined with the asymmetry of the north-south aligned San Joaquin River dominating the central part of the area. At least in the shallow parts of the system, the alignment of the San Joaquin River and its tributaries' channels and the physiography of the valley played an important role in the depositional history (Burow and others, 2004).

The deeper sediments may not reflect the orientation of the streams, especially in the northern San Joaquin Valley where the Tertiary sediments are much shallower. Although the depth intervals are consistent depths from the land surface, they represent potentially different depositional environments from north to south because of the differences in tectonic basin subsidence rates. For example, the coarse-grained sediments at 500 ft below land surface in the Kern Basin probably are Pleistocene sediments, whereas the sediments at 500 ft below land surface in the Modesto/Merced area probably are Tertiary in age and are more fine grained because of the difference in environment during deposition. The southern seaway also may have changed the course of the rivers, and some of them may have been oriented more north-south. During Pliocene and older ages, it is thought that the San Joaquin Valley drained to the south, thus, possibly affecting the orientation of streams and the location of fluvial/deltaic deposits in the south (Bartow, 1991).

In the northern part of the Northern San Joaquin domain, dissected uplands along the Sierra Nevada generally are fine-grained. The Calaveras River and Mokelumne River fans formed in a narrow part of the basin near the valley outlet (*fig. A14*). The Calaveras fan (*figs. A12* and *A14*) is not connected to glaciated parts of the Sierra Nevada, serving to limit the supply of readily available coarse-grained sediments (Weissmann and others, 2005). These fans exemplify these characteristics with their fine-grained texture. Conversely, as the Stanislaus and Merced Rivers leave the finer-grained, dissected uplands, the texture becomes coarser toward the valley axis at their confluences with the San Joaquin River, owing to the coarser sediments deposited by the San Joaquin River. Although these rivers connect to glaciated parts of the Sierra Nevada (like the very coarse-grained Kings River fan to the south), their relatively smaller drainage basins are at lower elevations and their outlets have a lower subsidence rate (Weissmann and others, 2005). Similarly, the Tuolumne River drainage basin is about the same size and elevation as that of the Kings River; however, its outlet has a lower subsidence rate. As expected, the Stanislaus, Merced, and Tuolumne River fans are moderately coarse-grained, but not as coarse-grained as the

Kings River fan. In addition, areas south of each of these three present-day channels are coarser grained, possibly indicating that the rivers have migrated north. In the southern-most part of the Northern San Joaquin domain (the Merced Basin south of Bear Creek), the basin geomorphic province reaches farther east, and this correlates with the extent of the finer-grained deposits mapped using the texture model (*fig. A14*).

The Chowchilla–Madera domain, dominated by the Chowchilla River fan and Fresno River fan (*figs. A12* and *A14*), generally is fine-grained. These fans have drainage basins that tap only non-glaciated parts of the Sierra Nevada (Weissmann and others, 2005). These fans did not experience large changes in the supply of sediment to the drainage basin, relative to the amount of water discharging from the basin (Weissmann and others, 2005); therefore, they did not develop the deep incised valleys, and they appear to have relatively moderate grain sizes throughout their extent. As expected, visually there is a correlation between the extent of the basin geomorphic province in this domain and the finer-grained texture (*fig. A14*).

The Kings domain, dominated by the San Joaquin River fan and Kings River fan, are much coarser grained than the alluvial fans to the north (*figs. A12A* and *A14*). Both fans are connected to glaciated parts of the Sierra Nevada. These glaciated sections provide an abundance of coarse-grained sediments to the basin. The San Joaquin River fan is similar in character to the Tuolumne River fan. It was developed in an area having relatively low subsidence rates, has a deep modern incised valley, and connects to the axial San Joaquin River (Weissmann and others, 2005). As a result, it is relatively coarse-grained, particularly near the river channel and its apex. It is finer grained in the basin geomorphic province outside the active channel to the southwest. The Kings River fan is an example of fan development in a part of the valley that is wide and has high subsidence rates (Weissmann and others, 2005). As a result, this fan has relatively thick deposits with vertical stacking and is one of the coarsest-grained areas in the Central Valley, particularly near its apex.

The texture data in layers 2 and 3 show coarse-grained deposits, some greater than 70 percent coarse, north of the present day Kings River and south of the current San Joaquin River (*figs. A12B*, *A14*, and *A15*), indicating that these rivers may have changed their course, migrating to the south and north, respectively. In contrast to the Kings River fan, the Kaweah River fan, which drains into the subsided area of the Tulare Lake Basin, generally is fine grained (*fig. A5A*); both fans have some coarse-grained deposits near their respective apex. This finer-grained nature may be related to the fact that the Kaweah River fan has a significantly smaller drainage basin with a lower contributing basin elevation. In addition, although its drainage basin was glaciated, it never had a large trunk glacier like the Kern, Kings, San Joaquin, Merced, and Tuolumne drainage basins (Matthes, 1960); rather, it had a series of separate, small glacial systems in tributary streams.

The Tulare/Kern domains are surrounded on three sides by mountains, and are drained internally. Most of the southern parts of the Tulare/Kern domains show a predominance of coarse-grained areas in the upper seven layers of the model (*figs. A12*, *A13,* and *A15*). The Tulare Lake bed in the northwestern part of the domain above and within the Corcoran Clay is predominantly fine-grained (*figs. A12A–C* and *A13*).

The domains in the western San Joaquin Valley (Tracy/Delta-Mendota and Westside regions) are relatively fine-grained (*fig. A12*). This is especially true in comparison to the eastern San Joaquin Valley and the Tulare/Kern domains. These finer textures reflect the source material: shales and marine deposits in the Coast Ranges. These rocks usually yield finer-grained sediments than the granitic rocks that are the sediment source for the fans on the eastern side of the Valley. The Westside domains, both above and beyond the extent of the Corcoran Clay, and the northern part of the Tulare/Kern domains are especially fine-grained. Except for the Corcoran Clay and the area around the Delta, the Westside domains are among the finest-grained areas in the Central Valley. This finer-grained nature may be attributed to flashy, debris flow fan type deposits from small drainage basins characteristic of this part of the Central Valley and (or) the fact that the area is internally drained with no outlet for exporting the finer-grained deposits (*fig. A14*). It is interesting to note that this area has more tile drains than any other area in the Central Valley. In addition, this area has the largest amount of pumping-induced subsidence recorded in the valley.

Despite this predominance of fine-grained deposits, coarse textures are found in the Westside and Tracy/Delta–Mendota spatial provinces. The western edge of these regions are coarser grained along the alluvial fans of the Coast Range, and coarse deposits are evident below a depth of 50 ft (*fig. A12B*) beneath land surface along the San Joaquin River. These coarser deposits correspond to the area identified by Laudon and Belitz (1991) as the Sierran Sands. Above the Corcoran Clay, the Tracy/Delta–Mendota domain generally is fine grained near the Delta and gets coarser to the southeast, particularly along the San Joaquin River. Similar trends continue farther below the land surface until an abrupt break at the Corcoran Clay.

Hydrologic System

The hydrologic system of the Central Valley comprises three principal components that govern the storage of water and affect its availability: the snowpack of the Sierra Nevada; an extensive system of rivers, streams, dams, lakes, and other storage and conveyance systems for surface water; and finally, the aquifer system that stores and conveys groundwater. Water is stored as snow generally accumulates in the Sierra Nevada during the late fall and winter and releases as snow melts during late winter, spring, and early summer. About 78 percent of the total unimpaired streamflow occurs from January through June (Williamson and others, 1989). During the past 100 years, much of this surface-water flow has been controlled by dams at the base of reservoirs (*fig. A12*). These dams capture

and store the surface water entering the Central Valley for use during the dry season.

Below these dams, a complex network of streams and canals distributes the water throughout the valley. Within the Central Valley, there are approximately 160 streams or rivers totaling 1,512 mi in length and 6,291 constructed agricultural channels with a total length of 19,812 mi (California Regional Water Quality Control Board, 1992). This network of streams and canals delivers surface water to Federal, State, local, and private water users. The water storage and delivery infrastructure —dams and canals—have been designed largely on the basis of the historical snowpack. A brief discussion of the surface-water system is presented in this section. *Chapter B* discusses this complex surface-water network in more detail.

Water supplied from aquifers is a less formal and less recognized contribution to California's water supply (California Department of Water Resources, 1998). Although some groundwater is used even when surface water is available, because groundwater generally is more expensive than surface water, it usually is used when surface water is not available. An overview of the groundwater system is presented in this section. The spatial and temporal patterns of groundwater development are discussed in more detail in *Chapter B*.

Climate variability affects the volume, and spatial and temporal distribution, of surface water as well as the potential recharge to, storage within, and increased discharge from the groundwater system. Climate variability also may affect the timing of snow melt, runoff, and other components of the Central Valley hydrologic system, including those associated with possibly prolonged growing seasons.

Climate

Climate affects each of the three principal components that govern the storage of water and affect its availability. Climate encompasses the temperatures, humidity, rainfall, and numerous other meteorological factors in a given region over long periods of time. The climate of a location is affected by its latitude, terrain, persistent snow cover, as well as nearby oceans and their currents. Hence, climate varies spatially and temporally. In the Central Valley, climate varies spatially from north to south as well as from east to west. Regional-scale topography is the major influence on precipitation. The source of precipitation to the Central Valley and adjacent mountain ranges is moist air masses that are swept inland from the Pacific Ocean on the prevailing westerlies as winter storm fronts. The mountain ranges cause orographic lifting of the moist air masses, which causes cooling, condensation, and precipitation—predominantly on the western slopes—and leaves a rain shadow on most eastern slopes. Accordingly, the eastern slopes of the Coast Ranges and the valley floor are in the rain shadow of the Coast Ranges, and heavy precipitation falls on the western slopes of the Sierra Nevada. This precipitation, occurring both as rainfall and snowfall on the Sierra Nevada, is the major source of water entering the valley (*fig. A16*). In particular, in most years the storms leave large accumulations of snow in the Sierra Nevada during the winter months.

The climate variability of moisture from the North Pacific, where the winter frontal storms originate, is reflected in the index known as the Pacific Decadal Oscillation (PDO) (Mantua and others, 1997; Mantua, 2006). Subtropical moisture from El Nino-Southern Oscillation (ENSO) events and monsoonal moisture from the North American monsoon system (NAMS) affect climate in the western United States (Hanson and others, 2006), and may affect climate in the Central Valley.

There also is a distinct variation in precipitation, volume of snowpack, and timing of snow melt from north to south. In terms of surface-water supply, the Central Valley is geographically dichotomous, with a surplus of water in the northern part of the valley and a deficit in the southern part of the valley. The northern half of the Central Valley (the Sacramento Valley) has more precipitation than the drier San Joaquin Valley (*fig. A5A*). Streamflow from the major drainages entering the valley reflect this dichotomy (*figs. A5* and *A16*). The Sacramento River drainage basin, which encompasses and feeds the Sacramento River, supplies approximately two-thirds of the surface water to the Central Valley. In contrast, the larger San Joaquin River drainage basin only contributes about one-third of the surface water (*fig. A16C*). Under the current climatic regime, streamflow from the major drainages entering the valley largely is a result of the melting of snowpack.

Recent studies indicate that the relative amounts and timing of precipitation and inflow from drainages entering the Central Valley are changing (Dettinger, 2005; Dettinger and Earman, 2007). Long-term trends in regional climate can be identified from a graph of the cumulative departure from the average precipitation (*fig. A17*). Wet periods represent the positively sloped limbs and the dry periods represent the negatively sloped limbs of the cumulative departure curve, respectively.

The cumulative departure graphs show wetter-than-median periods and drier-than-median periods since the late 1800s at several stations throughout the Central Valley. The precipitation at the various stations over the past several decades exhibit similar patterns throughout the valley (*fig. A17*). Based on these cumulative departures, wet and dry periods were defined (*fig. A17*). Even though there are many exceptions, the wet and dry periods generally are aligned with the variations in the cycles of the PDO index (*fig. A17*). Because annual precipitation in the San Joaquin Valley is much less than in the Sacramento Valley, the magnitude of the departure is less in the south (*figs. A16* and *A17*). Although somewhat masked by human activities, variations in stream flow at gages for water years 1962–2003 (*fig. A16A*) also demonstrate these wet and dry cycles.

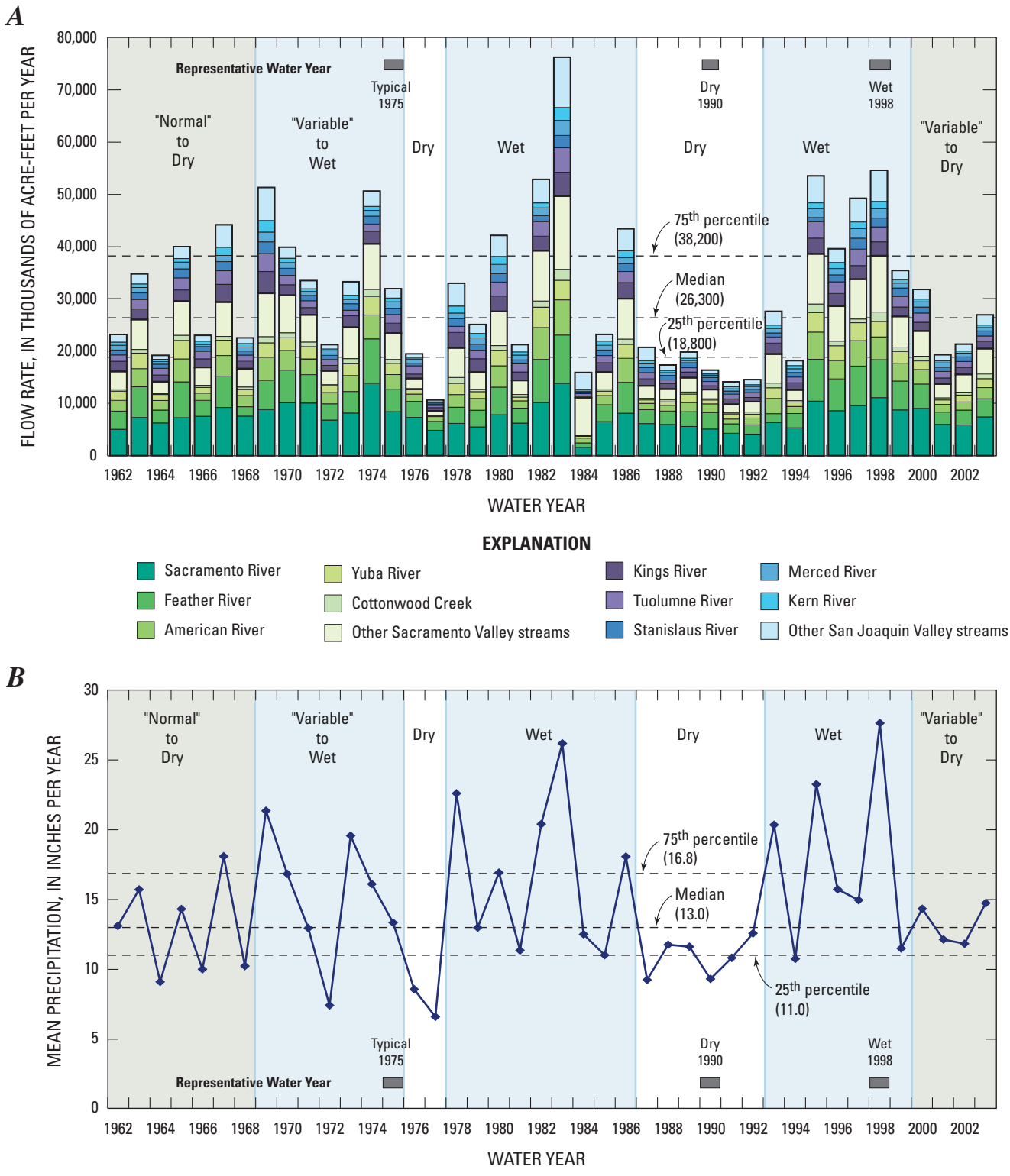

Figure A16. *A,* Total inflow from 44 gaged streams flowing into the Central Valley, California, water years 1962–2003. *B,* Average annual precipitation in the Central Valley, California, water years 1962–2003. *C*, Total surface-water flow into the Central Valley, California, water years 1962–2003.

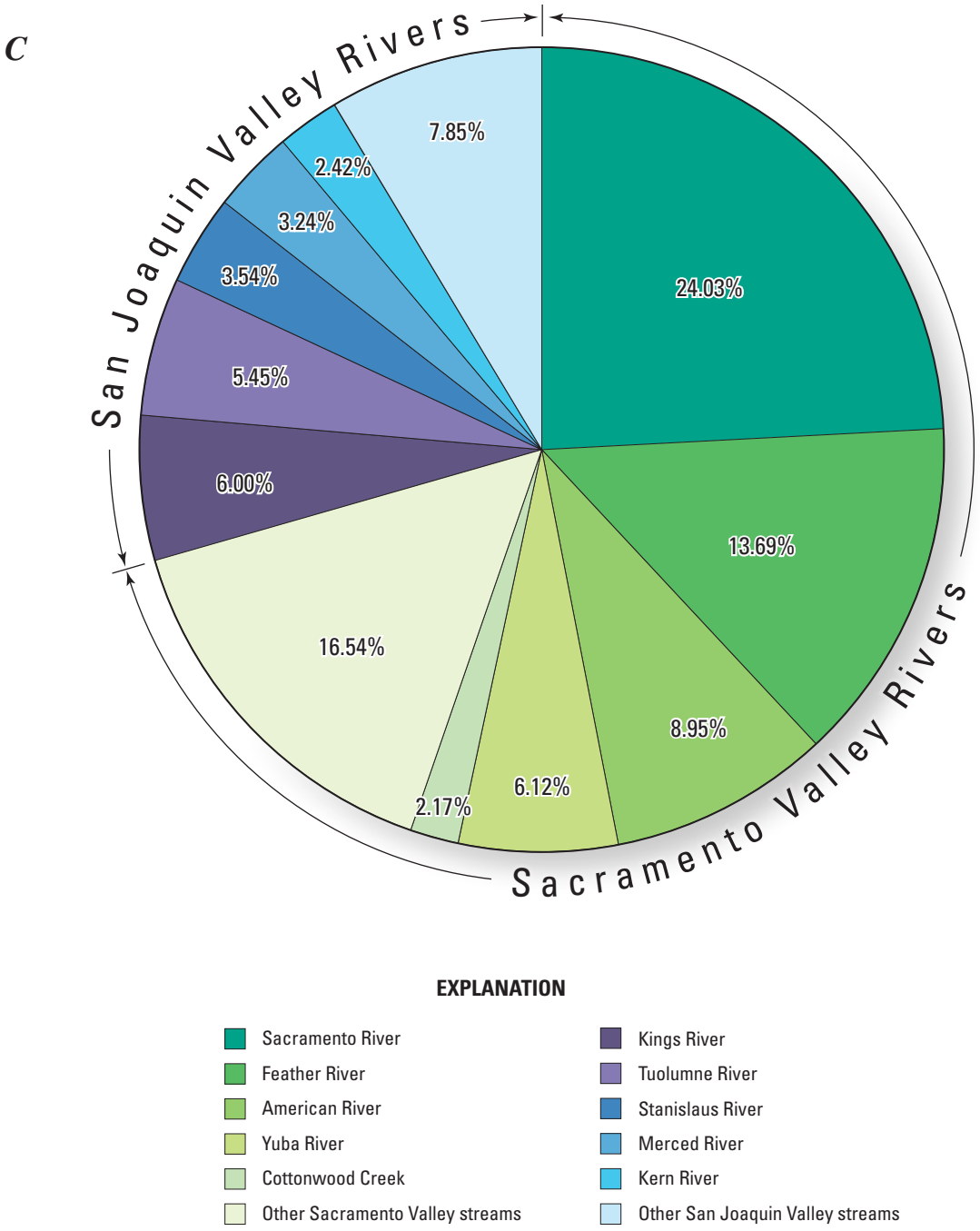

Figure A16. Continued.

Between 1875 and 2005, seven predominantly wet periods and six predominantly dry periods were identified. The cumulative departures from average shown in *figure A17* suggest that most areas have been subject to a precipitation deficit since the 1930s. This deficit grew during the 1950s and 1960s, and, with the exception of Red Bluff, underwent a gradual recovery thereafter. Most areas show trends of significant recovery in the 1990s. During the second half of the 20th century, California experienced multiyear droughts during 1959–61, 1976–77, and 1987–92 (California Department of Water Resources, 1998). These droughts are represented by the periods labeled "Dry" or "Variable to Dry" in *figure A17*.

There are some notable spatial differences in the cumulative departure of precipitation. For example, the southern part of the valley (Bakersfield station) shows an increase in precipitation from about 1935 to 2005, whereas the northern part of the valley (Red Bluff station) shows a dramatic decrease between 1945 and the early 1990s. However, other than during the 1987–92 drought, the pattern for all stations from the early 1980s to the present is characterized by above-average precipitation.

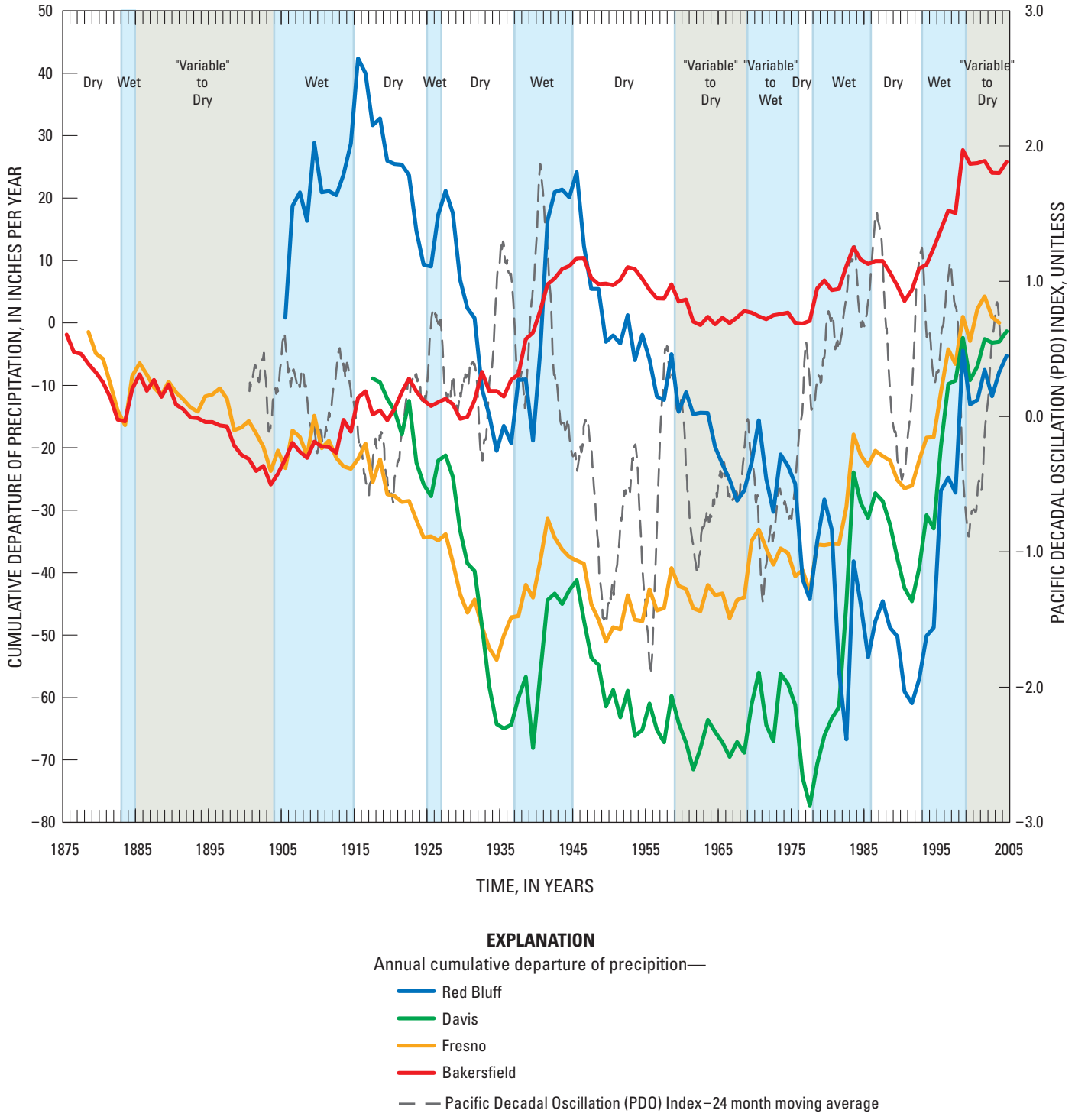

Figure A17. Cumulative departure from average annual precipitation at Redding, Davis, Fresno, and Bakersfield, California. For reference, a 24-month moving average of the Pacific Decadal Oscillation Index is also plotted.

This study focuses on water years 1962 through 2003 (*figs. A16* and *A18*). The first part of this period, 1962–77, is part of a cooler and drier (negative) PDO period, whereas the period 1978–2003 is warmer and wetter. The southern part of the valley shows smaller changes in average monthly precipitation, and all stations show small increases in summer precipitation that, nevertheless, are greatly exceeded by evapotranspiration (ET) (*figs. A5* and *A6*).

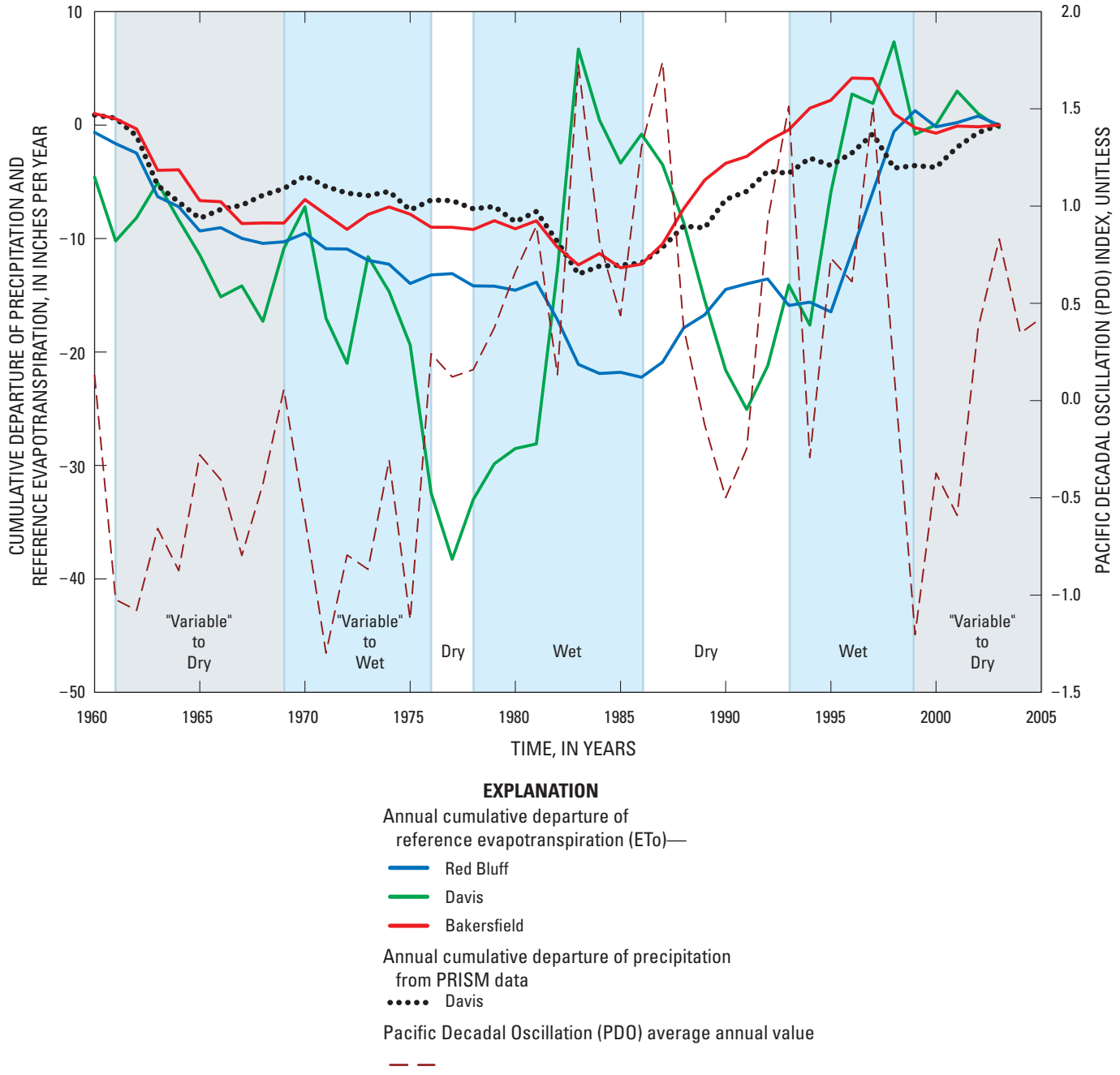

Figure A18. Cumulative departure of monthly precipitation (Parameter-elevation Regressions on Independent Slopes Model (PRISM) data from Davis, California), cumulative departure of the Pacific Decadal Oscillation (PDO) index, and cumulative departure of the monthly reference evapotranspiration (ETo) values (gridded values of California Irrigation Management Information System's (CIMIS) stations from Redding, Davis, and Bakersfield, 1960–2004).

ET, like precipitation and runoff, is affected by climate variability (*fig. A18*) and is directly dependent on a combination of temperature, wind, relative humidity, and net radiation. During periods of high cloudiness, ET is reduced. The PDO and the position and strength of the California Pressure Anomaly and the North Pacific High (and related Hadley cell) affect ET (Hidalgo and others, 2005). The cumulative departure curves for ET show less variation than precipitation (*fig. A18*). For example, the interannual and interdecadal cycles of ET generally are in opposite phase with the precipitation and PDO cycles. However, three Central Valley stations show less similarity in interannual cycles of ET since the end of the previous drought in 1992 (*fig. A18*) and are intermittently in phase with PDO cycles, which may suggest that other climate forcings, such as climate change as well as other climate cycles (for example, ENSO and NAMS), may be contributing to these

relations. Although generally showing similar trends, ET also has different magnitudes and patterns over the different areas of the Central Valley.

Surface Water

Streamflow is a critically important factor in the water supply of the Central Valley. The streamflow and reservoir storage almost entirely are dependent on precipitation and snowmelt in the Sierra Nevada and part of the Klamath Mountains in the north. Few perennial streams of any significant size enter the valley from the west. Snowpack and resulting surface-water flow in the northern part of the Central Valley is much greater than that in the southern part of the valley (*fig. A16*). Almost three-quarters of the inflow to the Central Valley is from the Sacramento River drainage basin, and more than three-quarters of this flow is from four rivers: Sacramento, Feather, American, and Yuba Rivers (*fig. A16C*). North of the Central Valley, the Sacramento River has its headwaters in the Trinity Mountains west of Mount Shasta, and a large quantity of flow is contributed to the Sacramento River from the Pit River. Several other large streams with steep gradients flow westward from the Sierra Nevada and join these rivers close to the axis of the Central Valley. Flows in the Sierran streams are seasonally variable, with high flows coinciding with the snowmelt that comes in the late spring. Many of these streams have been dammed, and outflows are stored for release as irrigation water, power generation, and urban supply along the Central Valley's vast natural and man-made surface-water system. Flows generally are intermittent in the smaller streams that drain eastward from the Coast Ranges.

Rivers feeding the San Joaquin River drainage basin are much smaller (*fig. A16C*). The Kings, Tuolumne, Stanislaus, Merced, Kern, and Mokelumne Rivers make up three quarters of the volume of water entering this drainage basin. The San Joaquin River has its headwaters in the Sierra Nevada. Prior to development of agriculture, flow in the San Joaquin River was sustained entirely from runoff from the western slope of the Sierra Nevada. Flow in the river is sustained by a combination of Sierra runoff, releases from upstream dams, and agricultural wastewater derived from drained fields that use irrigation water imported from outside the San Joaquin drainage area. Flows generally are intermittent in the streams that drain eastward from the Coast Ranges and typically do not reach the San Joaquin River. In the southern part of the valley, the Kings, Kaweah, Tule, and Kern Rivers flow into the internally drained Tulare Basin. Before development, flow was seasonally variable and spring runoff often would accumulate in Tulare Lake. Presently, the flows from these rivers are controlled by dams and have been redirected to various parts of the Central Valley and elsewhere in the State of California.

Streamflow in the Central Valley is highly variable. The median flow for water years 1962–2003 was 28.9 million acre-ft/yr (*fig. A16A*). The highest flow, 78 million acre-ft, was in1983. The highest combined flows coincided with the one of the highest average annual precipitation rates for the Central Valley (*fig. A16B*). Conversely, 1977 was a dramatically low-flow year with about one-third the median flow, 10 million acre-ft. The low flow in 1977 followed two consecutive years of drought. The total annual flow was within 10 percent of the median annual flow of these streams only for 8 years during 1961–2003 (*fig. A16A*).

The variation in precipitation from north to south produces differences in the timing of runoff in the two valleys. Peak runoff in the Sacramento Valley generally lags peak precipitation in the surrounding mountains by 1–2 months, whereas peak runoff in the San Joaquin Valley generally lags peak precipitation by 5 months (Williamson and others, 1989; Bertoldi and others, 1991). As a consequence of the geographic, seasonal, and climatic variations, the Sacramento Valley frequently floods, whereas rivers in the San Joaquin Valley alternately flood or have abnormally low flows during droughts (Bureau of Reclamation, 1994).

Streamflow in the Central Valley is influenced by variability in climate (Meko and Woodhouse, 2005) (*fig. A16A*). The cumulative departure of streamflow diversions from the Bear River shows consistency with wet/dry cycles (*fig. A19*). For example, there are larger streamflow diversions during wet years. It also shows a general alignment with the PDO climate index (Mantua and Steven, 2002) cycles. Interestingly, from 1968 to 1986 there is an increase in diversions and the PDO index. Between 1968 and 1975 there is a steady increase in diversions and the PDO index. During the drought in 1976–77, however, there is a sudden decline in diversions that is not reflected in the PDO index. After this short drought, the pattern of steady increase in diversions continues until the next drought begins in 1987. As with the previous drought, diversions from Bear River generally decrease during the 1987–92 drought. The first few years of this drought also are accompanied by a decrease in the PDO index. During the period 1960–92, changes in diversions generally lagged behind the PDO index by about 5 years (correlation of 0.45). Throughout the 1987–92 drought, there appears to be a systematic and sustained decrease in diversions that persisted for a couple years into the following wet period.

In contrast, since the 1987–92 drought, the demand for streamflow diversion appears to be inversely correlated with the cycles in the PDO index. After 1999, the streamflow diversion appears to become more inversely correlated with the PDO index and annual temperature differences. One interpretation of these data is that demand for surface water is constrained partly by climate as availability of surface water, but also is controlled by other factors. These factors may include agriculture growth, markets, changing crop types, and inter-annual variation in ET.

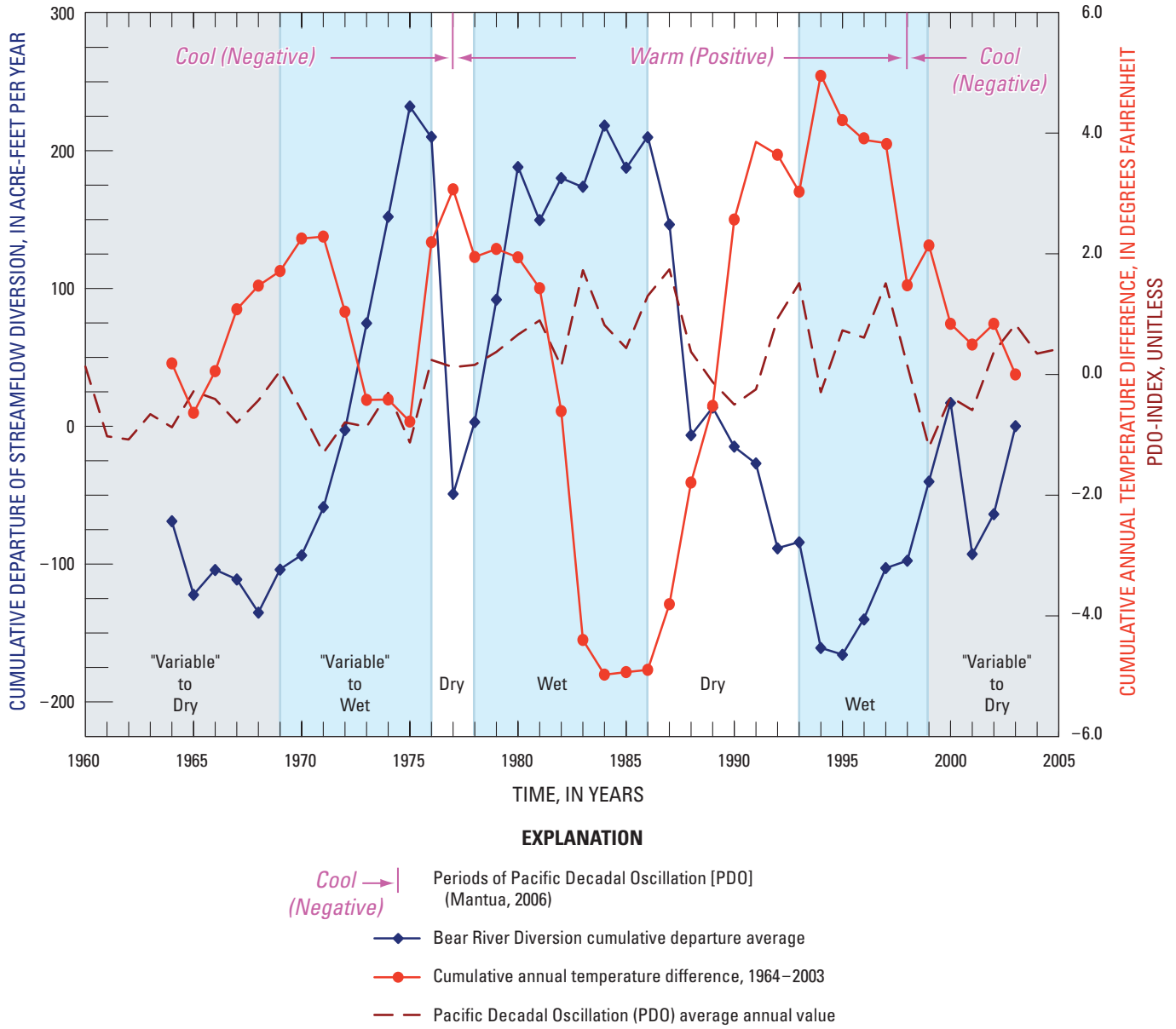

Figure A19. Cumulative departure of streamflow diversions from the Bear River by South Sutter Water District, California; cumulative annual temperature from California Irrigation Management Information System's (CIMIS) stations at Davis and the Pacific Decadal Oscillation (PDO) index, 1960–2004.

The timing and magnitude of precipitation and streamflow directly affects the availability and use of surface water for agriculture and the environment. Heavy winter and spring runoff do not correspond to the period of peak agricultural and urban water demand, which occurs in the summer. To ameliorate timing and distribution of surface-water supplies, California has developed and maintained a complex surface-water storage and distribution network (*fig. A7*). In addition, this distribution network is used for flood control, recreation, and regulating environmental flows.

Groundwater

Groundwater often is a more dependable source of water than surface water because of the high temporal and spatial variability associated with precipitation, runoff, and surface-water availability in the Central Valley. The principal sources of water to the present-day groundwater system are recharge from precipitation, leakage from streams and surface-water bodies, and return flow from irrigated agriculture (which currently is the vastly dominant source of recharge in the southern half of the valley, as discussed in this section).

Predevelopment Recharge, Discharge, Water Levels, and Flows

Prior to development, groundwater in both the confined and unconfined aquifers of the aquifer system generally moved from recharge areas in the upland areas surrounding the Central Valley toward discharge areas in the lowlands along the valleys axes and the Delta (Davis and others, 1959; Olmstead and Davis, 1961) (*figs. A1* and *A20*). Groundwater-flowed largely toward the Sacramento or San Joaquin Rivers or Tulare Lake. Areal recharge from precipitation provided about 75 percent of recharge, and seepage from stream channels provided the remaining recharge (Williamson and others, 1989). The eastern-valley streams carrying runoff from the Sierra Nevada and the Klamath Mountains provided the bulk of the recharge derived from streams (Bertoldi and others, 1991). Most of this occurred as mountain-front recharge in the coarse-grained upper alluvial fans where streams enter the basin.

Groundwater discharge occurred primarily through ET from marshes along the trough of the valley and through upward leakage to streams flowing toward the Delta (Williamson and others, 1989). The marshy discharge areas comprised wetland and riparian vegetation and intermittent lakes and sloughs. These areas generally corresponded with the areas of flowing, artesian wells mapped prior to 1900 along the valley trough (Hall, 1889; Mendenhall and others, 1916). These flowing wells and marshy discharge areas indicate that groundwater-flow was upward in the central part of the valley.

In the Tulare Basin, groundwater was discharged directly to Tulare Lake and through ET to the riparian areas surrounding the lake (*fig. A21*). Groundwater also discharged through ET prior to natural vegetation, including a mix of valley and foothill hardwoods in the Sacramento Valley, grasslands throughout the lower parts of the valley floor, and alkali desert scrub and chaparral in the San Joaquin and Tulare Basins (California State University, Chico, 2003) (*fig. A21*). Other than by ET, the Delta is the only outlet for natural discharge of surface or groundwater (Bertoldi and others, 1991, p. 17) (*fig. A21*). Direct groundwater outflow to the Delta is thought to have been negligible (Galloway and Riley, 1999).

Groundwater/Surface-Water Interaction

Under natural conditions, water flowed between the groundwater-flow system and the stream network within the Central Valley. Despite the fact that current surface-water flows are partly controlled by releases from dams, the surface-water system in the Central Valley still exchanges water with the groundwater system through gaining and losing sections of the streambed. Mullen and Nady (1985) quantified streamflow gains and losses of stream reaches throughout the Central Valley. The average results of their analyses are plotted in *figure A22*. As the streams flow into the valleys, much of the water percolates into the ground. Diverting streamflows to irrigation and lowering groundwater levels by pumping reduces the low summer flows of the streams. In the Sacramento Valley, streams issuing from the Coast Range generally are losing (Mullen and Nady, 1985). Conversely, the Feather River issuing from the Sierra Nevada generally is gaining, especially in the lower reaches. In the upper reaches, the streambed changes from gaining to losing based on climatic conditions. Further to the south, the American, Mokelumne, and lower reaches of the Calaveras Rivers all appear to be losing streams. The upper reaches of the streams appear to fluctuate between gaining and losing streams depending on the amount of flow coming out of the Sierra Nevada that year. In the northern parts of the San Joaquin Valley, Mullen and Nady (1985) show that the Stanislaus, Tuolumne, and Merced Rivers generally are gaining streams. More recent work by Phillips and others (2007) shows that these streams are losing in their upper and middle reaches and are becoming gaining streams in their lower reaches about two-thirds of the way toward the valley trough. The San Joaquin River north of Deadman's Creek along the valley trough generally is an area of groundwater discharge (gaining stream) and the river receives water from the aquifer system over most of its length. In the lower reaches such as this, streamflow entering the channel as groundwater discharge (base flow) generally is the primary component of streamflow; however, streamflow may be augmented by surface-water runoff during heavy precipitation events and irrigation return flows from agriculture. Conversely, Mullen and Nady (1985) found that streams issuing from the southern part of the Sierra Nevada and the Coast Ranges into the Tulare Basin generally are losing streams, particularly in the coarse-grained sediments adjacent to the mountain fronts (*fig. A22*).

Aquifer-System Storage

The quantity of groundwater in storage has been estimated by several investigators (Davis and others, 1959; Olmsted and Davis, 1961; Williamson and others, 1989). Williamson and others (1989) estimated the amount of water in storage from a study of several thousand well logs in which values of specific yield were assigned to depth intervals according to texture, as mapped by Page (1986). Approximately 800 million acre-ft of freshwater is reported to be stored in the upper 1,000 ft of sediments in the Central Valley (Bertoldi and others, 1991, p. 27). As has been pointed out by many investigators and most recently by Alley (2006, 2007), numbers such as these, although calculable, are impractical and likely misleading. Much of the water in storage cannot be extracted without serious consequences. Therefore, this type of calculation of volume of water in storage was not updated in this study. However, to address groundwater sustainability, the general magnitude of this number is discussed later in this report.

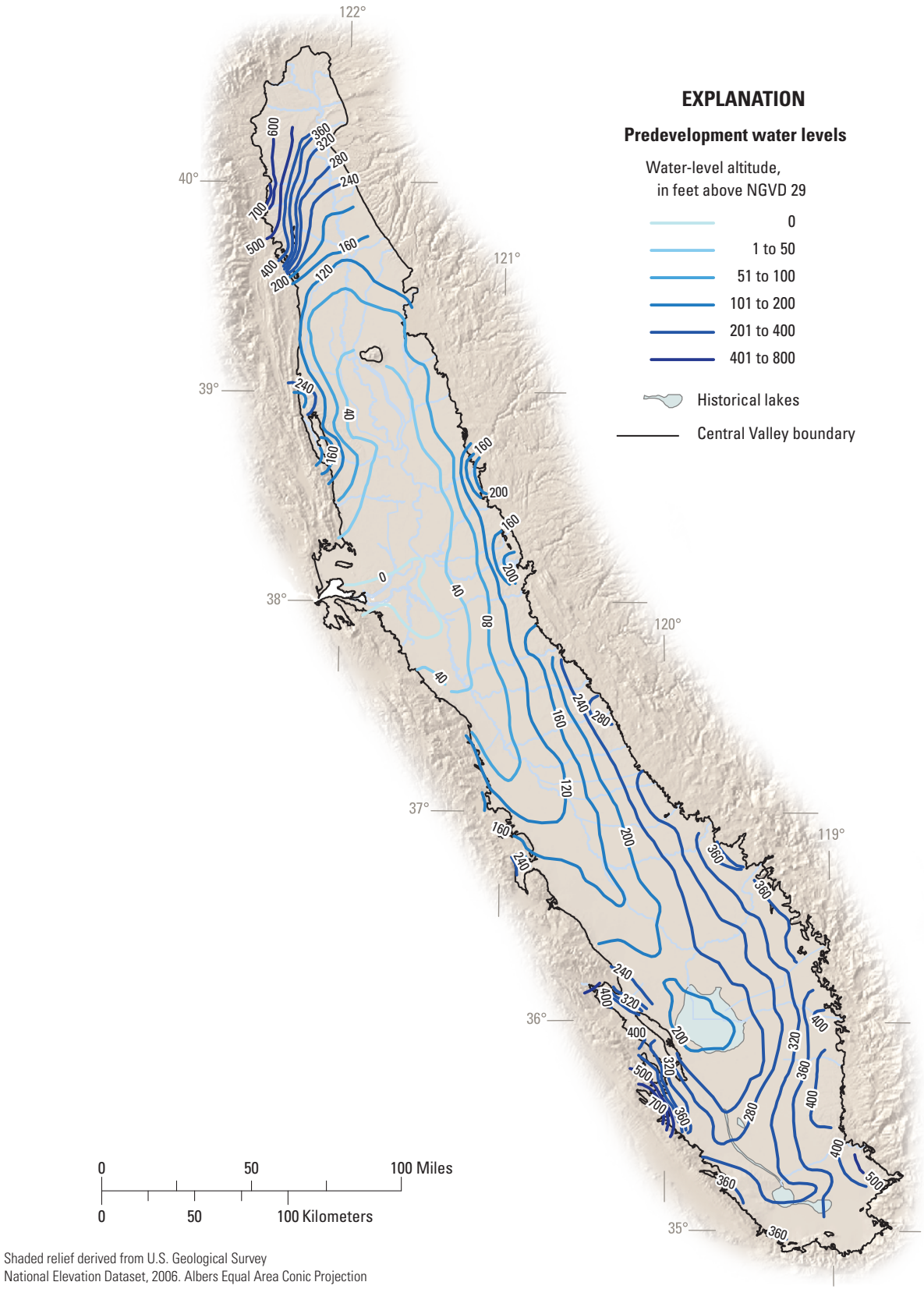

Figure A20. Pre-development groundwater map (modified from Williamson and others, 1989).

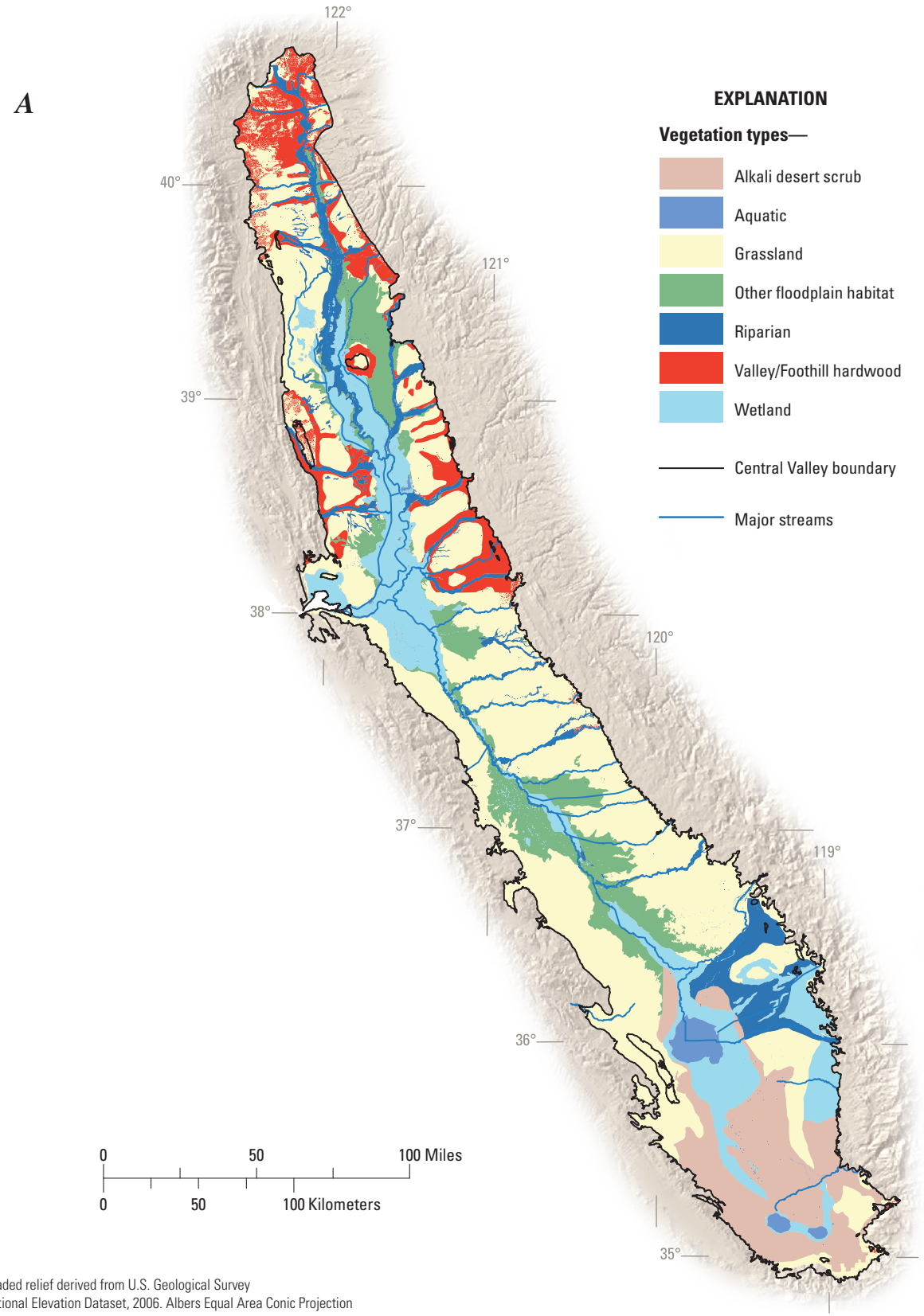

Figure A21. Distribution of *A,* Pre-1900 land-use patterns (modified from California State University, Chico, 2003), *B*, land-use patterns in 2000 (California Department of Water Resources, 2000) for the Central Valley, California.

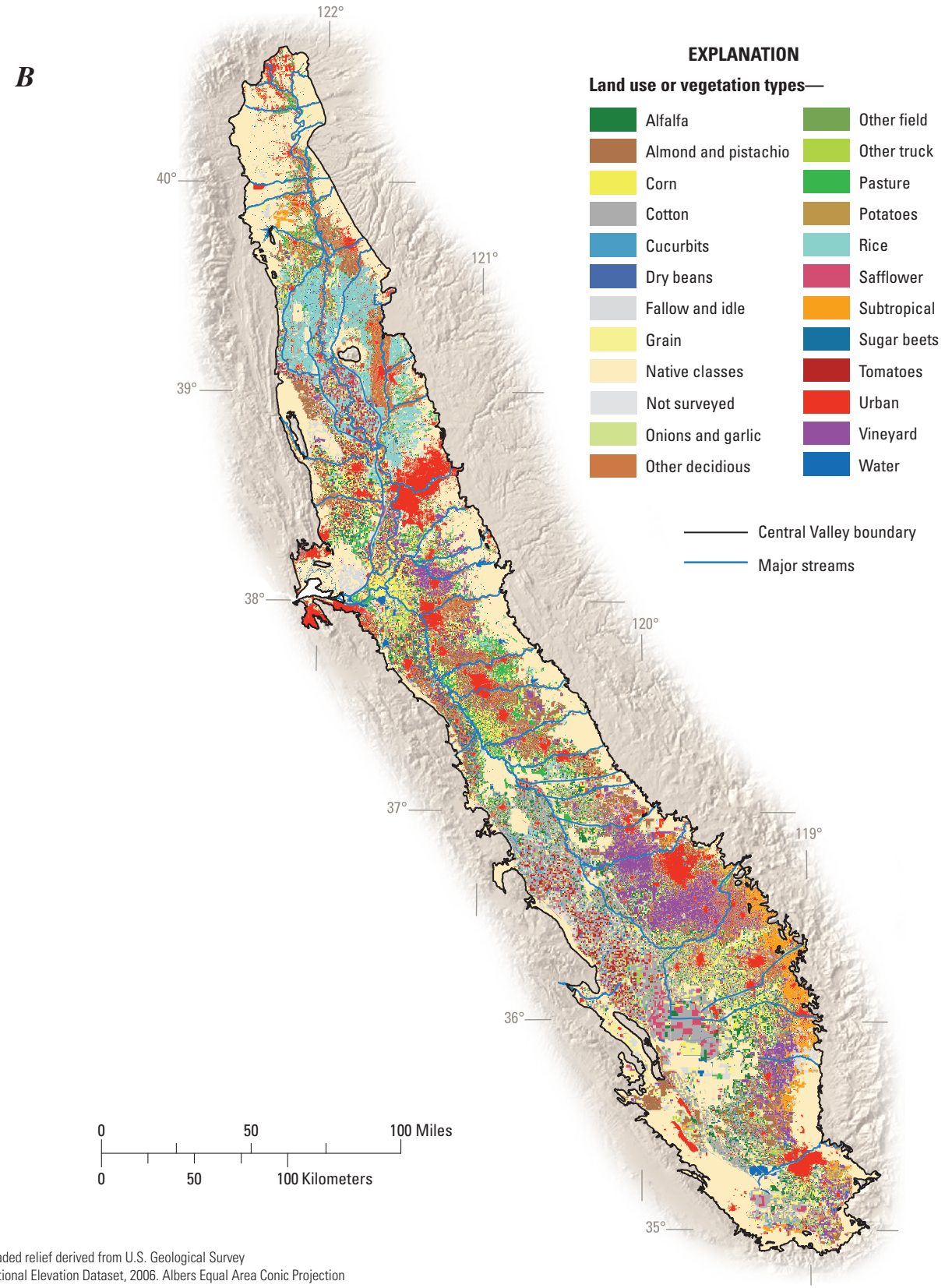

Figure A21. Continued.

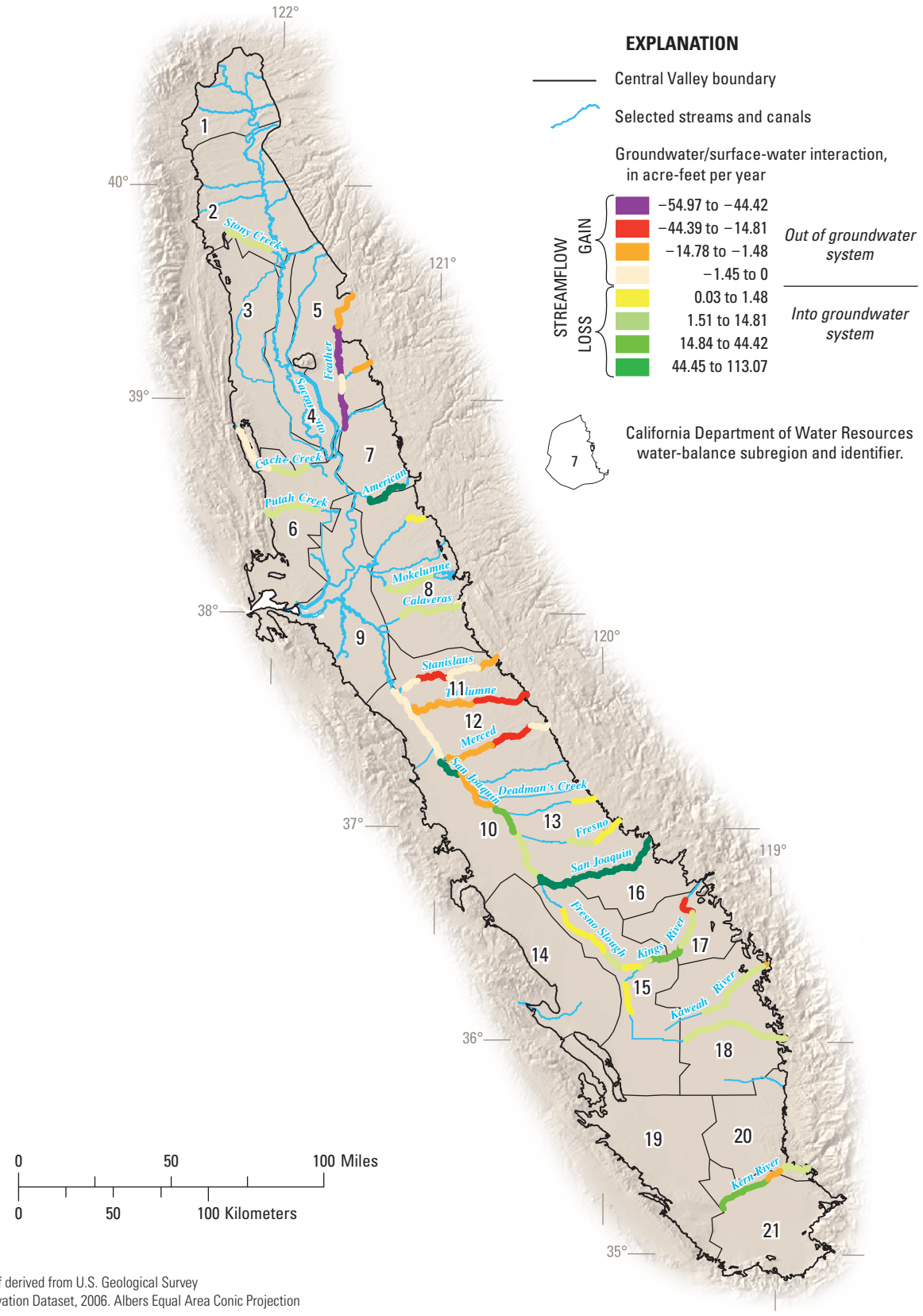

Figure A22. Distribution of selected streams and canals, and average estimated gains and losses for selected segments (Mullen and Nady, 1985).

Water Budget

Water development for irrigation has had a pronounced effect on the hydrologic budget of the Central Valley. The development of surface-water and groundwater resources in support of agriculture has fundamentally altered the recharge and discharge components of the Valley's water budget. *Chapter B* discusses the post-development hydrologic budget. Williamson and others (1989) developed a pre-development groundwater budget for the Central Valley that inherently accounts for the relation between the surface-water and groundwater systems. This budget is summarized here and in *figure A23*. During predevelopment conditions, the recharge and discharge of groundwater was about 1.5 million acre-ft per year (*fig. A23*). As described earlier, groundwater was recharged by infiltration from precipitation and surface-water leakage. Precipitation averaged about 12.4 million acre-ft per year. On average, an estimated 10.9 million acre-ft of this water directly evapotranspired before reaching the groundwater system (Williamson and others, 1989). This left an average 1.5 million acre-ft of precipitation to annually recharge the groundwater system. An average 31.7 million acre-ft of surface-water flowed annually into the Central Valley. Streamflow losses that are infiltrated from the surface-water system accounted for an annual average 0.5 million acre-ft of groundwater recharge.

Groundwater was discharged (withdrawn) to streams, springs, or seeps, evaporated to the atmosphere, and transpired by plants (*fig. A23*). An average 1.7 million acre-ft of groundwater was evapotranspired each year. Annually, an average 0.3 million acre-ft was lost to gaining reaches of streams. Prior to development, the groundwater system generally was in equilibrium; except for fluctuations caused by climatic changes, discharge was approximately equal to recharge, and the volume of water in storage remained relatively constant.

Acknowledgments

A project of this magnitude could not be completed without the help of many individuals and organizations. First, the authors acknowledge the U.S. Geological Survey's Groundwater Resources Program for their support of large-scale multidisciplinary studies of groundwater availability across the United States, including this study. The work would not have been possible without the data, technical input, and collaboration provided by the California Department of Water Resources (CA-DWR). In particular, Tariq Kadir, Charlie Brush, Emin C. Dogrul, Michael Moncrief, and Eric Senter provided invaluable assistance. We are grateful to our USGS colleagues Carol Sanchez, editor; Larry Schneider, illustrator; Steve Predmore, GIS specialist; and Steve Phillips and Brian Clark, technical reviewers. Finally, this work owes a debt of gratitude to the original CV-RASA studies and the accomplishments of Sandy Williamson, Dave Prudic, and many others.

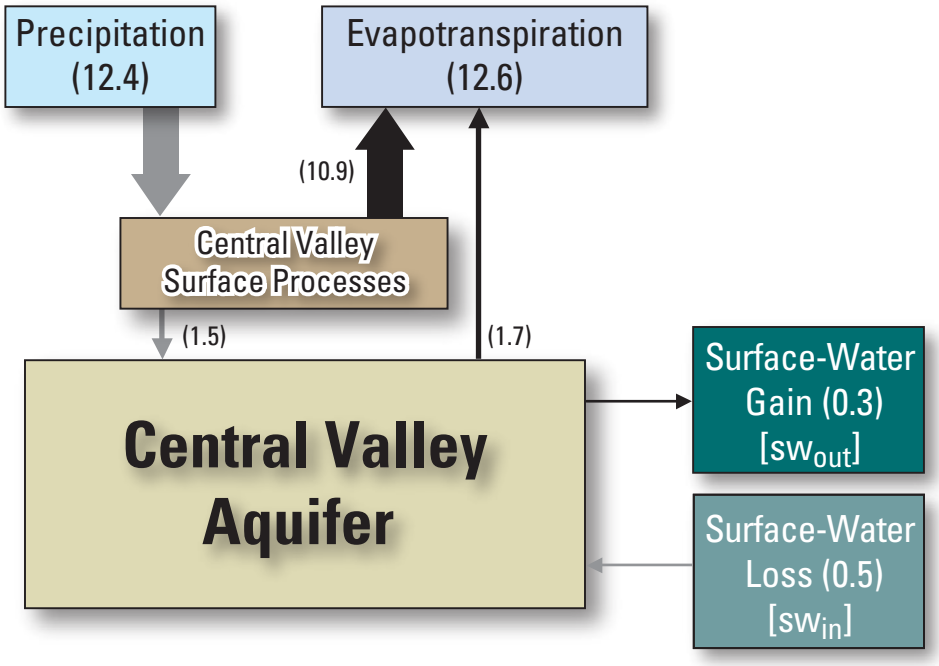

Figure A23. Pre-development water budget and post-development water budget. Values are in millions of acre-feet per year.

References Cited

Alley, W.M., 2006, Tracking U.S. ground-water reserves for the future: Environment, v. 48, no. 3, p. 10–25.

Alley, W.M., 2007, Another water budget myth: The significance of recoverable ground water in storage: Ground Water, v. 45, no. 3, p. 251.

Belitz, Kenneth, and Heimes, F.J., 1990, Character and evolution of the ground-water flow system in the central part of the western San Joaquin Valley, California: U.S. Geological Survey Water-Supply Paper 2348, 28 p.

Belitz, Kenneth, and Phillips, S.P., 1995, Alternative to agricultural drains in California's San Joaquin Valley: Results of a regional-scale hydrogeologic approach: Water Resources Research, v. 31, no. 8, p. 1845–1862.

Belitz, Kenneth, Phillips, S.P., and Gronberg, J.M., 1993, Numerical simulation of ground-water flow in the central part of the Western San Joaquin Valley, California: U.S. Geological Survey Water-Supply Paper 2396, 69 p.

Bertoldi, G.L., 1979, A plan to study the aquifer system of the Central Valley of California: U.S. Geological Survey Open-File Report 79–1480, 48 p.

Bertoldi, G.L., 1989, Ground-water resources of the Central Valley of California: U.S. Geological Survey Open-File Report 89–251, 2 p.

Bertoldi, G.L., Johnston, R.H., and Evenson, K.D., 1991, Ground water in the Central Valley, California—A summary report: U.S. Geological Survey Professional Paper 1401-A, 44 p.

Bloyd, R.M. Jr., 1978, Ground-water conditions in the Sacramento Valley, California 1912, 1961, and 1971: Report to the U.S. Geological Survey.

Brush, C.F., Belitz, Kenneth, and Phillips, S.P., 2004, Estimation of a water budget for 1972–2000 for the Grasslands Area, Central Part of the Western San Joaquin Valley, California: U.S. Geological Survey Scientific-Investigations Report 2004–5180, 51 p.

Brush, C.F., Dogrul, E.C., Kadir, T.N., Moncrief, M.R., Shultz, S., Tonkin, M., and Wendell, D., 2006, Modeling the evolution of a Regional Aquifer System with the California Central Valley ground-water-surface water simulation model (C2VSIM): American Geophysical Union, Fall Meeting 2006, abstract #H11A–1226.

Bureau of Reclamation, 1994, The Central Valley Project overview: Bureau of Reclamation History Program Research on Historic Reclamation Projects, accessed April 16, 2009, at *http://www.usbr.gov/dataweb/html/cvpintro.html*

Bryan, Kirk, 1923, Geology and ground-water resources of the Sacramento Valley, California: U.S. Geological Survey Water-Supply Paper 495, 285 p.

Burow, K.R., Shelton, J.L., Hevesi, J.A., and Weissmann, G.S., 2004, Hydrogeologic characterization of the Modesto area, San Joaquin Valley, California: U.S. Geological Survey Scientific–Investigations Report 2004–5232, 54 p.

California Department of Finance, 2007, E-4 population estimates for cities, counties and the State, 2001–2007, with 2000 Benchmark, Sacramento, California, accessed April 16, 2009, at *http://www.dof.ca.gov/HTML/DEMOGRAP/ReportsPapers/Estimates/E4/E4-01-06/HistE-4.asp*

California Department of Water Resources, 1977, Input data for 1980 and 2000 level Central Valley depletion studies, Memorandum dated August 22, 1977, 135 p.

California Department of Water Resources, 1998, California water plan update: Bulletin 160–98, 3 v., accessed April 16, 2009, at *http://rubicon.water.ca.gov/pdfs/b160cont.html*

California Department of Water Resources, 2000, Explanations of land use attributes used in database files associated with shape files: Land and Water Use Section, 11 p.

California Department of Water Resources, 2003, California's ground water, update 2003: California Department of Water Resources Bulletin 118, 246 p.

California Department of Water Resources, 2005, California water plan update 2005, Volume 1 – Strategic Plan: California Department of Water Resources Bulletin 160–05, CD.

California Department of Water Resources, 2007a, CALSIM-III, accessed April 16, 2009, at *http://bayDeltaoffice.water.ca.gov/modeling/hydrology/CalSimIII/index.cfm*

California Department of Water Resources, 2007b, IWFM: Integrated water flow model, accessed April 16, 2009, at *http://bayDeltaoffice.water.ca.gov/modeling/hydrology/IWFM/index.cfm*

California Regional Water Quality Control Board, Central Valley Region, 1992, Staff Report: Considerations of Water Body Designations to Comply with the Provisions of the Water Quality Control Plan for ISWP.

California State University, Chico, 2003, The Central Valley historic mapping project: California State University, Chico, Department of Geography and Planning and Geographic Information Center, 25 p.

Carle, S.F. and Fogg, G.E., 1996, Transition probability–based indicator geostatistics: Mathematical Geology, v. 28, p. 453–476.

Carle, S.F., Labolle, E.M., Weissmann, G.S., Vanbrocklin, D., and Fogg, G.E., 1998, Conditional simulation of hydrofacies architecture: a transition probability/Markov approach, in Fraser, G.S., and Davis, J.M., Hydrogeologic models of sedimentary aquifers: SEPM, Concepts in Hydrogeology and Environmental Geology, no. 1, p. 147–170.

Climate Source, 2006, Precipitation data from PRISM data, accessed April 16, 2009, at *http://www.climatesource.com/*

Davis, G.H., Green, J.H., Olmsted, F.H., and Brown, D.W., 1959, Ground-water conditions and storage capacity in the San Joaquin Valley, California: U.S. Geological Survey Water-Supply Paper 1469, 287 p.

Davis, G.H., Lofgren, B.E., and Mack, Seymour, 1964, Use of ground-water reservoirs for storage of surface water in the San Joaquin Valley, California: U.S. Geological Survey Water-Supply Paper 1618, 125 p.

Dettinger, M.D., 2005, From climate-change spaghetti to climate-change distributions for the 21st Century California: San Francisco Estuary & Watershed Science, v. 3, issue 1, article 4, 14 p., accessed April 16, 2009, at *http://repositories.cdlib.org/jmie/sfews/vol3/iss1/art4*

Dettinger, M.D. and Earman, S., 2007, Western ground water and climate change—Pivotal to supply sustainability or vulnerable in its own right?: Ground Water News and Views, v. 4, no. 1, p. 4–5.

Diamond, Jonathan, and Williamson, A.K., 1983, A summary of ground-water pumpage in the Central Valley, California, 1961–77: U.S. Geological Survey Water-Resources Investigations Report 83–4037, 70 p.

Dudley, Toccoy, Spangler, Debbie, Fulton, Alan, Staton, Kelly, Lawrence, Seth, Ehorn, Bill, and Ward, Michael, 2006, Seeking an understanding of the ground-water aquifer systems in the Northern Sacramento Valley: An update, accessed April 16, 2009, at *http://ucce.ucdavis.edu/files/filelibrary/2280/37336.pdf*

Farrar, C.D. and Bertoldi, G.L., 1988, Region 4, Central Valley and Pacific Coast Ranges, in Back, William, Rosenshein, J.S., and Seaber, P.R., eds., Hydrogeology: Boulder, Colorado, Geological Society of America, Geology of North America, v. O-2, p. 59–67.

Fogg, G.E., Carle, S., and Green, C.T., 2001, A connected network paradigm for the alluvial aquifer system, *in* Zhang, Dongxiao, and Winter, C.L., eds., Theory, modeling and field investigation in hydrogeology: GSA Special Publication, A Special Volume in Honor of Shlomo P. Neuman's 60th Birthday, 252 p.

Galloway, D.L., Jones, D.R., and Ingebritsen, S.E., 1999, Land subsidence in the United States: U.S. Geological Survey Circular 1182, 175 p.

Galloway, D.L., and Riley, F.S., 1999, San Joaquin Valley, California—Largest human alteration of the Earth's surface: *in* Galloway, D.L., Jones, D.R., and Ingebritsen, S.E., eds., Land Subsidence in the United States: U.S. Geological Survey Circular 1182, p. 23-34, accessed February 2, 2008, at *http://pubs.usgs.gov/circ/circ1182/*

Great Valley Center, 1998, Agricultural land conservation in the Great Central Valley, 32 p., accessed April 15, 2009, at *http://www.greatvalley.org/publications/agpubs/ag_land_conservation.pdf*

Great Valley Center, 1999, State of the great Central Valley: Assessing the region via indicators—The economy: State of the Great Central Valley Indicators Series, 56 p., accessed April 15, 2009, at *http://www.greatvalley.org/pub_documents/2005_1_7_16_55_28_Indicators%20-%20Economy%201.pdf*

Great Valley Center, 2005, State of the great Central Valley: Assessing the region via indicators—The economy: State of the Great Central Valley Indicators Series, 49 p., accessed April 15, 2009, at *http://www.greatvalley.org/pub_documents/2005_1_18_13_59_43_indicator_econ05_report.pdf*

Gronberg, J.A., and Belitz, K.R., 1992, Estimation of a water budget for the central part of the western San Joaquin Valley, California: U.S. Geological Survey Water-Resources Investigations Report 91–4192, 22 p.

Hackel, Otto, 1966, Summary of the geology of the Great Valley, p. 217–238, *in* Bailey, E.H. ed., Geology of Northern California: California Division of Mines and Geology Bulletin 190, 508 p.

Halford, K.J. and Hanson, R.T., 2002, User guide for the drawdown-limited, Multi-node well (MNW) package for the U.S. Geological Survey's modular three-dimensional finite-difference ground-water flow model, versions MODFLOW-96 and MODFLOW-2000: U.S. Geological Survey Open-File Report 02–293, 33 p., accessed April 16, 2009, at *http://pubs.usgs.gov/of/2002/ofr02293/text.html*

Hall, W.H., 1886, Physical data and statistics of California: State Engineering Department of California, 396 p.

Hall, W.H., 1889, Irrigation in California: National Geographic, v. 2, no. 4, p. 281.

Hanson, R.T., Dettinger, M.D., and Newhouse, M.W., 2006, Relations between climate variability and hydrologic time series from four alluvial basins across the southwestern United States: Hydrogeology Journal, v. 14, no. 7, p. 1122–1146.

Harbaugh, A.W., Banta, E.R., Hill, M.C., and McDonald, M.G., 2000, MODFLOW-2000: U.S. Geological Survey modular ground-water model—User guide to modularization concepts and the ground-water flow process: U.S. Geological Survey Open-File Report 00–92, 121 p.

Hidalgo, H.G., Cayan, D.R., Dettinger, M.D., 2005, Sources of variability of evapotranspiration in California: Journal of Hydrometeorology, v. 6, p. 3–19.

Hill, M.C., Banta, E.R, Harbaugh, A.W., and Anderman, E.R., 2000, MODFLOW–2000, The U.S Geological Survey modular ground-water model—User guide to the observation, sensitivity, and parameter-estimation processes and three post-processing programs: U.S. Geological Survey Open-File Report 00–184, 209 p.

Hoffmann, Jörn, Leake, S.A., Galloway, D.L., and Wilson, A.M., 2003, MODFLOW–2000 ground-water model—user guide to the subsidence and aquifer-system compaction (SUB) package: U.S. Geological Survey Open-File Report 03–233, 46 p.

Hull, L.C., 1984, Geochemistry of ground water in the Sacramento Valley, California: U.S. Geological Survey Professional Paper 1401-B, 36 p.

Ingebritsen, S.E., Ikehara, M.E., Galloway, D.L., and Jones, D.R., 2000, Delta subsidence in California: U.S. Geological Survey Fact Sheet 005–00, 4 p., accessed April 16, 2009, at *http://ca.water.usgs.gov/archive/reports/fs00500/fs00500.pdf*

Isaaks, E.H., and Srivastava, R.M., 1989, An introduction to applied geostatistics: New York, Oxford University Press, 561 p.

Jennings, C.W., 1977, Geologic map of California: California Division of Mines and Geology, Sacramento, scale 1:750,000, 1 sheet.

Johnson, A.I., Moston, R.P., and Morris, D.A., 1968, Physical and hydrologic properties of water-bearing deposits in subsiding areas in California: U.S. Geological Survey Professional Paper 497-A, 71 p.

Journel, A.G. and Huijbregts, C.J., 1978, Mining geostatistics: New York, Academic Press, 600 p.

Laudon, Julie, and Belitz, Kenneth, 1991, Texture and depositional history of Late Pleistocene–Holocene alluvium in the central part of the western San Joaquin Valley, California: Bulletin of the Association of Engineering Geologists, v. 28, no. 1, p. 73–88.

Lund, Jay, Hanak, Ellen, Fleenor, William, Howitt, Richard, Mount, Jeffrey, and Moyle, Peter, 2007, Envisioning futures for the Sacramento–San Joaquin Delta: San Francisco, California, Public Policy Institute of California, 284 p.

Mantua, N.J., 2006, The Pacific decadal oscillation (PDO) index: data obtained from the University of Washington's Joint Institute for the Study of the Atmosphere and Oceans web-page, accessed April 16, 2009, at *http://jisao.washington.edu/pdo/PDO.latest*

Mantua, N.J., Hare, S.R., Zhang, Y., Wallace, J.M., and Francis, R.C., 1997, A Pacific interdecadal climate oscillation with impacts on salmon production: Bulletin of the American Meteorological Society, v. 78, p. 1069–1079.

Mantua, N.J. and Steven, H., 2002, The Pacific decadal oscillation: Journal of Oceanography, v. 58, no. 1, p. 35–44.

Matthes, F.E., 1960, Reconnaissance of the geomorphology and glacial geology of the San Joaquin Basin, Sierra Nevada, California: U.S. Geological Survey Professional Paper 329, 62 p.

Meko, D.M., and Woodhouse, C.A., 2005, Tree-ring footprint of joint hydrologic drought in Sacramento and Upper Colorado River basins, western USA: Journal of Hydrology, v. 308, no. 1–4, pp. 196–213.

Mendenhall, W.C., Dole, R.B., and Stabler, Herman, 1916, Ground water in San Joaquin Valley, California: U.S. Geological Survey Water-Supply Paper 398, 310 p.

Miller, R.E., Green, J.H., and Davis, G.H., 1971, Geology of the compacting deposits in the Los Banos–Kettleman City subsidence area, California: U.S. Geological Survey Professional Paper 497-E, 45 p.

Moore, S.B., Winckel, J., Detwiler, S.J., Klasing, S.A., and Gaul, P.A., 1990, Fish and wildlife resources and agricultural drainage in the San Joaquin Valley, California: Sacramento, California, San Joaquin Valley Drainage Program, 974 p.

Mullen, J.R., and Nady, Paul, 1985, Water budgets for major streams in the Central Valley, California, 1961–77: U.S. Geological Survey Open-File Report 85–401, 87 p.

Olmstead, F.H., and Davis, G.H., 1961, Geologic features and ground-water storage capacity of the Sacramento Valley, California: U.S. Geological Survey Water-Supply Paper 1497, 287 p.

Page, R.W., 1983, Geology of the Tulare Formation and other continental deposits, Kettleman City area, San Joaquin Valley, California, with a section on ground-water management considerations and use of texture maps: U.S. Geological Survey Water-Resources Investigations Report 83-4000, 24 p.

Page, R.W., 1986, Geology of the fresh ground-water basin of the Central Valley, California, with texture maps and sections: U.S. Geological Survey Professional Paper 1401-C, 54 p.

Page, R.W., and Bertoldi, G.L., 1983, A Pleistocene diatomaceous clay and a pumiceous ash: California Geology, v. 36, no. 1, p. 14–20.

Parsons, J.J., 1987, A geographer looks at the San Joaquin Valley, 1987, Carl Sauer memorial lecture, accessed April 16, 2009, at *http://geography.berkeley.edu/ProjectsResources/Publications/Parsons_SauerLect.html*

Phillips, S.P. and Belitz, Kenneth, 1991, Calibration of a textured-based model of a ground-water flow system, western San Joaquin Valley, California: Ground Water, v. 29, no. 5, p. 702–715.

Phillips, S.P., Green, C.T., Burow, K.R., Shelton, J.L., and Rewis, D.L., 2007, Simulation of multiscale ground-water flow in part of the northeastern San Joaquin Valley, California: U.S. Geological Survey Scientific-Investigations Report 2007–5009, 43 p.

Planert, Michael, and Williams, J.S., 1995, Ground water atlas of the United States: Segment 1, California, Nevada: U.S. Geological Survey Hydrologic Atlas 730-B, 1 atlas, 28 p.

Prokopovich, N.P., 1987, Textural composition of near-surface alluvium in west-central San Joaquin California: Bulletin of the Association of Engineering Geologists, v. 24, no. 1, p. 59–81.

Prudic, D.E., Konikow, L.F., and Banta, E.A., 2004, A new streamflow-routing (SFR1) package to simulate stream-aquifer interaction with MODFLOW-2000: U.S. Geological Survey Open-File Report 04–1042, 95 p.

Reilly, T.E., 2005, Assessing the nation's ground-water resources: U.S. Geological Survey 125th Anniversary Articles, accessed April 16, 2009, at *http://www.usgs.gov/125/articles/groundwater.html*

Ritzi, R.W., Jr., 2000, Behavior of indicator variograms and transition probabilities in relation to the variance in lengths of hydrofacies: Water Resources Research, v. 36, p. 3375–3381.

Ryan, Holly, Gibbons, Helen, Hendley II, J.W., and Stauffer, P.H., 1999, El Niño sea-level rise wreaks havoc in California's San Francisco Bay Region: U.S. Geological Survey Fact Sheet 175–99, 4 p., accessed April 16, 2009, at *http://pubs.usgs.gov/fs/1999/fs175-99/fs175-99.pdf*

Schmid, W., Hanson, R.T., Maddock III, T.M., and Leake, S.A., 2006, User's guide for the Farm Process (FMP1) for the U.S. Geological Survey's modular three-dimensional finite-difference ground-water flow model, MODFLOW-2000: U.S. Geological Survey Techniques and Methods 6-A17, 127 p.

Sun, R.J., and Johnston, R.H., 1994, Regional Aquifer-Systems Analysis program of the U.S. Geological Survey, 1978-92: U.S. Geological Survey Circular 1099, 126 p.

U.S. Geological Survey, 2002, Concepts for national assessment of water availability and use: U.S. Geological Survey Circular 1223, 34 p.

Chapter B. Groundwater Availability in California's Central Valley

By Claudia C. Faunt, Kenneth Belitz, and Randall T. Hanson

Introduction

This chapter focuses on the availability of groundwater in the Central Valley. Therefore, the chapter includes a description of the effects of development and climate on the hydrologic system, a discussion of groundwater sustainability and management, and provides suggestions for monitoring the hydrologic system. A transient hydrologic model, referred to here as the Central Valley Hydrologic Model (CVHM), was developed as part of this study (*Chapter C*, this report). The CVHM incorporates monthly time-varying hydrologic-budget components for 21 water-balance subregions (WBSs) within the Central Valley for water years 1962 to 2003. The CVHM was used to evaluate the effects of climate, water-delivery systems, and land-use practices on the groundwater system. The descriptions of these effects are derived from this model as well as from the data and information gathered, compiled, and analyzed as part of this study. The chapter also incorporates information from the extensive literature on California's Central Valley.

Development and the Hydrologic System

The spatial and temporal differences between the natural distribution of water in the Central Valley, and the agricultural and urban demands for that water, have led to large-scale engineering of the hydrologic system. Simply stated, the mountains adjacent to the Central Valley have an average annual surplus of water, whereas the valley proper has an average annual water deficit (precipitation minus ET as much as –40 in.). Agricultural development and human population are concentrated in the precipitation-deficient valley. If applied irrigation-water requirement is added to the annual natural deficit, the average annual water deficiency is greater than 70 in. in places (*fig. A5*). Despite the magnitude of these numbers, they do not account for the seasonal and geographic water distribution issues. For example, the largest demand for water is in the drier spring-summer growing season of the drier and heavily agriculturally developed Tulare Basin.

As early as the 1870s, various plans were proposed to transfer "excess" water from the Sacramento River to the drier areas in the San Joaquin Valley (California Department of Water Resources, 1994). Dams were proposed to store water for release in the drier spring-summer growing season. Initially, these plans focused on surface water, but the plans began to include groundwater as well as time progressed. To meet the substantial water needs of California's growing agriculture and urban population, a massive surface-water diversion and delivery system was constructed by Federal, State, and local water purveyors (*fig. A7*). Because the surface-water diversion and delivery system cannot always meet all of the water demand, groundwater increasingly has been relied on to help rectify the imbalance.

Surface-Water and Groundwater Development History

The use of surface and groundwater has had a long history in the Central Valley. Development of surface water, primarily for irrigation, began in the 1700s (Bertoldi and others, 1991). By the late 1800s, gold rush settlers had begun ranching and dryland farming. Early farming was concentrated close to the Delta, where the water table was high year round and surface water was readily available. Since the 1860s, farmers around the Delta began to build levees and pump water to reclaim the land for agriculture.

As the gold mining began to diminish, agriculture grew in the Delta and Central Valley, as did the need for a reliable water supply. By the mid 1800s, it was clear that a major redistribution of the state's water would have to occur if farming were to continue in the San Joaquin Valley. Starting in the mid 1800s with the Miller and Lux agricultural enterprise, cooperatives and development companies formed, and by 1900 an extensive system of canals had been built to supply surface water to the southern San Joaquin Valley (Igler, 2001). Around 1880, during the same time that surface-water systems were being engineered, groundwater development began in the Central Valley (Bertoldi and others, 1991). Groundwater initially was developed in regions where shallow groundwater was plentiful. In particular, in the San Joaquin Valley, groundwater extraction enabled farms and cities to flourish.

This especially was true where flowing wells were commonplace near the central part of the valley near the historic lake basins (*fig. A21A*). After 1900, the yields of flowing wells had diminished as water levels declined, and it became necessary to install pumps in wells to sustain production rates. By 1913, the estimated annual groundwater extraction in the Central Valley was 360,000 acre-ft (Bertoldi and others, 1991, p. 22). Around 1930, the development of an improved deep-well turbine pump and rural electrification enabled additional groundwater development for irrigation (Galloway and Riley, 1999). For years, San Joaquin Valley farmers pumped the valley's groundwater, causing large and widespread declines in the water table and increased pumping costs. Many wells eventually went dry and thousands of acres of farmland were forced out of production. In addition, the constant threat of flooding was becoming an issue as was the encroachment of saltwater into Delta channels during the dry spring-summer growing season.

The Federal government has long played a major role in development of the West's surface-water resources. As early as 1875, the U.S. Army Corps of Engineers began work on the Sacramento and Feather Rivers to improve navigation. In 1919, shortly after retiring from the USGS, Lt. Col. R.B. Marshall proposed a comprehensive, statewide plan for conveyance and storage of California's Central Valley water supplies, which was published in 1920 by the California State Irrigation Association (Marshall, 1920). This plan served as the framework for the State Water Plan (SWP), which later formed the basis for the Federal Central Valley Project (CVP). The cornerstone of the CVP, officially formed in 1935, is the plan to use water from the San Joaquin and Sacramento Rivers to irrigate 12 million acres in the San Joaquin Valley. The CVP is a complex operation of interrelated projects built to control floodwaters, irrigate the semi-arid acreage of California's Central Valley, and where possible provide low cost power. As part of the CVP, in 1939, the entities that held Miller and Lux's (as well as others) historical water rights traded the rights to take water from the San Joaquin River for rights to Sacramento River water stored in Shasta Lake.

In the early 1900s, State water planners recognized that the Delta would be integral in supplying supplemental water to support the growing population of southern California and prevent increased groundwater overdraft in the Central Valley. Additionally, the need for flood control on the Feather River was recognized, as was the San Joaquin Valley's need for an outlet for saline irrigation drainage water. After years of debate and study, what was to become the State Water Project (SWP) officially was begun in the early 1950s. As a result of these two massive water projects, two main canals reroute water that would have gone to the San Joaquin River to be available for people holding pre-1914 water rights. Since the mid 1940s, the CVP has used the Madera and Friant–Kern Canals to divert San Joaquin River water southward to Kern County (*fig. A7*). In exchange, farmers on the west side of the San Joaquin Valley that had rights to the San Joaquin River began receiving water by way of the Delta–Mendota Canal (SWP) in 1951 based on Kern County's rights to water from Lake Shasta as part of the CVP (*fig. A7*).

Hence, the Central Valley relies on a combination of local and imported surface water and local groundwater. The CVP, SWP, and local agencies provide a network of diversions and deliveries throughout the Central Valley. The DWR C2VSIM model simulates this complex network as a series of 41 inflows, 66 diversions, and 21 subregions (C. Brush, California Department of Water Resources, written commun., February 21, 2007; *fig. A7*). Generally, when available, most farmers irrigate with surface water. When surface water is not available (such as later in the spring–summer growing season or during droughts) or not economical, farmers typically use groundwater.

This critical resource has not been redistributed without conflict. In the 1970s, growth in environmental awareness ultimately led to the inclusion of environmental factors into the water distribution process (California Department of Water Resources, 2005). These conflicts culminated in numerous environmental regulations and constraints embodied in the 1992 CVP Improvement Act (CVPIA). The CVPIA brought fundamental change to CVP operations and water allocation schemes. The results of this legislation have begun to be realized (California Department of Water Resources, 1994). Presently, environmental flows to protect critical components of the ecosystem, including the Delta smelt, are beginning to be enforced. These environmental flows may substantially reduce the amount of surface water available for farming and (or) urban uses and, thereby, increase reliance on groundwater. The potential increased reliance on groundwater is likely to lower groundwater levels, thereby increasing pumping costs, inducing further subsidence, and decreasing surface-water base flows.

Land Use

California's Central Valley is one of the most modified rural environments in the world (California State University, Chico, 2003). Abundant water (through irrigation) combined with the long growing season results in an exceptionally productive agricultural economy. Consequently, California's agricultural land-use patterns are dynamic. Market demand and resource limitations, particularly water, cause large shifts of land in and out of agricultural uses. Urbanization and development also have resulted in changes in land-use patterns. Because agricultural and urban land-use changes have had a dramatic effect on groundwater availability, an overview of agricultural and urban land use is given below.

Agricultural Land Use

Agriculture in the valley has developed through three overlapping stages: cattle ranching in the early days, followed by "dry-land" farming of small grains, and finally, specialized and intensified irrigated farming. Cattle ranching ended as a consequence of the disastrous drought of 1863–64, which resulted in the loss of almost all the cattle in California (Bureau of Reclamation, 1994). Combined with the demise of cattle ranching, population growth, the low cost of land, and the post 1869 development of the railroads shifted the agricultural focus toward grain production. Dry-land farming of wheat and barley expanded until the latter part of the 19th century and then declined as other grain-growing regions developed and irrigated farming proliferated (Bureau of Reclamation, 1994).

Mechanization greatly changed agriculture in the Central Valley. As transportation methods evolved, particularly the railroad, Central Valley agriculture expanded in the early 1900s. The invention of the deep-well turbine pump around 1930 allowed water to be pumped from greater depths. Mechanical harvesting of many crops was in place along with refrigerated railroad transportation to supplement or replace transportation by truck in the 1950s. This new form of transportation facilitated wider distribution of orchard (for example, citrus, avocados, and nuts) and truck (for example, tomatoes, melons, squash and lettuce) crops. The tomato harvester, and most recently the mechanical harvesting of grapes, also increased production (Parsons, 1987).

Water, soils, microclimate, pests, economic and historical factors, and the choices of individual farmers are all involved in deciding which crops to plant. Some crops, like almonds and alfalfa, are found almost everywhere in the Central Valley (*fig. A21B*). Other crops are confined sharply to restricted areas. For example, most of the orange growers are in a narrow thermal belt near the mountains on the east side of the San Joaquin Valley (California Department of Water Resources, 2000). Cotton generally is confined to the San Joaquin Valley, with most cotton grown west of the valley axis. Rice generally is confined to the fine-grained soils of the Sacramento Valley. Throughout the Central Valley, soils are deep and fertile and the growing season is long, allowing much of the valley to have crops grown and harvested two or three times in a year on a single field. Changing market conditions may lead to rapid shifts of land-use. Periodically, new crops are introduced, and new strains of crops always are being developed. For example, in the 1980s, safflower was added and, more recently, pistachios. More than half of all the grapes grown in the US now are produced in the San Joaquin Valley (Parsons, 1987; Great Valley Center, 2005). Nut crop plantings soared in the last few decades; almond acreage far exceeds that of any other tree crop, and in the late 1980s was nearly half of that of cotton. Dairies, moving from other parts of California, are beginning to locate to Tulare and Kings County. Despite the predominance of agriculture, the valley's economy is not fully dependent on agriculture. Kern County is one of the nation's largest oil-producing counties, and urban areas are expanding rapidly throughout the valley.

Agriculture still is the dominant land use in the Central Valley. The three major regions of the Central Valley (the Sacramento Valley, the San Joaquin Basin, and the Tulare Basin) had 1.9 million, 2 million, and 3 million irrigated crop acres, respectively, in 2000, representing 60 percent of the valley floor by area (California Department of Water Resources, 2000). In terms of production dollar value, the Sacramento Valley accounted for 12 percent of the agricultural production, while the San Joaquin Valley (San Joaquin and Tulare Basins combined; *fig. A1*) accounted for 88 percent. Between 1997 and 2002, growth of agricultural production increased by 4 percent in the valley as a whole. This represented a 6-percent increase in the San Joaquin Valley and a slight decrease in agricultural production in the Sacramento Valley (Great Valley Center, 2005).

Urban Land Use

The Central Valley is an important area for California's expanding urban population. Between 1970 and 2000, the population doubled in the Central Valley and reached 6.5 million in 2005. Future growth is expected to continue, according to Census Bureau projections, suggesting that the Central Valley's population will increase to 10 million by 2030. The vast majority of the population is in the major urban areas of Sacramento, Fresno, Bakersfield, Stockton, and Modesto (*fig. A1*). Fresno and Sacramento are two of the fastest growing cities in California (California Department of Finance, 2007).

These large increases in population have resulted in a shift in land-use in the Central Valley (California Department of Conservation, 2007). Between 1961 and 2000, urban areas have increased from 3 to 7 percent of the total area (California Department of Water Resources, 2000; California State University, Chico, 2003; *table C3*). During this same time frame, native vegetation decreased by at least 4 percent while croplands remained relatively constant. However, between 1990 and 2002, about 4 percent of the Central Valley's irrigated farmland was converted to other uses, primarily for housing and other urban uses (Great Valley Center, 2005). Hence, some of the land has had multiple changes in use. Between 1962 and 2003, pumpage of groundwater for municipal and industrial uses (urban) in the Central Valley increased more than threefold from about 0.6 to nearly 2 million acre-ft/yr, despite increased use of surface water and implementation of various urban conservation measures (California Department of Water Resources, 2005; C. Brush, California Department of Water Resources, written commun., February 21, 2007).

Population growth alone does not determine changes in land use. Where and how the growth is accommodated can make a difference. Development of the most productive farmland, rather than less productive land, places a premium on how efficiently the population is accommodated. Despite the urbanization of nearly 100,000 acres during the 1990s, the market value of Central Valley farm products increased (American Farmland Trust, 2006). Farmers have increased the value of output by shifting from "extensive" crops such as barley, oats, and sugar beets to higher-value fruits, nuts, vegetables, and ornamental horticultural crops. More than one-third of the increase in market value between 1992 and 2002 is attributed to a 56-percent increase in dairy production (American Farmland Trust, 2006).

Development and Changes to the Hydrologic Budget

As would be expected, the long history of agricultural and urban development has greatly altered the groundwater budget in the Central Valley (*figs. A23* and *B1*). *Chapter A* describes the groundwater budget prior to development. Presently, the agricultural and urban water demands are met by a combination of groundwater withdrawals and large imports of surface water. For nearly every city in the San Joaquin Valley, groundwater is the principal supply for municipal and industrial water demand. Because of the large effect that irrigated agriculture has on the system, the overall water budget for the system is separated into two linked parts for the purposes of analysis: a landscape budget, encompassing the surface processes (including most of the components of the agricultural part of the system), and a groundwater budget, encompassing fluxes into, through, and out of the aquifer system. Large volumes of water are moved into and out of these systems through groundwater pumpage and a surface-water delivery system.

This report primarily focuses on the groundwater part of the budget and its linkages to the landscape budget. The landscape budget includes inputs from precipitation, surface-water deliveries, and groundwater pumpage, and outputs of evapotranspiration (ET), runoff, and groundwater recharge. For accounting purposes, ET from groundwater is included in the landscape budget. In terms of the groundwater budget, the withdrawals from pumpage are balanced by a combination of increased recharge, decreased non-pumping discharge, and removal of water from storage. The aquifer receives recharge from precipitation, streamflow losses, and excess irrigation water. The excess irrigation water originates from a combination of surface-water deliveries and groundwater pumpage. Other than groundwater withdrawals from pumping wells, groundwater leaves the system predominantly through wells, ET, flux to streams and, to a small degree, through discharge to the Delta. When total recharge exceeds total discharge, water is added to storage; when the reverse is true, water is removed from storage, which can trigger aquifer-system compaction and associated land subsidence.

Recharge from a combination of precipitation and excess applied irrigation water and discharge by groundwater pumpage are the dominant stresses on the groundwater system (*fig. B1*). These stresses have had substantial effects on groundwater levels. These water-level changes (predominantly declines, but rises in some areas) have altered groundwater flow rates and directions, changed flows that are exchanged with streams and the adjacent aquifers and confining units in the aquifer system, altered groundwater quality, and resulted in a change in groundwater storage. More details on these stresses and elements of the groundwater budget are discussed in the next few sections. The discussion draws heavily on the results of updated numerical model (Central Valley Hydrologic Model [CVHM]) simulations conducted as a part of this study (*Chapter C*). Where necessary, the results of simulations by Williamson and others (1989) and summaries by Bertoldi and others (1991) are used to augment the discussion.

Hydrologic Budget Components

The inputs and outputs of the water budgets for the landscape and the groundwater systems are presented in *figures B2* and *B3* and tabulated in *tables B1* and *B2*, respectively. Because these systems are linked, many of the water-budget components pertain to both systems (*fig. B1*). The landscape and groundwater budgets vary significantly from year to year (*tables B1* and *B2* and *figs. B2* and *B3*). During wet years, relatively inexpensive surface water typically is used for irrigation, and during dry periods, many farms predominantly use groundwater. Because of great variability in the hydrologic conditions, a "typical" water year seldom is seen. In this report, a "typical" year is defined as one with annual precipitation and inflow that are near the long-term median values. In order to portray the system through its typical patterns and extremes, 3 recent years were selected: (1) 1975 was selected as a "typical" year because inflow is near the median value, even though precipitation is slightly lower than the median; (2) 1990 was selected as a representative dry year because of a prolonged series of low inflows and small precipitation rates during the drought 1987–92; (3) 1998 was selected as a typical wet year because it had relatively high inflows and extremely high precipitation. These 3 years will be used for the basis of discussion in many of the following sections. Where applicable, average hydrologic values for water years 1962–2003 also are used. Although an average year is rare and, as pointed out earlier, wet and dry extremes are more common, averages are used to the overall cumulative affect over the 42-year period. Water years that begin in October of the preceding calendar year are used because they represent the time period over which a complete annual hydrologic cycle normally occurs.

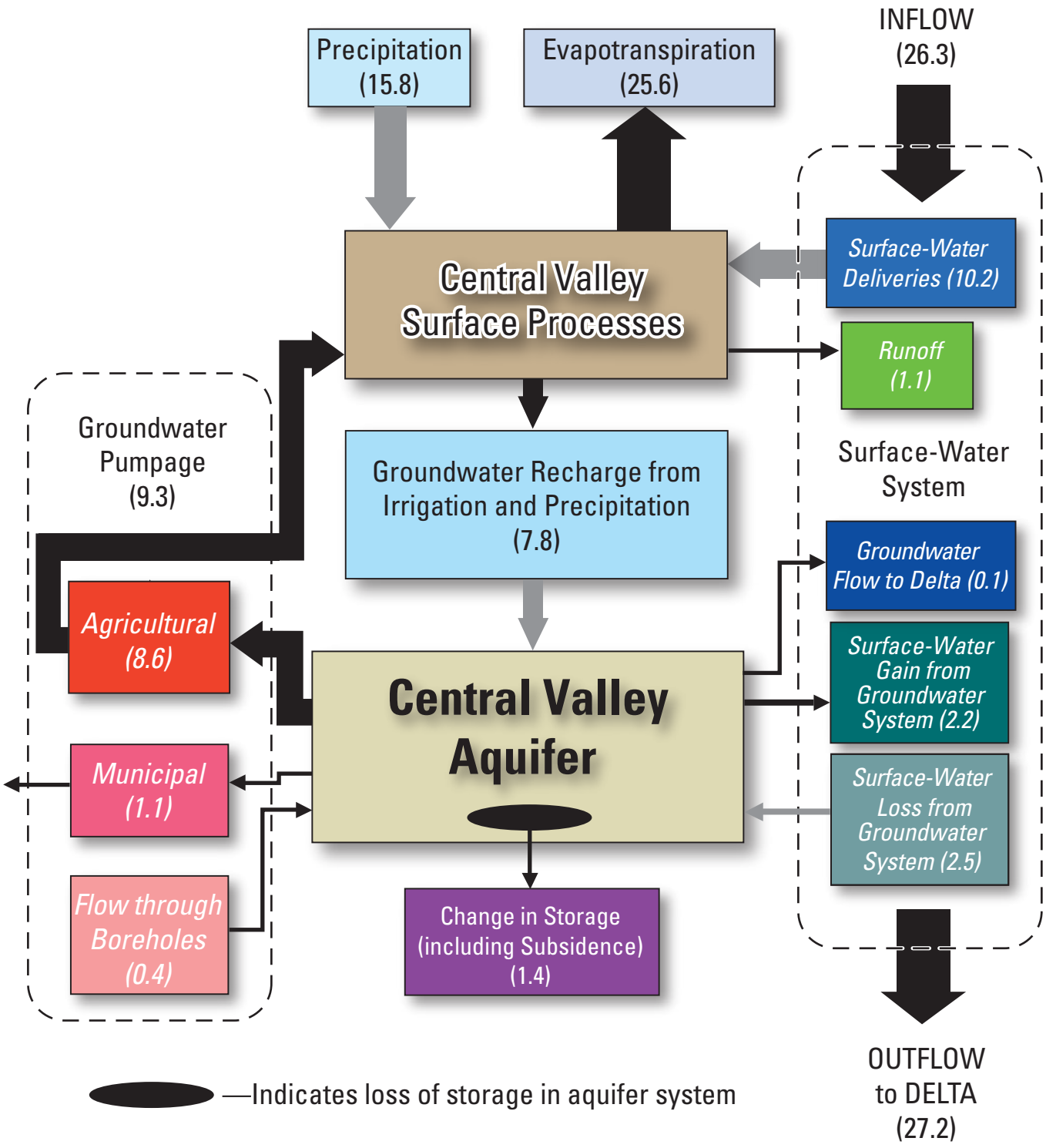

Figure B1. Average water budget for water years 1962–2003. This budget includes the landscape and groundwater components and their linkages. Values in millions of acre-ft/yr. A diagram showing the pre-development water budget is shown in *figure A23*.

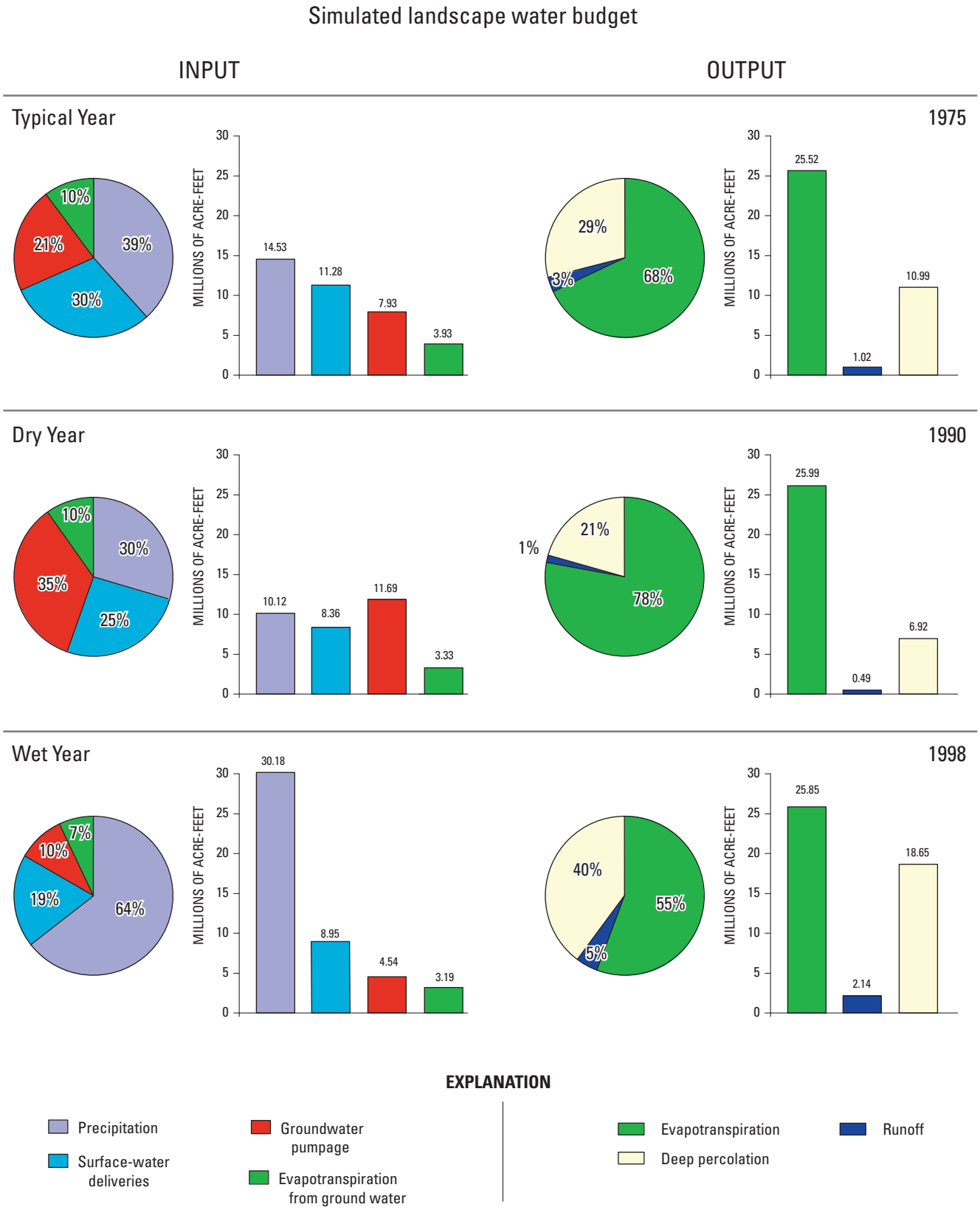

Figure B2. Simulated landscape budget for the Central Valley for typical (1975), dry (1990), and wet (1998) years.

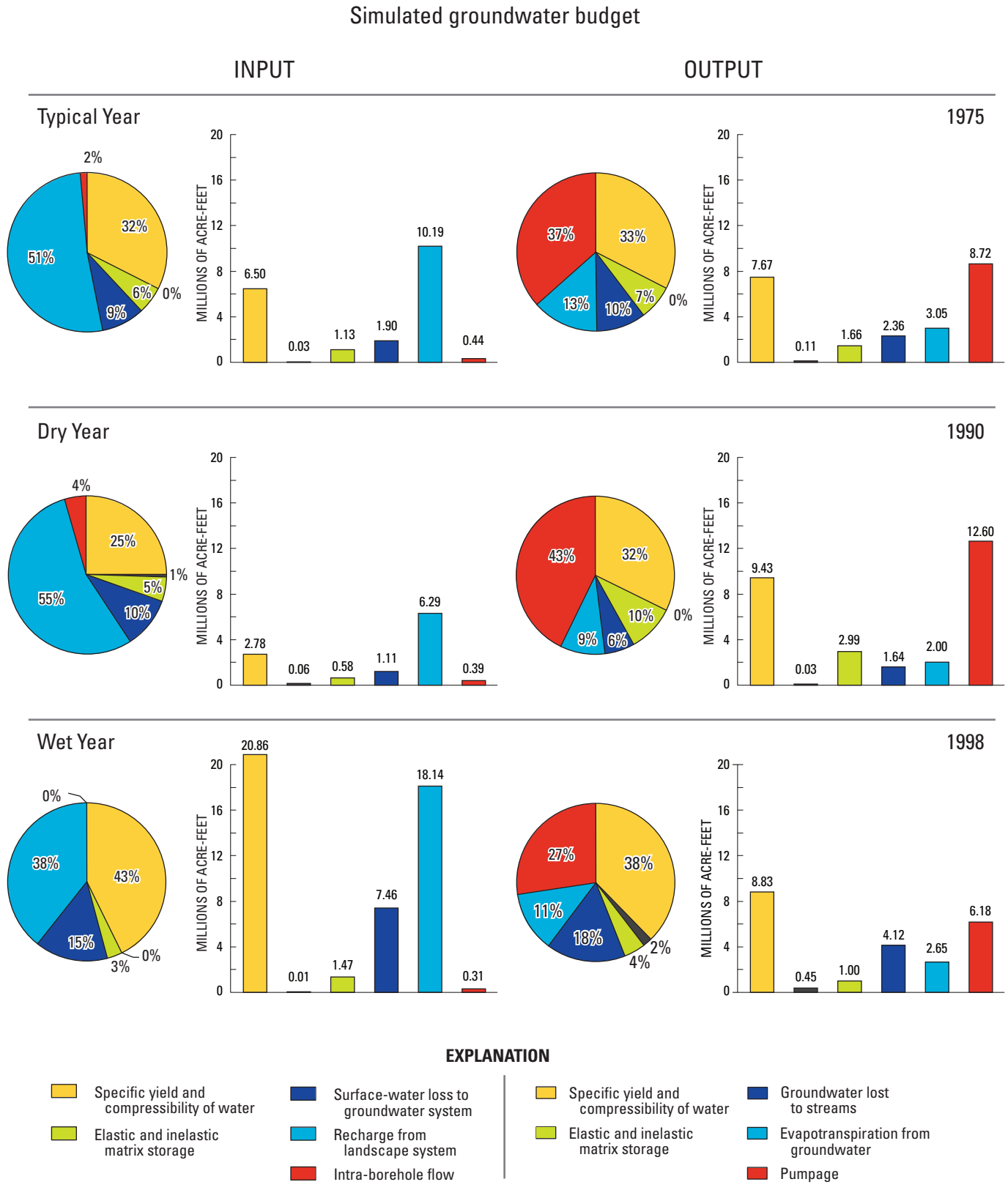

Figure B3. Simulated groundwater budget for the Central Valley for typical (1975), dry (1990), and wet (1998) years.

Table B1. Summary of the simulated landscape budget for average (water years 1962-2003), typical (1975), dry (1990), and wet (1998) years for the Central Valley, California.

[All values in millions of acre-feet per year. Totals may not agree because of rounding. Deep percolation is defined as excess water (irrigation and precipitation) beyond the active root zone (Schmid and others, 2006). Groundwater recharge: deep percolation – evapotranspiration from groundwater]

	Input to landscape system				Output from landscape system			
	Precipitation	Surface surface-water deliveries	Groundwater pumpage	Evapotranspiration from groundwater	Evapotranspiration	Runoff	Deep percolation	Groundwater recharge
Average	15.8	10.2	8.6	3.7	25.6	1.1	11.4	7.7
Typical	14.5	11.3	7.9	3.9	25.5	1	11	7.0
Dry	10.1	8.4	11.7	3.3	26	0.5	6.9	3.6
Wet	30.2	8.9	4.5	3.2	25.8	2.1	18.6	15.4

Table B2. Summary of the simulated groundwater budget for average (water years 1962-2003), typical (1975), dry (1990), and wet (1998) years for the Central Valley, California.

[All values in millions of acre-feet per year. Totals may not agree because of rounding. Pumpage includes urban and agricultural pumpage (groundwater pumpage into landscape system). Net recharge from landscape system matches net groundwater recharge from the landscape budget in *table B1*]

	Input to the groundwater system					
	Storage from specific yield and compressibility of water	Elastic and inelastic storage	Stream leakage to groundwater	Recharge from landscape process	Intra-borehole flow	General head boundaries
Average	8.1	1	2.6	10.7	0.4	0.0
Typical	6.5	1.1	1.9	10.2	0.4	0.0
Dry	2.8	0.6	1.1	6.3	0.4	0.1
Wet	20.9	1.5	7.5	18.1	0.3	0.0
	Output from the groundwater system					
	Storage (specific yield and compressibility of water)	Storage (elastic and inelastic compaction)	Groundwater inflow to streams	Discharge from landscape process	Pumpage	General head boundaries
Average	8.5	2	2.2	3.	9.7	0.1
Typical	7.7	1.7	2.4	3.1	8.7	0.1
Dry	8.8	3	1.6	2.6	12.6	0
Wet	18.9	1	4.1	2.6	6.2	0.5
	Net in relation to groundwater availability					
	Storage from specific yield and compressibility of water	Elastic and inelastic storage	Stream interaction	Recharge from landscape process	Pumpage	General head boundaries
Average	–0.3	–0.1	0.3	7.8	–9.3	–0.1
Typical	–1.2	–0.5	–0.5	7.1	–8.3	–0.1
Dry	–6.6	–2.4	–0.5	3.7	–12.2	0
Wet	12	0.5	3.3	15.5	–5.9	–0.4

Recharge and Discharge

Delivery of surface water for irrigation, combined with pumping for irrigation and public supply, has greatly altered the amount and distribution of recharge to, and discharge from, the groundwater system. Recharge rates from precipitation have not changed significantly from predevelopment times (Williamson and others, 1989).

Prior to development, natural recharge to, and discharge from, the system was in a dynamic steady state, with an estimated 2 million acre-ft/yr moving through the system (*fig. A20*). Soon after irrigated agriculture began in the late 1800s, water pumped for irrigation exceeded the amount of natural recharge. Recharge to the groundwater system comes from two main sources: percolation of water past the root zone, and stream losses. Prior to development, the source of percolating water was infiltration of precipitation.

During the period between 1962 and 2003, an average of 18.9 million acre-ft of water was required annually for irrigation, supplied in approximately equal proportions from groundwater and surface water (*table B1* and *fig. B2*). Part of this irrigation water was consumed by crops. However, it is important to recognize that not all irrigation water is consumed: some runs off and some returns to the groundwater system by deep percolation, canal leakage, and other mechanisms.

The primary source of recharge has become deep percolation of irrigation water past crop roots, sometimes referred to as recharge from excess applied irrigation water. Of the average 13.3 million acre-ft of groundwater recharged annually from 1962 to 2003, less than 1 percent was from infiltration from the Delta, 19 percent was from streams by way of stream-flow leakage, and 79 percent was from the landscape processes, which include recharge from excess applied irrigation water and from precipitation (*table B2* and *fig. B1*). Average annual groundwater recharge varies between typical, dry, and wet years; 12.1, 7.5, and 25.6 million acre-ft, respectively. During dry years, recharge is reduced to a little more than one-half the average recharge; recharge during wet years is almost double the average. In typical and dry years, the contribution from stream-flow leakage was about 15 percent. However, during wet years, the streams generally flow at higher rates for longer periods of time and the simulated contribution from stream-flow leakage increases to 24 percent.

Groundwater pumpage and ET from crops has replaced natural ET as the primary mechanism of discharge from the groundwater system (*fig. B1*). Groundwater flow out the Delta relatively is negligible (*fig. B3*). ET varies annually, but the total ET does not vary much from the average annual rate of 25.6 million acre-ft/yr. Roughly 15 percent of the ET is met directly from the uptake of shallow groundwater.

Groundwater pumpage is by far the largest discharge from the groundwater system. Pumpage is physically possible to measure; yet in the Central Valley it is one of the most uncertain components of the entire water budget. As a result, agricultural pumpage often is estimated from the consumptive use of water. Consumptive use of water in this context refers to all evaporation and transpiration by a particular crop. If this quantity is known, groundwater pumpage may be estimated by taking into account surface-water supply, effective precipitation, and irrigation efficiency. In this study, the numerical model CVHM was used to estimate groundwater pumpage. The CVHM employs the newly developed Farm Process for MODFLOW, which uses this method of estimating agricultural pumpage. Details of the model are found in *Chapter C* and *Appendix 1*.

For the 1962–2003 timeframe, the CVHM simulation indicates that average withdrawals from irrigation wells were about 8.6 million acre-ft/yr. Surface-water deliveries averaged 10.2 million acre-ft/yr (*table B1* and *fig. B1*). Hence, between 1962 and 2003, withdrawal from wells provided about 46 percent of the 18.8 million acre-ft of irrigation water required annually. As with recharge, annual surface-water deliveries and groundwater pumpage also vary with climatic variations. Typical, dry, and wet year surface-water deliveries were 11.3, 8.4, and 8.9, while agricultural groundwater pumpage was 7.9, 11.7, and 4.5 million acre-ft. Thus, even during wet years, about one-third of irrigation water is derived from groundwater pumpage. As expected, during drier years, this proportion increases.

Aquifer-System Storage

In the Central Valley, groundwater pumpage is the most significant human activity that affects the amount of groundwater in storage and the rate of discharge from the aquifer system (*table B2* and *figs. B1* and *B2*). A high concentration of broadly distributed wells and the multiple broadly distributed cones of depression have produced water-level declines across large areas (*fig. B4*). The principal areas of historical water-level changes prior to water year 1962 are shown in *figure B4A*. *Figure B4B* shows areas where additional changes in water levels have occurred between 1962 and 2003. In contrast to as much as 400 ft of drawdown since predevelopment, some areas of the San Joaquin Valley have recovered more than 300 ft since 1961, while others have had little recovery. Despite this recovery, the result of the changes in water levels since pre-development has been the extraction of millions of acre-ft of water from aquifer-system storage.

Storage of water within the aquifer system can be quantified in terms of the specific yield for unconfined groundwater flow, and the storage coefficient for confined flow, respectively. Specific yield represents gravity-driven dewatering of shallow, unconfined sediments at a declining water table, but also accommodates a rising water table. The specific yield is dimensionless and represents the volume of water released from or taken into storage per unit head change per unit area of the water table. Specific yield is a function of porosity and specific retention of the sediments in the zone of water-table fluctuation. Where the aquifer system is confined, storage change is governed by the storage coefficient, which is the product of the thickness of the confined-flow system and its specific storage. The specific storage is the sum of two component specific storages—the fluid (water) specific storage and the matrix (skeletal) specific storage, which are governed by the compressibilities of the water and skeleton, respectively (Jacob, 1940). Specific storage has units of 1 over length and represents the volume of water released from or taken into storage in a confined flow system per unit change in head per unit volume of the confined flow system. Therefore, the storage coefficient of a confined flow system is dimensionless and, similar to specific yield, represents the volume of water released from or taken into storage per unit head change.

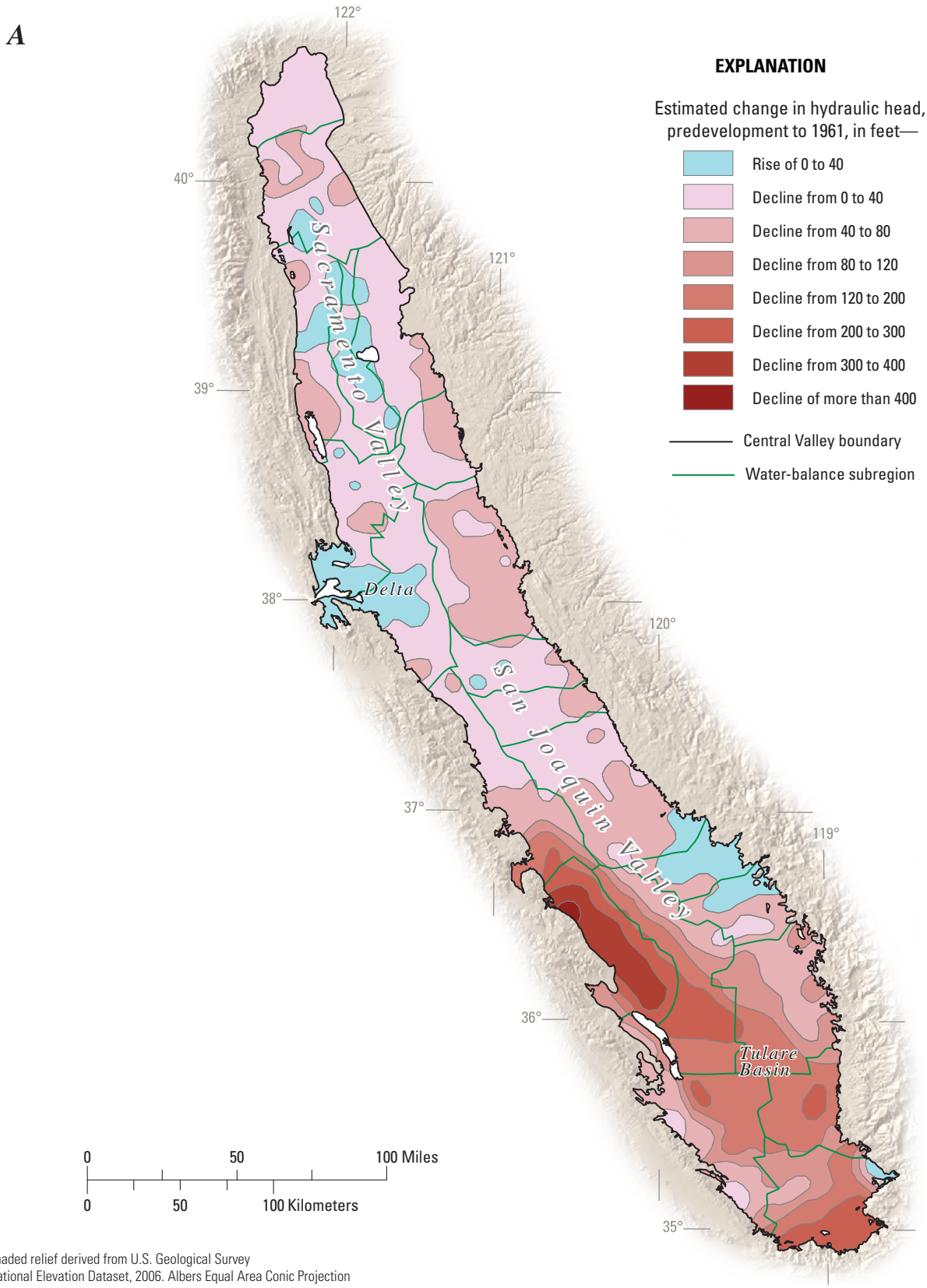

Figure B4. *A*, Estimated change in hydraulic head in upper part of the aquifer system from 1860 to 1961 (modified from Williamson and others, 1989; Bertoldi and others, 1991). *B*, Simulated change in hydraulic head in lower part of the aquifer system from spring 1962 to spring 2003.

B

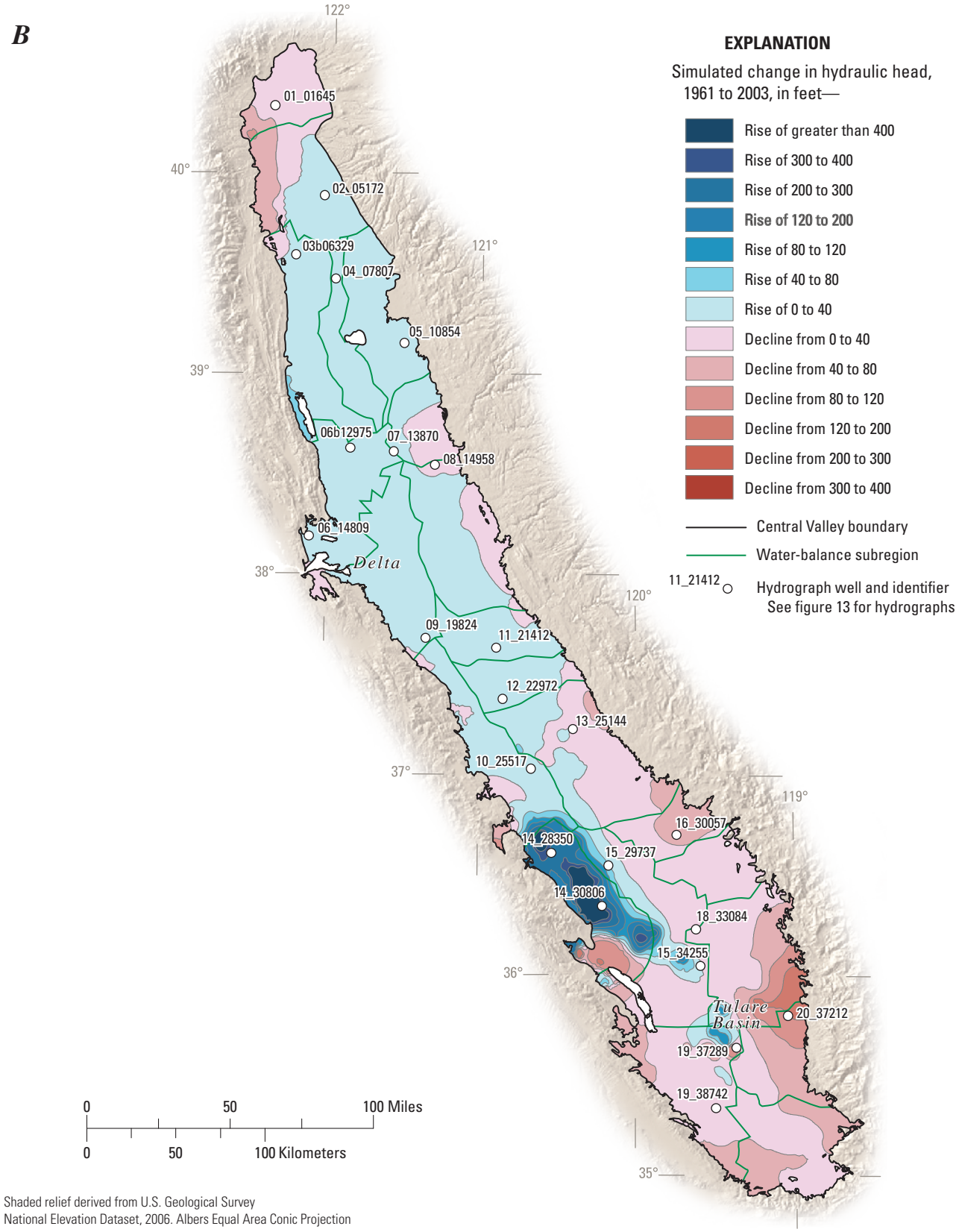

Shaded relief derived from U.S. Geological Survey National Elevation Dataset, 2006. Albers Equal Area Conic Projection

Figure B4. Continued.

Two skeletal compressibilities and, thereby, two skeletal specific storages and two storage coefficients can be further defined, one each for the elastic range of stress and one each for the virgin or inelastic range of stress. The elastic and inelastic stress ranges are defined by the previous maximum stresses imposed on the aquifer system (Terzaghi and Peck, 1948; Riley, 1969). The previous maximum stress can be expressed as a critical head—the previous minimum head, so that head changes in the stress range above the critical head (elastic stress range) result in elastic deformation (reversible compaction and expansion) of the aquifer system, and head declines in the stress range below the critical head (inelastic stress range) result in inelastic compaction (largely irreversible) of the aquifer system. A head decline below the previous critical head establishes a new critical head so that any subsequent head increase results in elastic expansion of the aquifer system.

This process governs the compaction of the aquifer system and the land subsidence that can accompany groundwater level declines in the Central Valley. Deformation of the aquifer system is proportional to the change in storage in the aquifer system. For confined flow systems in the elastic range of stress, the change in storage principally is governed by the elastic skeletal specific storage and the thickness of the aquifer system; and, in the inelastic range of stress, the change in storage principally is governed by the inelastic skeletal specific storage and the thickness of compressible fine-grained deposits in the aquifer system. In the Central Valley, the inelastic skeletal specific storage typically is 30 to several hundred times larger than the elastic skeletal specific storage (Ireland and others, 1984). Thus, depending on the thickness of fine-grained compressible deposits in the aquifer system, large storage changes and, thereby, significant amounts of permanent compaction and land subsidence, can accompany groundwater level declines below the critical head threshold. Hence, water released by the inelastic compaction of fine-grained deposits in the Central Valley aquifer system is a major source of water (*table B2*). Furthermore, the groundwater withdrawals have resulted in the permanent loss of storage capacity by the inelastic compaction of fine-grained sediments. This is discussed in more detail in the section of this report entitled "*Land Subsidence*."

Between 1962 and 2003, an average 9.1 million acre-ft of water went into storage annually, with an average removal from storage of about 10.5 million acre-ft/yr (*table B2* and *figs. B3* and *B4*). This average annual net loss in storage represents about 11 percent of net annual pumpage (*table B2*). In typical years, the average annual net loss in storage is about 1.4 million acre-ft. In dry years, about 9.0 million acre-ft of water are removed from storage, and during wet years more than 12.5 million acre-ft are returned to storage (*table B2*). Even though volumetrically, wet years exceed dry years in terms of changes in storage, overall water is being removed from storage.

Intra-Annual Variations in Typical, Dry, and Wet Years

Water use in the Central Valley varies seasonally and the sources of irrigation water vary greatly from season-to-season. Although some pumping occurs in all months, the vast majority of groundwater withdrawals occur during the spring-summer growing season (between March and September) (*fig. B5*), whether the climatic condition is dry, typical, or wet. In a typical year, almost 90 percent of groundwater is withdrawn in the spring-summer growing season and about 10 percent in the fall-winter dormant season (between October and February) (*fig. B5*).

Water typically is taken into storage during the wet winter months (December through March) and released from storage during the drier growing season (May through September) (*fig. B5A*). The timing and volume of these storage changes reflect the climatic regime (wet or dry year), groundwater pumpage, and the availability of precipitation and surface water (*fig. B5*). The spring-summer growing seasons relies on irrigation from groundwater pumpage and surface-water deliveries. The groundwater pumpage removes large amounts of water from storage in the aquifer system. This period of pumpage occurs when natural recharge rates are smallest, making the effects of pumpage largest during the spring-summer growing season. Although generally not as large of a volume as the pumpage, excess applied irrigation water recharges the shallow part of the aquifer during the growing season.

The relatively wet dormant period is a time of water-level recovery. During typical or wet years, the December through March period receives significant groundwater recharge (*fig. B5*). From year to year, whether the climate is dry, typical, or wet, significant groundwater recharge, mostly from precipitation, occurs in January and February. The vast majority of this recharge occurs in the Sacramento Valley. Even so, for the valley as a whole, there is little water removed from storage during the dormant period.

Water pumped from the aquifer system may not be quickly replenished. In some areas, particularly the wetter Sacramento Valley, groundwater that is pumped can be replenished annually during the non-irrigation season by recharge from precipitation and streams. In other areas, replenishment only occurs in years of abundant precipitation. Although urban land use may consume about an equivalent rate of water as agricultural land use, the timing of these withdrawals may be different. Hence, with land use shifting from agricultural to urban, the seasonal fluctuation of recharge and discharge may change. For example, in 1998, the relatively increased irrigation efficiency and large amount of evapotranspiration from groundwater overwhelms recharge in the spring-summer growing season (*fig. B5*).

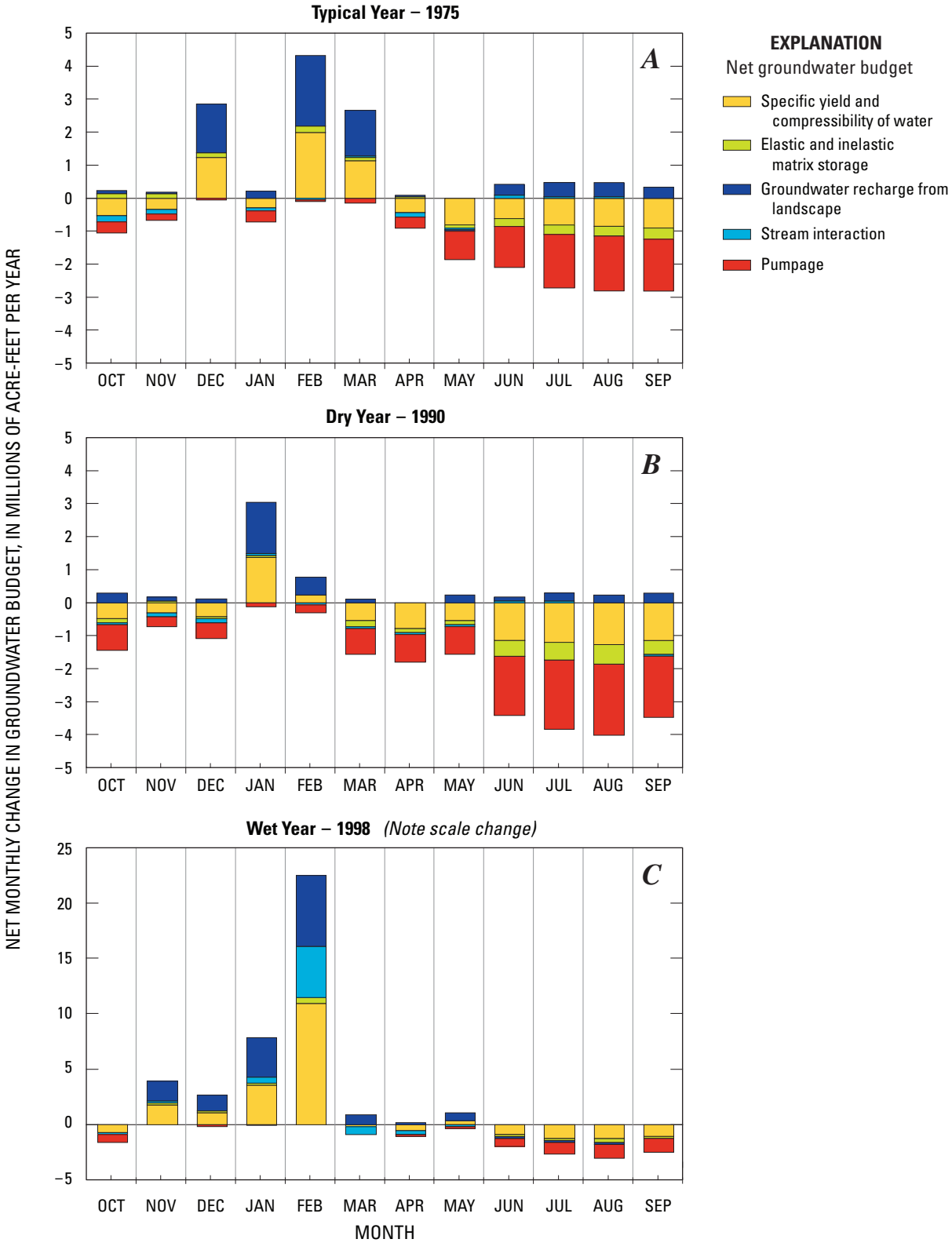

Figure B5. Monthly groundwater budget for the Central Valley for a dry year (1990), typical year (1975), and wet year (1998). Values are relative to water availability. Hence, an increase in storage is shown as a positive value.

Temporal Variation in the Hydrologic Budget

Hydrologic input and output to both the landscape and groundwater budgets, which vary through time, are represented in the 1962–2003 CVHM simulation. These variations predominantly are a result of the combined influences of climate variability, surface-water delivery systems, land-use changes, and farming practices. Climate variability can be seen in a graph of cumulative departure from average precipitation (*fig. A17*). In general, inflows of surface water follow the same climatic pattern as the precipitation (*fig. A16*). Since the second half of the 20th century, California experienced multiyear droughts in 1959–61, 1976–77, and 1987–92 (California Department of Water Resources, 1998). Based on climate variability, time periods can be classified as wetter periods, drier periods, and variations in between (*figs. A16* and *A17*). *Figure B6A* shows the classification of climate variability for water years 1962 through 2003 and the main components of the landscape system and their changes through time: delivery requirement (DR), landscape recharge, surface-water deliveries, and agricultural pumpage.

The DR fluctuates with changes in climate, land use, and farming practices. *Figure B6A* shows how the DR fluctuates with the climate. Warmer periods cause an increase in ET and, as a result, an increase in the demand for irrigation water. The 1976–77 and 1987–92 droughts show an increasing DR through each drought (*fig. B6A*). This partly is a result of an increase in potential ET, and partly a result of lowered water levels during each drought. When water levels drop too far, the plants that used to get all or part of their water from the water table must be irrigated. Overall, the wet period from 1978 through 1985 showed a gradual decrease in DR. In 1983, an extremely wet year, the DR decreased dramatically. The cooler wetter year caused many fields to flood. Where vegetation was growing, much of the demand was met by precipitation because the potential ET was lower. From 1993 through 1998, like the previous wet period, the DR decreased (*fig. B6A*). In this later wet period, the decrease was more dramatic. The decrease coincides with and likely is partially a result of changes in land use that, in many cases, included cultivation of more water-efficient crops and improved irrigation efficiencies.

Landscape recharge includes recharge from excess irrigation water as well as precipitation. Because of the large component of recharge from precipitation in the Sacramento Valley, landscape recharge shows the most direct correlation to the climate classifications (*fig. B6A*). During the droughts of 1976–77 and 1987–1992, the landscape recharge decreased. Superimposed on the climate effects is an inverse relation between landscape recharge and DR. The landscape recharge fluctuates inversely with the DR during the 1960s through the mid-1970s. The wet periods, 1978–1985 and 1993–1998, show larger magnitude landscape recharge fluctuations. Although not as dramatic as the decrease in DR because of the superimposed climatic effects, the agricultural pumpage shows a general decline in the 1990s. This decline most likely is a result of increased irrigation efficiencies.

The surface-water deliveries curve on *figure B6A* reflects the history of the surface-water delivery system, climate variability, and the DR. Abundant winter and spring precipitation are stored in reservoirs and released, as needed, to help control flooding and provide irrigation water. California's two largest water projects (CVP and SWP) form a complicated surface-water delivery system. This delivery system uses a series of reservoirs, streams, and canals to store and divert surface water throughout the valley. In particular, the system transfers the abundant water in the Sacramento and San Joaquin River systems south and southwest to drier parts of the valley (*fig. A7*). During the 1960s (*figs. B6* and *B7*), surface-water deliveries remained relatively constant. In the late 1960s, additional parts of the delivery system were completed and there was an increase in surface-water deliveries to the heavily irrigated Tulare Basin. The 1976–77 drought resulted in record low storage in surface reservoirs and a rapid decrease in surface-water deliveries (*fig. B6A*). Partly in response to the 1976–77 drought, there was an expansion of the delivery system and an increase in the importation of surface water on the west side of the San Joaquin Valley. The 1987–92 drought resulted in a decrease in surface-water deliveries to the lowest prolonged rate since the delivery system was put in place (*table B1* and *fig. B6A*). During and after this period, fiscal and environmental concerns slowed the development of new reservoirs. Nevertheless, except for the effects of climatic variability, on average the surface-water deliveries remained remarkably stable between 1962 and 2003.

On average, groundwater pumpage has decreased between 1962 and 2003. In general, groundwater pumpage is correlated directly to the DR because groundwater is used when surface water is not available. During the 1960s (*figs. B6* and *B7*), surface-water deliveries were relatively constant and groundwater pumpage fluctuated with the DR.

Climatic variations and the resulting surface-water supply directly affect the demand and the amount of groundwater required to meet agricultural and urban water demands (*fig. B6A*). During wet periods and the first part of a drought, surface-water reservoirs can be used to supply water for irrigation. In the later part of a drought, water in storage in surface reservoirs is depleted and farmers turn to pumping groundwater. Therefore, dry periods generally lead to increased pumping from wells. This is particularly apparent in severe short droughts or later periods of prolonged droughts. The groundwater pumpage in 1977 and 1990–1992 exemplify this increase in groundwater pumpage (*fig. B6A*).

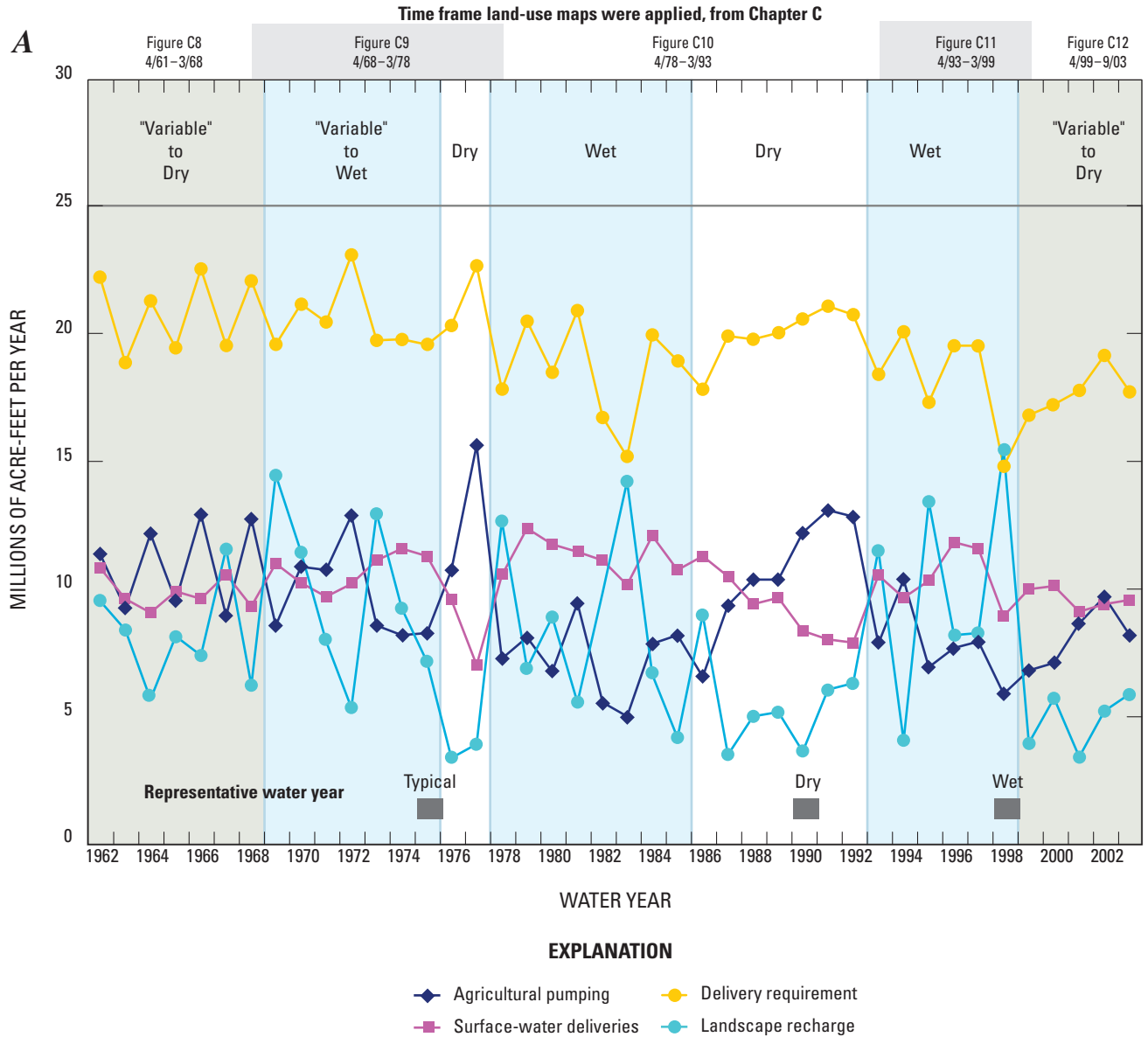

Figure B6. *A,* Annual delivery requirement, landscape recharge, surface-water deliveries, and agricultural pumpage. *B,* Annual groundwater withdrawals for agricultural and urban use for the entire Central Valley between 1962 and 2003. Other than urban pumpage, all values are simulated by the Central Valley Hydrologic Model (CVHM) (*Chapter C*). Urban pumpage compiled by California Department of Water Resources (C. Brush, California Department of Water Resources, written commun., February 21, 2007).

Figure B6B shows the relation of urban, agricultural, and total simulated pumpage during 1962–2003. In the last 40 years, millions of acre-ft/yr of water has been redistributed from agricultural production to urban and environmental uses (California Department of Water Resources, 1998; 2005). Between 1962 and 2003, withdrawals for urban uses ranged from 0.6 to 2.0 million acre-ft/yr. This pumpage for urban uses represents a steady increase from less than 5 percent in 1962 to about 30 percent in the late 1990s to early 2000s of the groundwater pumped in the Central Valley (*fig. B6B*). On average, 12 percent (1.2 million acre-ft/yr) of the withdrawals were for urban uses (*tables B1* and *B2* and *fig. B6B*).

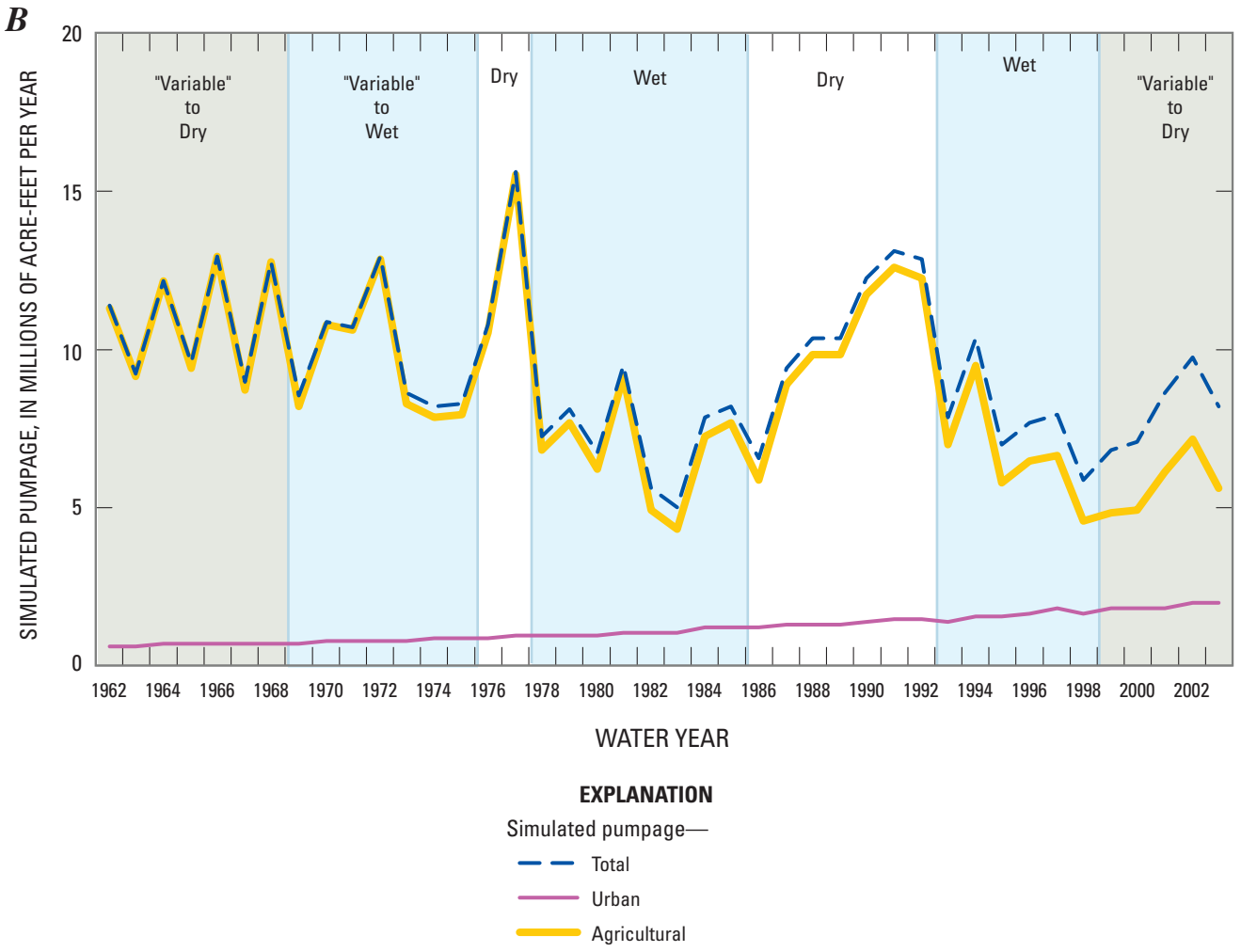

Figure B6. Continued.

Changes in land use, agricultural practices, surface-water deliveries, and urban pumpage have affected the groundwater system. *Figure B7* shows the simulated net annual changes to the groundwater system between 1962 and 2003. *Figure B8* shows just the storage components of the simulated groundwater budget. The yellow bars on the charts show net changes in storage resulting from compressibility of water in confined parts of the aquifer system and specific yield in unconfined parts of the aquifer system (for example, the water table). The green bars show changes in storage resulting from both elastic and inelastic compaction. *Figure B9* shows the cumulative change in storage from 1962 through 2003 for the Central Valley as a whole and for the individual major basins.

During1962–78, water predominantly was removed from storage (*figs. B8* and *B9*). During the relatively dry period 1962–68, before much of the surface-water delivery system was available to the Tulare Basin, groundwater was pumped at a high rate from wells in the Tulare Basin. In the late 1960s, increased importation of surface water to the heavily irrigated Tulare Basin combined with the somewhat wetter-than-average climate caused groundwater pumpage to decline, water levels to recover, and many wells to be unused (*figs. B6A* and *B7*). Despite the increased importation of surface water, during 1969–75, water still was released from storage in the Tulare Basin. However, water was taken into storage in the Sacramento Valley and the Central Valley as a whole, partially as a result of the relatively wetter climate during this period (*figs. B8* and *B9*).

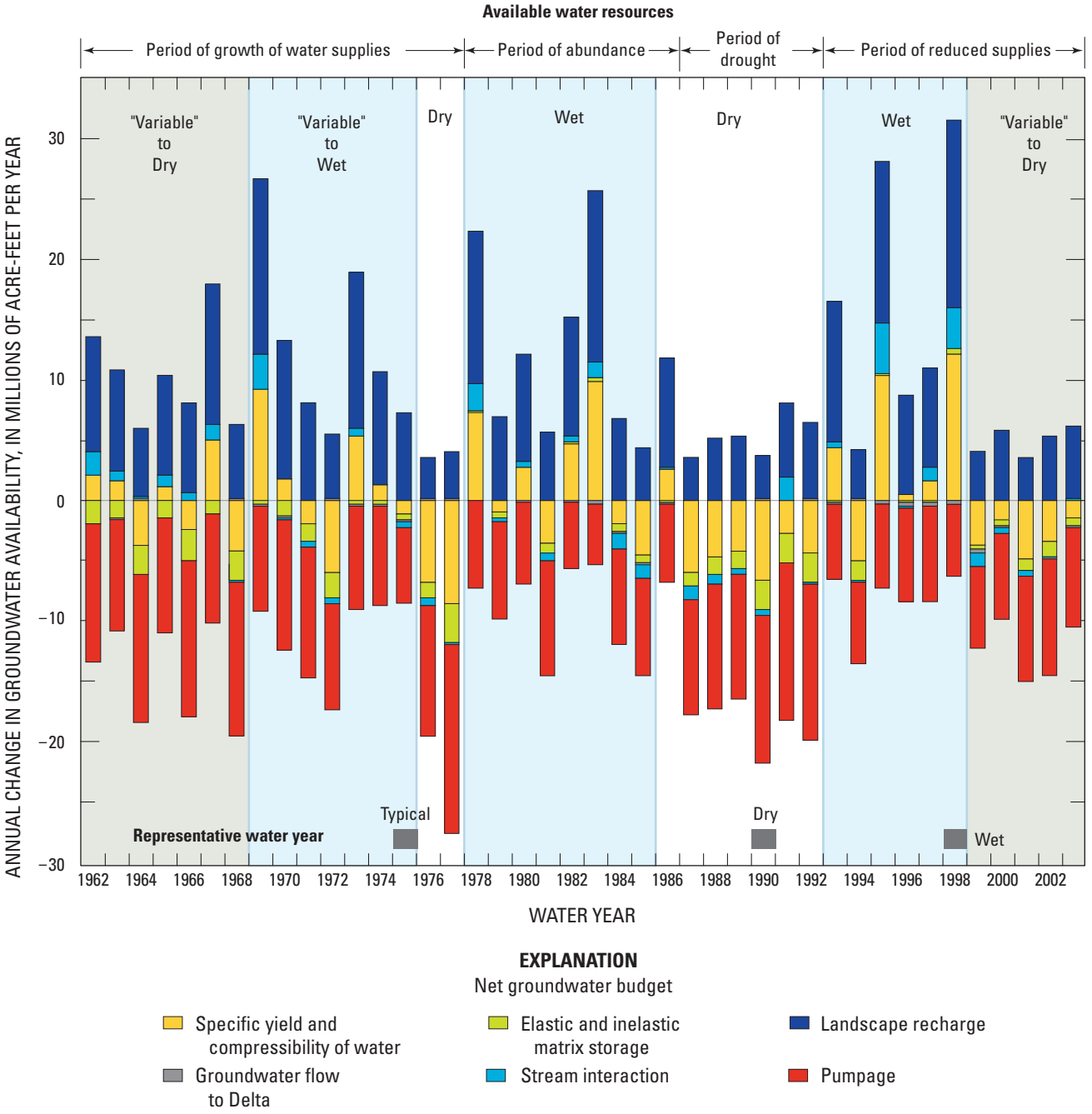

Figure B7. Simulated groundwater budget changes between water years 1962 and 2003 for the Central Valley, California.

The Central Valley's most severe recorded drought occurred during 1976–77. Two consecutive years of minimal precipitation (*fig. A8*) (fourth driest and the driest year in recorded history) resulted in record low storage in surface reservoirs and a rapid decrease in surface-water deliveries. This, in turn, caused an increase in groundwater pumpage and, as a consequence, extremely low groundwater levels. Socioeconomic and environmental impacts during these extreme drought conditions were severe (California Department of Water Resources, 2005). The simulated landscape and groundwater budgets reflect these drought conditions (*table B3*). During the 2-year drought, simulated recharge to the groundwater system reached a low of nearly 3.4 million acre-ft/yr, less than half of the average, and the simulated agricultural pumpage reached a high of 15.6 million acre-ft/yr (or about 1.7 times the average) (*fig. B6A*). Simulated surface-water deliveries (*fig. B6A*) reached an all-time low of 7.0 million acre-ft/yr; in turn, the percentage of irrigation water from groundwater peaked at 69 percent. This intense drought resulted in a large removal of water from storage. Through

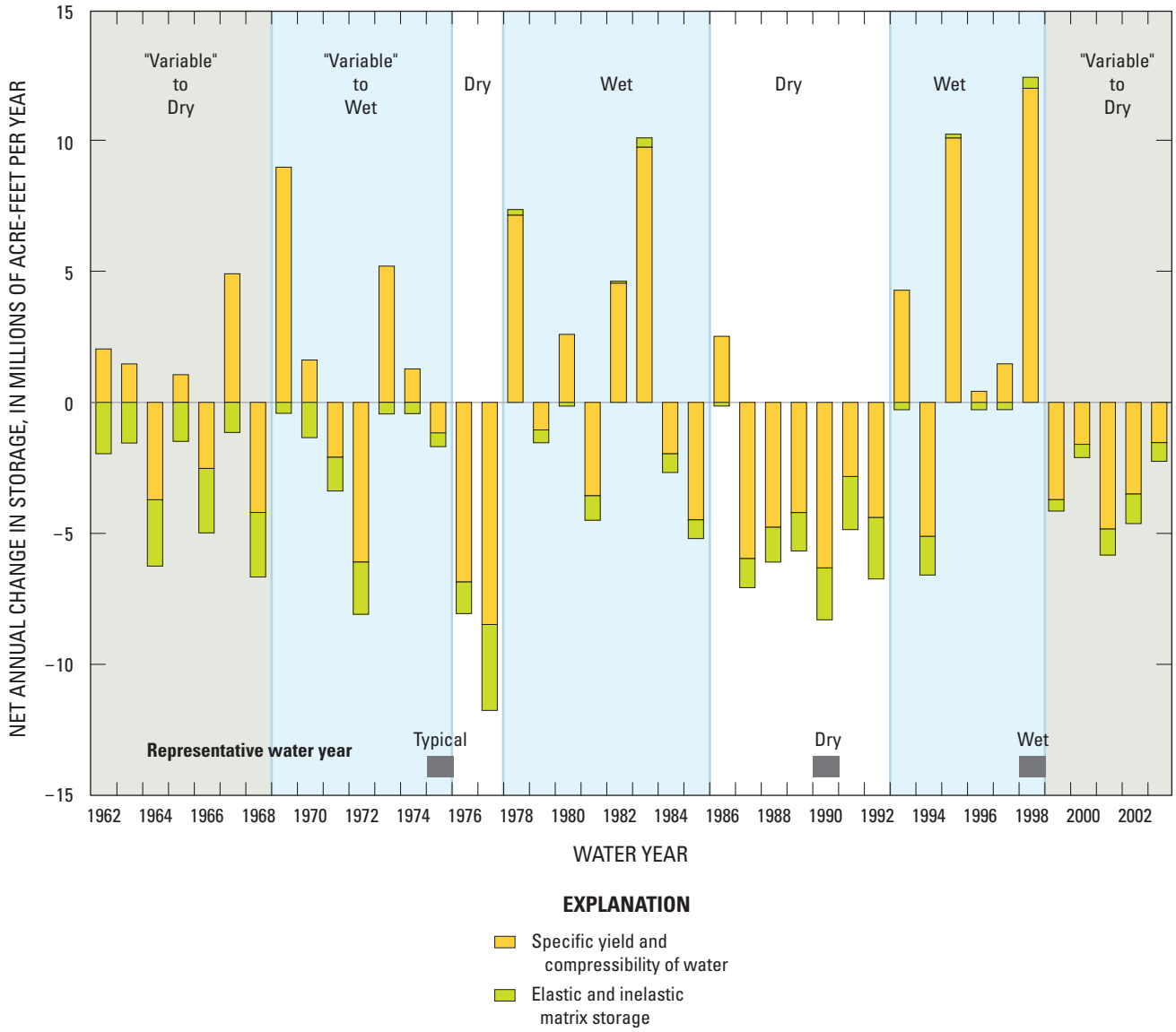

Figure B8. Simulated annual changes in aquifer-system storage between water years 1962 and 2003 for the Central Valley, California.

1977 the simulated cumulative loss in storage since 1962 was 33 million acre-ft with a total of 19.9 million acre-ft lost during these 2 extremely dry years, 1976–77 (*fig. B9*).

Between the droughts of 1976–77 and 1987–92, the climate was wetter and cropping patterns changed. During this period, the average irrigation efficiency increased from about 60 to 70 percent (California Department of Water Resources, 1994; 2005). This increase in irrigation efficiency is attributed largely to growers using more efficient drip and sprinkler irrigation as opposed to less efficient irrigation methods such as flood irrigation. Other improvements that contributed to the increased efficiencies include laser-leveling of furrow-irrigated fields, and shortening of furrows (particularly on large corporate farms). As an outcome, the DR decreased resulting in a reduction in applied water. Both surface-water deliveries and groundwater pumpage decreased (*fig. B6A*). Because groundwater pumpage decreased by a larger volume, the CVHM simulates the percentage of irrigation water met by groundwater pumpage reached a minimum of about 30 percent during the wet period from 1982 to 1983. With the reduced pumping rates, the simulation shows that local groundwater levels partially recovered, and depletion of groundwater storage virtually stopped. In years with more available water, significant volumes of water were taken into storage (*figs. B8* and *B9*). The CVHM simulates the amount of water entering storage during these 2 wetter years exceeded the amount removed by 14.8 million acre-ft.

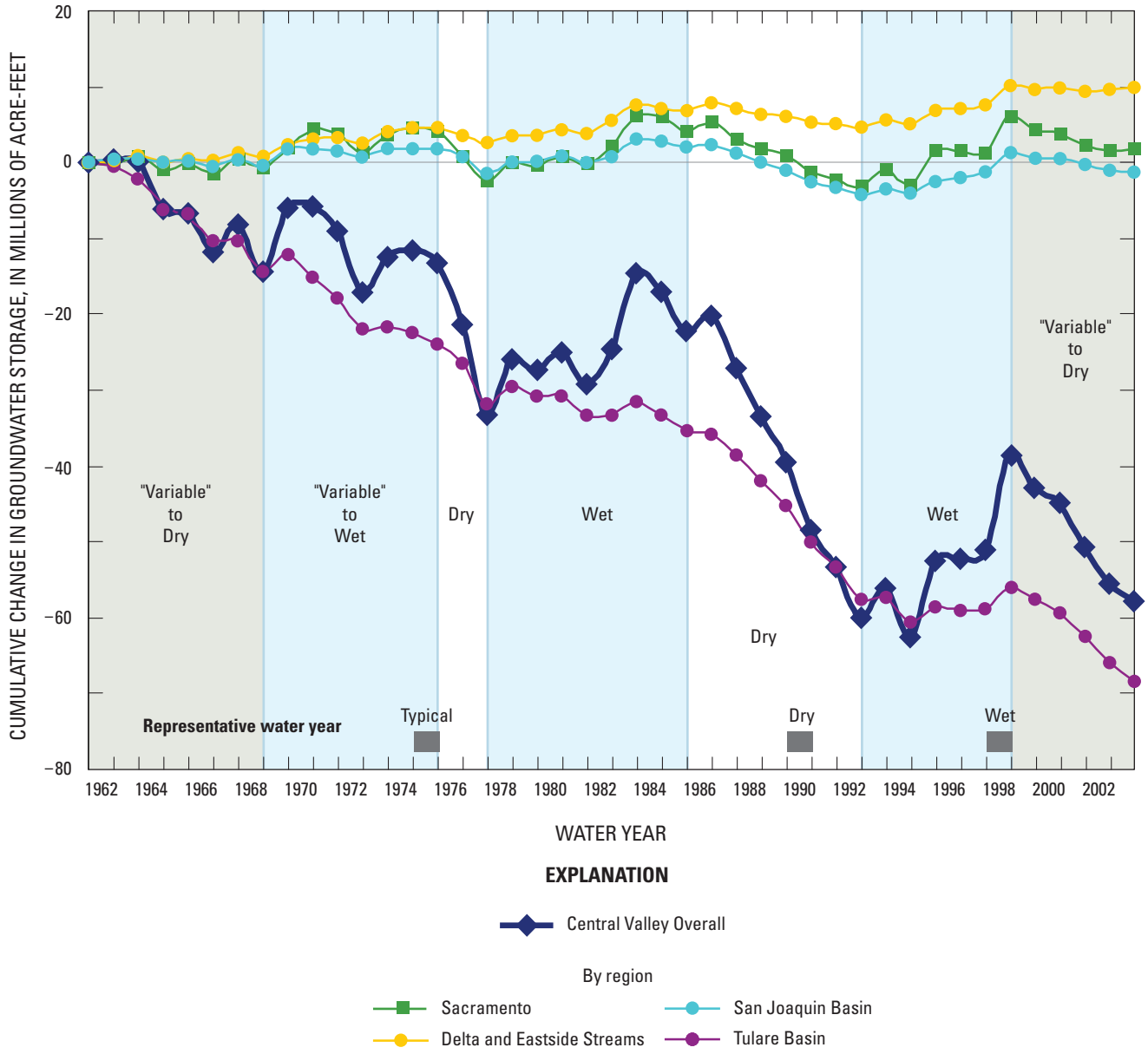

Figure B9. Simulated cumulative annual changes in aquifer-system storage between water years 1962 and 2003 for the Central Valley, California.

The 1987–92 drought was associated with increases in ET (*fig. A18*) and DR and a decrease in surface-water deliveries to the lowest prolonged rate in the study period (*table B1* and *fig. B6*). As a result, the CVHM shows that groundwater pumpage increased dramatically and exceeded surface-water deliveries (*fig. B6A*). Ultimately, pumpage increased to rates close to the 1970s levels. Although not as extreme as the 1970s, the CVHM shows that these high pumping rates continued for an extended period of time. During this prolonged drought, aquifer storage decreased at a dramatic rate, water levels declined, and subsidence briefly increased (*table B3* and *figs. B3*, *B8*, and *B9*). The CVHM simulates the cumulative change in storage reaching a maximum loss of 47.5 million acre-ft in the mid-1990s (*fig. B9*).

Between 1993 and 1998, with the return of a relatively wet climate, the CVHM simulates that surface-water deliveries increased, groundwater pumpage decreased, and except for 1994 surface-water deliveries, exceeded groundwater pumpage (*fig. B6*). Similar to the period between the previous droughts, groundwater levels partially recovered and approximately 24.3 million acre-ft of water returned to storage (*fig. B9*). During 1999–2003, with stable surface-water deliveries, more efficient irrigation systems, changes to lower-water-use crops, and overall relatively moderate-to-wet climate, the total average agricultural pumpage decreased to about 5.7 million acre-ft/yr (*fig. B6A*). Despite the relatively wet climate during this period, the decrease in excess irrigation water resulted in one of the lowest landscape recharge

Table B3. Selected average annual hydrologic budget components for water years 1962–2003 for each of the 21 water balance areas in the Central Valley, California.

[Values in acre-feet; totals may not sum because of rounding]

Water-balance subregion	Area (square miles)	Net storage from specific yield and compressibility of water[1]	Net elastic and inelastic storage[1]	Net stream leakage[2]	Net pumpage	Net recharge from landscape[3]	Precipitation	Evapotranspiration	Surface-water deliveries
1	611	36,000	13,000	–144,000	45,000	453,000	1,063,000	547,000	46,000
2	1,163	–17,000	23,000	–294,000	557,000	768,000	1,496,000	1,269,000	129,000
3	1,112	–39,000	3,000	–212,000	49,000	508,000	1,125,000	1,300,000	717,000
4	560	–34,000	0	–494,000	6,000	–19,000	562,000	635,000	78,000
5	957	–34,000	–1,000	–200,000	65,000	466,000	1,200,000	1,101,000	439,000
6	1,044	–47,000	10,000	34,000	506,000	522,000	1,137,000	1,315,000	329,000
7	534	2,000	4,000	–38,000	186,000	222,000	590,000	512,000	172,000
Sacramento Valley	**5,981**	**–99,000**	**52,000**	**1,348,000**	**1,414,000**	**2,920,000**	**7,173,000**	**6,6799,000**	**1,910,000**
Eastside Streams (8)	**1,362**	**–26,000**	**7,000**	**95,000**	**850,000**	**721,000**	**1,365,000**	**1,444,000**	**205,000**
Delta (9)	**1,026**	**–218,000**	**3,000**	**705,000**	**467,000**	**–200,000**	**975,000**	**1,603,000**	**64,000**
10	1,083	–36,000	29,000	64,000	60,000	89,000	588,000	1,465,000	983,000
11	664	–21,000	0	–98,000	85,000	251,000	509,000	901,000	643,000
12	540	–56,000	1,000	39,000	45,000	131,000	384,000	702,000	440,000
13	1,648	43,000	67,000	163,000	754,000	474,000	1,092,000	2,233,000	936,000
San Joaquin Basin	**3,935**	**–70,000**	**97,000**	**168,000**	**944,000**	**945,000**	**2,573,000**	**5,301,000**	**3,002,000**
14	1,071	179,000	165,000	6,000	934,000	418,000	432,000	1,631,000	716,000
15	1,423	26,000	146,000	239,000	1,603,000	708,000	607,000	2,225,000	757,000
16	478	89,000	35,000	33,000	202,000	212,000	299,000	518,000	358,000
17	569	54,000	28,000	170,000	445,000	348,000	358,000	852,000	442,000
18	1,358	158,000	198,000	104,000	1,135,000	710,000	715,000	2,237,000	821,000
19	1,365	85,000	133,000	0	754,000	334,000	494,000	1,275,000	367,000
20	705	74,000	92,000	19,000	252,000	240,000	295,000	892,000	610,000
21	1,105	83,000	81,000	130,000	324,000	272,000	414,000	1,333,000	1,096,000
Tulare Basin	**8,074**	**748,000**	**878,000**	**701,000**	**5,649,000**	**3,188,000**	**3,614,000**	**10,963,000**	**5,167,000**
Total	**20,378**	**300,000**	**1,000,000**	**300,000**	**9,300,000**	**7,600,000**	**15,700,000**	**25,900,000**	**10,300,000**

[1]Positive values indicate water levels are rising and water is being taken into storage, and negative values indicate water levels are falling and water is being released from storage.

[2]Positive values indicate water is leaving the surface-water system and recharging the groundwater system, and negative values indicate water is entering the surface-water system and discharging from the groundwater system.

[3]Positive values indicate water is leaving the landscape system and is recharging the groundwater system, and negative values indicate water is leaving the landscape system, predominantly through evapotranspiration, and discharging from the groundwater system.

rates in the simulation period of 3.4 million acre-ft/year in 2001 (*figs. A9* and *B6A*). It is interesting to note that despite increased irrigation efficiency, surface-water deliveries remained relatively constant. Even though agricultural pumpage decreased (*fig. B6A*), about 19.1 million acre-ft of water was released from storage between 1999 and 2003 (*figs. B8* and *B9*). The loss of storage can be explained by a decrease in excess irrigation water (2001 was the lowest recharge rate in the simulation period) resulting from increased urban pumpage, more efficient farming practices, and (or) decreased recharge from below-median precipitation.

In the Central Valley as a whole, the simulated magnitudes of the stream gains and losses generally are small and are similar from year to year. Principally during wet or variable-to-wet periods, streams lose water to the groundwater system. During dry and the 1998–2003 variable-to-dry periods, streams generally gain water from the groundwater system (*table B2* and *fig. B7*).

Likewise, in the Central Valley as a whole, during 1962–2003 there was a simulated net release of water from aquifer-system storage (*fig. B8*) and accompanying groundwater level declines (*fig. B4*). Simulated withdrawals from storage occur during most years. During years when more precipitation and imported surface water is available for irrigation, agricultural pumpage decreases and groundwater recharge is taken into storage (*fig. B7*). The difference between simulated annual groundwater recharge and discharge for the period 1962–2003 indicates a net loss of 57.7 million acre-ft from aquifer-system storage (*fig. B9*, *table B3*).

Spatial Variation in the Hydrologic Budget

The hydrologic budget for the Central Valley varies spatially (*figs. B9* and *B10*, and *table B3*). Precipitation is much larger in magnitude and is a larger percentage of recharge in the Sacramento Valley than in the southern areas of California (*table B3*). Likewise, streamflow interaction is a much larger percentage of the budget in the Sacramento Valley than the San Joaquin Valley *(fig. B10*). More agriculture and irrigation occur in the warmer and drier San Joaquin Valley. Although some surface-water deliveries reallocate water within the Sacramento Valley, the deliveries predominantly are to the San Joaquin Valley, especially to the Tulare Basin. In addition to surface-water deliveries, the irrigation requirements necessitate substantial groundwater pumpage. On average, 68 percent of pumpage in the Central Valley occurs in the San Joaquin Valley (11 percent from the San Joaquin Basin and 57 percent from the Tulare Basin). Groundwater recharge in the Sacramento Valley chiefly is from natural recharge (precipitation), whereas recharge in the San Joaquin Valley principally derives from excess applied irrigation water. However, on average, groundwater recharge in the Sacramento Valley volumetrically approximates recharge in the San Joaquin Valley.

The change in the amount of water in storage varies spatially because of the spatial variation in hydrologic stresses (*table B3* and *figs. B9* and *B10*). Somewhat surprisingly, the simulated and measured water levels indicate that water has been added to aquifer-system storage in and around the Delta and Eastside Streams *(fig. B10B)*. Volumetrically and historically, there has been very little overall change in storage in the Sacramento Valley (*fig. B10A*) and San Joaquin Basin (*fig. B10C*) (*table B3* and *fig. B9*). Conversely, despite the surface-water deliveries, a substantial amount of water has been removed from aquifer-system storage in the Tulare Basin (*table B2* and *figs. B9* and *B10D*). Changes in the amount of storage in each of the regions reflect the climate. During wetter periods there are increases in storage, and during drier periods there are decreases in storage. The magnitude of these changes is most evident in the Tulare Basin and most subdued around the Delta *(figs. B9* and *B10*). In the mid-1970s, there was a discernible reduction in the amount of pumpage on the west side of the San Joaquin Valley (Tulare Basin) because of increased availability of imported surface water for irrigation in that area. A general increase in storage occurs in the San Joaquin Basin, and relatively no change in storage in the Tulare Basin, from the mid 1970s until the 1987–92 drought when deliveries were curtailed (*fig. B9*). In addition, generally rising water levels also are evident in *figure B4B*.

Water Levels and Groundwater Flow

Groundwater levels and associated groundwater flows have responded to changes in the groundwater budget. Prior to development, the Central Valley aquifer system was driven by natural conditions in which natural discharge was in a long-term dynamic equilibrium with natural recharge, and longer-term changes in groundwater storage were negligible (Planert and Williams, 1995). Groundwater flowed from areas of higher altitude along mountain fronts to areas of discharge along rivers and marshes near the valley trough. Principally, this discharge occurred to the Sacramento and San Joaquin Rivers and Tulare Lake. Recharge predominantly was from rain and snowmelt in the mountains that became stream leakage at the valley margins in the northern and eastern parts of the valley. Precipitation falling on the valley floor was not consumed fully by ET, and some excess water infiltrated beyond the root zone, recharged the water-table, and subsequently flowed toward the rivers and surrounding marshes. At the valley margins the hydraulic gradient was downward—hydraulic head in the shallow part of the aquifer system was greater than the head in the deeper parts of the system; thus, groundwater moved downward. Conversely, the hydraulic gradient was upward in discharge areas near the valley trough, where water typically moved upward to discharge in rivers and marshes. Groundwater that was not evaporated or transpired by plants discharged either into the Sacramento and the San Joaquin Rivers that drained to the Delta or into the closed Tulare Basin from which it was consumed by ET (Planert and Williams, 1995). Most of the water in the San Joaquin Valley moved laterally, but a small amount leaked upward through the intervening confining unit (Planert and Williams, 1995). Upward vertical flow to discharge areas from the deep confined part of the aquifer system was impeded partially by confining clay beds, particularly the Corcoran Clay Member of the Tulare Formation (hereafter referred to as the Corcoran Clay). Because of the higher head in the confined part of the system during the early years of groundwater development, flowing wells were drilled into the deep aquifer in low-lying areas near rivers and marshes. Large-scale groundwater development for both agricultural and urban uses has modified the groundwater levels and flow patterns, relative to predevelopment conditions (*fig. B4*). Groundwater flow has become more rapid and complex. Groundwater pumpage and application of excess irrigation water has resulted in steeper hydraulic gradients as well as shortened flow paths between sources and sinks.

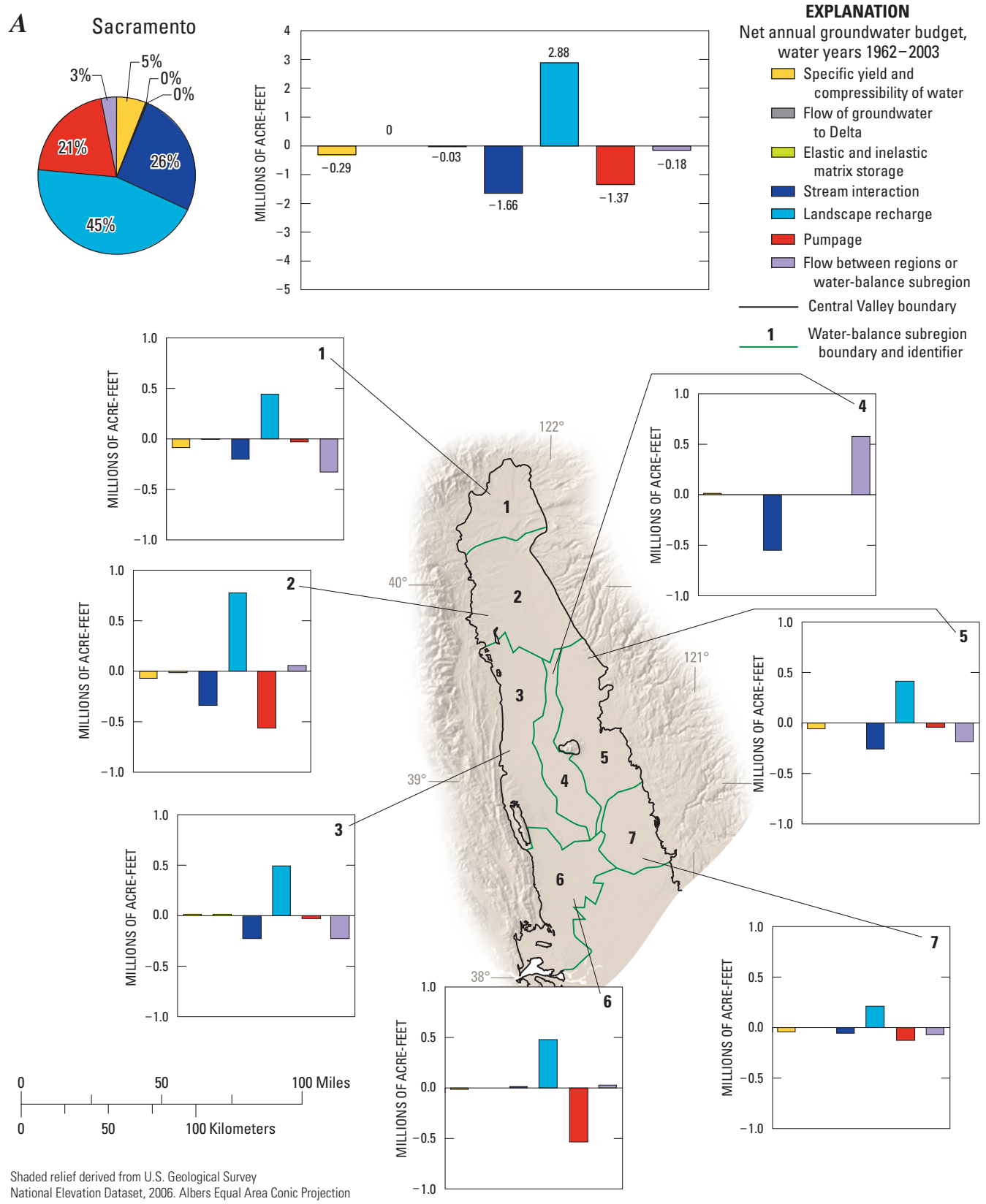

Figure B10. Average annual groundwater budget for the *A*, Sacramento Valley. *B*, Delta and Eastside Streams. *C*, San Joaquin Valley. *D*, Tulare Basin. Schematic bar charts of average annual groundwater budget for the 21 water-balance subregions (WBSs) in the Central Valley also are shown.

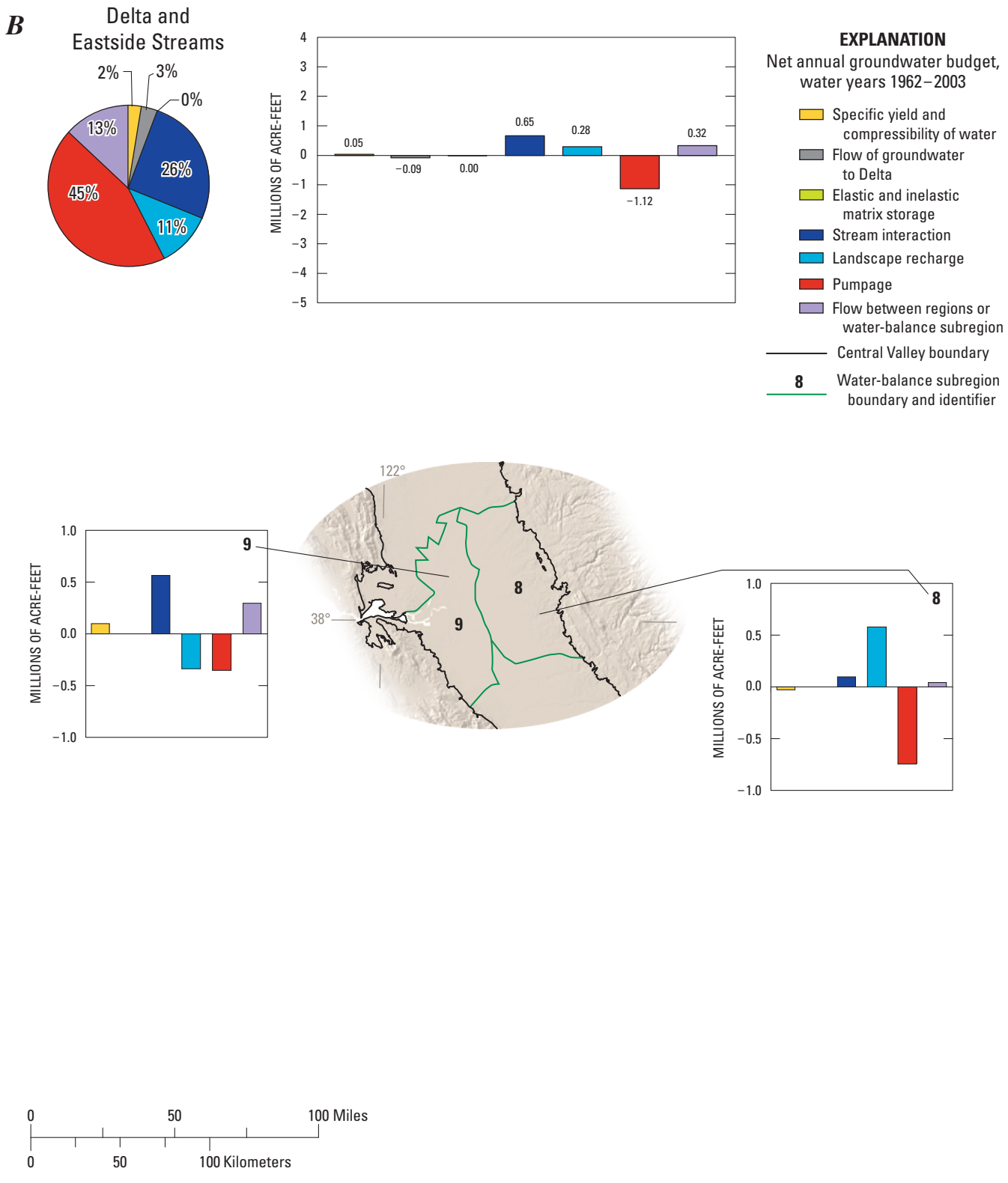

Shaded relief derived from U.S. Geological Survey National Elevation Dataset, 2006. Albers Equal Area Conic Projection

Figure B10. Continued.

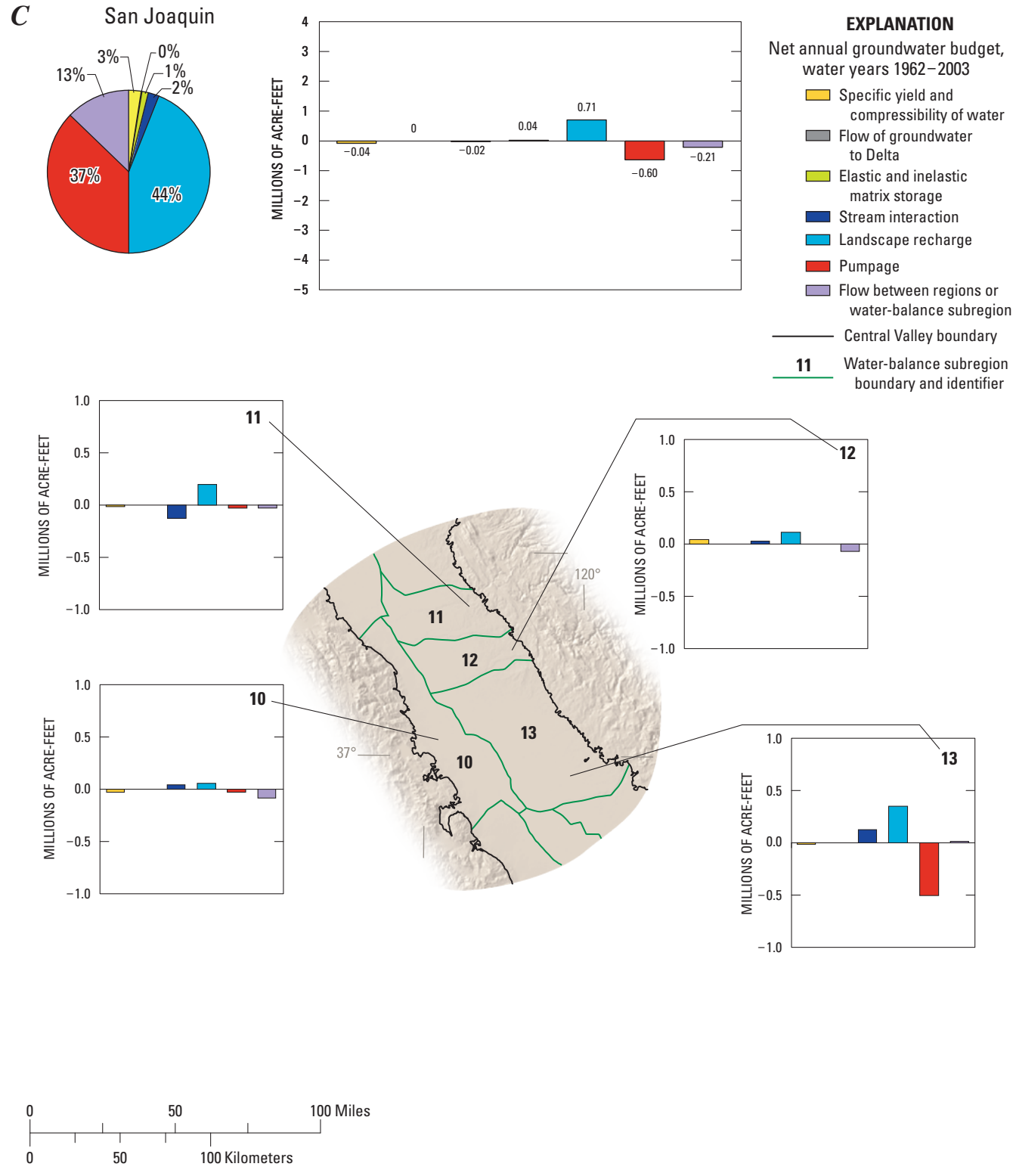

Shaded relief derived from U.S. Geological Survey National Elevation Dataset, 2006. Albers Equal Area Conic Projection

Figure B10. Continued.

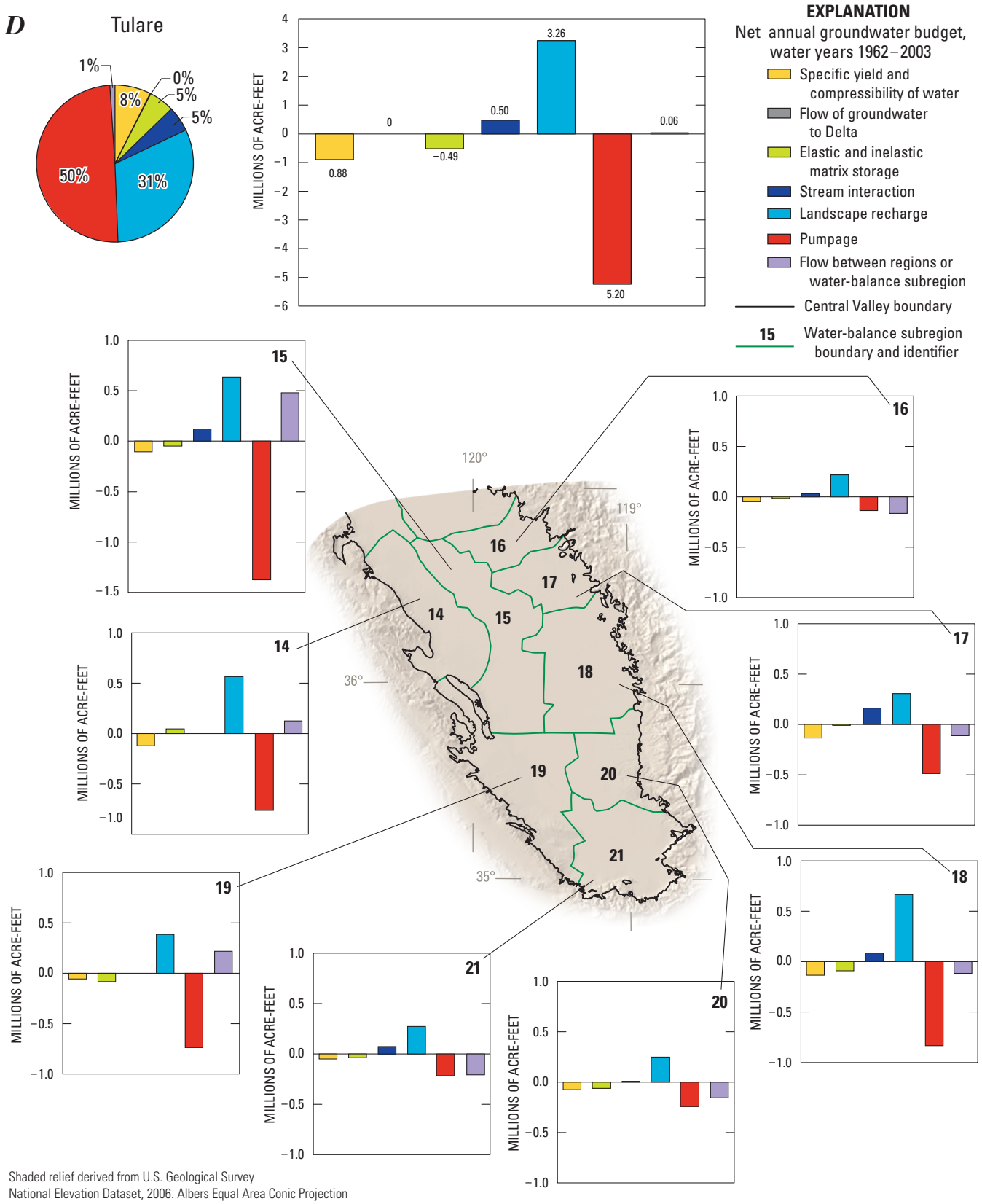

Shaded relief derived from U.S. Geological Survey
National Elevation Dataset, 2006. Albers Equal Area Conic Projection

Figure B10. Continued.

Well depths in the Central Valley are determined by the depth of permeable aquifer material and by the quality of the groundwater. In general, wells typically are less than 500 ft deep in the Sacramento Valley but are as deep as 3,500 ft in the San Joaquin Valley (Planert and Williams, 1995). The greater depth of well construction is necessitated by the low permeability of the unconfined part of the aquifer system in the western and southwestern San Joaquin Valley and the presence of highly mineralized water and water high in selenium in the upper parts of the aquifer system in the western San Joaquin Valley (Planert and Williams, 1995). The construction of about 100,000 irrigation wells, many of which have long intervals of perforated casing, has provided hydraulic connections between permeable zones within the aquifer system. Where these wells are open to the entire aquifer system, they allow flow through the boreholes (intra-borehole flow) between the shallow unconfined to semi-confined parts and the deep confined parts of the aquifer system. The resulting hydraulic connection, provided by these multi-zone wells, substantially increases the equivalent vertical hydraulic conductivity of the aquifer system, particularly the of the Corcoran Clay confining unit (*fig. B11*) (Page and Balding, 1973; Londquist, 1981; Williamson and others, 1989; Bertoldi and others, 1991; Gronberg and Belitz, 1992). The dramatic lowering of hydraulic heads in the confined parts of the aquifer system has resulted in a large, net downward movement of water through boreholes. This vertical flow through boreholes occurs in both pumped and non-pumped wells, and increases during the growing season and droughts when the hydraulic head gradient across the Corcoran Clay increases. The amount of water that flows downward through one large-diameter well is equivalent to the estimated natural leakage through the Corcoran Clay over an area of approximately 7 mi^2 (Williamson and others, 1989). If the multi-zone wells were absent, then the heads likely would adjust to accommodate the decreased vertical fluxes.

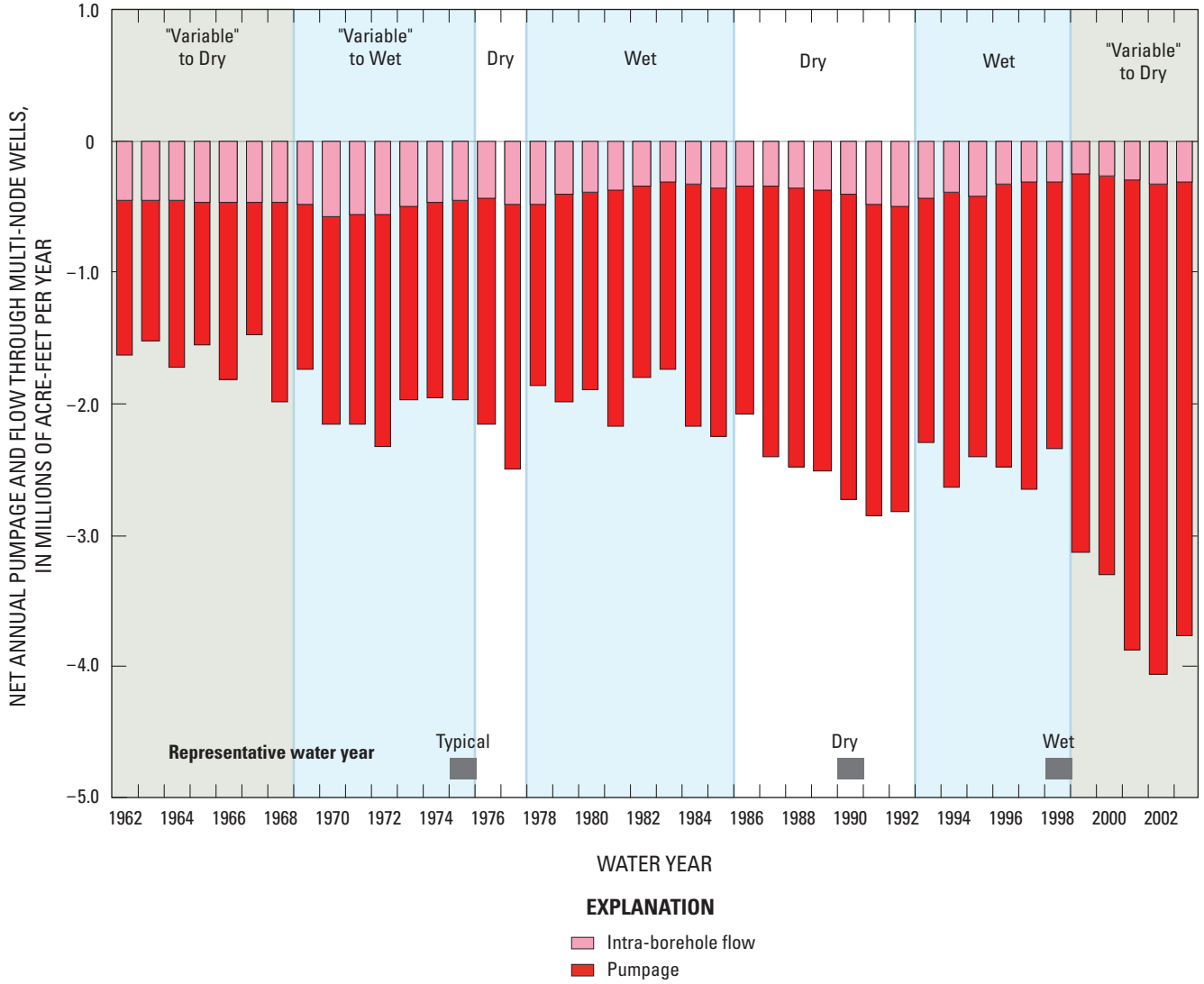

Figure B11. Simulated flow through multi-zone wells.

Between 1860 and the early 1960s, intensive groundwater development significantly lowered water levels and altered groundwater flow patterns. By the 1960s, excess irrigation water (predominantly from imported surface water) had become the dominant source of recharge. The rapid agricultural development and the associated increases in groundwater pumpage resulted in strong vertical head gradients, substantial vertical flow to wells pumping from the deeper part of the system, and significant head declines throughout the valley (*fig. B4A*). These areas of head declines often were widespread, attributable to the distributed pumpage for irrigated agriculture. The increased surficial recharge and groundwater withdrawal have increased vertical flow in the system. For example, water on a lateral flow path may be removed repeatedly by pumping and reapplied at the surface. By and large, the system still behaves this way. Water generally moves from irrigated areas toward pumping-induced broad head depressions in agricultural areas or toward cones of depression at urban pumping centers (Bertoldi and others, 1991). There still is a significant lateral and vertical component of flow toward the major rivers and streams where groundwater discharges to the surface-water system either along rivers and streams or in the Delta.

Three years; 1961, 1976, and 2000; were selected to show the configuration of the water table and potentiometric surface during the 1962–2003 period of study (*fig. B12*). The 1961 and 1976 maps were developed from measured data for the CV-RASA studies (Williamson and others, 1989) and the 2000 maps were developed from simulations developed for this study (*Chapter C*). The year 1961 represents the beginning of the study period, 1976 represents water levels for the early part of the study after the delivery of significant quantities of imported surface water had begun and prior to the intense 1976–77 drought, and 2000 represents more recent conditions. When compared, these potentiometric-surface maps show the cumulative effects of various combinations of pumpage, surface-water deliveries, and recharge from excess applied irrigation water from 1961 through 2003. Hydrographs from wells throughout the region show the changes through time *(fig. B13)*.

Changes to the system are both temporal and spatial in nature. Temporal variability of measured water levels generally is dominated on shorter time scales by the irrigation season and longer time scales by the natural climate. Simulations indicate that seasonal fluctuations reach several hundred feet in the deeper wells penetrating the confined part of the aquifer system on the west side of the San Joaquin Valley. Conversely, these fluctuations generally are less than 5 ft at the water table (*fig. B13*).

Adjacent to rivers, variability is dominated by river stage, and a combination of these factors influence water levels within about 1 mi of the rivers. Longer-term temporal variability predominately reflects the climate variability. The heads in the confined part of the aquifer system have varied significantly from year to year in some areas, declining in years of greater-than-average groundwater pumpage and recovering in years of reduced pumpage (*fig. B13*). Data from wells (*fig. B13*, wells 02_05172, 06b12975, 14_30806, 15_29737, and 19_37289) show that vertical hydraulic gradients from the water table to the deeper production zones associated with the major alluvial fans are strongly downward and larger during the spring-summer growing season than during the fall-winter dormant period. As one moves from the edges of the valley toward the valley trough, the gradients reverse. Under the valley trough, the gradient is in an upward direction (*fig. B13*, wells 04_07807, 15_34255). Over the Central Valley as a whole, the water levels in the water table wells (in general, this is layers 1 through 3 on *fig. B13)* remain fairly constant during the 1962–2003 period, with some fluctuations in intensively irrigated or pumped areas *(figs. B12A, B12C,* and *B13*).

By 1961, pumpage lowered water levels in the Sacramento Valley by 30–80 ft in the areas between major tributaries flowing from the Sierra Nevada (*fig. B4A*). In addition, water-level changes between 1860 and 1961 show a pumping center just north of the Delta. Similar water-level declines occur between the tributaries on the northeastern side of the San Joaquin Valley (*fig. B4A*). In general, water levels have declined slightly in the Sacramento Valley between 1962 and 2003 *(figs. B4B* and *B13*). Water levels have declined the most in the Sacramento and Stockton urban areas (*figs. B4B*, *B12B*, and *B12F*). Water levels have risen slightly in the area around the Delta. Much of this water-level rise is remediated by pumping local groundwater into a series of drainage canals.

In 2000, groundwater in the Central Valley generally was within 50 ft of the land surface in the northern, central, and western areas of the valley floor (*fig. B14*). In the San Joaquin Valley, the area where water was within 50 ft of land surface generally coincided roughly with the area of predevelopment flowing wells. The groundwater table generally is deeper along the southern and eastern margins of the valleys where generally coarse-grained alluvial fans allow the rapid infiltration of surface water and of any available precipitation (*fig. B14*). The western margin of the San Joaquin Valley has similar deeper water tables not shown at the scale of *fig. B14*.

A

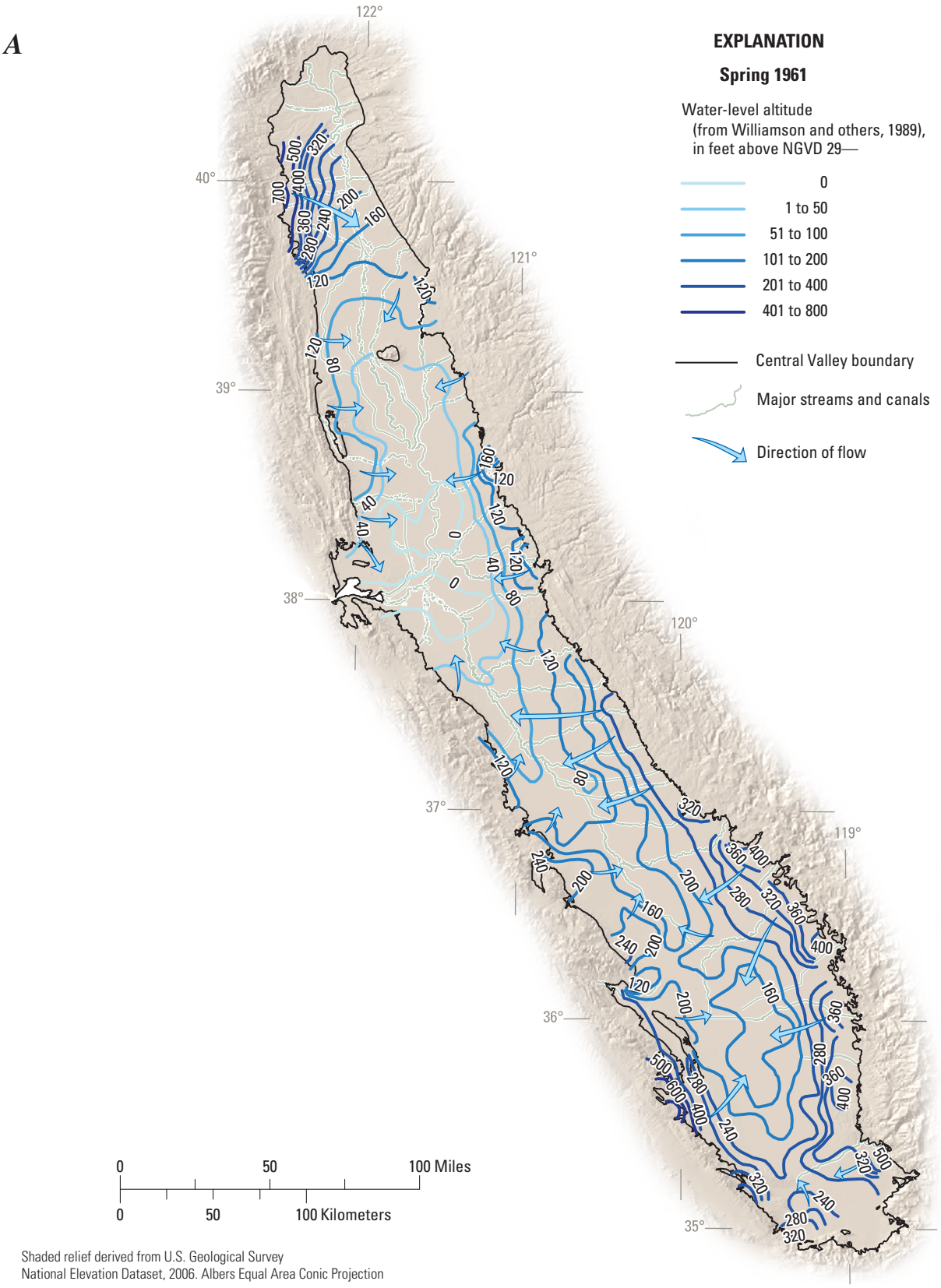

Figure B12. Altitude of the *A,* Water table in the unconfined part of the aquifer system (Williamson and others, 1989). *B*, Potentiometric surface of the confined part of the aquifer system for 1961 (Williamson and others, 1989). *C*, Unconfined part of the aquifer system (Williamson and others, 1989). *D*, Potentiometric surface of the confined part of the aquifer system for 1976 (Williamson and others, 1989. *E,* Unconfined part of the aquifer system (simulated, *Chapter C*). *F*, Potentiometric surface of the confined part of the aquifer system, for 2000 (simulated, *Chapter C*).

B

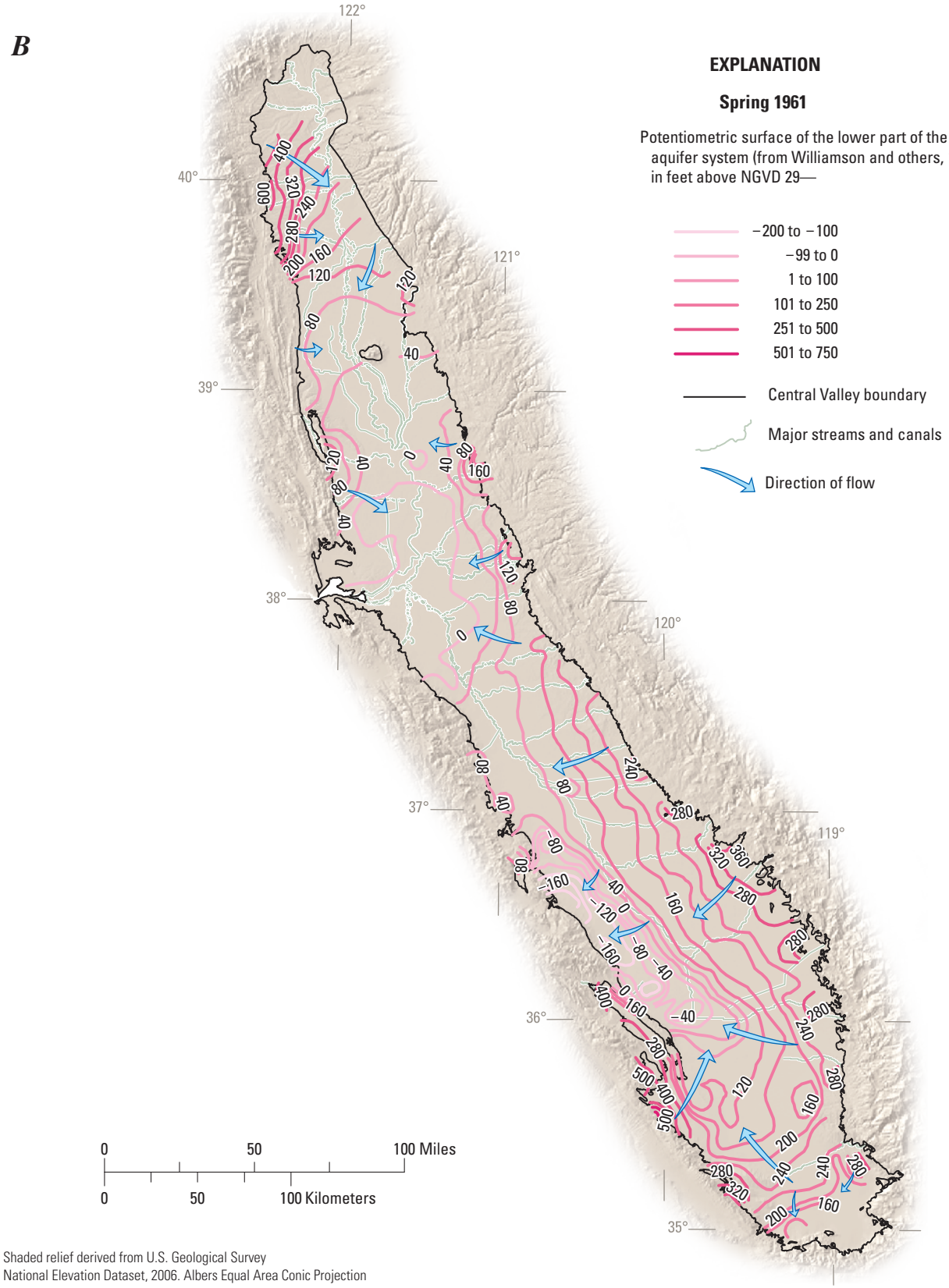

Figure B12. Continued.

C

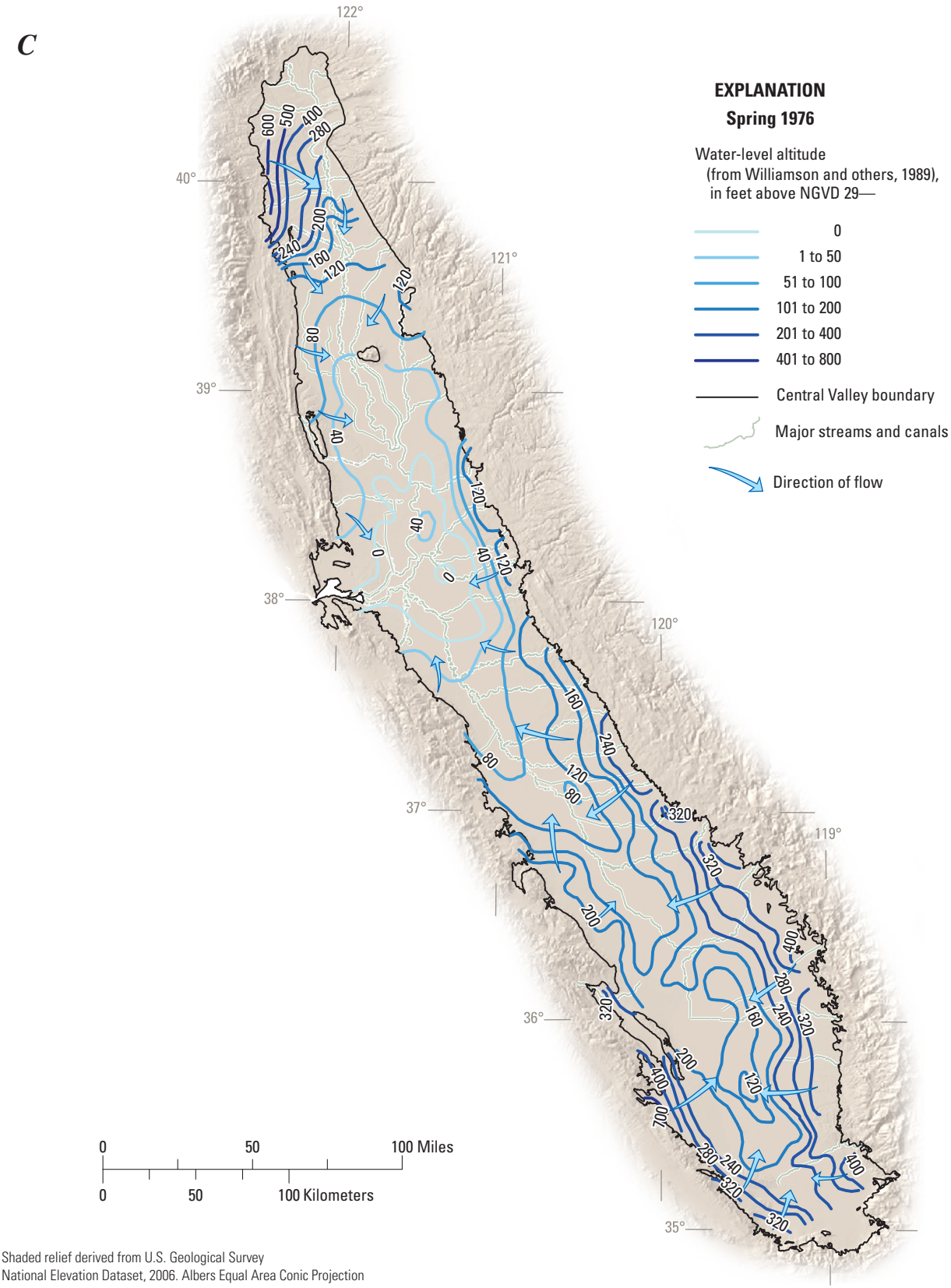

Shaded relief derived from U.S. Geological Survey
National Elevation Dataset, 2006. Albers Equal Area Conic Projection

Figure B12. Continued.

D

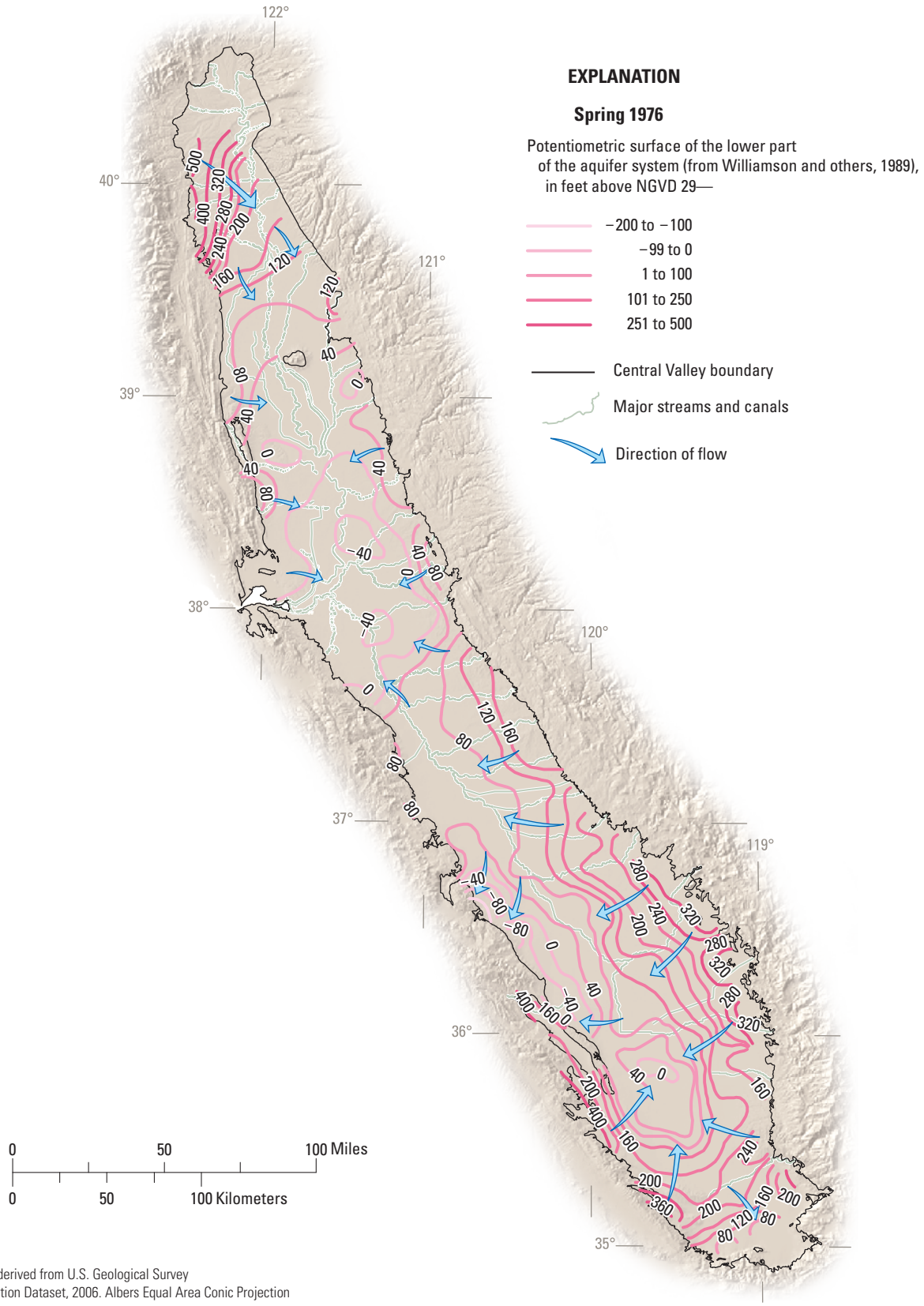

Figure B12. Continued.

E

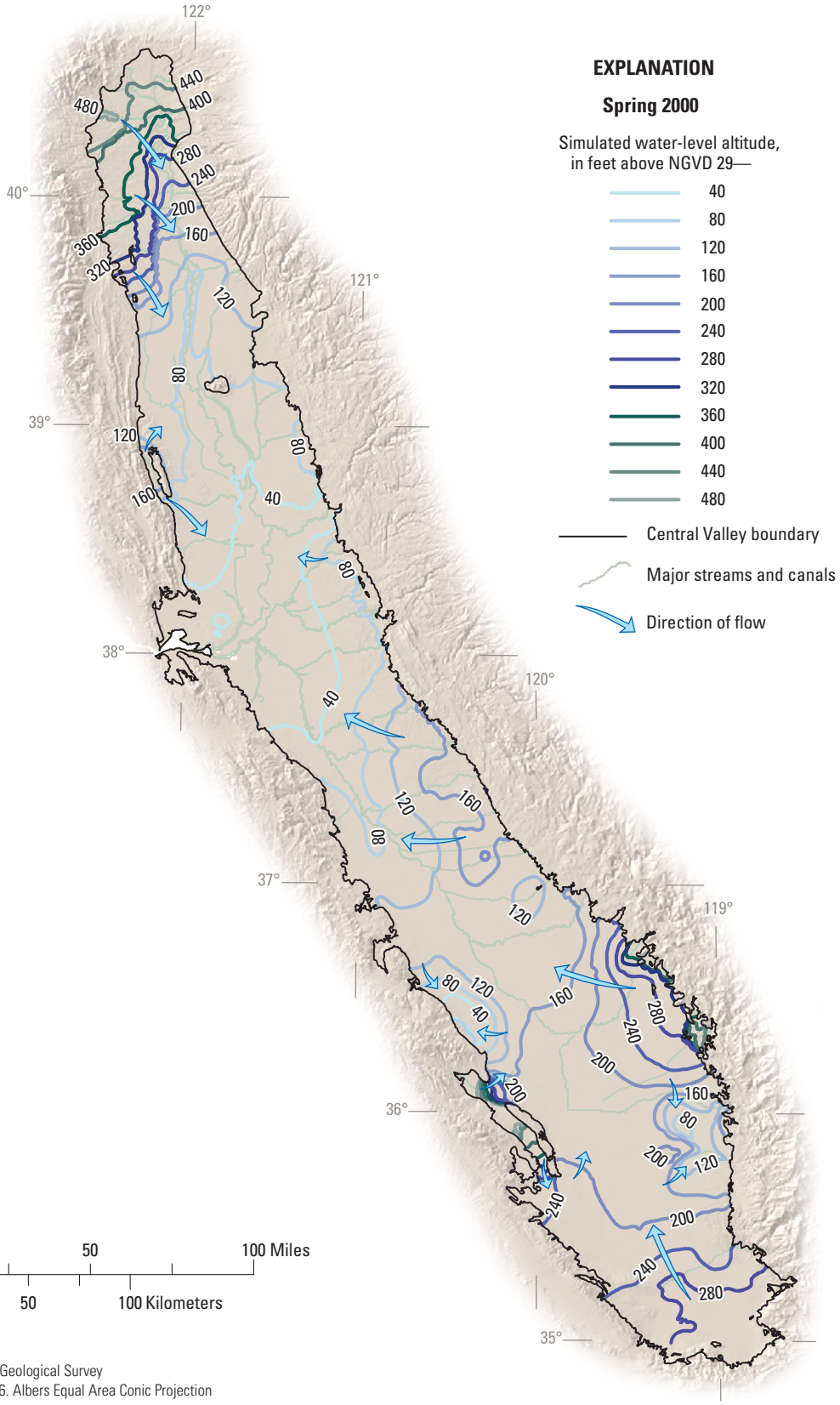

Shaded relief derived from U.S. Geological Survey National Elevation Dataset, 2006. Albers Equal Area Conic Projection

Figure B12. Continued.

F

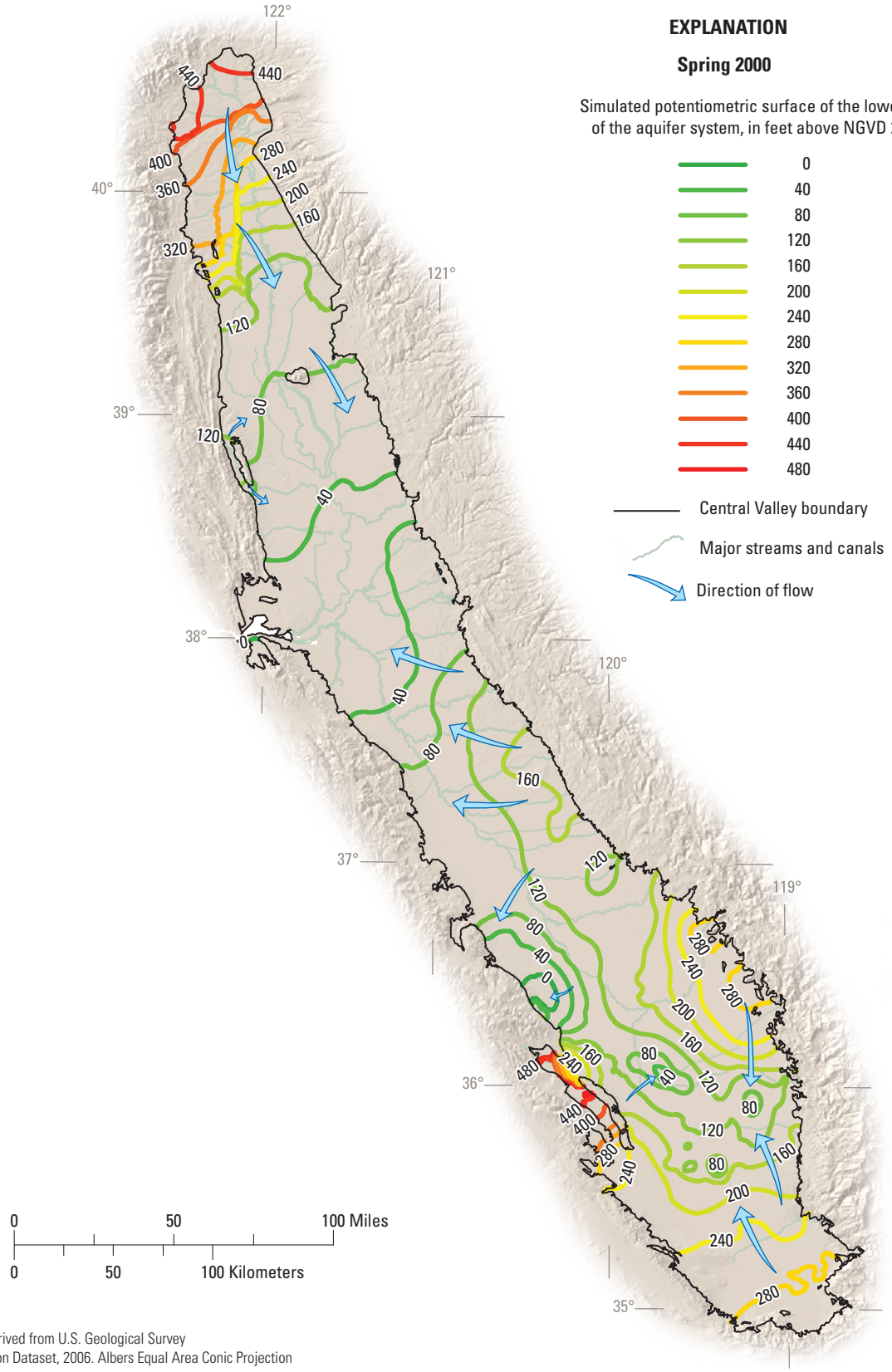

Shaded relief derived from U.S. Geological Survey National Elevation Dataset, 2006. Albers Equal Area Conic Projection

Figure B12. Continued.

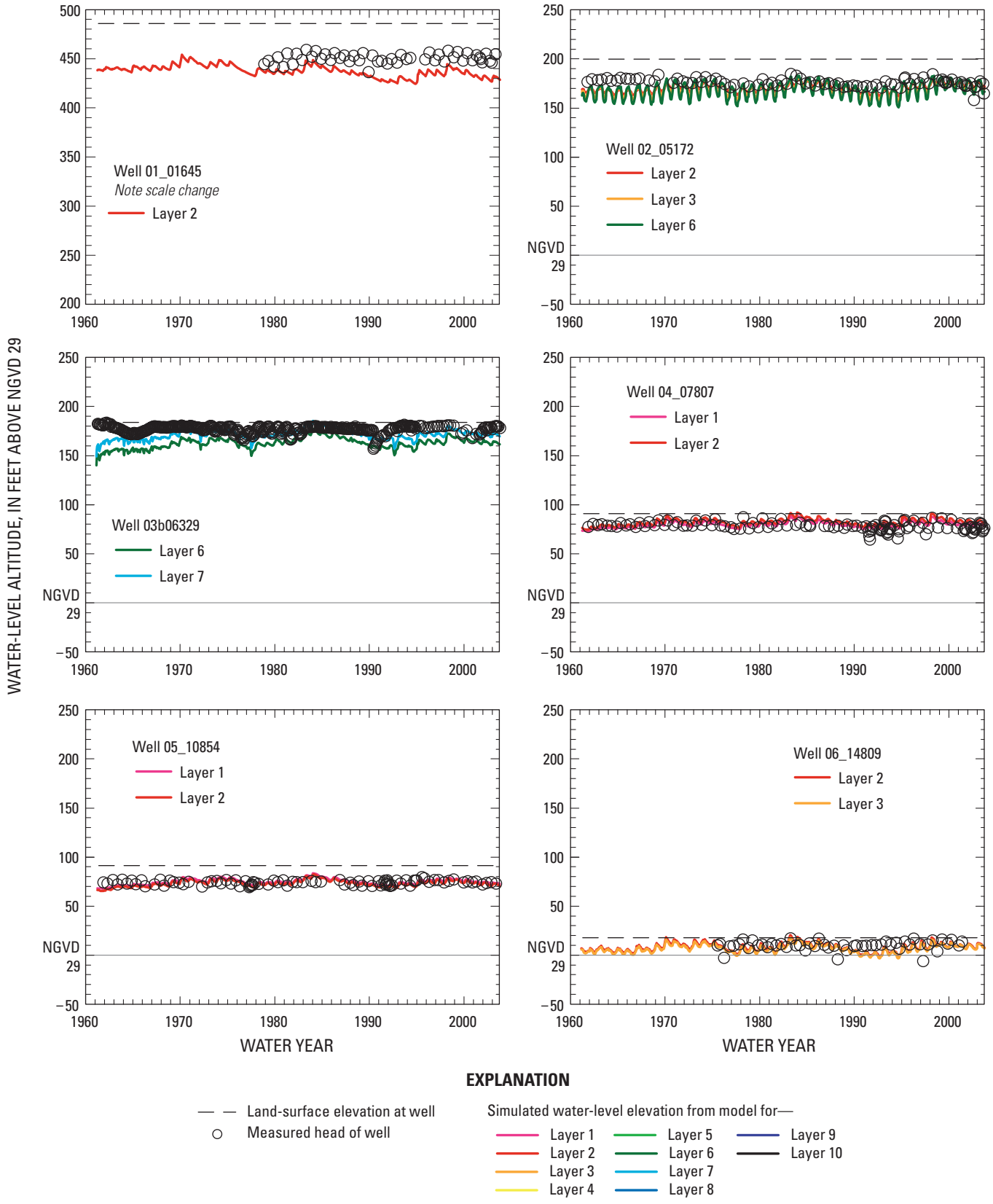

Figure B13. Hydrographs for representative wells in the Central Valley, California (locations shown in *figure B4B*).

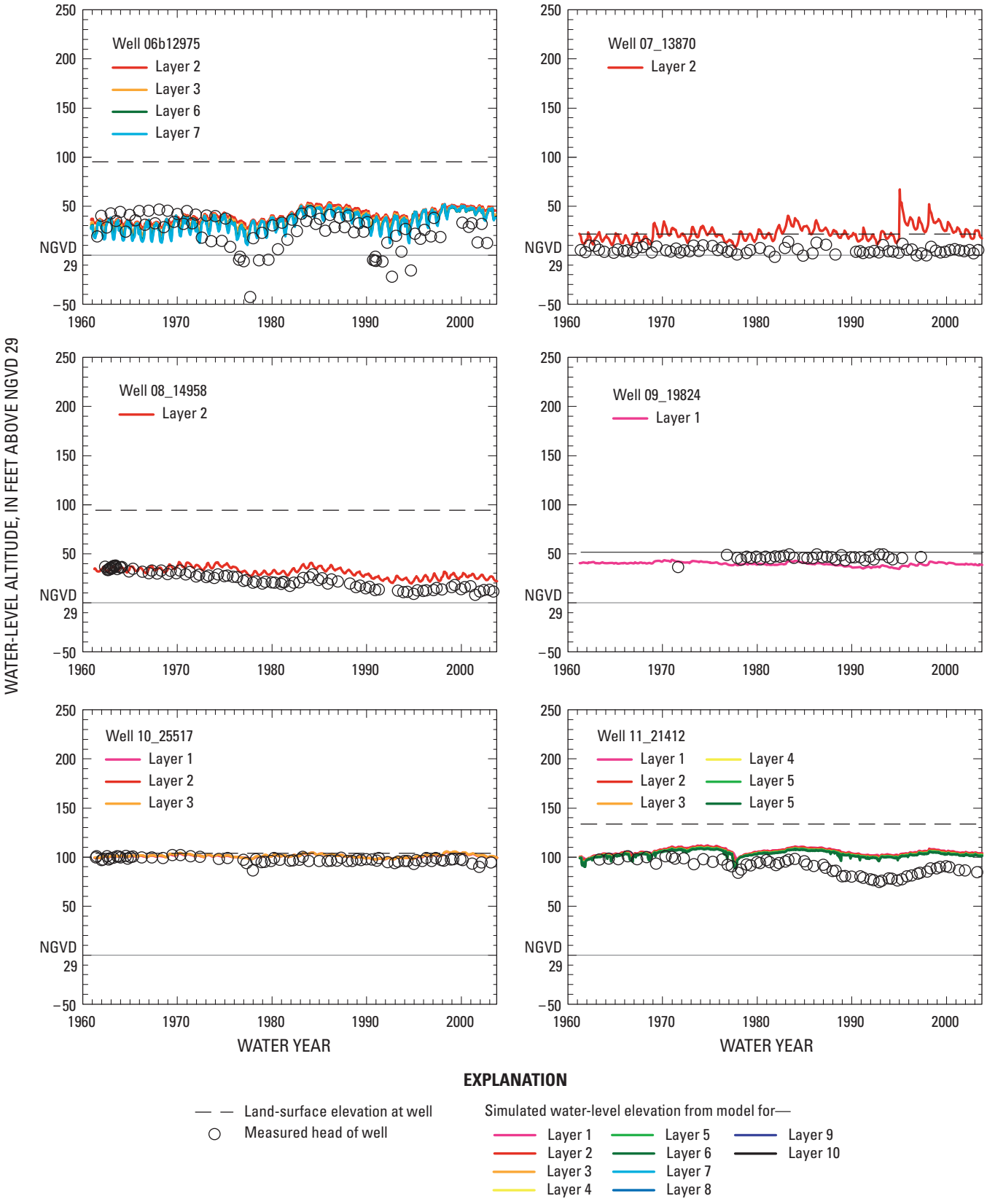

Figure B13. Continued.

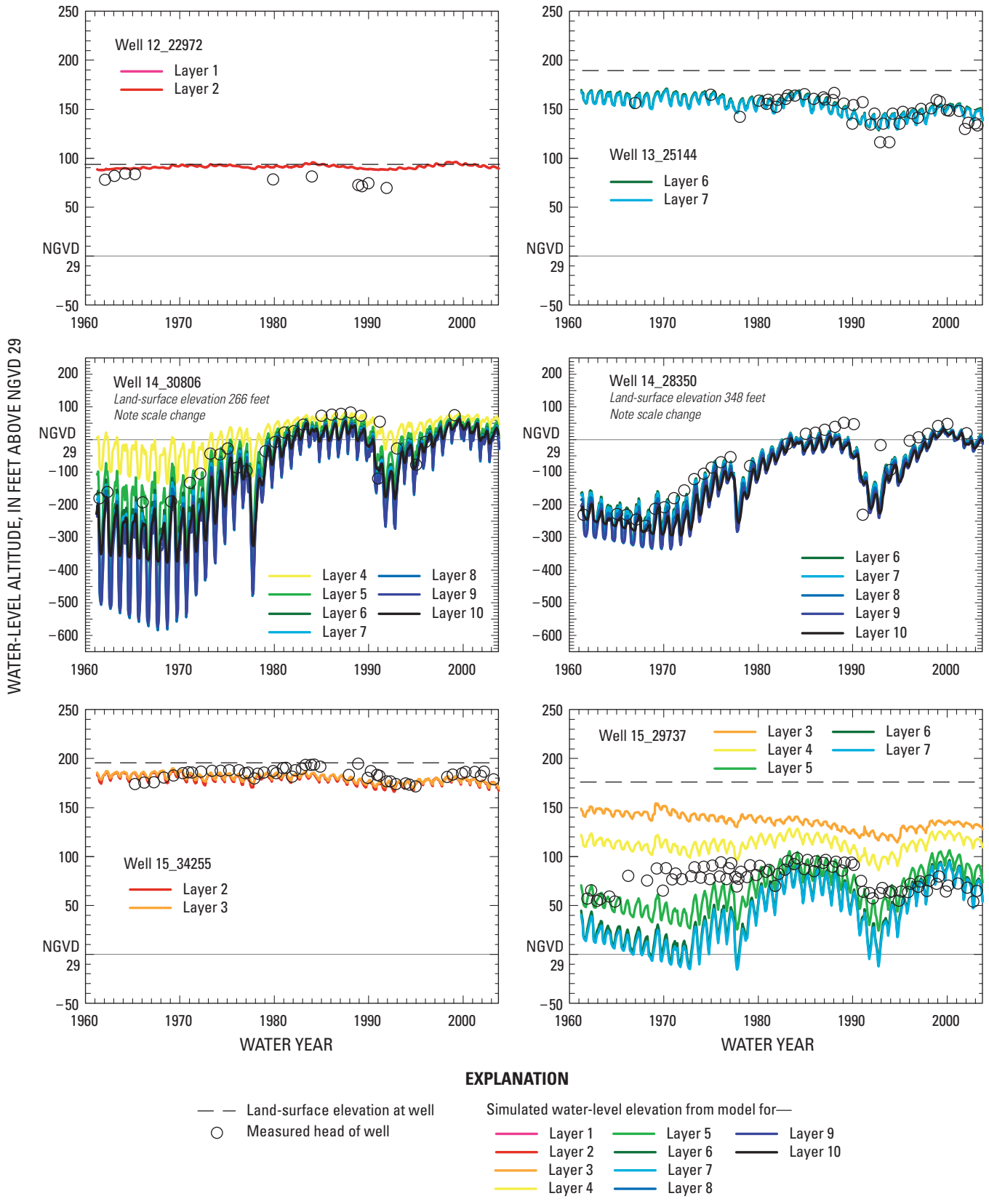

Figure B13. Continued.

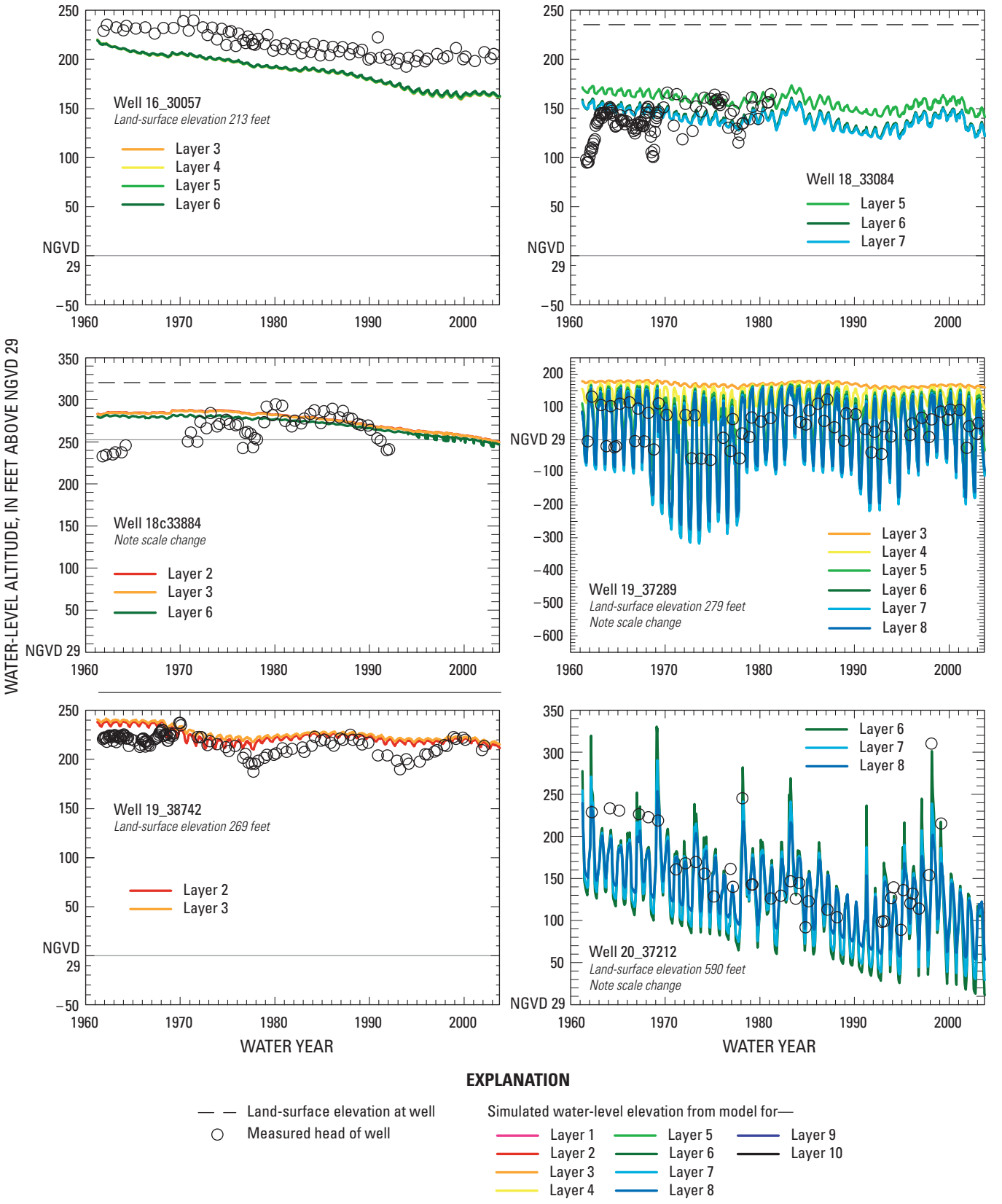

Figure B13. Continued.

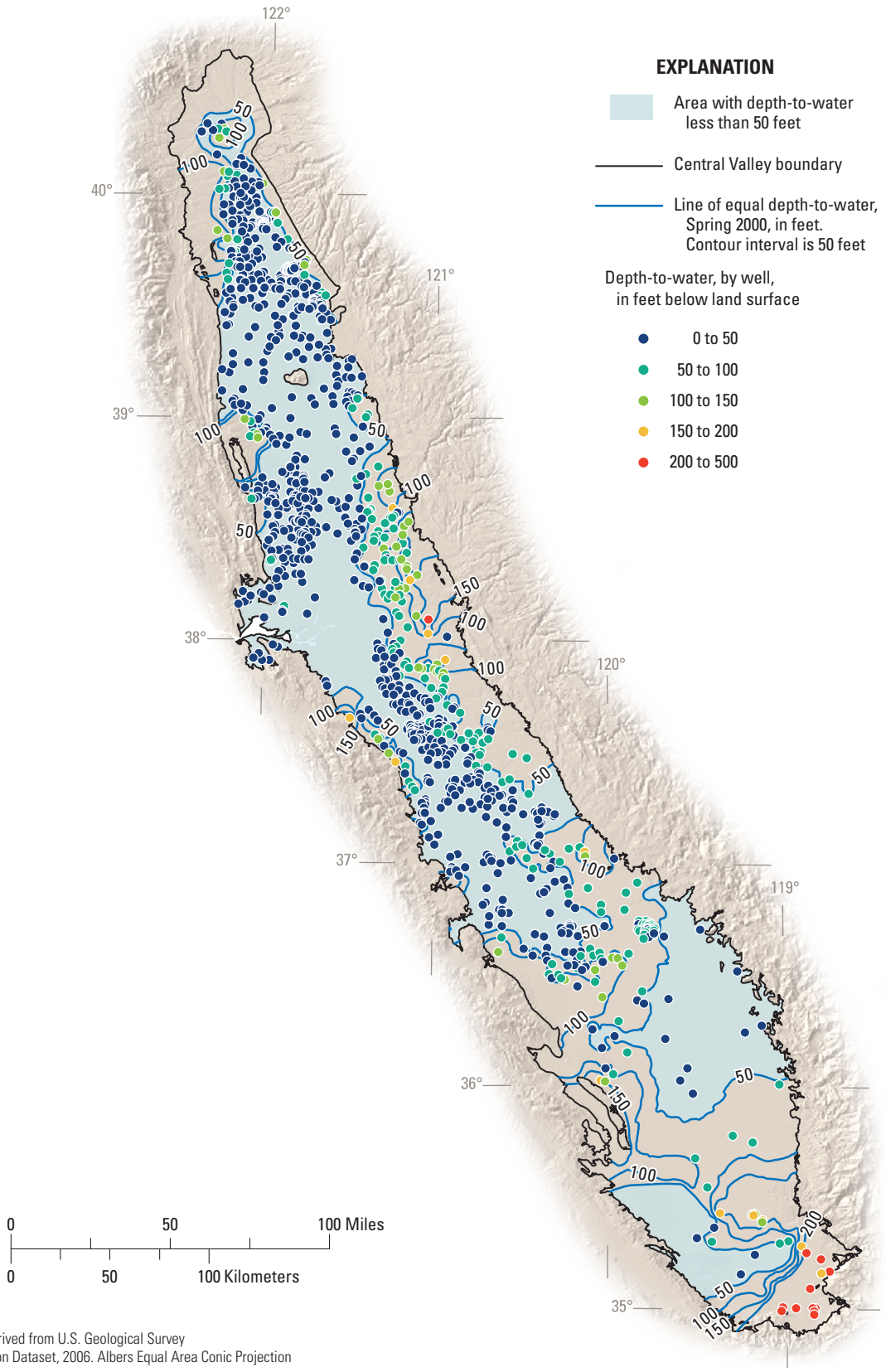

Figure B14. Estimated depth to water table in spring 2000.

The most obvious effects of development were in the western San Joaquin Valley. Although predevelopment flow generally was toward the San Joaquin River, large withdrawals from deep wells in the western and southern parts of the aquifer system reversed the direction of lateral flow in the confined part of the system until the water moved toward the withdrawal centers (Planert and Williams, 1995) (*figs. B4* and *B12*). Water levels in the confined part of the aquifer system declined as much as 400 ft by 1961 (Bull and Miller, 1975) (*fig. B4A*), and water levels reached record lows in the early-to-mid 1960s (Thomas and Phoenix, 1976). This decline was caused by heavy pumping from the confined part of the aquifer system below the Corcoran Clay combined with the resistance to vertical flow provided by the Corcoran Clay and other fine-grained lenses in the aquifer system (Bertoldi and others, 1991). Heads at depth originally were above land surface, and by 1961 were below sea level. This head decline also is notable because water levels declined more than 100 ft over an extensive area, indicating considerable depletion from storage. A significant part of this loss of water from storage is irreversible and came from the inelastic compaction of fine-grained deposits (Poland and others, 1975).

In the San Joaquin Valley, recharge from excess irrigation water has greatly exceeded the estimated predevelopment recharge rate. The combination of the magnitude of the withdrawals from the confined parts of the aquifer system and increased recharge to the water table reversed the vertical hydraulic gradient over much of the San Joaquin Valley. As a result, much of the water in the upper parts of the aquifer system that flowed laterally toward the San Joaquin River under predevelopment conditions began to leak downward through the confining beds into the confined part of the aquifer system. Groundwater pumpage reached a sustained maximum and confined water levels generally reached a low during the 1960s (*figs. B12* and *B13*).

Importation of surface water beginning in the late 1960s and early 1970s has, to some extent, decreased the magnitude of these anthropogenic changes by reducing the reliance on groundwater in the southwestern San Joaquin Valley (Belitz and Heimes, 1990) (*figs. B4*, *B6A*, and *B12*). The combined effect of increased availability of imported surface water and decreased groundwater pumpage was a large-scale, rapid recovery of the water table and heads in the confined part of the aquifer system (*figs. B12* and *B13*). In some parts of the western San Joaquin Valley, groundwater levels in the confined part of the aquifer system have recovered to pre-1960 levels. This is evident in the differences in the water table and potentiometric-surface maps between 1961 and 1976 (*figs. B12B* and *B12D*).

Figure B11 shows an overall trend of increased pumpage from wells penetrating both above and below the Corcoran Clay. However, there is a decreasing trend in intra-borehole flow. Because many of these wells are in urban areas where pumpage continued to increase, pumpage did not actually decrease when surface-water deliveries became available around 1972; it leveled off. Davis and others (1964) estimated that about 100,000 acre-ft/yr flowed through wells (intra-borehole flow) from the upper part of the aquifer system to the lower, confined part of the aquifer system in the western part of the San Joaquin Valley in the early 1960s. During the peak of the withdrawal season, net downward flow may be, on average, as much as 0.3 cubic foot per second per well (Planert and Williams, 1995). Simulations indicate that between 1962 and 2003, an average of 400,000 acre-ft/yr of water moved into the confined part of the aquifer system through intra-borehole flow (*table B2* and *fig. B11*). Williamson and others (1989) suggest that volumetrically the majority of intra-borehole flow may occur through multi-zone wells throughout the Central Valley that are outside the spatial extent of the Corcoran Clay. This is relative to the amount of intra-borehole flow across the Corcoran Clay.

In 1977, a severe drought caused a decrease in surface-water deliveries, resulting in a resumption of pumpage and a rapid decline in water levels (*fig. B13*). Groundwater pumpage reached a brief maximum and confined water levels generally reached a low during the 1977 drought. After this drought, irrigation efficiencies improved and surface-water deliveries increased, resulting in the rapid recovery of water levels to near pre-development levels (*fig. B13*). Water levels declined to near their prior 1977 lows during the 1987–92 drought (*fig. B13*). Following this drought, surface-water deliveries were re-established. In addition, many new water conservation techniques were applied. As a result, groundwater pumpage decreased and groundwater levels rose again in much of the San Joaquin Valley (*fig. B13*). However, in some isolated parts of the San Joaquin Valley where imported surface water generally has not been available, large withdrawals have continued and water levels have continued to decline. For example, on the southeastern side of the San Joaquin Valley, water levels dropped by more than 150 ft in the unconfined part of the aquifer system between 1962 and 2003 (*figs. B4B* and *B12*, and *B13*). Except for isolated areas, the groundwater flow patterns in the aquifer system are the same from the mid-1970s to 2003.

Increased surficial recharge from excess applied irrigation waters and decreased groundwater pumpage has caused the water table to rise dramatically in some areas (Belitz and others, 1993) (*figs. B12* and *B13*). When surface water was imported, groundwater pumpage decreased and irrigation increased because the imported water was less expensive. This influx of water, coupled with decreased discharge from wells, overwhelmed the permeability of the fine-grained system. The associated rise in hydraulic heads was large, as shown in *figure B4B*. For example, in the heavily irrigated San Joaquin Valley, fine-grained deposits limit the rate of downward flow (*fig. B14*). When irrigation occurs over a period of time, the water levels rise in the clayey deposits and eventually can drown the roots of crops. As a result of this and other factors, an extensive network of subsurface drains was installed on the west side (WBS 14) to limit the rise of the shallow water table. Likewise, in coarser grained areas, shallow wells have been installed to pump out the excess irrigation water.

Flow through the aquifer system has increased more than six fold, from about 2 million acre-ft/yr prior to development (Williamson and others, 1989) to an average of about 12 million acre-ft/yr (including ET directly from groundwater) between 1962 and 2003 (*figs. A20* and *B1*). The increased flow through the aquifer system predominantly is a result of increased pumpage and increased recharge. The increased recharge mostly is from excess applied irrigation water resulting from imported surface water or recirculated groundwater.

Land Subsidence

In the Central Valley, the typically slow process of draining fine-grained deposits has caused the permanent and irreversible compression or consolidation of fine-grained deposits. This consolidation has resulted in extensive land subsidence, particularly in the San Joaquin Valley. Galloway and others (1999) compiled a summary on the phenomena of land subsidence that includes the Central Valley. By far, the largest magnitude and areal extent of land subsidence in the Central Valley is attributable to aquifer-system compaction caused by groundwater pumpage (Poland and others, 1975; Ireland and others, 1984; Farrar and Bertoldi, 1988; Bertoldi and others, 1991; Galloway and Riley, 1999) (*fig. B15*). However, other processes have contributed to land subsidence locally in the Central Valley (Poland and Everson, 1966; Poland, 1984; Galloway and Riley, 1999), including principally: (1) oxidation and compaction of peat soils following drainage of marshland; (2) hydrocompaction resulting from compaction of moisture-deficient sediments following application of water; (3) compaction of sediments in petroleum reservoir rocks caused by withdrawal of fluids from oil fields; and (4) tectonic subsidence (Farrar and Bertoldi, 1988; Bertoldi and others, 1991) (*fig. B15*). Compaction of peat soils and subsequent land subsidence has occurred around the Sacramento–San Joaquin Delta (Poland and Evenson, 1966) (*fig. B15A*). Draining the islands of the Delta allowed the peat to oxidize, resulting in subsidence of the land surface on the developed islands in the central and western Delta at long-term average rates of 1–3 inches per year and resulting in large areas of many islands becoming more than 15 ft below sea level (Rojstaczer and others, 1991; Rojstaczer and Deverel, 1993; Deverel and Rojstaczer, 1996; Ingebritsen and Ikehara, 1999). Hydrocompaction, also known as "near-surface subsidence" refers to moisture-deficient and (or) poorly sorted deposits, "glued" together by clay, that compact following the first application of water. This type of subsidence has resulted in 5 to 10 ft (2 to 3 m) of subsidence in the dry areas along the western and southern margins of the San Joaquin Valley (Bull, 1961; Bull, 1964; Poland and Evenson, 1966; Bull, 1972, Bull, 1973; Galloway and Riley, 1999). Compaction of sediments due to the withdrawal of oil and gas has caused land subsidence locally; however, the magnitude is uncertain (Fielding and others, 1998; Galloway and Riley, 1999). Subsidence of up to 1 ft has been attributed to this process in the oil field near Bakersfield (Farrar and Bertoldi, 1988; Galloway and Riley, 1999). Although directly related to the large volume of sediments in the Tulare Basin, subsidence due to tectonic movement in the post-development period has been negligible compared to the other four processes (Williamson and others, 1989).

One of the earliest and most obvious results of groundwater pumpage was widespread land subsidence in the San Joaquin Valley (Poland and others, 1975; Bertoldi, 1989; Galloway and Riley, 1999). Subsidence from groundwater pumpage began in the mid-1920s (Bertoldi, 1989). By 1970, significant land subsidence (more than 1foot) due to the withdrawal of groundwater had occurred in about half of the San Joaquin Valley, or about 5,200 mi^2 (Poland and others, 1975) (*fig. B15*). One of the largest volumes of land subsidence in the world caused by human activities is in this part of the Central Valley (Poland and others, 1975; Bertoldi and others, 1991; Galloway and Riley, 1999). Prior to 1990, an estimated one-third of the volume of water pumped from storage in the Los Banos–Kettleman City area came from compaction of fine-grained beds that resulted in land subsidence (Poland and others, 1975).

The San Joaquin Valley has three principal areas of subsidence caused by groundwater withdrawals: (1) 1,500 mi^2 in the Los Banos–Kettleman City area, (2) 800 mi^2 in the Tulare–Wasco area, and (3) 400 mi^2 in the Arvin–Maricopa area (Poland and others, 1975; Thomas and Phoenix, 1976; Ireland and others, 1984) (*fig. B15*). In the Los Banos–Kettleman City area, head declines in the confined part of the aquifer system of as much as 500 ft due to groundwater withdrawals caused inelastic compaction of the clayey beds and resulted in as much as 28 ft of recorded land subsidence (Poland and others, 1975; Ireland and others, 1984; Galloway and Riley, 1999). This area is characterized by the highest percentage of fine-grained material (approximately 30 percent) within the upper 2,000 ft of the aquifer system in the San Joaquin Valley (*figs. A13* and *B6*). Although the largest concentration of clay is in the Corcoran Clay, little water has been extracted from these layers due to their low permeability, and a negligible fraction of the total simulated aquifer-system compaction in the San Joaquin Valley during 1962–2003 is attributable to the Corcoran Clay.

Small areas of the Sacramento Valley also have been affected by subsidence (*fig. B15*). Recent studies have documented that as much as 4 ft of subsidence has occurred in the Sacramento Valley since 1954 (Blodgett and others, 1990; Ikehara, 1994; Ikehara, 1995). In Yolo County, increased groundwater withdrawals caused land subsidence of several feet in the early 1990s (Ikehara, 1995).

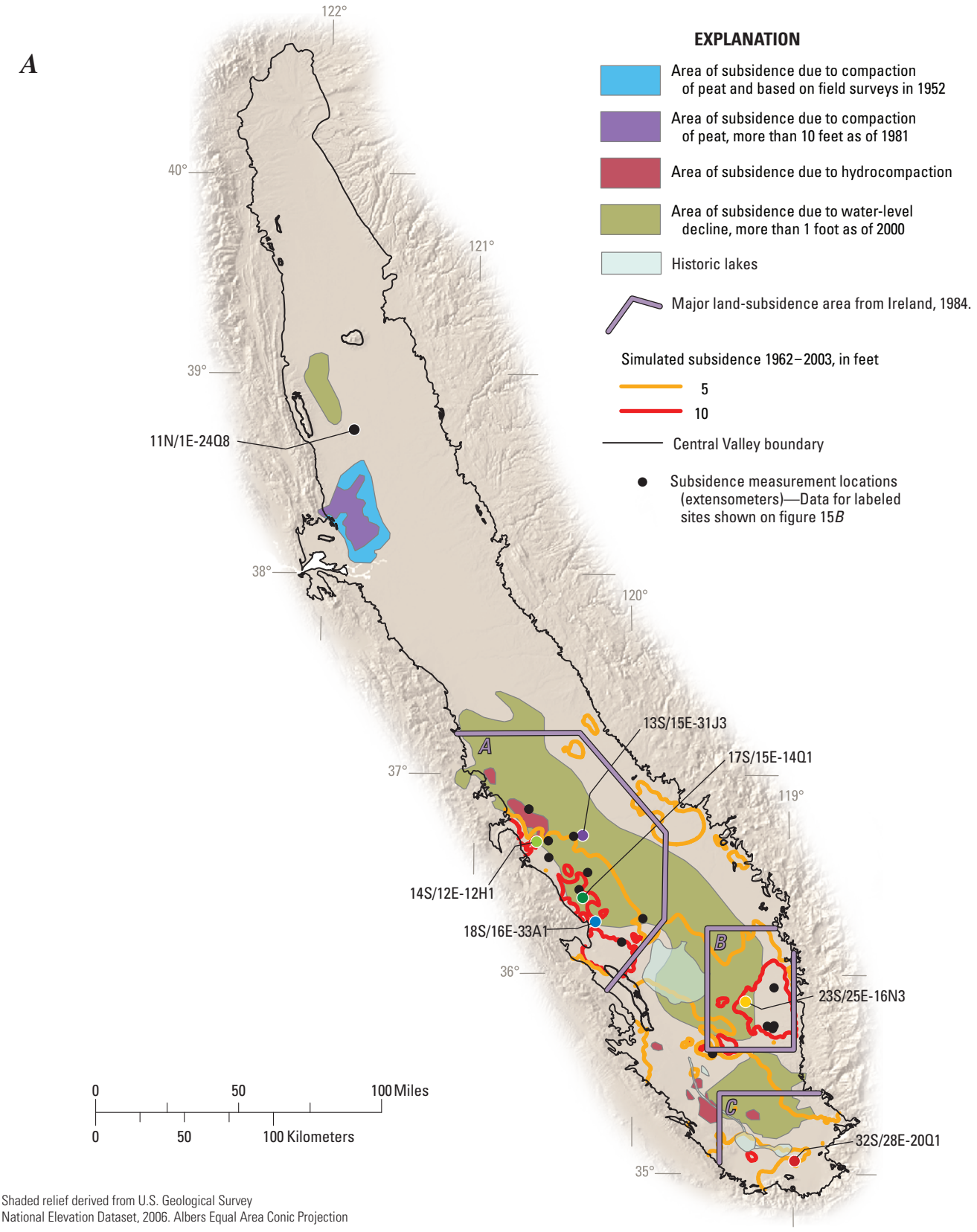

Figure B15. *A*, Areal extent of land subsidence in the Central Valley (modified from figure 9 Thomas and Phoenix, 1976; figure 11 Bertoldi and others, 1991) and locations of extensometers. Contours show simulated subsidence for water years 1962-2003. *B,* Compaction data from selected extensometers and total simulated pumpage in the Central Valley.

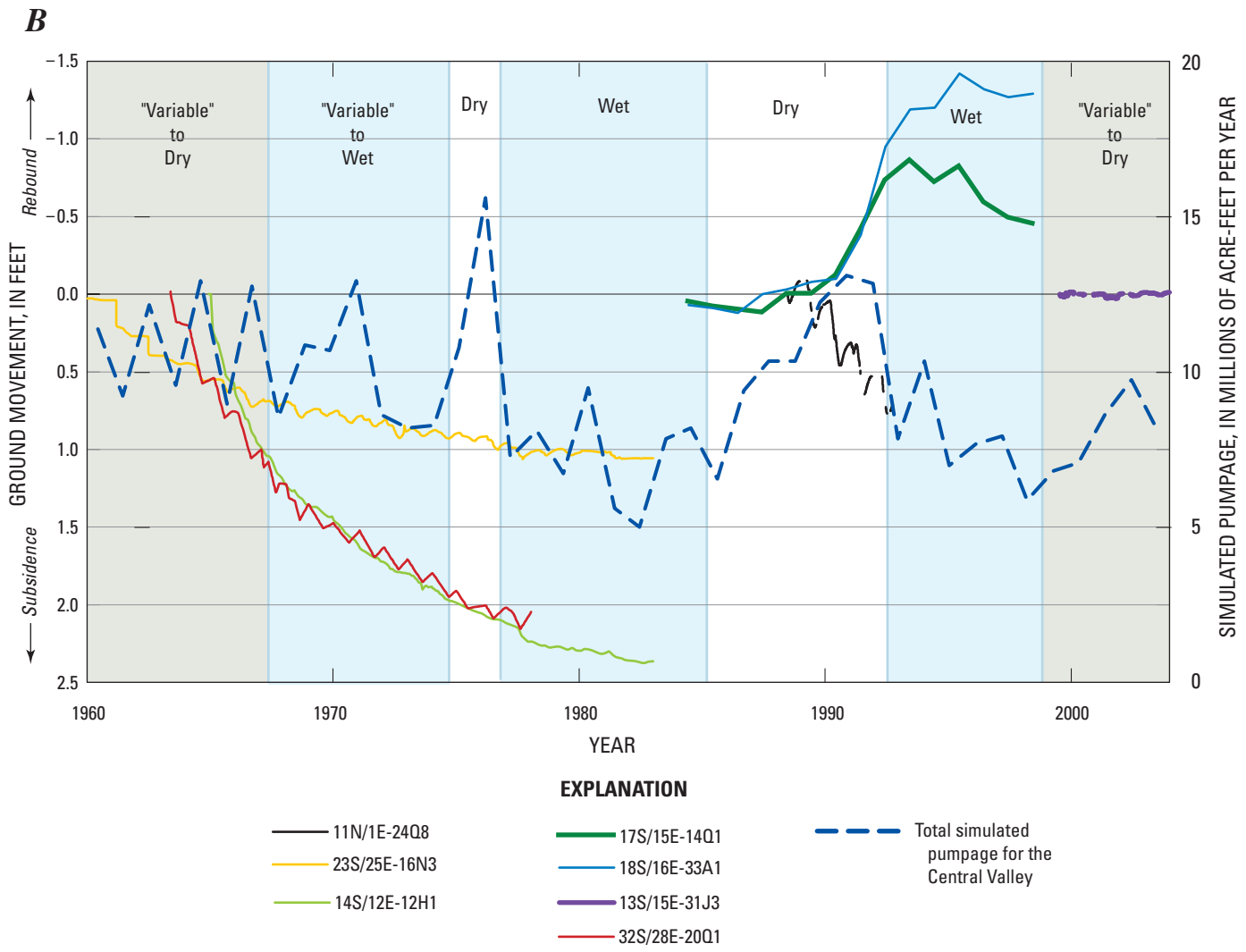

Figure B15. Continued.

Besides loss of water from inelastic compaction, subsidence throughout the Central Valley, particularly the San Joaquin Valley, has caused damage to structures such as aqueducts, roads, bridges, buildings, and well casings. Other important and expensive damages include the need for realignment of canals as they lose their constant gradient, and releveling of furrowed fields, many of which are laser-leveled for maximum irrigation efficiency. In addition, in low lying areas, subsidence has increased the potential for flooding and seawater encroachment (Bertoldi, 1989).

The measured compaction, in relation-to-water-level declines at a well in the southwestern San Joaquin Valley, demonstrates correlations between climate, groundwater use, and subsidence (*fig. B16*) (Galloway and others, 1999). This correlation can be summarized as follows. The1960s were marked by steady head decline and a high rate of compaction (*figs. B12*, *B13*, and *B16*). The importation of surface water and the associated decrease in groundwater pumpage in the early and middle 1970s was accompanied by a steady recovery of water levels and a reduced rate of compaction. During the severe drought of 1976–77, diminished deliveries of imported water prompted pumping of groundwater to meet irrigation demands. This was marked by a sharp decline in water levels and a short period of renewed compaction (*figs. B15* and *B16*). Ireland and others (1984) report that artesian heads generally declined 10 to 20 times faster during the drought than during the period of long-term drawdown and inelastic compaction that ended in the late 1960s. Thus, much of the water pumped during the drought probably was supplied by elastic storage, though some inelastic compaction did occur (*fig. B16*). Following the drought, recovery to pre-drought water levels was rapid and compaction virtually ceased. The negative compaction (rebound) measured immediately after pumpage returned to predrought levels indicates that part of the compaction during the drought was elastic (*fig. B16*). Between the 1970s and late-1980s, land subsidence greatly slowed or stopped in most areas (*fig. B15B*). The most recent prolonged Statewide drought lasted 6 years from 1987–92 (*fig. A9*). During these years, the groundwater extractions increased dramatically, especially in the San Joaquin Valley, which caused increased

compaction and land subsidence in some areas (*figs. B15B* and *B16*). Since the early 1990s, compaction has been slowed greatly or stopped in most areas (*fig. B15B*). In some areas, there has been a rebound of the land surface (Al Steele, California Department of Water Resources, written commun., 2004) (*fig. B15B*). However, subsidence has resumed locally in places. The vertical drainage of fine-grained deposits may proceed very slowly and lag far behind the changing water levels in the aquifer system (Galloway and others, 1999). Changes through time in the amount of subsidence or rebound are measured by compaction at extensometers at specific points in the valley (*fig. B15B*). Over larger areas, satellite-borne differential Interferometric Synthetic Aperture Radar (InSAR) can be used to map land-surface deformation (Galloway and others, 2000; Brandt and others, 2005; Galloway and Hoffmann, 2007). More details are discussed in the "*Subsidence*" subsection of the "*Monitoring the Hydrologic System*" section.

Surface Water and the Environment

In the Central Valley, as in most places, the environment and surface- and groundwater systems are intimately linked. Under predevelopment conditions and during the early period of development, the Central Valley had considerable swamps, marshes, sloughs, riparian habitat, and an extensive Delta region (*fig. A21A*). Many flow regimes no longer resemble natural conditions, largely because of efforts to manage water through diversions for agricultural and urban demands. Groundwater pumpage also has intercepted groundwater that previously discharged to these surface-water bodies and has induced infiltration of water from surface-water bodies (groundwater recharge). In some areas, groundwater pumpage has lowered the water table and surface water has been diverted in other areas. As a consequence, the surface-water bodies have reached or fallen below minimum stages or streamflows needed to support fish populations, wetland vegetation, and water conveyances (California Department of Water Resources, 2003; California Department of Water Resources, 2005). This has resulted in an extensive loss of riparian vegetation and wildlife habitat (*fig. A21B*). Examination of *figures A21A* and *A21B* shows the replacement of extensive marshlands with irrigated agriculture. In the Tulare Basin, most of these marshlands were drained and now are used for agriculture (*fig. A21B*). The Delta originally extended up the Sacramento and San Joaquin Rivers. It has been reduced substantially in area since predevelopment conditions by groundwater pumpage and surface-water diversions (*fig. A21B*).

A recent California Water Plan update (California Department of Water Resources, 2005) defines environmental water use as: dedicated flows in State and Federal wild and scenic rivers, Bay–Delta outflows, instream flow requirements, and applied water delivered to managed freshwater wildlife areas. Environmental water allocations have increased steadily since approval of the 1957 California Water Plan. A considerable amount of water now is dedicated to environmental water uses (California Department of Water Resources, 2003).

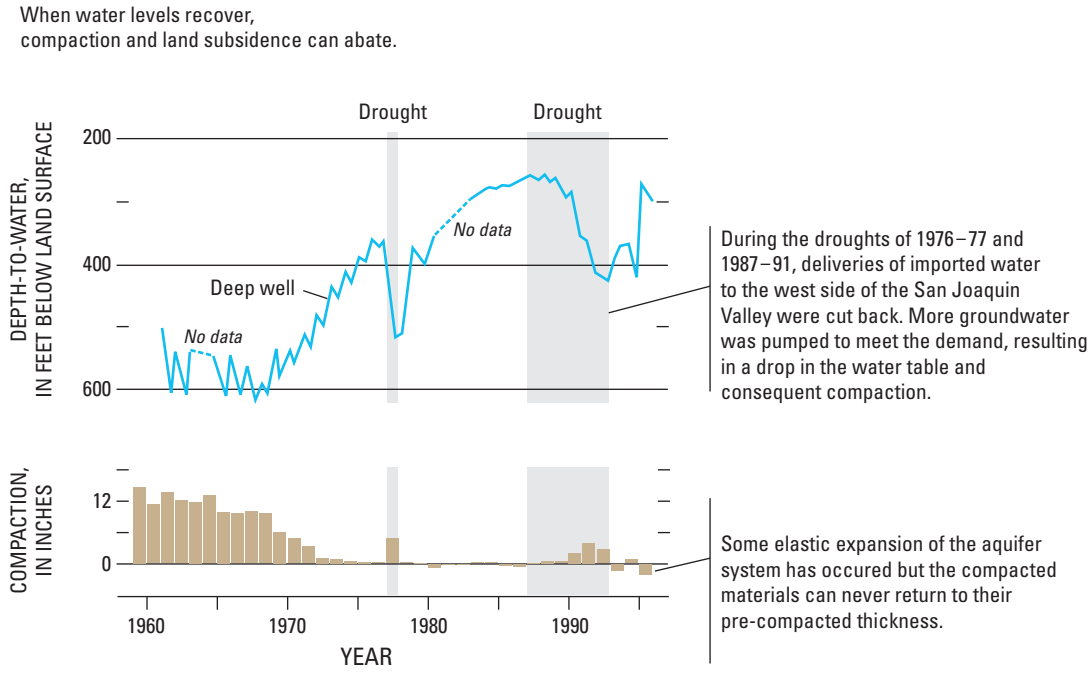

Figure B16. Measured compaction in relation to head decline in the San Joaquin Valley. The effects of drought on groundwater levels and associated subsidence also are evident. (Modified from Galloway and others, 1999; and Swanson, 1998.)

One of the major challenges in restoring the environment will be providing enough surface water of adequate quality to restore river habitat and fish populations along the San Joaquin River while maintaining water-supply reliability for other purposes. The river's historic salmon populations upstream of the Merced River were eradicated in the 1940s as a result of water being diverted with the construction of the Friant Dam. In 2004, a judge ruled that the U.S. Bureau of Reclamation (Reclamation) violated State Fish and Game codes by not providing sufficient water to sustain fish populations. To complicate matters, high salinity caused by agricultural drainage discharge and wastewater return flows already is a problem for fish in the lower San Joaquin River. With the mandate for the environmental flows, the long-term availability of the Sierra Nevada water supplies for agricultural and urban uses is a concern. The Reclamation is studying the feasibility of a new surface storage reservoir in the Upper San Joaquin basin to augment storage. In addition, artificial recharge and the pumping of additional groundwater to help meet environmental and other demands also are being evaluated. In years with below-average rainfall and surface-water inflows from the Sierra Nevada, all environmental, urban, and agricultural surface-water demands may not be met. As a result, meeting the long-term water demands, while balancing protections for water quality and environmental uses, will require groundwater resources.

Global Climate Change and Variability

California's water-delivery system and agriculture have been developed and operated based on the climatic record of the past century (California Department of Water Resources, 2005). The delivery system assumes a certain spatial distribution and amount of runoff, storage in snowpack, and timing coinciding with the growing season. During the study period (1962–2003), surface water generally has been available except during extreme droughts.

Past Climates

The effects of historical climate variability on the hydrologic system can be used to assess the system's responses to future climatic conditions. The response of the hydrologic system during dry years in the historical record can be used as an indicator of possible changes in the landscape and groundwater budgets in future droughts. Similarly, wet years in the historical record can be used as indicators of possible changes for future wet periods. The hydrologic period of record is about 100 years, with mostly qualitative information extending back another 100 years. Tree-ring indices provide a surrogate for hydrologic conditions. These indices have been used to reconstruct streamflow on the Sacramento River since more than 1,000 years prior to the historic period of record (Stine, 1994; Meko and Woodhouse, 2005). For example, on the basis of tree-ring indices, the 6-year drought of the 1930s was one of the most severe during the last few hundred years (California Department of Water Resources, 2005; 2006). Based on relict tree stumps, Stine (1994) showed that California experienced severe, sustained drought conditions with a duration of greater than 2 centuries before 1112 A.D. and a duration of greater than 140 years before 1350 A.D.

Total precipitation over the Sierra Nevada, from which all major drainages enter the Central Valley, decreases from north to south (*fig. A5A*). Contrary to the higher volumes of total precipitation in the north as compared to the south, annual snow accumulations are greater in the higher elevations of the southern Sierra Nevada (Bales and others, 2006). The period 1948–2002 had progressively higher average winter and spring temperatures. This warming trend is a result of a combination of effects related to Pacific Decadal Oscillation (PDO) inter-decadal cycles and to a springtime warming trend that spans the PDO cycles (Stewart and others, 2005; Knowles and others, 2006). These warmer temperatures have resulted in snowmelt runoff 1–4 weeks earlier (Stewart and others, 2005) and a growing season that has been extended by more than a month (California Department of Water Resources, 2006). In addition, since the 1950s, spring and early summer runoff has declined progressively (California Department of Water Resources, 2006). Data also show an overall decline in the amount of water stored annually in the northern Sierra Nevada snowpack. The same effect is noted, to a lesser degree, in the southern Sierra Nevada snowpack.

Future Climate Projections

Results from Global Climate Models (GCMs) indicate that California's hydrologic conditions will continue to shift from historical conditions (California Department of Water Resources, 2005). Although the extent and timing of the long-term changes remain unknown, the projections include increased temperatures, changes in precipitation (including reductions to the Sierra Nevada snowpack and more precipitation in the form of rain), an earlier snowmelt, possibly larger floods, a rise in sea level, and other phenomena (Dettinger and Cayan, 1995; California Department of Water Resources, 2005; Stewart and others, 2005).

The most common projection from GCMs is an increase in temperature of as much as 5°C (9°F) for California in the 21st Century (Dettinger, 2005). GCMs predict less groundwater recharge along mountain fronts because of the expected reduced Sierra Nevada snowpack (California Department of Water Resources, 2005; Dettinger and Earman, 2007). With increased temperatures, ET rates would be expected to increase. Other indirect effects of a temperature increase include earlier budding of orchard crops, premature ripening of crops (particularly grapes), the increased ability to grow more than one crop in a season, and reduced milk production from dairy herds (California Climate Change Center, 2006).

Projected climate changes could significantly alter California's precipitation pattern, intensity, and amount. Although the changes in regional precipitation are difficult to estimate, GCMs indicate modest changes in precipitation for California in the 21st Century (Dettinger, 2005) with changes becoming more significant with time. Simulated responses in GCMs for river basins contributing to the Sacramento Valley (American River Basin) and San Joaquin Valley (the Merced River Basin) suggest that seasonal runoff will occur a month earlier with only a 2.5°C (4.5°F) increase in temperature, but that the average annual streamflow may not change (Dettinger and others, 2004). However, less snowpack would mean less natural springtime replenishment of water storage in the surface-water reservoirs. More variability in rainfall, wetter at times and drier at times, could place more stress on the reliability of existing flood management and water-storage systems. Because most streamflow from the Sierra Nevada is dominated by snowmelt and because the Central Valley's engineered water-delivery system partially depends on the snowpack for storage, the timing and magnitude of snowmelt runoff may affect the supply of water.

GCMs project sea-level rises ranging from 7 to 23 inches above the 1980–99 average by 2100 (Intergovernmental Panel on Climate Change, 2007). The biggest effects of sea-level rise could be on the Delta, where sea-level rise would threaten levee stability, disrupt the environment including tidal wetland restoration, and increase salinity in surface water and groundwater in areas adjacent to the Delta. These effects to the Delta would threaten freshwater exports to southern California (24 million people).

Projected changes in other climate factors, such as solar radiation (for example, changes in cloud cover), relative humidity, and carbon dioxide concentrations, remain uncertain. A net reduction of net radiation and (or) an increase in humidity could help offset some of the effects of an increase in temperature (Hidalgo and others, 2005). Long-term increases in worldwide atmospheric carbon-dioxide concentrations may reduce plant water consumption (California Department of Water Resources, 2005). GCMs indicate that for the Sacramento Valley the increase in carbon dioxide likely is to mitigate many other aspects of climate change and provide a significant buffer for sustainable food production (Aerts and Droogers, 2004).

Increased ET would result in increased water demand for urban, agricultural, and environmental uses. The increased ET and associated water demand likely would occur simultaneously with a change in water supply. A warmer, wetter winter would increase the amount of runoff available for groundwater recharge; however, this additional runoff in the winter likely would occur when many surface-water reservoirs either are near or at maximum capacity. The water will require other forms of storage beyond the current surface-water reservoir capacity, such as managed aquifer recharge systems or additional surface-water reservoirs. Additionally, reductions in late spring and early summer runoff, and higher ET related to warmer temperatures, would reduce the amount of water available for recharge and surface storage during the dry season. If the total surface-water storage and the amount of surface water available during the dry season are reduced, the amount and timing of groundwater pumpage ultimately may be affected.

Groundwater Sustainability and Management

Groundwater sustainability can be defined as the achievement of an acceptable tradeoff between groundwater use and the long-term effects of that use (Alley, 2006). Sustainability requires an iterative process of monitoring, analysis, and application of management practices. Hence, groundwater availability and, ultimately, its sustainability in the Central Valley is an issue that is interrelated to groundwater management.

Groundwater Sustainability

The concept of sustainability is inherently subjective and ambiguous. This is because what is or is not considered sustainable is based, in part, on social and philosophical issues that can change with time (Alley and Leake, 2004). As a result, the term is not specifically defined in this report and factors that affect sustainability are discussed. Factors that limit sustainability include physical, chemical, economic, environmental, legal, philosophical, or institutional. This study focuses on the physical constraints that may affect groundwater sustainability.

The term "groundwater reserves" is used to emphasize the fact that groundwater, like other limited natural resources, can be depleted (Alley, 2006). Despite the fact that most groundwater resources can be replenished, this depletion is key. Depletion of aquifer-system storage by pumpage has had a substantial effect in the Central Valley. Water-level records and previous studies (Williamson and others, 1989) confirm that large amounts of water were removed from storage prior to 1960. Between 1962 and 2003, simulations indicate that aquifer-system storage has been depleted by 57.7 million acre-ft, and water-level altitudes have dropped significantly (*fig. B4*). The long-term decrease in aquifer-system storage between 1962 and 2003, although very large, represents only a small fraction of the approximately 800 million acre-ft of freshwater stored in the upper 1,000 ft of sediments in the Central Valley (Bertoldi and others, 1991, p. 27). As Alley (2007) points out, this volume of groundwater in storage is not by itself meaningful in analyses of water availability; it is used here for context. As a practical matter, it is impossible to remove all water from storage by pumpage. Many other factors limit the amount of water that can be recovered. Aquifer-system permeabilities, well yields, the cost of drilling wells, the cost of energy for lifting water, and the design of the well and pump can limit the availability of water. Similarly,

institutional factors, such as use restrictions, basin adjudication, and surface-water rights, in essence, limit the availability of water.

Depletion of the water in storage can have substantial related consequences. These consequences include changes in surface-water quality, quantity, temperature, and in land subsidence. In turn, these consequences factor into large environmental issues by changing and (or) degrading habitats. These related effects may constitute the primary constraint to groundwater development. For example, in the San Joaquin Valley, land subsidence is an important constraint on how much groundwater can be extracted in an area.

The Central Valley faces competing demands for water resources. These demands include providing water supply for growing urban areas, agriculture, and environmental uses. The population of the Central Valley is predicted to increase dramatically. Agricultural water demand is driven by climate, agricultural land use, crop selection, and farming practices. Because agricultural operations are businesses that seek to make profits, the crop mix typically is driven by market prices of agricultural commodities. The multi-faceted effects of global climate change on agriculture are not understood thoroughly.

The demand for water resources by people may directly compete with environmental uses such as maintaining minimum streamflows, preventing seawater inundation of coastal areas, and preserving habitats for fish and birds. Examination of changes in stream inflows and outflows, with respect to climate, may provide insight into how groundwater use may affect surface-water systems and, ultimately, the environment (*fig. B17*). In general, during wetter periods, streamflow gains and losses increase, particularly the losses. During periods of drought, streamflow gains and losses decrease, and the streams dependent on groundwater for baseflow may not have enough input from groundwater to sustain environmental flows. Both surface-water diversions and groundwater pumpage exacerbate this problem. In addition, runoff from irrigated agriculture and feedlot operations is beginning to be monitored, as it is a threat to water quality (California Department of Water Resources, 2005). This threat likely is to remain a significant and potentially expensive challenge with no simple solution.

Since the late 1970s, State and Federal water projects have not expanded with growing urbanization, agriculture, and environmental uses. Although irrigated agriculture continues to use the vast majority of groundwater, urban groundwater use increased dramatically between 1980 and 2003. The Central Valley's population reached 6.5 million people in 2005 and is projected to increase, possibly reaching 10 million by 2030 (California Department of Finance, 2007). Despite this projected increase in urban population, agriculture is expected to consume more water than would be consumed by urban users (*fig. B6B*). Although agricultural acreage has declined, agricultural yields and revenue have increased in the Central Valley. Recently, water deliveries for irrigation have been reduced in recognition of environmental needs. These trends are projected to continue.

During1962–2003, most water demands were met in most water years (California Department of Water Resources, 2005). In the future, competing demands for water for urban, environmental, and agricultural uses and the effects of global climate change may decrease the number of years in which water demands for agricultural uses are met. Thus far, farmers have adjusted their practices to grow more crops per acre-foot of applied water. The increased efficiencies result from changes in crop type, increased irrigation efficiency, improved productivity, and other improvements. For example, from 1980 to 2000, the annual statewide harvest increased by 50 percent as measured in tons of crops per acre foot of water applied (California Department of Water Resources, 2005). As a result of these improvements, the rate of groundwater storage loss has declined since 1998. Although the rate has decreased, based on an examination of simulated system conditions between 1998 and 2003, groundwater continues to be removed from storage (*fig. B9*). Hence, even disregarding the projected increased groundwater use accompanying climate change, historical usage indicates that the Central Valley groundwater system cannot meet competing demands indefinitely.

Projections based on GCMs indicate the likelihood of less surface water and precipitation along with increases in temperatures. These changes will lead to larger water demands. Assuming these projections are correct, then declines in storage likely are to continue. In addition, environmental uses, including reducing the amount of water pumped from the Delta to increase fish populations, may lead to even larger water demands. Thus, as discussed in the following section, meeting competing demands likely will benefit from an integrated water-management approach. Possible management actions include enhancements in conjunctive use of surface water and groundwater, artificial recharge, and the use of recycled or reclaimed water.

Groundwater Management

The effects of groundwater management may not be realized for many years. Therefore, groundwater sustainability requires a long-term view toward management of water resources. In the Central Valley, groundwater historically was viewed as a convenient resource that allowed for settlement nearly anywhere. Recently, the economic and environmental aspects of groundwater development have begun to be considered (Alley, 2006). In order to be sustainable, groundwater resources must be used and managed in a manner that can be maintained for an indefinite amount of time without causing unacceptable economic, environmental, or social consequences. This study has developed a tool, the CVHM (described in *Chapter C* of this report), which managers could use to help address implications of different management options.

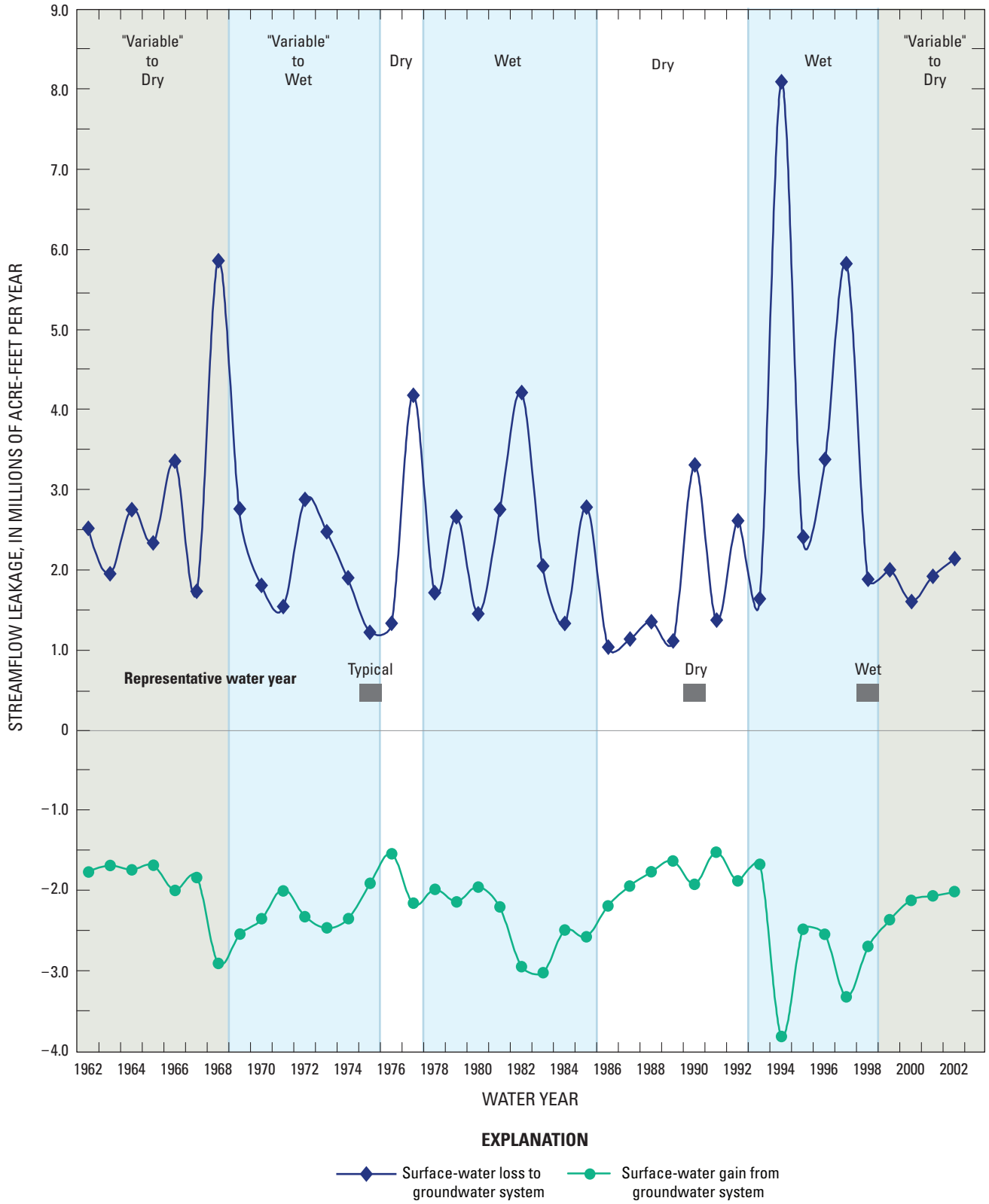

Figure B17. Streamflow gains and losses in the Central Valley between 1962 and 2003.

Over the past century, the Central Valley's water demand and water-management practices have changed significantly. Recent water demand can be separated into three categories: agricultural, urban, and environmental. Demand and management practices for all three categories have changed over time. Initially, water demand was largely local to support relatively small-scale irrigation agriculture near perennial streams (Bertoldi and others, 1991). In the 1800s, hundreds of miles of canals were constructed to transport water to where it was needed for gold-washing operations (Planert and Williams, 1995). This was the beginning of the surface-water delivery system. In the late 1800s, water demand mainly was for agricultural needs and was met through surface-water deliveries. Gradually both surface- and groundwater resources were used to meet demand.

Although groundwater and surface water are closely interconnected and considered a single resource by many (Winter and others, 1998), they are treated differently by State law. When the Water Commission Act defined the allocation of surface water rights in 1914, it did not address allocation of groundwater resources. Though the regulation of groundwater has been considered, the California Legislature has repeatedly held that groundwater management should remain a local responsibility (Sax, 2002). Legally, any landowner can pump groundwater as long as it is put to a reasonable and beneficial use (California Department of Water Resources, 2005). Counties and other local agencies can regulate groundwater resources within their boundaries (California Department of Water Resources, 2005). Some local agencies have adopted groundwater ordinances or groundwater management programs under a variety of statutory authorities. Many notable changes have occurred since the last extended drought of 1987–92. In some areas, water once used for irrigated agriculture is now used for urban uses, groundwater replenishment, and environmental restoration. For example, the State of California passed legislation in 1995 that requires higher flows to protect the Delta, and other legislation either exists or is proposed to protect other environmental systems.

Water can be managed in a sequence of both spatial and temporal uses that make additional surface water available for environmental systems. In many cases, careful water management can improve flows in the rivers. These flows can then be diverted and used consumptively by urban and (or) agricultural water users or to improve water quality.

GCMs indicate that warmer periods with less snowpack and more extreme precipitation events are likely. These factors could lead to increased demand for water by crops and reduced availability of surface water. At the same time, continued urbanization, agricultural development, and emerging water markets are expected to occur. Because of the long time frames involved with these processes and climate-change trends, and the physical and operational complexities of the Central Valley water resources, one feasible approach to evaluate the potential effects of different management alternatives would use the CVHM and linked GCM. For the long-term analyses, projections linked to GCMs may be useful to assess the future climatic effects on water supply and demand (California Department of Water Resources, 2005; Hanson and Dettinger, 2005).

Management strategies typically comprise a number of general approaches that can be used alone or in conjunction with each other. For example, aquifer systems can be effectively and economically used as subsurface reservoirs and conveyances to store as well as transmit groundwater. If surplus water is stored in aquifers during wet periods or periods of low water demand, a high percentage of the stored water typically can be recovered to meet water demands during dry periods or periods of high demand when surface-water supplies are less available. The major strategies applicable to the Central Valley are summarized in the next section.

The supply and demand of regional water resources typically is assessed at three temporal scales or levels of analysis. First, management analysis can occur on a daily to monthly level to determine allocations and to distribute water resources. Second, the analysis can occur on an inter-annual to inter-decadal level to assess actions related to development and water markets. Finally, analyses can occur on inter-decadal to century timeframes to assess policy and capital improvement projects that are required for long-term adaptation to climate change, growth, technology, and environmental issues. These levels of analyses include changes in water demands and regulations, improvements in conservation, and upgrades to water infrastructure. These changes can alter the current system and may alter the effects of future droughts. The CVHM is a tool that can be used to assess the effects of supply and demand at the second and third levels of analyses.

Conjunctive Use

Conjunctive use can be defined as the use of water from multiple sources to meet a demand. Water managers in the Central Valley have been applying conjunctive use for many decades. Because precipitation and runoff are distributed non-uniformly in space and time, the availability of surface-water supplies is variable. There is a long history of shifting between local groundwater, local surface water, and imported water in response to the spatial and temporal variability of surface-water supplies. Especially during droughts, allocations from the SWP and the CVP are susceptible to restrictions, cutbacks, and curtailments, thereby placing increased reliance on groundwater to meet water demand and (or) motivating users to reduce water consumption. Typically, for agricultural water users this is achieved by pumping more groundwater, switching to lower water-use crops and more efficient irrigation practices, and fallowing farmland.

During the past 50 years, the growing water demands of many Central Valley areas were met by large Federal (CVP), State (SWP), and interregional projects that moved water great distances across the state. Although these projects now serve as the backbone of California's water-supply system, they might not have sufficient future supplies to support California's growing population and environmental needs while, at the same time, maintaining agricultural production, particularly in the context of predicted climate change. The strains on the system are indicated by the continuing loss of aquifer-system storage as is shown in *figure B9*.

The traditional strategy for managing variations in the hydrologic cycle has been to build surface reservoirs. Reservoirs are used for surface-water storage on the major drainages entering the Central Valley. Generally, these surface reservoirs are used to store water for various uses: flood control, water supply, recreation, and (or) power generation. However, when a large snowpack melts rapidly in the Sierra Nevada or a big storm occurs, the available surface water may exceed the storage capacity of the local surface reservoirs. In addition, surface reservoirs are expensive to construct, can cause environmental damage, and allow for significant evaporation losses during long droughts (California Department of Water Resources, 2005). Furthermore, the recent trend has been toward dam removal. This trend cast doubt as to whether surface reservoirs can be used to solve the expanding water-supply problems. As a result, other options, such as aquifer-storage-and-recovery systems increasingly are being considered.

Regional partnerships have been formed to address many water-management problems. Every year, hundreds of water transfers (totaling hundreds of thousands of acre-ft) take place between water users for a wide variety of reasons (California Department of Water Resources, 2005). For example, the Sacramento Valley watershed provides water for much of the Central Valley and the rest of the State by way of the CVP and the SWP. Conversely, the Tulare Basin now imports more surface water than any other region in the State (Umbach, 1998). In the Tulare Basin, some agencies are trading water on a daily basis or are making in-lieu trades of surface water for groundwater to be used at a later date (groundwater banking).

As demand grows for high-quality water throughout California, water transfers from the Sacramento Valley are being evaluated more closely. Some counties have passed ordinances regulating out-of-basin water transfers. Conversely, projects such as State Water Resources Control Board's (SWRCB) Phase 8 Bay-Delta Water-Quality Control Plan propose exports of large amounts of water from the Sacramento Valley to the Delta and from the Delta to southern California metropolitan areas (State Water Resources Control Board, 1998). However, a recent report indicates that because of a variety of historical changes that have occurred in the Delta and in natural forces that will continue to operate there, fundamental changes to the Delta are inevitable (Lund and others, 2008). The report states that a peripheral canal is a necessary component in the long-term solution to the sustainability of the Delta. Hence, such water transfers from the Sacramento Valley to the south may need to occur through a peripheral canal.

Water Banking

In water banking, surplus water is "banked" in the groundwater system for the purpose of augmenting or restoring the water supply. Water banking is popular among some governmental and non-governmental organizations because a water bank generally involves far less change to the natural landscape than a surface-water reservoir, often provides wildlife habitat, and is less expensive than constructing a surface-water reservoir (California Department of Water Resources, 2005). The primary purpose of a water bank is to recharge, store, and recover water to improve water supply for its participants during periods of water shortage. During these water shortages, increased groundwater pumpage can be used to offset shortfalls in surface-water supplies. Thus, surface-water reservoirs and water banks can be used together to effectively coordinate the use of groundwater and surface water.

Three main options of water banking are available: (1) "in lieu" recharge, (2) artificial recharge by infiltration ponds and (or) well injection, and (3) pumpage designed to induce inflow of freshwater from surface waterways. "In lieu" recharge refers to using surface water in lieu of groundwater, thereby allowing the groundwater system to recover. The banked water is returned to the owner by release of entitlement and (or) pumping back to the surface-water system during times of water shortage. The second option, artificial recharge, includes engineered surface impoundments and direct-well injection. Surface impoundments involve excess surface water being placed in ponds and allowed to percolate into the ground. These surface impoundments fill quickly with runoff and slowly recharge the groundwater system. They can provide significant environmental benefits, including the enhancement of habitat for threatened and endangered species, waterfowl, and other wildlife. Surface impoundments are common in the Central Valley; injection wells are not. The final option, pumpage designed to induce inflow of freshwater from surface-water bodies, is not common in the Central Valley.

Water banking primarily is done through surface-water impoundments in the southern part of the Central Valley in Kern County. Kern County banks water from local rivers, the California Aqueduct, and the Friant–Kern Canal. The area conveniently is situated, in terms of geology and proximity, to water-supply and delivery systems. Most of the water banks are located on alluvial fans, consisting of sandy sediments on the valley floor in proximity to the mountains (*fig. A1*). These sandy sediments are highly permeable and, therefore, are

well suited for surficial recharge and later recovery by high-capacity wells.

The three major water banks (Arvin–Edison, the Kern Water Bank, and the Semitropic Water Storage District water bank), all located in Kern County, have a combined storage capacity of about 3 million acre-ft (Kern Water Bank Authority, 2007; Semitropic Water Storage District, 2007). That is more than five times the amount of water in Millerton Lake, one of the larger reservoirs feeding the Central Valley surface-water system. A new water bank, the Madera Ranch Project, is being proposed. This project would divert floodwaters from the Delta and possibly from the San Joaquin River during wet years, spread them over thousands of acres, and create a marsh habitat.

The existing banking system has yet to be tested with a severe drought. During such a drought, the water banks will pump groundwater out of storage and provide the water to their customers through the canals of the local, State, and Federal water projects. It is possible that a high rate of pumpage during recovery of stored water may have adverse effects of severely lowering hydraulic heads and possibly inducing subsidence.

A favorable location for an artificial recharge site is where coarse-grained deposits are present (*fig. A12*) and the water table is relatively deep (*fig. B14*). Hence, data gathered in this study can be used to identify favorable locations on a regional scale. The texture model indicates that most of the southeastern part of the valley is a good candidate for artificial recharge sites (*fig. A10*). More site-specific studies would be required to determine which of these areas would be most suitable. Other factors that need to be considered include local variations in the geology, the location of infrastructure such as canals to transport the water to the artificial recharge site and from the wells, and land ownership. One approach to mitigate groundwater depletion is to locate these artificial recharge sites in or near areas where large losses in groundwater storage have been identified.

The potential adverse effects of artificial recharge, particularly subsidence, also must be considered. Loading the water table increases geostatic loads on the underlying confined part of the aquifer system. If additional pumpage does not offset these increased loads, they may tend to exacerbate increased compaction in these units.

Other Management Strategies

In addition to conjunctive use and water banking, other management strategies are being considered and (or) used in the Central Valley. Groundwater pumpage is being controlled or regulated through implementation of restrictions on some types of water use, limits on withdrawal volumes, and establishment of critical levels for hydraulic heads (California Department of Water Resources, 2005). Advanced water conservation, improved water-use efficiency, and increased desalination and recycling of water sources techniques are practiced in many of the irrigation districts. In many areas, traditional flood-irrigation methods have been replaced by methods that use less water, such as drip systems or micro-sprinklers. The ability to monitor soil moisture and other crop-related data also are allowing for more efficient irrigation and harvesting schedules (California Department of Water Resources, 2005). California Department of Water Resources (1994) reported an average improvement in irrigation efficiency of 10 percent during the 1980s in the Central Valley.

There also are a variety of ways to prevent or mitigate subsidence induced by groundwater withdrawal. Though it is not possible to reverse the effects of this type of subsidence that has already occurred, additional subsidence can be stopped or slowed. When water levels are maintained above the critical heads, generally the historic low water levels reached in a specific location, aquifer-system compaction, and subsidence predominantly is elastic and recoverable. Only when water levels drop below this critical head does the aquifer system compact inelastically and the land subsidence becomes permanent (*fig. B18*). Hence, maintaining water levels above these critical heads will help prevent the occurrence of permanent subsidence. However, because of hydrodynamic lag, residual compaction may continue long after water-level declines in the aquifers essentially have stabilized (Galloway and Riley, 1999). To maintain water levels above these critical heads, options include stopping or reducing groundwater withdrawals, carefully managing the placement and production of groundwater supply wells, and using artificial recharge to offset withdrawals. Furthermore, it also may be possible to identify areas that most likely are susceptible to subsidence and limit usage of those areas to activities that likely are to suffer only minor effects from subsidence (Galloway and others, 1999).

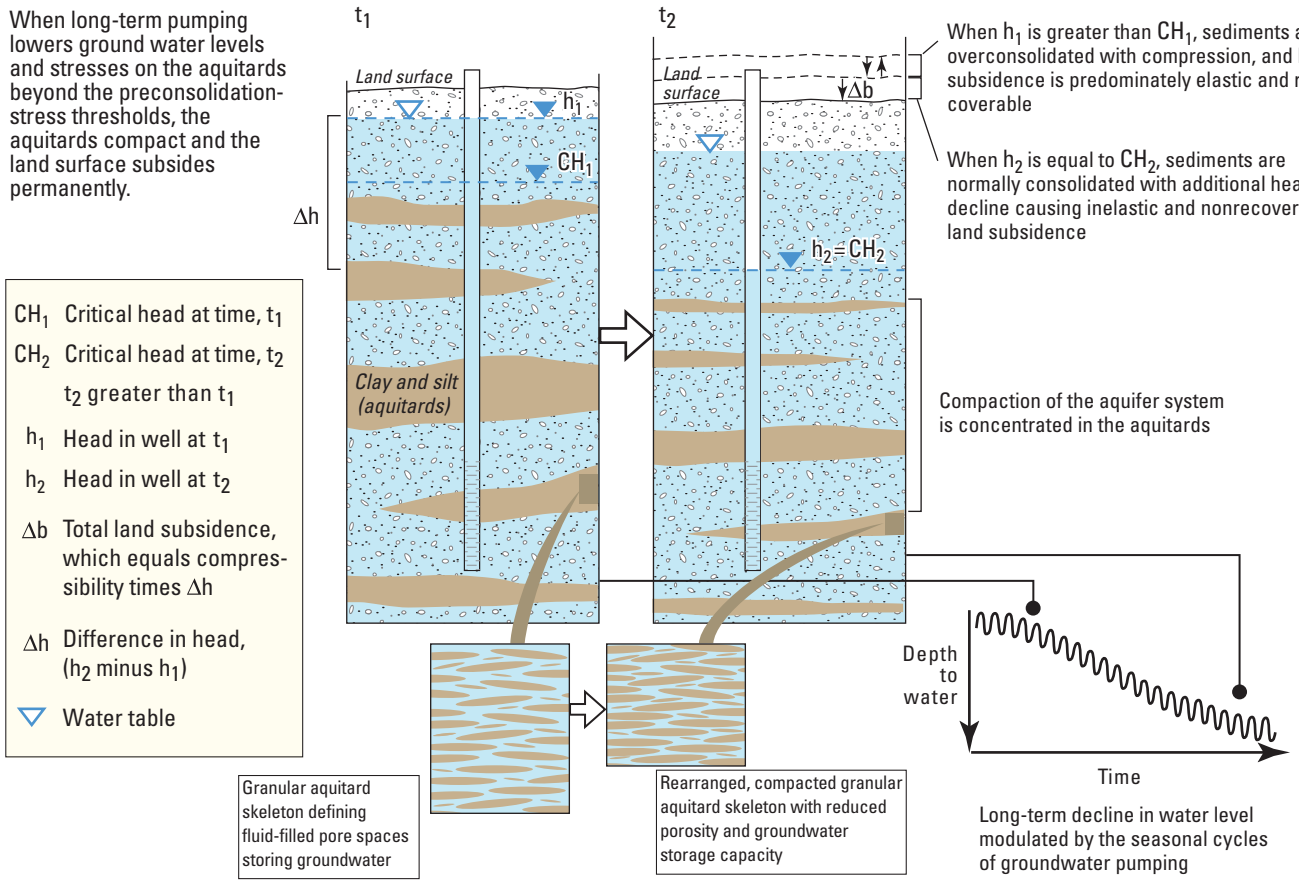

Figure B18. Relationship of water-level changes and critical heads to subsidence and inelastic compaction.

Monitoring the Hydrologic System

Management of the Central Valley's water-resources benefits from long-term monitoring of the hydrologic system, particularly the groundwater and surface-water systems at appropriate locations. An infrequent snapshot of conditions is important, but insufficient. It is important to incorporate comprehensive monitoring strategies designed to monitor the significant seasonal, annual, and multi-annual (decadal and longer) trends of key system variables. Some variables; such as surface-water flows, water quality, or compaction may help quantify information that is relevant to groundwater availability that water levels cannot directly measure, such as subsidence. Despite the size and value of its groundwater resource, California does not have an integrated, monitoring network for all the variables necessary for evaluating this resource. The reasons for this are many; one is that groundwater generally is locally controlled. State and Federal agencies become involved only when groundwater is directly related to the mission of a particular agency or if a local agency requests assistance. Many of these system variables have been identified, collected, and analyzed as part of this study. However, water-quality, which also is an important determinant of water availability, is beyond the scope of this study.

One of the main challenges in monitoring the Central Valley hydrologic system is managing the flow of information. A large variety of agencies produce vast arrays of hydrologic data. For example, this study found more than 873,000 water levels from more than 21,000 wells from multiple agencies for the 1962–2003 study period (*fig. A4*). Similarly, though more than 150,000 driller's logs were identified in the Central Valley, only a small part (approximately 9,000) of these logs was digitized for use in this study because of the large effort involved. Additionally, acreage data for more than 300 crop types from farms ranging in size from less than 1 acre to several square miles were identified for the recent period since the mid-1990s. On the other extreme, crop acreage data generally are unavailable for earlier years.

Tools are needed to manage, organize, and analyze these data. One such tool is a numeric model of the hydrologic system. Numerical models for simulating the groundwater system have played an increasing role in the evaluation of groundwater availability and management alternatives. The numerical model integrates many independent hydrologic stress variables to estimate dependent variables and, thus, is a useful tool for helping to monitor the groundwater system as a whole. The model is a quantitative means for evaluating the water balance of an aquifer system as it is affected by land use, climate, and groundwater withdrawals, and is a means of exploring how these changes affect different parts of the system, including streamflow, water levels, subsidence, and other system variables. Thus, modeling can provide a basis for designing and evaluating a monitoring network.

The CVHM can be considered a tool for identifying, organizing, and integrating the necessary monitoring data. The CVHM also can be used to formulate and answer important questions. The CVHM can be used to address groundwater depletion issues such as critically low groundwater levels and other consequences of groundwater storage depletion including subsidence, streamflow losses, and reduced availability of water for ET.

An inventory of existing data and data-management tools was compiled as part of the modeling task of this study. Key data gaps and tool needs were identified. Like many areas, the Central Valley needs better data, better access to existing data, and data-management tools to produce useful and integrated information. Given the vast quantities of water levels and well logs, among other types of data, the need for more data may seem contradictory. However, analyses of the wells during this study showed that the quality of the data, particularly the well-construction information, often was deficient. In some cases, the lack of information made the data that were available unusable. In addition, the spatial (laterally and vertically) and temporal distribution of data often were inadequate.

A complete and integrated monitoring network would include many of the inflows and outflows, as well as response attributes that reflect the state of the system. The more complete and integrated the monitoring network, the better analysis tools, like the CVHM, will be and will remain useful for helping with water-resources management.

Groundwater

Groundwater levels from wells are the key type of data in most groundwater monitoring networks. They are the primary sources of information about groundwater reserves, the hydrologic stresses on aquifers, and the effects of these stresses on groundwater recharge, storage, discharge, and, ultimately, its availability (Alley, 2006). Groundwater level is a dependent variable in the CVHM and reveals how the system has responded to stress. The long-term, systematic measurement of water levels, collected over years and decades, provides the essential data needed to evaluate temporal variability in groundwater availability; to monitor the long-term effects of aquifer-system development and management; to develop groundwater models, such as CVHM; to forecast trends; and to design, implement, and monitor the effectiveness of groundwater management and protection programs (Taylor and Alley, 2001).

As part of the development of the CVHM, 206 wells were identified to calibrate the model (*fig. C16*). These wells have detailed construction information and were selected to maximize the spatial and temporal distribution of data and information used to constrain the model. These measurements include water levels measured in wells open to different depths in order to monitor vertical gradients and to capture the three-dimensional nature of the groundwater flow system. Some wells were selected in close proximity to each other to cover the period of record and to make sure long-term water-level trends, as well as seasonal changes, were represented. Where necessary, additional wells were selected to make sure key climate periods (relatively wet and dry) were included. Thus, these wells, or a subset of these wells, could be used as a starting point to identify wells suitable for a comprehensive groundwater-level monitoring network. One specific observation made while compiling these hydraulic head data was the lack of construction data, specifically screen intervals, for many of the water-level monitoring wells in both the DWR and USGS databases. In particular, a few hundred wells for which there are hydraulic head data were not used for various purposes owing to missing construction and screen-interval data. Determining screen intervals for the observation wells with large data records would significantly increase the data available from monitoring the groundwater system. A cooperative effort among the stakeholders of the Central Valley groundwater resources could possibly go a long way toward resolving this data gap.

Currently, groundwater levels throughout the Central Valley are measured annually through the effort of the USGS, State (California Department of Water Resources), and local agencies. These agencies monitor some of their own wells, but mostly use private irrigation and (or) domestic wells to monitor water levels. However, the lack of coordination of this monitoring effort results in inefficiencies, and may result in inadequacies in the future if monitoring at key sites in the various monitoring networks is curtailed unilaterally. An analysis of available data and current data-collection activities is needed to determine whether current monitoring is adequate to support regional and broader-scale decision-making for effective water management.

The number of long-term monitoring wells in the Central Valley appears to be declining because of limitations in funding and human resources, among other factors. DWR (1998) summarizes several factors that have contributed to the reduction:

1. Funding for data programs in many agencies, which often was insufficient, has been reduced significantly.

2. When private properties change ownership, some new owners rescind permission for agency personnel to enter the property and measure the well.

3. Because the appropriateness of many private wells that have been monitored in the past is being brought into question, they are being dropped from monitoring networks. The appropriateness of using these private wells is questionable because they often are perforated over long intervals encompassing multiple aquifers in the subsurface and, in some cases, construction details for the well are unknown.

4. Some wells with long-term records actually reach the end of their usefulness because the casing collapses or something falls into the well, making the well unusable, or the groundwater level drops below the bottom of the well.

Despite the declining number of monitoring wells in the valley as a whole, at least 48 dedicated single or multi-completion monitoring wells have been installed since 1997 in the northern Sacramento Valley. Funding for these 48 wells was provided by grants awarded to Tehama, Butte, Colusa, and Glenn Counties through grant sources. At the request of the counties and (or) local agencies, DWR provided construction oversight and data analysis for these wells. These new monitoring wells now make it possible to measure groundwater levels and collect groundwater samples for laboratory analysis from different parts of the aquifer system. These data make it possible to measure the potential for water to move in a vertical direction between different geologic formations, and to evaluate whether these formations can be used to represent different aquifer systems. In particular, work needs to be done to determine if flow in the aquifer system is governed more by grain-size distribution or formation boundaries. Unconformities can cause permeability contrasts that tend to isolate the aquifers; if so, delineation of the extent of these unconformities would be an important step towards understanding recharge and three-dimensional groundwater flow in the Sacramento Valley aquifer system (Dudley and others, 2006).

In addition to water-level monitoring, geophysical techniques could be used to delineate water-level changes. Gravity methods can be used to measure gravitational changes that result from changes in groundwater storage either locally (microgravity) or regionally (satellite-based gravity measurements) (Yeh and others, 2006). Several satellite sensors (installed in current and near-future satellite missions) have demonstrated the capability for monitoring soil moisture, snow water equivalent, heights of inland water bodies (for example rivers, lakes, reservoirs), and changes in total water storage (the aggregate of all of the snow, surface waters, soil moisture and groundwater). In particular, the Gravity Recovery and Climate Experiment (GRACE) satellite mission provides monthly estimates of column integrated land water storage by observing variations of Earth's gravity field. These estimates include a contribution from all the components of land water storage, both above and below ground (Yeh and others, 2006). Combining these regional-scale techniques with well measurements may allow for an improved understanding of groundwater levels and storage.

InSAR can provide the areal extent of groundwater depletion where it is linked to subsidence and can detect uplift from artificial recharge (Galloway and Hoffmann, 2007). InSAR will be discussed in more detail in the *Subsidence* section of this report.

Surface Water

The status of groundwater resources needs to be placed in the context of the complete water budget. Because surface water and groundwater are linked inseparably, monitoring of both systems in the Central Valley is necessary.

The surface-water data needed include: inflow, diversions, deliveries, and gaged flows. These data often are unavailable or, when available, often the data have been collected by multiple agencies at different time intervals using different methodologies. There are 43 gaged inflows (*fig. A5A*) measured by a combination of the USGS, Reclamation, and DWR. The vast majority of these inflows are controlled by reservoir releases. However, the DWR has compiled the complex diversion and delivery history for 21 subregions (WBSs) covering the Central Valley. These data include 108 diversions from the surface-water system, compiled from a combination of Federal, State, and local agencies. Water from these diversions is delivered to the WBSs. The CVHM directly utilizes inflows, diversions, and streamflow-gage data. Indicators of surface-water availability, such as snowpack, streamflow, and surface-water storage, could be monitored to provide a more comprehensive status of the surface-water system.

Gaged streamflow rates are important for a number of reasons. Gaged flow rates are useful for calibration criteria and monitoring compliance with environmental regulations. Disputes over whether groundwater pumpage has had or will have an effect on a particular river or spring often is the driving force behind discussions about the sustainability of many groundwater systems (Alley, 2006). Changes in flow rates through time between various gages frequently can answer these questions. Streamflow measurements from 65 gages throughout the Central Valley are available from the USGS database. Unfortunately, many of these gages are no longer operated by the USGS; fortunately some are now measured by other agencies. The CVHM could be used to evaluate the effect of groundwater pumpage on streamflow and groundwater levels supporting marshes and lakes.

Subsidence

One of the generally unrecognized limitations in groundwater availability is subsidence from groundwater withdrawal. If pumpage demands are large enough, subsidence can occur (*fig. B4*). In the Central Valley, land subsidence has resulted in damage to buildings, aqueducts, well casings, bridges, and highways and has caused flooding. These damages have cost millions of dollars (Planert and Williams, 1995).

Several methods are available to monitor land subsidence (Galloway and others, 1999). The most basic approaches use repeat geodetic surveys such as conventional spirit leveling or GPS surveys. Another approach is to use compaction recorders or vertical (borehole) extensometers (Riley, 1969; 1986). These devices use a pipe or a cable inside a well casing. The pipe inside the casing extends from land surface to some depth through compressible sediments. A stable platform at land surface holds instruments that monitor change in distance between the top of the pipe and the platform. If the inner pipe and casing penetrate the entire thickness of compressible sediments, then the device measures actual land subsidence. If both groundwater levels and compaction of sediments are measured, then the data can be analyzed to determine elastic and inelastic storage properties that can be used to predict future subsidence (Riley, 1969). At least six extensometers and colocated monitoring wells were installed by the USGS in the San Joaquin Valley. Several of these still are being monitored, although irregularly, by DWR.

Recently DWR, together with 20 Federal, State, and local agencies, has installed and surveyed a land-elevation measurement network in the Sacramento Valley (California Department of Water Resources, 2008). This network allows land-surface elevations to be measured accurately with GPS at 339 survey monuments covering 10 counties in the Sacramento Valley. The monuments will be re-surveyed every 3 years. In addition to this GPS network, DWR monitors 13 extensometers and adjacent groundwater levels in monitoring wells in the Sacramento Valley. Several of the extensometers document subsidence and one site, Zamora, shows 0.5 ft of net subsidence from 1994 to 2007.

Another subsidence monitoring method uses InSAR, whereby individual radar images from satellites are compared and interferograms are produced. InSAR can provide hydrogeologic information for alluvial aquifer systems susceptible to aquifer-system compaction (Galloway and Hoffmann, 2007). InSAR makes high-density measurements over large areas using radar signals from Earth-orbiting satellites to measure changes in land-surface altitude at high degrees of measurement resolution and spatial detail (Galloway and others, 2000). Under the best conditions, land-surface elevation changes on the order of 0.2 to 0.4 inches can be determined. The InSAR information can provide the areal extent of groundwater depletion where it is linked to subsidence, and can detect uplift from artificial recharge. This method is the best approach for obtaining comprehensive spatial coverage of land subsidence over large regions like the Central Valley (Brandt and others, 2005). The main limitation for InSAR in the Central Valley is the loss of coherence owing to ground-surface disturbances caused by cultivation. Special techniques are required to extract stable points for observations in agricultural areas; reflector cubes also can be deployed as permanent monuments analogous to benchmarks. Some reflectors could be collocated with benchmarks to tie the leveling and InSAR monitoring systems together. The advent of permanent scatterer InSAR techniques (Feretti and others, 2001) shows promise in overcoming this principal limitation.

Water Quality

Groundwater-quality data are necessary for the protection of groundwater resources because deterioration of groundwater quality virtually may be irreversible, and treatment of contaminated groundwater can be expensive. Therefore, groundwater contamination from natural sources and human activities places constraints on groundwater availability (Alley, 2003; 2006). Various water-management actions potentially have groundwater-quality effects. Therefore, water quality needs to be considered in conjunction with information about changes in water levels and water in storage in evaluating the availability and sustainability of groundwater.

In general, freshwater is available throughout most of the Central Valley. Locally, dissolved solids, selenium, boron, nitrate, and pesticides are of concern and monitored (Planert and Williams, 1995). The water quality, particularly the concentration of dissolved solids, can reflect the chemical characteristics of the streams that recharge the aquifer and the depth of the water. Streams from the Cascade Ranges and the Sierra Nevada, which primarily are igneous rocks, have very small dissolved-solids concentrations. Streams that issue from the Coast Ranges, which predominantly are marine sedimentary rocks, have much higher dissolved-solids concentrations. Therefore, groundwater in the Sacramento Valley and eastern San Joaquin Valley has much smaller dissolved-solid concentrations than groundwater on the western side of the San Joaquin Valley (Planert and Williams, 1995). Groundwater in the agricultural areas has the tendency to become excessively saline and damaging to crops because evaporation of sprayed irrigation water and ET of soil moisture and shallow groundwater leaves behind dissolved salts. Shallow irrigation wells can worsen the problem by recirculating the shallow, saline groundwater. This is a particular problem that is being monitored in the Delta and the San Joaquin Valley. Several irrigation return-water drainage systems are being operated to help reduce this problem. In addition, dissolved-solids concentration generally increases with depth in the Central Valley. Because wells generally are deeper in the western and southern parts of the San Joaquin Valley, they are more likely to produce water with larger dissolved-solids concentrations than the shallower wells in the Sacramento Valley and the eastern part of the San Joaquin Valley (Planert and Williams, 1995).

Marine rocks form the western boundary of the San Joaquin Valley and contain relatively large amounts of selenium. This selenium is found in the soils and groundwater, and is concentrated in the soil by ET (Planert and Williams, 1995). Excess irrigation water applied for leaching salts from the soil leaches selenium from the soil and transports it to shallow groundwater or to surface drains. Large concentrations of dissolved selenium have been detected in shallow groundwater and surface drains (Planert and Williams, 1995). Boron is found in concentrations potentially harmful to plants in the northern and southwestern parts of the Sacramento Valley and in the southern part of the Tulare Basin (Planert and Williams, 1995). Large concentrations of boron also have been detected in shallow groundwater in the western part of the San Joaquin Valley. Excessive concentrations of nitrate, which are potentially harmful to humans and some crops, have been found in shallow groundwater in three areas in the Sacramento Valley and sporadically in the San Joaquin Valley (Planert and Williams, 1995). The source of the nitrate is attributed to effluent from waste-treatment facilities; discharge from septic tanks, feed lots, and dairies; or from leaching of nitrogen fertilizers. Agricultural use of pesticides is widespread; pesticides have been found in groundwater throughout the Central Valley, particularly in the San Joaquin Valley where they have been found in every county.

Sustainability, with respect to groundwater quality, only can be determined by observing groundwater quality over time. If conditions worsen, local managers may need to take steps to prevent further harm to groundwater quality. For these reasons, delineation of areas of contributing recharge to existing water supplies is important, as is identification of potential source areas for future water supplies. To create a serviceable monitoring network, Federal, State, and local agencies use private irrigation and (or) domestic wells along with agency-installed monitoring wells to monitor water quality. These monitoring wells include multi-zone wells, which are very important for understanding changes in water-quality with depth.

Design of a water-quality monitoring network is beyond the scope of this study. Several studies have included designs for such a network for large parts of the Central Valley. The USGS's San Joaquin and Sacramento Valley National Water Quality and Assessment (NAWQA) programs have established multiple water-quality networks in the Central Valley (Domagalski, 1998; Dubrovsky and others, 1998). The USGS's Priority Basin Project, a component of the California Water Board's Groundwater Ambient Monitoring and Assessment program (GAMA) program, is an ongoing comprehensive assessment of statewide groundwater quality. The program is designed to help better understand and identify risks to groundwater resources (Belitz and others, 2003). Groundwater is being sampled at many locations across the State, including the Central Valley, in order to characterize its constituents and identify trends in groundwater quality. The results of these tests will provide information for water agencies to address a variety of issues ranging in scale from local water supply to statewide resource management. The GAMA program was developed in response to the Groundwater Quality Monitoring Act of 2001 (Sections 10780-10782.3 of the Water Code): a public mandate to assess and monitor the quality of groundwater used as public supply for municipalities in California. The goal of the Groundwater Quality Monitoring Act of 2001 is to improve statewide groundwater quality monitoring and facilitate the availability of information about groundwater quality to the public.

Land Use and Climate

In addition to monitoring data on natural systems, estimation of water withdrawals and consumptive use is an essential part of computing a water budget for a developed aquifer system. Although groundwater pumpage is physically possible to measure, it is commonly not measured or tabulated in the valley because few wells are metered and because there is no requirement to do so for private wells. As a result, monitoring land use, particularly to the extent of monitoring native vegetation, urban areas, and irrigated agriculture (including crop type), is critical to the estimation of groundwater use, and, in turn, successful water-resource management. Because land use largely drives water use and consumption, land-use data need to be collected with adequate spatial and temporal detail that reflect the complexity of changing land use and the dynamics of agricultural activities. Most of the historical land-use information is based on interpreted high-altitude aerial photography. During the 1980s, Landsat's Thematic Mapper (TM) satellite sensor data were used to produce the North American Land Class Data (NLCD), which included the Central Valley. DWR has been collecting and mapping detailed land-use information by county on a rotating basis for several decades. Since 2000, DWR has begun to release detailed digital data sets (California Department of Water Resources, 2000). Several tools now available for monitoring land use from remotely sensed data include LANDSAT, MODIS, and InSAR. MODIS data are available as often as every 8 days at a spatial resolution ranging from 820 ft to 0.6 miles.

Mapping of the type and distribution of land use is integral to calculating the crop irrigation demand and, ultimately, the water use in the Central Valley. For a given land use, the demand can be calculated from two variables: crop coefficient (K_c) and reference evapotranspiration (ETo) (*Chapter C*). A number of studies report K_c values for most crops. The different studies report consistent values. ETo values change with climate and can be estimated from temperature. Hence, temperature data, currently available from DWR's California Irrigation Management Information System (CIMIS) stations, are a necessary part of the monitoring network. In addition to temperature, CIMISs 120 weather stations throughout California provide additional information useful in estimating crop water use. Estimated parameters (such as ETo, net radiation [Rn], dew point, temperature, etc.) and measured parameters (such as solar radiation [Rs], air temperature [T], relative humidity [RH], wind speed [u], etc.) are stored in the CIMIS database for unlimited free access by registered CIMIS data users.

Summary

This chapter focuses on the availability of groundwater in the Central Valley. The spatial and temporal differences between the natural distribution of water in the Central Valley, and the agricultural and urban demands for that water, have led to a massive surface-water diversion and delivery system. Because the surface-water diversion and delivery system cannot always meet all of the water demand, groundwater is relied upon to help rectify the imbalance.

Because of the large effect that irrigated agriculture has on the system, the overall water budget for the hydrologic system is separated into two linked parts for the purposes of analysis: a landscape budget, encompassing the surface processes (including most of the components of the agricultural part of the system), and a groundwater budget, encompassing fluxes in, through, and out of the aquifer system.

The hydrology of the Central Valley is driven by surface-water deliveries and associated groundwater pumpage, which in turn reflect spatial and temporal variability in climate, regional differences in water availability and agricultural practices, and temporal changes in the water-delivery system. In general, the Sacramento Valley receives more precipitation than the drier San Joaquin Valley. Historically, water managers have been able to respond to hydrologic challenges in the valley. Consequently, the San Joaquin Valley relies more heavily on groundwater pumpage than the Sacramento Valley. The surface-water delivery system developed for the valley redistributes this water from north to south through the Delta. The Delta is the heart of a massive north-to-south water-delivery system whose giant engineered arterials transport up to 7.5 million acre-feet per year southward (California Department of Water Resources, 1993). About 83 percent of this water is used for agriculture and the remainder for various urban uses in central and southern California. Two-thirds of California's population (more than 20 million people) get at least part of their drinking water from the Delta (Delta Protection Commission, 1995).

Monthly water budgets, computed as a part of this study, were used to examine the fate of water in the Central Valley. The aquifer receives recharge from precipitation, streamflow losses, and excess irrigation water. The excess irrigation water originates from a combination of surface-water deliveries and groundwater pumpage. Other than groundwater withdrawals from wells, groundwater leaves the system predominantly through ET, flux to streams, and, to a small degree, through discharge to the Delta. When total recharge exceeds total discharge, water is added to storage; when the reverse is true, water is removed from storage, which can trigger aquifer-system compaction and associated land subsidence.

Groundwater pumpage is the most significant human activity that affects the amount of groundwater in storage and the rate of discharge from the aquifer system. A high concentration of broadly distributed wells and the multiple broadly distributed cones of depression have produced water-level declines across large areas. Pumpage is physically possible to measure; yet in the Central Valley it is one of the least certain components of the entire water budget. In this study, the numerical model CVHM was used to estimate groundwater pumpage. During the 1962–2003 timeframe, the CVHM indicates that average withdrawals from irrigation wells were about 8.7 million acre-ft/yr.

Hydrologic input and output to the landscape and groundwater budgets vary with time. These variations predominantly are a result of the combined influences of climate variability, surface-water delivery systems, land-use changes, and farming practices. The monthly budgets indicate that precipitation and surface-water deliveries supply most of the consumption in the initial part of the growing season, whereas increased groundwater pumpage augments these supplies later in the season. Although some pumpage occurs in all months, the vast majority of groundwater withdrawals occur during the spring-summer growing season. As a result, water typically is taken into storage during the wet winter months (December through March) and released from storage during the drier growing season (May through September).

Groundwater levels and associated groundwater flows have responded to changes in the groundwater budget. Prior to development, the Central Valley aquifer system was driven by natural conditions in which groundwater flowed from areas of higher altitude along mountain fronts to areas of discharge along rivers and marshes near the valley trough. Large-scale groundwater development for both agricultural and urban uses has modified the groundwater levels and flow patterns, relative to predevelopment conditions. Groundwater flow has become more rapid and complex. Groundwater pumpage and excess irrigation water have resulted in steeper hydraulic gradients as well as shortened flow paths between sources and sinks.

Flow through the aquifer system has increased more than six fold, from about 2 million acre-ft/yr prior to development (Williamson and others, 1989) to an average of about 12 million acre-ft/yr (including ET directly from groundwater) between 1962 and 2003. The increased flow through the aquifer system predominantly is a result of increased pumpage and increased recharge. The increased recharge mostly is from excess applied irrigation water resulting from imported surface water or recirculated groundwater.

During recent decades, changes in the surface-water delivery system and climate have had large effects on the hydrologic system. In the late 1960s, the surface-water delivery system began to route water from the wetter Sacramento Valley to the drier, more heavily pumped San Joaquin Valley. In the San Joaquin Valley, prior to the late 1960s, groundwater pumpage exceeded surface-water deliveries, causing water levels to decline to historic lows on the west side of the San Joaquin Valley, which resulted in decreases in groundwater storage and large amounts of subsidence. The surface-water delivery system was fully functional by the early 1970s, resulting in water-level recovery in the northern and western parts of the San Joaquin Valley. Overall, the Tulare Basin, located in the southern part of the San Joaquin Valley, still is showing dramatic groundwater level declines and groundwater storage deficits. Because of the abundance of surface water and smaller amounts of pumpage, except locally, the Sacramento Valley and Delta have had little cumulative loss in groundwater storage.

The Central Valley hydrologic system responds to changes in the climate. During wet years, relatively inexpensive surface water typically is used for irrigation. During dry periods, many farms predominantly use groundwater. During dry years, groundwater pumpage exceeds recharge and water is removed from storage. For example, during the droughts of 1976–77 and 1987–92 when surface water was less available, more groundwater was pumped. As a result, water levels dropped and subsidence was reinitiated, particularly in the Tulare Basin of the San Joaquin Valley. During wet years where more precipitation and imported surface water were available for irrigation, pumpage decreased and groundwater was taken into storage. In most years, water was removed from storage, particularly in the Tulare Basin. In the Central Valley as a whole, during 1962–2003 there was a simulated net release of 57.7 million acre-ft of water from aquifer-system storage and accompanying groundwater-level declines.

The change in the amount of water in storage varies spatially because of the spatial variation in hydrologic stresses. On average, 68 percent of pumpage in the Central Valley occurs in the San Joaquin Valley (11 percent from the San Joaquin Basin and 57 percent from the Tulare Basin). Volumetrically, there has been very little overall change in storage in the Sacramento Valley and San Joaquin Basin. Conversely, despite the surface-water deliveries, a substantial amount of water has been removed from aquifer-system storage in the Tulare Basin.

In the Central Valley, the typically slow process of draining fine-grained deposits has caused the permanent and irreversible consolidation of fine-grained subsurface deposits. This consolidation has resulted in extensive land subsidence, particularly in the San Joaquin Valley. Significant land subsidence (more than 1 foot) due to the withdrawal of groundwater has occurred in about half of the San Joaquin Valley, or about 5,200 mi^2. Small areas of the Sacramento Valley also have been affected by subsidence.

In the Central Valley, as in most places, the environment and surface- and groundwater systems are intimately linked. Under predevelopment conditions and during the early period of development, the Central Valley had considerable swamps, marshes, sloughs, riparian habitat, and an extensive Delta region. Many flow regimes no longer resemble natural conditions, largely because of efforts to manage water through diversions for agricultural and urban demands. Groundwater pumpage also has intercepted groundwater that previously discharged to these surface-water bodies, and has induced infiltration of water from surface-water bodies (groundwater recharge).

California's water-delivery system and agriculture have been developed and operated based on the climatic record of the past century. The surface-water delivery system assumes a certain spatial distribution and amount of runoff, storage in snowpack, and timing coinciding with the growing season. During the study period (1962–2003), water generally has been available, except during extreme droughts.

California's water-management systems have been designed and operated in the context of the recent hydrologic record. Global Climate Models (GCMs) indicate that California's future hydrologic conditions may be different from those reflected in the past record. Although the extent and timing of the long-term changes remain uncertain, the projections include increased temperatures, changes in precipitation (including reductions to the Sierra Nevada snowpack and more precipitation in the form of rain), an earlier snowmelt, possibly larger floods, and a rise in sea level. These long-term changes in temperature and precipitation may lead to increased water usage, decreased surface-water availability, and, consequently, increased groundwater pumpage and reduced groundwater storage. The question remains as to whether the existing management strategies can accommodate the changed conditions.

Groundwater sustainability requires an iterative process of monitoring, analysis, and application of management practices. In the Central Valley, depletion of aquifer-system storage by pumpage has had a substantial effect. This depletion also has had substantial related consequences. These consequences include changes in surface-water quality, quantity, and temperature, and land subsidence. In turn, these consequences factor into large environmental issues by changing and (or) degrading habitats. These related effects may constitute the primary constraint to groundwater development.

The Central Valley faces competing demands for water resources. These demands include providing water supply for growing urban areas, agriculture, and environmental uses. The demand for water resources by people may directly compete with environmental uses such as maintaining minimum streamflows, preventing seawater inundation of coastal areas, and preserving habitats for fish and birds. Sustainable development likely will benefit from an integrated water-management approach. Possible management actions include enhancements in conjunctive use of surface water and groundwater, artificial recharge, and the use of recycled or reclaimed water.

In order to quantify groundwater availability and to evaluate the sustainability of the groundwater resources, continued and enhanced monitoring of the Central Valley's hydrologic system is needed. Because of the interconnection of the hydrologic system, a monitoring network should include groundwater levels, surface-water flows, subsidence, water quality, land use, and climate variables (including temperature, precipitation, and snowpack).

One of the main challenges in monitoring the Central Valley hydrologic system is managing the flow of information. The CVHM can be used as a tool for identifying, organizing, and integrating the necessary monitoring data into a form where scenarios of possible future consequences of natural and anthropogenic stresses on the hydrologic system can be simulated and evaluated. In particular, the CVHM can be used to address groundwater depletion issues such as: critically low groundwater levels and other consequences of groundwater storage depletion including subsidence, streamflow losses, and reduced availability of water for ET. Finally, the CVHM, used together with the GIS, has many other possible uses.

References Cited

Aerts, J., and Droogers, Peter, eds., 2004, Climate change in contrasting river basins: Adaptation strategies for water, food and environment: CABI Publishing, Manchester, England, 288 p.

Alley, W.M., 1993, General design consideration, *in* Alley, W.M., ed., Regional ground-water quality: New York, Van Nostrand Reinhold, 634 p.

Alley, W.M., 2006, Tracking U.S. ground-water reserves for the future: Environment, v. 48, no. 3, p. 12–25.

Alley, W.M., 2007, Another water budget myth: The significance of recoverable ground water in storage: Ground Water, v. 45, no. 3, p. 251.

Alley, W.M. and Leake, S.A., 2004, The journey from safe yield to sustainability: Ground Water, v. 42, no. 1, p. 12–16.

American Farmland Trust, 2006, The future is now: Central Valley farmland at the tipping point, accessed April 15, 2009, at *http://www.farmland.org/programs/states/futureisnow/default.asp*

Bales, R.C., Molotoch, N.P., Painter, T.H., Dettinger, M.D., Rice, R., Dozier, J., 2006, Mountain hydrology of the western United States: Water Resources Research, v. 42, W08432, doi:10.1029/2005WR004387, 13 p.

Belitz, Kenneth, Dubrovsky, N.M., Burow, K.R., Jurgens, Bryant, and Johnson, Tyler, 2003, Framework for a groundwater quality monitoring and assessment program for California: U.S. Geological Survey Water-Resources Investigations Report 03-4166, 78 p., accessed April 15, 2009, at *http://water.usgs.gov/pubs/wri/wri034166/*

Belitz, Kenneth, and Heimes, F.J., 1990, Character and evolution of the ground-water flow system in the central part of the western San Joaquin Valley, California: U.S. Geological Survey Water-Supply Paper 2348, 28 p.

Belitz, Kenneth, Phillips, S.P., and Gronberg, J.M., 1993, Numerical simulation of ground-water flow in the central part of the Western San Joaquin Valley, California: U.S. Geological Survey Water-Supply Paper 2396, 69 p.

Bertoldi, G.L., 1979, A plan to study the aquifer system of the Central Valley of California: U.S. Geological Survey Open-File Report 79–1480, 48 p.

Bertoldi, G.L., 1989, Ground-water resources of the Central Valley of California: U.S. Geological Survey Open-File Report 89–251, 2 p.

Bertoldi, G.L., Johnston, R.H., and Evenson, K.D., 1991, Ground water in the Central Valley, California—A summary report: U.S. Geological Survey Professional Paper 1401-A, 44 p.

Blodgett, J.C., Ikehara, M.E., and Williams, G.E., 1990, Monitoring land subsidence in Sacramento Valley, California, using GPS: Journal of Surveying Engineering, v. 116, no. 2, p. 112-130.

Brandt, J.T., Bawden, G.W., and Sneed, Michelle, 2005, Evaluating Subsidence in the Central Valley, CA, using InSAR: EOS. Transactions of the American Geophysical Union, v. 85, no. 52 , 2005 Fall Meeting Supplement, Abstract G51C-0851.

Brandt, J.T., Bawden, G.W., and Sneed, Michelle, 1964, Alluvial fans and near-surface subsidence, western Fresno County, California: U.S. Geological Survey Professional Paper 437-A, 71 p.

Brandt, J.T., Bawden, G.W., and Sneed, Michelle, 1972, Prehistoric near-surface subsidence cracks in western Fresno County, California: U.S. Geological Survey Professional Paper 437-C, 85 p.

Brandt, J.T., Bawden, G.W., and Sneed, Michelle, 1973, Geologic factors affecting compaction of deposits in a land subsidence area: Geological Society of America Bulletin, v. 84, p. 3783–3802.

Bull, W.B., 1961, Causes and mechanics of near-surface subsidence in western Fresno County, California: Short Papers in the Geologic and Hydrologic Sciences, U.S. Geological Survey Professional Paper 424-B, p. 187-189.

Bull, W.B., and Miller, R.E., 1975, Land subsidence due to ground-water withdrawal in the Los Banos-Kettleman City area, California; Part 1. Changes in the hydrologic environment conducive to subsidence: U.S. Geological Survey Professional Paper 437-E, 70 p.

Bureau of Reclamation, 1994, The Central Valley Project overview: Bureau of Reclamation History Program Research on Historic Reclamation Projects, accessed April 16, 2009, at *http://www.usbr.gov/dataweb/html/cvpintro.html*

California Climate Change Center, 2006, Our changing climate: Assessing the risks to California, accessed April 16, 2009, at *http://meteora.ucsd.edu/cap/pdffiles/CA_climate_Scenarios.pdf*

California Department of Conservation, 2007, Farmland conversion reports, accessed April 16, 2009, at *http://www.conservation.ca.gov/DLRP/fmmp/Pages/Index.aspx*

California Department of Finance, 2007, E-4 population estimates for cities, counties and the State, 2001–2007, with 2000 Benchmark, Sacramento, California, accessed April 16, 2009, at *http://www.dof.ca.gov/HTML/DEMOGRAP/ReportsPapers/Estimates/E4/E4-01-06/HistE-4.asp*

California Department of Water Resources, 1993, Sacramento-San Joaquin Delta atlas: Sacramento, State of California Department of Water Resources, 121 p.

California Department of Water Resources, 1994, California water plan update: Bulletin 160–93, 2 v., accessed April 16, 2009, at *http://rubicon.water.ca.gov/v1cwp/ause.html*

California Department of Water Resources, 1998, California water plan update: Bulletin 160–98, 3 v., accessed April 16, 2009, at *http://rubicon.water.ca.gov/pdfs/b160cont.html*

California Department of Water Resources, 2000, Explanations of land use attributes used in database files associated with shape files: California Department of Water Resources, Land and Water Use Section, 11 p.

California Department of Water Resources, 2003, California's ground water, update 2003: California Department of Water Resources Bulletin 118, 246 p.

California Department of Water Resources, 2005, California water plan update 2005: Volume 1 – Strategic Plan: California Department of Water Resources, Bulletin 160-05, CD.

California Department of Water Resources, 2006, Progress on incorporating climate change into management of California's water Resources: California Department of Water Resources Technical Memorandum Report, accessed April 16, 2009, at *http://baydeltaoffice.water.ca.gov/climatechange.cfm*

California Department of Water Resources, 2008, DWR to use GPS technology to measure land elevations: California Department of Water Resources news release, July 16, 2008, accessed April 16, 2009, at *http://www.water.ca.gov/news/newsreleases/2008/071608gpsevaluations.pdf*

California State University, Chico, 2003, The Central Valley historic mapping project: California State University, Chico, Department of Geography and Planning and Geographic information Center, 25 p.

Davis, G.H., Lofgren, B.E., and Seymour, Mack, 1964, Use of ground-water reservoirs for storage of surface water in the San Joaquin Valley, California: U.S. Geological Survey Water-Supply Paper 1618, 125 p.

Delta Protection Commission, 1995, Land use and resource management plan for the primary zone of the Delta: Walnut Grove, Delta Protection Commission, 60 p.

Dettinger, M.D., 2005, From climate-change spaghetti to climate-change distributions for the 21st Century California: San Francisco Estuary & Watershed Science, v. 3, issue 1, article 4, 14 p., accessed April 16, 2009, at *http://repositories.cdlib.org/jmie/sfews/vol3/iss1/art4*

Dettinger, M.D., and Cayan, D.R., 1995, Large-scale atmospheric forcing of recent trends toward early snowmelt runoff in California: Journal of Climate, v. 8, p. 606–623.

Dettinger, M.D., Cayan, D.R., Meyer, M.K., and Jeton, A.E., 2004, Simulated hydrologic responses to climate variations and change in the Merced, Carson, and American River Basins, Sierra Nevada, California, 1900–2099: Climatic Change, v. 62, p. 283–317.

Dettinger, M.D., and Earman, S., 2007, Western ground water and climate change—Pivotal to supply sustainability or vulnerable in its own right?: Ground Water News and Views: v. 4, no. 1, p. 4–5.

Deverel, S.J., and Rojstaczer, S.A., 1996, Subsidence of agricultural lands in the Sacramento-San Joaquin Delta, California: Role of aqueous and gaseous carbon fluxes: Water Resources Research, v. 32, p. 2,359–2,367.

Domagalski, J.L., Knifong, D.L., MacCoy, D.E., Dileanis, P.D., Dawson, B.J., and Majewski, M.S, 1998, Water quality assessment of the Sacramento River Basin, California; environmental setting and study design: U.S. Geological Survey Water-Resources Investigations Report 1997–4254, 31 p.

Dubrovsky, N.M., Kratzer, C.R., Brown, L.R., Gronberg, J.M., and Burow, K.R., 1998, Water quality in the San Joaquin–Tulare Basins, California, 1992–1995: U.S. Geological Survey Circular 1159, 38 p., accessed April 16, 2009, at *http://pubs.usgs.gov/circ/circ1159/*

Dudley, Toccoy, Spangler, Debbie, Fulton, Alan, Staton, Kelly, Lawrence, Seth, Ehorn, Bill, and Ward, Michael, 2006, Seeking an understanding of the ground-water aquifer systems in the northern Sacramento Valley: An update, accessed April 16, 2009, at *http://ucce.ucdavis.edu/files/filelibrary/2280/37336.pdf*

Farrar, C.D., and Bertoldi, G.L., 1988, Region 4, Central Valley and Pacific Coast Ranges, *in* Back, William, Rosenshein, J.S., and Seaber, P.R., eds., Hydrogeology: Boulder, Colorado, Geological Society of America, Geology of North America, v. O-2, p. 59–67.

Ferretti A., Prati C., and Rocca F., 2001, Permanent Scatterers in SAR Interferometry: IEEE Transactions on Geoscience and Remote Sensing, v. 39, no. 1, p. 8–20.

Fielding, E.J., Blom, R.G., and Goldstein, R.M., 1998, Rapid subsidence over oil fields measured by SAR interferometry: Geophysical Research Letters, v. 27, p. 3215–3218.

Galloway, D.L., and Hoffmann, Jörn, 2007, The application of satellite differential SAR interferometry-derived ground displacements in hydrogeology: Hydrogeology Journal, v. 15, no. 1, doi: 10.1007/s10040-006-0121-5, p. 133–154.

Galloway, D.L., Jones, D.R., and Ingebritsen, S.E., eds., 1999, Land subsidence in the United States: U.S. Geological Survey Circular 1182, 175 p., accessed February 2, 2008, at *http://pubs.usgs.gov/circ/circ1182/*

Galloway, D.L., Jones, D.R., and Ingebritsen, S.E., 2000, Measuring land subsidence from space: U.S. Geological Survey Fact Sheet 051–00, 4 p.

Galloway, D.L., and Riley, F.S., 1999, San Joaquin Valley, California—Largest human alteration of the Earth's surface: *in* Galloway, D.L., Jones, D.R., and Ingebritsen, S.E., eds., Land Subsidence in the United States: U.S. Geological Survey Circular 1182, p. 23–34, accessed February 2, 2008, at *http://pubs.usgs.gov/circ/circ1182/*

Great Valley Center, 2005, State of the great Central Valley: Assessing the region via indicators—The economy: State of the Great Central Valley Indicators Series, 49 p., accessed April 16, 2009, at *http://www.greatvalley.org/pub_documents/2005_1_18_13_59_43_indicator_econ05_report.pdf*

Gronberg, J.A., and Belitz, K.R., 1992, Estimation of a water budget for the central part of the western San Joaquin Valley, California: U.S. Geological Survey Water-Resources Investigations Report 91–4192, 22 p.

Hanson, R.T., and Dettinger, M.D., 2005, Ground-water/surface-water responses to global climate simulations, Santa Clara-Calleguas Basin, Ventura County, California, 1950–93: Journal of the American Water Resources Association, v. 43, no. 3, p. 517–536.

Hidalgo, H.G., Cayan, D.R., Dettinger, M.D., 2005, Sources of variability of evapotranspiration in California: Journal of Hydrometeorology, v. 6, p. 3–19.

Igler, David, 2001, Industrial Cowboys: Miller & Lux and the Transformation of the Far West, 1850–1920: University of California Press, 267 p.

Ikehara, M.E., 1994, Global Positioning System surveying to monitor land subsidence in Sacramento Valley, Califorinia, USA: Hydrological Sciences Journal, v. 29, no. 5, p. 417–429.

Ikehara, M.E., 1995, Data from Woodland land-subsidence monitoring station, Yolo County, California, water years 1988–92: U.S. Geological Survey Open-File Report 94-494, 77 p.

Ingebritsen, S.E., and Ikehara, M.E., 1999, Sacramento-San Joaquin Delta—The sinking heart of the state: *in* Galloway, D.L., Jones, D.R., and Ingebritsen, S.E., eds., Land Subsidence in the United States: U.S. Geological Survey Circular 1182, p. 83–94.

Intergovernmental Panel on Climate Change, 2007, Climate change 2007: The physical science basis, accessed April 16, 2009, at *http://www.aaas.org/news/press_room/climate_change/media/4th_spm2feb07.pdf*

Ireland R.L., Poland, J.F., and Riley, F.S., 1984, Land subsidence in the San Joaquin Valley, California, as of 1980: U.S. Geological Survey Professional Paper 437-I, 93 p., accessed August 18, 2008, at *http://pubs.er.usgs.gov/usgspubs/pp/pp437I*

Jacob, C.E., 1940. On the flow of water in an elastic artesian aquifer: American Geophysical Union Trans., pt. 2, p. 574–586.

Kern Water Bank Authority, 2007, accessed April 16, 2009, at *http://www.kwb.org/main.htm*

Knowles, Noah and Cayan, D.R., 2004, Elevation dependence of projected hydrologic changes in the San Francisco Estuary and watershed: Climatic Change, v. 62, p. 319–336.

Knowles, Noah, Dettinger, M.D., and Cayan, D.R., 2006, Trends in snowfall versus rainfall in the Western United States: Journal of Climate, v. 19, p. 4545–4559.

Lofgren, B.E., and Ireland, R.L., 1973, Preliminary investigation of land subsidence in the Sacramento Valley, California: U.S. Geological Survey Open-File Report, 32 p.

Londquist, C.J., 1981, Digital model of the unconsolidated aquifer system in the Modesto Area, Stanislaus and San Joaquin Counties, California: U.S. Geological Survey Water-Resources Investigations Report 81–12, 36 p.

Lund, Jay, Hanak, Ellen, Fleenor, William, Howitt, Richard, Mount, Jeffrey, and Moyle, Peter, 2007, Envisioning futures for the Sacramento–San Joaquin Delta: San Francisco, California, Public Policy Institute of California, 284 p.

Marshall, R.B., 1920, Outline of the Marshall plan: California State Irrigation Association, Sacramento, California, accessed April 16, 2009, at *http://www.sacramentohistory.org/admin/photo/1740_2172.pdf*

Mehl, S.W. and Hill, M.C., 2005, MODFLOW-2005, the U.S. Geological Survey modular ground-water model—Documentation of local grid refinement (LGR): U.S. Geological Survey Techniques and Methods 6-A12, 68 p.

Meko, D.M. and Woodhouse, C.A., 2005, Tree-ring footprint of joint hydrologic drought in Sacramento and Upper Colorado River basins, western USA: Journal of Hydrology, v. 308, no. 1–4, p. 196–213.

Page, R.W. and Balding, G.O., 1973, Geology and quality of water in the Modesto–Merced area, San Joaquin Valley, California: U.S. Geological Survey Water-Resources Investigations Report 73–6, 85 p.

Parsons, J.J., 1987, A geographer looks at the San Joaquin Valley, 1987, Carl Sauer memorial lecture, accessed April 15, 2008, at *http://geography.berkeley.edu/ProjectsResources/Publications/Parsons_SauerLect.html*

Planert, Michael, and Williams, J.S., 1995, Ground water atlas of the United States: Segment 1, California, Nevada: U.S. Geological Survey Hydrologic Atlas 730-B, 1 atlas, 28 p.

Poland, J.F., 1984, Guidebook to studies of land subsidence due to ground-water withdrawal: Studies and Reports in Hydrology 40, prepared for the International Hydrological Programme, Working Group 8.4, United Nations Educational, Scientific, and Cultural Organization (UNESCO), Paris, France, 305 p., 5 appendixes, accessed April 15, 2008, at *http://wwwrcamnl.wr.usgs.gov/rgws/Unesco/PDF-Chapters/Title.pdf*

Poland, J.F., and Evenson, R.E., 1966, Hydrogeology and land subsidence, Great Central Valley, California, Geology of Northern California: California Division of Mines and Geology, p. 239–247.

Poland, J.F., Lofgren, B.E., Ireland, R.L., and Pugh, A.G., 1975, Land subsidence in the San Joaquin Valley, California, as of 1972: U.S. Geological Survey Professional Paper 437-H, 78 p.

Riley, F.S., 1969, Analysis of borehole extensometer data from central California, *in* Tison, L.J., ed., Land Subsidence: Volume 2: Proceedings of the Tokyo Symposium, September 1969, International Association of Scientific Hydrology Publication 89, p. 423–431, accessed November 23, 2007, at *http://www.cig.ensmp.fr/~iahs/redbooks/a088/088047.pdf*

Riley, F.S., 1986, Developments in borehole extensometry, *in* Johnson, I.A., Carborgnin, Laura, and Ubertini, L., eds., Land subsidence: International Association of Scientific Hydrology Publication 151, p. 169–186.

Rojstaczer, S.A., and Deverel, S.J., 1993, Time dependence of atmospheric carbon inputs from drainage of organic soils: Geophysical Research Letters, v. 20, p. 1383–1386.

Rojstaczer, S.A., Hamon, R.E., Deverel, S.J., and Massey, C.A., 1991, Evaluation of selected data to assess the causes of subsidence in the Sacramento–San Joaquin Delta, California: U.S. Geological Survey Open-File Report 91-193, 16 p.

Sax, J.L., 2002, Review of the laws establishing the State water Resources Control Board's permitting authority over appropriations of ground-water classified as subterranean streams and the State water Resources Control Board's implementation of those laws: State water Resources Control Board, 92 p.

Schmid, Wolfgang, Hanson, R.T., Mattock III, T.M., and Leake, S.A., 2006, User's guide for the farm process (FMP) for the U.S. Geological Survey's modular three-dimensional finite-difference ground-water flow model, MODFLOW-2000: U.S. Geological Survey Techniques and Methods 6-A17, 127 p.

Semitropic Water Storage District, 2007, Groundwater Banking, accessed April 16, 2009, at *http://www.semitropic.com/GroundwaterBanking.htm*

State Water Resources Control Board, 1998, Revised notice of public hearing, Phase 8, Bay-Delta Water Quality Control Plan: State Water Resources Control Board, accessed April 16, 2009, at *http://www.waterrights.ca.gov/baydelta/html/6may98ntc.htm*

Stewart, I.T., Cayan, D.R., and Dettinger, M.D., 2005, Changes toward Earlier Streamflow Timing across Western North America: Journal of Climate, Vol. 18, p. 1136–1155.

Stine, S., 1994, Extreme and persistent drought in California and Patagonia during mediaeval time: Nature, v. 369, p. 546-549, doi:10.1038/369546a0

Swanson, A.A., 1998, Land subsidence in the San Joaquin Valley, updated to 1995, *in* Borchers, J.W., ed., Land subsidence case studies and current research: Proceedings of the Dr. Joseph F. Poland Symposium on Land Subsidence, Sacramento, Calif., October 4–5, 1995, Association of Engineering Geologists, Special Publication no. 8, p. 75–79.

Taylor, C.J., and Alley, W.M., 2001, Ground-water-level monitoring and the importance of long-term water-level data: U.S. Geological Survey Circular 1217, 68 p.

Terzaghi, Karl, and Peck, R. B., 1948, Soil mechanics in engineering practice, New York, John Wiley & Sons, Inc. 566 p.

Thomas, H.E. and Phoenix, D.A., 1976, Summary appraisal of the Nation's ground-water resources—California region: U.S. Geological Survey Professional Paper 813-E, 51 p.

Umbach, K.W., 1998, A statistical tour of California's great Central Valley—1998: California Research Bureau CRB-98-011, accessed April 16, 2009, *http://www.library.ca.gov/crb/98/11/98011.pdf*, .

U.S. Geological Survey, 2002, Concepts for national assessment of water availability and use: U.S. Geological Survey Circular 1223, 34 p.

Williamson, A.K., Prudic, D.E., and Swain, L.A., 1989, Ground-water flow in the Central Valley, California: U.S. Geological Survey Professional Paper 1401-D, 127 p.

Winter, T.C., Harvey, J.W., Franke, O.L., and Alley, W.M., 1998, Ground water and surface water a single resource: U.S. Geological Survey Circular 1139, 77 p.

Yeh, P.J., Famiglietti, J.S., Swenson, S.C., Rodell, M., 2006, Remote sensing of ground water storage changes using the gravity recovery and climate experiment (GRACE): Water Resources Research, v. 42, W12203, doi:10.1029/2006WR005374.

Chapter C. Numerical Model of the Hydrologic Landscape and Groundwater Flow in California's Central Valley

By Claudia C. Faunt, Randall T. Hanson, Kenneth Belitz, Wolfgang Schmid, Steven P. Predmore, Diane L. Rewis, and Kelly McPherson

Introduction

A numerical groundwater-flow model capable of being accurate at scales relevant to water-management decisions was developed for the Central Valley, California. This chapter documents (1) development of the transient three-dimensional, finite difference numerical flow model; (2) the procedure used to calibrate the flow model; (3) a summary of the model results; (4) a discussion of model uncertainty and limitations; and (5) suggestions for future work. The simulation incorporates time-varying stresses and can be used to evaluate the effects of both climatic and anthropogenic temporal changes in recharge and discharge on the hydrologic system between October 1961 and September 2003.

Model Development

Examination of the existing USGS's Central Valley Regional Aquifer System and Analysis (CV-RASA) numerical groundwater-flow model developed by Williamson and others (1989) indicated that updates were needed to maintain its usefulness. The Central Valley hydrologic system has continued to respond to the stresses imposed upon it, and new information on the surface-water and groundwater systems have become available. In addition to the new information, considerable advancements in numerical hydrologic models have occurred since the original model was developed. The finite-difference groundwater-modeling software MODFLOW-2000 (MF2K) (Harbaugh and others, 2000; Hill and others, 2000) incorporating an updated version of the Farm Process (FMP) (Schmid and others, 2006b; *Appendix 1*) has made it possible to do more detailed and realistic simulations of hydrologic systems. This numerical modeling software (MF2K-FMP) incorporates a dynamically integrated water supply-and-demand accounting within agricultural areas and areas of native vegetation, thus, enabling simulation of surface-water and groundwater-flow. MF2K-FMP was used to develop a model of the Central Valley hydrologic system, and its application to the Central Valley is referred to as the Central Valley Hydrologic Model (CVHM).

CVHM was constructed in five major phases. The first phase was the conversion of the CV-RASA model from the original pre-MODFLOW format into MF2K. Stan Leake (U.S. Geological Survey, written commun., 2005) did the initial transformation to MODFLOW-88 (McDonald and Harbaugh, 1988). As part of this study, the MODFLOW-88 version was converted to MF2K (*table C1*). The original discretization and water budget were maintained; however, new MODFLOW packages were utilized, particularly the Subsidence package (SUB). The second phase was the spatial re-discretization of the model at finer spatial scales, areally and vertically. Areally, the model grid was re-discretized from the 36 mi^2 CV-RASA model cells to 1 mi^2 cells for the CVHM. Vertically, the CV-RASA model had four layers representing 1,000–3,000 ft of freshwater-bearing deposits, and the thickness of the uppermost layer ranged from 200 to 300 ft. The updated model has 10 layers and the uppermost layer is 50 ft thick. This more detailed vertical discretization facilitates simulation of shallow groundwater-flow paths and compaction of fine-grained deposits. The third phase was the temporal re-discretization of the CVHM. The CV-RASA model had two stress periods per year representing the spring–summer growing season and the fall–winter dormant season from 1961 through 1977. The CVHM has monthly stress periods from 1961 through 2003. These monthly stress periods facilitate representation of the cyclical nature of irrigation, urban water use, and aquifer-system storage. The fourth phase was the implementation of an alternative water budget. The alternative water budget incorporates new climatic, land-use, and surface-water data. Much of the surface-water diversion and delivery information was compiled by the California Department of Water Resources (DWR) for 21 water-balance subregions (WBSs) covering the valley floor (C. Brush, California Department of Water Resources, written commun., February 21, 2007). The WBSs are used as accounting units for surface-water delivery and estimation of groundwater pumpage. Their boundaries generally represent hydrographic rather than political subdivisions and are described in more detail in *Chapter A* (*fig. A5*; *table A1*). The fifth and final phase was the incorporation of the texture model into the CVHM. *Table C1* summarizes the computer programs (processes and packages) used for CVHM.

Table C1. MODFLOW-2000 packages and processes used with the hydrologic flow model of the Central Valley, California.

Computer program (packages, processes, parameter estimation)	Function	Reference
Processes and Solver		
Global (GLO) and Groundwater Flow (GWF) Processes of MODFLOW-2000	Setup and solve equations simulating a basic groundwater flow model	McDonald and Harbaugh (1988), Harbaugh and others (2000), Hill and others (2000)
Preconditioned Conjugate-Gradient Package (PCG)	Solves groundwater flow equations; requires convergence of heads and(or) flow rates.	Hill (1990); Harbaugh and others (2000)
Farm process (FMP)	Setup and solve equations simulating irrigated agriculture.	Schmid and others (2006b)
Files		
Name File (Name)	Controls the capabilities of MODFLOW-2000 utilized during a simulation. Lists most of the files used by the GLO, OBS, and FMP Processes.	Harbaugh and others (2000)
Output Control Option (OC)	Used in conjunction with flags in other packages to output head, drawdown, and budget information for specified time periods into separate files.	Harbaugh and others (2000)
Global File	Output file for information that applies to model simulation as a whole.	Harbaugh and others (2000)
List File	Output file for allocation information, values used by the GWF process, and calculated results such as head, drawdown, and the water budget.	Harbaugh and others (2000)
Discretization		
Basic Package (BAS6)	Defines the initial conditions and some of the boundary conditions of the model.	Harbaugh and others (2000)
Discretization Package (DIS)	Space and time information.	Harbaugh and others (2000)
Multiplier Package (MULT)	Defines multiplier arrays for calculation of model-layer characteristics from parameter values.	Harbaugh and others (2000)
Zones (ZONE)	Defines arrays of different zones. Parameters may be composed of one or many zones.	Harbaugh and others (2000)
Aquifer Parameters		
Layer Property Flow Package (LPF)	Calculates the hydraulic conductance between cell centers.	Harbaugh and others (2000)
Subsidence (SUB)	Simulates aquifer-system compaction and land subsidence	Hoffman and others (2003b)
Hydrologic Flow Barriers (HFB6)	Simulates a groundwater barrier by defining a hydraulic conductance between two adjacent cells in the same layer	Hsieh and Freckleton (1993)
Boundary Conditions		
General Head Boundaries (GHB)	Head-dependent boundary condition used along the edge of the model to allow groundwater to flow into or out of the model under a regional gradient.	McDonald and Harbaugh (1988), Harbaugh and others (2000)
Recharge and Discharge		
Multi-node Wells (MNW1)	Simulates pumpage from wells with screens that span multiple layers.	Halford and Hanson (2002)
Streamflow Routing (SFR1)		Prudic and others (2004)
Output, Observations and Sensitivity		
Streamflow Observations (GAGE)		Prudic and others (2004)
Head Observation (HOB)	Defines the head observation and weight by layer(s), row, column, and time.	Hill and others (2000)
Observations (OBS)	Generates simulated values for comparison with observed values.	Hill and others (2000)
Hydmod (HYD)	Generates simulated values for specified locations at each time-step for subsidence, heads, and streamflow attributes.	Hanson and Leake (1998)
Sensitivity (SEN)	Specifies parameter values used in other packages. Because of calculations in the FMP Process and SFR1 Package make MF2K sensitivity calculations invalid, this process was not used.	Hill and others (2000)

The CVHM was adjusted during these phases, but calibrated primarily after the fifth phase, with the aid of automated parameter estimation. The parameter estimation code UCODE-2005 (Poeter and others, 2005) was used to calculate sensitivities and estimate parameters. The CVHM was calibrated to water-level altitudes, water-level altitude changes with time, streamflow losses, and subsidence. During construction and calibration of the CVHM, it became evident that several updates and enhancements were needed within MF2K, the FMP, and some post-processing software. The packages that were modified or updated include the Layer-Property Flow (LPF), Multiplier (MULT), Hydrograph Time Series (HYDMOD), and the Streamflow Routing (SFR1) packages (Hanson and Leake, 1998; Harbaugh and others, 2000; Prudic and others, 2004). Additional modifications also were made to the FMP (Schmid and others, 2006b). All of these modifications are summarized in *Appendix 1* of this report and in the release notes and online documentation of the source code for MF2K with the FMP (*http://water.usgs.gov/nrp/gwsoftware/mf2k-fmp/mf2kfmp.html* last updated May 6, 2006). The model components can be described in terms of the discretization, boundary conditions, stresses, "hydrologic landscape process," hydraulic properties, initial conditions, and water budget. The next few sections of this chapter discuss the development of these model components.

Discretization

The CVHM encompasses the alluvial deposits of the entire Central Valley extending from the Cascade Ranges on the north to the Tehachapi Mountains on the south and bounded on the east by the Sierra Nevada and on the west by the Coast Ranges (*fig. C1*). The only outlet is through Carquinez Strait, a narrow tidal strait that is part of the tidal estuary of the Delta of the Sacramento and San Joaquin Rivers (*fig. A1*).

The finite-difference model grid used to represent the deposits comprises a lattice of orthogonal cells. A detailed discussion of the use of finite–difference equations to simulate groundwater-flow is presented in McDonald and Harbaugh (1988). Model inputs include intrinsic characteristics of materials, such as hydraulic conductivity, represented by each model cell.

Spatial Discretization and Layering

The total active modeled area is 20,334 mi^2 on a finite-difference grid comprising 441 rows, 98 columns, and 10 layers (*table C2*; *fig. C1*). Slightly less than 50 percent of the cells are active. The model has a uniform horizontal discretization of 1 × 1 mi and is oriented parallel to the valley axis, 34 degrees west of north (*fig. C1*). The grid was oriented horizontally to coincide with the original CV-RASA grid; groups of 36 cells of the CVHM correspond to a single cell of the CV-RASA model.

The CVHM comprises 10 layers that generally thicken with depth (*table A3*). The top layer (layer 1) has an upper altitude of land surface and a base equal to 50 ft below land surface. Except where the Corcoran Clay Member of the Tulare Formation (hereafter referred to as the Corcoran Clay) exists, the layers range in thickness from 50 to 400 ft, increasing by 50 ft with each progressively deeper layer. Where the Corcoran Clay exists, the layers were morphed to explicitly represent the clay with layers 4 and 5 (*fig. A11*). The layering for the texture model and the flow model are the same; this is described in more detail in *Chapter A*.

The bottom boundary of the CV-RASA model was specified on the basis of the base of the post-Eocene continental deposits and the lowest altitude of freshwater (Williamson and others, 1989). The base of these deposits averages 2,400 ft below land surface, and ranges from less than 1,000 ft on the margins of the valley to more than 9,000 ft below land surface south of Bakersfield. The depth to the base of sediments saturated with freshwater (water with less than 1,000 milligrams per liter dissolved-solids concentration) varies greatly (Planert and Williams, 1995). In the Sacramento Valley, the base of freshwater generally coincides with the base of continental deposits. In the San Joaquin Valley, although the freshwater mainly is in continental deposits, the pattern is more complex. Freshwater also is in Tertiary marine rocks on the southeastern side of the valley and in pre-Tertiary igneous and metamorphic rocks. The thickness of the aquifer system saturated with freshwater in the San Joaquin Valley ranges from 100 to more than 4,000 ft (Berkstresser, 1973; Planert and Williams, 1995). In some local areas west and south of the Sutter Buttes and west of Stockton, the base of freshwater is less than 500 ft deep.

For the CVHM, the bottom of the model was specified on the basis of well-completion records to incorporate the part of the aquifer system that is stressed by pumpage. The model bottom extends to 1,800 ft below land surface, and where the Corcoran Clay is present, to 1,500 ft below the Corcoran Clay (*fig. A11*; *table A3*). For the most part, saline water is deeper than the model bottom and may be as much as 2,500 ft deep (Berkstresser, 1973; Planert and Williams, 1995). The deeper wells are simulated in model cells where wells are perforated and presumably freshwater is present. The CVHM does not simulate pumping in the lowermost model layer, 10. This layer, which is 400 ft thick, is included in the model as a buffer for flow.

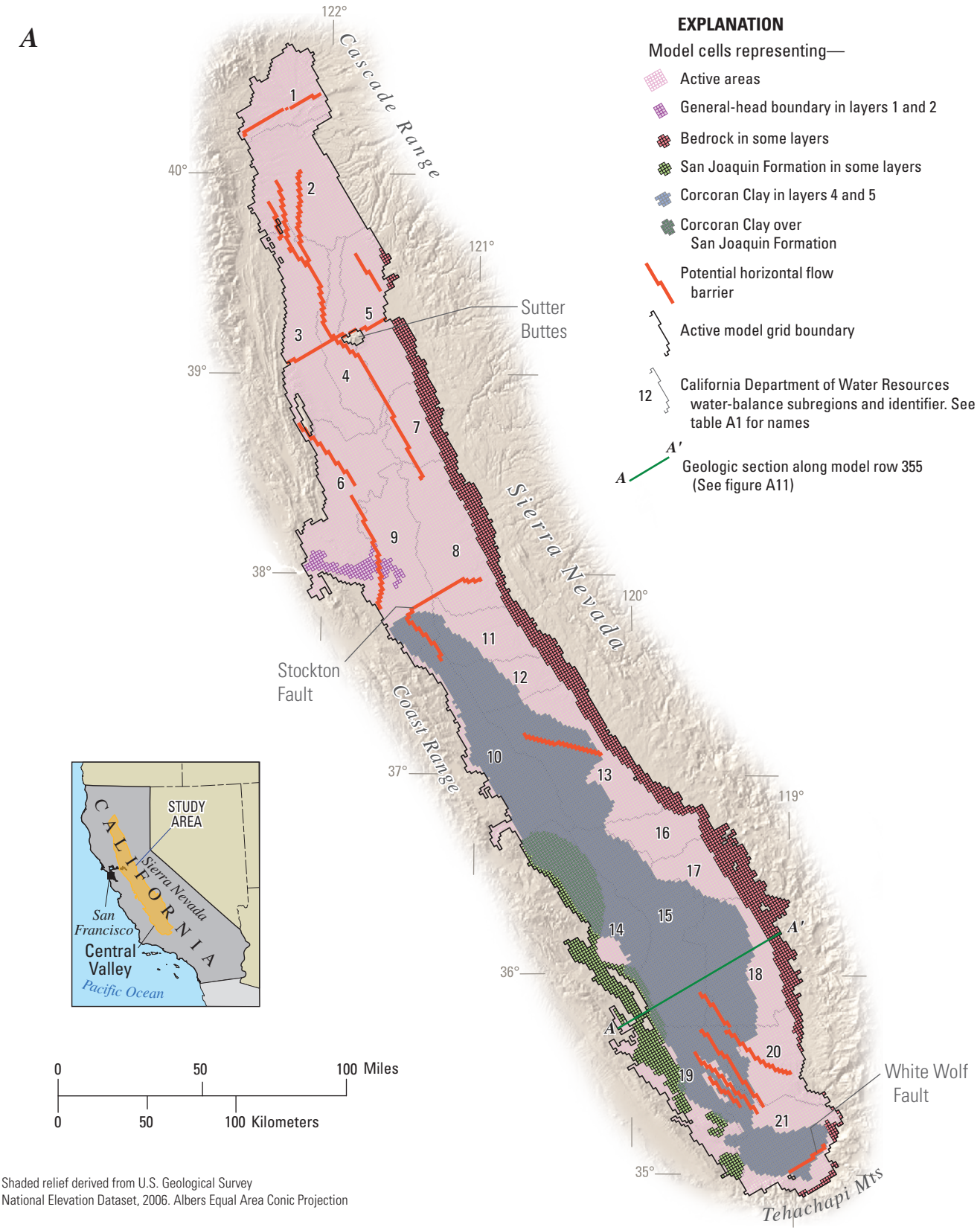

Figure C1. Central Valley Hydrologic Model grid: *A,* Extent of San Joaquin Formation, Corcoran Member of the Tulare Formation, crystalline bedrock, and horizontal flow barriers. *B,* Upper-most active layer.

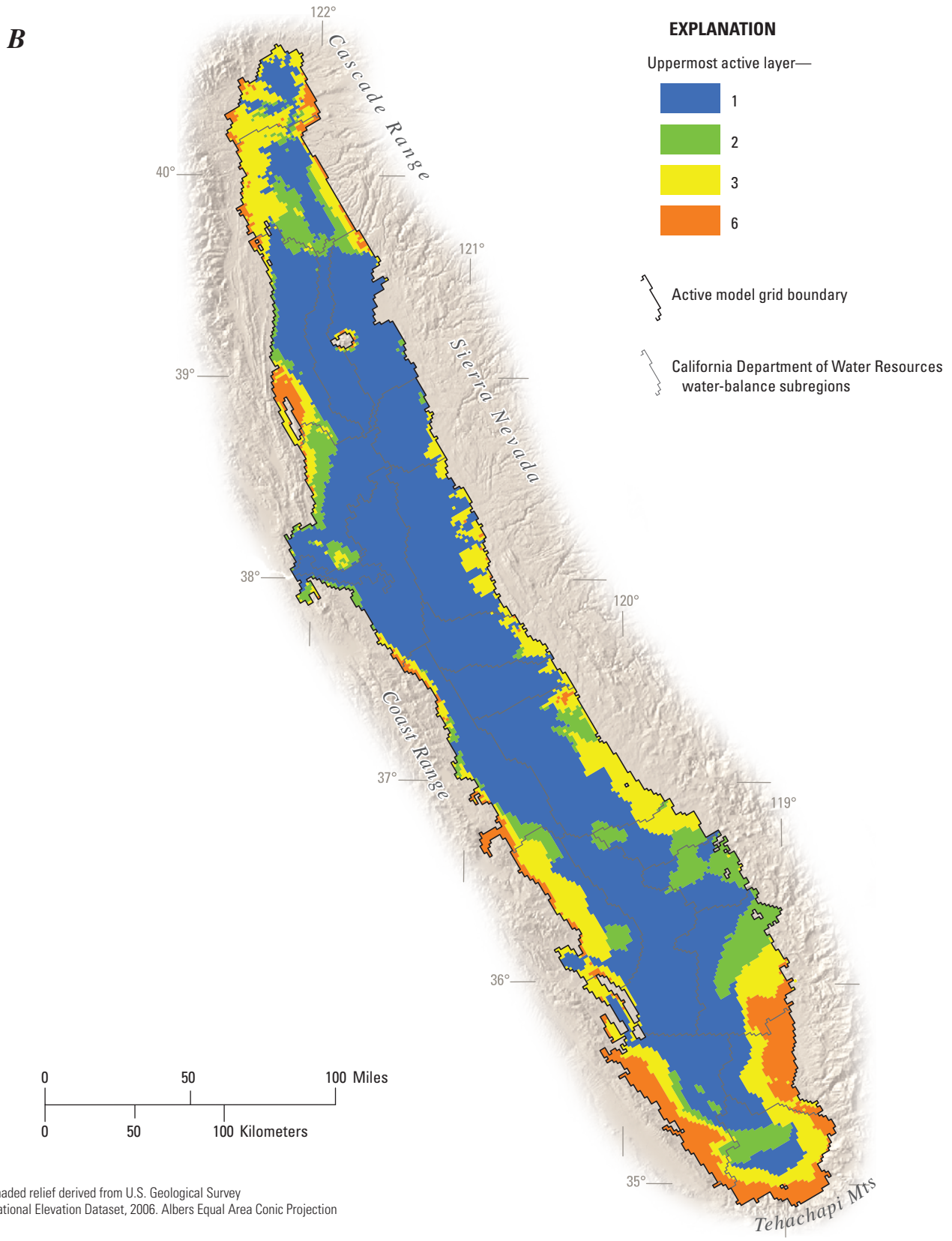

Figure C1. Continued.

Table C2. Coordinates of the Central Valley Hydrologic Model grid.

[Model grid is rotated 34 degrees west; coordinates below are calculated at the cell center of the model grid using the Albers projection using Central Meridian 120 degrees west, North American Datum 1983; each cell is 1 mile by 1 mile]

Corner of model grid	Model coordinates X (column)	Model coordinates Y (row)	Latitude (DMS)	Longitude (DMS)	Albers coordinates X (easting) (meters)	Albers coordinates Y (northing) (meters)
Northwest	1	1	39° 58' 34"	123° 46’ 49”	–319,957	1,890,733
Northeast	98	1	40° 43' 11"	122° 12’ 45”	–185,337	1,969,734
Southwest	1	441	34° 34' 54"	119° 34’ 24”	38,818	1,280,164
Southeast	98	441	35° 16' 26"	118° 04’ 36”	173,410	1,359,209

The upper part of the saturated groundwater-flow system—the unconfined to semi-confined zone (layers 1–3)—was more finely discretized in the CVHM to increase the accuracy in simulating (1) the altitude of the water table where it is shallow, (2) vertical hydraulic gradients, and (3) the interaction of the streams and crops with the shallow part of the groundwater system. Increasing the layer thickness with depth reflects a balance between the decreasing availability of data with increasing depth and the enhanced capability to simulate groundwater-flow processes near the land surface. The geometry and hydrogeology of the deeper units, particularly those below the Corcoran Clay, are not well understood and, for purposes of this study, are less critical. In addition, to partly correct for the inability of MF2K to simulate density-dependent flow, the hydraulic properties in the lowest layers represent a composite of the hydraulic conductivity and viscosity. Therefore, the minimal presence of saline waters in the model domain does not significantly affect the general flow patterns simulated.

During calibration, an additional modification to the layering was added where the water table is deeper than 50 ft (*fig. B11*). Where the water table is between 50 and 150 feet below land surface, the top layer was thickened to extend to 147 feet below land surface and layer 2 was configured as a 3-ft-thick dummy layer. Where the water table was between 150 and 300 ft below land surface, layers 1 and 2 were specified as inactive. Where the water table was deeper than 300 feet, layers 1–3 were specified as inactive.

Temporal Discretization

The CVHM is discretized into stress periods and time steps. In order to represent the growing season adequately, the annual hydrologic cycle was divided into 12 monthly stress periods. Specified inflows and outflows, including pumpage, precipitation, evapotranspiration (ET), surface-water diversions, and water deliveries are constant within each stress period. Variations in stresses are simulated by changing stresses from one stress period to the next. Stress periods were further divided into two time steps for which water levels and flows were calculated. The total simulation length was 42.5 years (or 510 monthly stress periods), from April 1961 through September 2003.

Boundary Conditions

Boundary conditions are prescribed over the boundary of the model domain, and are used to represent flow constraints within the groundwater-flow system. Two general types of boundary conditions are used in the CVHM: specified flow, and specified head-dependent flow or general head. For the transient simulation, the lower boundary and most of the lateral boundaries were simulated as no-flow (specified-flow equal to zero). A general-head boundary was used to quantify the amount of lateral flow into and out of the groundwater-flow system at the Delta (*fig. C2*). Boundary conditions representing flow and head-dependent flow constraints also were used within the model domain to simulate sources and sinks within the flow system. These include recharge to, and discharge from, the groundwater system. Recharge to the model includes stream leakage, precipitation, and excess applied irrigation water. Evaporation, transpiration, pumpage for agricultural and urban uses, and groundwater inflow to streams are the discharge mechanisms; the first three of these are specified in, or calculated by, the FMP. Although the evaporation and transpiration are a type of flow- and head-dependent flow boundary, they are implemented in the FMP. Because of the complexity of the FMP, it is discussed in the next section of this chapter.

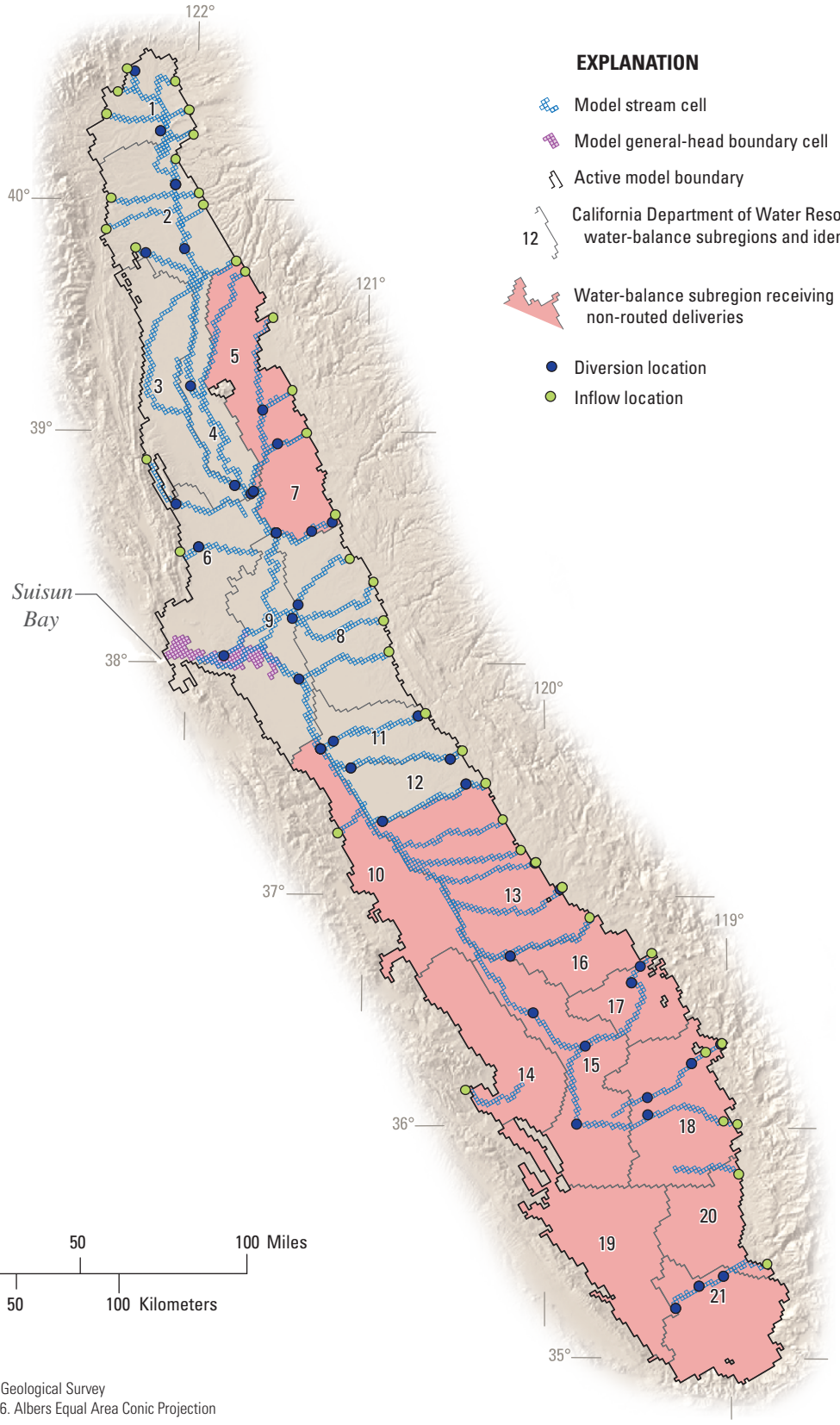

Figure C2. Distribution of general-head boundary cells and major streams and canals with streamflow-routing cells (including location of inflows and diversions). The water-balance subregions are described in *table A1*.

Specified-Flow Boundaries

The lower and lateral model boundaries are simulated as no-flow and the lateral boundaries generally are no-flow. As previously described, the lower boundary was located 1,800 ft below the land surface or 1,500 ft below the base of the Corcoran Clay, where it exists (*fig. A11*). Where bedrock intersected the model, model cells completely within the bedrock also were specified as no-flow (*fig. C1B*). Significant vertical flow at these depths or within the bedrock was considered unlikely. Lateral boundary conditions represent the contact between the mountain ranges and the unconsolidated alluvial sediments of the Central Valley (*fig. C1*). Except at the Delta, there are no-flow boundaries along the periphery of the Central Valley basin representing the Sierra Nevada, Coast Ranges, and surrounding mountains (*fig. C1*).

Pumpage

Groundwater pumpage is a major part of the groundwater budget of the Central Valley, and is grouped into two categories for this study: agricultural and urban (which includes municipal and industrial sources). Wells were simulated as a combination of "farm" wells (Schmid and others, 2006b) and multi-node wells (Halford and Hanson, 2002) (*fig. C3*). Farm wells are simulated in a manner similar to the WEL package (Harbaugh and others, 2000) and the pumpage is distributed among each of the farm wells (Schmid and others, 2006b). Agricultural pumpage is estimated through the FMP, whereas urban pumpage is specified using values compiled from DWR (C. Brush, California Department of Water Resources, written commun., February 21, 2007).

Agricultural Pumpage

Discharge from agricultural wells rarely is metered in the Central Valley (Diamond and Williamson, 1983), and, therefore, must be estimated by indirect means. The two most common methods are power consumption and consumptive use of water. Because groundwater pumpage was not metered, there can be no direct determination of the accuracy of the different methods of estimation. Power consumption historically has been used to estimate agricultural groundwater pumpage in the Central Valley, and was used for the original Central Valley RASA studies for the 1961–1977 time period (Diamond and Williamson, 1983). The power-consumption method involves estimating pumpage from the amount of power consumed by well pump motors. Although these estimates are very accurate under ideal conditions, this accuracy generally is not achievable and is not available for the entire valley or throughout the 1961–2003 simulation period of the CVHM (Diamond and Williamson, 1983). These data were tabulated for comparison purposes. Significant conversion from electrical to hydrocarbon-based energy sources in the 1980s and 1990s for agricultural pumpage limits the usefulness of electrical power records for estimating groundwater pumpage in later times.

Consumptive use of water in this context refers to all ET by a particular crop. If consumptive use can be quantified, groundwater pumpage may be estimated by taking into account surface-water supply, irrigation efficiency, and effective precipitation. Irrigation efficiency, as used in this report, is the percentage of water delivered to the WBS that is available for consumptive use (Diamond and Williamson, 1983). The newly developed FMP for MF2K uses this method (Schmid and others, 2006b). A disadvantage of this method is that it includes no direct measurement of pumpage; instead, it calculates pumpage as the residual irrigation demand. Because most of the wells in the Central Valley are not metered, and the power estimates are unavailable in many locations for much of the simulation period, the magnitude and distribution of pumpage was calculated using the FMP.

For the FMP, in each WBS, a single well was placed in each model cell where an irrigated crop was the predominant land use for a given time frame. Because the extent of irrigated agriculture changes through time, wells were added and deleted accordingly in the model during the simulation period. In general, wells were added through time because the extent of irrigated agriculture generally increases through time. In some areas, however, agricultural wells were replaced by urban wells in the model as the land use changed from agricultural to urban. In more limited areas, agricultural land was taken out of production and replaced by native vegetation; in these cases, the wells were removed. The single well per model cell represents the composite of all wells in each square-mile cell. Previous studies (Diamond and Williamson, 1983; Gronberg and Belitz, 1991) show that wells within the valley typically are at least this densely spaced.

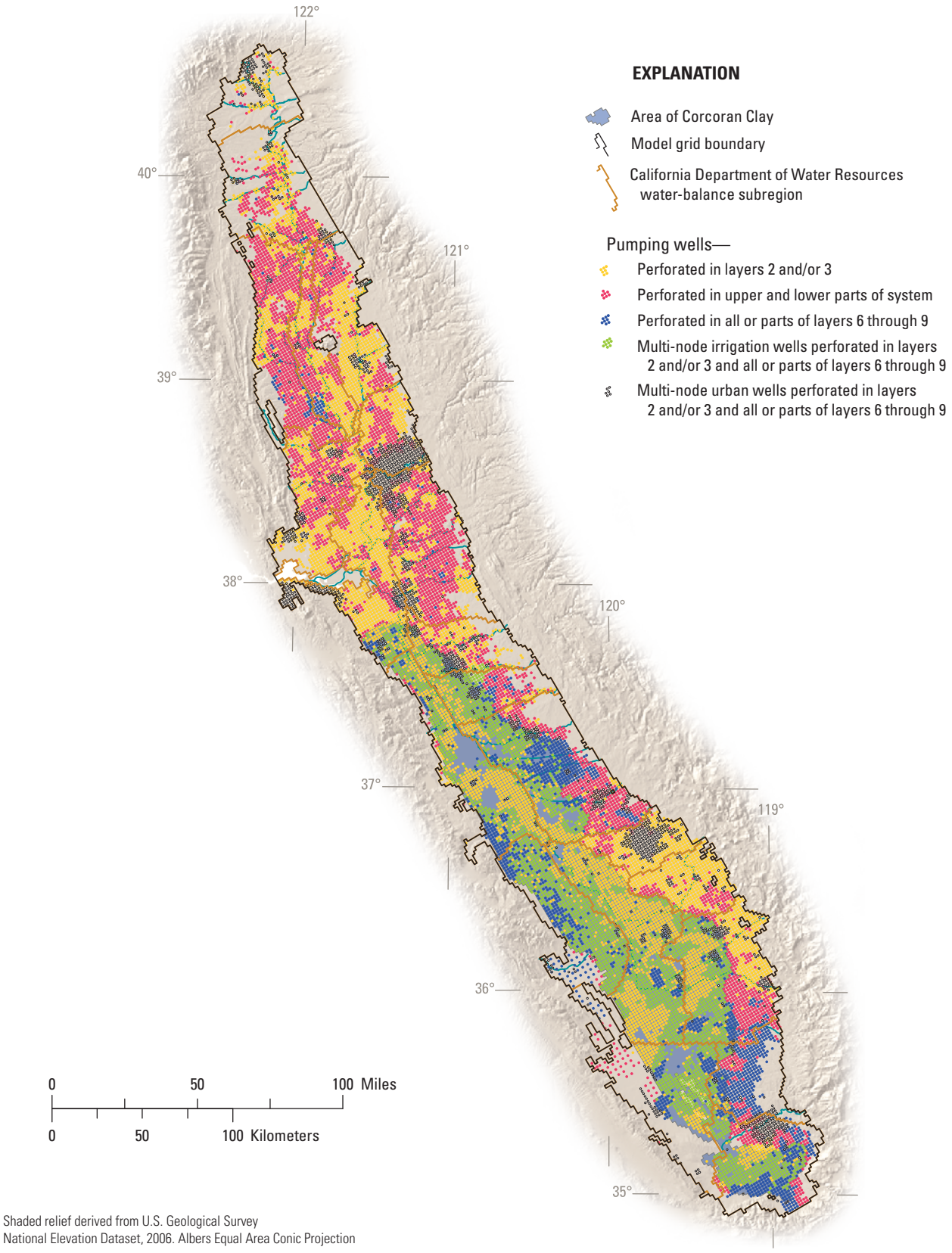

Figure C3. Distribution of urban and agricultural wells simulated in the Central Valley Hydrologic Model.

Pumpage was allocated to the layers, according to the construction information available from DWR and USGS files and databases. The open interval was used to identify the layers from which pumpage occurred. Specifically, the existing wells were analyzed, and the interval top and bottom for each model cell was assigned, based on wells in the area. Because pumpage was assumed to be minimal in the upper 50 ft of the system (layer 1), owing to typical construction of surface sanitary seals in production wells, and within blank-casing intervals in production wells across the Corcoran Clay (layers 4 and 5), pumpage was not simulated in these layers. Furthermore, no pumpage was simulated in the lowest layer, 10. Hence, depending on completion depths, pumpage was assumed to occur in layers 2–3 and in layers 6–9. Initially, where wells extended across multiple layers, the MNW package was used to simulate flow through the wellbore. Because of exceedingly long run times, only where wells are perforated above and below the Corcoran Clay was the MNW package used to simulate multi-aquifer pumpage and flow through the wellbores across the clay. Outside the area of the Corcoran Clay, a well was assigned to each model cell that was intersected by a wellbore. Because only a small amount of flow is thought to occur through well-bore flow outside this area, this simplification is thought to be reasonable. Estimated agricultural pumpage was restricted to wells in model cells corresponding to areas where active crops needed more water than was being supplied by precipitation or surface water. The FMP allocated the pumpage in these model cells on the basis of their specified hydraulic properties.

A substantial amount of agricultural pumpage has occurred in the western parts of the San Joaquin Valley and Tulare Basin. Diamond and Williamson (1983) and Gronberg and Belitz (1991) showed that more than 80 percent of this pumpage came from the deeper part of the system, below the Corcoran Clay. Because FMP distributes the amount of pumpage within a WBS evenly to all farm wells, including to multi-node wells, until the well's specified pumping capacity is reached (Schmid and others, 2006b), another way of adjusting the proportion of pumpage coming from the different parts of the system was needed. The capacity of the farm wells in the upper part of the system was set very low to approximate the estimated low pumpage from these wells (*fig. C3*). In addition, for farm wells perforated above and below the Corcoran Clay and simulated using the MNW package, the well skin factor was adjusted in the upper part of the system to force more simulated pumpage from the lower part of the well (*fig. C3*).

Urban Pumpage

Urban pumpage is a small percentage of the annual total estimated pumpage in each WBS (Diamond and Williamson, 1983) (*fig. B6B*). As with the agricultural pumpage data, urban pumpage data from the original USGS Central Valley RASA studies were available for 1961–1977 (Diamond and Williamson, 1983). The amount of urban pumpage also was compiled by DWR for C2VSIM for each WBS for the entire simulation period (C. Brush, California Department of Water Resources, written commun., February 21, 2007). In general, estimated pumpage from both compilations increase with time; however, overall, DWR's estimates are twice as much as those of the USGS (*fig. C4*). The larger estimates are most dramatic in the Sacramento metropolitan area where the USGS compilation may have had incomplete information (Diamond and Williamson, 1983). Because public-water suppliers are required to report the sources and volumes of water supply to the State (DWR), the DWR information is assumed to be more complete and accurate. Therefore, in order to have a complete and consistent data set for the entire simulation period, DWR's compilation of urban pumpage is used.

The location of urban wells in the CVHM, like agricultural wells, is based on land use. Where the majority of a corresponding model cell is occupied by urban land use, a single well is specified in the appropriate model layer(s) to represent the composite pumpage for urban use (municipal and industrial pumpage) within that cell. The total amount of urban pumpage per WBS per month is distributed evenly within each WBS to all urban cells. To allow for flow through the borehole, the MNW package is used to simulate all urban groundwater pumpage.

The vertical distribution of urban pumpage is segregated in a manner similar to the agricultural pumpage. Within the urban parts of each WBS, urban pumpage is allocated to the layers according to the well-completion information available from DWR and USGS files and databases. The open-screen interval is used to identify the layers from which pumpage occurred. Specifically, the existing wells were analyzed and the interval top and bottom for each cell is assigned on the basis of the perforated intervals of wells in the area. Pumpage is assumed to be minimal in the upper 50 ft of the system (layer 1) and within the Corcoran Clay (layers 4 and 5), and, generally, pumpage is not simulated in these layers. Where layer 1s thickness is increased to 147 feet, pumpage is allowed to occur in layer 1. Hence, as with agricultural pumpage, urban pumpage is simulated predominantly in layers 2–3 and in layers 6–9.

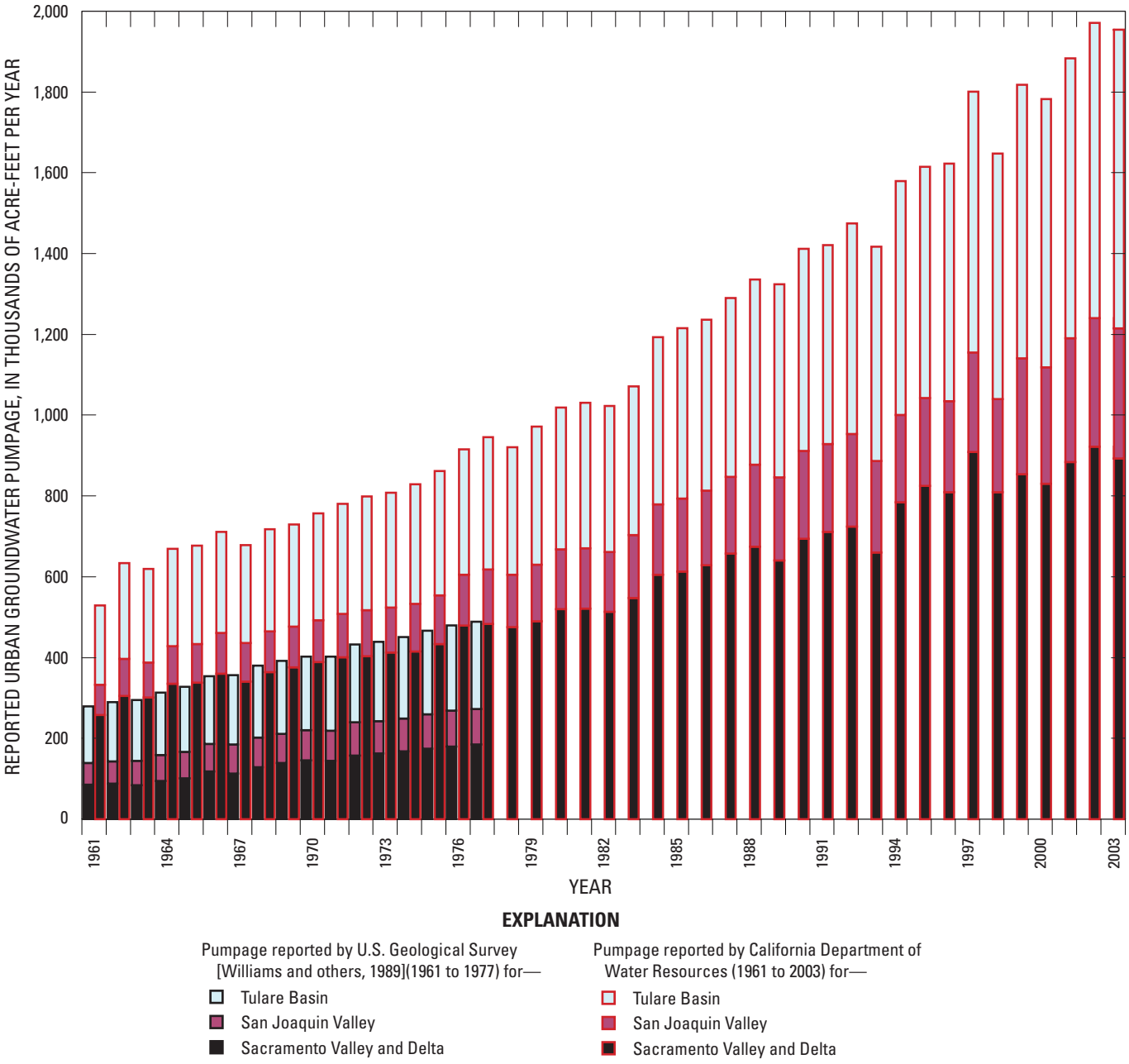

Figure C4. Urban pumpage from U.S. Geological Survey and California Department of Water Resources data (C. Brush, California Department of Water Resources, written commun., February 21, 2007).

Recharge from and Discharge to the Delta

The Delta is the only lateral-flow boundary simulated as a head-dependent flow boundary. This area was simulated by the MODFLOW General Head Boundary package (GHB) (McDonald and Harbaugh, 1988; Harbaugh and others, 2000) (*table C1*); general-head boundaries can both receive water from and contribute water to the aquifer system. General-head boundaries were specified in layers 1–3 at all cells throughout Suisun Bay (*fig. C2*). Water-level altitudes specified for the general-head boundary were estimated to be at sea level, and remained constant for the entire simulation period. The hydraulic conductance of the boundary was specified to be relatively large, compared to that of the adjacent cells. As a result, the texture-derived hydraulic conductivity of the aquifer-system sediments (in the adjacent cells) controls leakage to and from the Delta.

Recharge from and Discharge to Canals and Streams

A large number of streams and canals dissect the Central Valley. Forty-six key streams and canals (comprising 190 segments) were used to represent the major streams and water conveyance features (*fig. C2*). These features were simulated using the Streamflow Routing package (SFR1) (Prudic and others, 2004) (*table C1*); this head-dependent boundary condition allows groundwater discharge (gaining stream reaches), stream infiltration into the underlying aquifer (losing stream reaches), and the diversion of water for water supply or irrigation.

The SFR1 package also accounts for water that is routed through stream networks. This routing capability is used in the CVHM to route water from streams and canals as semi-routed deliveries to WBSs through the FMP. There are 41 major river inflows (*fig. A8*) and 66 diversions for irrigation simulated in the CVHM (*fig. A2*, *table A1*). Two of the river inflows each are divided into two additional inflows for book-keeping purposes, resulting in 43 simulated inflows. Two of the diversions are diverted out of the model area such that there only are 64 deliveries to WBSs (*table A1*).

The remainder of the streamflow that does not infiltrate as groundwater recharge or is not diverted and consumed for agriculture flows out of the Sacramento and San Joaquin River systems into the Delta (*fig. C2*). Some flow out of the Kern River (WBS 21, *fig. A2*) is simulated as a loss to the American Canal system, which represents water exported to Southern California.

Water-Table Simulation

In MF2K, model layers can be defined as either confined or convertible between confined and unconfined (Harbaugh and others, 2000). Confined layers are assigned a thickness that does not change during the simulation, regardless of the simulated value of hydraulic head. In this study, all layers were simulated as confined. For the CVHM, where the water table is deeper than 50 ft (*fig. B17*) for the entire 1961–2003 simulation period, the base of layer 1 is specified 147 ft below land surface, and layer 2 is specified as a dummy layer 3-ft thick with a large vertical conductivity and small horizontal conductivity. Where the water table is deeper than a model layer for the entire simulation, the model cells above the water table are inactivated. Because of the large percentage of fine-grained sediments in the Central Valley, Williamson and others (1989) concluded that sediments below the upper few hundred feet should be considered "confined" in the sense that the vertical permeabilities of the sediments are much lower than the horizontal permeabilities. Accordingly, in the CVHM, layers 8–10 are simulated as "confined". Storage properties in the upper layer are adjusted, as necessary, to represent the unconfined part of the system (see "*Storage Properties*" section). Because specific-yield properties apply at the water table and other storage properties are significantly smaller, layers with a water table are characterized by a storage coefficient equal to specific yield, but the saturated thickness is taken as a fixed value. The saturated thickness is based on the thickness of the model layer. Partly to decrease the magnitude of errors associated with saturated thickness, the layers are designed to be thinner near the water table and thicker with depth (*table A3*). These simplifications are thought to be acceptable for the intended use of the CVHM.

Despite simulating confined flow in the water table, a provision was made to represent unconfined-flow conditions by allowing model cells to activate (rewet) as the water table rose above the underlying cells; however, cell rewetting prohibitively increased numerical instability and computation time. Much of this instability was associated with cells where the water table intersects the Corcoran Clay. Ultimately, this rewetting provision was not implemented in this study, but could be incorporated with further refinements of the CVHM and (or) when better solvers become available.

Farm Process (FMP)

For the CVHM, the processes of evaporation, transpiration, runoff, and deep percolation to groundwater were estimated using the FMP. The FMP allocates water, simulates or approximates processes, and computes mass balances for defined subregions of the model domain; in the CVHM, these subregions, or "farms," are defined as the WBSs.

The FMP was developed for MF2K to estimate irrigation water allocations from conjunctively used surface water and groundwater (*fig. C5*). It is designed to simulate the demand components representing crop irrigation requirements and on-farm inefficiency losses, and the supply components representing surface-water deliveries and supplemental groundwater pumpage. The FMP also simulates additional head-dependent inflows and outflows such as canal losses and gains, surface runoff, surface-water return flows, evaporation, transpiration, and deep percolation of excess water.

The FMP is based on mass balances (Schmid and others, 2006a, b). A farm mass balance is maintained between all inflows to and outflows from a farm, and is calculated and balanced for each simulation time step (*fig. C5*). A soil-water balance is calculated between inflows into the soil zone and the ET outflow. The details of the soil-water balance are given by Schmid and others (2006b), and are not shown on *figure C5*. The FMP dynamically integrates irrigation water demand, surface-water and groundwater supply, and deep percolation.

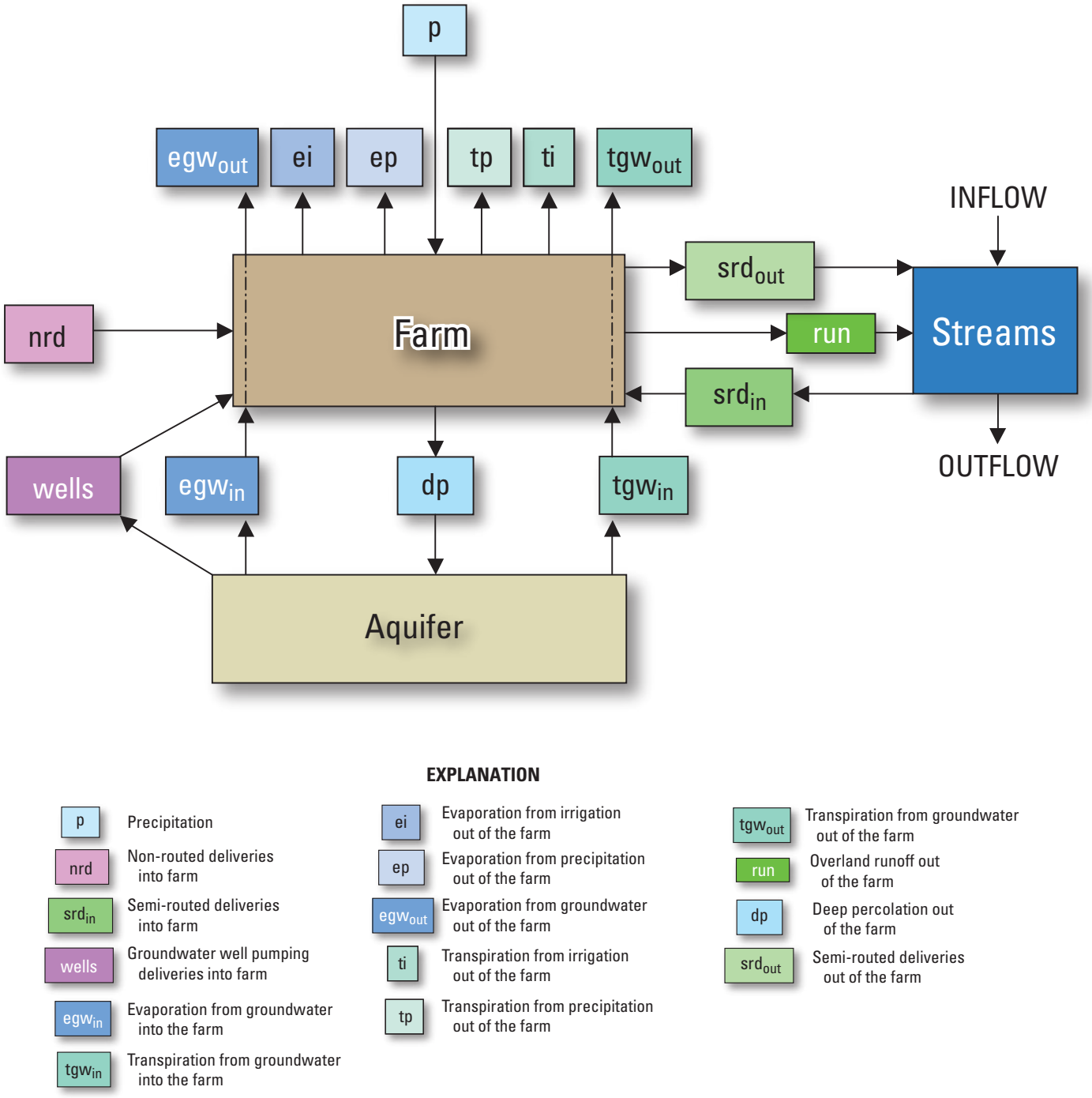

Figure C5. Flow chart of water inflows to and outflows from a "farm" as simulated by the Farm Process (FMP).

The FMP has the capability to estimate economically optimal allocations through acreage optimization of water supplied by surface-water and groundwater deliveries when demand exceeds supply. Other non-economic drought-response scenarios, such as deficit irrigation and water stacking, also are available. Combined with other MF2K packages such as SFR1 and MNW packages, the FMP helps to transform MF2K from a predominantly groundwater-flow model to a more complete hydrologic model. While the FMP contains many optional simulation features, only some of the available components are used for the Central Valley. More details on all the components of the FMP can be found in Schmid and others (2006b).

Few applications of this new MODFLOW capability are published because the FMP is a new process developed, in part, as part of this project and the ongoing research of the Groundwater Availability Program of the USGS. The first real-world application of MF2K with FMP and SFR1 was a micro-scale model for several hundred acres in the southern Rincon Valley, along the Lower Rio Grande of New Mexico within the Elephant Butte Irrigation District (Schmid and others, 2006a). In contrast to the micro-scale application in the Rincon Valley, the Central Valley represents a macro-scale application. The FMP components used in the simulation of the hydrologic flow system of the Central Valley are summarized in this chapter. Within MF2K, the FMP was used to simulate the surface-water and groundwater inflows and outflows needed by irrigated agriculture, native vegetation, and urban areas. For the purposes of this report, the WBS represents the basic accounting unit (farm) for water consumption. On the basis of cell-by-cell estimations for each WBS, the FMP first calculates crop-water demand as the transpiration from plant-water consumption and the related evaporation. The FMP then determines a residual crop-water demand that cannot be satisfied by precipitation and (or) by root uptake from groundwater. The FMP then equates this residual crop-water demand with the crop-irrigation requirement for the cells with irrigated crops (exclusive of any natural vegetation).

This crop irrigation requirement then is adjusted (increased) by accounting for evaporative losses from irrigation, and other losses owing to inefficiencies, to yield a final total farm delivery requirement (TFDR). In this report, the TFDR is equivalent to the delivery requirement (DR) discussed in *Chapter B* of this report. The FMP first attempts to satisfy the TFDR using surface water. The surface water can be obtained from source water that is not simulated in the stream network, referred to in this chapter as “non-routed,” or from water routed through the stream network and delivered to a WBS, referred to in this chapter as “semi-routed.” The non-routed surface-water supply components have first priority and surface-water deliveries have second priority. Lastly, if the TFDR is not met using surface water, the FMP computes the amount of supplemental groundwater necessary to extract from “farm” wells in order to satisfy the TFDR. The amount of excess water from irrigation and (or) precipitation that is not evaporated or consumed for plant growth then becomes either overland runoff to nearby streams or groundwater recharge. As mentioned earlier, a soil-water balance is calculated between inflows into the soil zone and the ET outflow. Thus, the FMP dynamically links the demand, supply, and related change in aquifer-system storage. All of the supply and demand components then are tabulated into a WBS budget that complements the groundwater-flow budget.

In order to do these calculations, the FMP integrates the components of supply and demand data, which can vary temporally. On the supply side, surface-water delivery and ”farm” well-construction data are needed to estimate the semi-routed and non-routed surface-water deliveries and the groundwater pumpage requirements, respectively. On the demand side, the FMP uses soil, land use, and consumptive irrigation requirement (CIR) to calculate demand.

The FMP dynamically simulates these supply and demand components for a WBS within MF2K by integrating the following computational components (*fig. C5*):

(1) TFDR, which depends on efficiency, changing climate (ET and precipitation), and variable shallow groundwater levels;

(2) Actual surface-water delivery to the WBS, which may be driven by TFDR, but limited by canal/stream inflow rates at the WBS’s diversion head gate, by allotments, or by semi- or non-routed deliveries;

(3) Supplemental groundwater pumpage, which is estimated as the TFDR minus the actual surface-water delivery, but is limited by a specified maximum farm well-pumping capacity on a well-by-well basis; and

(4) Net recharge (deep percolation) to groundwater, which is taken to be the sum of excess irrigation and precipitation minus the sum of surface-water runoff and ET from groundwater.

MF2K and the FMP maintain a dual mass balance of a WBS budget and a groundwater budget (*fig. C5*). Flows between these two budgets are accommodated by head-dependent inflows and outflows, such as the actual ET from groundwater. Quantities of interest, such as TFDR, surface-water and groundwater supply, and excess applied irrigation water depend on these head-dependent inflows and outflows. Thus, the use of FMP in MF2K represents the simulation of coupled flow of water through surface-water, land-use, and groundwater processes (Schmid and others, 2006a).

Delivery Requirement

The delivery requirement is defined as consumptive use of water by irrigated crops not met by natural precipitation plus any inefficient use from irrigation, with respect to plant consumption. In the CVHM, consumptive use is actual ET and includes both plant transpiration and evaporation (Schmid and others, 2006b). For the FMP, this consumptive use includes components estimated from both the landscape (predominantly met through irrigation) and groundwater systems. Thus, the amount of evaporation and transpiration from the groundwater table are computed. As a result, in the FMP, ET is a function of water-table altitude and the assumed wilting point of each crop.

Soils

The Central Valley soils were simplified into sandy loam, silty clay, and silt from the State Soil Geographic Database STATSGO (U.S. Department of Agriculture Natural Resources Conservation Service, 2005b) (*fig. C6*). The capillary fringe thickness also was estimated for each soil type (*fig. C6*). The FMP associates the distributed soil types with the specified capillary fringes and internal coefficients that allow individual analytical solutions for the calculation of evapotranspiration (Schmid and others, 2006a). The more detailed Soil Survey Geographic Database (SSURGO) (U.S. Department of Agriculture Natural Resources Conservation Service, 2005a) were not available for the entire Central Valley when this study began. Further refinement of soils information from SSURGO could be a future refinement of the CVHM.

Land Use

The FMP was used to estimate components of consumptive use for a wide variety of land uses, including vegetation in irrigated or non-irrigated agriculture, fallow fields, riparian or natural vegetation, and urban landscape settings. Similarly, FMP was used to simulate an assortment of irrigation methods and periods of transition between applied methods. The methods span the spectrum from flood irrigation such as for rice and cotton, to drip irrigation of truck crops and orchards. Although not used here, the FMP also can be used for applications with no, or nearly no, transpiration, such as for surface impoundments and spreading basins used for artificial recharge systems.

For the Central Valley, the land-use attributes are defined in the model on a cell-by-cell basis and include urban and agricultural areas, water bodies, and natural vegetation. The land use that covered the largest fraction of each 1-mi^2 model cell was the representative land use specified for that cell. Producing representative maps of land use, including crops, at regional scales is problematic because of the complex pattern that is subject to rapid change in the dynamic environment of modern agricultural processes. Despite the uncertainty and complexity, land-use maps were developed for five different time frames during the 42.5-year simulation period. Most of these maps were based on interpreted high-altitude aerial photography. Because land-use may vary gradationally or discretely in time, on the basis of climate variability, urbanization, or the farmer's free-market practices, criteria for selecting representative time frames were necessary. For this simulation, the five land-use patterns were aligned with the wet-dry climate cycle for which they were compiled (*fig. C7*).

Most of the valley floor is developed agricultural land (*table C3*). This agricultural land was further subdivided into agricultural classifications in the FMP. The agricultural classifications are based on the 12 DWR class-1 categories (California Department of Water Resources, 2000). The 12 class-1 categories were augmented with more general classes for earlier years when the delineation of land use was less detailed (*table C3*). In general, the 12 class-1 categories represent groups of vegetation that have similar amounts of water consumption and similar growth cycles that drive their consumption of water. These land-use categories, herein referred to as "virtual crops", are defined from land-use maps for 1960, 1973, 1992, 1998, and 2000 (*table C3*; *figs. C7–C12*). For simplicity, the land-use maps are named for the year the map represents. For the entire simulation period, the virtual crops are used to drive water movement and water use for each WBS. In total, there are 22 virtual crops. Each of the virtual crops is represented by a number in the FMP (*table C3*). Many of the virtual crops are amalgamations of the others (*table C3*, grouping of other classes). For example, virtual crops 19–22 are amalgamations of five or more virtual crops (*table C3*, grouping of other classes). Because the virtual-crop maps for the earlier time periods are more generalized, some of the more permanent or more established crop types mapped more recently are assumed to be active earlier and are embedded in the earlier maps on the basis of the most recent land-use period (2000 land use).

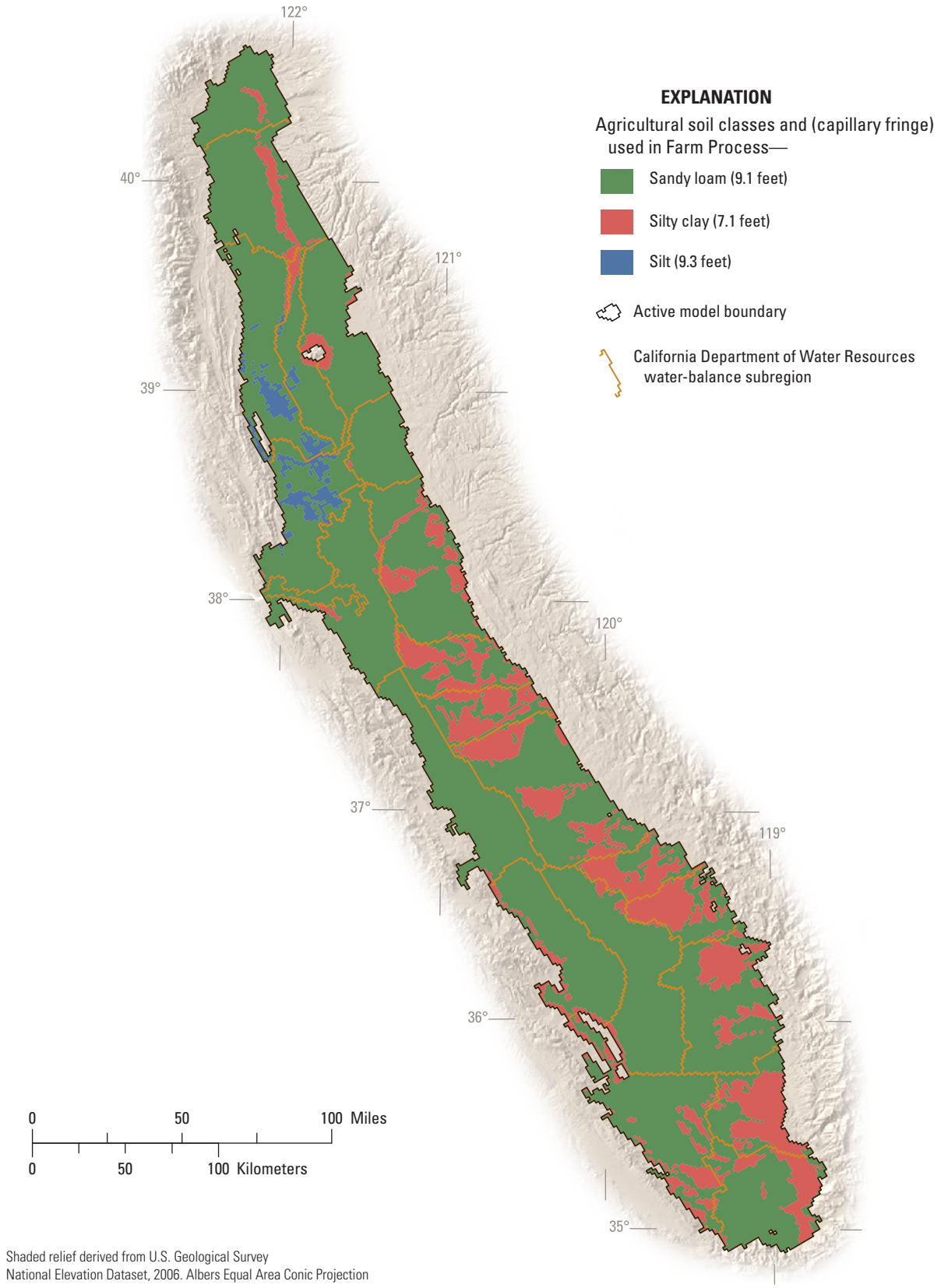

Figure C6. Agricultural soils for the Central Valley, California, derived from STATSGO data (U.S. Department of Agriculture Natural Resources Conservation Service, 2005b).

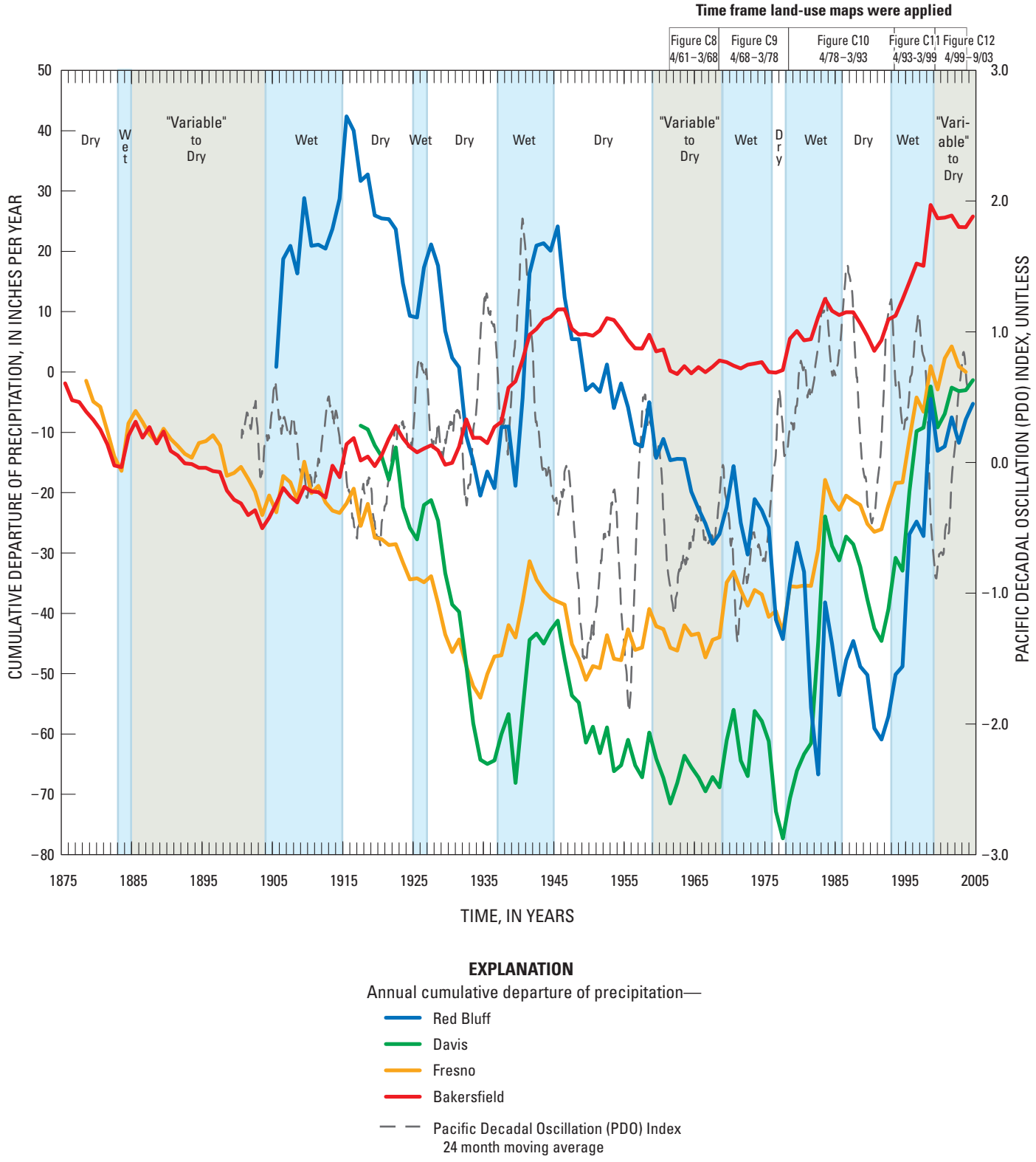

Figure C7. Cumulative departure of precipitation, Pacific Decadal Oscillation (PDO) Index, climate windows, and time frame land-use maps were applied.

Table C3. Land-use periods with acreage in square miles and percentage of different virtual crop categories.

Description	Irrigated	Area (square miles)					Percentage of active model area					Grouping of other classes[1]
		1961	1973	1992	1998	2000	1961	1973	1992	1998	2000	
1. Water	No	105	124	160	347	162	1	1	1	2	1	n/a
2 . Urban	No	641	765	1,043	894	1,528	3	4	5	4	7	n/a
3. Native classes[2]	No	7,355	4,809	6,237	5,102	6,639	36	23	30	25	32	n/a
4. Orchards, groves, and vineyards	Yes	n/a	312	553	263	n/a	n/a	2	3	1	n/a	10,12,16
5. Pasture/Hay	Yes	n/a	n/a	1,799	589	n/a	n/a	n/a	9	3	n/a	13,14
6. Row Crops	Yes	n/a	n/a	1,265	n/a	n/a	n/a	n/a	6	n/a	n/a	9,11,18
7.Small Grains	Yes	n/a	n/a	634	n/a	n/a	n/a	n/a	3	n/a	n/a	11,14,17
8. Idle/fallow[2]	Yes	241	104	1	n/a	372	1	1	<1	n/a	2	n/a
9. Truck, nursery, and berry crops[2]	Yes	889	923	640	934	958	4	4	3	5	5	n/a
10. Citrus and sub-tropical[3]	Yes	350	269	364	204	429	2	1	2	1	2	n/a
11. Field crops[2]	Yes	1,483	1,561	1,103	1,568	1,602	7	8	5	8	8	n/a
12. Vineyards[2]	Yes	1,098	675	1,095	915	1,209	5	3	5	4	6	n/a
13. Pasture[2]	No	1,198	1,366	788	862	1,448	6	7	4	4	7	n/a
14. Grain and hay crops[2]	Yes	708	821	497	810	893	3	4	2	4	4	n/a
15. Semi-agriculture [2,3]	Yes	4	n/a	n/a	n/a	5	0	n/a	n/a	n/a	0	n/a
16. Deciduous fruits and nuts[2]	Yes	2,075	1,010	1,921	1,683	2,344	10	5	9	8	11	n/a
17. Rice[2]	Yes	948	991	947	993	1,001	5	5	5	5	5	n/a
18. Cotton	Yes	1,635	1,891	1,486	1,917	1,943	8	9	7	9	9	n/a
19. Developed	Yes	1,803	n/a	n/a	n/a	n/a	9	n/a	n/a	n/a	n/a	8,9,10,11,12,13, 14,15,16,17,18
20. Cropland and pasture	Yes	n/a	4,912	n/a	n/a	n/a	n/a	24	n/a	n/a	n/a	9,11,13,14,17,18
21. Cropland	Yes	n/a	n/a	n/a	1,542	n/a	n/a	n/a	n/a	8	n/a	9,11,13,14,16,17,18
22. Irrigated Row and Field Crops	Yes	n/a	n/a	n/a	1,910	n/a	n/a	n/a	n/a	9	n/a	9,11,14,17,18

[1]Land-use category number of amalgamated crops from "descrition" in column 1.

[2]California Department of Water Resources class-1 categories (California Department of Water Resources, 2000).

[3]Semi-agricullture includes livestock feedlots, dairies, and poultry farms.

Virtual Crop Maps

For the simulation period of spring 1961 to spring 1968 ("1960" land-use map, *fig. C8*), land use was based on data gathered by California State University, Chico (2003), by using a geographic information system (GIS) to quantify vegetation changes over the previous 100 years. Maps were produced to identify major changes that have occurred in the valley due, in part, to hydrologic alterations associated with the Central Valley Project around 1945 and the California State Water project around 1968. The "1960" map (represented in the simulation period from 1961 to 1968) uses information on the extent of urban and agricultural areas from DWR land-use maps and native vegetation from earlier maps. As such, it is a patchwork of sources, scales, dates, accuracies, and completeness (California State University, Chico, 2003). The "1960" map includes nine vegetation classes. Eight of these classes are different types of native vegetation; one class, "urban/agriculture" represents developed land use. This study focuses on developed land uses. As a result, the native vegetation classes were lumped into one category for this study. Likewise, because of the generalized agricultural and urban classifications on this map, the best estimate for the extent of urban land uses available was from 1973. Therefore, the extent of urban areas was taken from the 1973 land-use map. Likewise, the "urban/agriculture" virtual crop class, where not identified as urban in 1973, was replaced with the virtual crop from the 2000 land-use map. For example, where the "urban/agriculture" class was specified and the area was not identified as urban on the 1973 land-use map, the virtual crops interpreted on the 2000 land-use map were embedded. This assumes the farmer would be growing the same type of crop in a given area over the 40-year time frame of the hydrologic simulation. In some cases, such as with orchards, this generally is a good assumption; in other cases, the crops may have changed several times. Approximately 36 percent of the valley was covered by native vegetation, 61 percent was covered by agricultural land (based on the urban and cropped land in 2000), and 3 percent was covered by urban development (*fig. C8*). The definition of early agricultural land use in the Central Valley is an aspect of the landscape hydrologic model that could use much improvement in future refinements of the CVHM.

For the period of spring 1968 to spring 1978, (1973 land-use map; *fig. C9*) land use was interpreted using the Anderson level II classifications (Anderson and others, 1976) and stored in the Geographic Information Retrieval and Analysis System (GIRAS) (U.S. Geological Survey, 1990). Data are gathered by quadrangle, and the dates range from the mid 1970s to the early 1980s (U.S. Geological Survey, 1990). Approximately 23 percent of the valley was covered by native vegetation, 71 percent was covered by agricultural land (24 percent was covered by undifferentiated cropland and pasture, 7 percent was covered by orchards and vineyards, and 40 percent was covered by other types of agriculture, based on 2000 land-use survey), 2 percent was covered by barren land or water, and 4 percent was covered by urban development (*fig. C9*). As Gronberg and others (1998) noted, the forested land predominantly is in the Sierras and rangeland predominantly is in the foothills of the Sierras and the Coast Ranges. Urban areas and agricultural land predominantly are on the valley floor; most orchards and vineyards are on the east side of the valley. Although the data are suitable for representing regional spatial patterns of land use, there are discrepancies across quadrangle boundaries and detail is lacking in specific crop types. In particular, the categorized agricultural land is limited to four classes: (1) cropland and pasture; (2) orchards, groves, vineyards, nurseries, and ornamental horticultural areas; (3) confined feeding operations; and (4) other agricultural land. As a result, these agricultural classifications were revised using information from the 2000 land-use survey in the same manner as the 1960 virtual-crop map. Because of the large extent and lack of definition in the "Cropland and Pasture" class, this class was further revised to "Native" where "Native" was identified in this area on the 1992 map or revised to the particular crop type where the crop type was identified in this area on the 1992 map. This revision smoothed the transition from 1973 to 1992 land-use maps.

For the period spring 1978 to spring 1993 (1992 land-use map, *fig. C10*), land use was based on the North American Land Class Data 1992 (NLCD) classification, a 21-class hierarchical, modified, Anderson Land Cover Classification (U.S. Geological Survey, 1999). The NLCD 1992 data are derived from images acquired by Landsat's Thematic Mapper (TM) sensor, as well as a number of ancillary data sources. Although the map is referred to as NLCD 1992, it represents land use for earlier years and actually is based on imagery acquired throughout the 1980s (U.S. Geological Survey, 1999). It is the first national land-cover data set produced since the early 1970s, effectively replacing the GIRAS data sets. NLCD 1992 data are an improvement over GIRAS data in that the herbaceous agricultural areas (Cropland and Pasture; Anderson Level II) are subdivided into four NLCD classes: Pasture/Hay, Row Crops, Small Grains, and Fallow. In addition, the 30-m resolution, raster-based NLCD was enhanced with GIRAS data to better represent orchards and residential areas (Gilliom and others, 2006). Approximately 30 percent of the valley was covered by native vegetation, 64 percent was covered by agricultural land (56 percent was covered by cropland and pasture and 8 percent was covered by orchards and vineyards), 1 percent was covered by barren land or water, and 5 percent was covered by urban development (*fig. C10*). Although the 1992 virtual crop map is much more detailed than the previous virtual-crop maps, the agricultural classes still were generalized. As with the other maps, some of the generalized agricultural classifications were revised using information from the 2000 land-use survey. The virtual crop "orchards, vineyards, and others" was divided into orchards, vineyards, and deciduous crops. Similarly, pasture and hay were separated, as were the row crops that were included in field and truck crops.

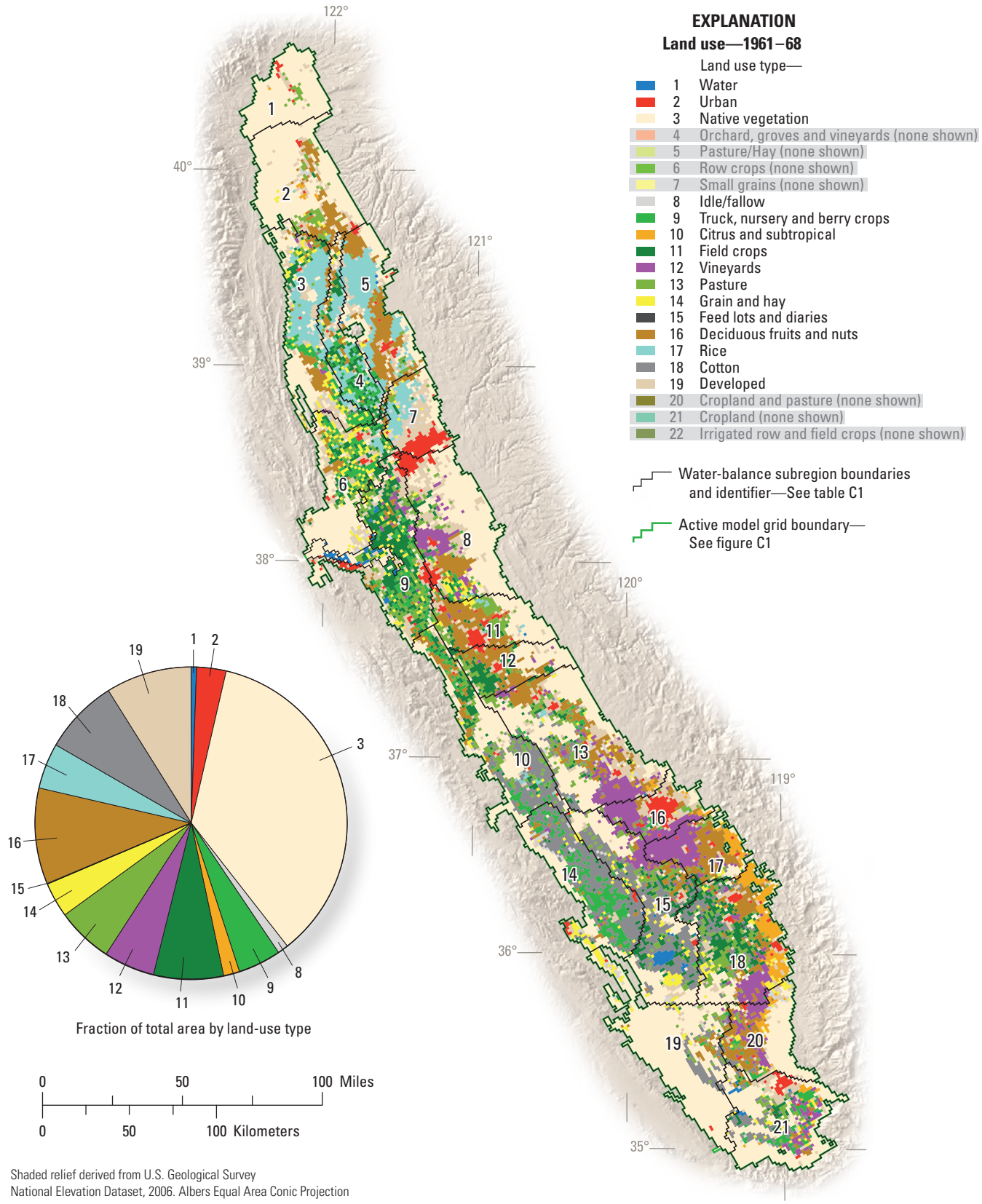

Figure C8. Virtual crops for 1960 (modified with 2000 data), including pie chart of percentage of different virtual crops (sources: California Department of Water Resources, 2000; California State University, Chico, 2003;). The water-balance subregions are described in *table A1*.

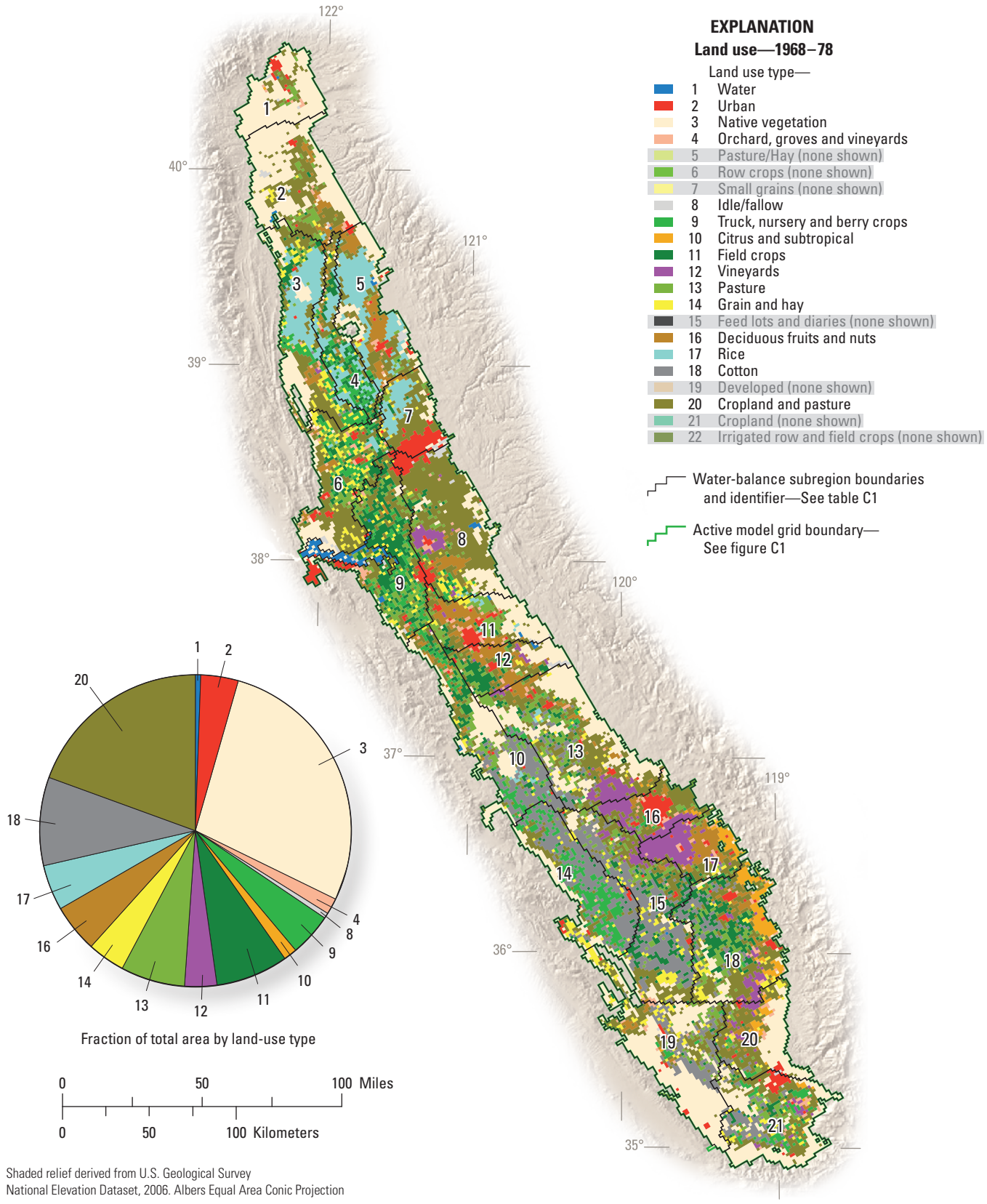

Figure C9. Virtual crops for 1973, including pie chart of percentage of different virtual crops (sources: U.S. Geological Survey, 1990; California Department of Water Resources, 2000). The water-balance subregions are described in *table A1*.

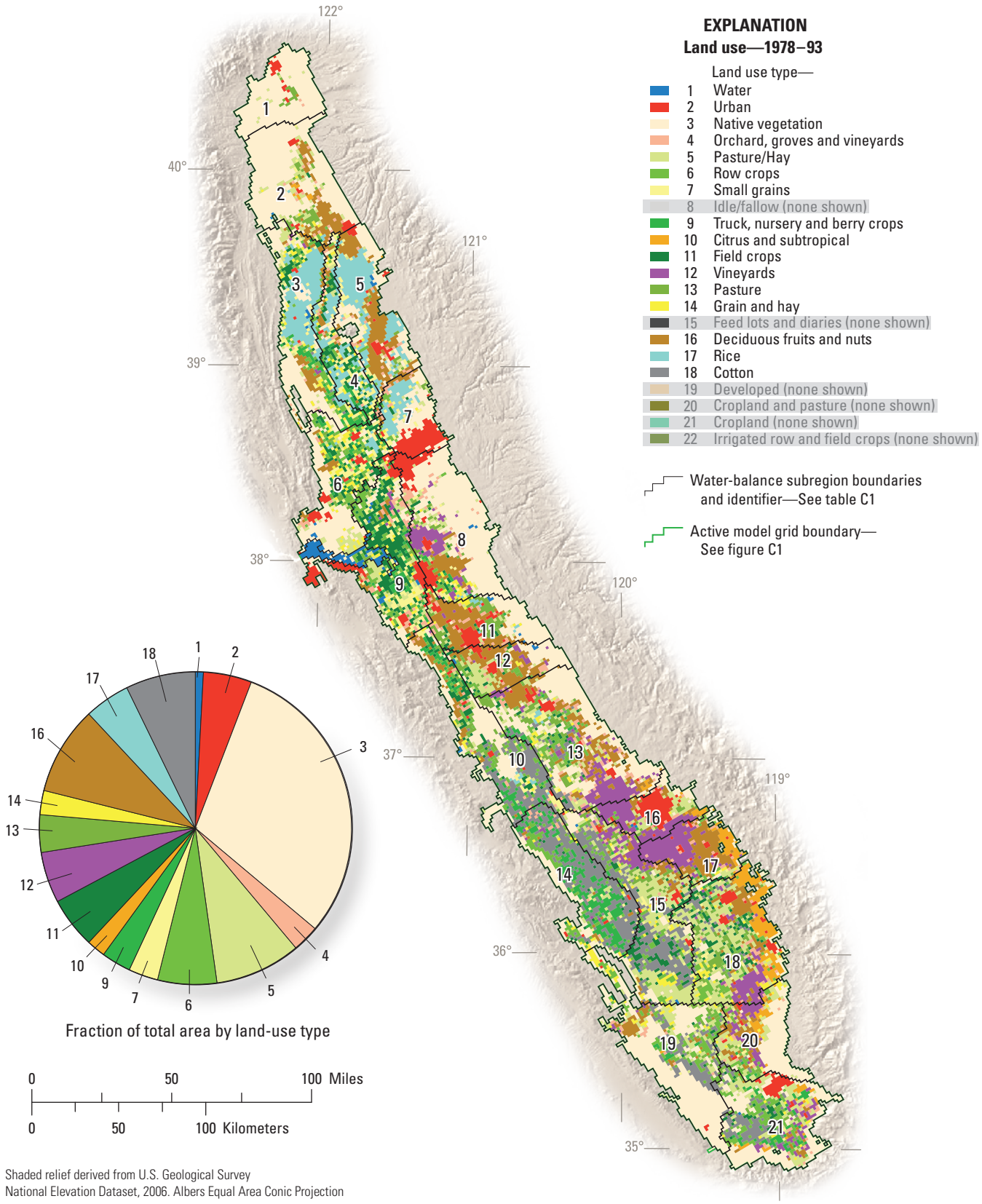

Figure C10. Virtual crops for 1992, including pie chart of percentage of different virtual crops (sources: Gilliom and others, 2006; California Department of Water Resources, 2000). The water-balance subregions are described in table A1.

For the period of spring 1993 to spring 1999 (1998 land-use map, *fig. C11*), land use was obtained from the "Gap Analysis" (Davis and others, 1998). The term "Gap Analysis" refers to the evaluation of the management status of plant communities, vertebrate species, and vertebrate species richness by GIS overlay of biological distribution data on a map of existing biological reserves (U.S. Geological Survey, 1990). Base information started with 1990 satellite and aerial photography data and was augmented extensively by local resources and field work. The date of 1998 is assigned to this land-use map although the land-use source information varies through the 1990s. Approximately 25 percent of the valley was covered by native vegetation, 69 percent was covered by agricultural land (63 percent was covered by cropland and pasture and 6 percent was covered by orchards and vineyards), 2 percent was barren land or water, and 4 percent was covered by urban development (*fig. C11*). The 1998 virtual-crop map has agricultural distributions representative for the time period and many individually mapped crops, such as rice, hay, orchards, and vineyards. However, some crops, such as row and field crops, are lumped together. Therefore, where appropriate, the agricultural classifications were revised using information from the 2000 virtual-crop survey, as with the previous virtual crop maps.

For the period spring 1999 to spring 2003 (2000 land-use map, *fig. C12*), land use was obtained in digital format (California Department of Water Resources, 2000). The county land-use survey data were developed by DWR through its Division of Planning and Local Assistance from aerial photography and extensive field surveys. The land uses that were compiled were detailed agricultural land uses, and lesser detailed urban and native vegetation land uses. The agricultural classifications can be correlated to the 12 DWR class-1 categories (California Department of Water Resources, 2000). This level of spatial detail is ideal for this study. The DWR prepares these detailed county maps of the agricultural land use on the valley floor every 6–7 years. Because the 2000 virtual crop map represents a composite map for land use from the late 1990s, this type of map also lacks the temporal detail needed to accurately reflect the dynamics of changing agriculture or urbanization. Although the data are suitable for representing regional spatial patterns of land use and crop patterns, there are some discrepancies across county boundaries. The agricultural classes were used instead of the more detailed crops that were identified. Approximately 32 percent of the valley was native vegetation, 60 percent was agricultural land (52 percent cropland and pasture, 8 percent orchards and vineyards), 3 percent was barren land or water, and 7 percent was urban (*fig. C12*; *table C3*). The distribution of crops generally reflects the distribution of soil texture and chemistry (Gronberg and others, 1998). About 9 percent of the irrigated land, generally on the southwest side of the valley, is planted in cotton, which is a salt-tolerant crop in its later growth stages. In contrast, 11 percent of the crop land, predominantly on the southeast side, is planted in deciduous fruit and nut trees, which are intolerant of salinity and some trace elements, such as boron, for citrus crops. Rice is grown in the finer-grained deposits in the north, covering about 5 percent of the valley. Together these account for about 25 percent of the total acreage of the crops in the valley. Because of the elimination of subsidies for growing cotton, these percentages recently have changed.

Crop-Type Data

The virtual crops provide a basis for estimating the consumptive use of water at the land surface, a key component of the TFDR (Schmid and others, 2006b). The TFDR largely is determined by the CIR. The CIR is determined from the product of ETo and an area-weighted crop coefficient on a cell-by-cell basis; these products are summed over the uppermost active model cells within each WBS. Because many factors affect ET (including weather parameters, soil factors, and plant factors), it is difficult to formulate an equation that can produce estimates of ET under different sets of conditions (California Department of Water Resources, 2007). Therefore, the idea of a reference crop ET was developed (California Department of Water Resources, 2007); ET from a standardized grass surface that commonly is denoted as ETo.

Specified root depths, suction pressures for the unsaturated root zone, crop coefficients, fractions of runoff, and fractions of transpiration and evaporation affect the consumption and movement of water for each crop category. For the CVHM, constant values of root depths and root uptake pressures were used for the entire simulation and were based on values from the literature and those developed for DWR's C2VSIM model of the Central Valley (C. Brush, California Department of Water Resources, written commun., February 21, 2007). These values are summarized in *table C4*. There is a positive (hydrostatic) and a negative pressure head component to the interval of heads for the root uptake interval for anoxia, optimal, and wilting (*table C4*; *appendix 1*). The positive pressure is used to simulate flooded crops such as rice and other vegetation that tolerates flooded environments. More detailed definitions of the root uptake pressures are given by Schmid and others (2006b).

Direct ET from the groundwater reservoir occurs when the water table is within reach of plant roots or when the capillary fringe reaches the land surface. This form of ET almost completely is eliminated when the water table is lowered below the root zone.

Runoff for each crop type is poorly known. The runoff values are based loosely on those developed for DWR's C2VSIM model of the Central Valley (C. Brush, California Department of Water Resources, written commun., February 21, 2007) and model calibration to surface-water flows in stream channels and out to the Delta.

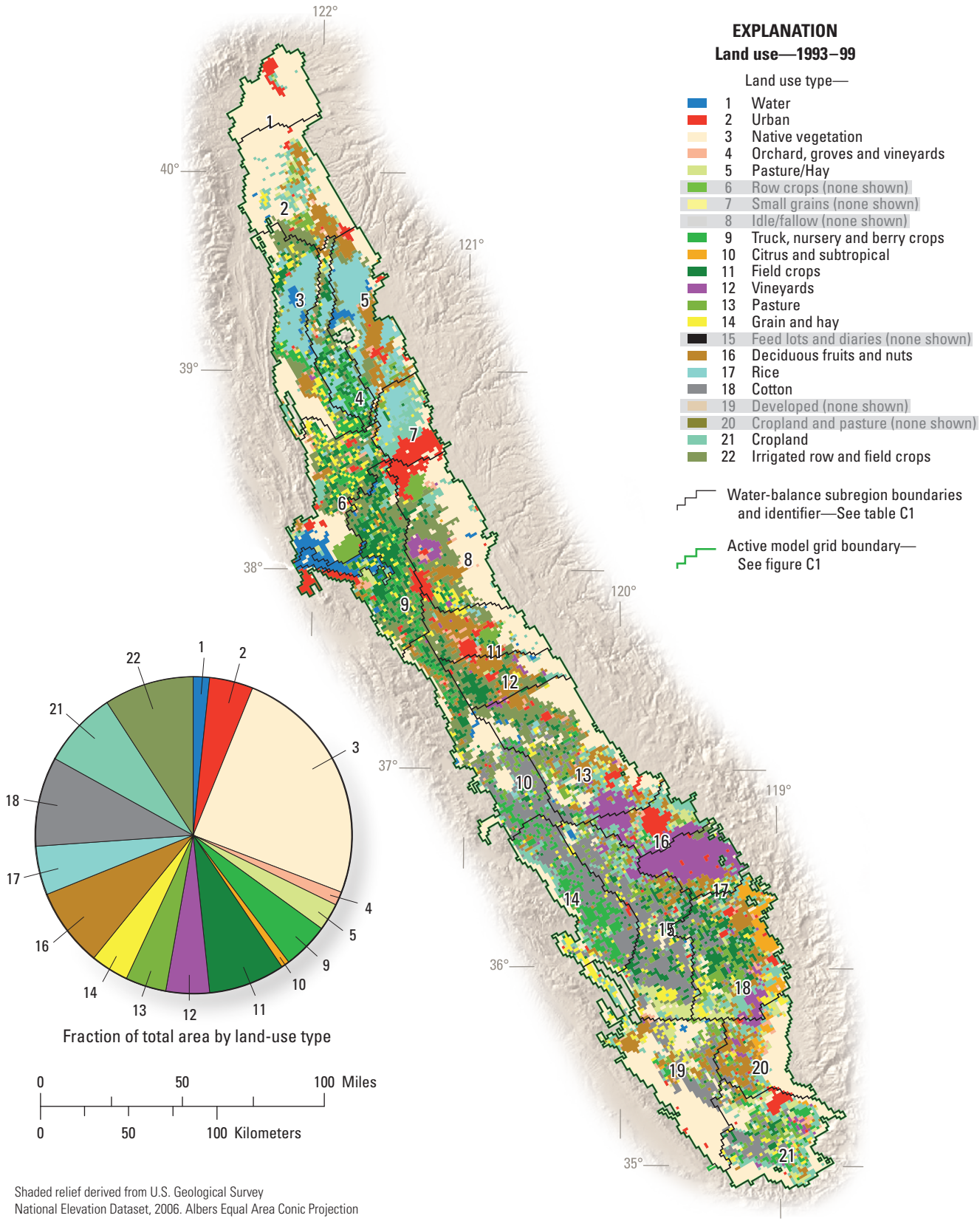

Figure C11. Virtual crops for 1998, including pie chart of percentage of different virtual crops (sources: Davis and others, 1998; California Department of Water Resources, 2000). The water-balance subregions are described in *table A1*.

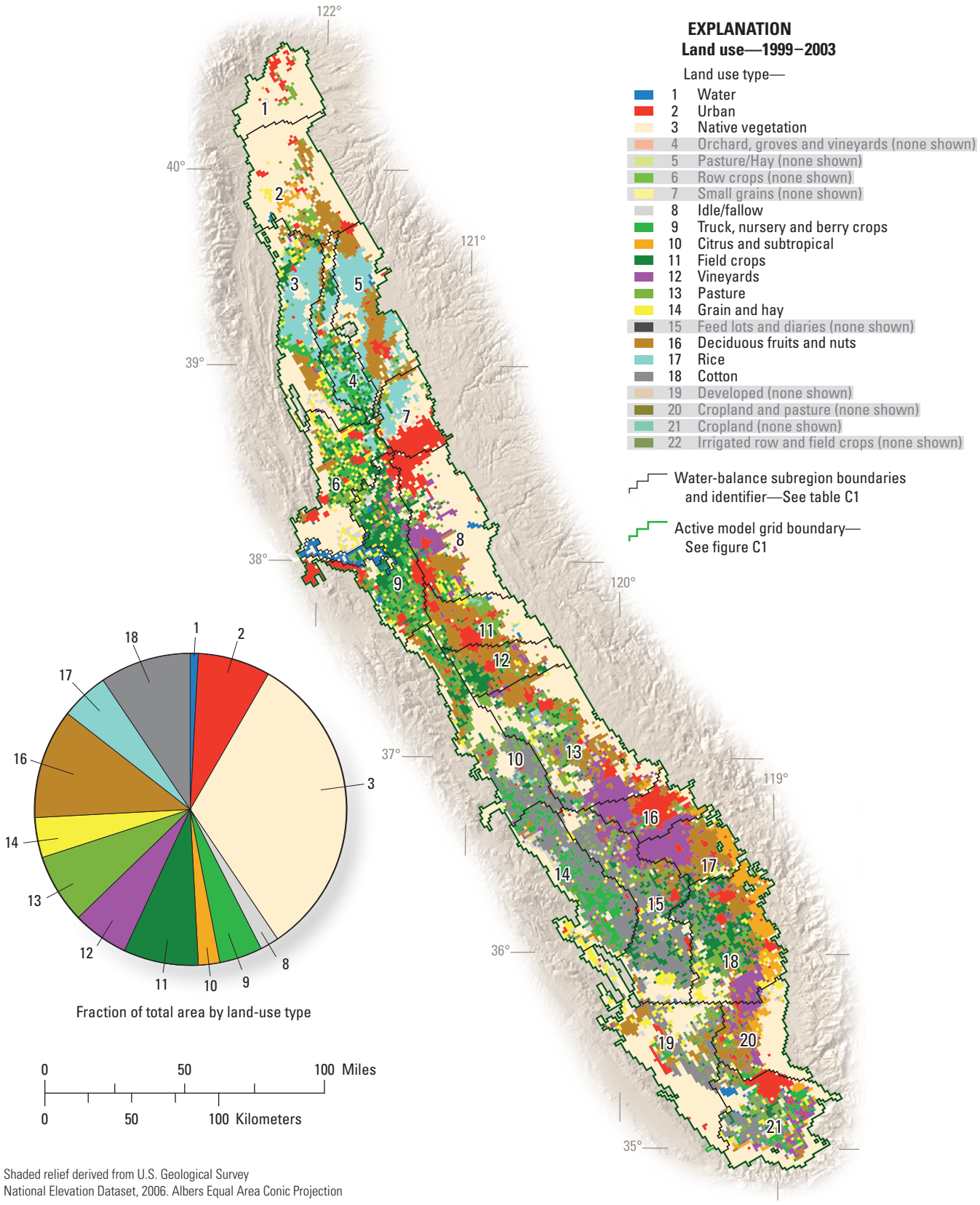

Figure C12. Virtual crops for 2000, including a pie chart of percentage of different virtual crops (California Department of Water Resources, 2000). The water-balance subregions are described in *table A1*.

Table C4. Summary of Central Valley, California, virtual crop categories and properties.

Virtual-crop crop category (number)	Root depth, in feet	Root uptake pressure heads, in feet				Fraction of surface-water runoff from precipitation /irrigation (dimensionless)
		Anoxia	Lower optimal range	Upper optimal range	Wilting	
Water (1)	3.6	1.6	0.3	–1.0	–1.3	0.05/0.01
Urban (2)	2.0	–0.4	–0.9	–37.4	–262.5	0.01/0.01
Native classes (3)	10.6	1.6	0.4	–27.1	–377.3	0.21/0.01
Orchards, groves, and vineyards (4)	6.0	–0.4	–0.9	–22.8	–291.4	0.10/0.01
Pasture/Hay (5)	5.3	–0.4	–0.9	–37.4	–262.5	0.10/0.02
Row Crops (6)	8.3	–0.5	–1.0	–17.9	–262.5	0.10/0.06
Small Grains (7)	4.0	–0.4	–0.9	–37.4	–262.5	0.10/0.04
Idle/fallow (8)	5.3	–0.2	–0.7	–27.1	–377.3	0.06/0.01
Truck, nursery, and berry crops (9)	6.3	–0.5	–1.0	–17.9	–262.5	0.10/0.10
Citrus and subtropical (10)	4.0	–0.5	–1.0	–19.7	–262.5	0.10/0.01
Field crops (11)	4.0	–0.5	–1.0	–98.4	–405.9	0.10/0.08
Vineyards (12)	5.0	–0.5	–1.0	–23.8	–262.5	0.01/0.01
Pasture (13)	5.3	0.0	–0.9	–37.4	–262.5	0.10/0.02
Grain and hay crops (14)	4.0	–0.5	–1.0	–170.9	–525.3	0.10/0.04
Semi–agricultural (livestock feedlots, diaries, poultry farms) (15)	3.6	–0.2	–0.7	–27.1	–377.3	0.32/0.35
Deciduous fruits and nuts (16)	6.0	–0.4	–0.9	–22.8	–377.3	0.11/0.05
Rice (17)	5.3	1.6	0.4	–5.8	–525.0	0.01/0.03
Cotton (18)	9.3	–0.2	–0.9	–91.3	–503.0	0.10/0.10
Developed (19)	5.3	–0.4	–0.9	–37.4	–262.5	0.10/0.08
Cropland and pasture (20)	4.9	–0.4	–0.9	–37.4	–262.5	0.10/0.08
Cropland (21)	6.3	–0.5	–1.0	–17.9	–262.5	0.10/0.08
Irrigated Row and Field Crops (22)	4.9	–0.4	–0.9	–37.4	–262.5	0.10/0.07

Crop water demand roughly can be related to the crop growth stage. The crop coefficient values used in this study were based on an idealized crop growth curve. This growth curve was divided into 12 monthly stages spanning the initial growth stage, the rapid growth stage, the mid-season stage, the late-season stage, and a period of no planting (*fig. C13*). Although the specific growth dates for each virtual crop vary with the planting date and climatic zone, no allowance is made for changes in growth dates with location in the valley. The only change in crop coefficient value at a location is based on a change in the virtual crop with land-use changes.

Crop coefficient values are available from several sources (Brush and others, 2004). When available, published crop coefficient values for the western San Joaquin Valley (Brush and others, 2004) were used; when no published crop coefficient values were available for the San Joaquin Valley, published crop coefficient values for another similar climatic area were used. In many cases, multiple crops were area-weighted to produce a composite, virtual crop coefficient. For example, the virtual crop "deciduous" is composed of almonds, walnuts, prunes, peaches, nectarines, pistachios, apples, plums, figs, pears, apricots, cherries, and other miscellaneous deciduous trees.

Other WBS and crop-related properties that were specified include the fraction of transpiration (Ftr), fraction of evaporation from precipitation (Fep), fraction of evaporation from irrigation (Fei), and the irrigation efficiencies. These fractions vary linearly with the respective area occupied by crops and the area open to soil-evaporation (Schmid and others, 2006a). Because the sum of cropped area and the exposed wetted area is the total area, Ftr plus Fep equals one. In addition, Fei must be less than or equal to Fep. The Ftr is assumed to be independent of whether the transpiratory consumptive use is satisfied by irrigation, precipitation, or groundwater uptake. The fraction of the consumptive use that is transpiratory (Ftr) or evaporative (Fep and Fei) depends highly on type of crop and growth stage. When the vegetation cover approaches 100 percent, Ftr = 1 while Fep and Fei = 0. As a result, the fractions of transpiration and evaporation vary by virtual crop for different months of the year (*table C5*).

A

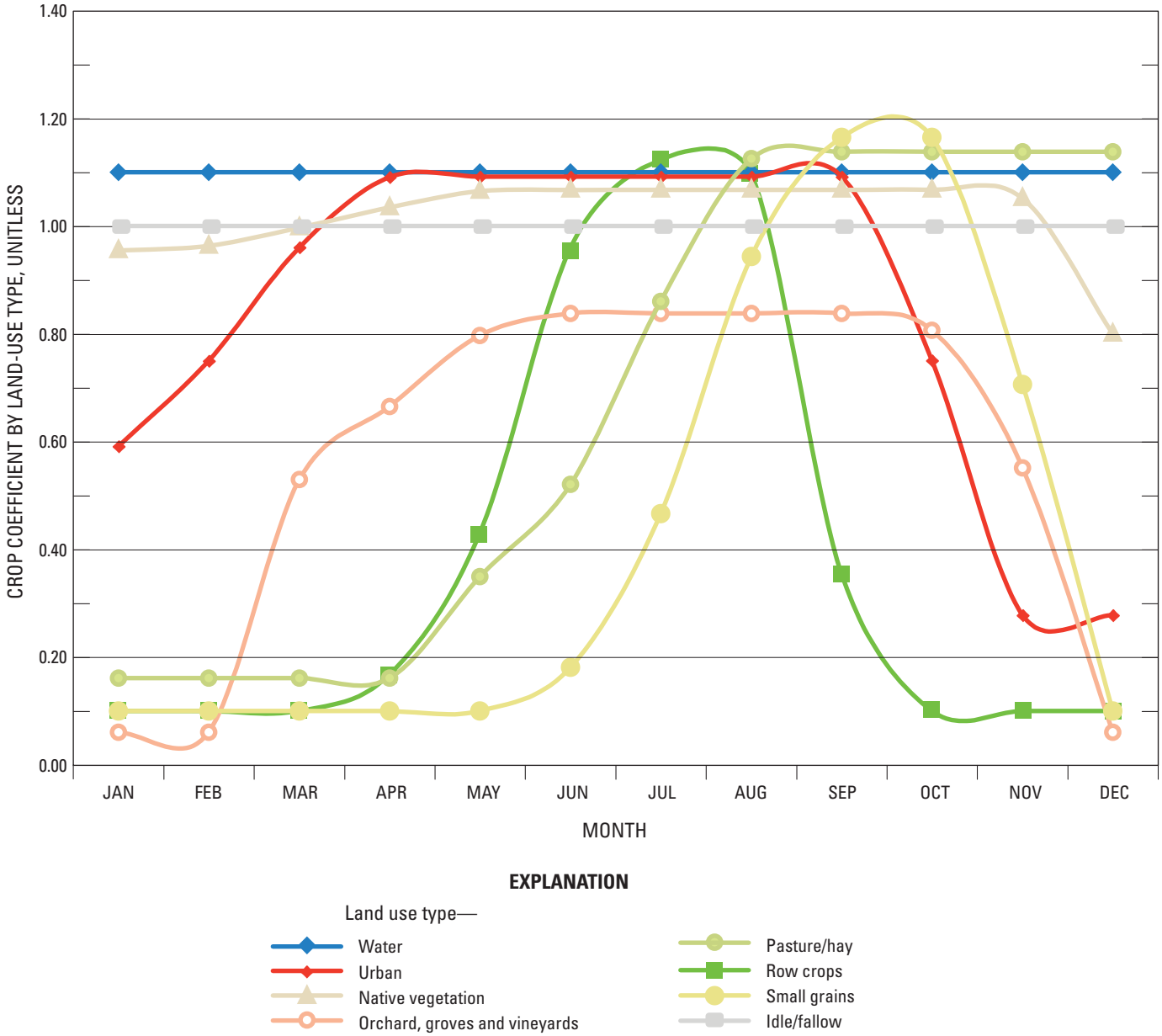

Figure C13. Monthly crop coefficients for virtual crops in the Central Valley, California (sources: Brouwer and others, 1985; Brouwer and Heibloem, 1986; Snyder and others, 1987a; Snyder and others, 1987b; Allen and others, 1998; Brush and others, 2004).

The irrigation efficiencies are defined as the consumptive use of applied water. Inefficiency is a result of losses to runoff and deep percolation as a result of excess irrigation and excess precipitation (Schmid and others, 2006b). In CVHM, the irrigation efficiencies are specified as a matrix of efficiencies for each WBS and each crop for each of the monthly stress periods. In this way, the efficiencies vary from crop to crop for different WBSs and they change through time. The average area-weighted composite efficiency, by decade, for each WBS in the simulations tabulated in *table C6*. Irrigation efficiencies are assumed to have varied in time, reflecting improvements in irrigation application technologies, increased use of tail-water return systems and recycling of drainage water, and changes in the cost and availability of water (Brush and others, 2004). In general, the efficiencies have improved through time with technological advances in sprinkler systems, drip irrigation, and changes in cropping patterns (California Department of Water Resources, 1994). California Department of Water Resources (1994) reports an average improvement in irrigation efficiency of 10 percent during the 1980s. This

B

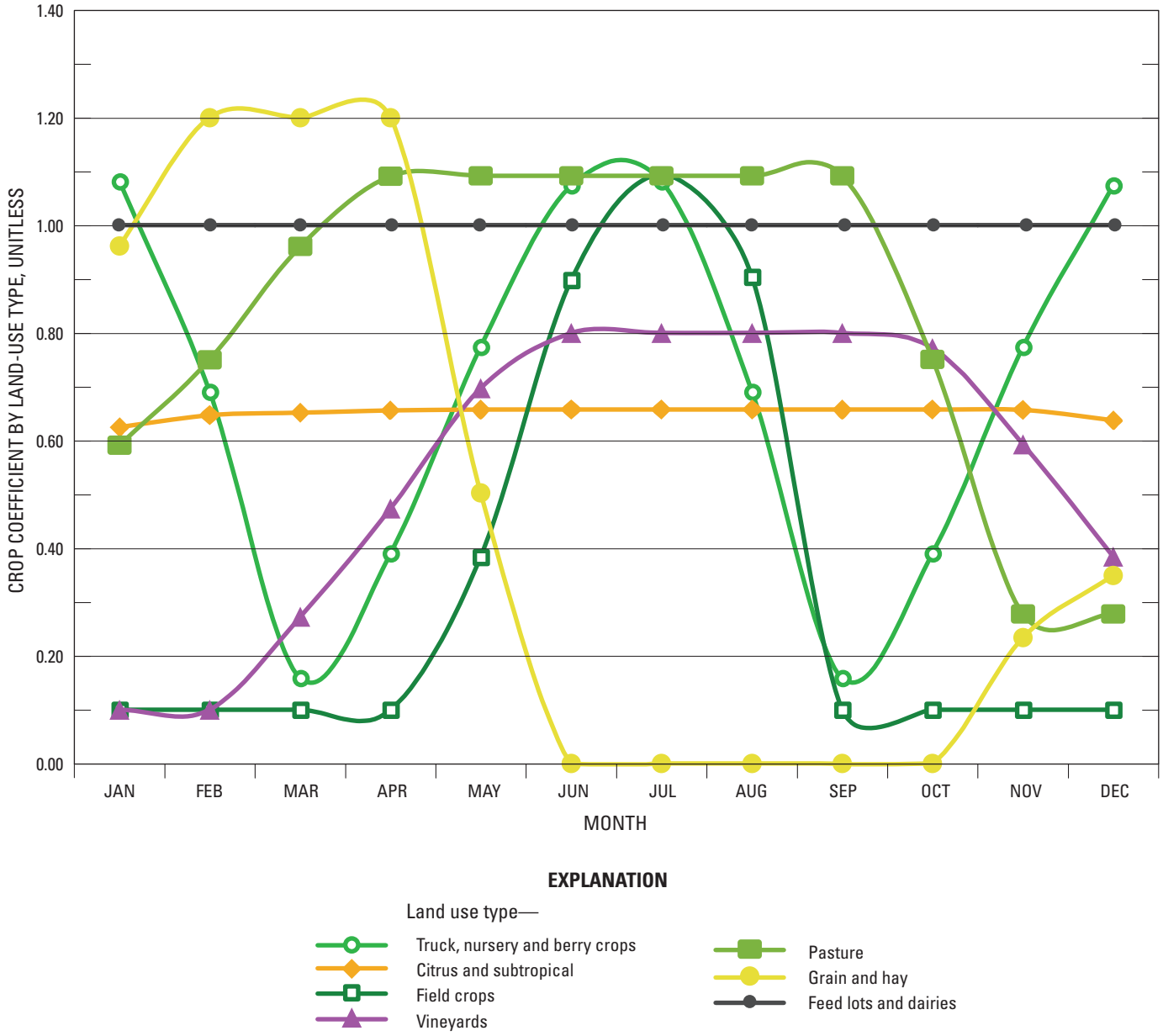

Figure C13. Continued.

particular increase in efficiency is taken into account with fractional irrigation efficiencies that increase by 1 percent per year in the 1980s and are reflected in efficiencies through that time period in *table C6*.

In general, irrigation efficiencies are poorly known (Williamson and others, 1989; California Department of Water Resources, 1994; Brush and others, 2004). Williamson and others (1989) report values averaging 59 percent, and ranging from 38 to 92 percent for the 1961–77 time period. DWR reports overall efficiencies of 60–70 percent for parts of the Central Valley (California Department of Water Resources, 1994). Because of the details incorporated in the FMP, some of what typically is included as inefficiency in irrigation in models (particularly uptake from the groundwater system) is accounted for in the FMP. Compared to previous simulations in the Central Valley, the CVHM efficiencies specified in the FMP typically are higher. For example, because rice is grown in flooded fields, rice has an extremely high irrigation efficiency of 88 percent in CVHM. Another example is WBS 14 in the central western San Joaquin Valley, which has had a large amount of scrutiny in the past (Williamson and others, 1989; Belitz and Heimes, 1990; Belitz and others, 1993; Brush

C

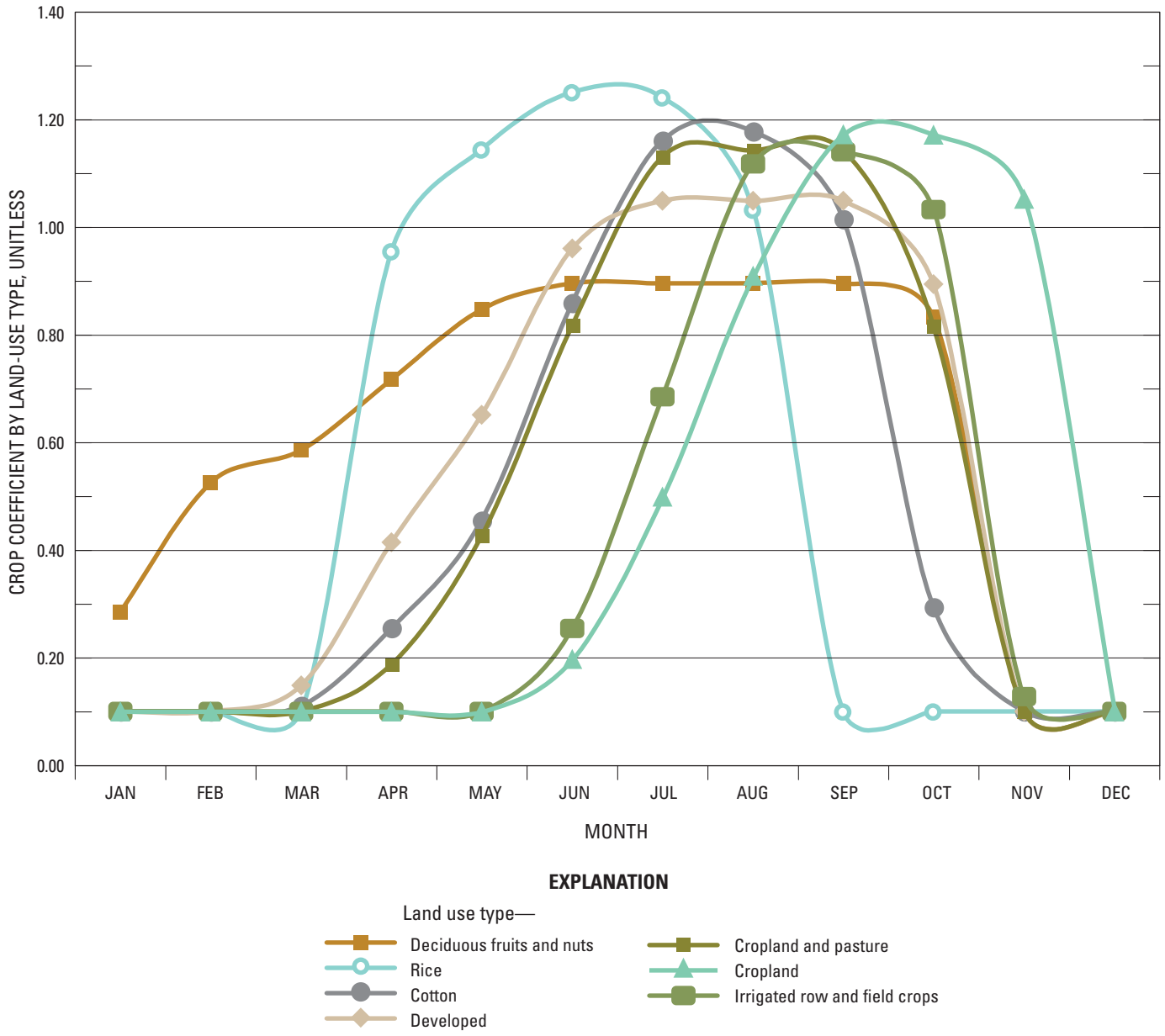

Figure C13. Continued.

and others, 2004). Williamson and others (1989) report efficiencies of 83–92 percent for this general area. Brush and others (2004) report efficiencies ranging from 70 to 80 percent, and averaging around 78 percent in this WBS between 1972 and 2000. By utilizing a completely closed pipeline system, the Westlands Water District claims an estimated 92-percent efficiency (California Department of Water Resources, 2003a). CVHM has average efficiencies for this WBS increasing from 68 percent in the 1960s to 87 percent in the 2000s. WBS 14 has tile drains to drain the fields and a canal system to reuse the water (Brush and others, 2004). As a result, the efficiencies in this area were increased by about 10 percent in the late 1970s to represent the reuse of this drainage water and canal leakage not simulated in the CVHM. Owing to a lack of data regarding long-term values and changes in efficiency, the efficiencies were adjusted during model calibration.

Table C5. Summary of fractions of transpiration and evaporation by month for Central Valley, California, virtual crops.

[Ftr, fraction of transpiration; Fep, fraction of evaporation from precipitation; Fei, fraction of evaporation from irrigation]

Virtual-crop crop category (number)	January (Ftr/Fep/Fei)	February (Ftr/Fep/Fei)	March (Ftr/Fep/Fei)	April (Ftr/Fep/Fei)	May (Ftr/Fep/Fei)	June (Ftr/Fep/Fei)
Water (1)	0.00/1.00/1.00	0.00/1.00/1.00	0.00/1.00/1.00	0.00/1.00/1.00	0.00/1.00/1.00	0.00/1.00/1.00
Urban (2)	0.25/0.75/0.02	0.25/0.75/0.02	0.25/0.75/0.02	0.25/0.75/0.02	0.25/0.75/0.02	0.25/0.75/0.02
Native classes (3)	0.28/0.72/0.72	0.28/0.72/0.72	0.66/0.34/0.34	0.66/0.34/0.34	0.66/0.34/0.34	0.66/0.34/0.34
Orchards, groves, and vineyards (4)	0.20/0.80/0.80	0.20/0.80/0.80	0.37/0.63/0.63	0.23/0.77/0.77	0.46/0.54/0.54	0.47/0.53/0.53
Pasture/Hay (5)	0.50/0.50/0.50	0.50/0.50/0.50	0.50/0.50/0.50	0.50/0.50/0.50	0.72/0.28/0.28	0.88/0.12/0.12
Row Crops (6)	0.11/0.89/0.89	0.11/0.89/0.89	0.11/0.89/0.89	0.09/0.91/0.91	0.36/0.64/0.64	0.46/0.54/0.54
Small Grains (7)	0.00/1.00/1.00	0.00/1.00/1.00	0.00/1.00/1.00	0.00/1.00/1.00	0.00/1.00/1.00	0.00/1.00/1.00
Idle/fallow (8)	0.00/1.00/0.00	0.00/1.00/0.00	0.00/1.00/0.00	0.00/1.00/0.00	0.00/1.00/0.00	0.00/1.00/0.00
Truck, nursery, and berry crops (9)	0.80/0.20/0.18	0.80/0.20/0.18	0.39/0.61/0.61	0.44/0.56/0.36	0.42/0.58/0.38	0.80/0.20/0.18
Citrus and subtropical (10)	0.27/0.73/0.73	0.27/0.73/0.73	0.46/0.54/0.14	0.46/0.54/0.14	0.46/0.54/0.14	0.46/0.54/0.14
Field crops (11)	0.01/0.99/0.99	0.01/0.99/0.99	0.01/0.99/0.99	0.15/0.85/0.85	0.15/0.85/0.85	0.94/0.06/0.06
Vineyards (12)	0.00/1.00/0.03	0.00/1.00/0.03	0.28/0.72/0.22	0.40/0.60/0.10	0.38/0.62/0.12	0.36/0.64/0.14
Pasture (13)	0.18/0.82/0.82	0.15/0.85/0.85	0.46/0.64/0.64	0.91/0.09/0.03	0.91/0.09/0.03	0.91/0.09/0.03
Grain and hay crops (14)	0.46/0.54/0.54	0.92/0.08/0.08	0.92/0.08/0.08	0.92/0.08/0.08	0.23/0.77/0.77	0.00/1.00/1.00
Semi-agricultural (15)	0.00/1.00/1.00	0.00/1.00/1.00	0.00/1.00/1.00	0.00/1.00/1.00	0.00/1.00/1.00	0.00/1.00/1.00
Deciduous fruits and nuts (16)	0.10/0.90/0.90	0.10/0.90/0.90	0.10/0.90/0.90	0.50/0.50/0.50	0.50/0.50/0.50	0.97/0.03/0.03
Rice (17)	0.20/0.80/0.50	0.20/0.80/0.50	0.20/0.80/0.50	0.75/0.25/0.25	0.75/0.25/0.25	0.80/0.20/0.10
Cotton (18)	0.75/0.25/0.25	0.75/0.25/0.25	0.75/0.25/0.25	0.43/0.57/0.17	0.75/0.25/0.20	0.75/0.25/0.20
Developed (19)	0.30/0.70/0.67	0.30/0.70/0.67	0.22/0.78/0.78	0.16/0.84/0.84	0.42/0.58/0.38	0.85/0.15/0.15
Cropland and pasture (20)	0.00/1.00/1.00	0.00/1.00/1.00	0.00/1.00/1.00	0.00/1.00/1.00	0.20/0.80/0.80	0.30/0.70/0.70
Cropland (21)	0.05/0.95/0.85	0.05/0.95/0.85	0.05/0.95/0.55	0.05/0.95/0.55	0.05/0.95/0.95	0.05/0.95/0.85
Irrigated Row and Field Crops (22)	0.05/0.95/0.55	0.05/0.95/0.55	0.05/0.95/0.75	0.05/0.95/0.75	0.20/0.80/0.78	0.85/0.15/0.10

Virtual-crop crop category (number)	July (Ftr/Fep/Fei)	August (Ftr/Fep/Fei)	September (Ftr/Fep/Fei)	October (Ftr/Fep/Fei)	November (Ftr/Fep/Fei)	December (Ftr/Fep/Fei)
Water (1)	0.00/1.00/1.00	0.00/1.00/1.00	0.00/1.00/1.00	0.00/1.00/1.00	0.00/1.00/1.00	0.00/1.00/1.00
Urban (2)	0.25/0.75/0.02	0.25/0.75/0.02	0.25/0.75/0.02	0.25/0.75/0.02	0.25/0.75/0.02	0.25/0.75/0.02
Native classes (3)	0.66/0.34/0.34	0.66/0.34/0.34	0.66/0.34/0.34	0.66/0.34/0.34	0.66/0.34/0.34	0.28/0.72/0.72
Orchards, groves, and vineyards (4)	0.47/0.53/0.53	0.47/0.53/0.53	0.47/0.53/0.53	0.47/0.53/0.53	0.45/0.55/0.55	0.20/0.80/0.80
Pasture/Hay (5)	0.95/0.05/0.05	0.96/0.04/0.04	0.96/0.04/0.04	0.96/0.04/0.04	0.96/0.04/0.04	0.96/0.04/0.04
Row Crops (6)	0.95/0.05/0.05	0.87/0.13/0.13	0.12/0.88/0.88	0.11/0.89/0.89	0.11/0.89/0.89	0.11/0.89/0.89
Small Grains (7)	0.20/0.80/0.80	0.50/0.50/0.50	0.90/0.10/0.10	0.90/0.10/0.10	0.00/1.00/1.00	0.50/0.50/0.50
Idle/fallow (8)	0.00/1.00/0.00	0.00/1.00/0.00	0.00/1.00/0.00	0.00/1.00/0.00	0.00/1.00/0.00	0.00/1.00/0.00
Truck, nursery, and berry crops (9)	0.80/0.20/0.18	0.80/0.20/0.18	0.80/0.20/0.18	0.80/0.20/0.18	0.80/0.20/0.18	0.80/0.20/0.18
Citrus and subtropical (10)	0.46/0.54/0.14	0.46/0.54/0.14	0.46/0.54/0.14	0.46/0.54/0.14	0.46/0.54/0.14	0.46/0.54/0.14
Field crops (11)	0.94/0.06/0.06	0.94/0.06/0.06	0.90/0.10/0.10	0.01/0.99/0.99	0.01/0.99/0.99	0.01/0.99/0.99
Vineyards (12)	0.36/0.64/0.14	0.36/0.64/0.14	0.36/0.64/0.14	0.36/0.64/0.14	0.36/0.64/0.14	0.38/0.62/0.12
Pasture (13)	0.96/0.04/0.04	0.91/0.09/0.03	0.91/0.09/0.03	0.46/0.64/0.64	0.15/0.85/0.85	0.15/0.85/0.85
Grain and hay crops (14)	0.00/1.00/1.00	0.00/1.00/1.00	0.00/1.00/1.00	0.00/1.00/1.00	0.16/0.84/0.84	0.35/0.65/0.65
Semi-agricultural (15)	0.00/1.00/1.00	0.00/1.00/1.00	0.00/1.00/1.00	0.00/1.00/1.00	0.00/1.00/1.00	0.00/1.00/1.00
Deciduous fruits and nuts (16)	0.97/0.03/0.03	0.97/0.03/0.03	0.97/0.03/0.03	0.10/0.90/0.90	0.10/0.90/0.90	0.10/0.90/0.90
Rice (17)	0.75/0.25/0.25	0.60/0.40/0.27	0.20/0.80/0.50	0.20/0.80/0.50	0.20/0.80/0.50	0.20/0.80/0.50
Cotton (18)	0.75/0.25/0.20	0.75/0.25/0.20	0.47/0.53/0.33	0.36/0.64/0.44	0.75/0.25/0.25	0.75/0.25/0.25
Developed (19)	0.90/0.10/0.10	0.90/0.10/0.10	0.90/0.10/0.10	0.50/0.50/0.50	0.30/0.70/0.70	0.30/0.70/0.67
Cropland and pasture (20)	0.85/0.15/0.15	0.95/0.05/0.05	0.90/0.10/0.10	0.50/0.50/0.50	0.00/1.00/1.00	0.00/1.00/1.00
Cropland (21)	0.05/0.95/0.85	0.75/0.25/0.25	0.95/0.05/0.05	0.94/0.06/0.06	0.93/0.07/0.07	0.00/1.00/1.00
Irrigated Row and Field Crops (22)	0.95/0.05/0.05	0.95/0.05/0.05	0.60/0.40/0.15	0.04/0.96/0.04	0.10/0.90/0.50	0.10/0.90/0.50

Table C6. Average area-weighted composite efficiency for each water-balance subregion of the Central Valley, California, through the simulation period.

[Efficiencies in percent]

Water-balance subregion	1960s	1970s	1980s	1990s	2000s
1	70	68	73	76	74
2	70	68	72	75	73
3	74	74	79	82	83
4	71	70	74	78	79
5	73	72	78	80	80
6	69	69	74	77	77
7	71	69	73	77	77
8	69	69	75	78	75
9	69	70	76	79	78
10	69	72	78	80	79
11	70	70	76	78	77
12	71	70	74	77	76
13	71	72	77	80	79
14	68	73	82	86	87
15	67	69	75	76	76
16	72	72	78	79	81
17	72	72	77	79	80
18	71	72	77	79	79
19	68	72	78	79	77
20	72	73	78	81	81
21	71	73	79	81	81

Climate Data

The consumptive use of water, specifically the TFDR, is related directly to the climate. Although several of the previously specified properties take into account yearly or monthly variations, and some have a climatic component, the main climatic contributors to the FMP are ETo and precipitation.

Reference Evapotranspiration (ETo)

Estimates of ETo can be derived using complex, parameter-based equations or simple, empirical equations. The main difficulty encountered when using parameter-based equations is the unavailability of accurate or complete data at sufficient spatial and temporal distributions. The detailed climatological data required for the parameter-based equations (such as the Penman-Monteith equation) are not available for many sites in California, especially prior to 1987. Empirical equations use a small number of parameters (usually air temperature and solar radiation) to estimate ETo and are well suited to estimating ETo for sites with limited climatological data. Samani (2000) determined that temperature and radiation explain at least 80 percent of ETo. Hidalgo and others (2005) determined the seasonal cycle of ETo can be fairly accurately when approximated from the seasonal cycle of net solar radiation (Rn) or average air temperature. The Hargreaves–Samani equation (Hargreaves and Samani, 1982, 1985; Hargreaves and others, 1985; Hargreaves, 1994; Hargreaves and Allen, 2003) provides a very accurate estimate of ETo (referred to as ETh) using a simple, reliable method with minimum data requirements and little sensitivity to weather station aridity (Hargreaves and Allen, 2003). ETh is calculated from the daily minimum and maximum air temperatures and the extraterrestrial solar radiation:

$$ETh = 0.0023Ra\left(\frac{T_{max}+T_{min}}{2\times 17.8}\right)\left(\frac{T_{max}-T_{min}}{2}\right)$$

where,

T_{max} is the maximum daily air temperature [°C],

T_{min} is the minimum daily air temperature [°C], and

Ra is the extraterrestrial solar radiation (megaJoule/m^2/day).

Jensen and others (1997) found the Hargreaves equation to be one of the simplest and most accurate of the empirical methods for estimating ETo. The Hargreaves method compared well with the Food and Agriculture Organization Penman–Monteith method (Allen and others, 1998) in most parts of California, with the greatest differences occurring for days with extreme values of wind speed or relative humidity (Temesgen and others, 2005). The Hargreaves equation also compared well with the Penman–Monteith method on a global scale using a high-resolution monthly data set (Droogers and Allen, 2002).

Monthly ETo values for the FMP in CVHM were estimated using the Hargreaves–Samani equation (Hargreaves and Samani, 1982, 1985) and temperature data. Gridded regional estimates of temperature were obtained at a 1.24-mi spatial resolution from the Climate Source (2006). A monthly minimum and maximum temperature value was interpolated to the center of each 1-mi^2 model cell using bilinear interpolation of the temperature data. ETo was calculated at each active cell for each month during the entire period of simulation using the Hargreaves–Samani equation. *Figure A2* shows the computed average annual ETo values over the entire Central Valley.

Since the 1980s, as part of the California Irrigation Management Information System (CIMIS), the DWR has

established more than 120 weather stations throughout California to measure ETo. CIMIS has been using a well-watered, actively growing, closely clipped grass that completely shades the soil as a reference crop. ETo values that were estimated using the Hargreaves–Samani equation are correlated highly with corresponding CIMIS ETo values but summer ETo values generally were underestimated and winter ETo values generally were overestimated (*table C7*) (California Department of Water Resources, 2007). Several studies have reported methods for adjusting the constants in the Hargreaves–Samani equation to correct for local climatological factors (Samani 2000; Droogers and Allen 2003). These methods correct differences between large ETo and ETh values but do not address differences between small ETo and ETh values. As a result, adjustments were made to correct for these potential errors during calibration by multipliers on the summer and winter crop coefficient values.

Precipitation

Precipitation for CVHM is specified through the FMP at the uppermost active model cell for every month for the period of simulation. Gridded regional estimates of precipitation are obtained at a 1.24-mi spatial resolution from the Climate Source (2006). A comparison of monthly precipitation data from five CMIS stations in the valley (Red Bluff, Davis, Modesto, Fresno, and Bakersfield) (*fig. A3*) indicates that the estimated precipitation from these gridded sources preserves the total mass of precipitation measured at these stations. A monthly precipitation rate is interpolated for the center of each 1 mi^2 model cell using bilinear interpolation of the precipitation data. A map of the average annual precipitation for the simulation period for the model domain is shown in *figure A2*. The precipitation is applied to the uppermost active cell at an average monthly rate. Parts of the precipitation are simulated as evaporation and transpiration from the WBS. If excess precipitation occurs, a part of this precipitation becomes runoff and the remaining part becomes deep percolation that is groundwater recharge. The parts of runoff from precipitation are user-specified and vary by crop type specified through the estimation of virtual-crop properties (*table C4*). The values of runoff are relatively unknown and are based on model calibration to surface-water flows in stream channels and out to the Delta.

Surface-Water Supply

In the Central Valley, surface-water supply is simulated using the SFR1 package (Prudic and others, 2004) as a combination of non-routed surface-water deliveries and semi-routed conveyances from diversions. The surface-water conveyances to and from the WBSs include a combination of transfers representing a variety of conveyance mechanisms from natural rivers to manmade canals and pipelines (*figs. C2* and *A4*). In addition, the multiple water transfers represent a combination of deliveries of water from private, State, and Federal sources of water. As a result, the WBSs often have a number of separate water transfers from multiple sources (*fig. A8* and *table A1*). Water-delivery and diversion data were obtained from DWR (C. Brush, California Department of Water Resources, written commun., February 21, 2007). To simulate the non-routed and semi-routed deliveries at the WBS scale, 110 diversion points from the streamflow-routing network were specified (two diversion points were inactive during the CVHM's simulation period, but were included for future use). Forty-two of the 108 active diversion points were specified non-routed surface-water diversions in the model and were used to move water to 12 of the WBSs without simulating the actual process of conveyance (*table A1*). The remaining 66 diversion points were specified semi-routed streamflow diversions in the model and routing to the respective head gate of the WBSs was simulated using the SFR1 (Prudic and others, 2004). Two of these diversions were delivered to areas outside the CVHM and only one WBS did not have a semi-routed delivery (WBS 14; *table A1*). In order to compile multiple deliveries to 18 of the WBSs, 18 "collector segments" were added to the SFR1 streamflow-routing network. The simulated diversions were routed through the SFR1 streamflow network to the collector segment and then delivered to the appropriate WBS (*fig. A4*). The distribution of surface water to model cells within the WBS is subject to transmission losses that implicitly are accounted for in the model by the WBS irrigation efficiencies.

When water transfers are specified as deliveries, they are the first water-supply components that are used by the FMP to satisfy the TFDR for each WBS. If more water is delivered than the WBS demands (TFDR), the excess deliveries are added to the furthest downstream, adjacent stream segment of the simulated streamflow-routing network. If the TFDR is not met by surface-water deliveries, the residual demand is supplied by groundwater pumped from wells assigned to each WBS.

Groundwater Supply

The groundwater supplied to each WBS is simulated by a series of single-layer "farm wells" or through multi-aquifer wells simulated with the MNW package (Halford and Hanson, 2002). The wells perforated above and below the Corcoran Clay were simulated as multi-node wells (see "*Agricultural Pumpage*" section of this chapter), because the amount of leakage across the Corcoran Clay through well-bore flow was of interest. Most wells simulating agricultural pumpage were simulated using "farm wells" in the FMP. A single well perforating and open to multiple aquifers represented in separate model layers was simulated by specifying separate wells for each model layer open to the well (Schmid and others, 2006b).

Agricultural groundwater pumpage requirements are estimated by the FMP after the TFDR is estimated and surface-water imports and exports from semi-routed and non-routed

Table C7. Average reference evapotranspiration (ETo) by month for the Central Valley, California, for 1961–2003 based on temperature data using the Hargreaves–Samani equation.

[ETo values in inches]

Water-balance subregion	January	February	March	April	May	June
1	1.13	1.79	2.43	3.68	5.00	6.32
2	1.24	1.93	2.61	3.91	5.15	6.32
3	1.39	2.15	2.91	4.22	5.34	6.55
4	1.36	2.18	2.92	4.22	5.35	6.58
5	1.28	2.08	2.81	4.14	5.32	6.54
6	1.28	2.14	2.77	4.06	5.19	6.34
7	1.15	1.96	2.65	4.00	5.24	6.45
8	1.29	2.14	2.84	4.04	5.17	6.22
9	1.24	2.09	2.79	4.01	4.98	5.94
10	1.63	2.33	3.11	4.16	5.26	6.40
11	1.53	2.43	3.16	4.24	5.35	6.44
12	1.53	2.37	3.16	4.28	5.37	6.48
13	1.75	2.54	3.29	4.39	5.57	6.72
14	1.72	2.40	3.18	4.33	5.43	6.57
15	1.61	2.32	3.15	4.39	5.51	6.60
16	1.70	2.50	3.30	4.49	5.76	6.99
17	1.70	2.51	3.30	4.52	5.72	6.79
18	1.90	2.70	3.46	4.64	5.77	6.80
19	2.10	2.62	3.33	4.38	5.38	6.48
20	2.21	2.73	3.41	4.34	5.38	6.53
21	2.28	2.70	3.31	4.19	5.13	6.24

Water-balance subregion	July	August	September	October	November	December
1	6.79	5.98	4.71	2.62	1.34	0.91
2	6.69	5.96	4.75	2.79	1.51	1.06
3	6.97	6.23	4.98	3.02	1.78	1.35
4	7.14	6.36	5.05	3.06	1.79	1.40
5	6.92	6.15	4.86	2.94	1.68	1.18
6	6.52	5.89	4.80	2.96	1.74	1.14
7	6.74	6.00	4.76	2.82	1.60	0.98
8	6.53	5.82	4.69	2.94	1.80	1.25
9	6.09	5.45	4.54	2.88	1.75	1.10
10	6.65	5.87	4.89	3.15	1.96	1.41
11	6.93	6.16	4.99	3.20	2.10	1.72
12	6.77	6.02	4.92	3.18	2.01	1.48
13	7.16	6.40	5.30	3.46	2.20	1.73
14	6.67	5.91	4.86	3.26	2.03	1.52
15	6.74	6.04	4.93	3.34	2.05	1.42
16	7.36	6.65	5.32	3.47	2.23	1.73
17	7.20	6.61	5.23	3.51	2.26	1.76
18	7.11	6.52	5.30	3.60	2.38	1.93
19	6.58	5.99	4.98	3.40	2.24	1.83
20	6.63	6.02	5.02	3.38	2.29	1.95
21	6.33	5.76	4.88	3.32	2.28	1.96

deliveries have been subtracted from the TFDR. If the TFDR was satisfied by the surface-water deliveries, then no groundwater pumpage was estimated for that stress period. Conversely, if not enough surface water was available for supply then groundwater from farm wells and multi-node wells was used to satisfy the residual demand.

Net Recharge

The net recharge in a WBS is defined as inefficiency losses due to excess irrigation and excess precipitation, reduced by losses to surface-water runoff and ET from groundwater (Schmid and others, 2006b). Alternatively, the net recharge can be defined in terms of consumptive use: the part of irrigation and precipitation not consumptively used by plants reduced by losses to surface-water runoff and ET from groundwater. The fraction of losses to surface-water runoff depends on whether the loss is related to irrigation or to precipitation. As in most areas, in CVHM, irrigation losses depend on the irrigation method, which, in turn, depends on the virtual crop type and other factors such as soil type and slope (*table C4*). ET from groundwater (even for irrigated areas) is subtracted from the potential net downward flux to the groundwater system. Hence, net recharge to groundwater can be defined by means of user-specified and head-dependent parameters. This definition of net recharge is physically valid, given the following assumptions: deep percolation beyond the active root zone is equal to groundwater recharge, recharge is simulated without delay and represents an instantaneous uptake into groundwater storage, and ET from groundwater represents an instantaneous release from groundwater storage within any monthly stress period (Schmid and others, 2006b). The net recharge to the groundwater is applied to the uppermost active cells in each WBS.

Hydraulic Properties

The hydraulic properties of an aquifer system govern the transmission and storage of groundwater in the system. The transmission properties of the Central Valley aquifer system are represented by hydraulic conductivity (K) and thickness in this study. Equivalent horizontal and vertical hydraulic conductivities are assumed to be correlated to sediment texture (the fraction of coarse-grained sediment). This assumption is based on the spatial correlation between saturated hydraulic conductivity and pore-size distributions in geologic media (Russo and Bouton, 1992). A method for estimating hydraulic conductivity based on this assumption has been applied successfully in previous groundwater-flow models of the central western San Joaquin Valley (Phillips and Belitz, 1991; Belitz and Phillips, 1995; C. Brush, U.S. Geological Survey, written commun., 2006) and northeastern San Joaquin Valley (Burow and others, 2004; Phillips and others, 2007). The method uses the estimated sediment texture for each cell and horizontal and vertical hydraulic conductivity estimates for each textural end member.

Brush and others (C. Brush, U.S. Geological Survey, written commun., 2006) reviewed the use of a power mean for defining hydraulic conductivity values and found it useful. A power mean is a mean of the form:

$$M^p(x) = \left(\frac{1}{n} \sum_{k=1}^{n} x_k^p \right)^{1/p}$$

where

x is the value being averaged (such as hydraulic conductivity),

p is the averaging power-mean exponent,

n is the number of elements being averaged, and

x_k is the k^{th} element in the list.

,

The horizontal hydraulic conductivity (k_{hi}) was calculated as the weighted arithmetic mean (p=1) of the hydraulic conductivities for each cell (i) of the coarse-grained (K_c) and fine-grained (K_f) lithologic end members and the distribution of sediment texture:

$$\mathrm{K_{h,i}} = \left[K_c F_{c,i} + K_f F_{f,i} \right]$$

where

$F_{c,i}$ is the fraction of coarse-grained sediment in a cell, estimated from sediment texture data as described earlier in Chapter A, and

$\mathrm{F}_{f,i}$ is the fraction of fine-grained sediment in a cell ($1 - F_{c,i}$).

Because K_f is much smaller that K_c, the arithmetic mean largely is influenced by the K and fraction of the coarse-grained end member.

Vertical hydraulic conductivity between layers ($K_{v,k+1/2}$) was calculated as the p^{th} weighted power mean of the hydraulic conductivities of the coarse-and fine-grained lithologic end members (C. Brush, U.S. Geological Survey, written commun., 2006):

$$K_{v,k+1/2} = \left[F_{c,k+1/2} K_c^p + F_{f,k+1/2} K_f^p \right]^{1/p}$$

where

k represents the layer,

$K_{v,k+1/2}$ is the fraction of coarse-grained sediment between layer midpoints, and

$F_{f,k+1/2}$ is the fraction of fine-grained sediment between layer midpoints.

The harmonic mean is a weighted power mean with $p = -1.0$. The geometric mean is a weighted power mean with $p = 0.0$. Phillips and Belitz (1991) determined that vertical conductivities could be calculated using either weighted harmonic or weighted geometric means. Belitz and others (1993) represented the vertical conductivities with the weighted harmonic mean. Brush and others (C. Brush, U.S. Geological Survey, written commun., 2006) calculated the vertical conductivities as power means in which p varied between –1.0 (the harmonic mean) and 0.0 (the geometric mean). Dimitrakopoulos and Desbarats (1993) determined that the value of p depends, to some extent, on the size and thickness of the grid blocks used to discretize the model domain; smaller grid cells result in smaller values of p.

Figure C14 shows the relation of hydraulic conductivity and percentage coarse-grained deposits, based on hydraulic conductivity end members and the exponent of the power mean. K_f is sensitive to the averaging method used. Both the harmonic and geometric means more heavily weight the fine-grained end members and, as a result, the vertical hydraulic conductivities are much lower than the horizontal hydraulic conductivities.

Some single-well hydraulic tests (slug tests) and some multiple-well hydraulic tests have been done in wells in the study area. Phillips and others (2007) report that 21 aquifer tests in the northeastern San Joaquin Valley resulted in hydraulic conductivity estimates ranging from 6.5 to 820 ft/d. Bertoldi and others (1991) tabulated the average horizontal hydraulic conductivity in the Central Valley from laboratory tests of core samples. These values ranged from 2 x 10^{-3} ft/d for silty clay to 13 ft/d for sand. Williamson and others (1989) estimated an average horizontal hydraulic conductivity of 6.5 ft/d for the Central Valley based on the calibration of the CV-RASA model. They also estimated the average hydraulic conductivity of the Sacramento Valley of about one-half the average for the San Joaquin Valley. They attributed this difference to the relative abundance of fine-grained volcanic-derived sediments in the Sacramento Valley. Belitz and Phillips (1995) estimated the hydraulic conductivity of the coarse-grained end member in the central western San Joaquin Valley (K_c) to be 104 ft/d for the Sierran Sands and 31 ft/d for the Coast Range sands. They estimated the fine-grained end member (K_f) to be 4.0×10^{-3} ft/d. Brush and others (C. Brush, U.S. Geological Survey, written commun., 2006) used similar values for

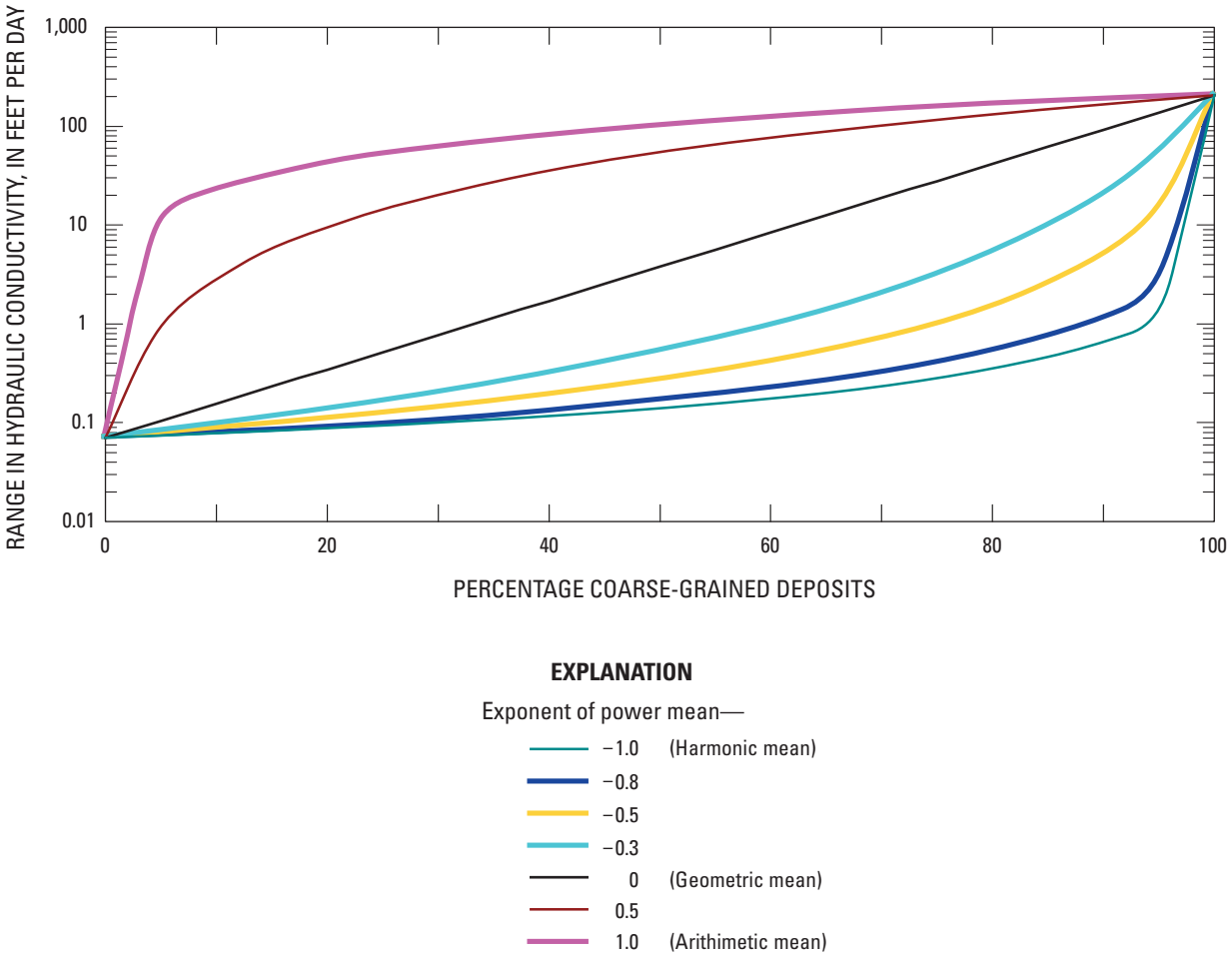

Figure C14. Relation between hydraulic conductivity and percentage coarse-grained deposits based on hydraulic conductivity end members and exponent of the power mean.

the crop coefficient, however, their estimate of K_f was about an order of magnitude lower at 4.3×10^{-4} ft/d (*table C8*). The Belitz and Phillips (1995) estimates are based on the harmonic mean ($p = -1.0$), and the Brush and others (C. Brush, U.S. Geological Survey, written commun., 2006) estimates are based on the power mean ($p = -0.8$). The harmonic mean more strongly weights the fine-grained end member than the power mean with a $p = -0.8$ (*fig. C14*).

Permeameter tests of cores from the Corcoran Clay have resulted in vertical hydraulic conductivity measurements of about 6.6×10^{-6} ft/d (Page, 1977). Johnson and others (1968) measured vertical hydraulic conductivities of 1.0×10^{-5}–2.0×10^{-5} ft/d in cores from the Corcoran Clay. Previous investigations, however, indicate that intra-borehole flow through the numerous wells perforated across the Corcoran Clay effectively have short-circuited the impedance to flow through this confining unit (Williamson and others, 1989; Belitz and Phillips, 1995). The estimated hydraulic conductivities of the Corcoran Clay used in previous models generally are higher than the permeameter and lab-derived results. Belitz and others (1993) compiled initial estimates of the conductivity of the Corcoran Clay from several modeling sources. These are tabulated in *table C8*. Based on the modeling of Williamson and others (1989), the mean values deduced for hydraulic conductivity for the Corcoran Clay are from 4.1×10^{-4} to 1.5×10^{-3} ft/d. Phillips and Belitz (1991) estimated that the hydraulic conductivity of the Corcoran Clay is 6.9×10^{-4} ft/d if harmonic averaging is used in the vertical direction, or 9.2×10^{-4} ft/d if geometric averaging is used in the vertical direction. The vertical hydraulic conductivity estimated by Belitz and Phillips (1995) is 5.2×10^{-4} ft/d. Brush and others (C. Brush, U.S. Geological Survey, written commun., 2006) used values of 3.9×10^{-4}–6.2×10^{-4} ft/d for the Corcoran Clay.

Hydraulic Conductivity

The lithologic end-member hydraulic conductivities used in this study are K_c, K_f, and K_{corc}. Parameter estimation was used in combination with the textural model developed for the region on the basis of the known stratigraphic units and kriged subsurface lithology, to estimate these end-member K values. These end members were used to estimate the horizontal and vertical K for each cell in the CVHM. The values of hydraulic conductivity in *table C8* represent final values derived from model calibration; calibration of the CVHM is discussed in the "*Model Calibration and Sensitivity*" section of this chapter.

The Sacramento and San Joaquin Valleys have somewhat different depositional environments and textural compositions that affect the end-member *K* values. The Sacramento Valley is much finer grained, has a strong volcanic influence, and, as a result, possibly has less layering of fine-grained deposits than does the San Joaquin Valley. Conversely, the San Joaquin Valley is known to have numerous lenticular clay deposits (Page, 1986; Williamson and others, 1989). Therefore, the hydraulic properties of each were estimated separately. For the Sacramento Valley, the calibrated value of K_f is 7.5×10^{-2} ft/d; K_c is $6.7\times10^{+2}$ ft/d. For the San Joaquin Valley, the calibrated value of K_f is 2.4×10^{-1} ft/d; K_c is $3.3\times10^{+3}$ ft/d. For both valleys, the distributions of horizontal and vertical K's are the same as those for the sediment texture (*fig. A9*). These values are significantly higher than values estimated for the western San Joaquin Valley by Belitz and others (1993), Belitz and Phillips (1995), and Brush and others (C. Brush, U.S. Geological Survey, written commun., 2006). Their values represent the finer-grained deposits characteristic of the western side of the San Joaquin Valley, whereas the values used in the CVHM are more representative of the coarser-grained sediments of the eastern side of the valley. In fact, a multiplier was used to decrease the *K* for the western side of the San Joaquin Valley (see "*Model Parameters*" section). The CVHM values are slightly higher than the values tabulated by Bertoldi and others (1991) and comparable with the range of values used by Williamson and others (1989) in the original CV-RASA model.

Unlike previous models where the hydraulic conductivity was specified for the Corcoran Clay as a unit, in the CVHM the hydraulic conductivity (K_{corc}) is based on the coarse- and fine-grained end member values. In general, finer-grained sediments are present in the area of the Corcoran clay. A "clay" designation on drillers logs within the Corcoran Clay has a much greater probability of being homogeneous and being clay, as opposed to silt or silty clay,. Hence, the Corcoran Clay forms a relatively continuous confining unit in the aquifer system as opposed to the clayey lenses or interbeds prevalent throughout the rest of the system. Decreased vertical flow through confining units and interbeds, particularly the Corcoran Clay, has resulted from the inelastic compaction of fine-grained materials within the aquifer system. As a result, the vertical hydraulic conductivity of the clays, including the Corcoran Clay, may have been reduced by 1.5 to 6 times from original laboratory values (Williamson and others, 1989). In addition, Riley (1998) concluded that aquitard permeabilities measured under no-load conditions (for example, permeameter tests) appear to have very limited applicability to field problems, although they presumably are significant, relative to each other (Riley, 1998).

In order to represent the impedance to flow through the clays and the enhanced impedance caused by compaction and other factors affecting the Corcoran Clay, the horizontal hydraulic conductivity of the Corcoran Clay was reduced by a factor of 0.01 from the value estimated by the arithmetic mean of the coarse- and fine-grained fractions. Likewise, the vertical conductivity was reduced by a factor of 0.002, resulting in vertical hydraulic conductivities of 100-percent fine-grained deposits about 4.8×10^{-4} ft/d ($0.002 * 2.4\times10^{-1}$ ft/d), close to the laboratory values. The local short-circuiting of flow through wells perforated across the Corcoran Clay was accomplished using intra-borehole flow with the MNW package.

Texture generally decreases with increasing distance from the original source of the sediments (adjacent mountain

Table C8. Measured and simulated hydraulic properties.

[K_c, hydraulic conductivity of coarse end member; K_f, hydraulic conductivity of fine-grained end member; K_c vertical hydraulic conductivity of Corcoran Clay; MNW, Multi-Node Well package; p, texture-weighted power-mean value; SY, specific yield; Ss, specific storage; ft, foot; ft/d, foot per day]

Hydraulic property	Field and laboratory values	Previously simulated values	Values simulated in this study
K_c	$8.2\times10^{+2}$ ft/d horizontal[1]; 10 ft/d vertical[5]	31 to 104 ft/d[2,3,4]	$6.7\times10^{+2}$ ft/d Sacramento Valley; $3.3\times10^{+3}$ ft/d San Joaquin Valley
K_f	2.0×10^{-3} ft/d vertical[5] to 9.8×10^{-6} ft/d vertical[5]	4.3×10^{-4} ft/d[4]; 4.7×10^{-2} ft/d[6]	7.5×10^{-2} ft/d Sacramento Valley; 2.4×10^{-1} ft/d San Joaquin Valley
K_{corc}	6.6×10^{-6} ft/d[7]	3.9 to 6.2×10^{-4} ft/d[4] 5.2×10^{-4} ft/d[2]; 6.9 to 9.2×10^{-4} ft/d[6]; 4.1×10^{-4} to 1.5×10^{-3} ft/d[9]	Varies with parameters in San Joaquin Valley; Horizontal K multiplied by factor of 1×10^{-2}; Vertical K multiplied by factor of 2×10^{-3} ; borehole leakage across clay included in MNW (previous simulations include borehole leakage by increasing K)
p	N/A	–0.8 San Joaquin Valley[4]	–0.5 Sacramento Valley; –0.8 San Joaquin Valley
Porosity (total)	0.25 to 0.65[5]	N/A	0.25 coarse-grained deposits; 0.50 fine-grained deposits
SY	0.0 to 0.35[5]	0.2 (lower layers) to 0.3 (upper layer)[4] 0.02 to 0.20[9]	Median value of 0.23 (0.09 to 0.40; scaled based on percentage of coarse-grained deposits)
Ss – elastic	Coarse-grained = 1.0×10^{-6} per ft[10–15]; Fine-grained = 2.0×10^{-6} to 7.5×10^{-6} per ft[10–15]; Compressibility of water = 1.4×10^{-6} per ft[10–15]	Coarse-grained = 1.4×10^{-6} per ft[9]; Fine-grained = 4.5×10^{-6} per ft[9] Ss – elastic and inelastic combined = 3.0×10^{-6} per ft[5]; 8.6×10^{-8} per ft[16]	Coarse-grained = 1.0×10^{-6} per ft; Fine-grained = 4.5×10^{-6} per ft; Compressibility of water = 1.4×10^{-6} per ft
Ss – inelastic	1.4×10^{-4} per ft to 6.7×10^{-4} per ft[15]	3.0×10^{-4} per ft[9]	1.4×10^{-4} per ft

[1]Phillips and others (2007).

[2]Belitz and others (1993).

[3]Belitz and Phillips (1995).

[4]Brush and others (2006).

[5]Bertoldi and others (1991).

[6]Phillips and Belitz (1991).

[7]Page (1977).

[8]Johnson and others (1968).

[9]Williamson and others (1989).

[10]Riley (1969).

[11]Riley (1984).

[12]Helm (1974).

[13]Helm (1975).

[14]Helm (1976).

[15]Helm (1977).

[16]Ireland and others (1984).

ranges) and with depth. This trend is observed in the observed aquifer-system sediments and texture model (*fig. A13*). Coarser-grained sediments were simulated near stream channels. Because the Sacramento Valley generally is finer grained than the San Joaquin Valley, average hydraulic conductivities in the Sacramento Valley are less than those in the San Joaquin Valley. An exception to this trend is in the southwestern part of the valley, where fine-grained deposits are common.

Intuitively, hydraulic conductivity decreases with depth because, among other things, (1) the geostatic load increases, thereby compressing deposits, and (2) older deposits tend to be more consolidated and (or) indurated with depth (age). Determining the value of the depth-dependence directly from hydraulic-conductivity data can be difficult because, in most situations, such data are scarce, depth decay is obscured by variability caused by other factors, and measurement error is substantial. Taylor and others (2001) and Whittemore and others (1993) show that hydraulic conductivity can decline systematically with depth. Though the most appropriate decay function to use is not always clear, exponential decay is commonly assumed (Anderman and Hill, 2003). Analyses and simulations indicated that depth was a significant factor in the variability of hydraulic conductivity in the Death Valley region (Faunt and others, 2004). Their study indicates that the hydraulic conductivity decreases rapidly for most rocks at depths less than 3,000 ft, particularly alluvial units. The exponential rate of decline of hydraulic conductivity estimated for alluvial units in Death Valley was used to specify depth-dependent hydraulic conductivity values in the CVHM. Adjustments to these specified values were made by estimating multipliers on the specified depth-dependent hydraulic conductivities during calibration.

Storage Properties

The hydraulic properties used to simulate the changes in storage of water within the aquifer system comprise three principal components:

1. Specific yield,
2. Elastic specific storage, and
3. Inelastic specific storage.

Specific yield (dimensionless) is unconfined storage and represents the fraction of gravity-driven drainage of a unit volume of saturated sediments following a decline of the water table or filling of drained porosity by a rising water table. Specific yield is a function of sediment porosity and its moisture-retention characteristics, and it cannot exceed the fractional sediment porosity. Specific storage is the volume of water that an aquifer system, or a specified hydrogeologic unit within the aquifer system, releases from or takes into storage per unit volume per unit change in head. Specific storage (units of inverse length) is equal to the storage coefficient (dimensionless) divided by the thickness (units of length) of the aquifer system or specified hydrogeologic unit within the aquifer system. Elastic and inelastic specific storage refers to the elastic and inelastic compressibilities of the aquifer-system material. Typically, coarse-grained material deforms elastically, and fine-grained material deforms elastically and inelastically, depending on the state of stress (Riley, 1969).

The first two principal storage components listed above, specific yield and the elastic specific storage, represent and govern the reversible uptake and release of water to and from storage. The elastic specific storage represents the component of confined storage owing to the compressibility of water and to the reversible compressibility of the matrix or the skeletal framework (skeleton) of the aquifer system. The inelastic specific storage governs the irreversible release of water from the inelastic compaction of the fine-grained deposits or permanent reduction of pore space. The values of inelastic specific storage are much larger than those of elastic specific storage, and the relative magnitudes of the corresponding inelastic and elastic storage coefficients are dependent on the relative aggregate thickness of the fine-grained sediments in the aquifer system or specified hydrogeologic unit within the system. Specific yield typically is orders of magnitude larger than the elastic storage coefficient and volumetrically is the dominant storage parameter; however, storage in fine-grained beds is a significant source of water where aquifers are developed and inelastic compaction occurs (Konikow and Neuzil, 2007). Given the fine-grained nature of the Central Valley aquifer system and its extensive development, water released by the compaction of the interbeds (discontinuous beds of fine-grained deposits) in the aquifer system most likely is a significant source of water in the valley. The water derived from inelastic compaction is a one-time, non-recoverable release of water from the fine-grained deposits. The release of water owing to compaction of fine-grained deposits results in land subsidence. The effects of long-term pumpage on lowering groundwater levels and compaction of the fine-grained deposits are shown in *figures B16* and *B18*.

In the CVHM, a combination of the LPF and SUB packages were used to define the storage properties. The LPF package was used to specify the compressibility of water for all model layers and the specific yield for the upper active layer (*fig. C1B*). Although all model layers are simulated as confined, the upper active layer represents unconfined (water table) conditions and, therefore, is assigned a specific yield.

Because porosity constrains specific yield, and because the product of fractional porosity and water compressibility determines the storage change in a confined aquifer system or hydrogeologic unit in the system owing to fluid

compressibility, it is worth reviewing some Central Valley aquifer-system porosity measurements and estimates. Previous modeling studies used porosities ranging from 0.25 to 0.65 in the Central Valley (Bertoldi and others, 1991). A porosity value of 0.25 for the channel sand and 0.35 for the mud, with an overall weighted average porosity of 0.31, was estimated on the basis of the hydrofacies models developed for the Modesto and Fresno areas of the San Joaquin Valley (Burow and others, 2004; Phillips and others, 2007). On the western side of the San Joaquin Valley in the Grasslands Drainage area, porosity is estimated to range from 0.31 to 0.56 with a mean of 0.42 for fine-grained sediments (Johnson and others, 1968); coarse-grained sediments are estimated to range from 0.28 to 0.50 with a mean of 0.41 (C. Brush, U.S. Geological Survey, written commun., 2006). These values were used for the western San Joaquin model (C. Brush, U.S. Geological Survey, written commun., 2006). Laboratory values of porosity range from 0.25 for silty sands to 0.65 for sands (Bertoldi and others, 1991).

Specific yields from previous models range from 0.02 to 0.20 for the entire Central Valley (Williamson and others, 1989) and from 0.20 to 0.30 for the Grasslands area of the western San Joaquin (Belitz and others, 1993). Williamson and others (1989, table 4) lists estimated aggregated specific yield values for the saturated sediment based on lithologic descriptions from about 17,000 well logs. They estimate an average specific yield of 0.07 for the Sacramento Valley, 0.08 for the Delta area, and 0.10 for the San Joaquin Valley and Tulare Basin. Laboratory values of specific yield range from less than 0.01 for clays to 0.35 for sands (Bertoldi and others, 1991). For the uppermost active model cells in the CVHM, specific yield was added to the compressibility of water. Specific yield was calculated using a linear relation between the fractions of coarse-grained deposits. Where there were no coarse-grained deposits, the specific yield was 0.09. Where the deposits are all coarse-grained, the specific yield was 0.40. Very few of the values reach the extreme ends of the range. The high end of this range is above previous measurements and estimates and only is used for coarsest-grained deposits representing very well-graded sand. Less than 17 percent of the uppermost active cells have specific yield values above 0.30 and less than 5 percent have specific yield values greater than 0.40. More than 50 percent of the model cells, where specific yield was specified, have values between 0.20 and 0.30. The median and average values are 0.23 and 0.24, respectively, well within previously estimated values of specific yield (*table C8*).

For the CVHM, porosity values of 0.25 and 0.50 were used for coarse-grained and fine-grained deposits, respectively. The products of these porosity values and the respective cell-by-cell average coarse- and fine-grained fractional aggregate thicknesses are summed and multiplied by the compressibility of water (1.4×10^{-6} per foot) to yield an aquifer-system specific storage value for each active cell of every layer.

Storage properties defining the matrix or skeletal components of specific storage were specified in the SUB package (Hoffmann and others, 2003b). The Subsidence (SUB) package was chosen over the Interbed Storage (IBS) package (Leake and Prudic, 1991) because SUB allows for time-dependent drainage. Realistically, the pore pressure of low-permeability units does not equilibrate instantaneously with changing hydraulic heads in the adjacent aquifer, as assumed in the IBS package. A time lag occurs that is dependent on the thickness, vertical hydraulic conductivity, and the specific storage of the low permeability units. Although the time-dependent drainage feature within SUB was not utilized, it was included to enable future use.

Both the elastic and inelastic components of skeletal specific storage were simulated with the SUB package. The elastic and inelastic skeletal storage coefficients were calculated as the product of the estimated elastic- and inelastic-specific storage values for coarse- and fine-grained materials and the aggregate thicknesses of those materials in each cell. The elastic skeletal storage coefficient of the coarse-grained deposits was estimated from the product of the aggregate thickness of coarse-grained deposits and the difference between an estimated elastic-specific storage and the specific storage representing the compressibility of water (Hanson, 1988). Reported values for aquifer-specific storage determined from selected aquifer tests typically range from 1×10^{-7} to 2×10^{-7} per foot (Riley, 1969, 1984; Helm, 1974, 1975, 1976, 1977). The average aquifer specific storage is reported to be 8.6×10^{-8} per foot for the San Joaquin Valley (Ireland and others, 1984). An initial elastic skeletal specific storage for aquifers of 1.0×10^{-6} per foot was specified in the model, based on reported values for coarse, alluvial sediments from the Central Valley and Arizona (Ireland and others, 1984; Hanson, 1988). The aquifer elastic skeletal-storage coefficient was estimated as the product of the aquifer skeletal-specific storage and the aggregate cell-by-cell thickness of the coarse-grained deposits for each layer. An initial elastic skeletal-specific storage for fine-grained units of 4.5×10^{-6} per foot was specified initially in the model. This value is based on reported values for alluvial sediments from the Central Valley and Arizona (Ireland and others, 1984; Hanson, 1988). During model calibration, this parameter was allowed to vary and the model solution was relatively insensitive to this parameter. Ultimately, the initial estimated value was used in the calibrated model. In a similar manner, the average elastic skeletal storage coefficient of the coarse-grained deposits was estimated to be 1.0×10^{-6} per foot. The composite aquifer-system elastic skeletal storage coefficient was the sum of the elastic skeletal storage coefficients for the coarse-grained and fine-grained deposits for each cell in each layer. An inelastic, skeletal-specific storage of 1.37×10^{-4} per foot was estimated. This value is consistent with the low end of the range of values determined from the analysis of extensometer and piezometer data of 1.4×10^{-4} per foot (Riley, 1969; Helm, 1977; Ireland and others, 1984). The inelastic skeletal storage coefficient was estimated as the product of the inelastic specific storage and the aggregate cell-by-cell thickness of the fine-grained deposits for each layer. With respect to matching subsidence observations, the model solution was

most sensitive to this parameter, and cell-by-cell parameter values were estimated during calibration.

Critical head is another parameter used by the SUB package that strongly affects storage changes, particularly the timing of those changes (*fig. B18*). Critical head is the equivalent head at which effective or intergranular stress is equal to the pre-consolidation stress. The equivalent critical head or pre-consolidation stress represents the threshold stress that determines whether changes in stress deform the granular skeleton elastically or inelastically. For head changes (whether positive or negative) in the range of heads greater than the critical head, the skeleton deforms elastically. For head changes in the range of heads less than the critical head, the mode of skeletal deformation depends on the sense of the head change—a positive change (head increase) causes elastic deformation, and a negative change (head decrease) causes inelastic deformation and re-establishes a new critical head. In the upper three model layers, specified initial critical-head values were equal to the water levels estimated for the spring of 1961 (starting head values used in CVHM). In the lower seven model layers, the initial critical heads initially were derived from those estimated by Williamson and others (1989). These heads are approximate and were interpolated from the minimum historical head values simulated in the CV-RASA model. In the final calibration, specified initial critical heads were equal to the head simulated in CVHM in September 1961. These values approximate the minimum historical head value in 1961.

Hydrogeologic Units

Because the 3D configuration of regionally extensive hydrogeologic units generally is unavailable for the Central Valley, only two stratigraphically defined units and the crystalline bedrock of the Sierra Nevada complex are explicitly incorporated in the CVHM. As described in *Chapter A*, the extent and thickness of the Corcoran Clay defined by Page (1986) and later modified by Burow and others (2004) was used to define model layers 4 and 5 (*fig. A8*). Where the San Joaquin Formation (Allegra Hosford Scheirer, U.S. Geological Survey, written commun., 2004) is present in the model domain, model cells within its mapped extent were identified. Similarly, model cells that coincide with the mapped extents of crystalline rocks of the Sierra Nevada complex also were identified. The uppermost model cell in each applicable column intersecting these crystalline rocks is zoned as upper bedrock and all lower cells were inactived. This bedrock intersection occurs only on the eastern edge of the model domain and leaves the bulk of the domain undefined by specific formations (*fig. C1*). The contribution of groundwater from the bedrock was assumed negligible.

Hydrogeologic Structures

As delineated in *Chapter A*, the basin is traversed by two cross-valley faults, the Stockton Fault and White Wolf Fault (Hackel, 1966) (*fig. C1*). In addition, several smaller structures also were identified as possibly affecting groundwater-flow during an examination of water levels throughout the valley (*fig. C1*). The Horizontal Flow Barrier package (Hsieh and Freckelton, 1993) was used to simulate resistance to flow across these two major structures and several smaller structures (*fig. C1*). Although the model solution is relatively insensitive to these features, the effectiveness of these barriers was evaluated through model calibration by estimating parameters representing the hydraulic conductance across the features. The only other prominent structure in the Central Valley is the Sutter Buttes, a Pliocene and Pleistocene volcanic plug that rises abruptly to an altitude of 2,000 ft (600 m) above the flat valley floor (*fig. C1*). The Sutter Buttes is about 9 mi in diameter and the area is represented by inactive cells within the model domain (*fig. C1*).

Initial Conditions

For transient models, initial conditions define the system state at the beginning of the simulation. There is a long history of groundwater development and irrigation in the study area. Despite the fact that the system has been under stress since the late 1800s, sufficient historical water levels and data for estimating stresses were not available until about the 1960s. The combined effects of irrigation and groundwater pumpage have greatly increased the vertical head gradients, particularly in the southwestern part of the CVHM (WBS 14, *fig. A4* and *B13*). The hydrologic system was in a transient state during the early 1960s owing to the changing vertical head gradients and the continued recovery of the potentiometric surface. As a result of these and possibly other conditions, steady-state simulations using 1961 stresses and water-level altitude constraints fail to capture the ongoing transient responses to pre-1961 stresses. Therefore, there is little choice but to begin the simulation with initial conditions derived from a combination of historical water-level-altitude data and model-derived initial water levels. Like CV-RASA, the groundwater-flow simulation starts in April 1961, for which there are sufficient data to map both the altitude of the water table and the groundwater levels in the confined part of the aquifer system (Williamson and others, 1989). Although the specified initial state of the system generally is inconsistent, to some degree, with the conservation equations and properties of the CVHM, it is considered an adequate starting point.

The initial heads for the transient simulation were specified using the approach employed for previous studies in the San Joaquin Valley (Belitz and others, 1993; C. Brush, U.S. Geological Survey, written commun., 2006). The 1961

heads and streamflows are used as initial conditions to begin the simulation and calibration period of April 1961 through September 2003. Specifically, the initial heads in the upper three model layers representing the shallow part of the system (the semi-confined zone) (described in *Chapter B*) were set equal to the water table altitudes defined by Williamson and others (1989; *fig. B12A*), and heads for layers 4–10 were set equal to groundwater levels defined by Williamson and others (1989; *fig. B12B*). Specifying hydrostatic initial conditions for the shallow and deep zones of the aquifer system ignores the vertical head gradients within those zones. However, the vertical head gradients were re-established in the first few months of simulation. Because of the importance of these gradients and the fact that the initial heads were coarse estimates, the CVHM was allowed to run forward 1 year to dissipate the transient effects caused by imposition of the poorly estimated initial heads. The resulting simulated heads were considered representative of heads in April 1961 and were used subsequently as initial heads for calibration of the CVHM as the April 1961 starting heads. During calibration of the CVHM, as various model parameter values were modified, this procedure to dissipate transient effects caused by inaccurate initial heads was repeated periodically.

Because the irrigation and pumpage stresses on the system change rapidly, the inconsistencies between the initially specified conditions and the simulated initial processes and properties generally are not problematic because the next stress regime soon dominates the solution (Hill and Tiedeman, 2007). This study and previous studies (Belitz and Phillips, 1995; C. Brush, U.S. Geological Survey, written commun., 2006) show that the time frame for the stabilization is on the order of several months of simulation. As a result, comparing observed and simulated values becomes meaningful after a relatively short simulation period.

Model Calibration and Sensitivity

Calibration of transient-state conditions was dependent on recharge (streamflow, farm net recharge) to, and discharge (pumpage, streamflow, and ET) from, the aquifer system and on hydraulic conductivity, storage, fault hydraulic characteristics, general-head boundary conductance, and streambed hydraulic conductivity. Many of the water-budget components are specified values. Specified model inputs that were not adjusted during calibration include precipitation, stream inflows at lateral boundaries, urban pumpage, semi-routed and non-routed diversions from streams and canals to WBSs, and many properties associated with WBSs and crops simulated in the FMP. The remaining water-budget components, calculated by the model, include streamflow gains/losses, inflow and outflow through the Delta, evaporation, transpiration, groundwater pumpage for agricultural uses, runoff, farm net recharge, leakage through multi-node wells, subsidence, and groundwater storage changes. The implementation of the MNW package maintained the net pumpage but redistributed groundwater-flow vertically between layers through intra-borehole flow.

Calibration of the CVHM was accomplished using a combination of trial-and-error and automated methods. For the CVHM, UCODE-2005 (Poeter and others, 2005) was used to help assess the ability of the CVHM to predict the effects of changing stresses on the hydrologic system. Simulated changes in water levels, streamflows, streamflow losses, and subsidence through time were compared to those measured in wells, at streamflow gages, and extensometer sites. Automated calibration adjustments were related to the combined fitting of the groundwater levels, groundwater level differences, streamflow losses, and subsidence measurements (locations shown in *fig. C15*). The observations were all compared to simulated values and provided a measure of model performance through space and time. The resulting error distributions constrain the parameter set and constitute a sensitivity analysis of these parameters. Maps of groundwater levels were used for qualitative comparisons but were considered less reliable than time-series data because the composite water-level altitude measurements and hand contours represent averaged conditions in many areas where there are large vertical-head differences within some parts of the aquifer system.

Observations Used in Model Calibration

Successful groundwater model calibration often is dependent on multiple observation types (Hill and others, 1998). However, parameter estimation, as used in groundwater model calibration, often uses hydraulic head data as the sole or highly dominant type of observation. The combination of flow observations, or other types of data, with water-level altitude data lead to a more accurate, rapid, and unique calibration. The availability and accessibility of other data types provide important observations that greatly aid in parameter estimation. Therefore, water levels, water-level altitude changes, and water-level and potentiometric-surface altitude maps; streamflows; boundary flows; subsidence; groundwater pumpage; water use; and water-delivery observations were used to constrain parameter estimates throughout the calibration of the CVHM.

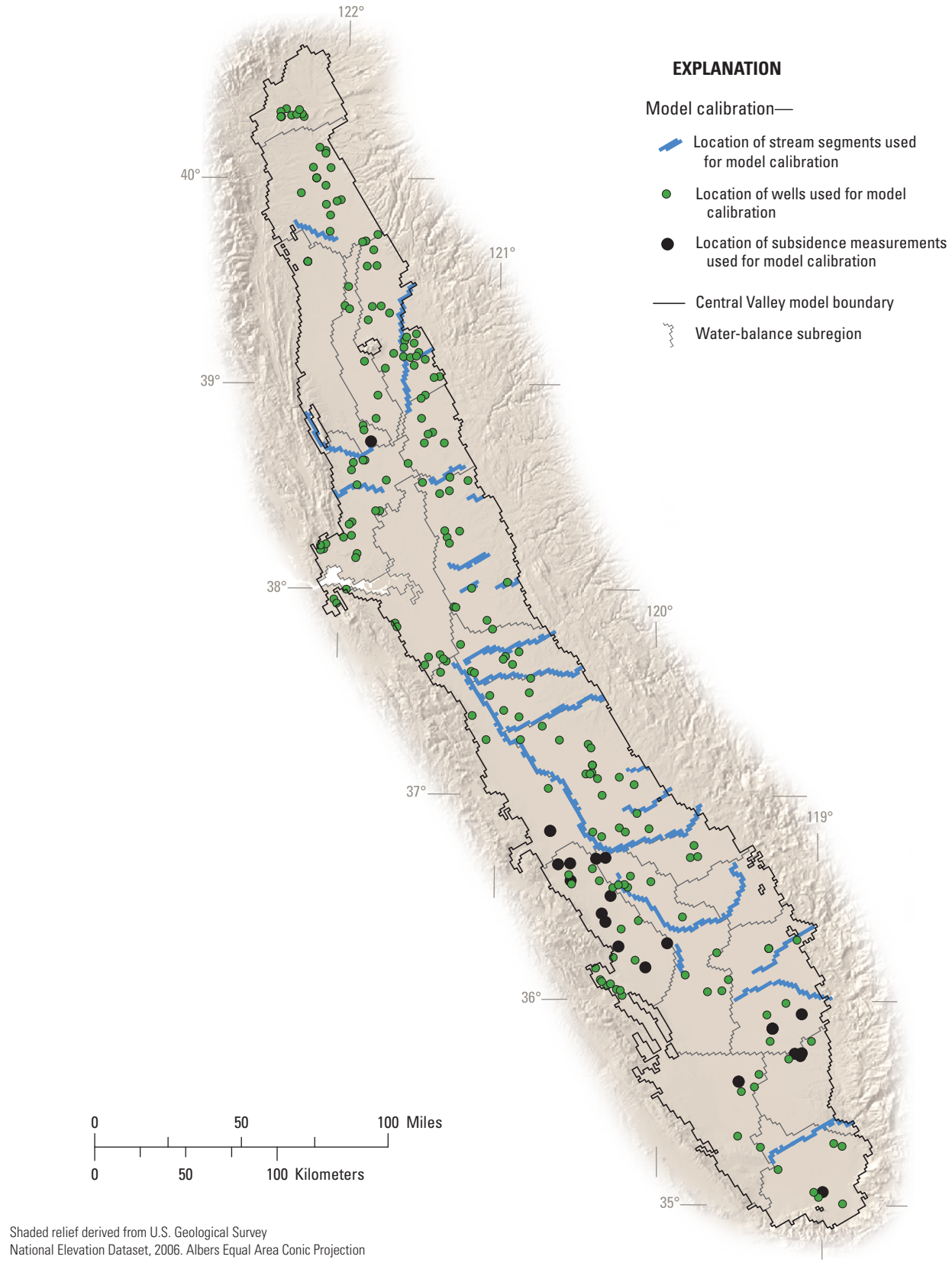

Figure C15. Distribution of calibration data (groundwater levels, gains and losses of streamflow, and subsidence observations).

Water-Level Altitudes, Water-Level Altitude Changes, and Water-Level Altitude Maps

The first calibration target was the groundwater-level altitudes and changes in these altitudes through time. The USGS and DWR maintain databases of key wells in the Central Valley that are web-accessible (*http://waterdata.usgs.gov* and *http://wdl.water.ca.gov/gw/*, respectively). These data were combined to form a database of available water levels throughout the Central Valley from 1961 to 2003. More than 850,000 water-level altitude measurements from more than 21,400 wells have been made by the USGS or DWR and have been entered into their respective databases (*fig. C16*). However, only a small proportion of these wells (590 wells) have both sufficient construction information to determine the well-perforation interval and water-level measurements for the simulation period.

For model calibration, water-level altitude data were needed that were (1) distributed spatially (both geographically and vertically) throughout the Central Valley, from the valley trough to the foothills; (2) distributed temporally throughout the simulation period (1961–2003); and (3) available during both wet and dry climatic regimes. From the available wells records, a subset of 170 comparison wells was selected on the basis of perforation depths, completeness of record, and locations throughout the Central Valley. In selecting the appropriate wells, shallow and deep wells were paired, where possible, and several nested or clustered monitoring wells were included. Even though the dataset containing 170 wells spanned the simulation period, the water-level altitude data were not always complete during the wettest and driest periods of the record. In order to ensure that the wet and dry years were adequately represented in the water-level-altitude calibration dataset, an additional analysis was done on the basis of perforation depths, water-level altitude measurements during the wet and dry periods (1961, 1965, 1969, 1976, 1977, 1980, 1983, 1991, 1998, and 2003; *fig. C7*), and the location of wells within the WBS and throughout the Central Valley. Thirty-six additional comparison wells were identified that best represent the wet and dry periods, for a total of 206 comparison wells (*fig. C16*). Because many wells had multiple measurements in a given monthly stress period, the minimum water-level altitude for each month was selected, resulting in 19,725 water-level altitude observations for the 206 comparison wells. These observations were used as calibration targets during parameter estimation.

In addition to simulating the measured water-level altitudes at a particular time, it is necessary to accurately simulate the trends in water-level altitudes throughout the valley. In order to represent these trends, a set of observations were compiled for each well based on the net change in water-level altitude for the period of record for each observation well. For comparison, the water-level altitudes at the observation wells ranged from –277 to 489 feet, and the average was 104 feet. The net change in measured water-level altitude in individual wells ranged from –150 to 250 ft and the average was 50 ft. The net change in simulated water-level altitude at these well locations ranged from –102 to 297 ft and the average was 80 ft. Both simulated and observed trends remained fairly flat in the northern part of the study area, increased dramatically in the deeper parts of the southwestern part of the study area and declined somewhat in the southeastern part of the study area.

A simple method of assessing overall model fit is to plot the simulated water-level altitude values against the measured water-level altitudes (*fig. C17*). For a perfect fit, all points should show a 1:1 relation (fall on the 1:1 diagonal line). The final model sum of squared weighted residuals (SOSWR) for water-level altitudes from the comparison wells was $3.82\times10^{7}\times10$ ft^2 for the 42.5-year simulation period 1961–2003. The root mean square error between measured and simulated water-level altitudes is 0.80 (*fig. C17*). Given the scale of the CVHM, simulated water-level altitudes reasonably matched measured water-level altitudes, as indicated by an average residual of –14 ft and a standard deviation of 43 ft; the residuals ranged from –277 to 384 ft. These extremes possibly represent errors in the databases, measurements that represent pumping conditions, or seasonal variations beyond the ability of the model to simulate. More than 50 percent of the simulated water-level altitudes are within 25 ft of observed water-level altitudes, more than 80 percent are within 50 ft, and more than 94 percent are within 75 ft. In general, the errors were distributed randomly and normally (*fig. C17*). In many WBSs, the measured water-level altitudes have a greater range in water-level altitude than the simulated water-level altitudes. This can be attributed to matching the average, more than the range, of water-level altitude values. Because the agricultural pumpage is distributed throughout all wells in a WBS, the CVHM tends to match the average more than the range of water-level altitude values. In reality, it is likely that some wells are pumping harder than others and would have a larger range in water-level altitude values. More detailed "farms," pumpage records, well-by-well pumping capacities, and delivery information could be used to better match the range of water-level altitude values.

The Central Valley aquifer system represents a range of unconfined, semi-confined, and confined conditions. As a result, water-level altitudes measured in wells and simulated with the CVHM represent all of these conditions. In this report, the term water-level altitude will be used to describe the altitude that the potentiometric surface would be at if penetrated by a well, whether unconfined, semi-confined, or unconfined.

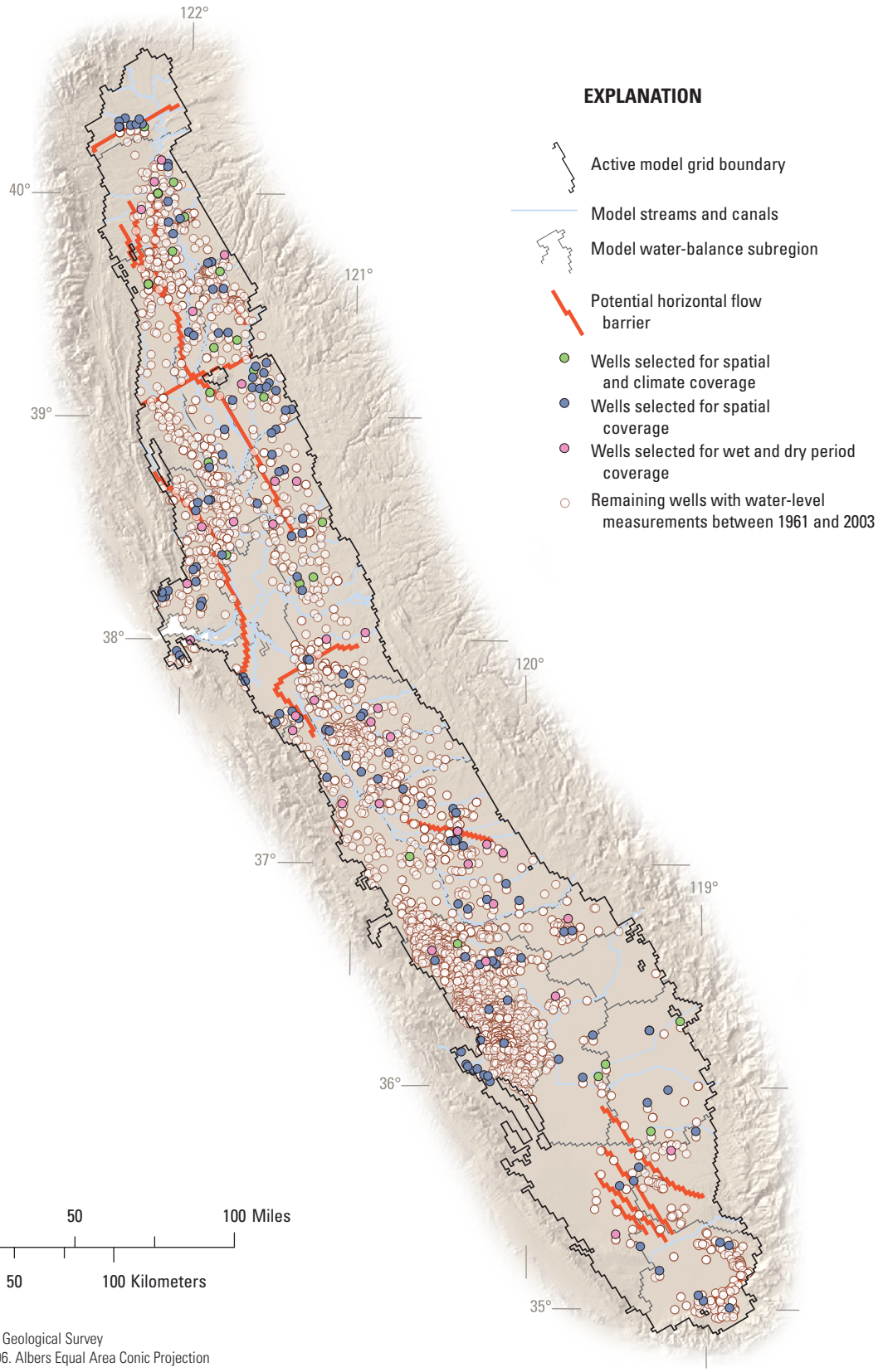

Figure C16. Distribution of wells with water-level-altitude data for the simulation period 1961–2003, and location of wells selected for model calibration. Only selected wells were used for calibration; other wells are shown to display the density of wells with water-level measurements in simulation period.

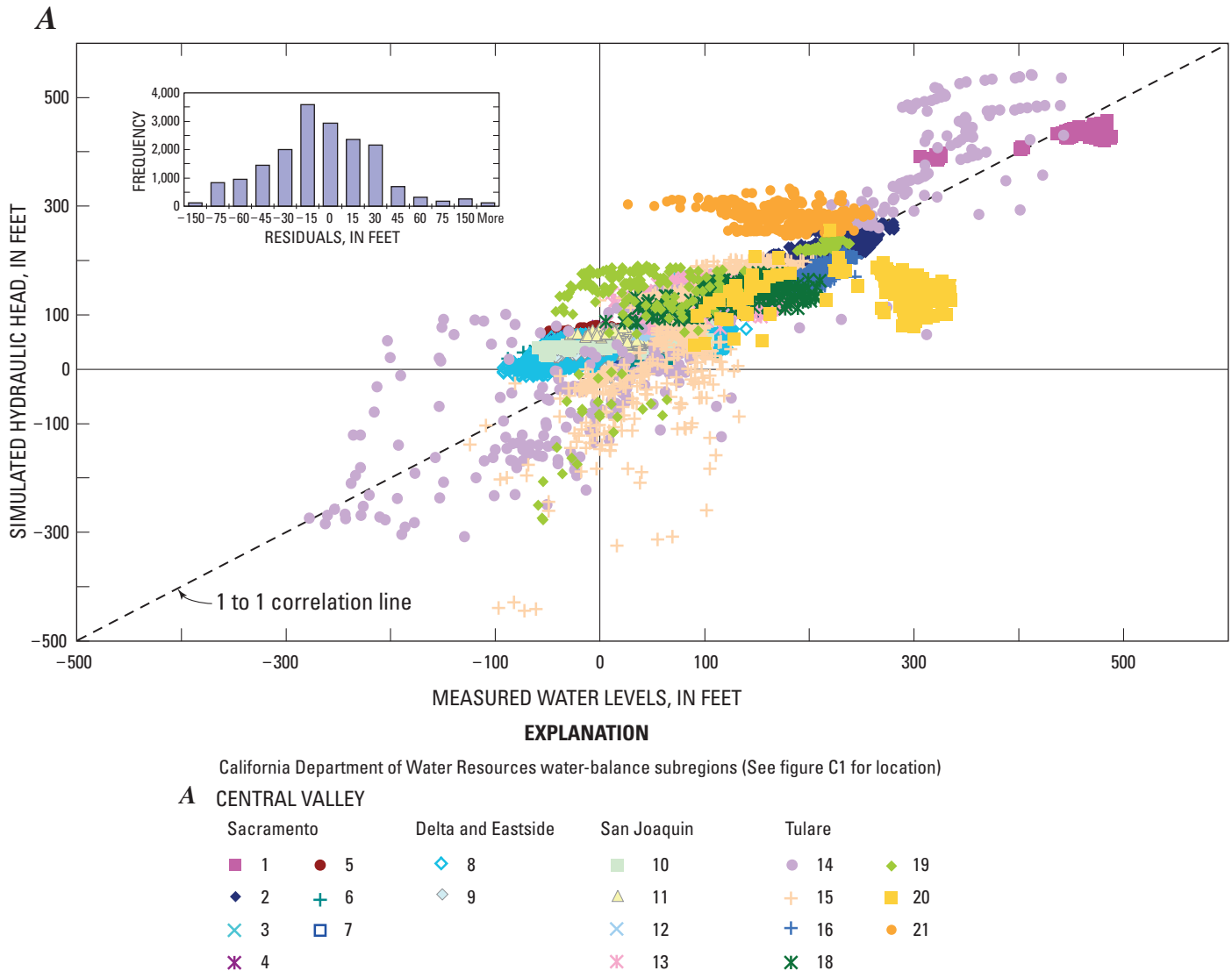

Figure C17. Plots of simulated water-level altitude values compared with the measured water-level altitudes for the *A,* Entire modeled area (and with inset with histogram of residuals). *B,* Sacramento Valley. *C,* Delta and Eastside. *D,* San Joaquin Basin. *E,* Tulare Basin.

Hydrographs comparing simulated and measured water-level altitudes for selected wells indicate how well the CVHM matches measured water-level altitudes in the upper and lower parts of the aquifer system above and below the Corcoran Clay (*fig. B13*). The minimum time period for which model simulations can reproduce accurate water-level altitude fluctuations in the groundwater-flow system (the response time of the model) varies with the depth to groundwater. Simulated annual water-level altitude fluctuations generally are greater than measured annual fluctuations. The reasons for this difference include the contrast between simulation and measurement frequency, and the fact that measurements generally are made after the well is turned off and, therefore, is more likely to represent quasi-static conditions.

The hydrographs indicate that CVHM-simulated water-level altitudes general fit the measured values (*fig. B13*). In both the simulated and measured water-level altitudes, the annual fluctuations are smallest at the water table and increase with depth below the land surface. This most likely is a result of the variability in storage, pumpage rates, and applications of irrigation water. The use of large WBSs, estimated pumpage rates, coarse land use, spatial and temporal crop distributions, uniform model layer thicknesses (except above and in the Corcoran Clay), lateral discretization of the model grid, and assumptions made in spatially distributing pumpage limit the performance of the CVHM. Given these limitations, the CVHM cannot be expected to accurately simulate time-series water-level altitude data from individual wells. Thus, the goal of the model calibration was not to match individual hydrographs, but to match the long-term change in water-level altitudes and to minimize the SOSWR for all simulated water-level altitudes.

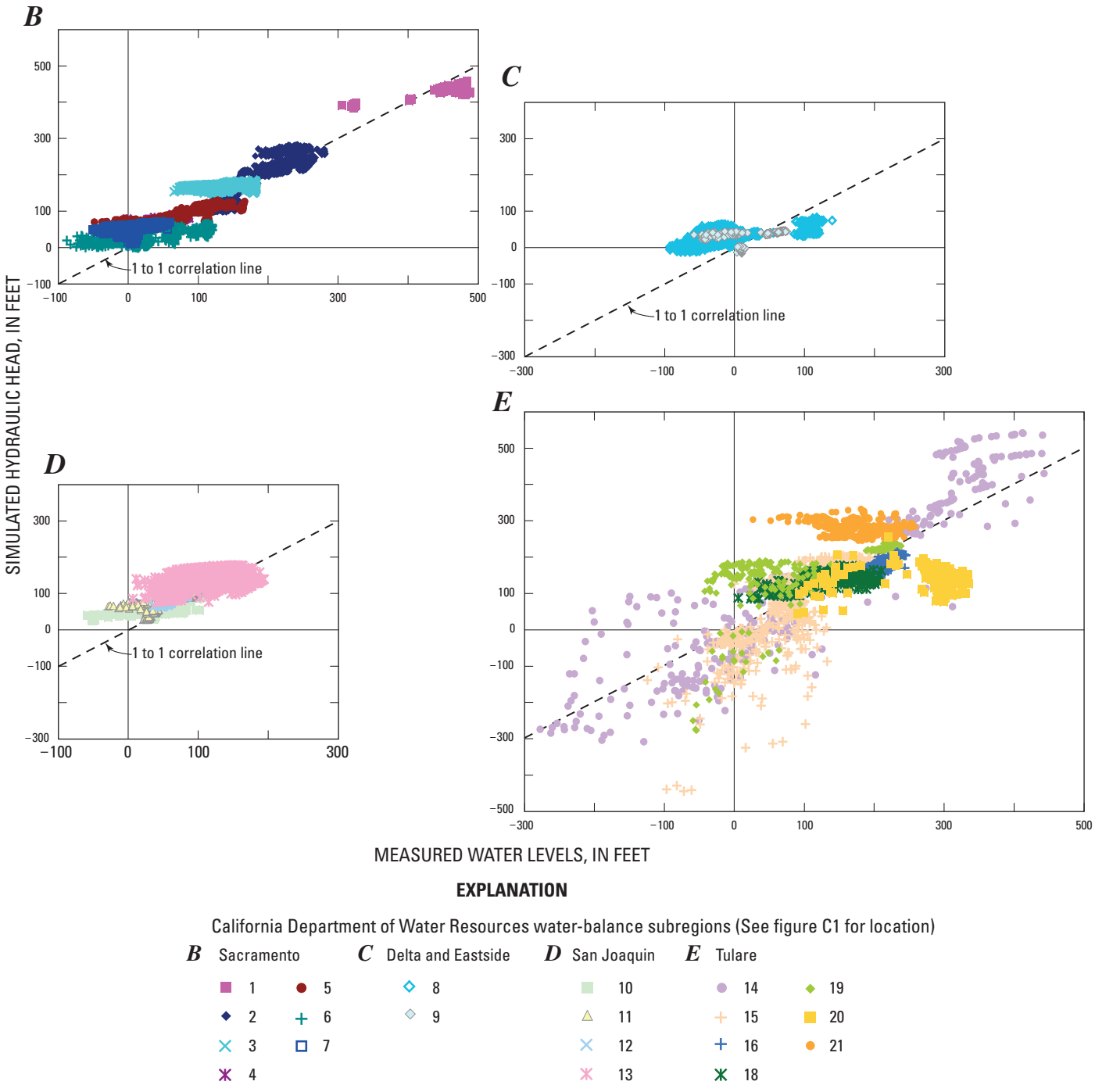

Figure C17. Continued.

A comparison of the simulated water levels suggests the CVHM is fairly accurate in the northern part of the study area where the system has not been stressed vigorously and the water table generally is flat, but performs poorly in the southeastern part of the study area (*fig. C17*). There was little change in the simulated water levels in the northern part of the study area but there were some dramatic changes in water-level altitudes in the southwestern part of the study area (*fig. B13*).

The CVHM closely matches measured water-level altitudes during some periods of time but overestimates or underestimates water-level altitudes at other times. This result likely is due to previously discussed assumptions about the simulated WBS budget, land use, and to the inability to represent at sufficient spatial and temporal detail, the land use (crops), well locations, and associated stresses throughout the simulation period. This is evident particularly in the southernmost part of the study area. Examination of the simulated water-level

altitudes shows that the CVHM reasonably represents seasonal changes and major features in the climate record. The effect of droughts during 1976–77 and 1987–91, and higher-than-normal precipitation during 1983–84 and 1998, are represented by changes in water-level altitudes (*fig. B4*). These changes are evident particularly in the highly stressed southwestern part of the San Joaquin Valley.

Water-Table and Potentiometric-Surface Maps

Water-table and potentiometric-surface maps for the Central Valley aquifer system for 1961 and 1976 are available from the CV-RASA study (*fig. B12*) (Williamson and others, 1989). The potentiometric-surface maps were compared with contoured model results to ensure similarity between hydraulic gradients and between water-level altitudes. The simulated water-level altitudes are in general agreement with the hand-contoured water-table and potentiometric-surface maps for the spring of 1976 (*fig. C18*). The water-table and potentiometric-surface maps for 1961 were used for starting water-level altitudes for the simulation.

The distribution of groundwater-level altitudes through time shows the effects of the time-varying recharge and pumpage on groundwater-flow. Cones of depression in major pumpage centers and water-level-altitude mounds in some fine-grained irrigation areas are evident. The water-level altitudes in the confined part of the aquifer system have varied significantly from year to year, declining in years of greater-than-average groundwater pumpage and recovering in years of reduced pumpage (*fig. B13*). The simulated and observed water-level altitudes in the water table wells (layers 1 through 3) remain fairly constant throughout the 1961–2003 period, with some variations in intensively irrigated or pumped areas (*figs. B4* and *B13*). The simulated hydrographs (*fig. B13*, wells 06b12975, 14_30806, 15_2973719_37289) show that vertical hydraulic gradients from the water table to the deeper production zones are strongly downward around the edges of the valley and larger during spring and summer than during fall and winter. Conversely, the gradient generally is upward in the vicinity of the valley trough (*fig. B13*, 03b06329 and 19_38742). Seasonally, simulated water-level altitudes fluctuate several hundred feet in the deeper wells on the west side of the San Joaquin Valley and generally fluctuate less than 5 ft at the water table (*fig. B13*). Temporal variability of measured water-level altitudes generally is dominated by irrigation. At rivers, variability is dominated by the river stage, and a combination of these factors influence areas nearby the rivers.

Sacramento Valley

In the Sacramento Valley, the hydraulic gradients generally are downward around the edges of the basin, while horizontal gradients, particularly in the upper part of the aquifer system, are toward the Sacramento River (*fig. C18*). In the Redding area, water-level altitudes seem relatively static over time (*fig. B13*, WBS 1), with water-level altitudes highest around the basin edges and decreasing toward the south and central part of the valley (*fig. C18*). Water-level altitudes in the wells in the northern Sacramento Valley have hydrograph signatures (peaks and troughs) which, although subdued, reflect the effect of wet, dry, and average precipitation years, and show seasonal fluctuations ranging from about 5 to 10 ft. The CVHM simulates the seasonal changes and some of the climatic effects accurately (*fig. B13*). Toward the south, water-level altitudes decline slightly, as indicated by the potentiometric surface maps (*fig. C18*). These changes partly are owing to topographic changes and may be partly owing to increased water demands caused by population growth. Hydraulic gradients near the Sacramento River (WBS 4) generally are upward, toward the gaining sections of the Sacramento River (*fig. B13*, well 04_07807). Measured and simulated water-level altitudes in wells closest to the Sacramento River respond only slightly to the dry years in the mid 1970s and early 1990s and specific periods in the mid 1980s and mid-to-late 1990s (*fig. B13*, well 02_05172, 03b06329, 07_13870, and 08_14958).

In the southern Sacramento Valley, numerous creeks drain runoff from the Coast Ranges that ultimately drains into the Sacramento River. The aquifer system in these areas is thicker; the deeper part of the system has upward hydraulic gradients and the shallow part of the system has downward gradients (*fig. B13*). These gradients partially are in response to pumpage. In addition, further south in the Sacramento Valley, water-level altitude changes reflect changes in pumpage activities, particularly during droughts. Near the North Fork of the American River, in the vicinity of the city of Sacramento, an area of water-level altitude declines likely represents urban pumpage (*fig. C18*). Although development-related stresses have only just begun by 1976 in parts of the Sacramento Valley, the initial effects seen in one interval of the aquifer system are not readily observable in deeper or shallower intervals of the system (*fig. C18*). This may indicate that major stratigraphic units, such as the Tuscan and Tehama Formations, form the primary aquifers in the Sacramento Valley.

Delta

Water-level altitudes in the Delta area are affected by human activity. Though surface-water-level altitudes in the canals, sloughs, and rivers between the island levees are above sea level, land-surface elevations of the islands generally are below sea level. Simulated and observed water-level altitudes generally decline toward the Delta (*fig. C18*); however, the Stockton area has a large pumpage depression that causes an influx of water from the Delta. This depression also is evident in the simulated potentiometric-surface maps (*fig. C18*). Although vertical hydraulic gradients generally are downward, particularly south of the Delta, they have varied over time with changes in pumpage activities. Locally, a number of faults (*fig. C16*) may affect water-level altitudes and groundwater-flow directions. Some faults were simulated in the CVHM, but not in this area.

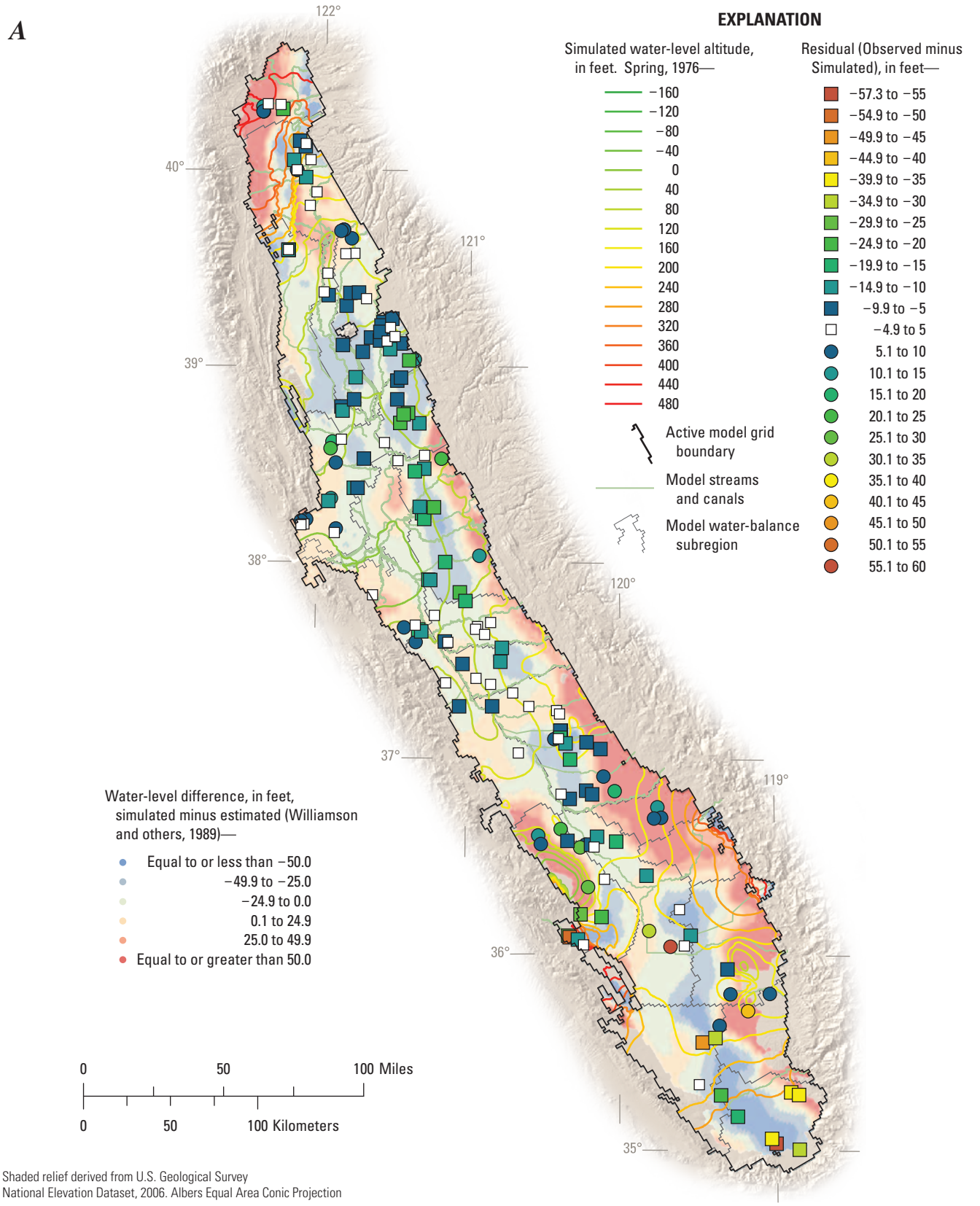

Figure C18. The simulated *A*, Water-table altitude in spring 1976. *B*, Potentiometric-surface altitude in spring 1976, for the calibrated transient groundwater-flow model of the Central Valley. Residuals at observation points and areal differences between hand-drawn altitude maps also are shown. Maps showing the simulated water-table altitude and potentiometric-surface altitude in spring of 2000 are shown in *figures B12E* and *B12F*.

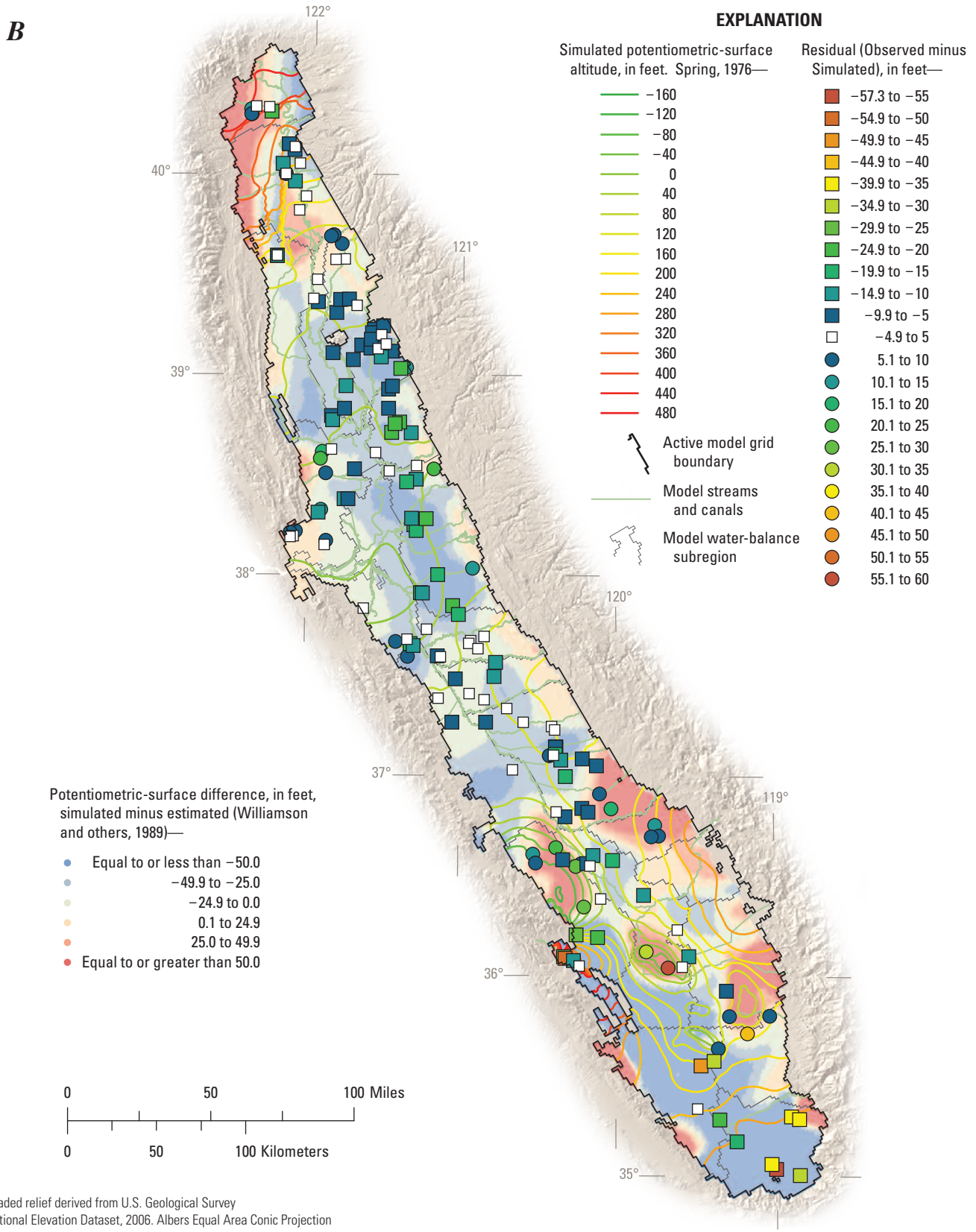

Figure C18. Continued.

San Joaquin Valley

Data from wells close to streams and rivers in the San Joaquin Valley exhibit a connection between the groundwater and surface-water systems. Along the edges of the basins, streams and rivers generally are losing water to the aquifer system; those near or along the axis of the valley generally are gaining. The potentiometric-surface maps show these relationships (*fig. C18*).

Water-level altitudes throughout most of the San Joaquin Valley are influenced by the Corcoran Clay, which acts as a confining unit, forming a confined part of the aquifer system. The vertical hydraulic gradients in the area of the Corcoran Clay generally are downward (*fig. B13*). This downward gradient is a result of the combined effect of a large amount of pumpage from the lower part of the aquifer system, and recharge of excess irrigation water to the shallow part of the system. Seasonal fluctuations range from about 15 to 100 ft, depending on the amount of pumpage (*fig. B13*). There was a substantial water-level-altitude decline associated with the 1987–92 drought and its after effects; pumpage increased during this period and water-level altitudes declined as much as 300 feet. As surface-water deliveries ramped up after the drought, water-level altitudes recovered to pre-drought levels (*fig. B13*).

In the San Joaquin Valley, water-level altitudes in the confined part of the aquifer system may be affected by variations in precipitation in the recharge area near the foothills and by drawdown cones from pumping wells. Both simulated and observed vertical hydraulic gradients on the eastern and western side of the San Joaquin Valley are downward. Measurements and other modeling in the Stanislaus to Merced River and Fresno areas indicate downward hydraulic gradients (Phillips and others, 2007). The measurements include multilevel piezometers (above and below the Corcoran Clay, where present) within, west of, and east of Modesto; near the Merced River; and in the mid-alluvial fan area near Fresno.

Water-level altitudes in the confined part of the aquifer system in the Chowchilla area are much different from those in the Merced area north of the Pre-Quaternary Fault; this suggests the fault may impede flow in the confined part of the aquifer system (*figs. C16* and *C18*). Water-level altitudes near the city of Fresno generally have been declining, which until very recently was the largest metropolitan area in the U.S. entirely dependent on groundwater (*figs. B13* and *C18*).

Extreme examples of changes in development and the effects on water-level altitudes occurred in the western San Joaquin Valley. These changes are replicated in the potentiometric-surface maps and hydrographs (*figs. B13* and *C18*). Groundwater pumpage reached a sustained maximum, and confined water-level altitudes generally reached a low during the 1960s. Pumpage in this area, predominantly from the lower part of the aquifer system, caused downward flow from the upper to the lower zone throughout the simulation period.

Tulare Basin

The Corcoran Clay extends throughout most of the Tulare basin. As on the west side of the San Joaquin Valley, water-level altitudes are heavily influenced by agricultural practices and the presence of the Corcoran Clay. On the eastern side of the Tulare basin, surface water is more available and groundwater pumpage has been less. Long-term, as well as seasonal, fluctuations in groundwater-level altitudes reflect changes in pumping activities in response to wet and dry years. Long-term water-level altitudes for several wells (*fig. B13*) indicate a downward vertical hydraulic gradient from the 1960s through 1972, and upward vertical gradients from 1973 through 1993. In the southern part of the basin, the confined part of the aquifer system has a higher water-level altitude, indicating an upward gradient. Wells located outside the extent of the Corcoran Clay (*fig. B13*) had declining water-level altitudes and several vertical hydraulic gradient reversals during the simulation period. On the southeastern side of the basin, simulated water-level altitudes decline at a faster rate than the observed rate of water-level altitude decline.

Streamflow Observations

Quantitative observations of streamflow gains and losses were available for 57 reaches of 20 major stream systems in the Central Valley for water years 1961–77 (Mullen and Nady, 1985). These observations were included in UCODE-2005's parameter estimation process and in the model-fit statistics. Water budgets for the Sacramento River were not included because estimates of gains (and losses) to groundwater are subject to larger errors in the Sacramento River than for other streams (Mullen and Nady, 1985). The 1961–77 period during which these data were collected reflects the cyclical characteristics of water supplies in the Central Valley and includes reliable records during a series of wet and dry years (Mullen and Nady, 1985). Phillips and others (2007) reported streamflow losses from the tributaries to the San Joaquin River in the Modesto area. Their work shows streamflow losses in the upper reaches and gains in the lower reaches.

Measured and simulated streamflow gains and losses are shown in *figure C19*. The simulated gaining and losing reaches generally are consistent with the observations from Mullen and Nady (1985) and the gaining and losing sections in the Modesto area (Phillips and others, 2007). The results of the simulation show gaining sections of the San Joaquin River with much larger gains than measured. The results of the simulation show the southern part of the Kern River as gaining when measurements indicate that this stream reach is losing water. High streambed hydraulic conductivities were assigned in the lower reaches of the Kern River to represent the artificial recharge area of the Kern Water Bank. The simulated gaining reaches may indicate that simulated water-level altitudes in the shallow part of the aquifer system are too high in this area.

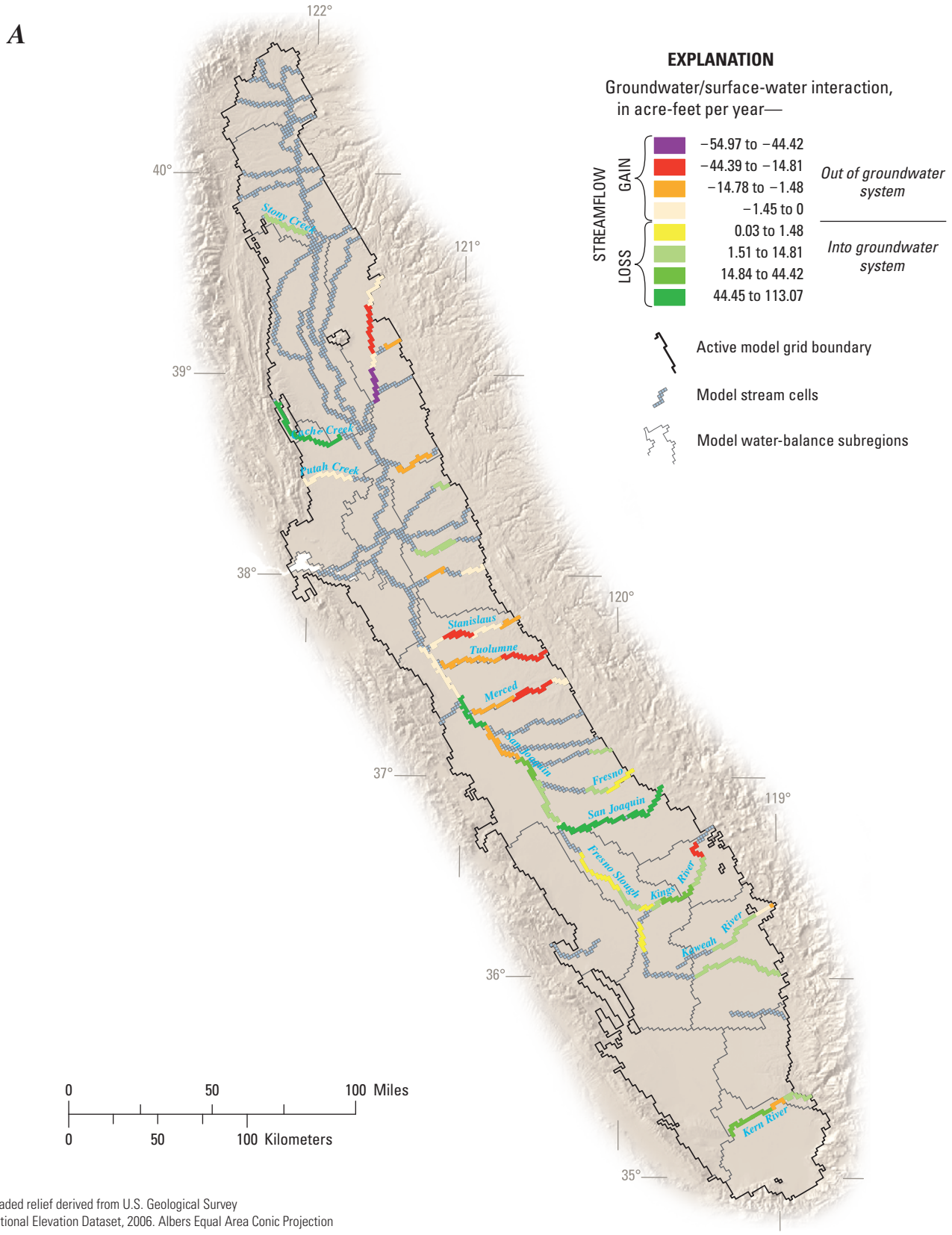

Figure C19. Distribution of stream gain/loss segments used for model calibration. *A*, Measured gaining and losing reaches for selected stream reaches for 1961–1977. *B*, simulated gaining and losing reaches for selected stream reaches for 1961–1977 for the Central Valley, California.

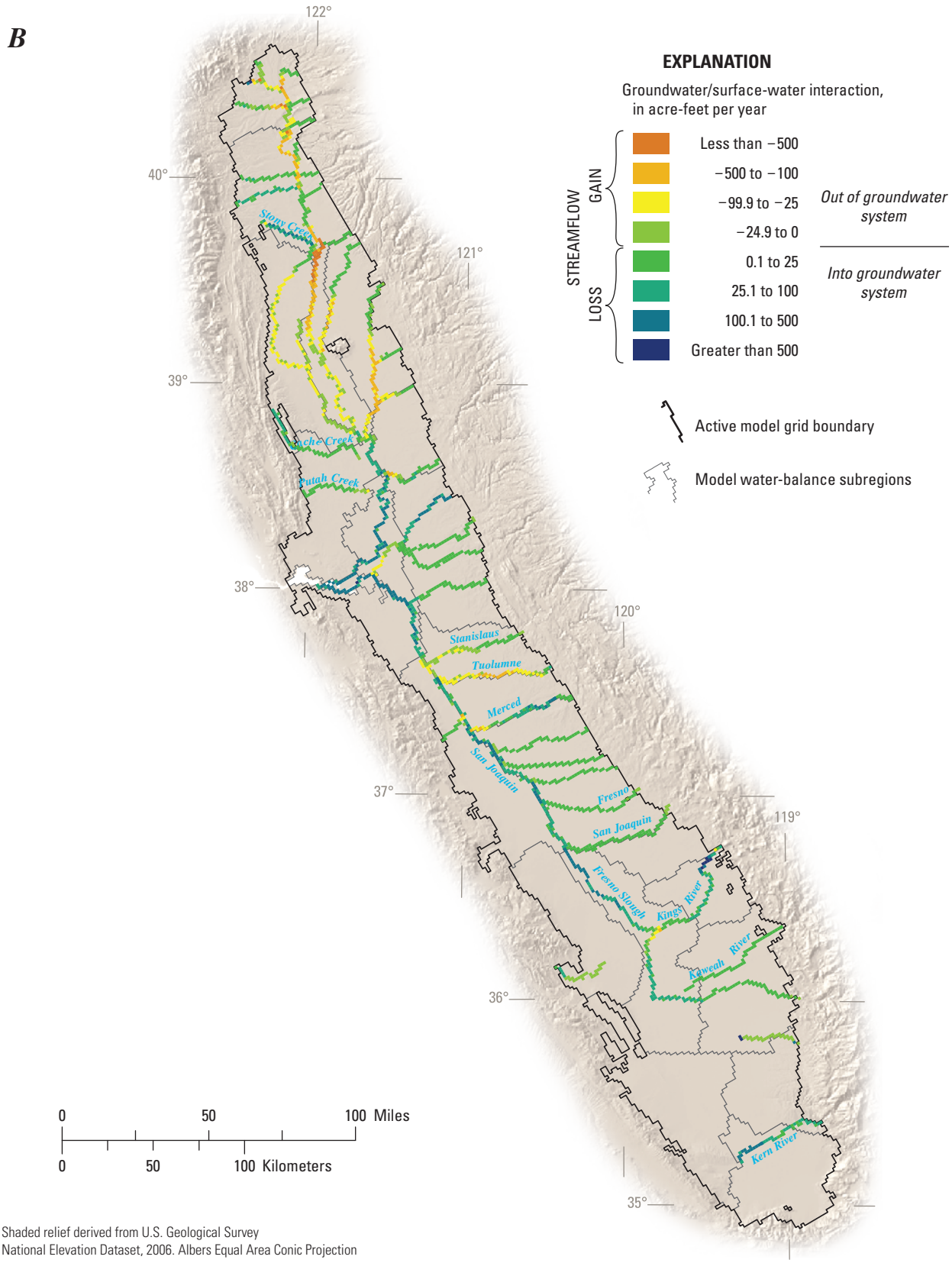

Shaded relief derived from U.S. Geological Survey National Elevation Dataset, 2006. Albers Equal Area Conic Projection

Figure C19. Continued.

Simulated streamflows at various gaging stations throughout the valley were monitored during calibration although, unlike streamflow gains and losses, these streamflow values were not a specific calibration target. The simulated streamflow generally matches measured streamflow, except in some low-flow situations.

Another model calibration constraint was the historical reported streamflow diversions from the 66 simulated diversions in the streamflow-routing network. Although not a specified calibration target used in the parameter estimation, the CVHM satisfies this constraint. This indirectly suggests that the streambed hydraulic conductivities for the stream segments upstream of these diversions allowed sufficient water to be conveyed by the various rivers to the points of diversion in the streamflow network.

The simulated streamflow gains and losses are approximately 1.5–2 times larger than those simulated by the CV-RASA model (Williamson and others, 1989). However, the net volume rate of streamflow gains and losses is a loss of 300,000 acre-ft per year. This net loss rate is of similar magnitude to the net loss rate simulated by the CV-RASA model (*fig. B1*), and represents a small part of the overall groundwater budget. The differences in magnitude of the gains, losses, and overall net rates likely are a result of the more detailed discretization of the shallow part of the aquifer system in the CVHM. The fact that simulated water-level altitudes in the shallow system are too high in places and that the net gain-loss rates compare well suggests that any additional groundwater-flow to streams flows quickly from streams to areas of lower groundwater level altitudes.

Boundary Flow Observations

Although little is known about the actual volume of groundwater discharge through the Delta, it is thought to be negligible, compared to the rest of the water budget (Williamson and others, 1989). The CVHM simulation indicates that less than 1 percent of the water is leaving the groundwater system through the general head boundaries (GHBs).

Flow from small watersheds surrounding the valley is poorly understood and, therefore, is not specified in the CVHM. This is a potential source of model error. In DWR's model (C. Brush, California Department of Water Resources, written commun., February 21, 2007), these small-watershed inflows average about 1 million acre-ft per year and account for less than 5 percent of the influx to the system. Brush (C. Brush, California Department of Water Resources, written commun., February 21, 2007) reports that these inflows are based on values published by Nady and Larragueta (1983). Although small, if these fluxes are correct, they represent a part of the total loss of storage simulated in the CVHM. Because simulated water-level altitudes are particularly low in the southeastern part of the Central Valley and DWR's estimated input to that area is relatively large, incorporating these inflows in the CVHM could improve model fit.

Subsidence Observations

Measured compaction from extensometers in the valley also was used as a calibration target. Subsidence monitoring observations can provide valuable information about hydrologic parameters such as elastic and inelastic skeletal specific storage (Riley, 1969; Hanson, 1988; Leake, 1990; Sneed and Galloway, 2000; Burbey, 2001; Larson and others, 2001; Sneed, 2001; Hoffmann and others, 2003a; Phillips and others, 2003, Pavelko, 2004; Halford and others, 2005). The CVHM was adjusted to fit the range of measured compaction at the extensometer sites utilizing UCODE-2005 and manual calibration. The calibration target was the measured compaction from several extensometers in the region (*figs. C15* and *C20*). Monthly simulation of stresses and associated water-level altitude changes improved the temporal resolution of simulated compaction over that in the CV-RASA model. A good match between simulated and measured compaction at extensometer sites was achieved though delayed drainage (and repressurizing) of aquitards was not simulated. In some areas, more seasonal variability in water-level altitudes is being simulated and, as a result, elastic rebound is overestimated (*fig. C20*). The trend of recovery of the land surface at some extensometers is not seen in the CVHM simulation, indicating some error in simulated water-level altitude or elastic properties and (or) the presence of delayed repressurization of aquitards. The simulated subsidence correlates well with measured climatic changes and surface-water deliveries. For example, the simulated subsidence shows multi-year elastic deformation related to the droughts (1976–77; 1980s) (*fig. C21*). Uplift also is evident in many of the plots (*fig. C21*).

Subsidence simulated by the revised CVHM was compared to estimated-subsidence maps. The simulated subsidence shows a similar spatial pattern of deformation, with respect to the spatial distribution derived from the historical subsidence (*figs. C20* and *C21*). As would be expected, the areal distribution and amount of subsidence generally has increased with time, particularly through the last major drought, 1987–92. The simulated subsidence is much larger than the measured subsidence in some areas, especially near township 24S/range 26E (*fig. C21*). In part, this subsidence likely is caused by the larger simulated water-level altitude declines, as compared to the measured declines, in these areas.

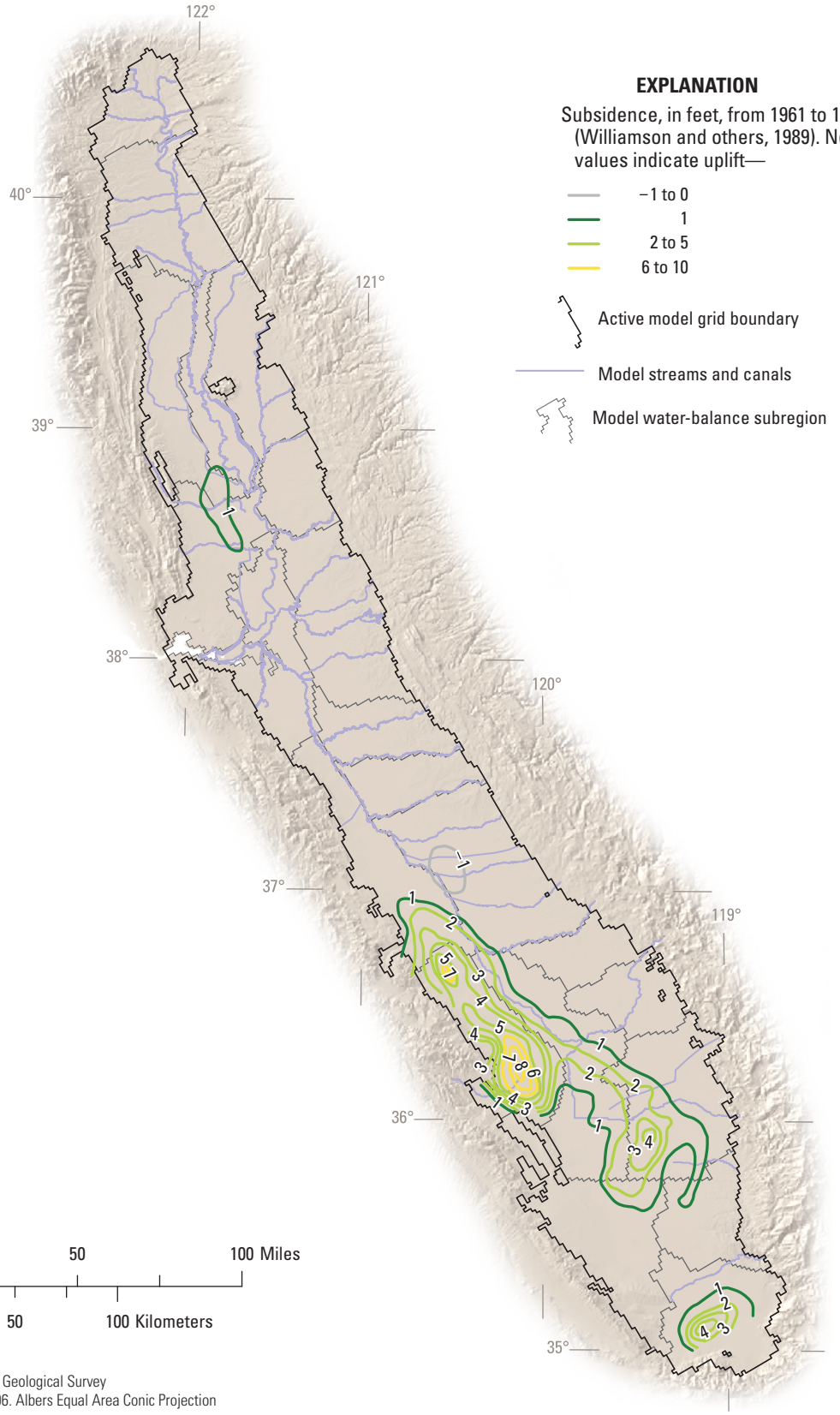

Figure C20. Distribution of historical subsidence, estimated from 1961 to 1977 extensometer data, Central Valley, California (modified from Williamson and others, 1989).

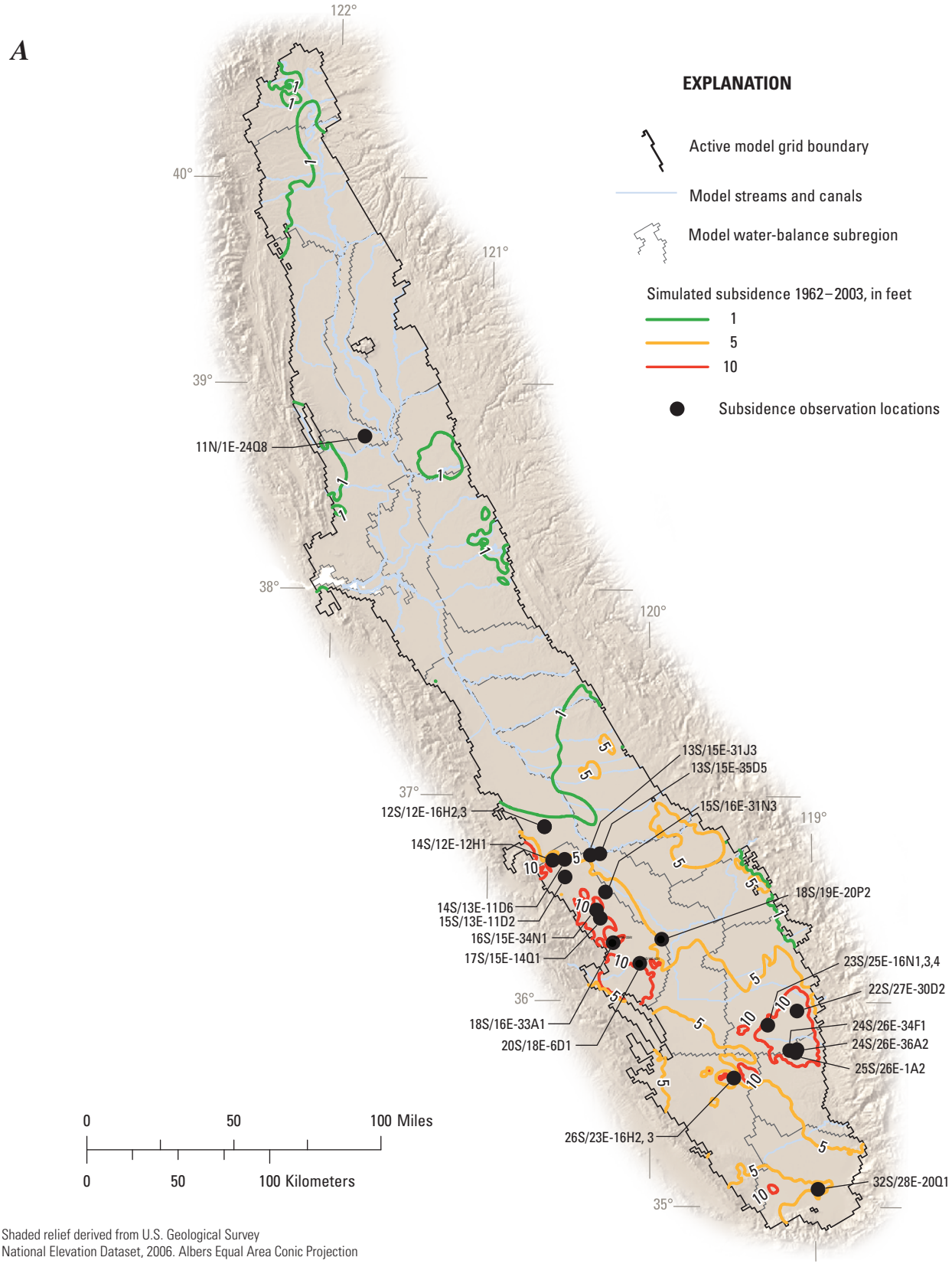

Figure C21. *A*, Distribution of total simulated subsidence for water years 1962 through 2003, and locations of subsidence measurements. *B,* Aggregate compaction measured at, and simulated subsidence for, selected extensometer locations, Central Valley, California.

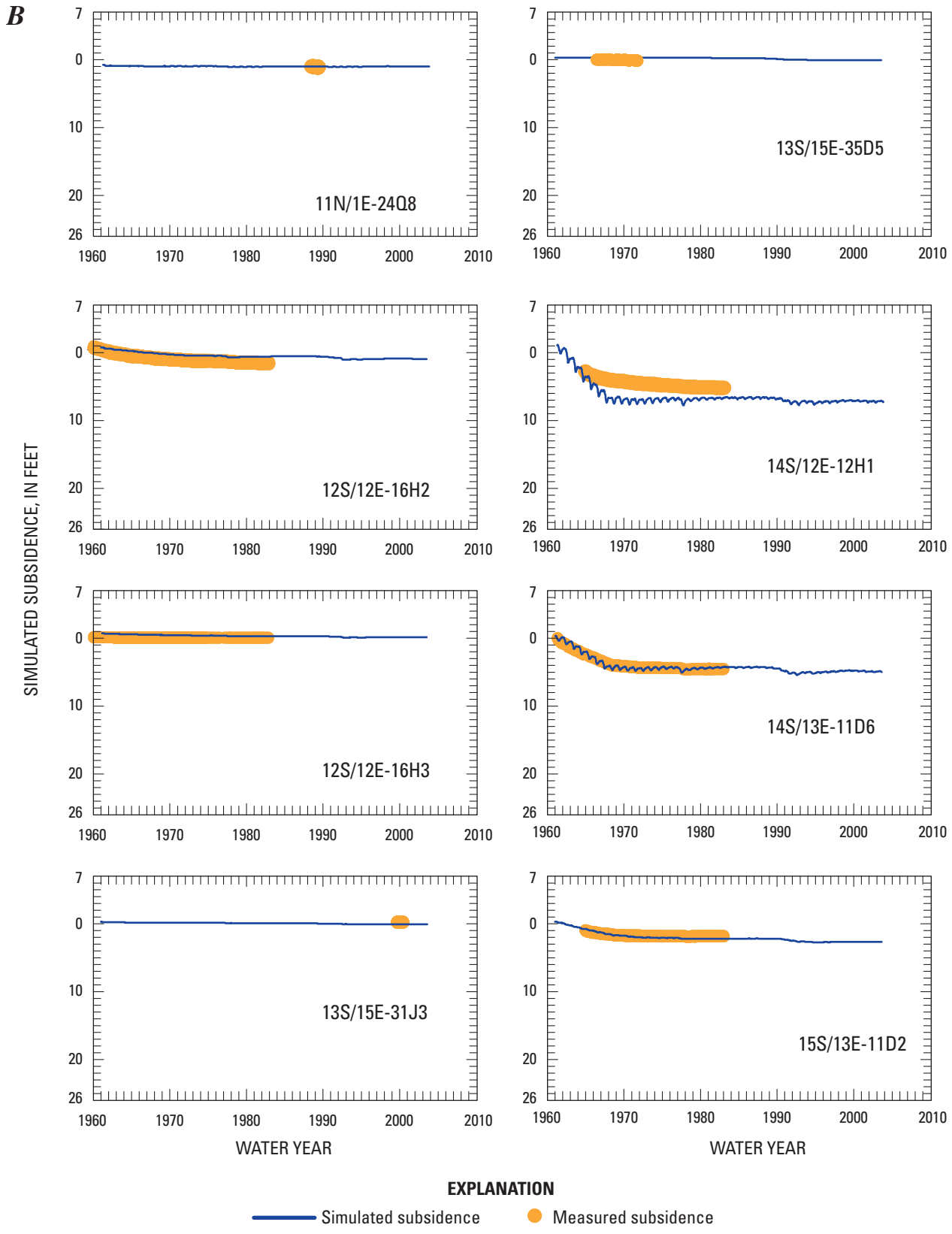

Figure C21. Continued.

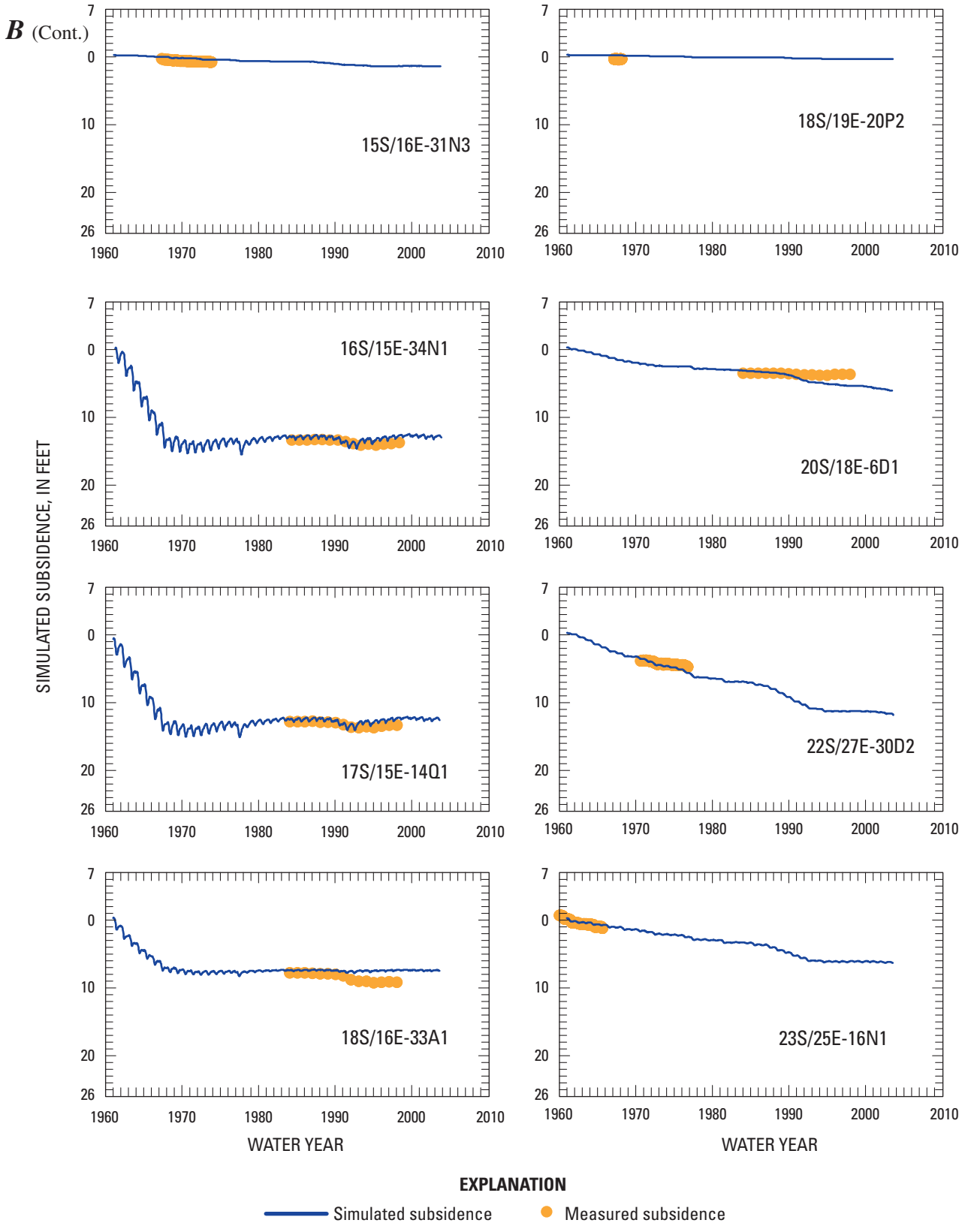

Figure C21. Continued.

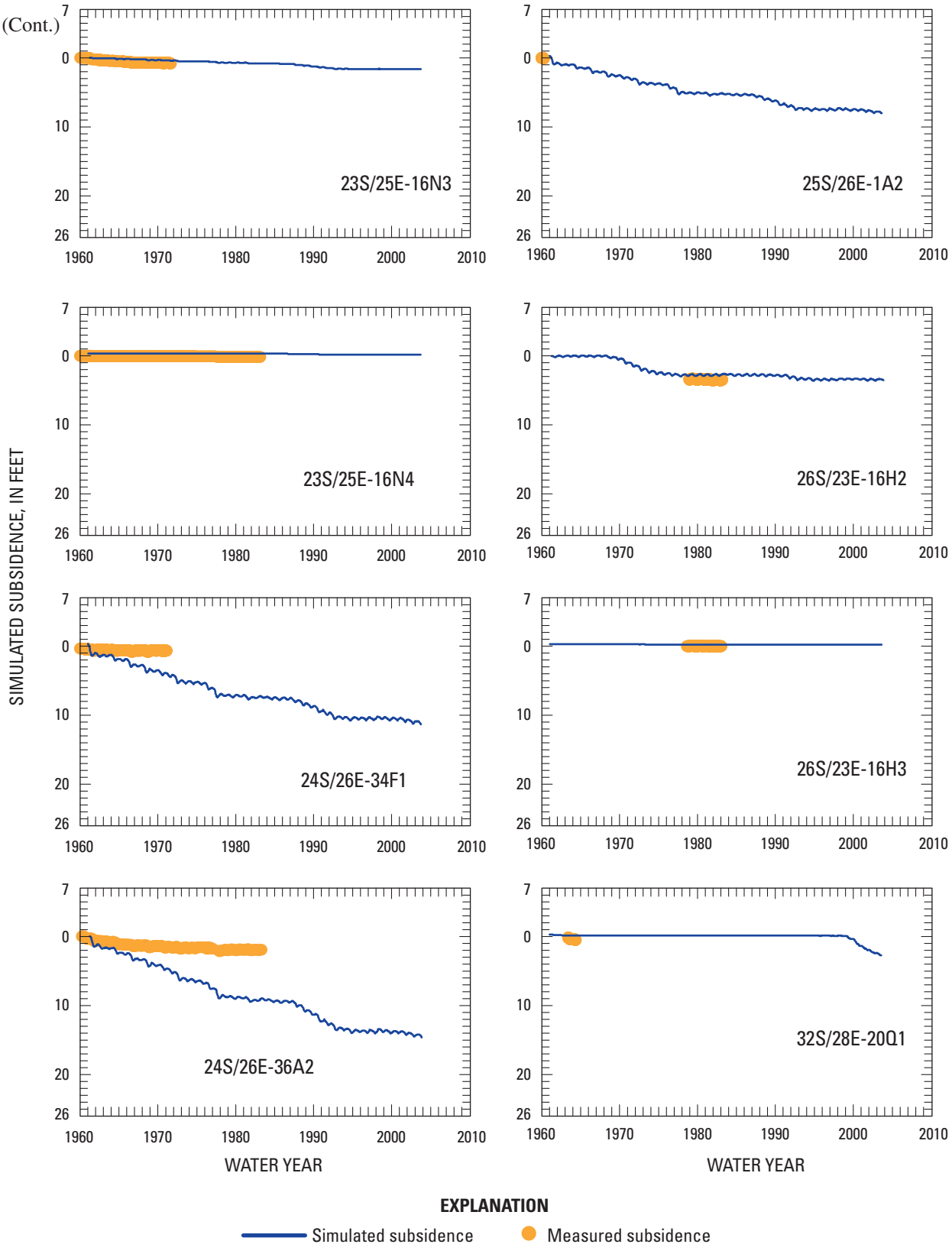

Figure C21. Continued.

When aquifer systems are developed, groundwater released from storage in fine-grained deposits often contributes a significant amount of the water supplied to pumping wells (Konikow and Neuzil, 2007). Because the fine-grained deposits constitute an average 64 percent of the unconsolidated sediments in the Central Valley (*Chapter B*), they likely represent a principal source of groundwater released from storage in the valley. In the original CV-RASA, many of the fine-grained units were simulated on the basis of the percentage of fine-grained deposits in a model cell. The confining units simply were represented by specifying impedance (reduced vertical conductance) between adjacent model layers, that is, without having the capacity to store groundwater. Although the original CV-RASA study did quantify storage losses attributed to compaction, storage changes in these confining units, such as the Corcoran Clay, were not simulated by the CV-RASA model and were not computed as a distinct component of the groundwater budget. The CV-RASA study and previous studies attributed most of the water derived from compaction to that of fine-grained interbeds and not from regional confining beds such as the Corcoran Clay (Ireland and others, 1984; Williamson and others, 1989). Because the fine-grained interbedded deposits and the confining units in the aquifer system are simulated explicitly in the CVHM, a more accurate accounting of the sources of water produced is now available. Simulated compaction in the CVHM corroborates the previous findings; since predevelopment, compared to storage losses from the fine-grained interbeds, a relatively significant volume of water has not yet been released from storage in the Corcoran Clay.

Pumpage Observations

Although not a defined calibration target, where available, agricultural pumpage estimates from power records (Diamond and Williamson, 1983) were compared with agricultural pumpage estimates from the CVHM (*fig. C22*). As mentioned previously, the USGS estimated groundwater pumpage from electric power consumption in the Central Valley prior to 1980. Estimates from these power records were compiled for the original CV-RASA study by township for the period 1961–77. Missing data during this period were computed by means of multiple regression models for each township by Diamond and Williamson (1983). Next, the agricultural groundwater pumpage per township was summed for each WBS. Although these power record estimates are reported to be accurate where they are complete (Diamond and Williamson, 1983), the data are not comprehensive for the Central Valley. Because these power-record based pumpage estimates were not available for the entire Central Valley, the estimates are considered minimum values. For the 1961–77 period, the estimated pumpage was compared to the CVHM simulated pumpage values for the entire Central Valley (*fig. C22*). Comparison of simulated and estimated pumpage for this period shows good general agreement between these values (*fig. C22*). In particular, the trends are matched. The simulation matches closely in drier periods and is simulated at lower rates in wet periods.

For the 1960s and 1970s, the CVHM estimates that an average of approximately 20 million acre-ft of irrigation water was required annually, about one-half from groundwater and one-half from surface-water. These values closely match the proportions and total 21 million acre-ft of annual farm delivery requirement, as reported by Williamson and others (1989).

The development of groundwater involved the construction of about 100,000 irrigation wells, many with long intervals of perforated casing that provide a hydraulic connection between permeable zones within the aquifer system. The vertical leakage of the aquifer system was increased substantially because of the hydraulic connection provided by the wells completed in multiple zones (*fig. C13*) (Page and Balding, 1973; Londquist, 1981; Williamson and others, 1989). This vertical flow through wellbores occurs through both pumped and non-pumped wells. Davis and others (1964) estimated that about 100,000 acre-ft/yr flowed between these zones through wells in the western part of the San Joaquin Valley in the early 1960s. The CVHM suggests that between 1961 and 2003, 400,000 acre-ft/yr flowed into the lower aquifer through well-bore flow (*fig. C13*). This most likely is a low estimate, because, for computational reasons, only urban wells and agricultural wells penetrating both above and below the Corcoran Clay were simulated using MNW. Williamson and others (1989) suggest that more intra-borehole flow may occur through wells in the rest of the Central Valley than intra-borehole flow across the Corcoran Clay. Unfortunately, given its current configuration, the CVHM cannot confirm or contradict this.

Water-Use Observations

As with pumpage estimates, water-use data were not a defined calibration target. Few data exist for water use and most of the factors used in its calculation are indirect measurements, such as temperature or crop coefficient values, or are estimates, such as percentage of runoff. However, as part of the CV-RASA, Williamson (1982) calculated the evapotranspiration of applied water (ETaw) for the Central Valley during 1957–78. *Table C9* lists Williamson's estimated ETaw values, along with CVHM simulated values, for the Central Valley. The simulated values of ETaw (which do not include uptake of groundwater) fall within the range of values estimated by Williamson (1982). Of note, the average ETaw value simulated, in some cases, is less than those estimated by Williamson (1982). This may be the result of changes in crop types, increased irrigation efficiencies, and groundwater uptake simulated in the 1962–2003 time period. The estimated and simulated ETaw generally increase toward the south. Although the area of irrigated agriculture increased (*table C3*), the amount of

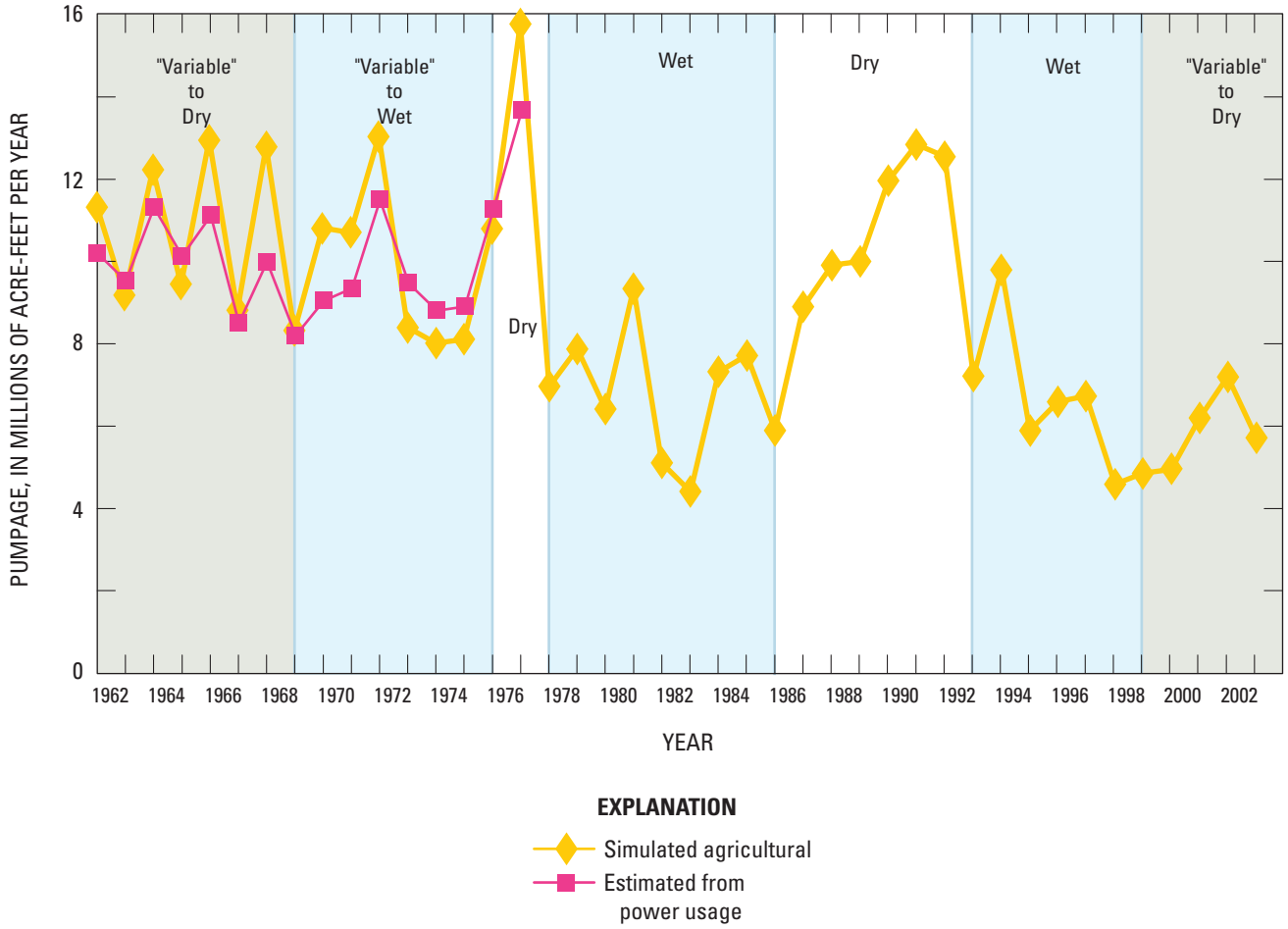

Figure C22. Agricultural pumpage from 1961–77 estimated from power records (Diamond and Williamson, 1983) compared to Central Valley Hydrologic Model simulated agricultural pumpage for the Central Valley, California.

Table C9. Estimated and Central Valley Hydrologic Model-simulated average and unit evapotranspiration of applied water (ETaw) for the Central Valley, California.

[Unit ETaw values in feet; Average ETaw values in millions of acre-feet per year; source of estimates, Williamson (1982)]

Basin	Area (square miles)	Estimated unit (average)			
		ETaw 1957–1961	ETaw 1966-–1973	ETaw 1968–1978	Simulated ETaw average (1962–2003)
Sacramento Valley	5,981	2.4 (2.49)	2.3 (2.84)	1.9 (3.04)	1.8 (2.20)
Delta and Eastside Streams	2,388	2.2 (1.86)	2.1 (1.96)	1.8 (1.91)	1.9 (1.00)
San Joaquin Valley	3,782	2.5 (2.76)	2.0 (2.48)	2.3 (3.16)	2.3 (2.90)
Tulare Basin	7,780	2.1 (4.46)	2.2 (6.390)	2.2 (7.13)	2.3 (8.20)
Central Valley	**19,389**	**2.3 (11.57)**	**2.1 (13.67)**	**2.1 (15.24)**	**2.1(14.30)**

ETaw increased at a smaller rate, most likely the result of using lower water-use crops (Williamson, 1982). In the Tulare Basin, the increase in ETaw is attributed to the delivery of surface water for irrigation by the California Aqueduct, beginning in 1967 (Williamson, 1982).

Water-Delivery Observations

Water-delivery data were not a calibration target, but were used to refine the CVHM. In some areas and in many years, particularly in wetter years, available surface-water deliveries exceeded the used surface-water deliveries. This was particularly evident on the west side of the San Joaquin Valley (WBS 14) (*fig. C23A*). During these years, a significant part of the unused available deliveries occurred during the winter months (*fig. C23B*). These winter-month deliveries are used partly for double cropping and partly for on-farm storage and pre-wetting of fields. Double cropping was estimated by adjusting the crop-coefficients to have a second peak during the winter (*fig. C25*).

On-farm storage of surplus water deliveries and its delayed release is not simulated currently in the FMP. This modification will require adding 'farm-water storage' to the farm mass balance (Schmid and others, 2006a). Because these values are important on the heavily irrigated Central Valley's west side (WBS 14), a method was developed for simulating the use of some of these deliveries for storing and pre-wetting the soils. In general, truck crops and cotton are grown in this area; therefore, the crop-coefficients were adjusted for both cotton and truck crops. In order to preserve mass balance of water usage, the adjustment was made keeping the average total ET constant for WBS 14. For example, a percentage of the total ET was taken from the initial summer growing months (April through July). This volume of water then was added equally to December through February by adjusting the crop coefficient values for each month (*fig. C25*). Based on the best match with deliveries, it was estimated that for WBS 14, about 20 percent of the volume of ET was used for on-farm storage and pre-wetting of soils.

Model Parameters

Following Hill and Tiedeman (2007), the term "parameter" is used to define model inputs. Because the CVHM includes many complex processes that require that parameters be distributed widely in space and time, the potential number of model parameters that could be estimated is large and computationally prohibitive. Therefore, model parameterization and the approach to parameter estimation were designed to estimate a limited number of parameter values that sufficiently define the simulated processes. The parameter values were adjusted by a combination of best guesses and a systematic application of the parameter estimation method to narrow the range of possible solutions to produce simulated values that best matched the measured observations. Many of the parameters were defined beforehand, and about 50 parameters were estimated during the automated calibration process, with less than ten estimated at any one time. These parameters included hydraulic properties of the aquifer system, streambed hydraulic conductivities, and parameters related to the FMP (*table C10*). Additional parameters could be estimated and others could be added, as needed. However, longer model execution times pose a practical limit on the number of estimated parameters.

Initial input parameters were adjusted within ranges of reasonable values to best fit hydrologic conditions measured in the aquifer system, including measured water-level altitudes and associated long-term trends, estimated streamflow losses, and subsidence. Because the CVHM utilized the SFR1 package and FMP process, MF2K could not be used directly for sensitivity analyses and parameter estimation. A separate code for sensitivity analyses, such as UCODE or PEST must be used. A combination of UCODE-2005 (Poeter and others, 2005) and manual adjustments were used to conduct the parameter estimation and sensitivity analyses.

As described in the "Hydraulic Properties" section of this report, K_h and K_v were estimated for every cell in the CVHM on the basis of sediment texture, end-member hydraulic conductivity values (K_c and K_f), and averaging method (weighted arithmetic average for K_h; power mean for K_v). These end-member hydraulic conductivity values were adjusted by UCODE-2005 to minimize model error. During initial calibration efforts, the same end-member hydraulic conductivities and averaging-method parameter (the p value used in the power mean) were used for the entire Central Valley. As calibration progressed, it became evident that more hydraulic parameters would be necessary to represent the system with sufficient accuracy. A K_c and K_f were defined separately for each of the Sacramento and San Joaquin Valleys because of the somewhat different depositional environments in the two valleys (*Chapter A*). In addition, a separate power mean was used for these two areas. A relatively larger value of the power mean (p = –0.5 versus –0.8) was estimated in the Sacramento Valley to represent the less layered nature of the aquifer system there (*fig. C14*). The estimated end-member hydraulic conductivities for the Sacramento and San Joaquin Valleys were similar and the Kv differed according to the power mean (*table C10*).

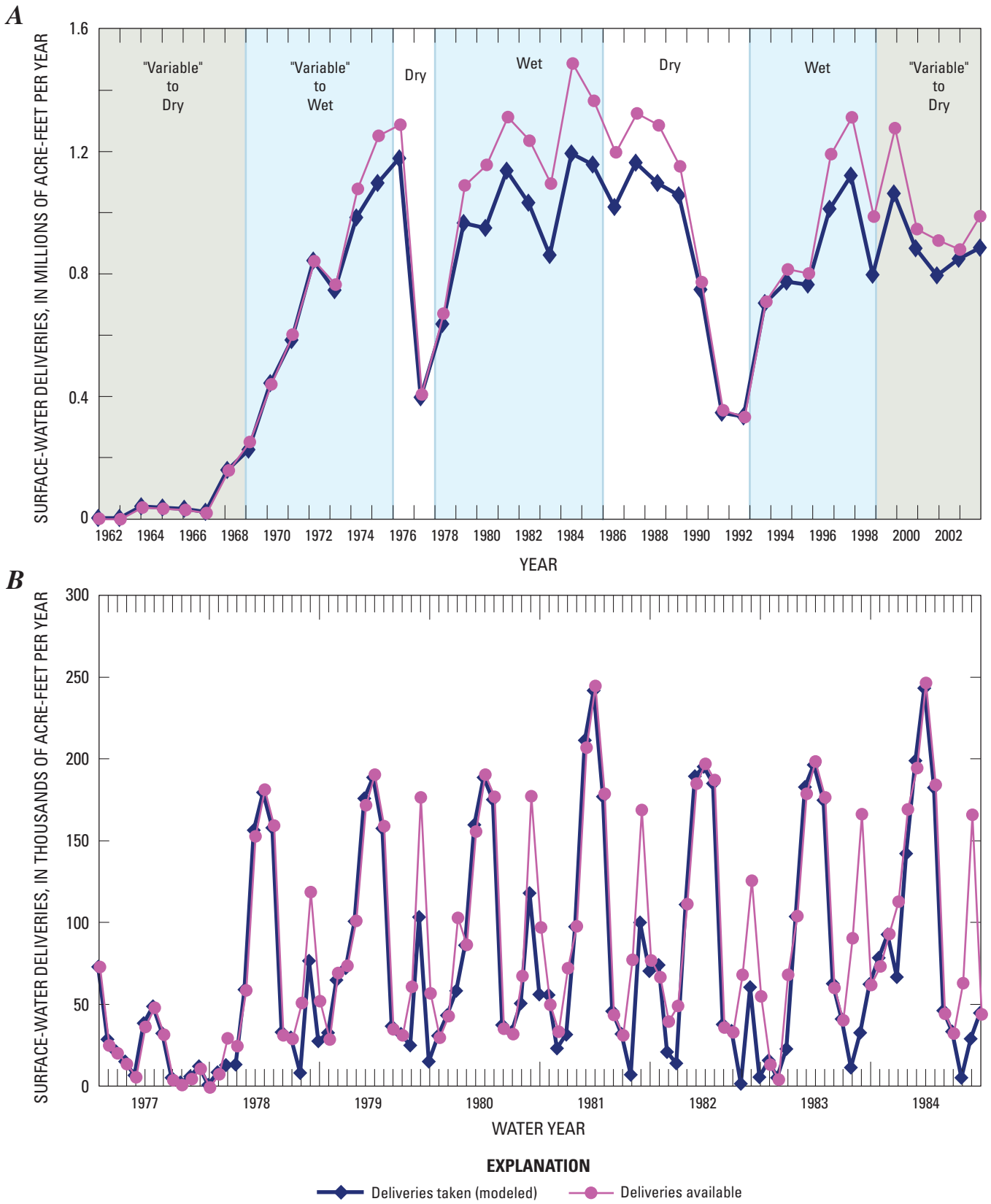

Figure C23. *A,* Annual water deliveries. *B,* monthly water deliveries from the mid 1970s to mid 1980s for water-balance subregion 14.

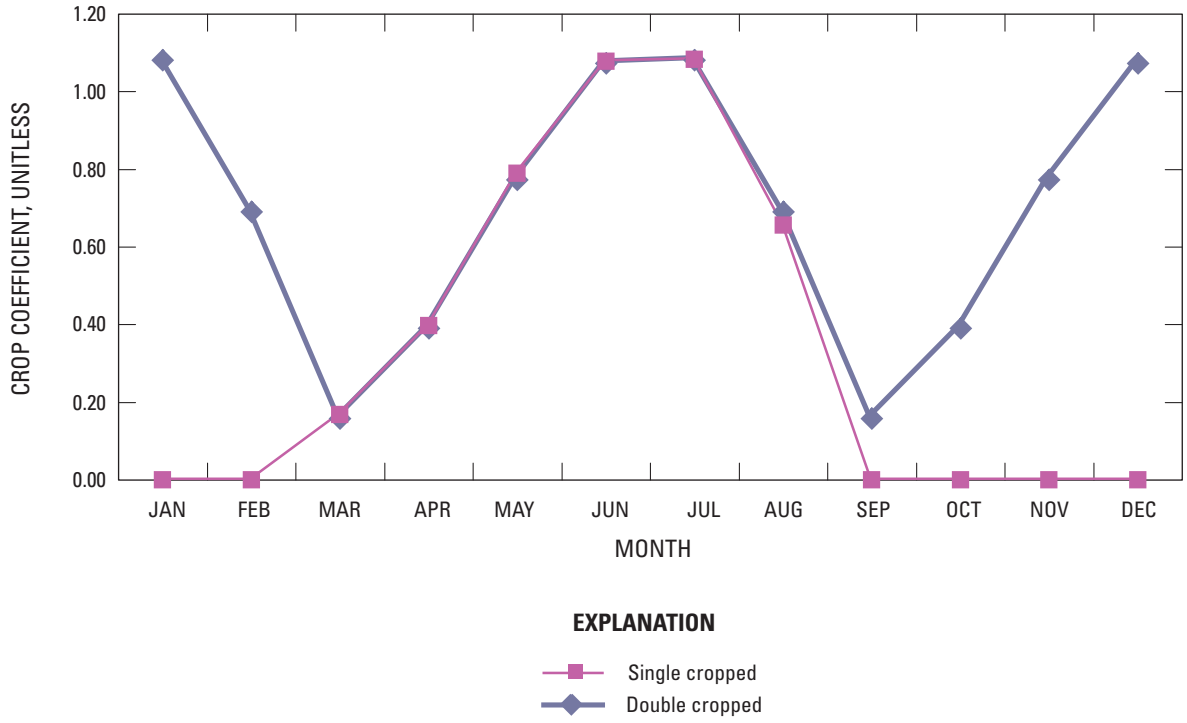

Figure C24. Single and double cropped crop coefficient values for truck crops.

As calibration continued, it became evident that too much flow was occurring through the lower parts of the aquifer system. Because the texture model does not incorporate depth decay of horizontal and vertical hydraulic conductivity, a set of multipliers were included in the CVHM to represent these changes. Initially, the exponential rate of decline of hydraulic conductivity estimated for alluvial units in Death Valley was used to decrease the hydraulic conductivity values. Although the multipliers varied slightly by location and for horizontal and vertical *K*, the values generally are 1.0 for the upper three model layers and 0.5, 0.37, 0.24, 0.15, and 0.08 for layers 6–10, respectively. Adjustments to this rate of decline were made by estimating multipliers on the hydraulic conductivity with depth during calibration (*table C10*).

The streambed hydraulic conductivity parameters also were estimated. Seven streambed hydraulic conductivity zones were identified (*fig. C26* and *table C10*) and low streambed hydraulic conductivities were used as initial estimates and adjusted during calibration (*table C10*). The GAGE package was used to calculate flow at upstream and downstream gage points (*fig. C26*). Yearly streamflow losses between gage points were used to estimate streambed hydraulic conductivities that reproduced the average annual streamflow losses for 1961–77. Streamflow depths were not calibrated and were specified at 3 ft.

A multiplier on the range of specific-yield values was adjusted during calibration. This value was modified to scale the range in specific yield and minimize the error for all observations. Parameters representing both the elastic and inelastic storage properties also were estimated. Adjustments to the elastic and inelastic storage properties allowed for better matches to subsidence data. The skeletal inelastic specific storage was estimated directly (*table C10*). A multiplier on the elastic specific storage for both the coarse and fine-grained end members also was estimated (*table C10*). Trends in subsidence that are inaccurately simulated indicate some error in the simulated water-level altitude, the elastic properties, or both. Elastic specific storage appears to be the most difficult parameter to estimate accurately.

In order to match water-level altitudes in the western San Joaquin Valley, wells penetrating the Corcoran Clay and perforated above and below the clay were simulated as multinode wells. During calibration, the skin factor in the MNW package was found to affect the interlayer flow and related water-level altitude difference between layers. This value was adjusted manually to best match observed water-level altitudes. The skin factor representing resistance to flow between the wellbore and the aquifer system was decreased both above and below the Corcoran Clay, but more so below the Corcoran Clay.

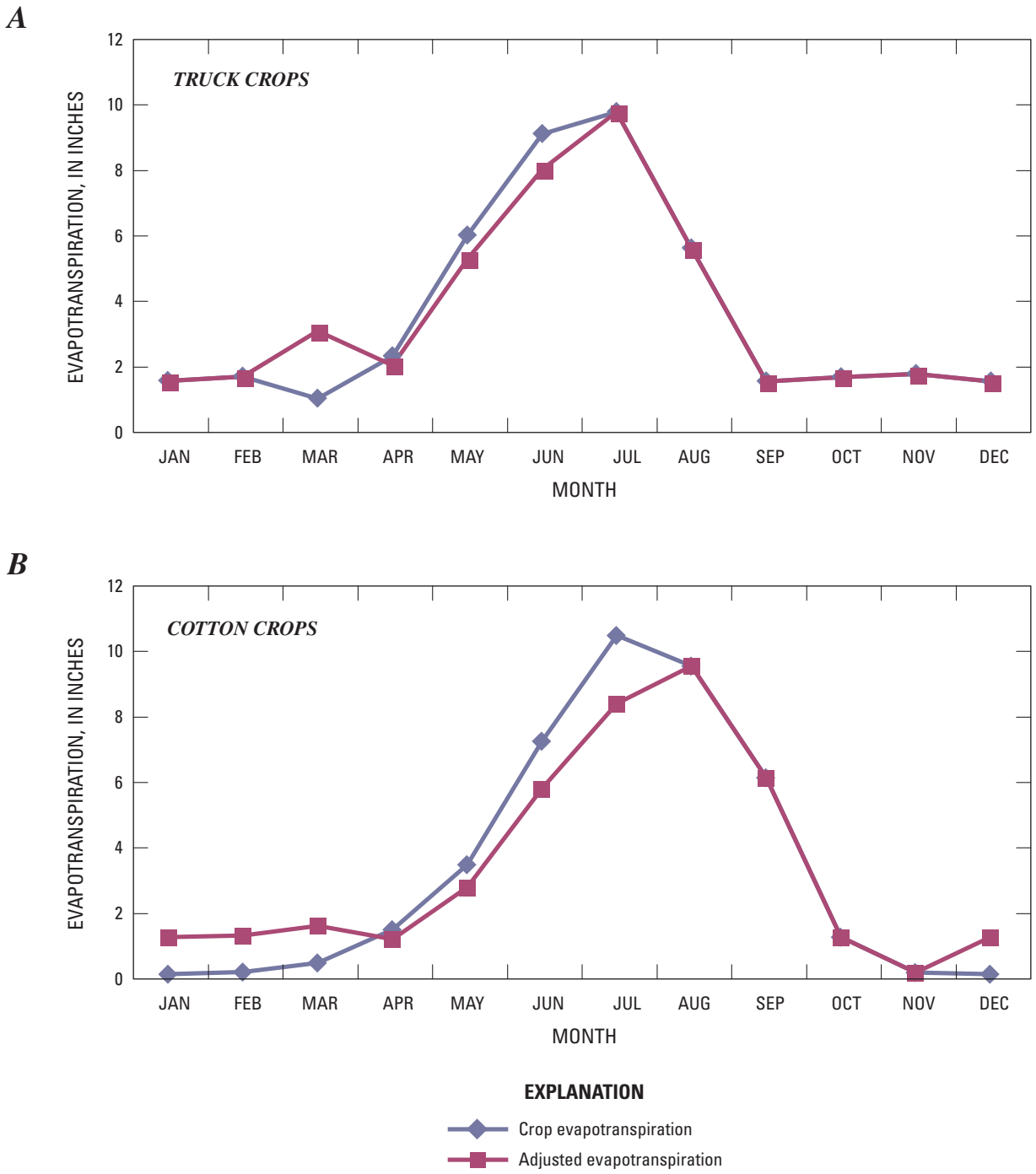

Figure C25. Original and adjusted crop coefficient values for truck and cotton crops.

Table C10. Parameter values estimated for the Central Valley Hydrologic Model.

[WBS, water-balance subregion]

Parameter name	Parameter description	Value	Units	Estimated using automated methods	Composite scaled sensitivity	Parameter group
		Land-use Properties				
NAT_ROOT	Rooting depth of natural vegetation	10.55	feet	yes	1.37	Farm Process properties
KC_S	Multiplier for crop coefficients in summer growing season (April–September)	0.98	multiplier	yes	1.18×10^{2}	Farm Process properties
KC_W	Multiplier for crop coefficients in winter dormant season (October–March)	1.18	multiplier	yes	2.20×10^{1}	Farm Process properties
		Runoff				
H2O_PRO	Percent runoff from precipitation for water land-use class	5.00	percentage	yes	1.67×10^{10}	Farm Process properties
URB_PRO	Percent runoff from precipitation for urban land-use class	1.50	percentage	yes	1.23	Farm Process properties
NAT_PRO	Percent runoff from precipitation for natural vegetation land-use class	20.71	percentage	yes	3.76	Farm Process properties
PRECIP_RO	Percent runoff from precipitation for various land-use classes	10.25	percentage	yes	1.41	Farm Process properties
IDL_PRO	Percent runoff from precipitation for idle land-use class	6.04	percentage	yes	1.38	Farm Process properties
VIN_PRO	Percent runoff from precipitation for vineyards land-use class	1.30	percentage	yes	3.64	Farm Process properties
SEM_PRO	Percent runoff from precipitation for semi-agriculture land-use class	32.29	percentage	yes	6.67×10^{9}	Farm Process properties
DEC_PRO	Percent runoff from precipitation for deciduous land-use class	10.67	percentage	yes	1.34	Farm Process properties
RIC_PRO	Percent runoff from precipitation for rice land-use class	10.62	percentage	yes	3.52	Farm Process properties
CIT_IRO	Percent runoff from irrigation for citrus land-use class	1.00	percentage	yes	1.23	Farm Process properties
PAS_IRO	Percent runoff from irrigation for pasture land-use class	1.72	percentage	yes	2.67×10^{11}	Farm Process properties
ROW_IRO	Percent runoff from irrigation for row crop land-use class	6.08	percentage	yes	1.01	Farm Process properties
SGR_IRO	Percent runoff from irrigation for grains and small grain land-use class	4.46	percentage	yes	1.23	Farm Process properties
TRK_IRO	Percent runoff from irrigation for truck crop land-use class	10.00	percentage	yes	1.40	Farm Process properties
FLD_IRO	Percent runoff from irrigation for field crops land-use class	7.72	percentage	yes	1.24	Farm Process properties
VIN_IRO	Percent runoff from irrigation for vineyards land-use class	1.20	percentage	yes	1.40	Farm Process properties
DEC_IRO	Percent runoff from irrigation for deciduous land-use class	4.82	percentage	yes	3.66	Farm Process properties
RIC_IRO	Percent runoff from irrigation for rice land-use class	3.00	percentage	yes	1.00×10^{10}	Farm Process properties
COT_IRO	Percent runoff from irrigation for cotton land-use class	10.16	percentage	yes	2.00×10^{10}	Farm Process properties
UDE_IRO	Percent runoff from irrigation for other land-use class	7.76	percentage	yes	1.28	Farm Process properties

Table C10. Parameter values estimated for the Central Valley Hydrologic Model.—Continued

[WBS, water-balance subregion]

Parameter name	Parameter description	Value	Units	Estimated using automated methods	Composite scaled sensitivity	Parameter group
		Soil Properties				
CAPFR_SICL	Length of capillary fringe for silty-clay	9.08	feet	yes	3.51	Farm Process properties
CAPFR_SILT	Length of capillary fringe for silt	7.10	feet	yes	1.12	Farm Process properties
CAPFR_SALO	Length of capillary fringe for sandy-loam	9.32	feet	yes	3.81	Farm Process properties
		Irrigation efficiency				
EFF_MLT1	Multiplier on irrigation efficiency for April 1961 through September 1964	0.971	multiplier	yes	2.47×10^{1}	Farm Process properties
EFF_MLT2	Multiplier on irrigation efficiency for October 1964 through September 1977	0.991	multiplier	yes	1.53×10^{10}	Farm Process properties
EFF_MLT3	Multiplier on irrigation efficiency for October 1977 through March 1978	1.030	multiplier	no	6.75×10^{1}	Farm Process properties
EFF_MLT4	Multiplier on irrigation efficiency for April 1978 through March 1980	1.040	multiplier	no	2.46	Farm Process properties
EFF_MLT5	Multiplier on irrigation efficiency for April 1980 through March 1982	1.050	multiplier	no	2.42	Farm Process properties
EFF_MLT6	Multiplier on irrigation efficiency for April 1982 through March 1984	1.060	multiplier	no	1.86	Farm Process properties
EFF_MLT7	Multiplier on irrigation efficiency for April 1984 through March 1990	1.065	multiplier	no	3.06	Farm Process properties
EFF_MLT8	Multiplier on irrigation efficiency for April 1990 through March 1996	1.070	multiplier	no	6.66	Farm Process properties
EFF_MLT9	Multiplier on irrigation efficiency for April 1996 through September 2003	1.074	multiplier	yes	1.32×10^{1}	Farm Process properties
EFF_75G	Irrigation efficiency for generally less known regions and months	60.30	percentage	yes	4.51	Farm Process properties
EFF_RICE	Irrigation efficiency for rice	80.00	percentage	yes	1.21	Farm Process properties
		Hydraulic Conductivity				
KC	Hydraulic conductivity of coarse-grained deposits in San Joaquin Valley and Tulare Basin	672.93	feet/day	yes	4.09×10^{11}	Hydraulic conductivity
KF	Hydraulic conductivity of fine-grained deposits in San Joaquin Valley and Tulare Basin	0.24	feet/day	yes	1.26×10^{1}	Hydraulic conductivity
KC_SAC	Hydraulic conductivity of coarse-grained deposits in Sacramento Valley	4921.50	feet/day	yes	2.71	Hydraulic conductivity
KF_SAC	Hydraulic conductivity of fine-grained deposits in Sacramento Valley	0.08	feet/day	yes	4.42	Hydraulic conductivity
HK_BEDRX	Horizontal hydraulic conductivity of Bedrock	1.57	feet/day	yes	4.17×10^{7}	Hydraulic conductivity
HK_SJ	Horizontal hydraulic conductivity of San Joaquin Formation	0.17	feet/day	yes	1.33	Hydraulic conductivity multipliers
HK_QPC	Horizontal hydraulic conductivity of the dissected uplands	0.68	feet/day	yes	1.40×10^{1}	Hydraulic conductivity
VK_BEDRX	Vertical hydraulic conductivity of bedrock	1.57	feet/day	yes	1.26	Hydraulic conductivity multipliers

Table C10. Parameter values estimated for the Central Valley Hydrologic Model.—Continued

[WBS, water-balance subregion]

Parameter name	Parameter description	Value	Units	Estimated using automated methods	Composite scaled sensitivity	Parameter group
VK_SJ	Vertical hydraulic conductivity of San Joaquin Formation	0.17	feet/day	yes	2.64	Hydraulic conductivity multipliers
VK_QPC	Vertical hydraulic conductivity of the dissected uplands	0.68	feet/day	yes	1.93	Hydraulic conductivity multipliers
	Multiplier on hydraulic properties of Corcoran Clay					
HK_CC_MULT	Multiplier on horizontal hydraulic conductivity of Corcoran Clay	0.010	multiplier	yes	1.35	Hydraulic conductivity multipliers
VK_CC_MULT	Multiplier on vertical hydraulic conductivity of Corcoran Clay	0.002	multiplier	yes	7.45	Hydraulic conductivity multipliers
	Horizontal Conductivity Depth Decay					
HK_UN_VF	Multiplier for layers 1–3 Sacramento Valley	1.000	multiplier	no	2.35	Hydraulic conductivity multipliers
HK_US_VF	Multiplier for layers 1–3 San Joaquin Valley	1.000	multiplier	no	1.83×10^{11}	Hydraulic conductivity multipliers
HK_UWS_VF	Multiplier for layers 1–3 Western San Joaquin Valley (WBS 10 and 14)	0.181	multiplier	yes	2.08×10^{10}	Hydraulic conductivity multipliers
HK_LN6_VF	Multiplier for layer 6 Sacramento Valley	0.914	multiplier	yes	1.46	Hydraulic conductivity multipliers
HK_LS6_VF	Multiplier for layer 6 San Joaquin Valley	0.614	multiplier	yes	3.84×10^{11}	Hydraulic conductivity multipliers
HK_WS6_VF	Multiplier for layer 6 Western San Joaquin Valley (WBS 10 and 14)	0.100	multiplier	no	9.59	Hydraulic conductivity multipliers
HK_LN7_VF	Multiplier for layer 7 Sacramento Valley	0.370	multiplier	no	4.19×10^{1}	Hydraulic conductivity multipliers
HK_LS7_VF	Multiplier for layer 7 San Joaquin Valley	0.240	multiplier	no	1.00×10^{11}	Hydraulic conductivity multipliers
HK_WS7_VF	Multiplier for layer 7 Western San Joaquin Valley (WBS 10 and 14)	0.075	multiplier	no	8.59	Hydraulic conductivity multipliers
HK_LN8_VF	Multiplier for layer 8 Sacramento Valley	0.240	multiplier	no	4.17×10^{1}	Hydraulic conductivity multipliers
HK_LS8_VF	Multiplier for layer 8 San Joaquin Valley	0.180	multiplier	no	4.17×10^{10}	Hydraulic conductivity multipliers
HK_WS8_VF	Multiplier for layer 8 Western San Joaquin Valley (WBS 10 and 14)	0.060	multiplier	no	4.36	Hydraulic conductivity multipliers
HK_LN9_VF	Multiplier for layer 9 Sacramento Valley	0.150	multiplier	no	1.52	Hydraulic conductivity multipliers
HK_LS9_VF	Multiplier for layer 9 San Joaquin Valley	0.040	multiplier	no	1.84	Hydraulic conductivity multipliers
HK_WS9_VF	Multiplier for layer 9 Western San Joaquin Valley (WBS 10 and 14)	0.040	multiplier	no	3.14	Hydraulic conductivity multipliers
HK_LN10_VF	Multiplier for layer 10 Sacramento Valley	0.080	multiplier	no	1.00×10^{11}	Hydraulic conductivity multipliers
HK_LS10_VF	Multiplier for layer 10 San Joaquin Valley	0.020	multiplier	no	1.73	Hydraulic conductivity multipliers
HK_WS10_VF	Multiplier for layer 10 Western San Joaquin Valley (WBS 10 and 14)	0.020	multiplier	no	1.42×10^{11}	Hydraulic conductivity multipliers

Table C10. Parameter values estimated for the Central Valley Hydrologic Model.—Continued

[WBS, water-balance subregion]

Parameter name	Parameter description	Value	Units	Estimated using automated methods	Composite scaled sensitivity	Parameter group
Vertical Conductivity Depth Decay						
VK_UN_VF	Multiplier for layers 1–3 Sacramento Valley	1.000	multiplier	no	1.61	Hydraulic conductivity multipliers
VK_US_VF	Multiplier for layers 1–3 San Joaquin Valley	1.000	multiplier	no	5.94	Hydraulic conductivity multipliers
VK_UWS_VF	Multiplier for layers 1–3 Western San Joaquin Valley (WBS 10 and 14)	0.180	multiplier	no	2.18	Hydraulic conductivity multipliers
VK_LN6_VF	Multiplier for layer 6 Sacramento Valley	0.663	multiplier	yes	1.67	Hydraulic conductivity multipliers
VK_LS6_VF	Multiplier for layer 6 San Joaquin Valley	0.463	multiplier	yes	5.34	Hydraulic conductivity multipliers
VK_WS6_VF	Multiplier for layer 6 Western San Joaquin Valley (WBS 10 and 14)	0.150	multiplier	no	1.61	Hydraulic conductivity multipliers
VK_LN7_VF	Multiplier for layer 7 Sacramento Valley	0.370	multiplier	no	1.40	Hydraulic conductivity multipliers
VK_LS7_VF	Multiplier for layer 7 San Joaquin Valley	0.200	multiplier	no	2.14	Hydraulic conductivity multipliers
VK_WS7_VF	Multiplier for layer 7 Western San Joaquin Valley (WBS 10 and 14)	0.100	multiplier	no	1.53	Hydraulic conductivity multipliers
VK_LN8_VF	Multiplier for layer 8 Sacramento Valley	0.240	multiplier	no	1.62	Hydraulic conductivity multipliers
VK_LS8_VF	Multiplier for layer 8 San Joaquin Valley	0.150	multiplier	no	1.78	Hydraulic conductivity multipliers
VK_WS8_VF	Multiplier for layer 8 Western San Joaquin Valley (WBS 10 and 14)	0.060	multiplier	no	1.66	Hydraulic conductivity multipliers
VK_LN9_VF	Multiplier for layer 9 Sacramento Valley	0.150	multiplier	no	1.94	Hydraulic conductivity multipliers
VK_LS9_VF	Multiplier for layer 9 San Joaquin Valley	0.040	multiplier	no	4.17×10^{10}	Hydraulic conductivity multipliers
VK_WS9_VF	Multiplier for layer 9 Western San Joaquin Valley (WBS 10 and 14)	0.040	multiplier	no	1.51	Hydraulic conductivity multipliers
VK_LN10_VF	Multiplier for layer 10 Sacramento Valley	0.080	multiplier	no	4.00×10^{11}	Hydraulic conductivity multipliers
VK_LS10_VF	Multiplier for layer 10 San Joaquin Valley	0.020	multiplier	no	2.52	Hydraulic conductivity multipliers
VK_WS10_VF	Multiplier for layer 10 Western San Joaquin Valley (WBS 10 and 14)	0.020	multiplier	no	1.25×10^{10}	Hydraulic conductivity multipliers

Table C10. Parameter values estimated for the Central Valley Hydrologic Model.—Continued

[WBS, water-balance subregion]

Parameter name	Parameter description	Value	Units	Estimated using automated methods	Composite scaled sensitivity	Parameter group
		Conductance				
DELTA	Conductance of Delta Sediments	3281.00	feet/day	no	1.36	Delta
		Stream Bed Hydraulic Conductivity				
K_SACRIV	Hydraulic conductivity of the stream bed of the northern Sacramento River	0.04	feet/day	yes	1.70	Streambed hydraulic conductivity
K_SACRIV	Hydraulic conductivity of the stream bed of the Sacramento River	0.16	feet/day	yes	1.10×10^{11}	Streambed hydraulic conductivity
K_SJRIV	Hydraulic conductivity of the stream bed of the San Joaquin River	0.48	feet/day	yes	4.58	Streambed hydraulic conductivity
K_SO_RIV	Hydraulic conductivity of the stream bed of the river channel in trough of valley south of San Joaquin River	2.71	feet/day	yes	1.49	Streambed hydraulic conductivity
K_TRIB_NE	Hydraulic conductivity of the stream bed of the Sacramento Valley tributaries east of Sacramento River	0.33	feet/day	yes	1.21	Streambed hydraulic conductivity
K_TRIB_NW	Hydraulic conductivity of the stream bed of the Sacramento Valley tributaries west of Sacramento River	5.64	feet/day	yes	2.37×10^{11}	Streambed hydraulic conductivity
K_TRIB_SE	Hydraulic conductivity of the stream bed of the San Joaquin Valley and Tulare Basin Tributaries east of valley trough	3.31	feet/day	yes	1.33×10^{10}	Streambed hydraulic conductivity
K_TRIB_SW	Hydraulic conductivity of the stream bed of the San Joaquin Valley and Tulare Basin tributaries west of valley trough	0.19	feet/day	yes	1.40	Streambed hydraulic conductivity
		Storage Properties				
SY_MULT	Multiplier on specific yield values based on percentage of coarse-grained deposits	1.33	multiplier	yes	5.93	Storage properties
PHI_C	Porosity of the coarse-grained deposits	25.00	percentage	no	1.26	Storage properties
PHI_F	Porosity of the fine-grained deposits	50.00	percentage	no	2.37×10^{11}	Storage properties
SS_QPC_MULT	Multiplier on storage values of the dissected uplands	1.00	multiplier	yes	3.33×10^{9}	Storage properties
SUB_E	Multiplier on elastic storage coefficients	1.00	multiplier	yes	5.73	Storage properties
SUB_I	Inelastic storage coefficient	1.37E-04	per foot	yes	6.67×10^{9}	Storage properties

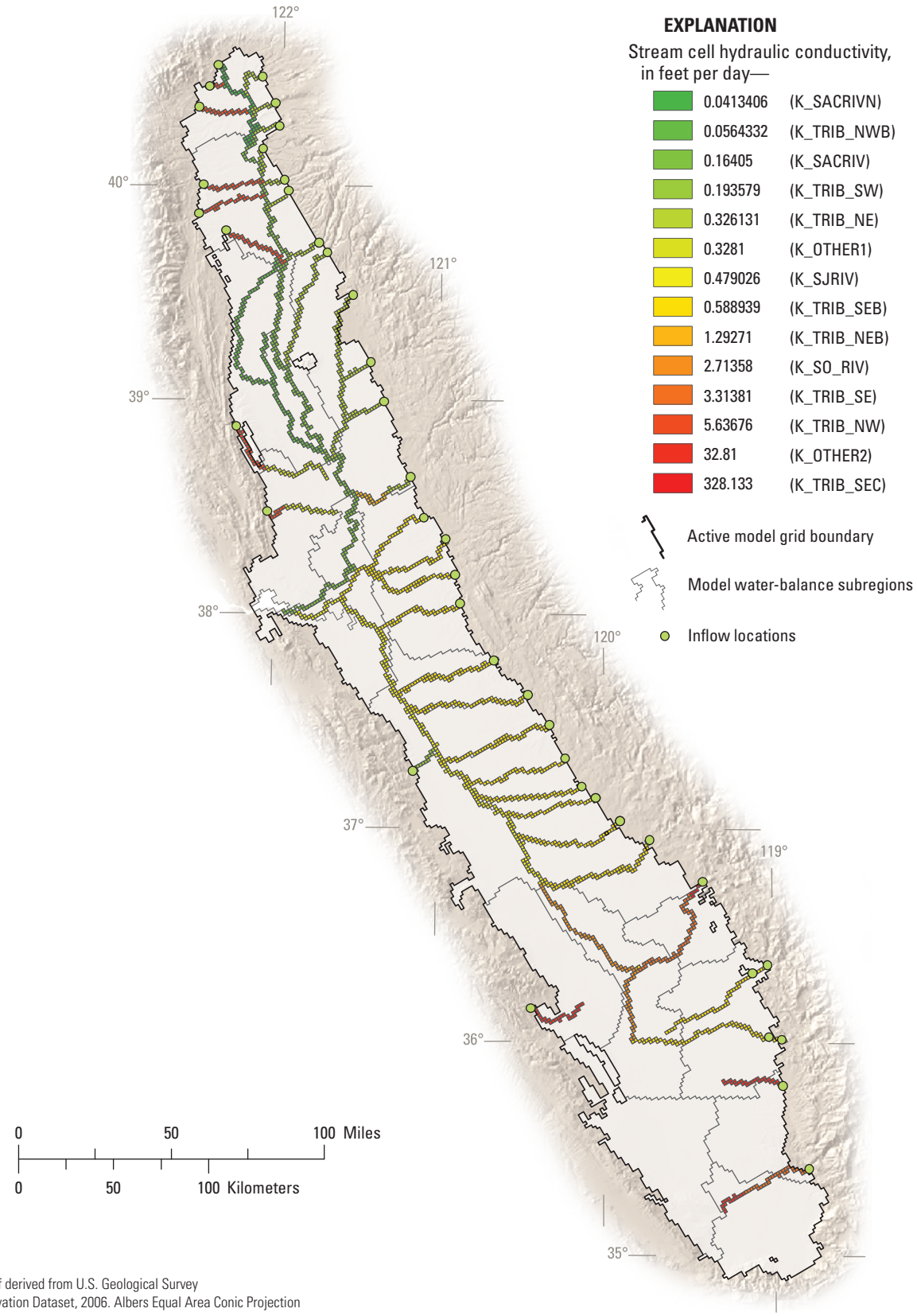

Figure C26. Distribution of cells used for streams, colored by streambed hydraulic conductivity values for cells estimated during calibration.

Sensitivity Analysis

The CVHM was extremely sensitive to changes in certain hydraulic properties. In particular, the CVHM failed convergence when some of the model parameters were perturbed out of the range of the final set of specified values. This, in part, limited the use of systematic parameter-estimation techniques to estimate model parameters and related sensitivities. However, it was generally possible to use systematic parameter-estimation techniques based on perturbation approaches for selected parameters. The sensitivity process in UCODE-2005 identifies the sensitivity of computed values at the locations of measurements to changes in model parameters, and was used to identify the parameters to include in the parameter estimation and to adjust during calibration. More than 100 parameters related to hydraulic properties, storage properties, streambed hydraulic conductivities, and various parameters in the FMP were included in the sensitivity process. Composite scaled sensitivity (CSS) values are used here to show relative sensitivity; the definition and derivation are described in Hill and others (2000). Although more than 100 parameters were identified, 24 parameters had relatively large and similar CSS values. Very few of the parameters actually were estimated using automated calibration (*table C10*). Results of the UCODE-2005 sensitivity process indicate that the CVHM was sensitive to a variety of different types of parameters (*fig. C27*). The CVHM was most sensitive to the hydraulic conductivity of the coarse-grained fraction in the San Joaquin Valley (K_c). Several multipliers on different hydraulic conductivity parameters also were fairly sensitive. Runoff from irrigation from pastures (PAS_IRO) had one of the highest CSS values (*fig. C27*). Some streambed hydraulic conductivities and storage properties also were relatively sensitive.

The CVHM also was extremely insensitive to changes in certain hydraulic properties. Streambed hydraulic conductivities of the eastern tributaries generally are insensitive. Because of the relatively low estimated values, the majority of the multipliers on the vertical hydraulic conductivity were relatively insensitive. Except for the cases shown on *fig. C27*, in general, the fractions of runoff from precipitation and irrigation were insensitive. Multipliers on efficiencies since the late 1970s also are generally insensitive. As would be expected, many parameters were insensitive within a certain range. When they were moved outside this range, they became much more sensitive. As a result, the sensitivities of parameters changed through the calibration process.

Simulation Results and Budget

A quantitative understanding of a basin's water balance provides key information about groundwater availability (Grannemann and Reeves, 2005). The water balance for the Central Valley was compiled and summarized by describing the components of the groundwater budget through the 42-year simulation. This chapter focuses on the simulation of the groundwater part of the budget and its linkages to surface water and the farm budget. More detailed discussions of the budget and groundwater availability, based on the simulation, are the focus of *Chapter B*.

In terms of the post-development groundwater budget, withdrawals from pumpage are balanced by a combination of increased recharge from irrigation, decreased discharge to streams, decreased evaporation, and release of groundwater from storage. The aquifer receives recharge from precipitation, streamflow losses, and agricultural return flow. Groundwater leaves the system predominantly through wells, ET, discharge to streams, and (to a small degree) discharge to the Delta. Depending on the magnitude, distribution, and timing of recharge and discharge, groundwater is both released from and taken into storage. Storage depletion often is accompanied by aquifer-system compaction and land subsidence.

Recharge from a combination of precipitation and excess applied irrigation water, and groundwater pumpage, are the dominant hydrologic stresses on the groundwater system (*table C3*; *figs. C28* and *C29*). Groundwater-level altitudes respond to these stresses. Groundwater pumpage has altered groundwater-flow rates and directions, reduced flow to streams, captured water from streams and other parts of the aquifer system, and altered groundwater quality. From 1961 to 2003 there has been a net depletion of groundwater in storage in the Central Valley.

Figure C30 shows an example of how the TFDR is met by a combination of surface-water deliveries and pumpage that varies through the irrigation cycle. The TFDR first is met by non-routed surface-water deliveries and then semi-routed surface-water deliveries. When the TFDR exceeds the total surface-water deliveries, groundwater is pumped to meet the remaining agricultural water demand. When the surface-water deliveries exceed the TFDR, the excess deliveries are returned to the surface-water system.

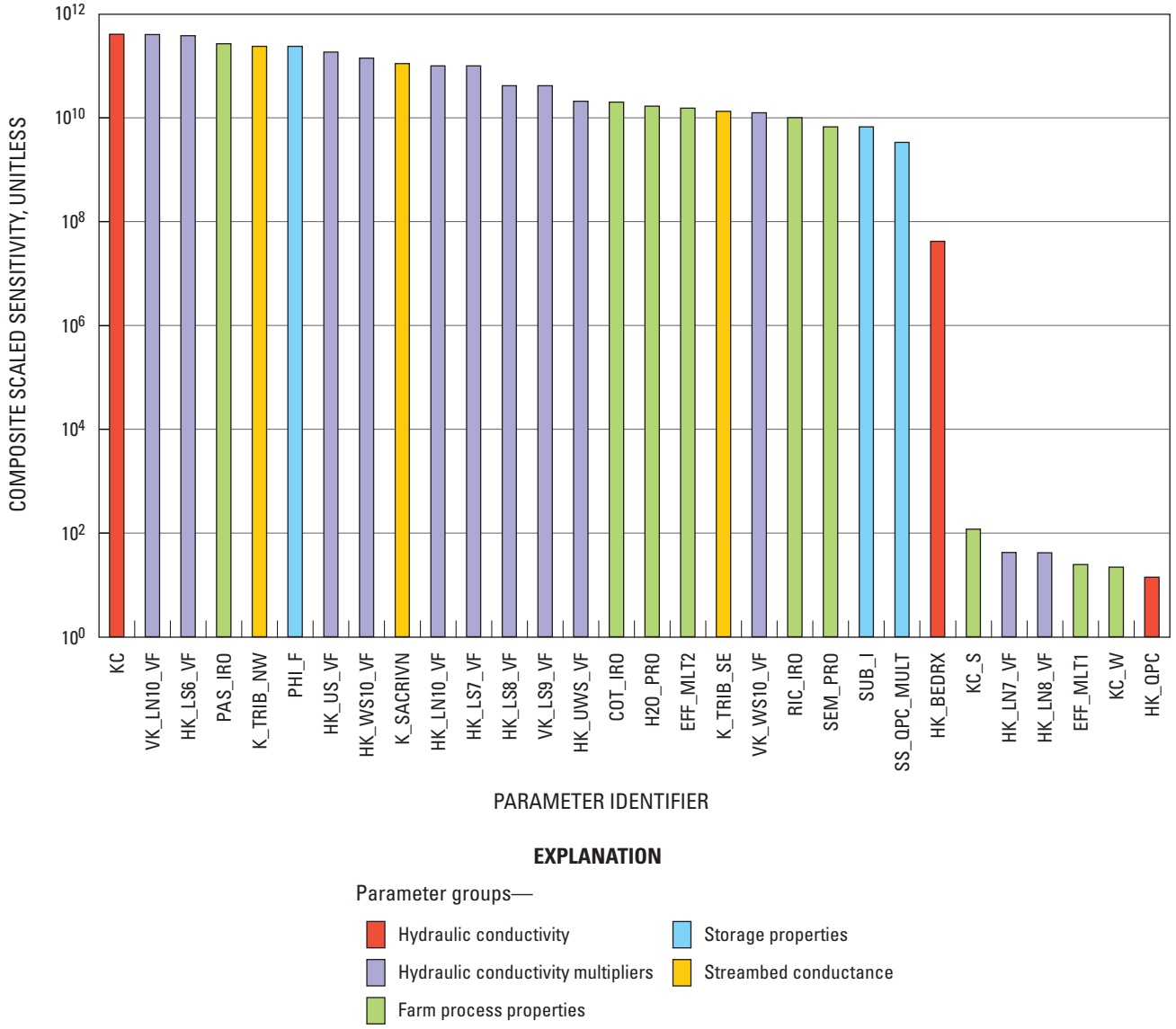

Figure C27. Relative composite sensitivity of computed water-level altitudes, flows, and subsidence information at calibration points to changes in parameters. Composite scaled sensitivity values are used here to show relative sensitivity; the definition and derivation are described in Hill and others (2000). The top 30 composite scaled sensitivities are plotted.

Recharge and Discharge

Delivery of surface water for irrigation, combined with pumpage for irrigation and public supply, have greatly altered the amount and distribution of recharge and discharge in the Central Valley. Prior to development, recharge and discharge were about 2 million acre-ft per year (*fig. A23*). As expected, simulated groundwater-flow to the Delta (General Head Boundary) was negligible (*fig. C31*). Since irrigated agriculture began in the late 1800s, the amount of groundwater pumped for irrigation has been greater than the natural (pre-development) recharge and discharge. During the period from 1962 to 2003, an average of 18.7 million acre-ft of irrigation water was required annually, about one-half from groundwater and one-half from surface-water (*tables C11* and *C12* and *fig. C29*). It is important to recognize that that not all irrigation water necessarily is consumed by ET; some water runs off and returns to the surface-water flow system and some returns to the groundwater system by deep percolation and other mechanisms.

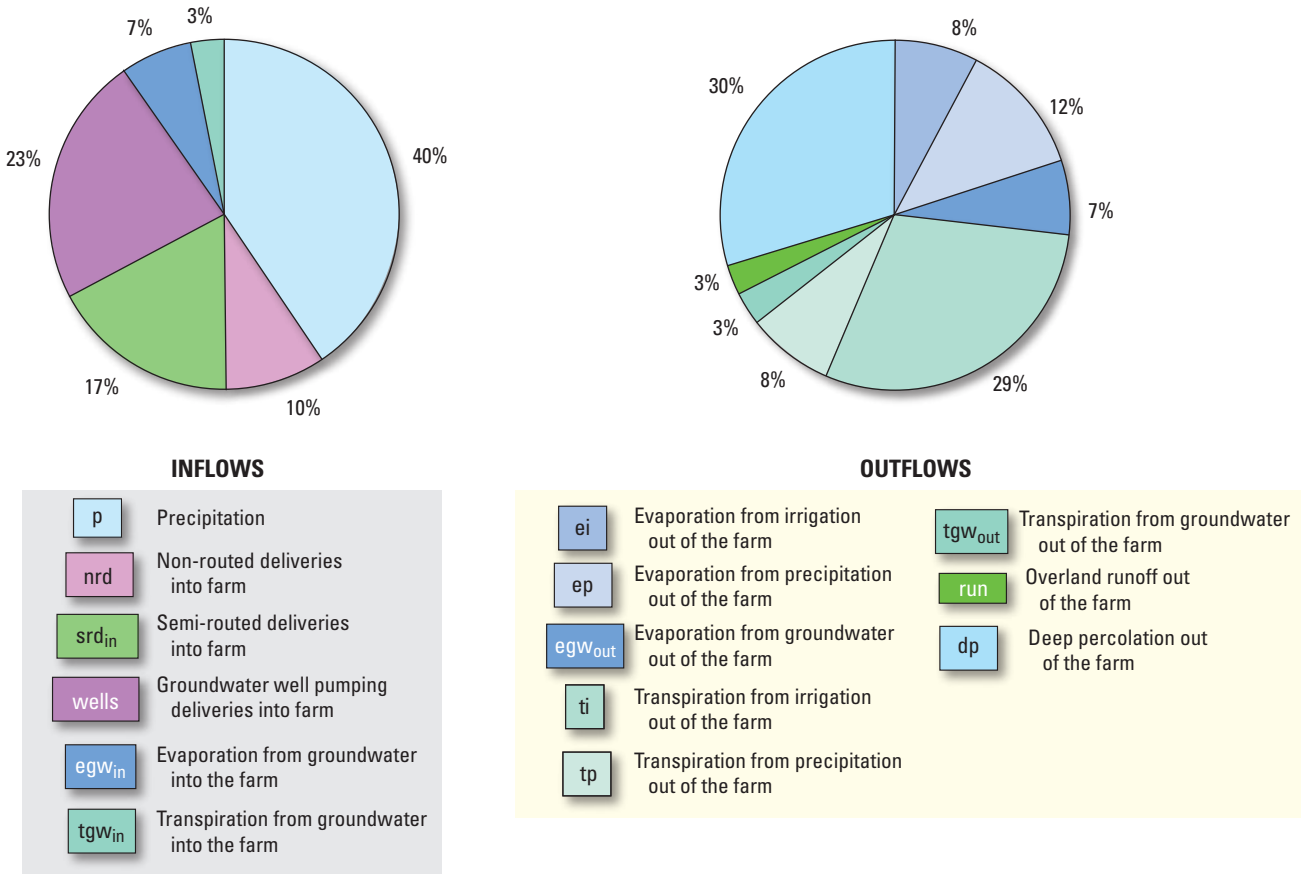

Figure C28. Average annual components of farm budget for water years 1962–2003.

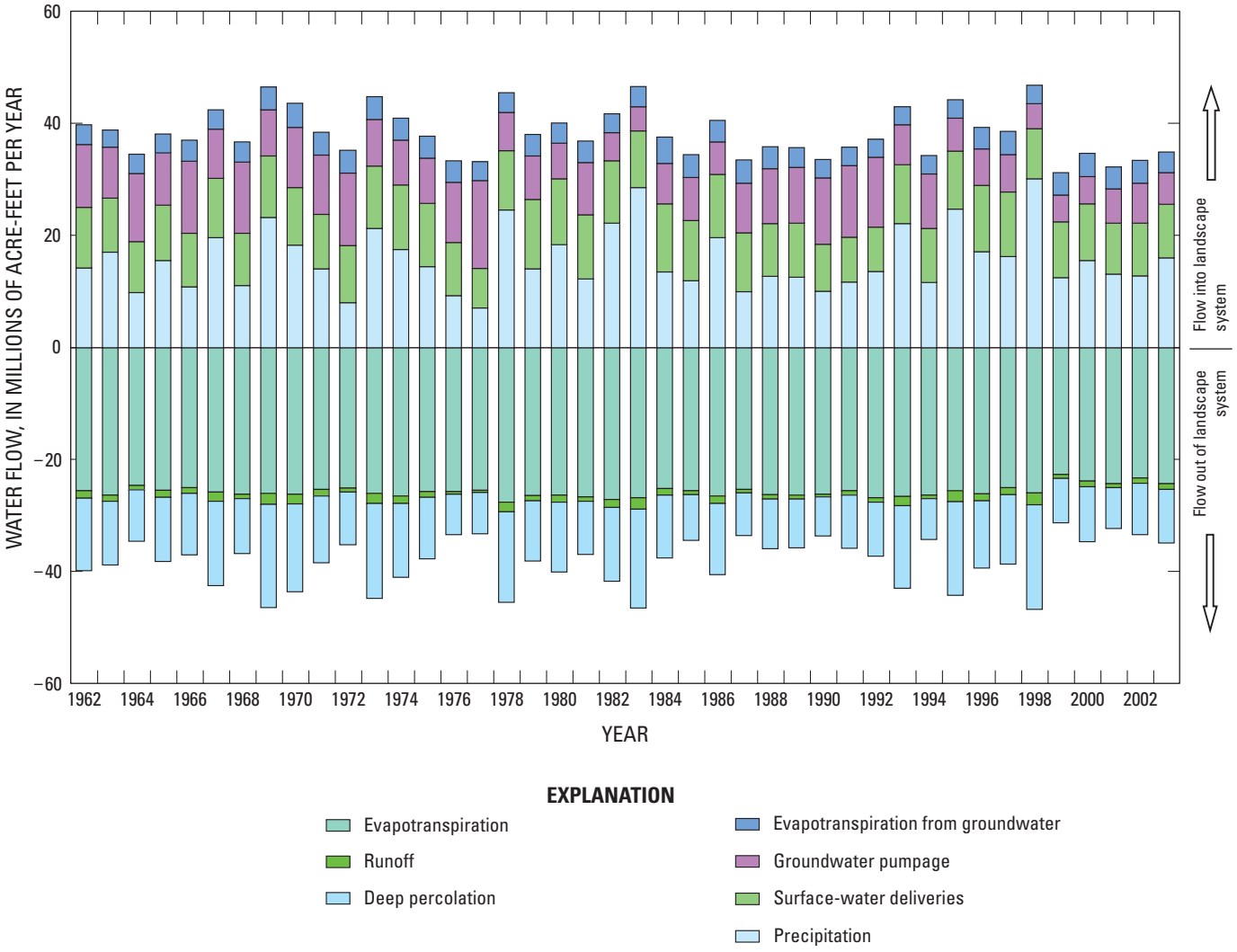

Figure C29. Farm budget changes through time for the Central Valley, California.

Recharge and discharge from the various budget components changes through the 1962–2003 time period as a result of climatic changes, land-use changes, and farming practices (*tables C11* and *C12* and *figs. C28*, *C29*, and *C31*). Between 1962 and 2003, *figure C29* shows that groundwater pumpage and surface-water deliveries for irrigation are a larger component of recharge to the landscape system than precipitation. As a result, percolation of irrigation water past crop roots has replaced infiltration of precipitation and stream water as the primary mechanism of recharge. With increases in irrigation efficiencies, however, the recharge from groundwater pumpage and surface-water deliveries (excess irrigation water), relative to precipitation, has declined (*fig. C28*). Recharge rates from precipitation are thought to have not changed significantly from pre-development times (Williamson and others, 1989). However, because the shallow part of the system now is simulated in more detail, the streamflow gains and losses are of much larger magnitude than previous estimates by Williamson and others (1989) (*fig. C31A*). Discharge of water through wells and the resulting loss of storage have replaced natural ET as the primary mechanism of discharge (*fig. C31*).

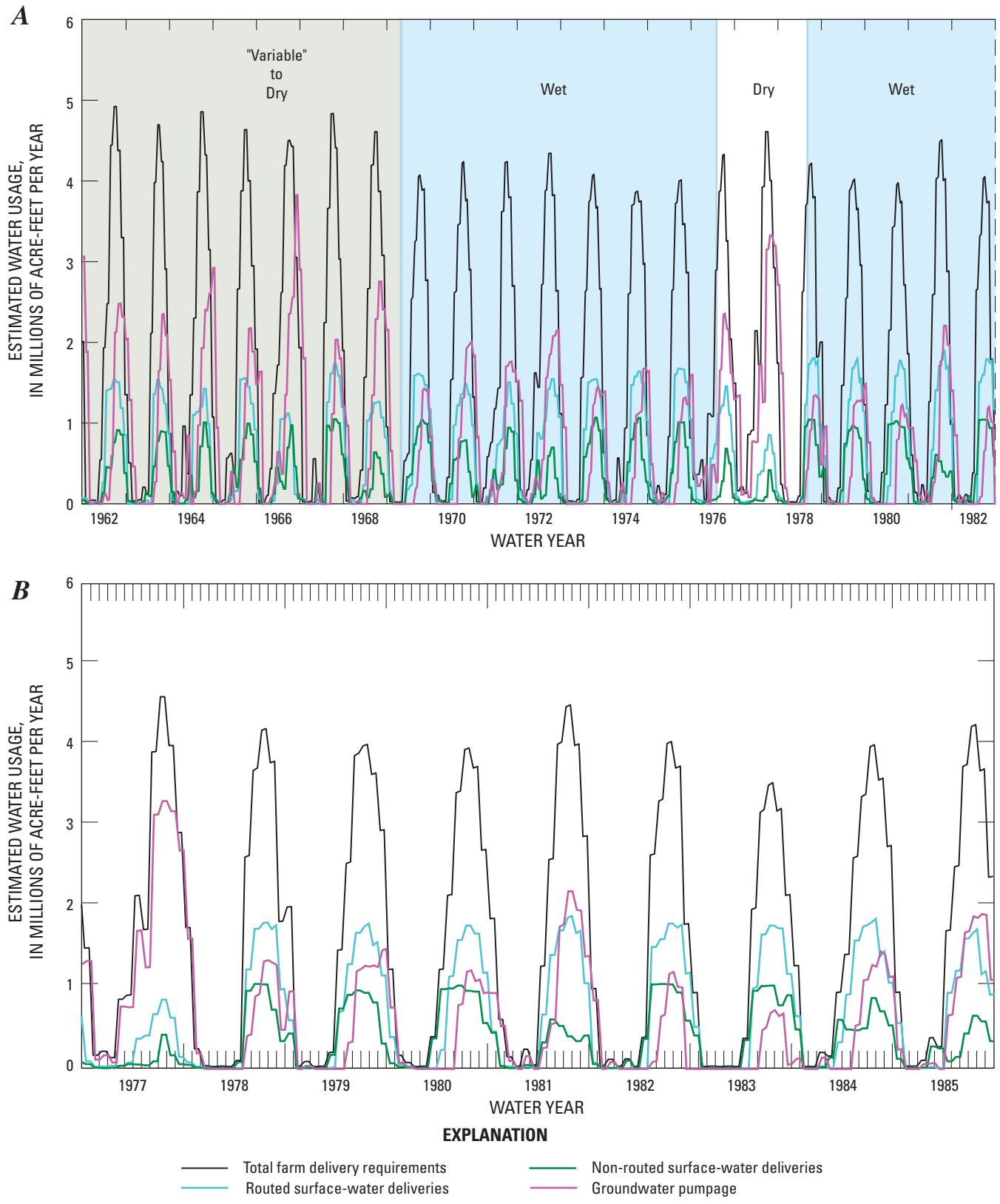

Figure C30. Farm budget changes through time for water-balance subregion 13, western San Joaquin Valley, Central Valley, California. *A,* Water years 1962–2003. *B,* Water years 1977–1985.

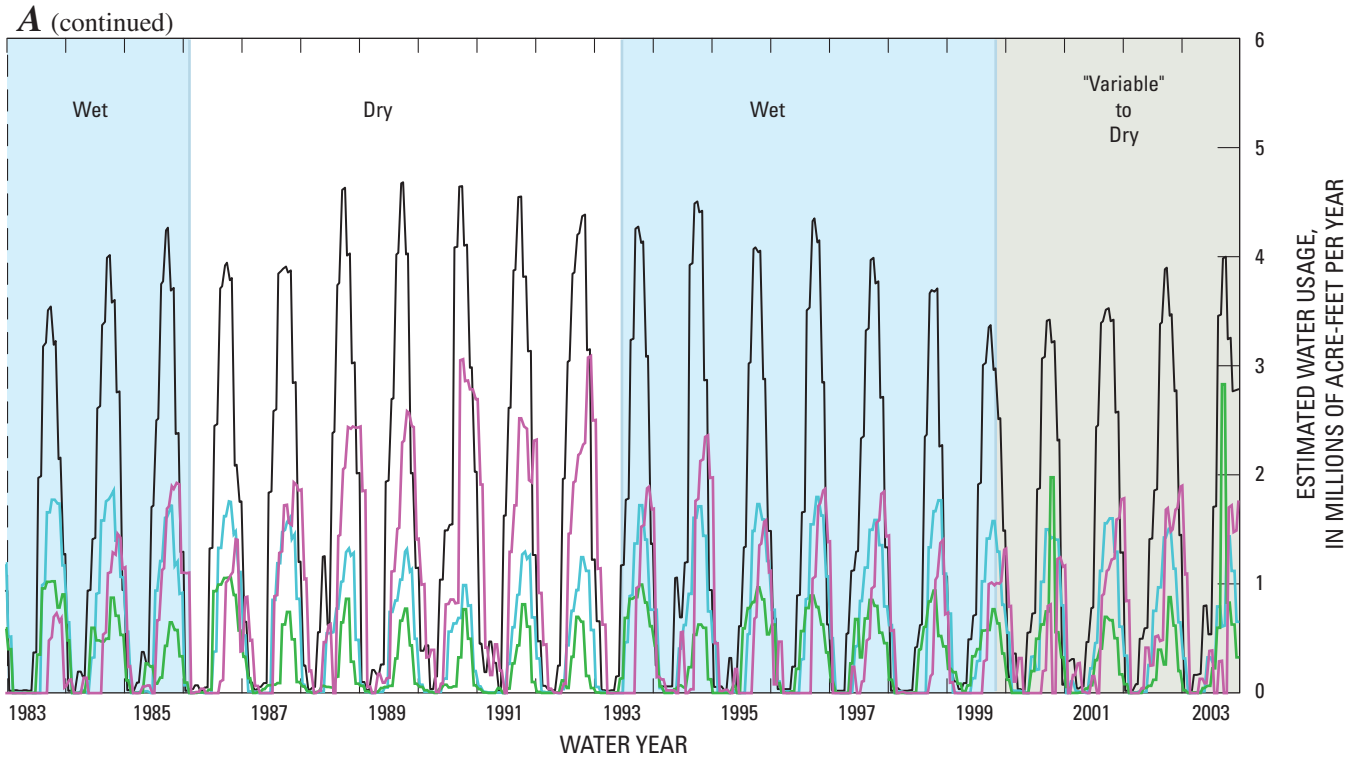

Figure C30. Continued.

The sources of irrigation water vary greatly from year to year and month to month (*fig. C30*). Dry periods generally lead to increased pumpage from wells and associated losses from storage, and reduced recharge associated with fallowing and changes to lower water-use crops. Wet periods have the opposite effects.

Water pumped from the aquifer system may or may not be replenished quickly. In some areas, groundwater that is pumped can be replenished annually during the non-irrigation season by recharge from precipitation and streams. In other areas, replenishment only occurs in years of abundant precipitation. In still other areas, most notably the southwestern San Joaquin Valley and Tulare basin, pumpage caused substantial water-level altitude declines and subsidence during periods of drought. Recently, artificial recharge projects have been implemented in the Tulare basin. Examples of these recharge projects are the recharge ponds developed by the Kern Water Bank (Kern Water Bank Authority, 2007) and in-lieu recharge projects started by SemiTropic Water Storage District (Semitropic Water Storage District, 2007). The potential effects of these projects are discussed in more detail in later sections of this report.

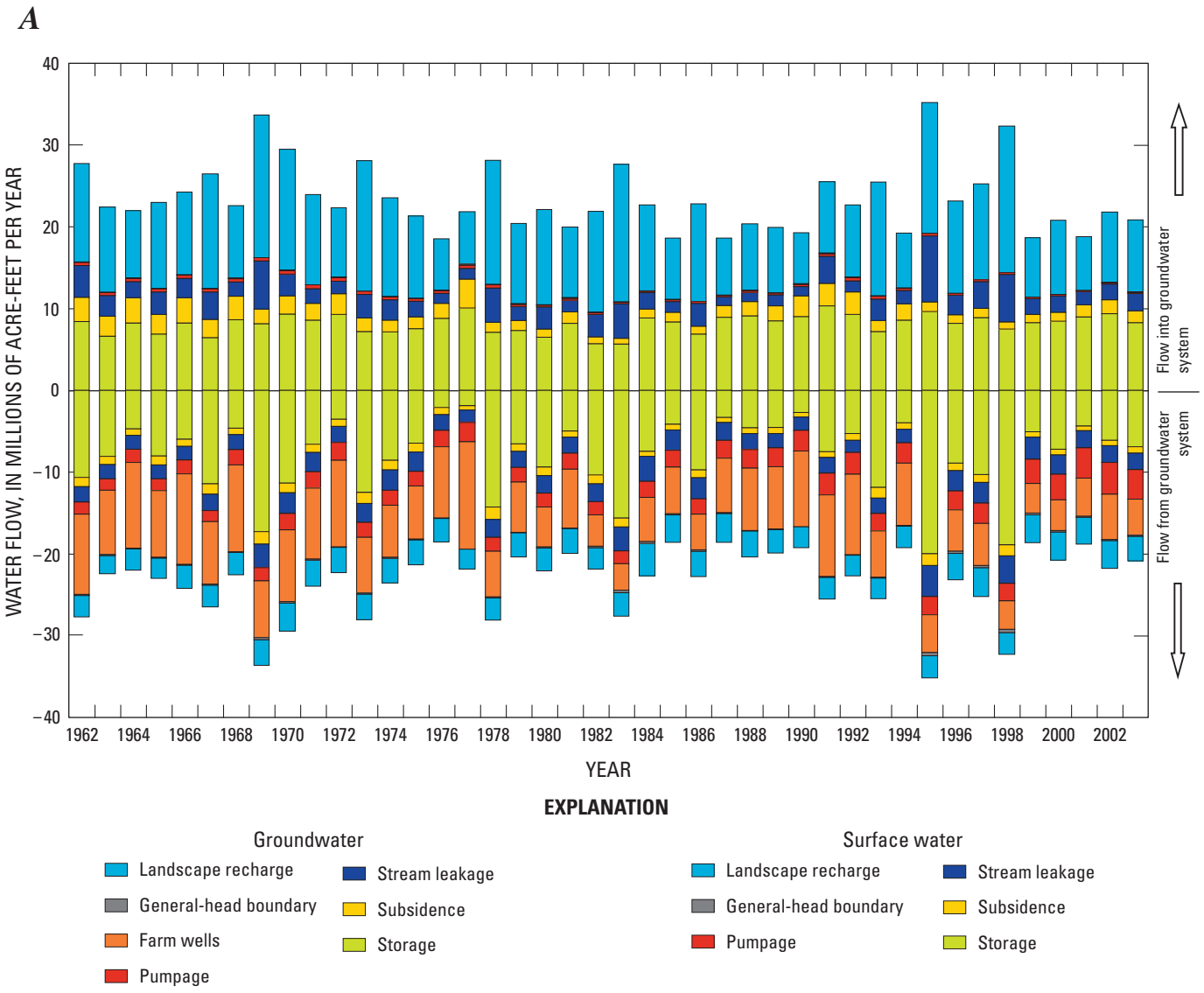

Figure C31. Groundwater budget changes through time for the Central Valley. *A,* All values. *B,* Net values.

Aquifer-System Storage

During the simulation period (1961–2003) there has been a depletion of millions of acre-ft of aquifer-system storage (*table C12* and *fig. C31*). Generally, the water removed from storage may be replaced by precipitation, stream leakage, excess applied irrigation water, artificial recharge, or any combination of the above (*fig. C31*). However, the withdrawals also have caused the permanent loss of storage by the inelastic compaction of fine-grained sediments. About 10 million acre-ft of water are taken into and released from groundwater storage annually (*table C12* and *fig. C31*). Year-to-year (and season-to-season) changes in storage reflect groundwater pumpage and the availability of precipitation and surface water. The difference between simulated annual groundwater discharge and recharge indicates an overall average net removal of about 1 million acre-ft/yr of groundwater from storage.

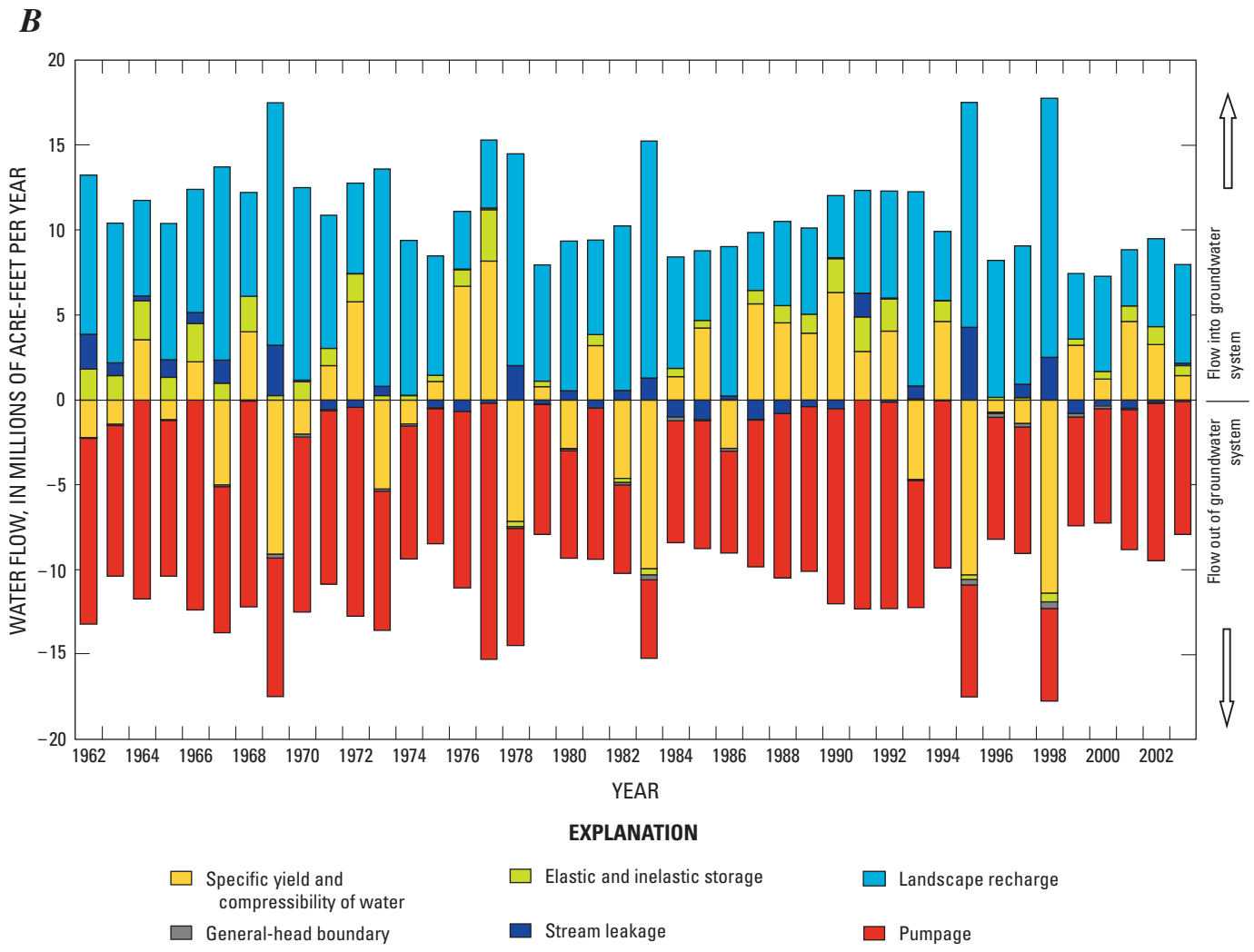

Figure C31. Continued.

Table C11. Simulated farm budget for the Central Valley, California, in acre-feet per year.

Typical (1975) highlighted in **bold italic**, dry (1990) highlighted in **bold**, and wet (1998) years highlighted in ***italic***.

Year	Precipitation	Surface-water deliveries	Groundwater pumpage	Evapotrans- piration	Runoff	Evapotrans-piration from groundwater	Deep percolation
1962	14,281,000	10,808,000	11,271,000	25,505,000	1,310,000	3,522,000	12,967,000
1963	17,119,000	9,625,000	9,096,000	26,300,000	1,097,000	3,056,000	11,391,000
1964	9,877,000	9,079,000	12,156,000	24,584,000	795,000	3,484,000	9,108,000
1965	15,590,000	9,915,000	9,355,000	25,448,000	1,221,000	3,337,000	11,425,000
1966	10,876,000	9,619,000	12,918,000	24,920,000	1,071,000	3,663,000	10,976,000
1967	19,718,000	10,583,000	8,743,000	25,748,000	1,652,000	3,514,000	15,012,000
1968	11,127,000	9,322,000	12,734,000	26,118,000	820,000	3,639,000	9,798,000
1969	23,300,000	11,002,000	8,231,000	25,937,000	2,015,000	4,039,000	18,433,000
1970	18,345,000	10,261,000	10,738,000	26,122,000	1,675,000	4,342,000	15,723,000
1971	14,102,000	9,701,000	10,569,000	25,198,000	1,159,000	4,114,000	11,973,000
1972	8,042,000	10,200,000	12,875,000	25,015,000	716,000	4,139,000	9,394,000
1973	21,343,000	11,136,000	8,253,000	25,934,000	1,772,000	4,043,000	16,914,000
1974	17,548,000	11,581,000	7,854,000	26,366,000	1,311,000	3,966,000	13,154,000
1975	***14,527,000***	11,279,000	7,925,000	25,525,000	1,024,000	3,927,000	10,995,000
1976	9,301,000	9,560,000	10,558,000	25,581,000	453,000	3,894,000	7,177,000
1977	7,152,000	7,034,000	15,551,000	25,389,000	436,000	3,445,000	7,279,000
1978	24,651,000	10,546,000	6,768,000	27,474,000	1,755,000	3,521,000	16,088,000
1979	14,134,000	12,364,000	7,661,000	26,325,000	941,000	3,857,000	10,657,000
1980	18,453,000	11,735,000	6,230,000	26,189,000	1,257,000	3,616,000	12,472,000
1981	12,350,000	11,440,000	9,108,000	26,510,000	810,000	3,965,000	9,435,000
1982	22,260,000	11,133,000	4,956,000	26,990,000	1,386,000	3,360,000	13,176,000
1983	28,589,000	10,166,000	4,341,000	26,664,000	2,050,000	3,532,000	17,703,000
1984	13,603,000	12,098,000	7,258,000	25,091,000	1,148,000	4,640,000	11,233,000
1985	11,972,000	10,760,000	7,647,000	25,435,000	700,000	4,055,000	8,204,000
1986	19,712,000	11,273,000	5,836,000	26,435,000	1,324,000	3,809,000	12,738,000
1987	10,048,000	10,509,000	8,843,000	25,282,000	581,000	4,171,000	7,620,000
1988	12,796,000	9,390,000	9,815,000	26,129,000	792,000	3,880,000	8,850,000
1989	12,632,000	9,663,000	9,830,000	26,131,000	741,000	3,549,000	8,662,000
1990	**10,121,000**	8,356,000	11,690,000	25,993,000	487,000	3,331,000	6,919,000
1991	11,763,000	8,009,000	12,549,000	25,424,000	793,000	3,436,000	9,395,000
1992	13,684,000	7,889,000	12,229,000	26,666,000	821,000	3,334,000	9,546,000
1993	22,192,000	10,538,000	6,958,000	26,430,000	1,645,000	3,262,000	14,726,000
1994	11,690,000	9,676,000	9,522,000	26,196,000	617,000	3,332,000	7,295,000
1995	24,818,000	10,345,000	5,737,000	25,428,000	1,913,000	3,366,000	16,739,000
1996	17,151,000	11,843,000	6,485,000	25,973,000	1,240,000	3,814,000	11,969,000
1997	16,299,000	11,567,000	6,644,000	24,859,000	1,294,000	4,120,000	12,347,000
1998	*30,177,000*	8,946,000	4,535,000	25,846,000	2,139,000	3,190,000	18,646,000
1999	12,511,000	10,006,000	4,831,000	22,538,000	757,000	3,969,000	7,885,000
2000	15,602,000	10,116,000	4,887,000	23,765,000	1,019,000	4,157,000	9,822,000
2001	13,197,000	9,099,000	6,127,000	24,232,000	673,000	3,925,000	7,316,000
2002	12,868,000	9,425,000	7,137,000	23,175,000	943,000	4,050,000	9,238,000
2003	16,050,000	9,571,000	5,643,000	24,252,000	1,009,000	3,695,000	9,554,000
Average	15,752,000	10,171,000	8,621,000	25,598,000	1,128,000	3,740,000	11,427,000

Table C12. Simulated groundwater budget for the Central Valley, California, in acre-feet per year.

[Values in this table are relative to flow in and out of the groundwater system as modeled. Typical (1975) highlighted in **bold italic**, dry (1990) highlighted in **bold**, and wet (1998) years highlighted in **italic**. GHB, General Head Boundary; IN, into groundwater system; OUT, out of groundwater system; NET, IN minus OUT]

Year	Specific yield and compressibility of water IN	GHB IN	Elastic and inelastic storage IN	Stream leakage IN	Farm recharge IN	Pumpage IN[1]
1962	8,613,000	57,000	3,150,000	3,791,000	12,166,000	439,000
1963	6,688,000	32,000	2,582,000	2,619,000	10,597,000	448,000
1964	8,424,000	58,000	3,320,000	1,957,000	8,299,000	451,000
1965	6,990,000	49,000	2,559,000	2,715,000	10,638,000	452,000
1966	8,331,000	63,000	3,369,000	2,171,000	10,197,000	465,000
1967	6,527,000	37,000	2,389,000	3,284,000	14,196,000	463,000
1968	8,849,000	59,000	3,206,000	1,684,000	8,957,000	464,000
1969	8,351,000	35,000	1,950,000	5,879,000	17,582,000	479,000
1970	9,620,000	23,000	2,515,000	2,425,000	14,898,000	565,000
1971	8,774,000	25,000	2,326,000	1,891,000	11,129,000	558,000
1972	9,570,000	56,000	2,859,000	1,445,000	8,511,000	557,000
1973	7,424,000	26,000	1,839,000	2,919,000	16,122,000	490,000
1974	7,262,000	20,000	1,643,000	2,398,000	12,247,000	463,000
1975	***7,667,000***	***29,000***	***1,664,000***	***1,901,000***	***10,189,000***	***436,000***
1976	9,005,000	60,000	2,099,000	1,224,000	6,313,000	430,000
1977	10,460,000	102,000	3,827,000	1,347,000	6,436,000	477,000
1978	7,231,000	46,000	1,409,000	4,261,000	15,387,000	478,000
1979	7,636,000	42,000	1,429,000	1,719,000	9,930,000	395,000
1980	6,741,000	29,000	1,195,000	2,600,000	11,765,000	374,000
1981	8,560,000	47,000	1,693,000	1,405,000	8,731,000	367,000
1982	5,916,000	21,000	995,000	2,781,000	12,536,000	343,000
1983	5,928,000	8,000	827,000	4,266,000	17,069,000	301,000
1984	9,222,000	12,000	1,340,000	1,825,000	10,613,000	313,000
1985	8,734,000	22,000	1,457,000	1,387,000	7,597,000	356,000
1986	7,199,000	17,000	1,177,000	2,712,000	12,106,000	340,000
1987	9,340,000	25,000	1,782,000	1,062,000	7,085,000	338,000
1988	9,462,000	34,000	2,136,000	1,211,000	8,202,000	344,000
1989	8,803,000	42,000	2,198,000	1,300,000	8,065,000	362,000
1990	**9,428,000**	**62,000**	**2,991,000**	**1,113,000**	**6,292,000**	**394,000**
1991	10,969,000	67,000	3,188,000	3,908,000	8,830,000	470,000
1992	9,813,000	67,000	3,153,000	1,324,000	8,941,000	497,000
1993	7,367,000	40,000	1,589,000	2,339,000	14,114,000	425,000
1994	8,959,000	55,000	2,310,000	1,417,000	6,773,000	381,000
1995	10,261,000	26,000	1,337,000	8,331,000	16,185,000	414,000
1996	8,420,000	20,000	1,237,000	2,296,000	11,452,000	312,000
1997	9,249,000	22,000	1,277,000	3,735,000	11,851,000	299,000
1998	*8,831,000*	*11,000*	*1,017,000*	*7,460,000*	*18,138,000*	*305,000*
1999	8,626,000	17,000	1,133,000	1,715,000	7,381,000	248,000
2000	8,730,000	20,000	1,245,000	1,862,000	9,176,000	264,000
2001	9,324,000	25,000	1,622,000	1,680,000	6,716,000	283,000
2002	9,699,000	26,000	1,877,000	2,011,000	8,686,000	316,000
2003	8,533,000	24,000	1,560,000	2,197,000	8,950,000	305,000
Average	8,465,000	37,000	2,011,000	2,561,000	10,739,000	401,000

Table C12. Simulated groundwater budget for the Central Valley, California, in acre-feet per year—Continued.

[Values in this table are relative to flow in and out of the groundwater system as modeled. Typical (1975) highlighted in **bold italic**, dry (1990) highlighted in **bold**, and wet (1998) years highlighted in ***italic***. GHB, General Head Boundary; IN, into groundwater system; OUT, out of groundwater system; NET, IN minus OUT]

Year	Specific yield and compressibility of water OUT	GHB OUT	Elastic and inelastic storage OUT	Stream leakage OUT	Farm recharge OUT[2]	Pumpage OUT[3]	Farm wells OUT
1962	10,634,000	105,000	1,153,000	1,850,000	2,648,000	1,628,000	10,185,000
1963	8,192,000	120,000	1,007,000	1,738,000	2,209,000	1,513,000	8,170,000
1964	4,694,000	53,000	809,000	1,689,000	2,618,000	1,720,000	10,911,000
1965	8,013,000	98,000	1,058,000	1,729,000	2,493,000	1,548,000	8,449,000
1966	5,811,000	65,000	864,000	1,667,000	2,807,000	1,815,000	11,548,000
1967	11,462,000	132,000	1,259,000	1,983,000	2,630,000	1,468,000	7,948,000
1968	4,601,000	56,000	793,000	1,814,000	2,729,000	1,986,000	11,220,000
1969	17,398,000	263,000	1,537,000	2,905,000	3,122,000	1,738,000	7,290,000
1970	11,241,000	182,000	1,164,000	2,558,000	3,439,000	2,151,000	9,297,000
1971	6,685,000	126,000	1,030,000	2,361,000	3,197,000	2,158,000	9,129,000
1972	3,466,000	46,000	875,000	1,976,000	3,168,000	2,328,000	11,119,000
1973	12,662,000	165,000	1,406,000	2,333,000	3,169,000	1,962,000	7,109,000
1974	8,543,000	154,000	1,201,000	2,457,000	2,999,000	1,953,000	6,708,000
1975	***6,496,000***	***115,000***	***1,125,000***	***2,361,000***	***3,060,000***	***1,963,000***	***6,752,000***
1976	2,127,000	39,000	892,000	1,922,000	2,945,000	2,154,000	9,037,000
1977	1,918,000	10,000	531,000	1,552,000	2,527,000	2,502,000	13,593,000
1978	14,447,000	164,000	1,564,000	2,131,000	2,736,000	1,862,000	5,889,000
1979	6,590,000	86,000	935,000	1,982,000	3,040,000	1,984,000	6,516,000
1980	9,350,000	142,000	1,081,000	2,146,000	2,845,000	1,885,000	5,242,000
1981	4,987,000	61,000	787,000	1,963,000	3,168,000	2,173,000	7,641,000
1982	10,469,000	182,000	1,122,000	2,225,000	2,660,000	1,799,000	4,123,000
1983	15,728,000	331,000	1,134,000	3,009,000	2,858,000	1,737,000	3,583,000
1984	7,235,000	232,000	666,000	3,051,000	3,966,000	2,169,000	5,988,000
1985	4,195,000	118,000	772,000	2,504,000	3,400,000	2,247,000	6,298,000
1986	9,712,000	186,000	1,006,000	2,597,000	3,133,000	2,070,000	4,825,000
1987	3,336,000	94,000	673,000	2,203,000	3,586,000	2,398,000	7,321,000
1988	4,666,000	68,000	778,000	1,957,000	3,182,000	2,481,000	8,238,000
1989	4,546,000	55,000	756,000	1,775,000	2,894,000	2,505,000	8,221,000
1990	**2,779,000**	**33,000**	**582,000**	**1,641,000**	**2,635,000**	**2,724,000**	**9,871,000**
1991	8,216,000	99,000	728,000	2,041,000	2,785,000	2,847,000	10,702,000
1992	5,346,000	49,000	856,000	1,547,000	2,644,000	2,820,000	10,513,000
1993	11,676,000	116,000	1,325,000	1,881,000	2,584,000	2,290,000	5,992,000
1994	3,835,000	52,000	818,000	1,686,000	2,728,000	2,627,000	8,133,000
1995	20,424,000	384,000	1,475,000	4,125,000	2,756,000	2,398,000	4,970,000
1996	8,814,000	231,000	933,000	2,510,000	3,245,000	2,475,000	5,509,000
1997	10,716,000	249,000	1,012,000	2,610,000	3,568,000	2,645,000	5,614,000
1998	*20,861,000*	*454,000*	*1,472,000*	*4,126,000*	*2,649,000*	*2,347,000*	*3,833,000*
1999	4,894,000	240,000	688,000	2,793,000	3,422,000	3,130,000	3,938,000
2000	7,112,000	195,000	732,000	2,411,000	3,468,000	3,306,000	4,052,000
2001	4,471,000	137,000	636,000	2,166,000	3,284,000	3,869,000	5,068,000
2002	6,189,000	130,000	710,000	2,086,000	3,448,000	4,053,000	5,979,000
2003	6,966,000	137,000	879,000	2,041,000	3,046,000	3,768,000	4,712,000
Average	8,131,000	142,000	972,000	2,240,000	2,988,000	2,314,000	7,410,000

Table C12. Simulated groundwater budget for the Central Valley, California, in acre-feet per year—Continued.

[Values in this table are relative to flow in and out of the groundwater system as modeled. Typical (1975) highlighted in **bold italic**, dry (1990) highlighted in **bold**, and wet (1998) years highlighted in ***italic***. GHB, General Head Boundary; IN, into groundwater system; OUT, out of groundwater system; NET, IN minus OUT]

Year	Net specific yield and compressibility of water	Net GHB	Net elastic and inelastic storage	Net stream leakage	Net farm recharge	Net Pumpage[4]
1962	–2,021,000	–48,000	1,997,000	1,941,000	9,519,000	–11,373,000
1963	–1,504,000	–89,000	1,575,000	881,000	8,388,000	–9,236,000
1964	3,730,000	4,000	2,511,000	268,000	5,681,000	–12,180,000
1965	–1,023,000	–49,000	1,500,000	986,000	8,145,000	–9,544,000
1966	2,521,000	–2,000	2,505,000	504,000	7,389,000	–12,898,000
1967	–4,935,000	–94,000	1,129,000	1,301,000	11,566,000	–8,953,000
1968	4,247,000	2,000	2,413,000	–130,000	6,229,000	–12,742,000
1969	–9,047,000	–229,000	413,000	2,974,000	14,460,000	–8,550,000
1970	–1,621,000	–159,000	1,351,000	–134,000	11,459,000	–10,883,000
1971	2,089,000	–102,000	1,296,000	–470,000	7,932,000	–10,729,000
1972	6,103,000	10,000	1,984,000	–531,000	5,343,000	–12,890,000
1973	–5,238,000	–139,000	433,000	586,000	12,953,000	–8,581,000
1974	–1,282,000	–134,000	442,000	–59,000	9,247,000	–8,198,000
1975	***1,171,000***	***–86,000***	***539,000***	***–461,000***	***7,129,000***	***–8,279,000***
1976	6,878,000	22,000	1,208,000	–698,000	3,368,000	–10,762,000
1977	8,542,000	92,000	3,296,000	–205,000	3,909,000	–15,618,000
1978	–7,216,000	–117,000	–155,000	2,130,000	12,651,000	–7,272,000
1979	1,046,000	–44,000	494,000	–263,000	6,890,000	–8,104,000
1980	–2,609,000	–113,000	114,000	454,000	8,920,000	–6,752,000
1981	3,573,000	–15,000	906,000	–557,000	5,562,000	–9,447,000
1982	–4,553,000	–161,000	–127,000	556,000	9,877,000	–5,579,000
1983	–9,800,000	–323,000	–307,000	1,258,000	14,211,000	–5,020,000
1984	1,987,000	–220,000	674,000	–1,225,000	6,647,000	–7,844,000
1985	4,539,000	–96,000	685,000	–1,117,000	4,197,000	–8,188,000
1986	–2,514,000	–170,000	171,000	116,000	8,973,000	–6,556,000
1987	6,004,000	–69,000	1,109,000	–1,141,000	3,499,000	–9,381,000
1988	4,796,000	–35,000	1,358,000	–745,000	5,020,000	–10,375,000
1989	4,257,000	–13,000	1,442,000	–475,000	5,171,000	–10,365,000
1990	**6,649,000**	**29,000**	**2,409,000**	**–528,000**	**3,657,000**	**–12,201,000**
1991	2,753,000	–32,000	2,460,000	1,868,000	6,045,000	–13,078,000
1992	4,467,000	18,000	2,297,000	–223,000	6,297,000	–12,836,000
1993	–4,309,000	–76,000	264,000	459,000	11,531,000	–7,857,000
1994	5,124,000	3,000	1,492,000	–269,000	4,045,000	–10,379,000
1995	–10,163,000	–358,000	–139,000	4,206,000	13,428,000	–6,954,000
1996	–394,000	–211,000	303,000	–214,000	8,206,000	–7,672,000
1997	–1,467,000	–227,000	266,000	1,125,000	8,283,000	–7,960,000
1998	*–12,030,000*	*–443,000*	*–455,000*	*3,334,000*	*15,489,000*	*–5,874,000*
1999	3,732,000	–222,000	445,000	–1,078,000	3,959,000	–6,820,000
2000	1,619,000	–175,000	513,000	–549,000	5,708,000	–7,095,000
2001	4,853,000	–111,000	986,000	–486,000	3,432,000	–8,654,000
2002	3,510,000	–103,000	1,168,000	–75,000	5,237,000	–9,717,000
2003	1,566,000	–113,000	680,000	155,000	5,904,000	–8,175,000
Average	334,000	–105,000	1,039,000	321,000	7,751,000	–9,323,000

[1]Pumpage IN refers to flow into the borehole from the aquifer system.

[2]Farm recharge OUT is equivalent to evapotranspiration from groundwater.

[3]Pumpage OUT includes urban pumpage and farm pumpage through multi–node wells.

[4]Net Pumpage = Pumpage IN – Pumpage OUT – Farm Wells OUT.

Model Uncertainty and Limitations

The goal of this modeling activity was to develop a model capable of being accurate at scales relevant to water-management decisions. The intent of developing the CVHM was not to reproduce every detail of the hydrologic system, but to portray its general characteristics. Although the CVHM doesn't completely represent all parts of the system, it is relevant for developing a better understanding of the flow system at a regional scale and contains sufficient fundamental detail to facilitate addition of more detailed features that may be relevant at a sub-regional scale.

Though the development of the CVHM has employed some of the latest modeling methods available at the time of the study, the use of numerical models to simulate hydrologic systems still has inherent limitations. Limitations of the modeling software, data limitations, assumptions made during model development, conceptual model error (Bredeheoft, 2005), and results of model calibration and sensitivity analysis all are factors that constrain the appropriate use of hydrologic models, including the CVHM. Differences between simulated and actual hydrologic conditions arise from a number of sources and are known collectively as model error (Walter and Whealan, 2005). One component of model error relates to discretization. The CVHM represents the hydrologic system as a series of discrete spatial units, through which intrinsic properties and stresses were simulated as locally uniform. For example, spatially the CVHM is discretized into 1-mi^2 model cells and features smaller cells that are not simulated. In reality, the model is likely only to represent features accurately at a scale of approximately 5 mi^2. Temporally, the CVHM is discretized into a series of discrete, monthly stress periods during which hydrologic stresses (user-specified inflows and outflows) are constant. Temporal discretization introduces additional sources of model inaccuracy. These were minimized by choosing monthly stress periods, which are an appropriate temporal interval to address the changes in irrigated agriculture and disparities between supply and demand components of the hydrologic budget. Model errors also may arise from the numerical solution that is based on head and flow closure criteria. These errors were minimized by constraining acceptable model solutions to mass-balance residuals of less than 0.1 percent of the total mass of flow in the Central Valley.

An additional component of model error arose from how accurately model-input values represent the actual hydrologic system. The degree to which the CVHM simulation provides a reasonable representation of the hydrologic system was evaluated by comparing simulated hydrologic conditions with those observed in the field. The CVHM's performance and accuracy are constrained primarily by groundwater-level altitudes, streamflow losses, the database used to synthesize the texture distribution, and subsidence values. These comparisons were used to ensure that the simulation of the regional hydrologic system is consistent with historical measurements of responses to stresses throughout the Central Valley.

Although simplifying assumptions were made of an inherently complex, developed hydrologic system in developing the CVHM model, this perhaps is the most detailed model of the entire Central Valley that has been developed to date. The CVHM solves for average conditions within each model cell, these cells range in volume from about 32,000 acre-ft near the land surface to 256,000 acre-ft at depth. Within each of these cells, the hydraulic properties are interpolated or extrapolated from measurements and (or) estimated during model calibration. Long-term hydrographs indicate that the water-level altitudes have been changing with time. Because the initial conditions specified in the CVHM were derived from a period of transient groundwater-flow, errors related to these transients may be significant in places during the early part of the simulation. However, discrepancies in the initial conditions are quickly dissipated with time. Based on sensitivity tests of the initial heads (±5 ft), errors associated with misspecification of the initial condition are negligible after the first 6 months. Thus, care must be taken in interpreting CVHM results and analyses that depend on the early part of the simulation. As a result, model output only was used for analyses after this first 6-month stabilization period.

Several elements of the CVHM remain uncertain and will require additional investigation. The hydrologic stresses in the CVHM are a combination of measured values, adjustments to represent conceptualizations of the system, and values specified through the GHB, HFB, LPF, MNW, MULT, and SFR1 packages and the FMP. Hydrologic features that remain uncertain include hydraulic properties, the location and properties of flow barriers, and critical-head distributions. Hydraulic properties that remain uncertain include horizontal and vertical hydraulic conductivities and storage properties.

The CVHM model-layering is, in part, uncertain because it is based on layers that were derived by using a uniform thickness with depth except where the Corcoran Clay is present. Although the sequence stratigraphic and facies changes may be somewhat depth dependent, the model layers generally do not coincide with the actual glacial cycles of sedimentation sequences in the alluvial deposits. The representation of sedimentary layering and additional formations might improve the model accuracy. However, the inclusion of the Corcoran clay is a unique feature that was not explicitly present in other models of the Central Valley. The representation of sedimentary layering and formations needs to be improved before the CVHM is suitable for particle-tracking simulations or for simulating solute-transport. The implicit inclusion of the volcanic units and the sedimentary Tuscan and Tehama Formations in the Sacramento Valley inadequately defines the sequence stratigraphic detail and the geologically controlled flow paths in the groundwater-flow system. In addition, depth decay was implemented during calibration but remains an uncertain feature. In some areas, the change in saturated thickness as well as changes in porosity and specific yield with depth may affect the CVHM.

The application of the SFR1 package makes several assumptions that may affect the accuracy of the streamflow infiltration, streambed hydraulic conductivity, and the related groundwater/surface-water interactions. In particular, the assumption of a linear change in streambed altitude may be a poor approximation. Errors in this approximation may result in an over or under estimation of streambed infiltration. In addition, the assumption that the streamflow stage-discharge relation remains constant over entire stream segments with a wide variety of geomorphic conditions may lead to model error in streamflow infiltration and stream-bed conductivities. Finally, the distribution of streambed hydraulic conductivities is poorly defined. Uncertainty exists in surface-water inflows, surface-water deliveries, and surface-water diversions. These uncertainties can have a significant effect on the accuracy of the CVHM and can represent thousands of acre-feet of error per month. As a result, these uncertainties may indirectly affect the amount of groundwater pumpage required to satisfy irrigation requirements.

The effectiveness of simulated barriers used in the HFB package to represent selected fault systems that may be partial barriers to groundwater-flow remains uncertain. Limited water-level altitude observations across faults were used to constrain flow-barrier conductances during model calibration. Additional water-level altitude observations would be required to constrain these features.

Overall, the application of multi-aquifer pumpage to dynamically redistribute the pumpage between layers temporally and spatially still is a significant improvement over other models of the Central Valley. Despite this improvement, multi-aquifer pumpage, which is simulated by a combination of farm wells and the MNW package has several elements of significant uncertainty. The use of virtual wells instead of actual wells, and the lack of pumping capacity information to locally constrain non-uniform pumpage, may affect the accuracy of the model on a local basis. A large component of multi-node well pumpage uncertainty is the distribution of wellbore properties such as well depths, well radii, pumping capacities of individual wells, and the skin factor used to represent friction and entrance losses. In particular, the value of the skin factor is uncertain. This skin factor promotes or inhibits wellbore flow between model layers. As with agricultural pumpage, urban pumpage is not metered for the major urban centers. The estimates of urban pumpage are based on population. Finally, all the agricultural wells outside the extent of the Corcoran Clay could not be simulated feasibly as multi-aquifer wells. Both the MNW package and the FMP can have extremely non-linear solutions. When simulated together, the solutions were unfeasibly slow and unstable. As a result, these wells were simulated as single-aquifer wells with the FMP and intra-borehole flow between model layers was not simulated in these areas.

Some of the inputs to the FMP that are necessary to calculate water use were estimated for some regions of the Central Valley but remain uncertain in other areas. For example, the temporal and spatial distribution of land use and crop distributions are very coarse. Temporally, land-use distributions were based on only five multi-year maps. Many of the stresses related to these land uses varied throughout the simulation period, driven by climatic conditions as well as cultivation periods. Hence, the changes simulated by the FMP with these few land-use estimates are simulated seasonally and by climatic-driven events that can be yearly or multi-year in length. Anthropogenic changes are incorporated minimally through land-use changes and surface-water deliveries. The CVHM includes some double cropping and K_c values that reflect the winter versus summer growing periods. The growing periods for some crops vary annually and generally are uncertain. This especially is true with climatic changes, where wet spring seasons may delay planting, dry spring seasons may require additional supplemental irrigation, and additional warm months may allow for prolonged growing seasons. In addition to K_c values, consumptive use is based on ETo. In the CVHM, these ETo values are estimated from empirical equations based on temperature data. Limitations of the FMP include its inability to simulate soil moisture storage and "on-farm" storage. This limitation is most important during months when fields are rewetted prior to cultivation and in areas of natural vegetation during prolonged droughts. This limitation may have little effect on areas where repetitive agricultural irrigation minimizes the changes in soil moisture or where the water table is near the surface and groundwater uptake is occurring.

Some of the boundary conditions of the CVHM are incomplete, which may be a minor source of model error. Though most surface inflow occurs through the 43 rivers simulated in CVHM, some minor intermittent flows from smaller watersheds surrounding the valley is poorly understood and is not specified in the CVHM. Recent work by DWR (C. Brush, California Department of Water Resources, written commun., February 21, 2007) and estimates from Nady and Larragueta (1983) report that these influxes make up less than 2 percent of the influx to the system. However, this may be a local source of model error and may affect the local accuracy of the CVHM. In addition, the CVHM does not simulate any surface-water bodies, such as the intermittently wet Tulare Lake, Kern Lake, and Buena Vista Lake bed areas. The CVHM also does not simulate the emergent artificial recharge projects in the Tulare Basin. These water banks now recharge thousands of acre-ft/year (Kern Water Bank Authority, 2007; Semitropic Water Storage District, 2007).

Not all of the major canals were simulated within the streamflow routing network. In addition, land subsidence can reduce the gradient and elevation on canals and streams, which may result in a reduction in conveyance and freeboard capacity. Although this subsidence was simulated, the effects of subsidence on streamflow and canal conveyance were not simulated. The total surface-water delivery system that represents water passed through the Delta, and then pumped into the major canals, was not accounted for in the streamflow-routing network. These deliveries were simulated as non-routed deliveries. In addition, the component of diversions that was used for maintenance of habitat or maintenance of water rights was not accounted for in the model, neither within the streamflow routing network nor as surface-water deliveries through the FMP water-rights features. These omissions may result in reported streamflow diversions being much larger than the crop irrigation demand estimated with the FMP for some WBSs. Drainage pumpage in the San Joaquin Valley, particularly WBS 14, and the Delta also is not accounted for in the CVHM. Omission of this pumpage may be part of the inaccuracy water-level altitudes in these regions. Simulation results indicate that flows across these poorly constrained boundaries make up a small part of the groundwater budget (*table C12*). The boundary flows may be significant locally but insignificant in the regional groundwater budget because these flows are simulated partially in the streamflow and landscape budgets.

The accuracy of CVHM results is related strongly to the quality and spatial distribution of input data and of measurements of the system (such as water-level altitudes, subsidence, and streamflow) that are used to constrain the calibration. The CVHM may not accurately simulate locally intense drawdowns in the potentiometric surfaces. This limitation is a function of several factors, including the allocation of relatively uniform pumpage per virtual well in cells where crops were grown within each WBS, in cell size, and limited unsaturated zone processes simulated with the FMP where the water table is deep. For example, the CVHM does not adequately simulate the magnitude of the subsidence and water-level altitudes on the southern-most part of the domain. Water-level altitude declines and the amount of subsidence both are over estimated. This most likely is a result of limitations in the methods used to represent pumpage distribution with virtual wells and no spatially varying pumping capacities or local detail of irrigation schedules within a WBS, unknown hydraulic properties, and fluxes from the edges of the domain. Another example is the match with depth of simulated water-level altitudes. The difference between simulated and measured water-level altitudes generally increases with depth below the land surface.

A related topic is the scarcity of information in the textural database with increasing depth below the land surface and, therefore, the decreasing accuracy of the simulated texture distribution with depth used to estimate the hydraulic conductivities. In addition, the texture method assumes that all coarse/fine-grained units of the same percentage have the same hydraulic conductivity over very large regions. This may not necessarily be true even though the texture estimates were completed sub-regionally to reflect more localized depositional features.

The use of relatively large WBSs facilitated computation of surface-water deliveries but may have degraded the local variability of changes in water use and groundwater storage. In particular, the composite surface-water deliveries and coarse land-use and crop distributions are used to estimate pumpage without spatially varying pumpage rates, based on local irrigation needs or pumping capacities. As a result, the CVHM is best suited to quantify the conceptual understanding of the flow system and to quantify and analyze the responses at the scale of these 21 WBSs.

Given these limitations, the CVHM cannot be expected to accurately simulate time-series data from individual wells, but can be expected to represent the longer term changes and larger spatial trends in groundwater storage. Thus, the goal of the model calibration was not to match individual hydrographs, subsidence records, and streamflow losses, but to match general trends and to minimize the SOSWR for all simulated water-level altitudes, changes in water-level altitudes, land subsidence, and streamflow losses. Despite these limitations, the CVHM does an adequate job of matching water-level altitudes, changes in water-level altitudes, land subsidence, and streamflow. Furthermore, the CVHM adequately represents groundwater conditions for the entire Central Valley and is capable of simulating regional and sub-regional groundwater-flow and land subsidence.

Future Work

The performance, utility, detail, and accuracy of the CVHM could be improved in several ways. These improvements can be classified as limitations to address and as potential enhancements. Limitations that could be improved can be further categorized into simulation-code features, conceptual features, and input and comparison data. Simulation-code features include potential improvements to the SUB, LPF, MNW, and SFR packages, FMP, and the numerical solver. These enhancements may create more accurate or realistic simulations. In order for these simulations to be as accurate and realistic as possible, the CVHM will need to be updated frequently with new data and new capabilities. Doing this would make the model more dynamic and allow it to overcome some of the limitations of the current state of the model. The simulation of subsidence in the CVHM could be enhanced by both data updates and code enhancements. First, the simulation possibly could be improved by incorporating hydrodynamic lag in the simulation of aquifer-system compaction. Thick interbeds and the Corcoran Clay both should be included. Overestimated water-level altitudes and subsidence in the western San Joaquin Valley could be related to the limitations of simulating the instantaneous release from storage and compaction. For

example, delay interbeds could be assigned in the SUB package and the model re-layered with the Corcoran Clay split into four or more model layers to approximate delayed drainage in the confining unit. Secondly, geostatic load changes owing to recharge to the water table from irrigation return flows could be included through the addition of the new SUB-WT package (Leake and Galloway, 2007). A potential enhancement to the SUB package would be the ability to separate the water derived from elastic and inelastic compaction through the SUB package. Because a large part of the water pumped historically into the San Joaquin Valley was derived from inelastic compaction, the ability to make this distinction will allow water-resource managers to better assess the effects of sustained pumpage during droughts or from climate change.

The representation of sedimentary layering and formations could be improved, particularly the volcanic units and the sedimentary Tuscan and Tehama Formations in the Sacramento Valley. Additional estimates of horizontal hydraulic conductivity could be obtained from additional slug tests at monitoring-well sites.

In the CVHM, the model layers all are simulated as having a constant saturated thickness. This simplification results in an over estimation of transmissivity in areas with relatively large water-level altitude declines. Similarly, the transition from confined to unconfined storage also would affect the estimates and magnitude of changes in groundwater storage and their potential effects on streamflow infiltration and recharge. In the future, allowing the water table to fluctuate in the uppermost layers utilizing the wetting and drying capabilities of MODFLOW may result in a more accurate simulation. Although not a large source of error, allowing the layers to convert between confined and unconfined storage would result in a more accurate flow solution, provided that the drying and rewetting algorithms provided a smooth transition with improved solvers such as the Newton-Raphson solution schemes (Richard Niswonger, U.S. Geological Survey, written commun., 2008).

Recharge was applied to the water table without accounting for delays associated with travel through the unsaturated zone. Unsaturated zones range from a few feet in the San Joaquin Valley to more than 200 feet in the southern San Joaquin Valley. Transient storage in the unsaturated zone is not accounted for in the CVHM. This storage may play an important role in the water budget if artificial recharge projects are simulated. Linkage to the Unsaturated Zone Flow (UZF1) package would allow for the simulation of these delayed recharge features below the root zone (Niswonger and others, 2006). In addition, linkages between the FMP and SFR would facilitate the simulation of artificial recharge projects. The linkage to the UZF1 package also would facilitate a more realistic simulation of runoff during exceptionally wet periods when rainfall greatly exceeds the saturated vertical hydraulic conductivity.

Transition to the new SFR2 package (Niswonger and Prudic, 2005) would facilitate unsaturated infiltration under streambeds in the alluvial fan regions and would allow for a more realistic representation of reach elevations. The SFR2 package allows altitudes to vary by reach. This altitude representation, along with connections to the Lake (LAK) (Merritt and Konikow, 2000), UZF1 packages, and FMP would allow a more complete and detailed simulation of the surface-water deliveries. Combined with the optional connection of SFR2 and FMP with the SUB package, the SFR2 can be used to simulate canals and streamflows that also are affected by land subsidence owing to groundwater and petroleum production and related changes in runoff from precipitation and irrigation from FMP.

The magnitude and extent of surface-water/groundwater interactions are poorly defined. These interactions could be better quantified through field studies and more detailed classification of streambed sediments or temperature profiles. The CVHM also could be improved by including more-detailed estimates of the extent of leakage from canals, the nature of inflow and outflow that could affect seawater intrusion along the San Francisco Bay and the distribution and application of artificial recharge.

Changes in soil-water storage are less important to long-term, large-scale models and are less important in regions where irrigation from agriculture is frequent (Schmid and others, 2006a), but can make a difference for regions where pre-wetting of soils prior to the irrigation season are required or for natural vegetation that is subjected to prolonged droughts. The connection of FMP to UZF1 may address some of these issues but an additional discrepancy may remain between a transient ET and fluxes into the root zone without soil moisture storage for shorter time frames. Adding soil moisture storage to the FMP may allow for a transition of additional ET into the pre-wetting phase for some types of crops that would occur in these settings.

FMP does not simulate “on-farm” storage of delivered water and its delayed use or reuse for irrigation. This likely is an issue where WBSs have local reservoirs or reuse of water. To provide this feature, an ‘on-farm-water storage’ will need to be added to the FMP mass balance (Schmid and others, 2006a).

A potential enhancement to the CVHM would be the improvement of the accuracy of input data. In particular, land-use data, crop acreage, amount and area of double cropping, and ETo could be improved. Updates to the land-use distributions could reflect other factors such as urbanization and economic factors such as migrating to more profitable truck crops, to vineyards, and to orchards. In theory, the land-use distributions could be based on land-use distributions that change monthly or seasonally to capture more of the changes in supply and demand. Finally, the ETo estimates in the CVHM could be improved, particularly where CIMIS data are available. Furthermore, use of remotely sensed ET data, particularly MODIS, could be used to replace the current methods for calculating consumptive use.

The lack of information regarding the rate and the spatial and temporal distribution of groundwater pumpage is a significant shortcoming; in particular, the depth from which water is being pumped is lacking. Construction information on municipal and agricultural wells and wellbore profiles would help to refine the uncertain distribution of multi-aquifer pumpage that was simulated within CVHM. In particular, the value of the skin factor is uncertain. The skin factor could be refined spatially if additional wellbore flow or head-difference data were available to better constrain this parameter during model calibration. Urban pumpage potentially could be improved by including the dynamic use of water in urban settings that is subject to climate variability, variable efficiencies, and non-uniform growth. Simulating all the agricultural wells with multi-node wells with the FMP and intra-borehole flow between model layers will allow more accurate simulations.

The scale of spatial distribution of deliveries used in the CVHM is equally limiting. If deliveries were known in greater spatial detail, groundwater pumpage could be estimated in greater detail. For example, the Eastside Water District, southeast of Modesto, is a large water district that has no surface-water rights and, therefore, has experienced development of a large cone of depression (Phillips and others, 2007). This is not reflected in the CVHM because of the spatial scale of delivery data.

The CVHM is designed to be readily updateable to allow for coupling with forecasts from Global Climate Models (GCMs). Implementation of the FMP using GIS facilitates the use of remotely sensed ET data and, therefore, allows for the spatial and temporal input data for the CVHM to be updated more efficiently. This capability, in turn, facilitates using the CVHM with climate forecasts derived from GCMs. The input to the crop-based water budget is consistent with output from the GCMs. This consistency will provide the State of California and other stakeholders an ability to forecast the potential supply of surface-water deliveries, associated demand for groundwater, and, ultimately, the change in groundwater storage in the Central Valley.

In the future, coupling CVHM with optimization tools would improve the ability to identify and quantitatively evaluate water-management strategies. With the aid of the GIS, the CVHM could be used as a platform to connect simulation of groundwater/surface-water flow with the water allocation/optimization model called CALSIM (California Department of Water Resources, 2003b), and to transition to the more detailed water accounting units if they become available. Likewise, the CVHM could be used for evaluation of subregional issues, such as exportation of water from the Sacramento Valley to Southern California or the upcoming restoration of the salmon habitat of the San Joaquin River. These types of subregional issues could be assessed using the CVHM as-is, or by nesting finer-gridded subregional models within the CVHM that are linked dynamically using the embedded-model technology of the local grid refinement (LGR) package in MODFLOW (Mehl and Hill, 2005) or similar technology.

References Cited

Allen, R.G., Pereira, L.S., Raes, D., and Smith, M., 1998, Crop evapotranspiration—Guidelines for computing crop water requirements: Food and Agriculture Organization of the United Nations, Irrigation and Drainage Paper 56, 300 p., accessed April 16, 2009, at [*http://www.fao.org/docrep/X0490E/X0490E00.htm*] Errata sheet, accessed April 16, 2009, at *http://www.kimberly.uidaho.edu/water/fao56/index.html*

Anderman, E.R. and Hill, M.C., 2003, MODFLOW-2000, The U.S. Geological Survey modular ground-water flow model—Three additions to the hydrogeologic-unit flow (HUF) package—Alternative storage for the uppermost active cells (STYP parameter type), flows in hydrogeologic units, and the hydraulic conductivity depth-dependence (KDEP) capability: U.S. Geological Survey Open-File Report 03–347, 36 p., accessed April 16, 2009, at *http://water.usgs.gov/nrp/gwsoftware/modflow2000/modflow2000.html*

Anderson, J.R., Hardy, E.E., Roach, J.T., and Witmer, R.E., 1976, A land use and land cover classification system for use with remote sensor data: U.S. Geological Survey Professional Paper 964, 28 p.

Belitz, Kenneth, and Heimes, F.J., 1990, Character and evolution of the ground-water flow system in the central part of the western San Joaquin Valley, California: U.S. Geological Survey Water-Supply Paper 2348, 28 p.

Belitz, Kenneth, and Phillips, S.P., 1995, Alternative to agricultural drains in California's San Joaquin Valley: Results of a regional-scale hydrogeologic approach: Water Resources Research, v. 31, no. 8, p. 1845–1862.

Belitz, Kenneth, Phillips, S.P., and Gronberg, J.M., 1993, Numerical simulation of ground-water flow in the central part of the Western San Joaquin Valley, California: U.S. Geological Survey Water-Supply Paper 2396, 69 p.

Berkstresser, C.F., Jr., 1973, Base of fresh ground-water —approximately 3,000 micromhos—in the Sacramento Valley and Sacramento–San Joaquin Delta, California: U.S. Geological Survey Water-Resources Investigations 40-73, 1 map.

Bertoldi, G.L., Johnston, R.H., and Evenson, K.D., 1991, Ground water in the Central Valley, California—A summary report: U.S. Geological Survey Professional Paper 1401-A, 44 p.

Bredehoeft, John, 2005, The Conceptualization Model Problem—Surprise: Hydrogeology Journal, v. 13, p. 37–46.

Brouwer, C., Goffeau, A., and Heibloem, M., 1985, Irrigation water management: Training manual no. 1—Introduction into Irrigation: Food and Agriculture Organization of the United Nations, Land and Water Development Division, 91 p.

Brouwer, C. and Heibloem, M., 1986, Irrigation Water Management: Training manual no. 3–Irrigation Water Needs: Food and Agriculture Organization of the United Nations, Land and Water Development Division, 89 p.

Brush, C.F., Belitz, Kenneth, and Phillips, S.P., 2004, Estimation of a water budget for 1972–2000 for the Grasslands Area, Central Part of the Western San Joaquin Valley, California: U.S. Geological Survey Scientific Investigations Report 2004–5180, 51 p.

Burbey, T.J., 2001, Stress–strain analyses for aquifer-system characterization: Ground Water, v. 39, no. 1, p. 128–136.

Burow, K.R., Shelton, J.L., Hevesi, J.A., and Weissmann, G.S., 2004, Hydrogeologic characterization of the Modesto area, San Joaquin Valley, California: U.S. Geological Survey Scientific-Investigations Report 2004–5232, 54 p.

California Department of Water Resources, 1994, California water plan update: Bulletin 160-93, California Department of Water Resources, Sacramento, California.

California Department of Water Resources, 2000, Explanations of land use attributes used in database files associated with shape files: Land and Water Use Section, 11 p.

California Department of Water Resources, 2003a, California's groundwater, Update 2003: California Department of Water Resources Bulletin 118, 246 p.

California Department of Water Resources, 2003b, CALSIM II simulation of historical SWP/CVP operations, California: Department of Water Resources Technical Memorandum Report November 2003.

California Department of Water Resources, 2007, California Irrigation Management Information System, accessed April 16, 2009, at *http://wwwcimis.water.ca.gov/cimis/welcome.jsp*

California State University, Chico, 2003, The Central Valley historic mapping project: California State University, Chico, Department of Geography and Planning and Geographic information Center, 25 p.

Climate Source, 2006, Precipitation data from PRISM data, accessed April 16, 2009, at *http://www.climatesource.com/*

Davis, G.H., Lofgren, B.E., and Mack, Seymour, 1964, Use of ground-water reservoirs for storage of surface water in the San Joaquin Valley, California: U.S. Geological Survey Water-Supply Paper 1618, 125 p.

Davis, F.W., Stoms, D.M., Hollander, A.D., Thomas, K.A., Stine, P.A., Odion, D., Borchert, M.I., Thorne, J.H., Gray, M.V., Walker, R.E., Warner, K., and Grace, J., 1998, The California Gap Analysis Project—Final Report: University of California, Santa Barbara, California, accessed April 16, 2009, at *http://www.biogeog.ucsb.edu/projects/gap/gap_rep.html*

Diamond, J., and Williamson, A.K., 1983, A summary of ground-water pumpage in the Central Valley, California, 1961–1977: U.S. Geological Survey Water-Resources Investigations Report 83-4037, 70 p.

Dimitrakopoulos, Roussos, and Desbarats, A.J., 1993, Geostatistical modeling of grid block permeabilities for 3D reservoir simulators: Reservoir Engineering, v. 8, p. 13–18.

Droogers, Peter, and Allen, R.G., 2002, Estimating reference evapotranspiration under inaccurate data conditions: Journal of Irrigation and Drainage Systems, v. 16, p. 33–45.

Faunt, C.C., Blainey, J.B., Hill, M.C., D'Agnese, F.A., and O'Brien, G.M., 2004, F. Transient flow model, *in* Belcher, W.R., ed., Death Valley regional ground-water flow system, Nevada and California—Hydrogeologic framework and transient ground-water flow model: U.S. Geological Survey Scientific-Investigations Report 2004–5205, p. 257–352, accessed April 16, 2009, at *http://water.usgs.gov/pubs/sir/2004/5205/*

Gilliom, R.J., Barbash, J.E., Crawford, C.G., Hamilton, P.A., Martin, J.D., Nakagaki, Naomi,Nowell, L.H., Scott, J.C., Stackelberg, P.E., Thelin, G.P., Wolock, D.M., 2006, Pesticides in the nation's streams and ground water, 1992–2001: U.S. Geological Survey Circular 1291, 180 p.

Granneman, N.G. and Reeves, H.W., 2005, Great Lakes Basin water availability and use: U.S. Geological Survey Fact Sheet 2005–3113, 4 p.

Gronberg, J.M., and Belitz, K.R., 1991, Estimation of a water budget for the central part of the western San Joaquin Valley, California: U.S. Geological Survey Water-Resources Investigations Report 91-4192, 22 p.

Gronberg, J.M., Dubrovsky, N.M., Kratzer, C.K., Domagalski, J.L., Brown, L.R., and Burow, K.R., 1998, Environmental setting of the San Joaquin–Tulare Basins, California: U.S. Geological Survey Water-Resources Investigations Report 97–4205, 45 p.

Hackel, Otto, 1966, Summary of the geology of the Great Valley, p. 217–238, *in* Bailey, E.H., ed., Geology of Northern California: California Division of Mines and Geology Bulletin 190, 508 p.

Halford, K.J. and Hanson, R.T., 2002, User guide for the drawdown-limited, Multi-Node Well (MNW) Package for the U.S. Geological Survey's modular three-dimensional finite-difference ground-water flow model, versions MODFLOW-96 and MODFLOW-2000: U.S. Geological Survey Open-File Report 02–293, 33 p., accessed April 16, 2009, at *http://pubs.usgs.gov/of/2002/ofr02293/text.html*

Halford, K.J., Laczniak, R.L., and Galloway, D.L., 2005, Hydraulic characterization of over pressured tuffs in central Yucca Flat, Nevada Test Site, Nye County, Nevada: U.S. Geological Survey Scientific Investigations Report 2005–5211, 36 p.

Hanson, R.T., 1988, Aquifer-system compaction, Tucson Basin and Avra Valley, Arizona: U.S. Geological Survey Water-Resources Investigation Report 88–4172, 69 p.

Hanson, R.T. and Leake, S.A., 1998, Documentation for HYDMOD, A program for time-series data from the U.S. Geological Survey's modular three-dimensional finite-difference ground-water flow model: U.S. Geological Survey Water-Resources Investigations Report 98-564, 57 p.

Harbaugh, A.W., Banta, E.R., Hill, M.C., and McDonald, M.G., 2000, MODFLOW-2000: U.S. Geological Survey Modular Ground-Water Model—User Guide to Modularization Concepts and the Ground-Water Flow Process: U.S. Geological Survey Open-File Report 00–92, 121 p.

Hargreaves, G.H., 1994, Defining and using reference evapotranspiration: Journal of Irrigation and Drainage Engineering, v. 120, no. 6, p. 1132–1139.

Hargreaves, G.L., and Allen, R.G., 2003, History and evaluation of the Hargreaves evapotranspiration equation: Journal of Irrigation and Drainage Engineering, v. 129, no. 1, p. 53–63.

Hargreaves, G.H., and Samani, Z.A., 1982, Estimating potential evapotranspiration: Journal of Irrigation and Drainage Engineering, v. 108, no. 3, p. 225–230.

Hargreaves, G.H., and Samani, Z.A., 1985, Reference crop evapotranspiration from temperature: Applied Engineering in Agriculture, v. 1, no. 2, p. 96–99.

Hargreaves, G.L., Hargreaves, G.H., and Riley, J.P., 1985, Irrigation water requirements for Senegal River Basin: Journal of Irrigation and Drainage Engineering, v. 111, no. 3, p. 265–275.

Helm, D.C., 1974, Evaluation of stress-dependent aquitard parameters by simulating observed compaction from known stress history: Berkeley, California, University of California, doctoral dissertation, 175 p.

Helm, D.C., 1975, One-dimensional simulation of aquifer-system compaction near Pixley, California, 1, Constant parameters: American Geophysical Union, Water Resources Research, v. 11, no. 3, p. 465–478.

Helm, D.C., 1976, One-dimensional simulation of aquifer-system compaction near Pixley, California, 2, stress-dependent parameters: American Geophysical Union, Water Resources Research, v. 12, no. 3, p. 375–391.

Helm, D.C., 1977, Estimating parameters of compacting fine-grained interbeds within a confined aquifer system one-dimensional simulation of field observations, in International Symposium on Land Subsidence, 2d, Anaheim, California, 1976, Proceedings: International Association of Hydrological Sciences Publication 121, p. 145–156.

Hidalgo, H.G., Cayman, D.R., Hettinger, M.D., 2005, Sources of variability of evapotranspiration in California: Journal of Hydrometeorology, v. 6, p. 3–19.

Hill, M.C., Banta, E.R., Harbaugh, A.W., and Anderman, E.R., 2000, MODFLOW-2000, The U.S Geological Survey modular ground-water model—user guide to the observation, sensitivity, and parameter-estimation processes and three post-processing programs: U.S. Geological Survey Open-File Report 00-184, 209 p.

Hill, M.C., Cooley, R.L., and Pollock, D.W., 1998, A controlled experiment in ground-water flow model calibration: Ground Water, v. 36, no. 3, p. 520–535.

Hill, M.C., and Tiedeman, C.R., 2007, Effective groundwater model calibration: with analysis of data, sensitivities, predictions, and uncertainty: New York, Wiley and Sons, 464 p.

Hoffmann, Jon, Galloway, D.L., and Secker H.A., 2003a, Inverse modeling of interbred storage parameters using land subsidence observations, Antelope Valley, California: Water Resources Research, 39, doe: 10.1029/2001WR001253.

Hoffmann, Jon, Leake, S.A., Galloway, D.L., and Wilson, A.M., 2003b, MODFLOW-2000 ground-water model—User guide to the subsidence and aquifer-system compaction (SUB) package: U.S. Geological Survey Open-File Report 03–233, 46 p.

Hsieh, P.A., and Freckelton, J.R., 1993, Documentation of a computer program to simulate horizontal-flow barriers using the U.S. Geological Survey's modular three-dimensional finite-difference ground-water-flow model: U.S. Geological Survey Open-File Report 92-477, 32 p.

Ireland R.L., Poland, J.F., and Riley, F.S., 1984, Land subsidence in the San Joaquin Valley, California, as of 1980: U.S. Geological Survey Professional Paper 437-I, 93 p.

Jensen, D.T., Hargreaves, G.H., Temesgen, B., and Allen, R.G., 1997, Computation of ETo under no ideal conditions: Journal of Irrigation and Drainage Engineering, v. 123, no. 5, p. 394–400.

Johnson, A.I., Muston, R.P., Morris, D.A., 1968, Physical and hydrogeologic properties of water-bearing materials in subsiding areas in central California: U.S. Geological Survey Professional Paper 497-A, 71p.

Kern Water Bank Authority, 2007, accessed April 16, 2009, at *http://www.kwb.org/main.htm*

Konikow, L.F. and Neuzil, C.E., 2007, A method to estimate groundwater depletion from confining layers, Water Resources Research, 43, W07417, doi:10.1029/2006WR005597.

Larson, K.J., Basagaolu, H., and Mario, M., 2001, Numerical simulation of land subsidence in the Los Banos-Kettleman City area, California: University of California Davis Water Resources Center Technical Completion Report Contribution no. 207, 83 p.

Laudon, Julie, and Belitz, Kenneth, 1991, Texture and depositional history of Late Pleistocene–Holocene alluvium in the central part of the western San Joaquin Valley, California: Bulletin of the Association of Engineering Geologists, v. 28, no. 1, p. 73–88.

Leake, S.A., 1990, Interbed storage changes and compaction in models of regional ground-water flow: Water Resources Research, v. 26, no. 9, p. 1939–1950.

Leake, S.A., and Galloway, D.L., 2007, MODFLOW groundwater model—user guide to the Subsidence and Aquifer-System Compaction Package (SUB-WT) for Water-Table Aquifers: U.S. Geological Survey Techniques and Methods, Book 6, Chap. A23, 42 p.

Leake, S.A., and Prudic, D.E., 1991, Documentation of a computer program to simulate aquifer-system compaction using the modular finite-difference ground-water flow model: U.S. Geological Survey Techniques of Water-Resources Investigations, book 6, chap. A2, 68 p.

Londquist, C.J., 1981, Digital model of the unconsolidated aquifer system in the Modesto Area, Stanislaus and San Joaquin Counties, California: U.S. Geological Survey Water-Resources Investigations Report 81-12, 36 p.

McDonald, M.G., and Harbaugh, A.W., 1988, A modular three-dimensional finite-difference ground-water flow model: U.S. Geological Survey Techniques of Water-Resources Investigations Report, book 6, chap. A1, 586 p.

Mehl, S.W., and Hill, M.C., 2005, MODFLOW-2005, The U.S. Geological Survey modular ground-water model—Documentation of shared node local grid refinement (LGR) and the boundary flow and head (BFH) package: U.S. Geological Survey Techniques and Methods 6-A12, 68 p.

Merritt, L.M., and Konikow, L.F., 2000, Documentation of a computer program to simulate lake-aquifer interaction using the MODFLOW ground-water flow model and the MOC3D solute-transport model: U.S. Geological Survey Water-Resources Investigations Report 00-4167, 146 p.

Mullen, J.R., and Nady, Paul, 1985, Water budgets for major streams in the Central Valley, California, 1961–77: U.S. Geological Survey Open-File Report 85-401, 87 p.

Nady, Paul, and Larragueta, L.L., 1983, Estimated average annual streamflow into the Central Valley of California: U.S. Geological Survey Hydrologic Investigations Atlas HA-657.

Niswonger, R.G., and Prudic, D.E., 2005, Documentation of the Streamflow-Routing (SFR2) Package to include unsaturated flow beneath streams—a modification to SFR1: U.S. Geological Survey Techniques and Methods, Book 6, Chap. A13, 47 p.

Niswonger, R.G., Prudic, D.E., and Regan, R.S., 2006, Documentation of the unsaturated-zone flow (UZF1) package for modeling unsaturated flow between the land surface and the water table with MODFLOW-2005: U.S. Geological Survey Techniques and Methods 6–A19, 74 p.

Page, R.W., 1977, Guide for data collection to calibrate a predictive digital ground-water model of the unconfined aquifer in and near the city of Modesto, California: U.S. Geological Survey Water-Resources Investigations Report 76-41, 46 p.

Page, R.W., 1986, Geology of the fresh ground-water basin of the Central Valley, California, with texture maps and sections: U.S. Geological Survey Professional Paper 1401-C, 54 p.

Page, R.W. and Balding, G.O., 1973, Geology and quality of water in the Modesto–Merced area, San Joaquin Valley, California: U.S. Geological Survey Water-Resources Investigations Report 73-6, 85 p.

Pavelko, M.T., 2004, Estimates of hydraulic properties from a one-dimensional numerical model of vertical aquifer-system deformation, Lorenz Site, Las Vegas, Nevada: U.S. Geological Survey Water-Resources Investigations Report 03–4083, 35 p., accessed April 16, 2009, at *http://pubs.usgs.gov/wri/wri034083/*

Phillips, S.P., and Belitz, Kenneth, 1991, Calibration of a textured-based model of a ground-water flow system, western San Joaquin Valley, California: Ground Water, v. 29, no. 5, p. 702–715.

Phillips, S.P., Carlson, C.S., Metzger, L.F., Howled, J.F., Galloway, D.L., Sneed, Michelle, Ichihara, M.E., Hunt, K.W., and King, N.E., 2003, Analysis of tests of subsurface injection, storage, and recovery of freshwater in Lancaster, Antelope Valley, California: U.S. Geological Survey Water-Resources Investigations Report 03–4061, 122 p., accessed April 16, 2009, at *http://ca.water.usgs.gov/pubs/wrir_03-4061.pdf*

Phillips, S.P., Green, C.T., Burow, K.R., Shelton, J.L., and Rewis, D.L., 2007, Simulation of multistage ground-water flow in part of the Northeastern San Joaquin Valley, California: U.S. Geological Survey Scientific-Investigations Report 2007–5009, 43 p.

Poeter, E.P., Hill, M.C., Banta, E.R., Mehl, Steffen, and Christensen, Steen, 2005, UCODE_2005 and six other computer codes for universal sensitivity analysis, calibration, and uncertainty evaluation: U.S. Geological Survey Techniques and Methods 6-A11, 283 p.

Prudic, D.E., Konikow, L.F., and Banta, E.A., 2004, A new streamflow-routing (SFR1) package to simulate stream-aquifer interaction with MODFLOW-2000: U.S. Geological Survey Open-File Report 04–1042, 95 p.

Riley, F.S., 1969, Analysis of borehole extensometer data from Central California, in Tyson, L.J., ed., Land Subsidence: Tokyo, International Association of Hydrological Sciences Publication 89, v. 2, p. 423–431.

Riley, F.S., 1984, Developments in borehole extensometer, in International Symposium on Land Subsidence, 3d, Venice, Italy, 1984, Proceedings: International Association of Hydrological Sciences Publication 151, p. 169–186.

Riley, F.S., 1998, Mechanics of aquifer systems—The scientific legacy of Dr. Joseph F. Poland, *in* Borchers, J.W., ed., Land subsidence case studies and current research: Proceedings of the Dr. Joseph F. Poland Symposium on Land Subsidence, Association of Engineering Geologists Special Publication no. 8, p. 13–27.

Russo, David, and Bouton, Moshe, 1992, Statistical analysis of spatial variability in unsaturated flow parameters: Water Resources Research, v. 28, no. 7, p. 1911–1925.

Samani, Z.A., 2000, Estimating solar radiation and evapotranspiration using minimum climatological data: J. Irrigation and Drainage Engineering, v. 126, no. 4, p. 265–267.

Schmid, Wolfgang, Hanson, R.T., and Mattock III, T.M., 2006a, Overview and advances of the farm process for MODFLOW-2000: Managing Groundwater Systems —Conference Proceedings, International Ground Water Modeling Center, Golden, Colorado, May 21–24, 2006 , p. 23–27

Schmid, Wolfgang, Hanson, R.T., Mattock III, T.M., and Leake, S.A., 2006b, User's guide for the farm process (FMP) for the U.S. Geological Survey's modular three-dimensional finite-difference ground-water flow model, MODFLOW-2000: U.S. Geological Survey Techniques and Methods 6-A17, 127 p.

Semitropic Water Storage District, 2007, accessed April 16, 2009, at *http://www.semitropic.com/index.htm*

Sneed, Michelle, 2001, Hydraulic and mechanical properties affecting ground-water flow and aquifer-system compaction, San Joaquin Valley, California: U.S. Geological Survey Open-File Report 01-35, 26 p.

Sneed, Michelle, and Galloway, D.L., 2000, Aquifer-system compaction and land subsidence: Measurements, analyses, and simulations - the Holly Site, Edwards Air Force Base, Antelope Valley, California: U.S. Geological Survey Water-Resources Investigations Report 00-4015, 65 p., accessed April 16, 2009, at *http://ca.water.usgs.gov/archive/reports/wrir004015/*

Snyder, R.L., Lamina, B.J., Shaw, D.A., and Pruitt, W.O., 1987a, Using reference evapotranspiration (ETo) and crop coefficients to estimate crop evapotranspiration (Etch) for agronomic crops, grasses, and vegetable crops: Berkeley, Calif., Leaflet 21427, Cooperative Extension of the University of California Division of Agriculture and Natural Resources, 12 p.

Snyder, R.L., Lamina, B.J., Shaw, D.A., and Pruitt, W.O., 1987b, Using reference evapotranspiration (ETo) and crop coefficients to estimate crop evapotranspiration (Etch) for trees and vines: Berkeley, Calif., Leaflet 21428, Cooperative Extension of the University of California, Division of Agriculture and Natural Resources, 8 p.

Taylor, A., Hume, P., Hughes, A., and Ruston, K.R., 2001, Representation of variable hydraulic conductivity with depth in MODFLOW: *In*: Proceedings of MODFLOW 2001 and Other Modeling Odysseys Conference, Golden, CO, Sep. 11–14, v. I, p. 24–30.

Temesgen, Berkeley, Echoing, Simon, Davidoff, Baryohay, and Frame, Kent, 2005, Comparison of some reference evapotranspiration equations for California: Journal of Irrigation and Drainage Engineering, v. 131 no. 1, p. 73–84.

U.S. Department of Agriculture Natural Resources Conservation Service, 2005a, Soil Survey Geographic (SSURGO) Database: USDA Natural Resources Conservation Service, accessed April 16, 2009, at *htttp://www.soils.usda.gov/survey/geography/ssurgo/*

U.S. Department of Agriculture Natural Resources Conservation Service, 2005b, State Soil Geographic (STATSGO) Database: USDA Natural Resources Conservation Service, accessed April 16, 2009, at *http://www.soils.usda.gov/survey/geography/statsgo/*

U.S. Geological Survey, 1990, Land use and land cover digital data from 1:250,000- and 1:100,000-scale maps. Data User Guide 4, Reston, Virginia.

U.S. Geological Survey, 1999, National land cover digital data, accessed April 16, 2009, at *http://edc.usgs.gov/products/landcover/nlcd.html*

Walter, D.A. and Whealan, A.T., 2005, Simulated water sources and effects of pumping on surface and ground water, Sagamore and Monomoy flow lenses, Cape Cod, Massachusetts: U.S. Geological Survey Scientific Investigations Report 2004–5181, 85 p.

Whittemore, D.O., Macfarlane, P.A., Doveton, J.H., Butler, J.A., Jr., Chu, T.M., Bassler, R., Smith, M., Mitchell, J., and Wade, A., 1993, The Dakota Aquifer Program Annual Report, FY92, Kansas Geological Survey, Open-File Report 93-1, 170 p.

Williamson, A.K., 1982, Evapotranspiration of applied water, Central Valley, California, 1957–78: U.S. Geological Survey Water-Resources Investigations Report 81-45, 56 p.

Williamson, A.K., Prudic, D.E., and Swain, L.A., 1989, Ground-water flow in the Central Valley, California: U.S. Geological Survey Professional Paper 1401-D, 127 p.

Appendix 1. Supplemental Information—Modifications to Modflow-2000 Packages and Processes

By Wolfgang Schmid and R.T. Hanson

Introduction

The modification of selected packages was required to align the functionality of MODFLOW-2000 with the hydrologic and geologic architecture of the Central Valley. The packages that were modified or updated include the Layer-Property Flow (LPF), the Multiplier (MULT), Hydrograph Time Series (HYDMOD) (Hanson and Leake, 1998), and the Streamflow Routing (SFR1) (Prudic and others, 2004) packages. Additional improvements also were made to the Farm Process (Schmid and others, 2006). All of these modifications are summarized in the release notes and online documentation of the source code for MODFLOW-2000 version 1.15.03 (MF2K) with the Farm Process. (*http://water.usgs.gov/nrp/gwsoftware/mf2k-fmp/mf2kfmp.html*).

Layer-Property Flow Package (LPF)

The modifications to the LPF package remove the vertical leakance correction for conditions in which a partially saturated cell is immediately below a fully or partially saturated cell (Harbaugh and others, 2000, p. 31–33; McAda and Barroll, 2002) and are implemented for MF2K. The vertical leakance correction in MF2K adds an additional nonlinear term to the model, which simulates perched conditions within an aquifer system (McAda and Barroll, 2002). The modified version of the LPF package, incorporating changes documented by McAda and Barroll (2002), reduced simulated perching of the water table in areas where it has not been measured.

Multiplier Package (MULT)

The MULT package was modified to include exponentiation as an additional binary operator that could be performed on scalars or arrays, as specified in the MULT package input. The ability to perform exponentiation facilitates the expression of power functions for calculating vertical hydraulic conductivities. The distribution of vertical hydraulic conductivity now can uniformly grade between the harmonic and geometric mean by the specification of the power function to multiplier arrays that are based on sedimentary textural data estimated on a cell-by-cell basis (*Chapter C*, this volume). This approach first was recognized by Belitz and others (1993) and then implemented externally in the development of the revised groundwater-flow model for the central part of the western San Joaquin Valley within the Central Valley (C. Brush, U.S. Geological Survey, written commun., 2006). With this modification, the estimation of power functions of hydraulic conductivity distributions can be performed internally with MF2K. This resulted in modification of the subroutine GLO1BAS6RP. The exponentiation imposes absolute value on the operand; therefore, the operand must be greater or equal to zero. The exponentiation operator can be positive, negative, or zero. To use exponentiation in the MULT package, the user simply uses the "^" as a binary operator similar to the other binary operators provided by the MULT package—addition, subtraction, multiplication, and division (Harbaugh and others, 2000, p. 47–48). The MULT package does not restrict the number of binary operations specified by the user. The specified operations are performed in order from left to right. If exponentiation needs to occur prior to other mathematical operations, the user should make this binary operation a separate input command prior to other mathematical operations.

Time-Series Package (HYDMOD)

The modifications to the HYDMOD package allow the capture of time series from the Subsidence package (SUB) (Hoffmann and others, 2003) and from the SFR1 packages (Prudic and others, 2004). Input specifications of locations for retrieval of time-series data in HYDMOD are the same for SUB as originally specified for the Interbed Storage package and the same for SFR1 as the first Streamflow Routing package (STR1). However, the input item that specifies the package that time-series data are retrieved from (PCKG) is specified as 'SUB' for the Subsidence package and as 'SFR1' for SFR1 and STR1. Note that time series of compaction and subsidence for non-delay interbeds is available with these modifications and time series for delayed compaction currently are not available.

Streamflow Routing Package (SFR1)

The modifications to SFR1 (version 1.4) (Prudic and others, 2004) includes an additional option to compute streambed elevation for canal reaches (reaches of SFR diversion segments), which allows the streambed slope to follow the slope of ground surface at a defined depth. Details of these changes were documented in Schmid and others (2006). These changes to SFR1 are independent of the linkage between the Farm Process and SFR1.

The Farm Process (FMP1)

Additional improvements made to the Farm Process include:

1. Root uptake under variably saturated conditions;
2. Matrix of on-farm efficiencies not only by farm, but also by crop;
3. Nonirrigated vegetation;
4. Additional consumptive use types that include the use of crop coefficients and reference evapotranspiration;
5. A modification to the specification of a point of diversion for semi-routed deliveries;
6. Semi-routed return flows to specified reaches of the stream network;
7. Restrictions on farm-well pumping, where no irrigation requirement exists; and
8. Additional budget components.

With the ability to simulate root-zone pressure heads that span from negative to positive values, the FMP now can simulate the growing of crops that take up water from saturated conditions such as rice or some types of riparian vegetation. A more distributed specification of on-farm irrigation efficiencies allows the user to specify efficiencies as a matrix by farm and by crop for the entire simulation or each stress period. The addition of an input flag to the consumptive-use data allows the differentiation between irrigated vegetation and nonirrigated vegetation. Nonirrigated vegetation can represent dryland farming or natural vegetation settings such as rangeland, forests, or riparian settings. This flag prevents irrigation water from surface-water deliveries and groundwater pumpage from being applied to the nonirrigated vegetation. The expansion of the consumptive-use features allows the specification of consumptive use as the product of the crop coefficients and reference evapotranspiration for each crop for the entire simulation or for each stress period. This, in turn, allows the simulation of demand that is in alignment with the growth stages of each crop group the user is simulating. Locations along the streamflow network, where runoff from farms can be returned to the streamflow network, now can be specified. The additional restriction of farm wells now allows for restricting pumpage to farm wells that are located in cells, where vegetation requires irrigation water. The additional budget components facilitate output of a detailed time series of all the inflows to and outflows from each farm (water-balance subregion). The input-data options and specifications for each of these new features are described in the following input-data instructions.

Concepts and Input Instructions for New FMP1 Features

New FMP1 features that are add-on options to existing FMP1 features are described below in the order of their occurrence within the FMP input instructions in the FMP1 user guide (Schmid and others, 2006, p. 65 and 66). The following table highlights, in yellow, the position of changed or new items within the existing numbering scheme of data-input items. Changes to existing flags or parameters are displayed in blue fonts and new flags or parameters are displayed in red fonts. For explanations of the table, for example, for footnotes indicating which Array-Reading Utility Modules was used, refer to the user guide (Schmid and others, 2006, p. 64–69).

Data for each Simulation

Item No.	Input instruction for each item	
0	[#Text] read if '#' is specified (can be repeated multiple times)	
1	[PARAMETER NPFWL MXL] read if word 'PARAMETER' is specified	
2	MXACTW NFARMS NCROPS NSOILS IRTFL **ICUFL** IPFL IFTEFL IIESWFL IEFFL IEBFL IROTFL IDEFFL {IBEN} {ICOST} ICCFL INRDFL {MXNRDT} **ISRDFL** IRDFL **ISRRFL** IALLOT {PCLOSE} IFWLCB IFNRCB ISDPFL {IOPFL} {IPAPFL} **IFBPFL** **{Option}** read	
3	[PARNAM PARTYP PARVAL NLST] read if NPFWL > 0	Repeat items 3 + 4 NPFWL times
4	[Layer Row Column Farm-Well-ID Farm-ID QMAXfact] **[xyz]** read* NLST times with [3] if NPFWL > 0	Repeat items 3 + 4 NPFWL times
5	GSURF(NCOL,NROW) read* with [2]	
6	FID(NCOL,NROW) read* with [1]	
7	[Farm-ID OFE] **or [Farm-ID OFE(FID,CID$_1$), OFE(FID,CID$_2$), … , OFE(FID,CID$_{NCROPS}$)]** read* NFARMS times with [5] if IEFFL = 1	
8	SID(NCOL,NROW) read* with [1]	
9	Soil-ID CapFringe [A-Coeff B-Coeff C-Coeff D-Coeff E-Coeff], or Soil-ID CapFringe [Soil-Type] (parameters in brackets only if ICCFL = 1) read* NSOILS times with [6]	
10	[CID(NCOL,NROW)] read* with [1] if IROTFL >= 0	
11	[Crop-ID ROOT] read* NCROPS times with [4] if IRTFL = 1	
12	[Crop-ID FTR FEP FEI] read* NCROPS times with [5] if IFTEFL = 1	
13	[Crop-ID FIESWP FIESWI] read* NCROPS times with [5] if IIESWFL = 1	
14	[Crop-ID **PSI(1) PSI(2) PSI(3) PSI(4)**] read* NCROPS times with [5] if ICCFL = 1	
15	[Crop-ID BaseT MinCutT MaxCutT C_0 C_1 C_2 C_3 BegRootD MaxRootD RootGC **{NONIRR}**] read* NCROPS times with [5] if IRTFL = 3, or ICUFL = 3, or IPFL = 3	
16	[TimeSeriesStep MaxT MinT Precip ETref] read* LENSIM times with [5] if IRTFL = 3, or ICUFL = 3, or IPFL = 3 (LENSIM = length of simulation expressed as total number of time-series steps; length of time-series step defined by ITMUNI in the Discretization File)	
17	[Crop-ID IFALLOW] read* NCROPS times with [7] if IDEFFL = -2	
18	[Crop-ID WPF-Slope WPF-Int Crop-Price] read* NCROPS times with [5] if IDEFFL > 0 and if IBEN = 1	
19	Farm-ID GWcost1 GWcost2 GWcost3 GWcost4 SWcost1 SWcost2 SWcost3 SWcost4] read* NFARMS times with [5] if IDEFFL > 0 and ICOST = 1	
20	[Farm-ID Row Column Segment **Reach**] read* NFARMS times with [7] if ISRDFL = 1	
New Item	**[Farm-ID Row Column Segment Reach]** read* NFARMS times with [7] if ISRRFL = 1	

Data for each Stress Period

Item No.	Input instruction for each item
21	ITMP NP read
22	[Layer Row Column Farm-Well-ID Farm-ID QMAX] [xyz] read* ITMP times with [3] if ITMP > 0
23	[Pname] read NP times if NP > 0
24	[Farm-ID OFE] or [Farm-ID OFE(FID,CID_1), OFE(FID,CID_2), … , OFE(FID,CID_{NCROPS})] read* NFARMS times with [5] if IEFFL = 2
25	[CID(NCOL,NROW)] read* with [1] if IROTFL = -1
26	[Crop-ID ROOT] read* NCROPS times with [4] if IRTFL = 2
27	[Crop-ID CU {NONIRR}] read* NCROPS times with [4] if ICUFL = 2
New item	ETR(NCOL,NROW) read with [1] if ICUFL = 1 or -1
28	[Crop-ID FTR FEP FEI] read* NCROPS times with [5] if IFTEFL = 2
29	[Crop-ID FIESWP FIESWI] read* NCROPS times with [5] if IIESWFL = 2
30	[PFLX(NROW,NCOL)] read* with [2] if IPFL = 2
31	[Crop-ID WPF-Slope WPF-Int Crop-Price] read* NCROPS times with [5] if IDEFFL > 0 and if IBEN = 2.
32	[Farm-ID GWcost1 GWcost2 GWcost3 GWcost4 SWcost1 SWcost2 SWcost3 SWcost4] read* NFARMS times with [5] if IDEFFL > 0 and ICOST = 2.
33	[Farm-ID (NRDV NRDR NRDU)$_1$, (NRDV NRDR NRDU)$_2$, … , (NRDV NRDR NRDU)$_{MXNRDT}$] read* NFARMS times with [5] if INRDFL = 1. A maximum number of MXNRDT types of nonrouted deliveries is read for each farm. One set of variables NRDV, NRDR, and NRDU is read for a certain unranked type t of a nonrouted delivery by (NRDV NRDR NRDU)$_t$.
34	[Farm-ID Row Column Segment Reach] read* NFARMS times with [7] if ISRDFL = 2
New Item	[Farm-ID Row Column Segment Reach] read* NFARMS times with [7] if ISRRFL = 2
35	[ALLOT] read if IALLOT = 1
36	[Farm-ID CALL] read* NFARMS times with [5] if IALLOT = 2

Root Uptake Under Variably Saturated Conditions (PSI specified in Item 14)

The currently released version of the FMP allows only the simulation of transpiration uptake from unsaturated root zones. A water level rising into the root zone causes saturated conditions, under which the stress response of natural vegetation or crops becomes zero. A new concept was developed that allows the simulation of natural vegetation or crops (for example, rice and willow trees) that do not reduce their uptake as a result of anoxic conditions in the unsaturated zone and maintain maximum uptake even under saturated conditions until, eventually, they reduce their uptake as positive pressure heads increase. We will review the current concept before elaborating on the new concept. The review of the current concept makes reference to text and graphs in the FMP1 user guide (Schmid and others, 2006). Therefore, the reader is referred to the user guide, which is available under (*http://water.usgs.gov/nrp/gwsoftware/mf2k-fmp/mf2kfmp.html*).

Current Concept of Root Uptake from Unsaturated Conditions

The FMP assumes that the actual transpiration of crops is reduced proportionally to the reduction of the total root zone, TRZ, to an active root zone by wilting and anoxia. Prior to the current FMP modifications, this concept extended only to crops, whose stress response to water does not allow any uptake from saturated conditions.

The conceptualization of root uptake from an unsaturated root zone in FMP is described in detail in Schmid and others (2006, p. 11, 15, 46, and 76) and in Schmid (2004, p. 80, 83, 84, and 86). Varying hydraulic pressure heads within a root zone impose different levels of stress on a crop resulting in water uptake ranging between a maximum and zero. The functionality between dimensionless water uptake, α, ($0 \le \alpha \le 1$) and pressure head, ψ, is called a water stress response function. Such a crop-specific water stress response function can be defined by four negative critical pressure heads at which water uptake ceases as a result of either anoxia or wilting (ψ_1 ψ_4) or at which water uptake is at its maximum (ψ_2, ψ_3). The FMP simplifies this stress response function to a step function, where water uptake is considered at maximum between the averages of ψ_1 and ψ_2, and of ψ_3 and ψ_4(Schmid and others, 2006, fig. 8A, p. 15). These averages then are compared with pressure heads found by an analytical solution of the vertical pressure head configuration across the root zone (Schmid and others, 2006, fig. 8B, p. 15). In the FMP, regions of the root zone with negative pressure heads smaller than the average of ψ_4 and ψ_3 or greater than the average of ψ_2 and ψ_1 are considered inactive wilting and anoxia zones, respectively (WZ, AZ) (Schmid and others, 2006, fig. 8B, p. 15). For a water level at the bottom of the root zone (h_b), the residual active unsaturated root zone (AURZ) is equal to the TRZ minus WZ and AZ. As the groundwater level rises, the vertical pressure head distribution is shifted upward. The WZ at the top end of the pressure head distribution becomes gradually eliminated and the active root zone remains constant until the water level reaches a point, where the depth of the WZ is zero (water level at that point = h_{w0}). For water levels rising beyond this point, the AURZ is reduced linearly until the top of the anoxia fringe above the water level reaches the ground-surface elevation (GSE). At this position of the water level, transpiration reaches extinction (water level at that point = h_{ux}).

$$AURZ(h) = \begin{cases} TRZ - AZ - WZ, & h_b h \ge h_{w0} \\ GSE - AZ - h, & h_{w0} h \ge h_{ux} \\ 0 & h \ge ux \end{cases} \quad (1)$$

For water levels at or above the bottom of the root zone, the root uptake from groundwater from unsaturated conditions can be formulated as:

$$T_{gw-act-unsat}(h) = T_{c-pot}, AURZ(h) / TRZ \quad (2)$$

with :

T_{c-pot} = potential transpiration;

$T_{gw-act-unsat}$ = actual transpiration (root uptake) from groundwater.

Expanded Concept of Root Uptake from Variably Saturated Conditions

An expansion of the current concept was needed because certain crops and riparian vegetation (for example, rice and willow trees) do not reduce their uptake as a result of anoxic conditions in the unsaturated zone. However, they eventually do reduce their uptake as positive pressure heads increase in the saturated root zone or, for ponding conditions, above the ground-surface elevation.

For deep root zones and for groundwater levels ranging within the root zone, particular cases are possible, where uptake from both unsaturated and saturated conditions occurs. Above the groundwater level, zero or full uptake may occur from unsaturated conditions within the WZ and the AURZ, respectively. For crops characterized by positive critical pressure heads ψ_1 and ψ_2, the AURZ is not restricted by anoxia (AZ = 0) (*fig. 1-1*, above groundwater level). Below the groundwater level, full or reduced uptake may occur from saturated conditions within the active saturated root zone (*fig. 1-1*, below groundwater level):

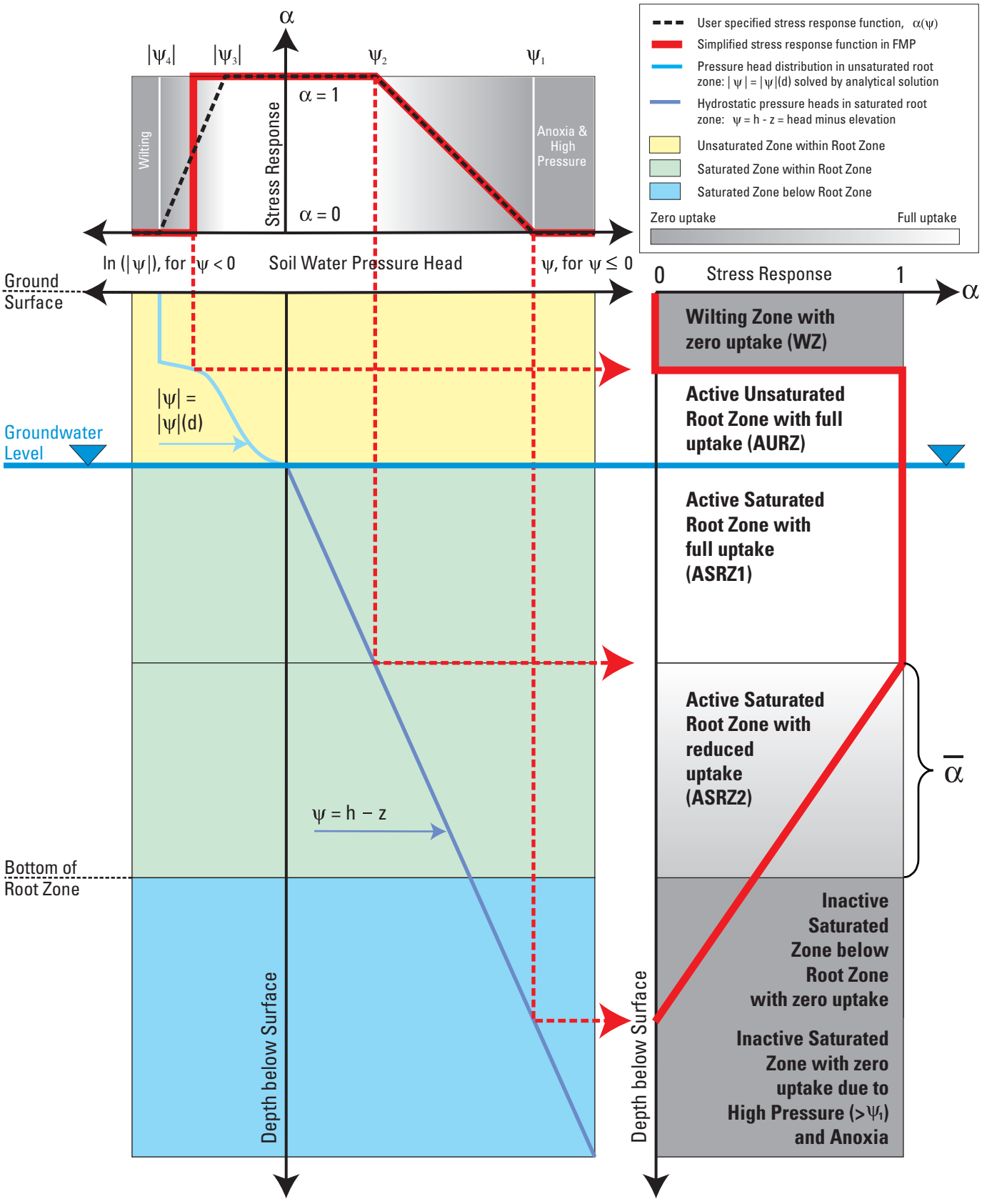

Figure 1-1. Evaluation of active and inactive parts of a variably saturated root zone in FMP (Concept of stress response, α, as a function of pressure heads, ψ, varying over depth, d).

Full uptake from saturated conditions occurs for a region of positive pressure heads within the root zone ranging between zero at the groundwater level and the user-specified pressure head ψ_2. This region of the root zone is defined as Active Saturated Root Zone 1, ASRZ1. Within this zone, the stress response to water uptake, a, is equal to 1, meaning full uptake is possible. For water levels rising above the GSE (not displayed in *fig. 1-1*), the ASRZ1 extends from the GSE to where the critical pressure head ψ_2 is found.

Reduced uptake from saturated conditions occurs for a region of positive pressure heads ranging between ψ_2 (full uptake) and the lesser of ψ_1 (zero uptake) and the pressure head at the bottom of the root zone. This region of the root zone is defined as the Active Saturated Root Zone 2, ASRZ2. Within this zone, the stress response to water uptake, α, is taken to be equal to the average of stress responses, $\bar{\alpha}$, owing to pressure heads that are found within the root zone between ψ_2 and the lesser of ψ_1 and the pressure head at the bottom of the root zone. *Figure 1-1* displays a case where ψ_1 is not found within but is found below the bottom of the root zone. That is, in this case, ASRZ2 is not bound by ψ_1 but by the pressure head at the bottom of the root zone, where the stress response owing to this pressure head is not yet zero.

For water levels at and above the bottom of the root zone, the uptake from saturated conditions is formulated as (T-notations see eq. 2):

$$T_{gw-act-sat}(h) = T_{c-pot} \bullet \left(ASRZ1(h) + ASRZ2(h) \bullet \bar{\alpha}(h) \right) / TRZ \quad (3)$$

For water levels at and above the bottom of the root zone, the total uptake is formulated as:

$$T_{gw-act}(h) = T_{c-pot} \bullet \left(AURZ(h) + ASRZ1(h) + ASRZ2(h) \bullet \bar{\alpha}(h) \right) / TRZ \quad (4)$$

ASRZ1, ASRZ2, and $\bar{\alpha}$ depend on the vertical location of the hydrostatic pressure heads ψ_1 and ψ_2. Because ψ_1 and ψ_2 move vertically up or down as the water level rises or falls, the terms ASRZ1, ASRZ2, and $\bar{\alpha}$ depend on the simulated groundwater level and, therefore, are head-dependent terms. In order to avoid the term $ASRZ2(h) \bullet \bar{\alpha}(h)$ becoming nonlinear in head, we evaluate ā based on the head of the previous iteration (k-1), while ASRZ2 is related to the head of the current iteration (k):

$$T_{gw-act}(h^k) = T_{c-pot} \bullet \left(AURZ(h^k) + ASRZ1(h^k) + ASRZ2(h^k) \bullet \bar{\alpha}(h^{k-1}) \right) / TRZ \quad (5)$$

Schmid and others (2006) explained how $T_{gw\text{-}act\text{-}unsat}$ can be split into non-head-dependent and head-dependent terms. Similarly, $T_{gw\text{-}act\text{-}sat}$, is separated into terms either dependent or not dependent on the head of the current iteration. While *figure 1-1* demonstrates a situation for a particular water-level elevation, *figure 1-2* illustrates the conceptual approximation to the change of all transpiration and evaporation components with varying groundwater level (*fig. 1-2*, Example 1). Only the transpiration components are discussed in this appendix, the evaporation components are explained in the FMP user guide (Schmid and others, 2006) and as no expansions to them were made here.

This concept allows the simulation of water uptake and irrigation requirements of natural vegetation or crops (for example, rice, willows) rooting in soils that are fully or partially saturated by the groundwater rising into the root zone or even above ground surface (for example, in alluvial valleys). Under such conditions, irrigation only is required for vegetation specified as irrigated crops for special cases, where uptake from groundwater does not fully satisfy the potentially possible transpiration.

Depending on where the water level is positioned (above, within, or below the root zone), this new concept of FMP considers five different cases of combinations of up to four transpiration components. These components are fed either by capillary rise from groundwater (unsaturated root zone), by direct uptake from groundwater (saturated root zone), by irrigation, or by precipitation. For instance, for Case 3 (*fig. 1-2*, Example 1), the water level rises only slightly above the bottom of the root zone and wilting still might occur in the drying top soil. Transpiration is fed by groundwater uptake from the unsaturated and saturated part of the root zone. The deficit between the transpiration from groundwater and the maximum possible transpiration may be supplemented by precipitation or irrigation. However, if the water level rises further (*fig. 1-2*, Example 1, Case 2), all possible transpiration will occur by groundwater uptake from the unsaturated and saturated root zone. Finally, when the water level rises above the ground surface and ponding occurs, then uptake only will take place from the saturated, inundated root zone (*fig. 1-2*, Example 1, Case 1).

Examples 1, 2, and 3 (*fig. 1-2*) show how the total transpiration uptake from the saturated root zone (light green curve) is composed of the uptake from the fully active and partially active part of the saturated root zone. The uptake from the fully active root zone (light blue curve) is a piecewise linear approximation. The uptake from the partially active root zone (purple curve) depends on the product of two head-dependent terms, the depth of this zone and the average stress response, $\bar{\alpha}$, within that zone. Therefore, as shown in *figure 1-2*, this part of the uptake is nonlinear with changing head (eq. 4). For select positive ψ_1 and ψ_2 values, the range of positive pressure heads with reduced uptake ($\psi_1 - \psi_2$) may be less than the thickness of the total root zone. In this case, the "partial uptake zone," ASRZ2, and the average stress response, $\bar{\alpha}$, within that zone may remain constant with a moving water level, as long as the elevation where ψ_2 is found (head - ψ_2) is less than the ground-surface elevation, and as long as the elevation where ψ_1 is found (head - ψ_2) is greater than the bottom of the root zone.

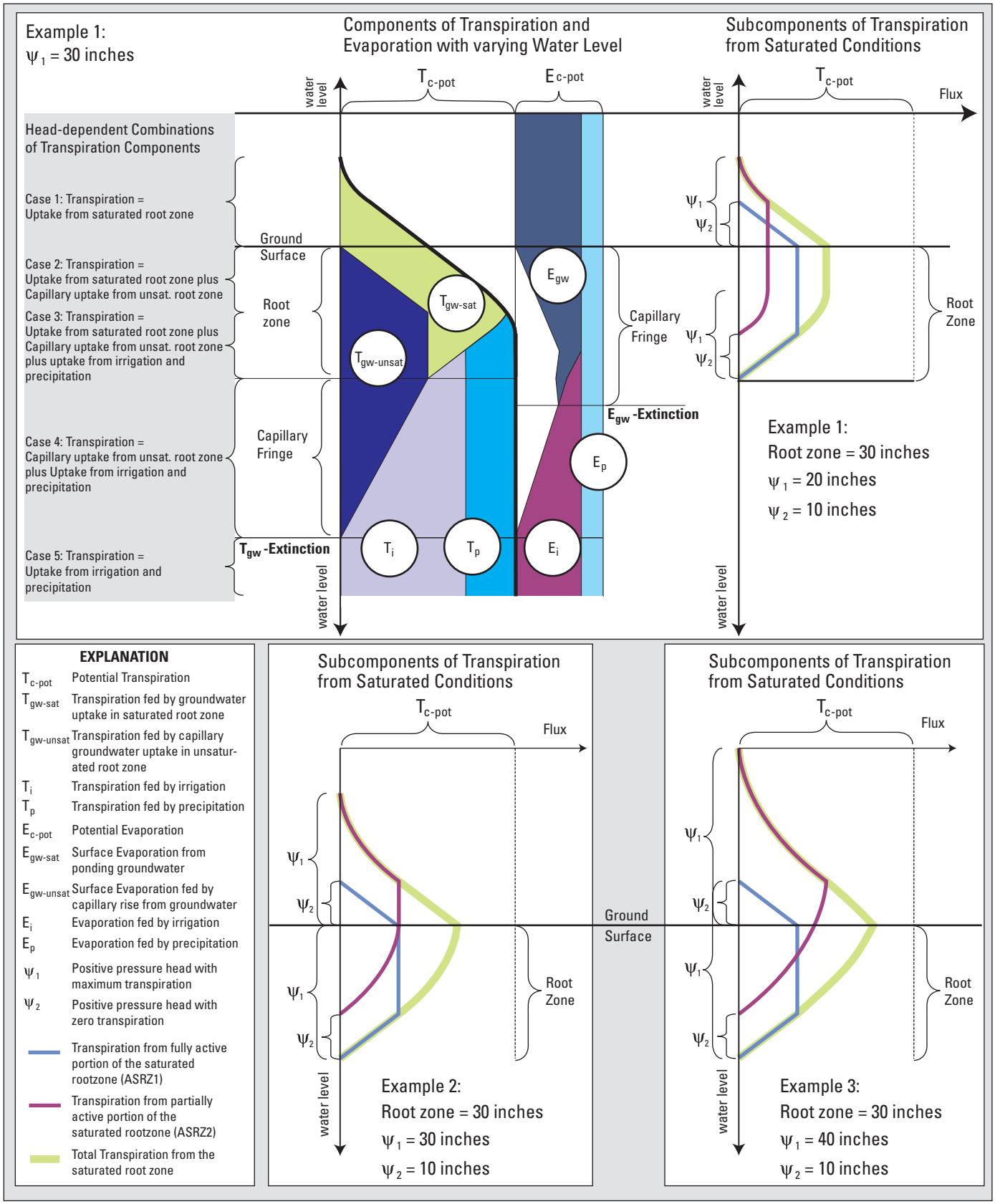

Figure 1-2. Conceptualization to the change of transpiration uptake from a saturated root zone with varying water level (Three examples with different ψ_1 values; example 1 at top includes conceptualization of all transpiration and evaporation components with varying water level).

Input Instructions

Until now, the use of the FMP was limited to natural vegetation and crops that consume water only from unsaturated conditions. The original input requirements for crop-specific stress response functions required absolute values of negative pressure heads, between which, root uptake is at maximum and at which uptake becomes zero due to wilting and anoxia. For new FMP1 features, the parameter and input item number of the FMP input instructions are referenced in parenthesis after the section titles.

The new, expanded concept of consumptive use allows the simulation of natural vegetation or crops that take up water from parts of the root zone with both negative and positive pressure heads. Therefore, the user must be able to enter any pressure head at which root uptake is at maximum or zero. For saturation-intolerant natural vegetation or crops, the user is required to enter negative pressure head values for the stress-response function for unsaturated conditions. For natural vegetation or crops that tolerate saturated conditions, ψ_1 and ψ_2 have to be positive pressure heads. These values describe a linear decrease of uptake from optimal (at ψ_2) to zero (at ψ_1) due to anoxia and increasing pressure. The critical pressure heads ψ_3 and ψ_4 remain negative, since they represent the diminishing of uptake from maximum (at ψ_3) to zero (at ψ_4) due to wilting in drying, unsaturated conditions.

The input instructions for item 14 (Schmid and others, 2006, p. 76) have changed to:

PSI(1) Negative or positive pressure head, at which root uptake becomes zero due to anoxia or high pressure [L]

PSI(2) Negative or positive pressure head, at which root uptake is at maximum and from which uptake decreases with rising pressure head due to anoxia [L]

PSI(3) Negative pressure head, at which root uptake is at maximum and from which uptake decreases with falling pressure head due to wilting [L]

PSI(4) Negative pressure head, at which root uptake becomes zero due to wilting [L]

Matrix of On-Farm Efficiencies (OFE specified in Items 7 or 24)

In addition to just reading one value of on-farm efficiency per farm, a matrix of efficiencies for any farm and any crop now can be read (rows: farm ID; columns: crop type ID). The user also may specify efficiencies varying from crop to crop for some farms while specifying one efficiency (not varying by crop) for other farms. In the latter case, the efficiency entered in column 2 of item 7 or item 24 (column 1 = farm ID) is assumed to be valid for all other crops and the matrix fields do not have to be filled for other crops.

Input Requirements

For a matrix of on-farm efficiencies, the required data input is as follows:

[FID OFE(FID,CID=1), OFE(FID,CID=2), … , OFE(FID,CID=NCROPS)] read NFARMS times for each simulation if IEFFL = 1 (item 7) or for each stress period if IEFFL = 2 (item 24). (FID= Farm ID; CID = Crop-ID)

In matrix form (NFARMS = number of farms; NCROPS = number of crops):

	Column 1	Column 2	Column 3	...	Column NCROPS+1
Row 1	1	$OFE_{1,1}$	$OFE_{1,2}$	…	$OFE_{1,NCROPS}$
Row 2	2	$OFE_{2,1}$	$OFE_{2,2}$	…	$OFE_{2,NCROPS}$
…	…	…	…	…	…
Row NFARMS	NFARMS	$OFE_{NFARMS,1}$	$OFE_{NFARMS,2}$	…	$OFE_{NFARMS,NCROPS}$

CAUTION: Comments for each farm neither can be entered to the right of efficiencies specified by crop nor to the right of just one value per farm in column 2. If the user enters a comment, the following input error is printed to the list file: ERROR CONVERTING "…" TO A DP-REAL NUMBER IN LINE ... .

Data Output

For each farm, an output "composite efficiency" is printed together with the farm demand and supply budget for each iteration, each time step, or selected time steps either to the list file, to an ASCII file called FDS.OUT, or to a binary file as specified by the Farm Supply and Demand Print Flag, ISDPFL. This "composite efficiency" is an area-weighted average of either specified efficiency values (IEBFL=1) or simulated head-dependent efficiencies (IEBFL=2,3) of all model cells in a farm, weighted by the area of each cell.

Non-Irrigation Crops (NONIRR Specified in Items 15 or 27)

Non-irrigation crops are designated by NONIRR=1 in column 3 of the data list in item 27 (ICUFL≤2). This is required if, a potential crop evapotranspiration flux value for each crop is specified for each stress period in item 27 (ICUFL=1,2). This also is required if, for each crop, a potential crop evapotranspiration flux value is derived as the product of crop coefficients specified in item 27 for each stress period and a reference evapotranspiration-inserted item after item 27 for each stress period (ICUFL=–1). Non-irrigation crops are designated by NONIRR=1 in column 12 of the crop list in item 15 (ICUFL=3), if, for each crop, a potential crop evapotranspiration flux value is derived for each time step from time-series of climate data and growing-degree-day coefficients as explained in Schmid and others (2006, p. 47–48). For irrigated crops, NONIRR=0 or no data entry is required in column 3 of item 27 (ICUFL= 2), or in column 12 of item 15 (ICUFL=3), respectively.

The Farm Process does not calculate an irrigation requirement or excess irrigation return flows for non-irrigation crops. However, it does account for transpiration and evaporation parts supplied by precipitation and groundwater uptake, as well as for excess precipitation runoff-return flows and deep percolation.

For Non-irrigation crops, the required data input is as follows:

[Crop-ID CU NONIRR] read NCROPS times if ICUFL = –1, 1, or 2 (item 27)

	Column 1	Column 2	Column 3
Row 1	1	CU_1	$NONIRR_1$
Row 2	2	CU_2	$NONIRR_2$
…	…	…	…
Row NCROPS	NCROPS	CU_{NCROPS}	$NONIRR_{NCROPS}$

Or

[Crop-ID BaseT MinCutT MaxCutT C0 C1 C2 C3 BegRootD MaxRootD RootGC NONIRR] read NCROPS times if IRTFL = 3, or ICUFL = 3, or IPFL = 3 (item 15)

	Column 1	Column 2	Column 3–11	Column 12
Row 1	1	$BaseT_1$	…	$NONIRR_1$
Row 2	2	$BaseT_2$	…	$NONIRR_2$
…	…	…	…	…
Row NCROPS	NCROPS	$BaseT_{NCROPS}$	…	$NONIRR_{NCROPS}$

Consumptive Use Options (ICUFL Specified in Item 2; ETR Specified as New Item)

1. If ICUFL=3, then a time series of crop-specific crop coefficients (K_c) is calculated. A time series of reference evapotranspiration (ETo) is read and available to be used for multiplication with a Kc value (K_c*ETo=$ET_{c\text{-}pot}$) and for fallow cells (ICID(IC,IR)=–1). The ETo is assumed to be 100 percent evaporative for fallow cells.

2. If ICUFL=2, then a list of crop specific consumptive use fluxes is read for every stress period (crop consumptive use = potential crop evapotranspiration). No fallow cells (ICID(IC,IR)=–1) can be used. In this case, no ETo is read because cropped cells (ICID(IC,IR>0) are associated with a lumped consumptive user for the entire stress period.

3. NEW: If ICUFL=1, then a list of crop-specific consumptive use fluxes is read as item 27 for every stress period (crop consumptive use = potential crop evapotranspiration). An ETo is assigned to optional fallow cells (ICID(IC,IR)=-1). In this case, a constant or a 2D array of ETo is read directly after item 27 (Crop-ID, Consumptive Use). The ETo is assumed to be 100 percent evaporative for fallow cells.

4. NEW: If ICUFL=-1, then a list of crop-specific crop coefficients (K_c) are read as item 27 for every stress period. A constant or a 2D array of ETo is read directly after item 27 (Crop-ID, K_c) in order to be multiplied with a K_c value (K_c*ETo=$ET_{c\text{-}pot}$) and to be assigned to optional for fallow cells (ICID(IC,IR)=-1). The ETo is assumed to be 100 percent evaporative for fallow cells.

For ETo, the required data input after item 27 is as follows:

ETR(NCOL,NROW) read by utility module U2DREL as constant or as 2D real array if ICUFL = 1 or –1 (new item after item 27).

Semi-Routed Delivery (ISRDFL in Item 2; REACH in Items 20 or 34)

Previously in the FMP, a stream-reach number required to specify a point of diversion for a semi-routed delivery was defined as a sequential number of a reach from zero to the total number of reaches that are active during the simulation, as specified in the SFR1 input file (NSTRM, item 1, Prudic and others, 2004, p. 40). This option allowed defining the diversion point uniquely by just the reach number (option 5 in Schmid and others, 2006, pages 54, 61, and 78) but made it difficult for the user to keep track of which segment the reach belongs to. The reach number of the diversion point is now aligned in FMP with the reach numbering scheme per segment in the SFR1 input instructions (IREACH, item 2, Prudic and others, 2004, p. 41). A unique definition of a diversion point for complex cases, where multiple reaches may exist within one model cell, now requires the entry of both a segment number and reach number. Therefore, option 5 became obsolete and was deleted.

Semi-Routed Surface-Water Runoff-Return Flow (ISRRFL in Item 2 and ROW COLUMN SEGMENT REACH Specified as New Item)

A "Semi-Routed Surface-Water Runoff-Return flow" Flag, ISRRFL, is available to simulate surface-water runoff-return flow from excess irrigation and (or) excess precipitation that is allocated as non-routed return flow to a point of recharge at a specified reach of the stream network and then routed further downstream. The ISRRFL flag was added to the existing surface-water flags after the delivery-related flags and before the water-rights related flags. That is, it is inserted between flags IRDFL and IALLOT:

ISRRFL Semi-Routed Runoff-Return flow Flag:

- 0 = No locations along the stream network are specified for any farm, where semi-routed runoff-return flow is recharged into the stream network. Runoff either is automatically prorated over tributary-segment reaches crossing through or adjacent to a farm, or automatically recharged into one tributary-segment reach nearest to the lowest elevation of the farm.
- 1or 2 = For each farm, a location is specified anywhere along the stream network, where semi-routed runoff-return flow is recharged. A farm-related list of row and column coordinates or segment and reach numbers for a point of runoff-return flow recharge is read (only if SFR1 is specified in Name File).
- 1 = List of row and column coordinates or segment and reach numbers is read for the entire simulation.
- 2 = List of row and column coordinates or segment and reach numbers is read for each stress period.

If ISRRFL=0, the FMP attempts by first priority to automatically detect tributary-segment reaches adjacent or within a farm. If none of these are found, then, by second priority, the FMP automatically locates one remote reach of a tributary segment that is situated nearest to the lowest elevation of the farm. If tributary-segment reaches are adjacent or within a farm, then the surface-water runoff of a farm is prorated over these reaches weighted by their reach lengths. We define this form of return flow as "automatic fully routed return flow." If, instead, a remote tributary-segment reach was detected, then the total runoff of a respective farm was recharged into the tributary at this reach. This form of return flow is called "automatic semi-routed return flow."

Unlike reaches receiving automatic fully or semi-routed return flow (ISRRFL=0), reaches receiving the new "specified semi-routed return flow" can be located on any type of segment. Notice that multiple farms may discharge into the same runoff-return flow reach.

A list of row and column coordinates, segment and reach numbers of a return flow reach has to be specified to receive semi-routed return flow from a specific farm. This farm-specific list is read as a new item after current item 20 or 34 (list of coordinates for semi-routed deliveries), depending on whether these data are entered for the entire simulation or for each stress period. If ISRRFL=1 and a semi-routed runoff-return flow location is specified for a particular farm, then a potentially existing automatic, fully routed runoff-return flow is disabled. For a farm, where no runoff-return flow location is known, zero coordinates and zero segment and reach numbers have to be entered. If ISRRFL=1 and no return-flow location is specified for a farm, then the FMP applies just for that particular farm either "automatic fully routed runoff return flow" or "automatic semi-routed runoff return flow," as described above for all farms if ISRRFL=0. Clearly, setting ISRRFL=1 allows the user to specify return-flow locations for farms where they are known, but still assures invoking automatic features of the FMP for other farms to find stream reaches that receive the return flow. This warrants that simulated crop-inefficient losses from a farm to surface-water runoff are indeed sent as return flow from the respective farm to the stream network. This prevents loosing mass to an open system. Simulating runoff outflows from farms without reallocating them back into the stream network would require the assumption that the runoff leaves the model domain. In the FMP, this assumption applies only if the SFR1 package is not specified in the MF2K Name File.

Farm-Related Data List for Semi-Routed Runoff-Return Flow Locations (New Item Added After Items 20 or 34):

Farm-ID	Farm identity to which the parameters below are attributed
Row	Row number of point of recharge of runoff-return flow
Column	Column number of point of recharge of runoff-return flow
Segment	Number of stream segment, in which the runoff-return flow reach is located. This number must be equal to the segment number of the identical stream reach, as specified in column 4 of the data list in the SFR1 input file for the entire simulation.
Reach	Number of reach within a segment, into which the runoff-return flow is recharged. This number must be equal to the sequential number of a reach within a particular stream segment.

Four options of data input are available in order to uniquely identify the point of recharge of runoff-return flow within a cell:

Row	Column	Segment	Reach	Comments	
x	x	x	x	full set of information is available	maximum information
x	x	x	__	if more than one segment pass through the cell	identification of location by coordinates
x	x	__	__	if just one segment passes through the cell	
0	0	x	x	if more than one segment pass through the cell	identification of location by reach and segment numbers

x = data input; 0 = input of zero; __ = no input or zero input

Additional Auxiliary Variable (AUX NOCIRNOQ Specified in Item 2)

The specification of the optional flag "AUX NOCIRNOQ" for {option} in item 2 will prompt the FMP1 to limit the distribution of farm pumpage to farm wells, whose row and column coincides with a top layer cell with a current irrigation requirement from active crops. "NOCIRNOQ" is "no crop irrigation requirement (CIR), no pumping (Q)." This feature is implemented by setting the maximum capacity of select farm wells to zero if, during a particular time step, no crop irrigation requirement of the top layer cell exists. At each new time step, the maximum capacity of such a select well will be reset to the default value. If some wells of a farm are deactivated, the remaining active wells will receive a higher demand to satisfy the pumping requirement.

The variable "AUX NOCIRNOQ" has to be specified in the entry line that contains all FMP1 flags (item 2) after the optional auxiliary variable "AUX QMAXRESET," if set, and before optional flag "NOPRINT." The optional flag "AUX NOCIRNOQ" requires FMP1 to read an auxiliary variable [xyz] either from column 7 of the farm-wells list (items 4 or 22) if "AUX QMAXRESET" is not set, or from column 8 of the farm-wells list (items 4 or 22) if "AUX QMAXRESET" is set. The auxiliary variable for "AUX NOCIRNOQ" is a binary parameter that specifies wells selected for the NOCIRNOQ option. If a "1" is read, then the respective well is selected and its maximum capacity is set equal to zero if no crop irrigation requirement of the top layer cell exists during a particular time step. The maximum capacity of such a select well is reset to the default value at each new time step.

Farm Budget Output Options (IFBPFL Specified in Item 2)

A Farm Budget print flag IFBPFL may be entered in item 2 after mandatory flag ISDPFL and between optional flags {IPAPFL} and {Option}. The IFBPFL flag allows for the following print option:

IFBPFL = 1 A compact list of Farm Budget components (flow rates and cumulative volumes into and out of a farm) is saved on ASCII file "FB_COMPACT.OUT" for all time steps:

PER	Stress period
STP	Time step
DAYS	Time unit chosen in discretization file
FID	Farm ID
Flow rates into a farm:	
Q-p-in	Precipitation
Q-sw-in	Surface-water inflow
Q-gw-in	Groundwater inflow
Q-ext-in	External deliveries
Q-in-tot	Total inflows
Flow rates out of farm:	
Q-et-out	Evapotranspiration outflow
Q-ineff-out	Inefficient losses
Q-sw-out	Surface-water outflow (excess non-routed deliveries back into canal)
Q-gw-out	Groundwater outflow (excess non-routed deliveries injected into farm wells)
Q-tot-out	Total outflows
Q-in-out	Inflows minus Outflows
Q-Discrepancy[%]	Percent discrepancy

Cumulative volumes into and out of a farm are denoted by "V" analogous to "Q" for flow rates (e.g.: V-p-in = cumulative precipitation into a farm)

IEBPFL=2 A detailed list of Farm Budget components (flow rates and cumulative volumes into and out of a farm) is saved on ASCII file "FB_DETAILS.OUT" for all time steps:

PER	Stress period
STP	Time step
DAYS	Time unit chosen in discretization file
FID	Farm ID
Flowrates into a farm:	
Q-p-in	Precipitation
Q-nrd-in	Non-routed deliveries
Q-srd-in	Semi-routed deliveries
Q-rd-in	Fully routed deliveries
Q-wells-in	Groundwater well pumping deliveries
Q-egw-in	Evaporation from groundwater into the farm
Q-tgw-in	Transpiration from groundwater into the farm
Q-ext-in	External deliveries
Q-in-tot	Total inflows
Flowrates out of a farm:	
Q-ei-out	Evaporation from irrigation out of the farm
Q-ep-out	Evaporation from precipitation out of the farm
Q-egw-out	Evaporation from groundwater out of the farm
Q-ti-out	Transpiration from irrigation out of the farm
Q-tp-out	Transpiration from precipitation out of the farm
Q-tgw-out	Transpiration from groundwater out of the farm
Q-run-out	Overland runoff out of the farm
Q-dp-out	Deep percolation out of the farm
Q-nrd-out	Non-routed deliveries from the farm
Q-srd-out	Semi-routed deliveries out of the farm (in form of excess non-routed deliveries recharged back into 'remote' head-gate)
Q-rd-out	Fully routed deliveries out of the farm (in form of excess non-routed deliveries recharged back into a head-gate within or adjacent to the farm)
Q-wells-out	Injection from farm into farm-wells (excess non-routed deliveries injected into farm-wells)
Q-tot-out	Total outflows
Q-in-out	Inflows minus outflows
Q-Discrepancy[%]	Percent discrepancy

The FMP Farm Budget has to be viewed as a 'reference interface' on the ground surface rather than a 'reference volume.' At this stage, the Farm Budget does not include soil-water storage or on-farm water storage.

References Cited

Belitz, Kenneth, Phillips, S.P., and Gronberg, J.M., 1993, Numerical simulation of ground-water flow in the central part of the Western San Joaquin Valley, California: U.S. Geological Survey Water-Supply Paper 2396, 69 p.

Brush, C.F. Belitz, Kenneth, Phillips, S.P., Burow, K.R., and Knifong, D.L., 2006, MODGRASS: Update of a groundwater flow model for the Central Part of the Western San Joaquin Valley, California: U.S. Geological Survey Scientific Investigations Report 2005-5290, 81 p.

Hanson, R.T., and Leake, S.A., 1998, Documentation for HYDMOD, A program for time-series data from the U.S. Geological Survey's modular three-dimensional finite-difference ground-water flow model: U.S. Geological Survey Open-File Report 98-564, 57 p, accessed April 16, 2009 at *http://pubs.er.usgs.gov/usgspubs/ofr/ofr98564*

Harbaugh, A.W., Banta, E.R., Hill, M.C., and McDonald, M.G., 2000, MODFLOW-2000: U.S. Geological Survey Modular Ground-Water Model—User Guide to Modularization Concepts and the Ground-Water Flow Process: U.S. Geological Survey Open-File Report 00-92, 121 p.

Hoffmann, J., Leake, S.A., Galloway, D.L., and Wilson, A.M., 2003, MODFLOW-2000 ground-water model—user guide to the subsidence and aquifer-system compaction (SUB) package: U.S. Geological Survey Open-File Report 03–233, 46 p.

McAda, D.P., and Barroll, P., 2002, Simulation of groundwater flow in the middle Rio Grande Basin between Cochiti and San Acacia, New Mexico: U.S. Geological Survey Water-Resources Investigations Report 02–4200, 88 p.

Prudic, D.E., Konikow, L.F., and Banta, E.A., 2004, A new Streamflow-Routing (SFR1) Package to simulate stream-aquifer interaction with MODFLOW-2000: U.S. Geological Survey Open-File Report 04-1042, 95 p.

Schmid, W., 2004, A Farm Package for MODFLOW-2000: Simulation of Irrigation Demand and Conjunctively Managed Surface-Water and Ground-Water Supply; PhD Dissertation: Department of Hydrology and Water Resources, The University of Arizona, 278 p.

Schmid, W., Hanson, R.T., Maddock III, T.M., and Leake, S.A., 2006, User's guide for the Farm process (FMP) for the U.S. Geological Survey's modular three-dimensional finite-difference ground-water flow model, MODFLOW-2000: U.S. Geological Survey Techniques and Methods 6-A17, 127 p.

Manuscript appproved on April 16, 2009
Prepared by the USGS Publishing Network,
Publishing Service Center, Sacramento, California

For more information concerning the research in this report, contact the
California Water Science Center Director,
U.S. Geological Survey, 6000 J Street
Sacramento, California 95819
http://ca.water.usgs.gov

Groundwater Availability of the Central Valley Aquifer, California

USGS

Faunt — Groundwater Availability of the Central Valley Aquifer, California

Professional Paper 1766

ISBN 978-1-4113-2515-9